वार्षिक प्रतिवेदन

ANNUAL REPORT

2013-14

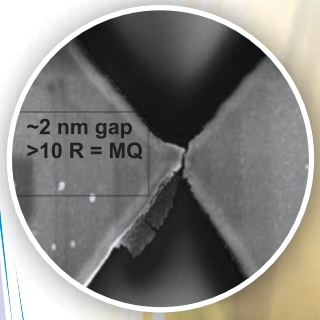

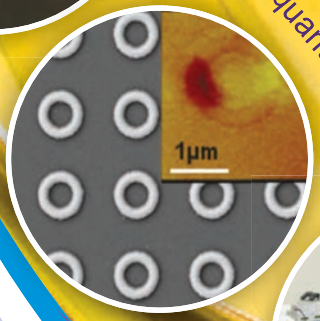

CSIR-NPL towards excellence in quantum phenomena based research

सीएसआईआर-एनपीएल के क्वान्टम परिघटना आधारित उन्नत शोध में बढ़ते कदम

सीएसआईआर-राष्ट्रीय भौतिक प्रयोगशाला
CSIR-National Physical Laboratory
New Delhi 110 012

Dr Sanjay Kumar Srivastava receiving the CSIR Young Scientist Award 2013 in Physical Sciences (including instrumentation) from the Hon'ble Minister for Science & Technology and Earth Sciences, Govt. of India and Vice President CSIR, Sri Jaipal Reddy on the CSIR Foundation Day at VigyanBhawan, 26th September, 2013.

Dr Parveen Saini receiving the CSIR Young Scientist Award 2013 in Engineering Sciences from the Hon'ble Minister for Science & Technology and Earth Sciences, Govt. of India and Vice President CSIR, Sri Jaipal Reddy on the CSIR Foundation Day at VigyanBhawan, 26th September, 2013.

Ms Anjali Sharma (Scientist), Ms Bhawna Guglani (SO) and Sh Upendera Kumar (FAO) receiving the Outstanding Achieving Award and CSIR-NPL's Institutional Award for Enterprise Resource Planning (ERP) on 26th September 2013, from DG, CSIR.

वार्षिक प्रतिवेदन

ANNUAL REPORT

2013-14

With Best Compliments from

Prof. R. C. Budhani
Director

CSIR-National Physical Laboratory
Dr. K.S. Krishnan Marg, New Delhi-110012
Tel. : +91-11 45609201, 45609301
Fax : + 91-11 45609310
E-mail : dnpl@nplindia.org
URL : www.nplindia.org

सीएसआईआर-राष्ट्रीय भौतिक प्रयोगशाला
CSIR-National Physical Laboratory
New Delhi 110 012

निदेशक
प्रो आर सी बुधानी
दूरभाष: +91-11-45609201, 45609301
ई-मेल: dnpl@nplindia.org

सम्पादन, संकलन एवं प्रकाशन
डा. रश्मि
डा. ए के श्रीवास्तव
डा. गोविंद
डा. दिवि हरनाथ
डा. टी के मंडल
डा. आशीष अग्रवाल
डा. नीता दिलावर
डा. अनुराग गुप्ता
श्री जे एन उपाध्याय
श्री अशोक कुमार
डा. एस सुधाकर
श्री राजीव शर्मा (छायांकन)
श्री एन के वाधवा

आभार
विभागाध्यक्ष
गतिविधि प्रमुख
प्रशासन नियंत्रक
नियंत्रक, वित्त एवं लेखा
नियंत्रक, भंडार एवं क्रय
डा. वीरेंद्र शंकर
श्री विश्व दीपक अरोड़ा

वेबसाइट: www.nplindia.org
फैक्स: +91-11-45609310
कार्य समय: 0900 to 1730
साप्ताहिक अवकाश: शनिवार एवं रविवार

प्रकाशन
निदेशक
सीएसआईआर-राष्ट्रीय भौतिक प्रयोगशाला
डा. के एस कृष्णन मार्ग
नई दिल्ली-110012

मुद्रण
सीएसआईआर-निस्केयर
डा. के एस कृष्णन मार्ग
नई दिल्ली-110012

Director
Prof R C Budhani
Tel.:+91-11-45609201, 45609301
Email: dnpl@nplindia.org

Editing, Compilation & Publication
Dr. Rashmi
Dr. A K Srivastava
Dr. Govind
Dr. D Haranath
Dr. T K Mandal
Dr. Ashish Agarwal
Dr. Nita Dilawar
Dr. Anurag Gupta
Sh. J N Upadhyay
Sh. Ashok Kumar
Dr. S Sudhakar
Sh. Rajiv Sharma (Photographs)
Sh. N K Wadhwa

Acknowledgements
Divisional Heads
Activity Leaders
COA
CO(F&A)
CO(S&P)
Dr. Virendra Shanker
Sh. Vishwa Deepak Arora

Website: www.nplindia.org
Fax: +91-11-45609310
Working Hours: 0900 to 1730
Weekly Off: Saturday & Sunday

Published by
Director
CSIR-National Physical Laboratory
Dr. K S Krishnan Marg
New Delhi - 110012

Printed by
CSIR-NISCAIR
Dr. K S Krishnan Marg
New Delhi – 110012

विषय सूची/Contents.....

प्रभागीय गतिविधियां/Divisional Activities

परिशिष्ट/Appendices

निदेशक की लेखनी से .....

मुझे सी एस आई आर – राष्ट्रीय भौतिक प्रयोगशाला की वर्ष 2013–2014 की वार्षिक रिपोर्ट आपके समक्ष प्रस्तुत करते हुए अत्यन्त प्रसन्नता हो रही है । सी एस आई आर – एन पी एल, भौतिक विज्ञान के क्षेत्र में एक अग्रणी अनुसंधान प्रयोगशाला तथा भारत का राष्ट्रीय मापिकी संस्थान है जो कि सी एस आई आर तंत्र के तहत स्थापित प्रथम पाँच राष्ट्रीय प्रयोगशालाओं में से एक है। इस प्रयोगशाला का प्राथमिक उद्देश्य मापन के राष्ट्रीय मानकों को बनाए रखना तथा अनुसंधान द्वारा उनका निरंतर अनुरक्षण करना है, जिसके लिए क्वांटम मानकों तथा मापन विज्ञान के उदीयमान क्षेत्रों में महत्त्वपूर्ण अनुसंधान किया गया है । प्रयोगशाला द्वारा ऊर्जा संचयन प्रौद्योगिकी, नैनोटेक्नोलॉजी, उन्नत पदार्थों, क्वांटम संघनित द्रव्य तथा रेडियो एवं वायुमण्डलीय विज्ञान के विभिन्न क्षेत्रों में अनुसंधान तथा विकास गतिविधियों को भी प्रोत्साहित किया गया है । देश के औद्योगिक, सामाजिक तथा पर्यावरणीय क्षेत्रों के प्रति अपने उत्तरदायित्वों से प्रयोगशाला परिचित है तथा ज्ञान आधारित प्रौद्योगिकियाँ प्रदान कर और विज्ञान, प्रौद्योगिकी एवं नवीनता के एकीकृत क्रियान्वयन द्वारा ज्ञान में निरन्तर उन्नति द्वारा योगदान कर रही है । भौतिक विज्ञान में एक अग्रणी तथा विश्वव्यापी स्तर पर मान्यता प्राप्त प्रयोगशाला बनने की दिशा में सी एस आई आर – एन पी एल का धीरे–धीरे तथा निरन्तर रूपातंरण हो रहा है । वर्ष 2013–14 के दौरान, यह प्रक्रिया चलती रही तथा प्रयोगशाला में पहले से उपलब्ध विश्व – स्तरीय अनुसंधान अवसंरचना को और अधिक विस्तृत किया गया । $-272.99^{0}C$ तक पदार्थ अनुसंधान सुविधा, प्रत्येक परमाणु को प्रतिबिंबित करने तथा उनकी संयोजी अवस्था को सुनिश्चित करने के लिए इलेक्ट्रॉन माइक्रोस्कॉपी की व्यवस्था के साथ नवोन्नत मापिकी बिल्डिंग तथा सौर ऊर्जा स्वच्छ कक्ष की सुविधा प्रयोगशाला की अवसंरचना में महत्त्वपूर्ण परिवर्धन हैं।

इन सभी प्रयासों के फलस्वरूप वर्ष के दौरान संवर्धित तथा महत्त्वपूर्ण अनुसंधान एवं विकास हुआ । हमारे दो युवा वैज्ञानिक, डा. संजय कुमार श्रीवास्तव और डा. प्रवीन सैनी ने

अपने असाधारण योगदान के कारण क्रमशः भौतिक विज्ञान तथा अभियांत्रिकी विज्ञान के क्षेत्र में प्रतिष्ठित सी एस आई आर युवा वैज्ञानिक पुरस्कार, 2013 सी एस आई आर के उद्यम संसाधन योजना (ई आर पी) प्रयास में सी एस आई आर – एन पी एल के उत्कश्ष्ट प्रदर्शन के सम्मान में सुश्री अंजली शर्मा, सुश्री भावना गुगलानी तथा श्री उपेन्द्र कुमार को उत्कृष्ट उपलब्धि पुरस्कार तथा सी एस आई आर – एन पी एल का संस्थागत पुरस्कार, 2013 प्राप्त हुआ ।

प्रयोगशाला के विषय – समर्पित सभी सात प्रभागों, यानि ऊर्जा संचयन भौतिकी, पदार्थ भौतिकी तथा अभियांत्रिकी, रेडियो एवं वायुमण्डलीय विज्ञान, समय तथा आवृत्ति, शीर्ष स्तरीय मानक एवं औद्योगिकी मापिकी, क्वांटम परिघटना एवं अनुप्रयोग और परिष्कृत तथा विश्लेषणात्मक यंत्र में महत्त्वपूर्ण अनुसंधान कार्य किया गया । राष्ट्रीय तथा अंतरराष्ट्रीय पेटेण्ट दाखिल करने तथा प्रौद्योगिकियों को उद्योगों को हस्तांतरित करने के साथ–साथ इन प्रभागों के प्रतिफल को प्रतिष्ठित वैज्ञानिक जर्नल्स में प्रकाशित किया गया है ।

ऊर्जा संचयन भौतिकी प्रभाग ने पॉलीमर सौर सेल के विकास, क्रिस्टलीय सिलिकन प्रकाशवोल्टीय उपकरणों हेतु यूनिट प्रक्रियाओं के सृजन, उपकरण गुणवत्ता नैज तथा मादित अक्रिस्टलीय/माइक्रोक्रिस्टलीय सिलिकन तनु फिल्मों की वृद्धि तथा ग्रेफिन सहित विभिन्न कार्बन के बहुरूपकों की वृद्धि हेतु प्रक्रिया मापदण्डों के इष्टतमीकरण में और अधिक प्रगति की गयी । इस प्रभाग से जुड़े वैज्ञानिक कोलायडल मार्ग द्वारा बहु–तात्त्विक अर्धचालक फिल्मों, लेजर तथा आण्विक रश्मि पुंज, एपीटैक्सी सहायता प्राप्त आर एफ प्लाज़्मा का उपयोग कर सम/विषम एपीटैक्सीय III-नाइट्राइड्स के संश्लेषण तथा एम्बीपोलर क्षेत्र प्रभाव ट्रांजिस्टर्स (FET) तथा कार्बनिक प्रकाश उत्सर्जी ट्रांजिस्टर्स की संविरचना में भी लगे हुए हैं।

पदार्थ भौतिकी तथा अभियांत्रिकी प्रभाग ने इस वर्ष भी आधारभूत तथा अनुप्रयोग अनुसंधान, दोनों पर बल दिया । इस प्रभाग की मुख्य उपलब्धियों में उच्च प्रदर्शन माइक्रोवेव अवशोषण शील्ड, कार्डियक बायोमार्कर्स के लेबल मुक्त संसूचन हेतु लिक्विड क्रिस्टल सेंसर, इलैक्ट्रोस्पिनिंग का उपयोग कर PAN तथा PVA पॉलीमर से निरंतर कार्बन नैनोतंतु तथा Li-ion बैटरी के लिए एक एनोड के रूप में नैनो साइज SnO_2 - कार्बन नैनोट्यूब कम्पोजिट पर आधारित स्टैंडिंग बाइंडर लेस कंडक्टिंग पेपर का डिजाइन सम्मिलित है । इस समूह के वैज्ञानिकों ने नवीन ताप वैद्युत पदार्थों के संश्लेषण में महत्त्वपूर्ण उन्नति की है, ताकि ताप वैद्युत पावर जेनरेटर्स का भविष्य में विकास किया जा सके । दुर्लभ मिट्टी रहित स्थायी चुंबकीय पदार्थों के संश्लेषण हेतु एक मेल्ट स्पिनिंग सुविधा की भी शुरूआत की गयी । अत्यधिक समर्थ आतिथेय (host) YVO_4 में लैंथेनाइड आयन Er^{3+}, Yb^{3+}, Eu^{3+} के युगपत् मादन के कारण सौर सेल अनुप्रयोग हेतु द्वि–उत्तेजन तथा द्वि–उत्सर्जन संदीपक का विकास हो सका । एन एम आर टेसलामीटर के परिशुद्ध अंशांकन की क्षमता का विकास किया गया तथा एक सीज़ियम चुंबकत्वमापी को बतौर प्राथमिक मानक स्थापित किया गया ।

रेडियो विज्ञान के क्षेत्र में, सेलुलर संचार प्रणाली के सिस्टम पैरामीटर्स का अनुमान लगाने के लिए विद्युत–चुंबकीय मॉडल के सत्यापन हेतु विस्तार से कार्य किया गया । आयनमण्डलीय अध्ययनों हेतु नवोन्नत उपस्कर डिजिसोंड प्राप्त किया गया है तथा इसकी संस्थापना प्रगति पर है । इस प्रभाग के वैज्ञानिक ने ट्रेस गैसों तथा भारत के विभिन्न भागों से एकत्रित किए गए विविक्त पदार्थ का विस्तृत मापन किया । इस प्रभाग ने ध्रुवीय आयनमण्डल तथा मानचित्र ऐरोसॉल विकिरणशील गुणधर्मों के अध्ययन हेतु 32 वें अंटार्कटिक अभियान में भी भाग लिया । C, N तथा S समस्थानिकों का प्राकृतिक के साथ–साथ कृत्रिम ऑर्गेनिक तथा सल्फर युक्त ठोस नमूनों के रूप में सटीक तथा परिशुद्ध मापन करने के लिए निरन्तर प्रवाह मोड में तात्विक विश्लेषक के साथ युग्मित, हाल में प्राप्त किए गए स्थिर समस्थानिक अनुपात द्रव्यमान – स्पेक्ट्रोमीटर का मानकीकरण किया गया । अंतरराष्ट्रीय परमाण्विक ऊर्जा संस्था, वियना द्वारा सप्लाई किए गए प्रमाणित अंतरराष्ट्रीय मानकों के समूह द्वारा इस यंत्र का अंशांकन किया गया तथा अंतरराष्ट्रीय ख्याति के अन्य संस्थानों द्वारा उपयोग किए गए कई इन–हाउस प्रयोगशाला मानकों से इसकी दोबारा जाँच की गयी ।

समय तथा आवृत्ति प्रभाग अति स्थिर परमाण्विक आवृत्ति स्रोतों के क्षेत्रों में कार्य कर रहा है जिसमें प्रथम एवं द्वितीय Cs फाउंटेन, अंतरिक्ष अनुप्रयोग हेतु विकसित Rb परमाण्विक घड़ी, एकल प्रगहण Yb आयन प्रकाशिक आवृत्ति मानक तथा परिशुद्ध कालमापन पद्धति सम्मिलित है । देश का टाइमकीपर होने के नाते सी एस आई आर – एन पी एल ने सफलतापूर्वक भारतीय मानक समय (IST), इसके प्रकीर्णन को बनाए रखा तथा अति–परिशुद्ध सेटेलाइट लिंक का उपयोग कर इसे अंतरराष्ट्रीय बाट एवं मापन ब्यूरो (BIPM) के साथ अनुमार्गणीय बनाए रखा । इस वर्ष की प्रमुख वैज्ञानिक उपलब्धियों में प्रथम Cs फाउंटेन की अंतरराष्ट्रीय अंतर–तुलना, परमाण्विक आवृत्ति मानकों पर उच्च परिशुद्ध प्रयोगों में सहायता करने के लिए विभिन्न इलेक्ट्रॉनिक यंत्रों का स्वदेशीय विकास, BEL में Rb मानक का सफलतापूर्वक दूरस्थ अंशांकन तथा आयन प्रग्रहण, वैक्यूम चैम्बर, हैलीकेल रिसोनेट तथा प्रकाशिक आवृत्ति मानक हेतु प्रकाशिक सैट–अप के डिजाइन को पूर्ण करना सम्मिलित है । द्वितीय Cs फाउंटेन का वांछित क्लॉक अवस्था में बढ़ती परमाण्विक जनसंख्या हेतु प्रकाशिक पम्पिंग के प्रभाव का इसकी स्थिरता बढ़ाने के लिए अध्ययन किया गया । रूबिडियम परमाण्विक घड़ी के प्रदर्शन को बेहतर बनाने के लिए प्राकृतिक Rb बल्बों को समस्थानिक ^{87}Rb से समृद्ध किया गया था ।

शीर्षस्तरीय मानक तथा औद्योगिक मापिकी प्रभाग राष्ट्रीय मानकों को स्थापित करने, अनुरक्षित करने और उनका उन्नयन करने तथा भौतिक यांत्रिक विद्युतीय तथा इलैक्ट्रानिक्स मानक के क्षेत्र में अन्य अधिकृत प्रयोगशालाओं को अनुमार्गणीयता प्रदान करने के लिए उत्तरदायी है । वर्ष के दौरान विज्ञान तथा प्रौद्योगिकी में मापन नवीनता (MIST) शीर्षक वाली 12 वीं पंचवर्षीय योजना परियोजना तथा विस्तारित 11 वीं पंचवर्षीय योजना परियोजना "मापिकी में उन्नति सी एस आई आर/एन डब्ल्यू पी -45" के तहत इस प्रभाग में महत्त्वपूर्ण योगदान दिया । नवीन गतिविधि आरंभ की गयी, जैसे–वॉट संतुलन के विकास हेतु आरंभिक जांच की शुरूआत/ब्रिनेल, रॉकवेल (सतही रॉकवेल सहित), विकर्स तथा सूक्ष्म–विकर्स कठोरता हेतु द्वितीयक कठोरता मानकीकरण मशीन की स्थापना, पराश्रव्य शक्ति मूल्यांकन में वोल्टता मापन हेतु शिखर से शिखर मापन मॉड्यूल के डिजाइन, AC-DC धारा ट्रांसफर मापन सुविधा की सीमा का विस्तार, विकिर्ण शक्ति घनत्व हेतु मानकों के स्वदेशीय विकास द्वारा प्रभाग की सुविधाओं को और अधिक सुदृढ़ किया गया । ट्रांसफार्मर हानि मापन सिस्टम (TLMS) अंशांकन हेतु नवीन सुविधा और वायु गुणवत्ता मूल्यांकन हेतु 1 किमी. की ऊंचाई तक वायुमण्डलीय सीमा परत के परिवीक्षक की क्षमता युक्त मोनो–स्थिर (SODAR) के नमूना, विकास तथा संविरचना को पूर्ण किया गया । इस प्रभाग ने बी आई पी एम तथा ए पी एम पी कार्यक्रम के तहत अंतरराष्ट्रीय अंतर–तुलनाओं में सक्रिय रूप से भाग लिया । सार्क देशों के एन एम आई के साथ विभिन्न अंतर–प्रयोगशाला तुलनाओं में सी एस आई आर– एन पी एल पथ प्रदर्शक प्रयोगशाला भी थी ।

क्वांटम परिघटना तथा अनुप्रयोग प्रभाग का मुख्य बल नैनो–संरचना, क्वांटम परिघटना तथा मापिकी की दिशा में है। पेराक्स्काइट आक्साइड, मल्टिफेरोइक, लंब अनिसोट्रोपिक चुंबकीय पदार्थ जैसे CoFeB, FePt, CoPt तथा अर्ध – धात्विक हुसेलर मिश्रधातु जैसे Co_2 FePt, Co_2 MnSi की तनु फिल्मों/विषमसंरचनाओं की वशद्धि हेतु एक स्पंदित लेसर निक्षेपण सुविधा का सफलतापूर्वक उपयोग किया गया है । विभिन्न नैनो उपकरणों जैसे अतिचालकीय नैनो–तार एवं ग्रेफिन पर संधि स्थल की संविरचना तथा प्लैज्मॉनिक एंटीना की शुरूआत हेतु केन्द्रित आयन बीम मीलिंग का अत्यधिक उपयोग किया गया । विभिन्न ज्यामीति के पर्मएलॉय नैनो वलयों के पुनरूत्पादनीय प्रतिरूप तैयार करने के लिए ई–बीम लिथोग्राफी का उपयोग किया गया । निम्न तापमान

तथा उच्च चुंबकीय क्षेत्र में सभी उपकरणों/संरचनाओं पर उच्च परिशुद्ध चुंबकीय तथा विद्युत मापन से निरंतर रोचक परिणाम प्राप्त हो रहे हैं । क्वांटम विशिष्टता पर और अधिक चर्चा करते हुए, -10mK के निम्न तापमान पर पहुँचने की क्षमता वाले एक डिल्यूशन रेफ्रिजरेटर को सफलतापूर्वक संस्थापित किया गया । नवीन आविष्कृत Sro.5 Lao.5 FBiS2 अतिचालकों में दाब–आश्रित अतिचालकीयता से रोचक परिणाम प्राप्त हुए । ज्योति–तीव्रता तथा अन्य प्रकाशमितीय पैरामीटर्स के वर्तमान स्केल में मैग्नीट्यूड के कम से कम दो क्रमों तक अनिश्चितता को पुनर्परिभाषित तथा कम करने के लिए क्रायोजेनिक रेडियोमीटर को संसूचक आधारित प्राथमिक मानक के रूप में संस्थापित किया गया है । स्वतः पैरामीट्रिक डाउन कनवर्जन (SPDC) का 355 nm पर उत्सर्जन करने वाली 25ps स्पंद चौडाई के Nd-YAG लेसर के साथ प्रदर्शन किया गया है । कुल 256, 116 जोसेफसन संधियों जो 3 संधियों के ढेर में संगठित तथा 32 माइक्रोतरंग समतलीय तरंग निर्देश लाइन में वितरित हैं, युक्त 10V चिप को 'राष्ट्रीय मानकों' के अंशांकन के माध्यम से भारत में 'वोल्ट' मात्रक के प्रकीर्णन हेतु उपयोग किया जाता है ।

कृत्रिम विश्लेषणात्मक यंत्र प्रभाग में एक्स–रे विश्लेषण, इलेक्ट्रॉन तथा आयन माइक्रोस्कोपी (EIM); इलेक्ट्रॉन अनुचुंबकीय अनुनाद (EPR); विश्लेषक रसायन समूह हाउस उच्च गुणवत्ता नवोन्नत सुविधाएं सम्मिलित है । यह प्रभाग आकृति विज्ञान के पदार्थों/रासायनिक संयोजन/शुद्धता/संरचना (दोष सहित)/क्रिस्टलीय पूर्णता के अभिलक्षणन हेतु एक विश्वसनीय केन्द्रीय सेवा प्रदाता के रूप में महत्त्वपूर्ण भूमिका अदा कर रहा है ।

एक्स–रे विश्लेषण समूह के पास क्रिस्टल वृद्धि विशेषज्ञता तथा नवीन वृद्धि प्रक्रियाओं जैसे नेकिंग, बीजारोपण, CZ तकनीक में ठोस–द्रव अंतरफलक का नियंत्रण, आक्सीकरण/परिवर्तन, पोलिंग आदि को अपनाने का अनुभव है तथा तापवैद्युत पदार्थों के उत्कृष्ट गुणवत्ता युक्त बल्क एकल क्रिस्टल का सफलतार्वूक विकास किया है । ई आई एम समूह विभिन्न अनुसंधान तथा विकास परियोजनाओं हेतु वास्तविक तथा व्युत्क्रम/पारस्परिक अधर में भी पदार्थों का सूक्ष्म–संरचनात्मक विश्लेषण उपलब्ध करवाता है । यह समूह विभिन्न नैनो–पदार्थों के विकास कार्य को भी अंजाम दे रहा है । ई पी आर तथा चुंबकीय तरल गतिविधियों में फेरोफ्लूड, फेरोजेल, फेरोफाइबर तथा चुंबकीय तनु फिल्म बनाने में उपयोगी नैनो क्रिस्टलीय चुंबकीय पदार्थों का विकास सम्मिलित है । रसायन में मापिकी (MiC) तथा प्रमाणित संदर्भ पदार्थ (सी आर एम) गतिविधि समूह मानक गैस मिश्रण, अजैविक तात्विक विलयन तथा वायु/जल गुणवत्ता की निगरानी में लगा हुआ है ।

वर्ष के दौरान, कुल 342 वैज्ञानिक तथा तकनीकी पेपर एस सी आई जर्नल में प्रकाशित हुए, 10 पेटेंट भारत में दर्ज किए गए और 4 पेटेंट विदेश में दर्ज किए; पिछले वर्ष दर्ज किए गए 8 अंतरराष्ट्रीय पेटेंट तथा 2 भारतीय पेटेंट को वर्ष 2013–14 के दौरान मंजूर किया गया; 13 नई परियोजनाएँ आरंभ की गयी तथा 3102 अंशांकन रिपोर्ट जारी की गयी जिससे 528 लाख की निधि प्राप्त हुई । उन्नत पदार्थ भौतिकी तथा अभियांत्रिकी में स्नात्तकोत्तर अनुसंधान कार्यक्रम अभियांत्रिकी (PGRPE) हेतु वैज्ञानिक तथा नवीन अनुसंधान अकादमी (AcSIR) के अंतर्गत 7 विद्यार्थियों को प्रवेश दिया गया । वर्ष के दौरान भारी संख्या में शोध छात्र प्रयोगशाला में भर्ती हुए तथा देश भर में फैले विभिन्न शैक्षणिक संस्थानों से एम.एस.सी/एम.टेक/एम.सी.ए डिग्री करने वाले छात्रों को तकनीकी प्रशिक्षण प्रदान करने हेतु अनवरत प्रयास किए गए ।

प्रयोगशाला द्वारा विशिष्ट विषय पर सम्मेलन, विचार–गोष्ठी औद्योगिक प्रशिक्षण पाठ्यक्रम आयोजित किए जाते रहे । इसमें ध्वानिकी पर अंतरराष्ट्रीय सम्मेलन काफ्रेंस (11–13 नवम्बर, 2013), बायो–मेडिकल सांइस तथा प्रौद्योगिकी पर राष्ट्रीय सम्मेलन (हिन्दी में) (21–22 नवम्बर, 2013) तथा मापिकी/मानक एवं गुणवत्ता प्रबंधन के क्षेत्र में 6 औद्योगिक प्रशिक्षण पाठयक्रम शामिल हैं । औद्योगिक प्रशिक्षण पाठयक्रमों में मापिकी अधिकारियों, विभिन्न उद्योगों तथा परीक्षण एवं अंशांकन प्रयोगशालाओं के कर्मचारियों ने भाग लिया । विद्यालयों, महाविद्यालयों, विश्वविद्यालयों तथा वैज्ञानिक एवं तकनीकी

संगठनों के छात्रों और अध्यापकों तक पहुंचने के लिए हमारे पास सुदृढ़ कार्यक्रम हैं ।

प्रयोगशाला द्वारा 'दैनिक जीवन में मापन' थीम के तहत 20.05.2013 को विश्व मापिकी दिवस–2013 मनाया गया । इसी दिन राष्ट्रीय प्रौद्योगिकी दिवस भी मनाया गया जिसमें समारोह के मुख्य अतिथि प्रो. अशोक चन्द्र द्वारा वैज्ञानिकों तथा तकनीकी कर्मचारी–वर्ग को उनके पेटेंट, सॉफ्टवेयर कॉपीराइट तथा प्रौद्योगिकी हस्तातंरण हेतु पुरस्कार प्रदान किए गए । 25 सितम्बर, 2013 को 71 वां सी एस आई आर स्थापना दिवस मनाया गया । प्रो. आर. के. शेवगांवकर, निदेशक – आई आई टी दिल्ली द्वारा 'रेडियो यूनिवर्स' पर स्थापना दिवस व्याख्यान दिया गया । (27 सितम्बर, 2013 को) इस उत्सव के भाग के रूप में सी एस आई आर – एन पी एल ओपन–डे आयोजित किया गया । स्थानीय महाविद्यालयों तथा विद्यालयों से लगभग 2500 छात्रों ने विभिन्न प्रभागों की अनुसंधान तथा विकास गतिविधियों को समझने के लिए प्रयोगशाला का भ्रमण किया ।

सर सी वी रमन को श्रद्धांजलि देते हुए 28.02.2014 को राष्ट्रीय विज्ञान दिवस 2014 आयोजित किया गया जिसमें डा. आर मुरलीधरन, निदेशक, एस एस पी एल ने "इलैक्ट्रॉनिक पदार्थ तथा उपकरण रक्षा प्रौद्योगिकी" हेतु संबल' विषय पर एक व्याख्यान दिया । इस समारोह में सी एस आई आर–एन पी एल के छात्रों में उत्साहपूर्वक भाग लिया और आकर्षक पोस्टर कार्यशाला में अपने कार्यों का प्रदर्शन किया तथा पुरस्कार हेतु 4 श्रेष्ठ पोस्टर चुने गए । यह प्रयोगशाला के लिए गर्व की बात रही कि 17 फरवरी, 2014 को प्रो. सर रिचर्ड फ्रेंड, केवेंडिश प्रोफेसर तथा कार्बनिक इलैक्ट्रॉनिक्स के क्षेत्र में विश्व विख्यात अनुसंधानकर्त्ता द्वारा 35 वां कृष्णन् स्मृति व्याख्यान दिया गया ।

शैक्षणिक के साथ–साथ अन्य गतिविधियों में भी सी एस आई आर–एन पी एल ने अपनी उपस्थिति दर्ज की । प्रयोगशाला ने आई ए आर आई – दिल्ली में आयोजित वार्षिक पूसा बागवानी प्रदर्शनी में भाग लिया तथा पिछले वर्ष की भांति, प्रदर्शन की विभिन्न श्रेणियों में अनेक पुरस्कार प्राप्त किए । वृक्षारोपण अभियान के भाग के रूप में, स्वतंत्रता दिवस पर एन पी एल के वैज्ञानिकों तथा स्टाफ सदस्यों द्वारा भारी संख्या में पौधे लगाए गए । प्रयोगशाला द्वारा 21–24 अक्तूबर, 2013 के दौरान 45 वां शांति स्वरूप भटनागर खेलकूद – प्रतियोगिता (आउटडोर) आयोजित किया गया । इसमें सी एस आई आर की विभिन्न प्रयोगशालाओं से प्रतिभागियों ने भाग लिया । वर्ष के दौरान आयोजित कुछ अन्य कार्यक्रमों में हिन्दी पखवाड़ा और हिन्दी दिवस, सतर्कता जागरूकता सप्ताह, कौमी एकता सप्ताह तथा एन पी एल क्लब खेल सप्ताह शामिल है । सी एस आई आर–एन पी एल द्वारा पिछले कई वर्षों से वर्ष में दो बार आयोजित होने वाली सी एस आई आर – नेट परीक्षा का संयोजन भी किया जा रहा है ।

मैं, प्रयोगशाला की प्रगति में सी एस आई आर – एन पी एल कर्मचारी–वर्ग तथा छात्र समुदाय के प्रत्येक सदस्य के बिना शर्त के सहायता तथा निष्ठापूर्व योगदान के लिए उनकी ईमानदारी से सराहना करता हूँ । यह स्पष्ट करना महत्त्वपूर्ण है कि उनके उदार एवं समर्पित सहयोग के बिना बहुत सी उपलब्धियाँ हमारे लिए हासिल कर पाना संभव नहीं हो पाता । मैं, इस अवसर पर सी एस आई आर मुख्यालय, अनुसंधान परिषद् और प्रबंध परिषद् से प्राप्त महत्त्वपूर्ण मार्गदर्शन एवं सहायता, जो हमारे लक्ष्यों को पूरा करने में अत्यधिक सहायक सिद्ध हुई, के लिए आभार व्यक्त करता हूं । राष्ट्रीय एवं अंतरराष्ट्रीय विशेषज्ञों का प्रयोगशाला दौरा तथा उनकी हमारे अनुसंधानकर्त्ताओं के साथ अंत:क्रिया सर्वाधिक फलदायी एवं प्रेरणादायी रही । अंत में, मैं इस विवरण को समय से प्रकाशित करने के लिए प्रकाशन समिति एवं इसकी अध्यक्षा डा. रश्मि का उनके योगदान के लिए आभार व्यक्त करता हूं । पी एम ई समूह एवं सभी प्रभागों/गतिविधियों/यूनिटों के प्रमुख का सहयोग एवं विशेष प्रयास अत्यधिक सराहनीय है ।

प्रो. आर सी बुधानी
निदेशक

From the Director's Desk.....

I am delighted to present you the Annual Report of the CSIR-National Physical Laboratory (NPL) for the Year 2013-14. CSIR-NPL, a premier research laboratory in the field of Physical Sciences and the National Metrology Institute (NMI) of India is one of the first five National Laboratories set up under the CSIR system. The primary mandate of this laboratory is to keep and maintain continuously by research the National Standards of Measurements, for which front-line research in the emerging areas of quantum standards and measurements science has been carried out.The laboratory has also promoted Research and Development (R&D)activities in various fields of energy harvesting technologies, nanotechnology, advanced materials, quantum condensed matter and radio & atmospheric sciences.

The laboratory is aware of its responsibility towards industrial, societal and environmental sectors of the country and has been contributing by providing knowledge-based technologies and continuous advancement in knowledge through integrated implementation of science, technology and innovation. CSIR-NPL has been steadily and continuously undergoing transformation to be a frontline and globally recognized laboratory in Physical Sciences. During the year 2013-14, this process continued and further additions were made to the already existing world class research infrastructure of the laboratory. A state-of-the-art metrology building and a solar energy clean room facility have been the important additions to the infrastructure of the laboratory along with setting up of facilities for materials research down to -272.99°C, and electron microscopy to image individual atoms and to ascertain their valence states.

All these efforts culminated into enhanced and important R&D accomplishments during the year. Two of our young scientists, Dr. Sanjay Kumar Srivastava and Dr. Parveen Saini with their exceptional contributions bagged the coveted CSIR Young Scientist Award, 2013 in the areas of Physical Sciences

and Engineering Sciences respectively. In recognition of the outstanding performance of CSIR-NPL in the Enterprise Resource Planning (ERP) endeavor of the CSIR, Ms. Anjali Sharma,Ms. BhawnaGuglani and Sh. Upendra Kumar received the Outstanding Achievement Award and the CSIR-NPL's Institutional Award 2013.

Important research was carried out in all the seven theme-dedicated Divisions of the laboratory; namely, Physics of Energy Harvesting, Materials Physics and Engineering, Radio & Atmospheric Sciences, Time & Frequency, Apex Level Standards & Industrial Metrology, Quantum Phenomenon & Applications and Sophisticated & Analytical Instruments. The output of these Divisions has been published in scientific journals of repute along with filing of national and international patents and transfer of technologies to industry.

The Physics of Energy Harvesting Division made further advancements in the development of polymer solar cells, creation of unit processes for crystalline silicon photovoltaic devices, optimization of process parameters for the growth of device quality intrinsic and doped amorphous /microcrystalline silicon thin films and growth of various polymorphs of carbon including graphene. The scientists of this Division are also engaged in the synthesis of multi-elemental semiconductor films by colloidal route, homo/ hetero-epitaxial III-nitrides using laser and RF plasma assisted molecular beam epitaxy and fabrication of ambipolar field effect transistors (FET) and organic light emitting transistors.

Materials Physics and Engineering Division has continued to emphasize on both fundamental and application oriented research this year as well.The major achievements of this Division include design of high performance microwave absorption shields,FETs for label free detection of cardiac biomarkers, a DNA biosensor, liquid crystal sensor for detection of total cholesterol, continuous carbon nanofibres from PAN and PVA polymers using electrospinning and a free standing binder-less conducting paper based on nanosize SnO_2-carbon nanotube composite as an anode for Li-ion batteries. The scientists of this group have also made significant advances in the synthesis of novel thermoelectric materials to enable future development of thermoelectric power generators.A melt spinning facility has also been commissioned for the synthesis of rare earth free permanent magnetic materials. Simultaneous doping of lanthanide ions Er^{3+}, Yb^{3+}, Eu^{3+} in a highly efficient host YVO_4 has enabled the development of a dual excitation, dual emission phosphor for solar cell application. Capabilities for precise calibration of NMR Teslameter were developed and a Cesium Magnetometer was installed as a primary standard.

In the area of Radio Science, further work for verification of electromagnetic model for predicting system parameters of cellular communication systems has been carried out.A state-of-the-art equipment digisonde for ionospheric studies has been acquired and its installation is in progress. The scientists of this Division have carried out extensive measurements of trace gases and particulate matter collected from various parts of India.The Division also participated in the 32nd Antarctic expedition to study the polar ionosphere and map aerosol radiative properties. Standardization of a newly acquired stable isotope ratio mass-spectrometer coupled with elemental analyzer in a continuous flow mode was carried out for making accurate and precise measurements of C, N and S isotopes in a variety of natural as well as synthetic organic and sulfur containing solid samples. The instrument was calibrated using a suite of certified international standards supplied by International Atomic Energy Agency Vienna and cross-checked against several in-house laboratory standards used by other institutions of international repute.

The Time and Frequency Division is working in the areas of ultra stable atomic frequency sources that include the first and second Cs Fountain, Rb atomic clock developed for space applications, single trap Yb ion optical frequency standard and precise timing systems. CSIR-NPL being the timekeeper of the Nation successfully continued to maintain the Indian Standard Time (IST), its dissemination, and keeping it traceable to the International Bureau of Weights and Measures (BIPM) using ultra-precise satellite links. Major scientific achievements this year included international inter-comparison of the first Cs fountain, indigenous development of a variety of electronic instruments to support high precision experiments on atomic frequency standards, successful remote calibration of an Rb standard at BEL, and completion of the design of the ion trap, vacuum chamber, helical resonator and optical set-up for the optical frequency standard.Effect of optical pumping for increasing atomic population in the desired clock state in the second Cs fountain was studied to increase its stability.Natural Rb bulbs were isotopically enriched with 87Rb to improve the performance of Rubidium Atomic Clock.

Apex Level Standards and Industrial Metrology Division is responsible for establishing, maintaining and upgrading the National Standards and providing traceability to other accredited laboratories in the field of physico-mechanical, electrical and electronics standards.The division made significant contributions during the year under the 12th Five Year Plan project entitled 'Measurement Innovation in Science & Technology' (MIST) and the extended 11th Five Year Plan project 'Advances in Metrology - CSIR/NWP-45'. New activities such as initiation of preliminary investigations for development of a Watt balance were undertaken. Facilities of the division were further strengthened through establishment of secondary hardness standardizing machines for Brinell, Rockwell (including superficial Rockwell), Vickers and micro-Vickers hardness,design of a peak-to-peak measurement module for voltage measurement in the ultrasonic power evaluation,extension of the range of AC-DC current transfer measurement facility and indigenous development of Standards for Radiated Power Density. A new facility for the calibration of Transformer Loss Measuring System (TLMS) and design, development and fabrication of a mono-static SODAR with capability of monitoring atmospheric boundary layer up to a height of 1 km for air quality assessment were completed. The division was actively involved in international inter-comparisons under the BIPM and APMP programmes. CSIR-NPL was also the pilot laboratory for various inter-laboratory comparisons with the NMIs of SAARC countries.

Major impetus of the Quantum Phenomenon and Applications Division has been in the directions involving nanostructures, quantum phenomena and metrology. A pulsed laser deposition facility has been successfully used to grow thin films/heterostructures of perovskite oxides, multiferroics, perpendicular anisotropic magnetic materials such as CoFeB, FePt, CoPt and half-metallic Heusler alloys such as Co_2FeSi, Co_2MnSi. Focused ion beam milling was extensively used to fabricate various nanodevices like superconducting nano-wires and junctions on graphene, and initiation of plasmonic antennas. E-beam lithography was employed to create reproducible patterns of permalloy nanorings of varying geometry. High precision magnetic and electrical measurements on all the devices/structures at low temperatures and high magnetic fields have continued to yield interesting results. To address the quantum peculiarities further, a dilution refrigerator capable of reaching temperature as low as ~ 10 mK has been successfully installed. Interesting results of pressure-dependent superconductivity in newly discovered $Sr_{0.5}La_{0.5}FBiS_2$ superconductors have been obtained. To redefine and to reduce uncertainties by at least two orders of

magnitude in the existing scale of luminous intensity and other photometric parameters, cryogenic radiometer has been installed as detector based primary standard. Spontaneous parametric down conversion (SPDC) has been demonstrated with an Nd-YAG laser of 25ps pulse width emitting at 355nm. The 10 V chip with a total of 256,116 Josephson junctions organized in stacks of three junctions and distributed into 32 microwave coplanar waveguide lines is put to use for the dissemination of unit 'volt' in India through the calibration of 'National Standards'.

Sophisticated Analytical Instruments Division consisting of X-Ray Analysis; Electron & Ion microscopy (EIM); Electron paramagnetic resonance (EPR); Analytical Chemistry Groups house high quality state-of-the-art facilities. The division is playing an important role as a credible central analytical service provider for characterization of materials for morphology/ chemical composition/ purity/ structure (including defects)/ crystallographic perfection.

The X-ray Analysis group has crystal growth expertise and experience in adopting novel growth processes like necking, seeding, control of solid-liquid interface in CZ technique, oxidation/ reduction, poling etc. and has successfully grown excellent quality bulk single crystals of thermoelectric materials. The EIM group provided micro-structural analysis of materials even at atomic scale in real and reciprocal space for various R&D projects. The group is also involved in development of a variety of nano-materials.The EPR and magnetic fluid activities encompassed the development of nano crystalline magnetic materials useful for making ferrofluids, ferrogels, ferrofibers and magnetic thin films. The metrology in chemistry (MiC) and certified reference materials (CRM) activities group is engaged in the development of standard gas mixtures, inorganic elemental solutions and air/ water quality monitoring.

During the year, a total of 342 scientific and technical papers were published in SCI Journals; 10 patents were filed in India and 4 patents were filed abroad; 8 international patents and 2 Indian patents filed in previous years were granted during 2013-14; 13 new projects (sponsored and consultancy) were undertaken and 3102 calibration reports were issued, which contributed to the generation of funds to the tune of 528 lakhs. Under the Academy of Scientific and Innovative Research (AcSIR) for Post Graduate Research Programme in Engineering (PGRPE) in Advanced Materials Physics & Engineering, seven students were admitted. A large number of research fellows joined the laboratory during the year and sustained efforts were made to provide technical training to students pursuing M Sc/M Tech/MCA degree from different academic institutions spread all across the country.

The laboratory continued to organize conferences, seminars, industrial training courses on specialized themes. These include the International Conference on Acoustics (Nov. 11 to 13, 2013), National Conference on Biomedical Science and Technology (in Hindi) (Nov. 21 to 22, 2013), and six industrial training courses in the area of Metrology/ Standards and Quality Management. The industrial training courses were attended by legal metrology officers, personnel belonging to various industries and test and calibration laboratories. We also have a strong outreach programme for students and teachers of schools, colleges, universities, and S&T organizations.

The laboratory celebrated the World Metrology Day-2013 on 20-05-2013 under the theme 'Measurements in Daily Life'. The National Technology Day was also observed on the same day during which awards were given to scientists and technical staff for their patents, software copyrights and technology transfers by the Chief Guest of the function Prof. Ashok Chandra. The 71st CSIR Foundation Day was celebrated on September 25, 2013. Prof R.K. Shevgaonkar,

Director - I.I.T. Delhi, delivered the Foundation Day lecture titled'The Radio Universe'. As a part of this celebration, the CSIR-NPL Open-Day was held on 27th September, 2013. About 2500 students from local colleges and schools visited the laboratory to see various R&D activities of several Divisions.

As a tribute to Sir C.V. Raman,the National Science Day 2014 was celebrated on 28-02-2014 with a lecture of Dr. R. Murlidharan, Director-SSPL titled 'Electronic Materials and Devices - Enablers for Defence Technology'. This function attracted enthusiastic participation of CSIR-NPL students who displayed their works in a vibrant Poster Workshop and four best posters were selected for awards.It was an honour for the laboratory to have the 35th Krishnan Memorial Lecture delivered by Prof. Sir Richard Friend,Cavendish Professor and a world renowned researcher in the area of Organic Electronics on February 17, 2014.

Along with the academics, CSIR-NPL made a mark in other activities as well. It participated in the Annual Pusa Horticulture Show held at IARI - Delhi, and like previous years, bagged a large number of prizes in various categories of display. As a part of the Tree Plantation Drive, a large number of saplings were planted by the scientists and staff members of NPL on the Independence Day. The laboratory also organized 45th Shanti Swarup Bhatnagar Tournament (outdoors) during the period 21 to 24 October, 2013. It attracted participation from various laboratories of the CSIR. Some of the other functions of the Year included Hindi Pakhwara and Hindi Divas, Vigilance Awareness Week, QaumiEkta Week and NPL Club Sports Week. CSIR-NPL has also been coordinating the CSIR-NET examination held twice a year for the past several years.

I earnestly appreciate the unconditional support and sincere contributions of each and every member of the CSIR-NPL staff and student community towards the progress of the laboratory. It is important to emphasize that without their wholehearted and dedicated cooperation, much of our accomplishment would not have been possible. I also wish to acknowledge the valuable guidance and support provided by the CSIR Head Quarters, our Research Council and Management Council in achieving our goals. The visits of national and international experts to the laboratory and their interactions with our researchers had been most rewarding and motivational. Finally, I wish to acknowledge the contribution of the Publication Committee and its Chairperson Dr. Rashmi in bringing out this report. The cooperation and special efforts of the PME group and all divisional/ activity/unit Heads are deeply appreciated.

(R C Budhani)
Director

प्रस्तावना

सी एस आई आर – राष्ट्रीय भौतिक प्रयोगशाला, सी एस आई आर के तहत स्थापित की जाने वाली पहली प्रयोगशालाओं में से एक थी। भारत के प्रथम प्रधानमंत्री स्वर्गीय पण्डित जवाहरलाल नेहरू ने 4 जनवरी, 1947 को इसकी आधारशिला रखी । स्वर्गीय डा. के एस. कृष्णन्, एफ आर एस, प्रयोगशाला के प्रथम निदेशक थे । तत्कालीन उप–प्रधानमंत्री स्वर्गीय सरदार बल्लभ भाई पटेल ने 21 जनवरी, 1950 को मुख्य बिडिंग (भवन) का उद्घाटन किया था।

घोषणा–पत्र

एन पी एल का मुख्य उद्देश्य (अ) मापन के राष्ट्रीय मानकों की स्थापना, रख–रखाव तथा सुधार करना और अन्तरराष्ट्रीय पद्धति पर आधारित मात्रक ज्ञात करना; (ब) भौतिकी के क्षेत्रों की पहचान करना तथा उनमें अनुसंधान करना, जो राष्ट्र की आवश्यकताओं तथा क्षेत्र की उन्नति के लिए सर्वाधिक उपयुक्त हों, (स) परिशुद्ध मापन, अंशांकन, उपकरणों, प्रक्रियाओं के विकास तथा भौतिकी से संबंधित अन्य संबद्ध समस्याओं के समाधान द्वारा उद्योगों, राष्ट्रीय तथा अन्य अभिकरणों की उनके विकासात्मक कार्यों में सहायता करना तथा (द) स्वयं को सूचित रखना तथा भौतिकी की अवस्था का गंभीर अध्ययन करना रहा है ।

मापन के राष्ट्रीय मानकों का संरक्षक भारत एवं मापन अधिनियम 1956 (1976 अधिनियम के तहत 1988 में पुनः प्रकाशित) के अधीनस्थ विधानों के तहत अन्तरराष्ट्रीय पद्धति (एस आई मात्रक) पर आधारित भौतिक मापन के मात्रकों को ज्ञात करना राष्ट्रीय भौतिक प्रयोगशाला का उत्तरदायित्व है । मापन के राष्ट्रीय मानकों तथा विभिन्न प्राचलों हेतु अंशांकन सुविधाओं की स्थापना, रख–रखाव तथा उन्हें अद्यतन करना भी एन पी एल का सांविधिक दायित्व है । सात एस आई बेस मात्रक हैं : मीटर, किलोग्राम, सेकण्ड, केल्विन, एम्पीयर, कैण्डेला तथा मोल और एस आई पूरक मात्रक है :– रेडियन (rad) तथा स्टैरेडियन (sr) । भौतिक मापन के अन्य व्युत्पन्न मात्रक, जिनका प्रयोगशाला द्वारा वर्तमान में रख–रखाव किया जा रहा है, इस प्रकार हैं :– बल, दाब, निर्वात, ज्योति अभिवाह, ध्वनि दाब, पराश्रव्य शक्ति; एसी वोल्टता; धारा एवं विद्युत; निम्न आवृत्ति वोल्टता; प्रतिबाधा एवं विद्युत; उच्च आवृत्ति वोल्टता, संकीर्णन तथा शोर; सूक्ष्मतंरग विद्युत तथा अवृत्ति ।

राष्ट्रीय शीर्ष अंशांकन निकाय

यह प्रयोगशाला देश में शीर्ष स्तरीय अंशांकन सेवा प्रदान करती है, यह देश के राष्ट्रीय प्रत्यायन निकाय – राष्ट्रीय परीक्षण एवं अंशांकन प्रत्यायन बोर्ड को (i) आवेदक प्रयोगशाला की श्रेष्ठ मापन क्षमता स्थापित करने हेतु आवश्यक अपने योग्य निर्धारक; (ii) प्रत्यायन हेतु आवेदक प्रयोगशाला की उपयुक्तता का निर्णय करने हेतु एन ए बी एल को तकनीकी सहयोग तथा (iii) परीक्षण प्रयोगशालाओं को उनके मापन में अनिश्चितता के आकलन हेतु प्रशिक्षित करने के लिए अपनी फैकल्टी उपलब्ध करवाती है ।

इसके अतिरिक्त, प्रयोगशाला प्रमाणित संदर्भ पदार्थों का विकास करने में जुटी है ताकि गुणवत्ता पद्धति (IS/ISO/IEC-17025 : 2005) तथा एन ए बी एल की अनिवार्य आवश्यकताओं को पूर्ण करने के लिए राष्ट्रीय/अंतरराष्ट्रीय मापन पद्धति (S I मात्रक) के अनुरूप विश्लेषणात्मक उच्च गुणवत्ता मापन तथा विश्लेषणात्मक मापन की अनुमार्गणीयता सुनिश्चित की जा सके ।

प्रमुख उपलब्धियाँ

राष्ट्रीय भौतिक प्रयोगशाला की अगण्य उपलब्धियों की सूची तैयार करना मुश्किल है, कुछ मुख्य उपलब्धियाँ उनमें से इस प्रकार हैं :– (1) भारत में मापन की मात्रिक पद्धति की शुरूआत, (2) अमिट स्याही का विकास – भारतीय लोकतंत्र को अमिट योगदान, (3) भारत से उत्सर्जित मीथेन गैस का आकलन – पर्यावरण सुरक्षा में देशव्यापी हित करने वाला राष्ट्रव्यापी मापन अभियान, (4) इलेक्ट्रॉनिक घटकों (फैराइट) के विकास हेतु पायलट संयत्र की स्थापना जिससे 1973 में सेन्ट्रल इलेक्ट्रॉनिक्स लि; (CEL) नामक सार्वजनिक क्षेत्र इकाई की स्थापना का मार्ग प्रशस्त हुआ; (5) स्वेदशी पदार्थों का उपयोग कर विद्युतस्थैतिक फोटोकॉपी मशीन की तकनीकी जानकारी का विकास तथा (6) भारतीय मानक समय ।

अनुसंधान एवं विकास के प्रमुख क्षेत्र :–

(ए) मापिकी

- उद्योगों को अंशांकन एवं परीक्षण सेवाएँ
- वैद्युत एवं इलेक्ट्रॉनिक मानक
- भौतिक – यांत्रिक मानक
- रसायन विज्ञान मापिकी
- नैनो मापिकी
- प्राथमिक मानक
- एस आई यूनिटों का प्रापण

(बी) पदार्थ विज्ञान

- हल्के वजन एवं उच्च शक्ति के धात्विक पदार्थ
- बल्क नैनोधात्विक एवं नैनोसम्मिश्र पदार्थ
- कार्बन एवं कार्बन सम्मिश्र
- प्लाज्मा प्रसंस्कृत पदार्थ
- कार्बनिक एवं अकार्बनिक फोटोवोल्टाइक
- प्रदीप्त पदार्थ
- कार्बनिक प्रकाश उत्सर्जक डायोड
- चालक बहुलक एवं सम्मिश्र
- अतिचालक पदार्थ एवं अतिचालकता
- ईंधन सेल
- संवेदक (जैव, गैस, रासायनिक एवं एम ई एम एस)
- उन्नत अभिलक्षणन प्रौद्योगिकी

(सी) रेडियो एवं वायुमण्डलीय विज्ञान

- आयनमण्डल एवं क्षोभमण्डल
- वायुमण्डलीय पर्यावरण
- वैश्विक जलवायु परिवर्तन
- अंटार्कटिका एवं आर्कटिक अध्ययन
- रेडियो संचलन
- संचार (स्थिर, मोबाइल एवं समुद्री)

संगठन एवं प्रबंधन

प्रयोगशाला की सभी गतिविधियों को सात वैज्ञानिक निर्णयण इकाइयों में गठित किया गया है । ये इकाइयाँ हैं :– (i) ऊर्जा संचयन भौतिकी (ii) पदार्थ भौतिकी एवं अभियांत्रिकी (iii) रेडियो एवं वायुमण्डलीय विज्ञान (iv) समय एवं आवशत्ति मानक (v) शीर्षस्तरीय मानक एवं औद्योगिक मापिकी (vi) क्वांटम परिघटना एवं अनुप्रयोग (vii) परिष्कृत एवं विश्लेषणपरक उपकरण

इनके अतिरिक्त, संगठन एवं प्रबंधन हेतु आठ सहायक इकाइयों को स्थापित किया गया है । ये हैं :– (i) प्रशासन (ii) वित्त एवं लेखा (iii) भण्डार एवं क्रय (iv) कार्य एवं सेवाएँ (v) कर्मशाला एवं क्रायोजेनिक्स (vi) संगणन एवं नेटवर्क सुविधाएँ (vii) निदेशालय (viii) बौद्धिक संपदा एवं मानव संसाधन

Preamble

CSIR-National Physical Laboratory is one of the first National laboratories set-up under CSIR. Its foundation stone was laid by the first Prime Minister of India, late Pandit Jawaharlal Nehru on 4th January 1947. Late Dr. K.S. Krishnan, FRS, was the first Director of the laboratory. The main building was opened by the Deputy Prime Minister, late Sardar Vallabhbhai Patel on 21st January 1950.

CHARTER

The main objectives of NPL have been a) to establish, maintain and improve National Standards of Measurements and to realize the Units based on International system, b) to identify and conduct research in areas of Physics, which are most appropriate to the needs of the Nation and for the advancement of the field, c) to assist industries, national and other agencies in their developmental tasks by precision measurements, calibration, development of devices, processes and other allied problems related to physics and d) to keep itself informed of and study critically the status of physics.

CUSTODIAN OF NATIONAL STANDARDS OF MEASUREMENT

National Physical Laboratory has the responsibility of realizing the units of physical measurements based on the International System (SI units) under the subordinate legislations of Weights & Measures Act 1956 (reissued in 1988 under the 1976 Act). NPL also has the statutory obligation to establish, maintain and update the national standards of measurement & calibration facilities for different parameters. The seven SI base units are metre, kilogram, second, Kelvin, Ampere, candela, mole and the SI supplementary units are radian (rad) & steradian (sr). The other derived units for physical measurement, that the laboratory currently maintains, are: force, pressure, vacuum, luminous flux, sound pressure, ultrasonic power; ac voltage; current and power; low frequency voltage; impedance and power; high frequency voltage; attenuation and noise; microwave power and frequency.

NATIONAL APEX BODY FOR CALIBRATION

The laboratory provides apex level calibration services in the country, offering National Accreditation Board for Testing and Calibration (NABL), the national accreditation body in the country, (i) its qualified assessors as needed for establishing best measurement capability of the applicant laboratory; (ii) its technical input to enable NABL to decide the suitability of the applicant laboratory for accreditation, and (iii) its faculty to train testing laboratories for estimation of uncertainty in their measurements.

Besides, the laboratory is engaged in development of Certified Reference Materials to ensure high quality measurement and traceability of analytical measurements to national/international measurement system (SI unit) in order to fulfill the mandatory requirement of quality systems (IS/ISO/IEC-17025:2005) and of the NABL.

MAJOR ACHIEVEMENTS

National Physical Laboratory has to its credit innumerable number of achievements, a few major achievements are: a) Introduction of Metric system of measurements in India, b) Development of Indelible ink- the indelible contribution to Indian democracy, c) Estimation of methane gas emission from India- a nationwide measurement campaign giving countrywide advantage in environment protection, d) Setting up a pilot plant for development of Electronic Components (ferrites), which led to setting up a public sector Unit called Central Electronics Ltd. (CEL) in 1973, e) Development of know-how of the Electrostatic Photocopying machine using indigenous materials and f) Indian Standard Time.

THE MAJOR THRUST AREAS OF R & D

(A) Metrology

- Calibration & Testing Services to Industries
- Electrical & Electronic Standards
- Physico - Mechanical Standards
- Metrology in Chemistry
- Nano Metrology
- Primary Standards
- Realization of SI units

(B) Materials

- Light weight, high strength metallic materials
- Bulk Nanometallic and Nanocomposite materials
- Carbon & Carbon composites
- Plasma Processed Materials
- Organic and Inorganic Photovoltaics
- Luminescent Materials
- Organic Light Emitting Diodes
- Conducting Polymers & Composites
- Superconducting materials and Superconductivity
- Fuel cells
- Sensors (based on Bio, Gas, Chemicals, MEMS)
- Advanced Characterization Techniques

(C) Radio and Atmospheric Sciences

- Ionosphere & Troposphere
- Atomospheric Environment
- Global Climate Change
- Antarctica and Arctic studies
- Radio-Propagation
- Communications (fixed, mobile and marine)

ORGANIZATION AND MANAGEMENT

The laboratory has structured its total activities under seven scientific decision units. These are: (i) Physics of Energy Harvesting, (ii) Materials Physics and Engineering, (iii) Radio and Atmospheric Sciences, (iv) Time and Frequency Standards, (v) Apex Level Standards and Industrial Metrology, (vi) Quantum Phenomena and Applications (vii) Sophisticated and Analytical Instruments.

In addition, it has set-up eight support units for its organization and management. These are (i) Administration (ii) Finance & Accounts, (iii) Stores & Purchase, (iv) Works and Services, (v) Workshop and Cryogenics, (vi) Computation & Network Facility, (vii) Directorate, (viii) Intellectual Property and Human Resource.

सी एस आई आर - एन पी एल
संगठन संरचना

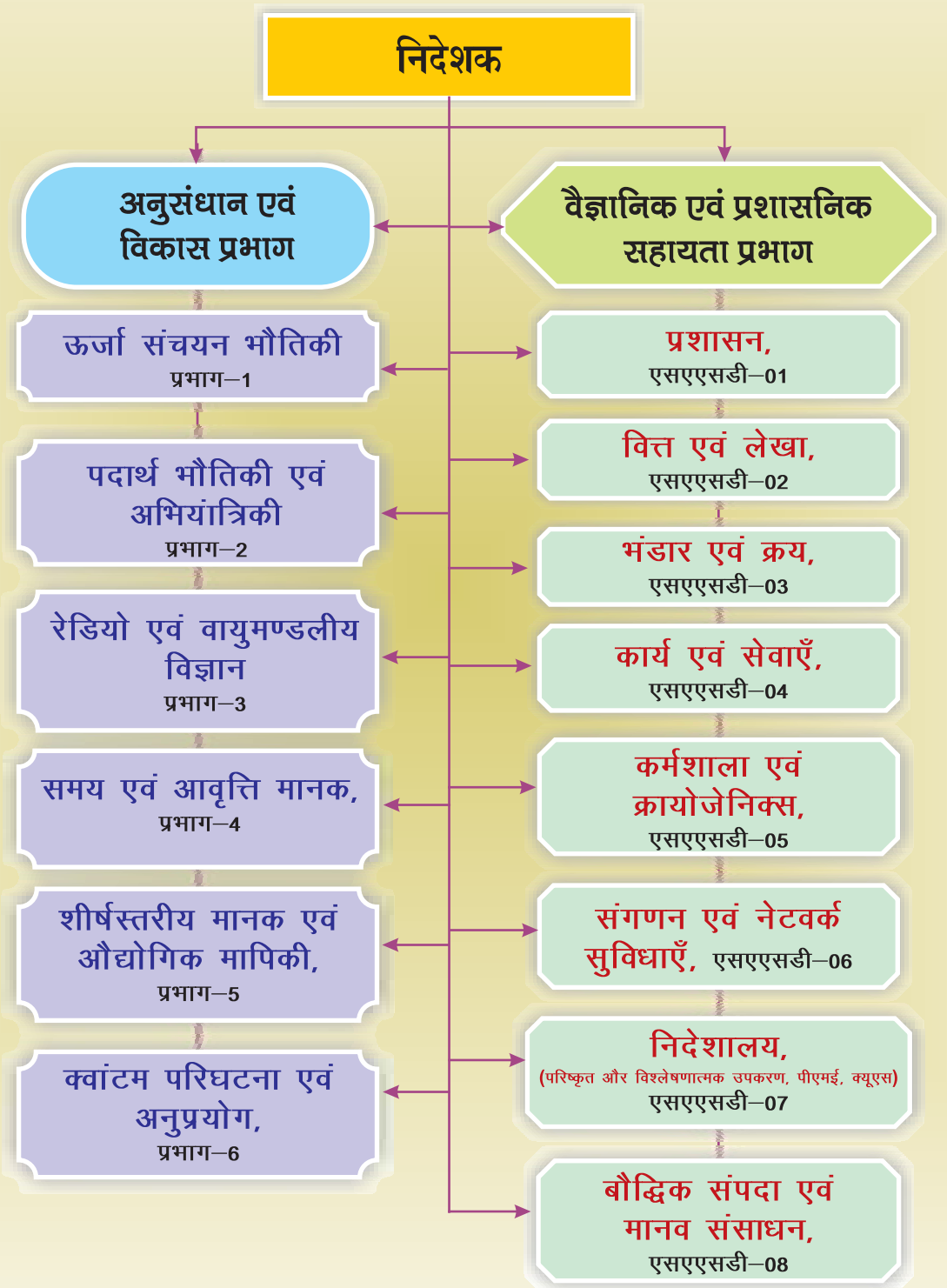

CSIR–NPL
Organizational Structure

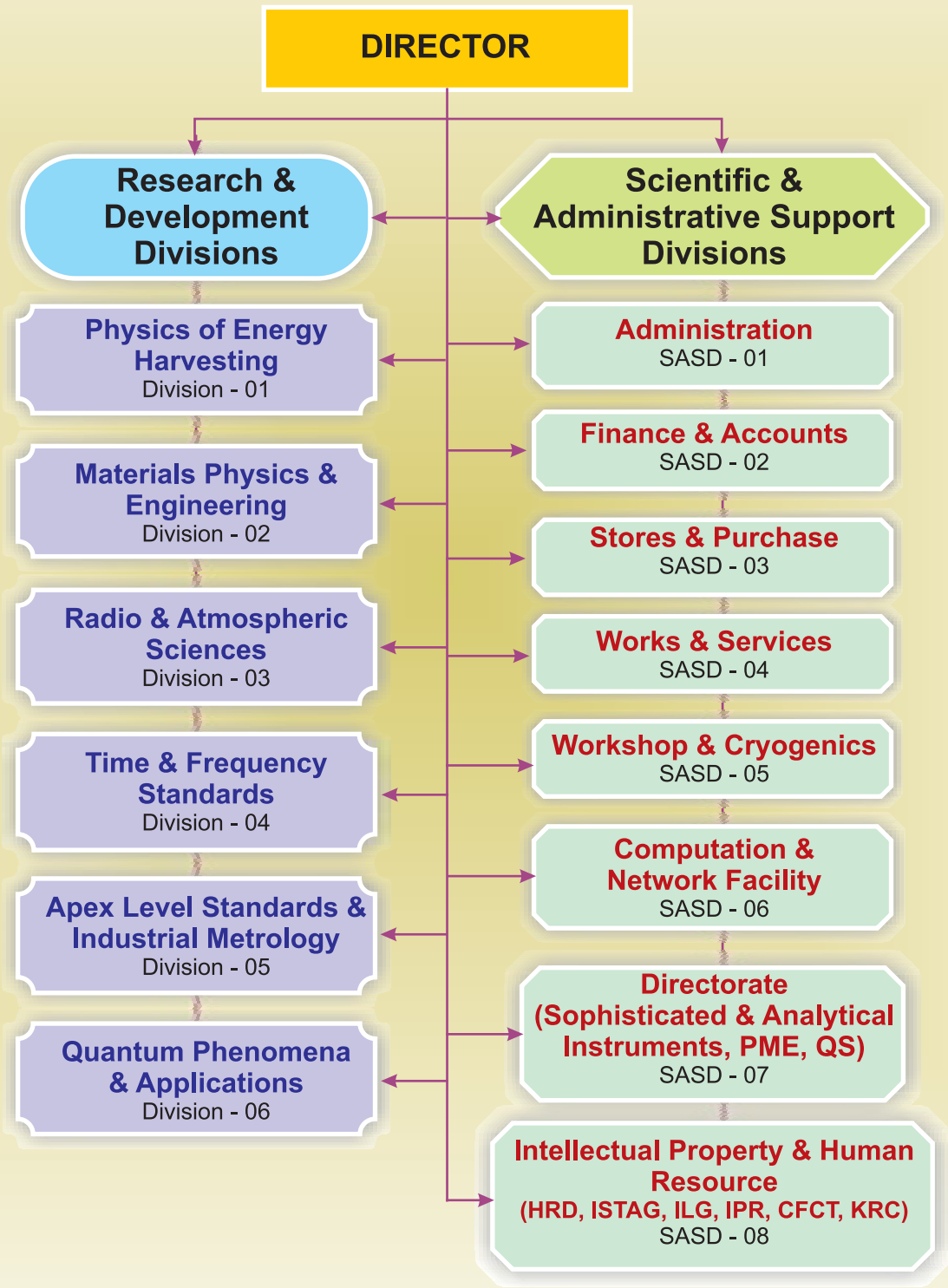

आगन्तुक पुस्तिका से ...

From the visitors book ...

निष्पादन संकेतक

Performance Indicators

PUBLICATIONS

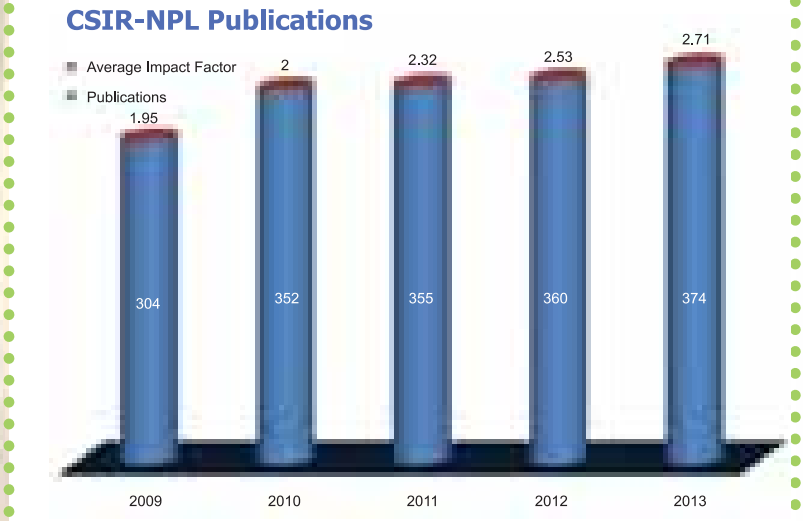

PATENTS FILED

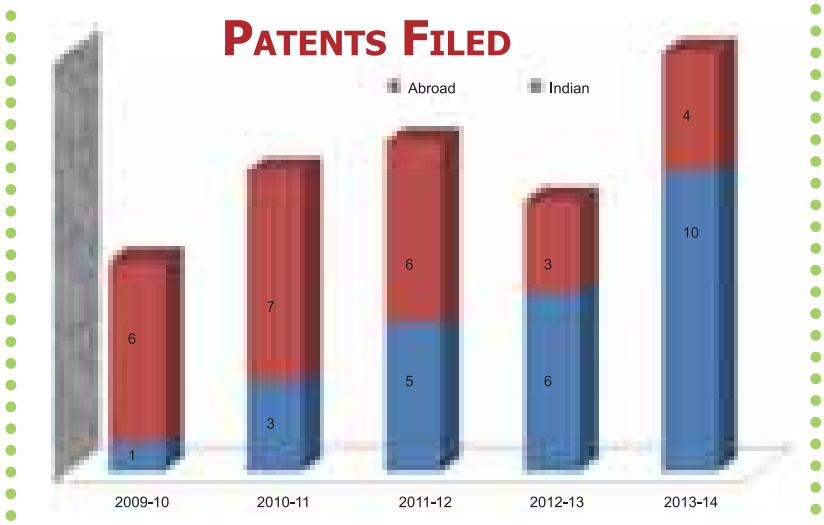

PATENTS GRANTED

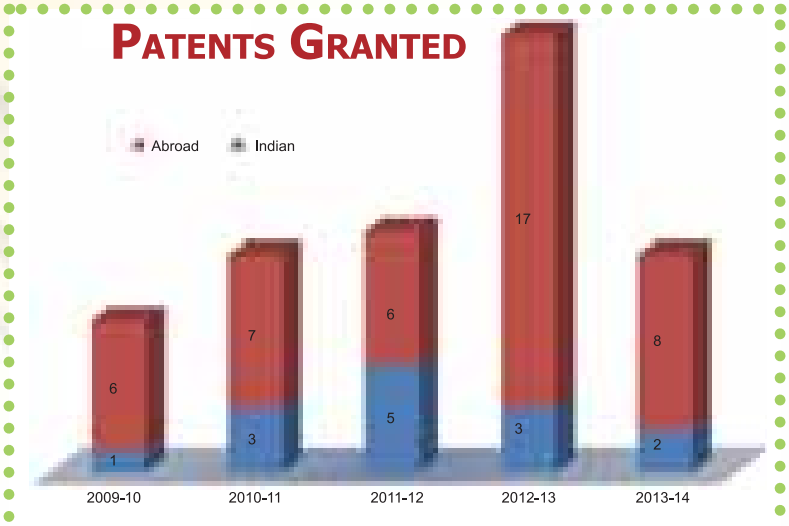

Calibration and Testing at CSIR-NPL

Earnings

(₹ in Lakhs)

Calibration and Testing at CSIR-NPL

(Number of Reports)

Regular Staff (as on 31-03-2014) =698

Average Age of Total Staff: 47.02

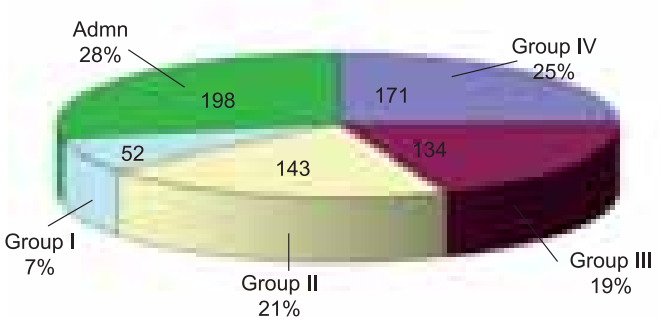

आगन्तुक पुस्तिका से ...

From the visitors book ...

वैज्ञानिक एवं नवीन अनुसंधान अकादमी

एसीएसआईआर, (वैज्ञानिक एवं नवीन अनुसंधान अकादमी) की स्थापना संसद अधिनियम (भारत का राजपत्र सं. 15 दिनांकित 7 फरवरी, 2012 तथा 3 अप्रैल, 2012 को अधिसूचित) द्वारा की गयी। एसीएसआईआर एक विश्व– स्तरीय अनुसंधान अकादमी है । यह वैज्ञानिक तथा औद्योगिक अनुसंधान परिषद् की, जीव–विज्ञान, भौतिक, रासायनिक तथा अंभियांत्रिकी विज्ञान से जुड़ी, 37 राष्ट्रीय प्रयोगशालाओं, 6 इकाइयों तथा 39 विस्तार केन्द्रों के साथ मिलकर कार्य कर रही है जिसके पास देश की सर्वश्रेष्ठ मूलभूत सुविधाएँ हैं । एसीएसआईआर की स्थापना विज्ञान तथा अभियांत्रिकी के समाकलनात्मक (इंटीग्रेटीव) तथा अंतर्विषयक क्षेत्रों में अनुसंधानकर्त्ताओं की संख्या में महत्त्वपूर्ण बढ़ोतरी के उद्देश्य से की गयी थी। इसका मुख्य फोकस अनुसंधान करना तथा विज्ञान एवं प्रौद्योगिकी के उन्नत ज्ञान का प्रसार कर तथा सीमांत क्षेत्रों में शिक्षण तथा अनुसंधान के अवसर प्रदान कर उन क्षेत्रों में शिक्षण प्रदान करना है जो समस्त भारत के नियमित शैक्षणिक विश्वविद्यालयों में आमतौर पर नहीं पढ़ाए जाते ।

एसीएसआईआर के तहत, सी एस आई आर – राष्ट्रीय भौतिक प्रयोगशाला (एनपीएल), नई दिल्ली, जो भौतिक एवं संबंधित विज्ञानों के क्षेत्र में भारत की एक अग्रणी अनुसंधान प्रयोगशाला है, में एम. टेक, पी.एच.डी तथा एकीकश्त एम.टेक तथा पी.एच.डी का संचालन किया जाता है । सी एस आई आर – एन पी एल द्वारा उन्नत पदार्थ भौतिकी तथा अभियांत्रिकी में पी एच.डी. कार्यक्रम तथा एकीकृत एम.टेक – पी.एच.डी. (आईएमपी) कार्यक्रम का संचालन किया जा रहा है । इस कार्यक्रम का महत्त्वपूर्ण पहलू यह है कि इसके कोर्स वर्क को इस प्रकार डिजाइन किया गया है कि इसमें पदार्थ भौतिकी के मूल सिद्धांतों के सैद्धान्तिक पहलू तथा घटकों एवं उपकरणों के विकास हेतु पदार्थ अभियांत्रिकी, दोनों पर बल दिया गया है । नवोन्नत अनुसंधान सुविधाओं तथा फैकल्टी के तौर पर कार्य कर रही प्रयोगशाला की वैज्ञानिक श्रमशक्ति की वैज्ञानिक विशेषज्ञता के कारण यह कार्यक्रम अनूठा तथा विशिष्ट बन गया है ।

भौतिक विज्ञान के मुख्य अनुसंधान क्षेत्रों में नवोन्नत अनुसंधान सुविधाओं के साथ सश्जनात्मक तथा नवीन सोच को प्रोत्साहित करने वाला उत्कृष्ट वातावरण प्रदान करने के लिए विख्यात वर्तमान में सी एस आई आर – एन पी एल के साथ (एसीएसआईआर), आई आई टी, एन आई टी, डी टी यू तथा अन्य प्रतिष्ठित विश्वविद्यालयों के तहत 117 छात्र पंजीकश्त है तथा भौतिक विज्ञान एवं प्रौद्योगिकी के अग्रणी अनुसंधान क्षेत्रों में कार्यरत लगभग 150 अनुभवी वैज्ञानिकों के समुच्चय के पर्यवेक्षण में कार्य कर रहे हैं । विभिन्न सत्रों के दौरान पी एच डी तथा आई एम पी कार्यक्रम के अंतर्गत प्रस्तुत विभिन्न कोर्स इस प्रकार है :–

- इलेक्ट्रॉनिक पदार्थों तथा अर्धचालक उपकरणों के मूलभूत सिद्धांत
- तुन फिल्म भौतिकी तथा प्रौद्योगिकी
- उन्नत पदार्थ अभिलक्षणन तकनीकें
- नैनो–संरचनात्मक पदार्थ
- क्वांटम प्रकाशिकी तथा उन्नत ठोस अवस्था प्रकाशिक उपकरण
- अभियांत्रिकी पदार्थ
- अनुसंधान कार्य पद्धति, तकनीकी लेखन तथा संचार कौशल
- अतिचालकीय तथा चुंबकीय पदार्थ
- उन्नत मापन तकनीकें तथा मापिकी
- उन्न अभिकलनात्मक भौतिकी

पी.एच.डी. कार्यक्रम

- अगस्त 2013 बैच में 23 छात्रों को प्रवेश दिया गया ।
- जनवरी 2014 बैच में 18 छात्रों को प्रवेश दिया गया
- मार्च 2014 में पंजीकश्त छात्रों की कुल संख्या 117 रहीं ।

एकीकृत एम.टेक – पी.एच.डी (आईएमपी) कार्यक्रम

- अगस्त 2013 सत्र में, इस कार्यक्रम के तहत सी एस आई आर – एन पी एल में 7 छात्रों को प्रवेश दिया गया ।
- मार्च 2014 तक, इस कार्यक्रम के तहत छात्रों की (2013–2014) में कुल संख्या 16 थी ।

Academy of Scientific & Innovative Research

AcSIR, (Academy of Scientific Innovative Research) was established by an Act of Parliament, (The Gazette of India No.15 dated February 7, 2012 and notified on April 3, 2012). AcSIR is a world class research academy functioning with 37 national laboratories, 6 units and 39 extension centres, encompassing biological, physical, chemical and engineering sciences, of the Council of Scientific & Industrial Research (CSIR) that have the country's best infrastructural facilities. AcSIR has been established with an aim to substantially increase the number of researchers in integrative and interdisciplinary areas of science and engineering. The primary focus is on research and in imparting instructions in areas not commonly taught in regular academic universities across India, by disseminating advanced knowledge in science & technology and by providing teaching and research opportunities in frontier areas.

Under AcSIR, the CSIR-National Physical Laboratory (NPL), New Delhi, a premier research laboratory in India in the field of Physical & related Sciences conducts the M.Tech. , Ph.D. and Integrated M.tech and Ph.D. CSIR-NPL is running a Ph.D. program and an integrated M.Tech. - Ph.D. (IMP) programme in Advanced Materials Physics and Engineering. The important aspect of the programme is that the course work has been designed in such a manner to provide emphasis on both, the theoretical aspects of fundamentals of material physics and engineering of materials for development of components and devices. The state of the art research facilities and research expertise of scientific manpower of the laboratory acting as the faculty makes the programme very unique and different.

Known for providing an excellent ambience that fosters creativity and innovative thinking along with state-of-the-art research facilities in frontline research areas of Physical Sciences, CSIR-NPL has currently about 117 students registered under (AcSIR), IITs, NITs, DTU and other prestigious universities and working under the supervision from a pool of about 150 experienced scientists working in cutting-edge research areas of Physical Science and Technology.

Various courses offered during different semesters under the Ph.D. & IMP programme are as follows:

- Fundamentals of Electronic Materials & Semiconductor Devices
- Physics & Technology of Thin films
- Advanced Materials Characterization Techniques
- Nanostructured Materials
- Quantum Optics & Advanced Solid State Optical Devices
- Engineering Materials
- Research Methodology, Technical writing & Communication Skills
- Superconducting & Magnetic materials
- Advanced Measurement Techniques & Metrology
- Advanced Computational Physics

Ph.D. Programme

- 23 students were enrolled in August 2013 batch.
- 18 students were enrolled in January 2014 batch.
- As on March 2014 total number of students registered were 117

Integrated M.tech – Ph.D. (IMP) programme

- In August 2013 session, 7 students were enrolled at CSIR-NPL under this programme.
- As on March 2014, total number of students (2013-2014) under this programme were 16.

आगन्तुक पुस्तिका से ...

From the visitors book ...

बारहवीं पंचवर्षीय योजना-परियोजनाएं

XII Five Year Plan - Projects

Supra-Institutional, Network & Interagency Projects

(12th FYP New Projects started in yr. 2013-14)

Sr. No.	Title	Nodal Scientist	Nodal Lab	Supra / Network / Interagency	Project Code	Total cost NPL (₹ In Lakhs)
1	CSIR-Knowledge Gateway & Open Source Private Cloud Infrastructure. (CSIR-KNOWGATE)	Sh. N K Wadhwa	NISCAIR		ISC 0102	11.93
2	Development of Novel CSIR Technologies for Manufacturing Tailored and Patient-Specific Bioceramic Implants and Biomedical Devices at Affordable Cost. (BIOCERAM)	Dr. G Summana	CGCRI		ESC 0103	100.20
3	Very high Power Microwave Tubes: Design and Development Capabilities. (MTDDC)	Dr R B Mathur	CEERI PILANI		PSC 0101	180.12
4	Intelligent Coatings. (IntelCoat)	Dr. S K Dhawan	IICT		CSC 0114	108.50

List of all 12th 5 years plan projects

S. No.	Project title	Project code	Project leader
1.	Novel approaches for solar energy conversion. (under TAPSUN)	NWP-54	Dr. Suresh Chand
2.	Efficient Silicon Photovoltaics with Smart Electronics and Lighting System. (under TAPSUN)	NWP-55	Dr. P K Singh
3.	Innovative solutions for solar energy storage. (under TAPSUN)	NWP56	Dr. R B Mathur Dr. S K Dhawan
4.	Research and Development on Single Trapped ion based Frequency Standard (STIOS). (SUPRA Institutional Project)	PSC 0207	Dr. A Sengupta
5.	Advance Quantum Research and Innovation with Ultra Small Systems (AQuaRIUS).	PSC 0158	Dr. H C Kandpal
6.	Research initiative on Nano-devices and Nano-sensors (R-Nano).	PSC 0152	Dr. R K Kotnala

7.	Development of Advanced for Next-Generation Energy-Efficient Devices (D-NEED).	PSC 0109	Dr. R S Mathur
8.	Measurement for Innovation in Science & Technology for Improvement of Quality & Economy of Life (MAITRIQUE).	PSC 0111	Dr. A K Bandyopadhyay
9.	Probing the Changing Atmosphere and its Impacts in Indo-Gangetic Plains (IGP) and Himalayan Regions (AIM-IGPHim).	PSC 0112	Dr. Chhemendra Sharma
10.	Very high Power Microwave Tubes: Design and Development Capabilities (MTDDC)	PSC 0101	Dr R S Mathur
11.	Nanotechnology: Impact on Safety, Health and Environment (NanoSHE).	ESC 0112	Dr. A K Srivastava
12.	Development of Novel CSIR Technologies for Manufacturing Tailored and Patient-Specific Bioceramic Implants and Biomedical Devices at Affordable Cost (BIOCERAM).	ESC 0103	Dr. G Summana
13.	CSIR-Knowledge Gateway & Open Source Private Cloud Infrastructure (CSIR-KNOWGATE)	ESC 0102	N K Wadhwa
14.	Intelligent Coatings (IntelCoat)	CSC 0114	Dr. S K Dhawan

List of 11th 5 years plan completed projects (2013-14)

S. No.	Project title	Project code	Project leader
1.	R&D on Photovoltaics and Other Energy applications (SUPRA PROJECT)	MP 07	Dr. P K Singh

S. No.	Project title	Project code	Project leader
1.	Advancement in Metrology	NWP-45	Dr. V N Ojha

आगन्तुक पुस्तिका से ...

From the visitors book ...

उल्लेखनीय उपलब्धियाँ

Significant Achievements

नव स्थापित मानक

New Standards Established

Time and Frequency Standards

India's first Cs Fountain Clock, India-CsF1, contributes to the International Atomic Timescale with fractional uncertainty of the time interval below 10^{-15}.

Vibration Standards

National Primary Standard of Low Frequency Vibration realized at CSIR-NPL, India

Force Standards

New Secondary Hardness Standardizing Facility for Micro Vickers Hardness.

नवसृजित सुविधाएँ

Major Facilities Established

LF & HF Voltage, Current and Microwave Standards

AC-DC Current Transfer Measurement Facility Extended up to 80A

AC high voltage and AC high current Standards

New Facility for Calibration of Transformer Loss Measurement System by using High Precision C & Tanδ Measuring System

Quantum Phenomena and Applications

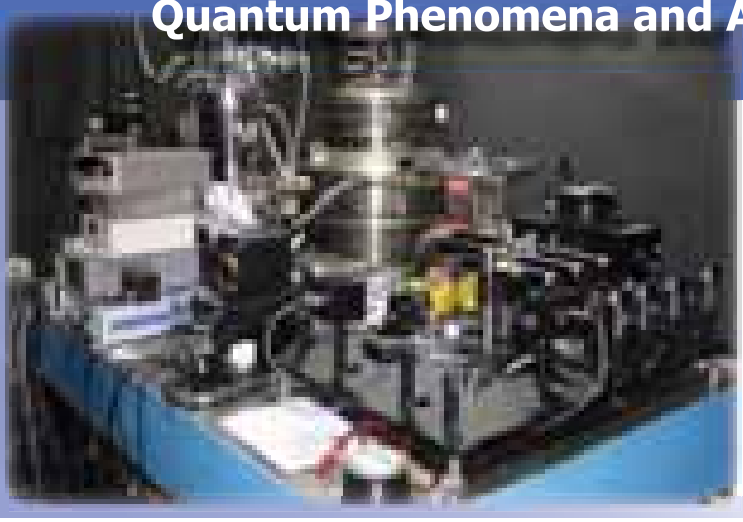

Uncertainty reduced by two orders of magnitude in the existing Scale of Luminous Intensity by the newly established Cryogenic Radiometer Facility

नवसृजित सुविधाएँ

Major Facilities Established

Temperature Standards

High temperature calibration facility has been enhanced for IR-radiation thermometer in the range from 600 °C to 3000 °C.

Quantum Phenomena and Applications

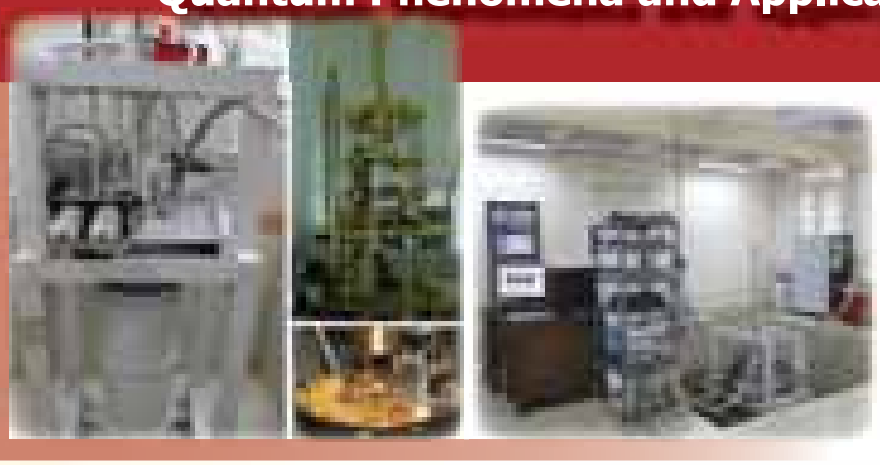

Cryo-free Dilution Refrigerator Facility for Research in Condensed Matter Physics at low temperature research (in mK range).

Vacuum Standards

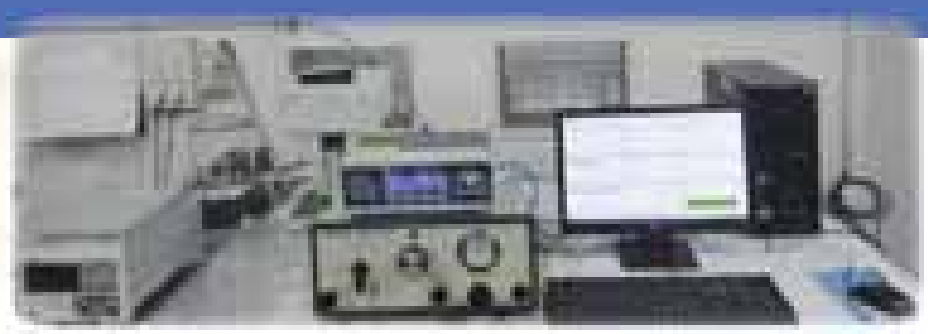

Upgradation of Ruska Air Piston gauge with gauge controller, data acquisition system with Windows based softwares

नवसृजित सुविधाएँ

Major Facilities Established

Melt Spinning Unit

Fluid Flow Standards

Water Flow Calibration Standard (i.e. Primary Standard of Flow) of size DN100

Weighing Tanks, Fishtail and Diverter

PC based flow measurement system comprising of Electromagnetic Flowmeters, digital multimeter, load cell indicators, universal counter, barometric pressure gauge, temperature and humidity indicator

नवसृजित सुविधाएँ

Major Facilities Established

Capacitance Voltage Profiler

Electrochemical Capacitance Voltage Profiler for doping profile measurement in silicon with a capability of carrier concentration range 10^{13}-10^{20} cm^{-3} with a depth resolution of 1nm.

MW-PECVD System

A 2.45 GHz microwave plasma enhanced chemical vapor deposition (MW-PECVD) system equipped with substrate heating facility designed and developed indigenously to synthesize graphene, carbon nanotubes and other carbon nanostructures on metal and ceramic substrates.

Technology Development: Choestrol Biosensor

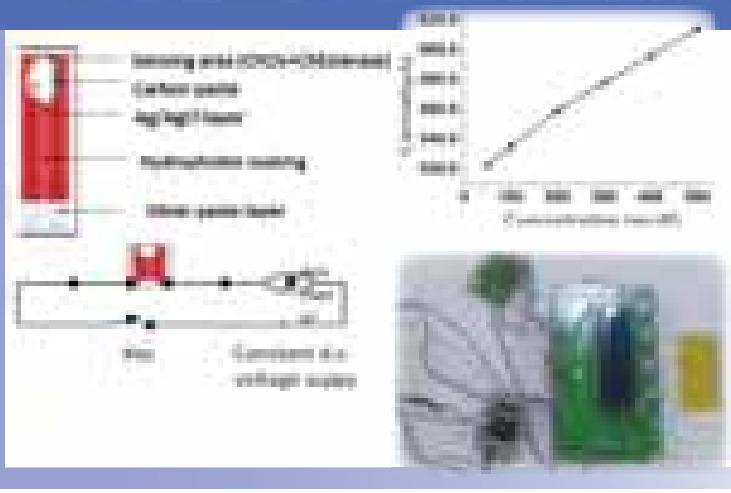

*The technology is ready for transfer

Detection Range: 50-500 mg/dl (normal range 70- 200mg/dl)

Stability of strips: 4 months

Strips are cost effective (Rs 20/-)

Validation is being done with clinical samples

* Reproducibility: +95%

नवसृजित सुविधाएँ

Major Facilities Established

CSIR-NPL ERP Data Centre

CSIR-NPL ERP Data Centre established with Application & DB Clustering and 20 TB SAN storage.

Metrology Building

Solar Energy Clean Room Complex

आगन्तुक पुस्तिका से ...

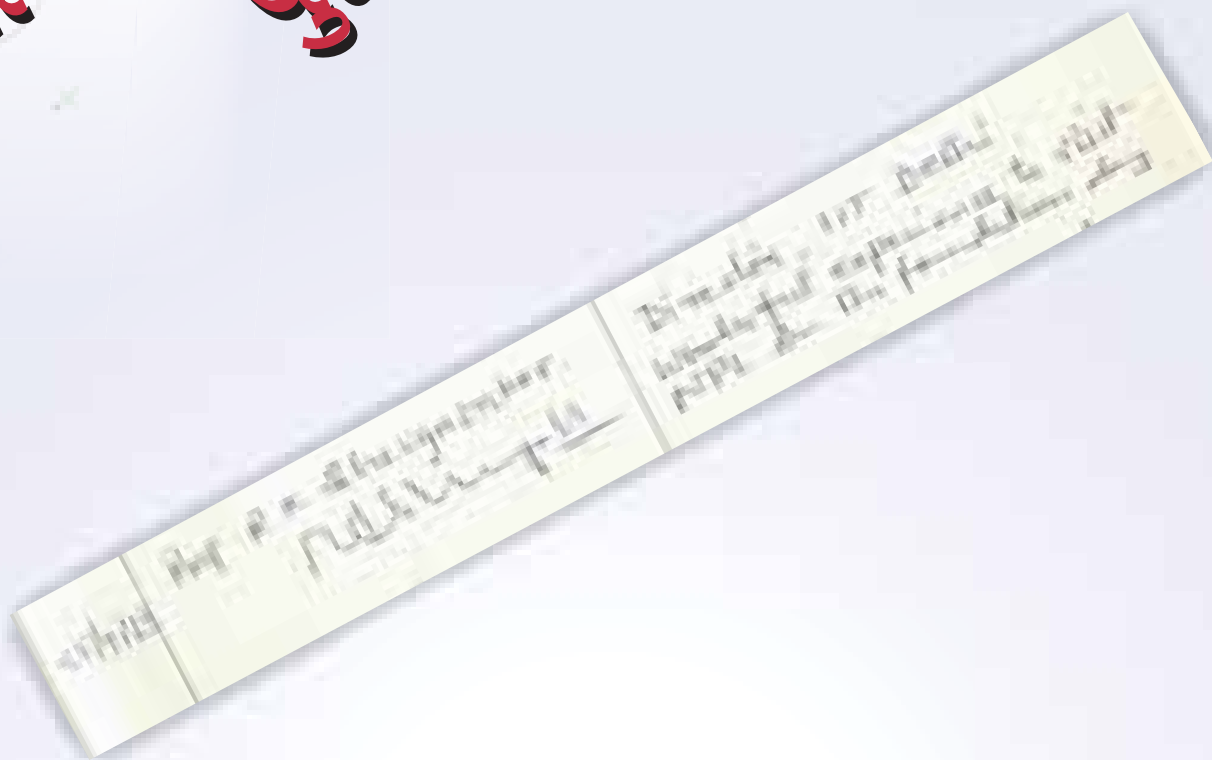

From the visitors book ...

उच्च प्रभाव कारक जर्नल में प्रकाशित शोध पत्र

Research Papers in High Impact Factor Journals

Research Papers of CSIR-NPL Scientists Published in High Impact Factor Journals during 2013-2014

S. No. Source Title
IF 2013

1.
Multiple Quantum Criticality In A Two-Dimensional SuperconductorJ. Biscaras, N. Bergeal, S. Hurand, C. Feuillet-Palma, A. Rastogi, **R. C. Budhani**, M. Grilli,S. Caprara, J. Lesueur *Nature Materials Volume: 12 Issue: 6 Pages: 542-548 Published: Jun 2013* (IF:36.425)

2.
Efficient Solution-Processed Small-Molecule Solar Cells With Inverted StructureAung Ko Ko Kyaw, Dong Hwan Wang, **Vinay Gupta**, Jie Zhang, **Suresh Chand** ,Guillermo C. Bazan, Alan J. Heeger *Advanced Materials Volume: 25 Issue: 17 Pages: 2397-2402 Published: May 7 2013* (IF:15.409)

3.
Enhanced Efficiency Parameters Of Solution-Processable Small-Molecule Solar Cells Depending On Ito Sheet ResistanceDong Hwan Wang , Aung Ko Ko Kyaw , **Vinay Gupta** , Guillermo C. Bazan, Alan J. Heeger *Advanced Energy Materials Volume: 3 Issue: 9 Pages: 1161-1165 Published: Sep 2013* (IF:14.385)

4.
Magnetic Switching Of Ferroelectric Domains At Room Temperature In Multiferroic PztftD.M. Evans, A. Schilling, **Ashok Kumar**, D. Sanchez, N. Ortega, M. Arredondo, R.S. Katiyar, J.M. Gregg, J.F. Scott *Nature Communications Volume: 4 Article Number: 1534 Published: Feb 2013* (IF:10.742)

5.
Effect Of Voltage Sweep Direction On The Performance Evaluation Of P3ht:Pcbm Solar Cells**Pankaj Kumar, Abhishek Sharma**, Dwijendra Pratap Singh *Progress In Photovoltaics Volume: 21 Issue: 5 Pages: 950-959 Published: Aug 2013* (IF:9.696)

6.
Room Temperature Nanoscale Ferroelectricity In Magnetoelectric Gafeo3 Epitaxial Thin FilmsSomdutta Mukherjee, Amritendu Roy, **Sushil Auluck,** Rajendra Prasad, Rajeev Gupta, Ashish Garg *Physical Review Letters Volume: 111 Issue: 8 Article Number: 087601 Published: Aug 21 2013* (IF:7.728)

7.
A Highly Efficient Microfluidic Nano Biochip Based On Nanostructured Nickel Oxide**Md. Azahar Ali, Pratima R. Solanki, Manoj K. Patel Hemant Dhayani,Ved Varun Agrawal**, Renu John and Bansi D. Malhotra *Nanoscale Volume: 5 Issue: 7 Pages: 2883-2891 Published: 2013* (IF:6.739)

8.
Cationic Poly(Lactic-Co-Glycolic Acid) Iron Oxide Microspheres For Nucleic Acid Detection**Chandra Mouli Pandey, Aditya Sharma, Gajjala Sumana,** Ida Tiwari, **Bansi Dhar Malhotra** *Nanoscale Volume: 5 Issue: 9 Pages: 3800-3807 Published: 2013* (IF:6.739)

9.
Electrophoretically Deposited Reduced Graphene Oxide Platform For Food Toxin Detection**Saurabh Srivastava,** Vinod Kumar**, Md Azahar Ali, Pratima R. Solanki**, Anchal Srivastava, **Gajjala Sumana**, Preeti Suman Saxena, **Amish G. Joshi,** B. D. Malhotra *Nanoscale Volume: 5 Issue: 7 Pages: 3043-3051 Published: 2013* (IF:6.739)

10.
High Permittivity Polyaniline-Barium Titanate Nanocomposites With Excellent Electromagnetic Interference Shielding Response**Parveen Saini, Manju Arora, Govind Gupta, Bipin Kumar Gupta, Vidya Nand Singh,** Veena Choudhary *Nanoscale Volume: 5 Issue: 10 Pages: 4330-4336 Published: 2013* (IF:6.739)

11.
Microstructural And Electrochemical Impedance Characterization Of Bio-Functionalized Ultrafine Zns Nanocrystals-Reduced Graphene Oxide Hybrid For Immunosensor Applications**Sujeet K. Mishra, Avanish K. Srivastava**, Devendra Kumar,**Ashok M. Biradar, Rajesh** *Nanoscale Volume: 5 Issue: 21 Pages: 10494-10503 Published: 2013* (IF:6.739)

12.
Nanostructured Graphene/Fe3o4 Incorporated Polyaniline As A High Performance Shield Against Electromagnetic PollutionKuldeep Singh, Anil Ohlan, Viet Hung Pham, Balasubramaniyan R.,**Swati Varshney**, Jinhee Jang, Seung Hyun Hur, Won Mook Choi, Mukesh Kumar, **S. K. Dhawan**, Byung-Seon Kong, Jin Suk Chung Nanoscale Volume: 5 Issue: 6 Pages: 2411-2420 Published: 2013 (IF:6.739)

13.
Temperature Tuned Defect Induced Magnetism In Reduced Graphene OxideGeetika Khurana, **Nitu Kumar**, **R. K. Kotnala**, Tashi Nautiyal, R. S. Katiyar *Nanoscale Volume: 5 Issue: 8 Pages: 3346-3351 Published: 2013* (IF:6.739)

14.
Silver Nanoprism Enhanced Fluorescence In $Yvo_4:Eu^{3+}$ Nanoparticles**Zubair Buch, Vineet Kumar,** Hitesh Mamgain**, Santa Chawla** *Chemical Communications Volume: 49 Issue: 82 Pages: 9485-9487 Published: 2013* (IF:6.718)

15.
Silver Nanoprisms Acting As Multipolar Nanoantennas Under A Low-Intensity Infrared Optical Field Exciting Fluorescence From Eu3+**Zubair Buch, Vineet Kumar**, Hitesh Mamgain, **Santa Chawla** *Journal Of Physical Chemistry Letters Volume: 4 Issue: 22 Pages: 3834-3838 Published: Nov 21 2013* (IF:6.687)

16.
Biocompatible Nanostructured Magnesium Oxide-Chitosan Platform For Genosensing Application**Manoj Kumar Patel, Md.Azahar Ali**, Md.Zafaryab, **Ved Varun Agrawal**, M. Moshahid Alam Rizvi, Z.A.Ansari, S.G.Ansari, Bansi D. Malhotra *Biosensors & Bioelectronics Volume: 45 Pages: 181-188 Published: Jul 15 2013* (IF:6.451)

17.
Magnesium Oxide Grafted Carbon Nanotubes Based Impedimetric Genosensor For Biomedical Application**Manoj Kumar Patel, Md.Azahar Ali, Saurabh Srivastava, Ved Varun Agrawal,**S.G. Ansari, **Bansi D. Malhotra** *Biosensors & Bioelectronics Volume: 50 Pages: 406-413 Published: Dec 15 2013* (IF:6.451)

18.
Multiwalled Carbon Nanotube/Cement Composites With Exceptional Electromagnetic Interference Shielding Properties**Avanish Pratap Singh, Bipin Kumar Gupta, Monika Mishra, Govind,** Amita Chandra, **R.B. Mathur, S.K. Dhawan** *Carbon Volume: 56 Pages: 86-96 Published: May 2013* (IF:6.16)

19.
Fabrication Of Artificially Stacked Ultrathin Zns/Mgf2 Multilayer Dielectric Optical FiltersGarima Kedawat, Subodh Srivastava, Vipin Kumar Jain, **Pawan Kumar, Vanjula Kataria, Yogyata Agrawal, Bipin Kumar Gupta,** Yogesh K. Vijay *ACS Applied Materials & Interfaces Volume: 5 Issue: 11 Pages: 4872-4877 Published: Jun 12 2013* (IF:5.9)

20.
Influence Of Silver Incorporation On The Structural And Electrical Properties Of Diamond-Like Carbon Thin Films**Neeraj Dwivedi, Sushil Kumar,** J. David Carey, **R. K. Tripathi,** Hitendra K. Malik, **M. K. Dalai** *ACS Applied Materials & Interfaces Volume: 5 Issue: 7 Pages: 2725-2732 Published: Apr 10 2013* (IF:5.9)

21.
Organic And Inorganic Markers And Stable C-, N-Isotopic Compositions Of Tropical Coastal Aerosols From Megacity Mumbai: Sources Of Organic Aerosols And Atmospheric Processing**S. G. Aggarwal,** K. Kawamura, G. S. Umarji, E. Tachibana, R. S. Patil, **P. K. Gupta** *Atmospheric Chemistry And Physics Volume: 13 Issue: 9 Pages: 4667-4680 Published: 2013* (IF:5.298)

22.
Platinum Nanoflowers Decorated Three-Dimensional Graphene-Carbon Nanotubes Hybrid With Enhanced Electrocatalytic Activity**Rajesh,** Rajat K. Paul, Ashok Mulchandani *Journal Of Power Sources Volume: 223 Pages: 23-29 Published: Feb 1 2013* (IF:5.211)

23.
Barium: An Efficient Cathode Layer For Bulk-Heterojunction Solar Cells**Vinay Gupta,** Aung Ko Ko Kyaw, Dong Hwan Wang, **Suresh Chand,** Guillermo C. Bazan, Alan J. Heeger *Scientific Reports Volume: 3 Article Number: 1965 Published: Jun 11 2013* (IF:5.078)

24.
Highly Efficient Bienzyme Functionalized Nanocomposite-Based Microfluidics Biosensor Platform For Biomedical Application**Md. Azahar Ali, Saurabh Srivastava, Pratima R. Solanki,** Venu Reddy, **Ved V. Agrawal,** Cheol Gi Kim, Renu John, **Bansi D. Malhotra** *Scientific Reports Volume: 3 Article Number: 2661 Published: Sep 27 2013* (IF:5.078)

25.
Biological Delignification Of Paddy Straw And Parthenium Sp Using A Novel Micromycete Myrothecium Roridum Lg7 For Enhanced Saccharification Rameshwar Tiwari, Sarika Rana, Surender Singh, Anju Arora, Rajeev Kaushik, **Ved Varun Agrawal**, Anil Kumar Saxena, Lata Nain *Bioresource Technology Volume: 135 Pages: 7-11 Published: May 2013* (IF:5.039)

26.
Influence Of Emitter Bandgap On Interdigitated Point Contact Back Heterojunction (A-Si:H/C-Si) Solar Cell Performance **R. Jeyakumar, T.K. Maiti, Amit Verma** *Solar Energy Materials And Solar Cells Volume: 109 Pages: 199-203 Published: Feb 2013* (IF:5.03)

आगन्तुक पुस्तिका से ...

From the visitors book ...

महत्वपूर्ण समारोहों की झलकियाँ

Glimpses of Important Events

World Metrology Day and National Technology Day Celebrations,

20th May, 2013

TAPSUN-APEX Meeting, 7th June, 2013

58th RC Meeting, 1st November, 2013

35th K S Krishnan Memorial Lecture, 17th February, 2014

National Conference on Bio-medical Sciences and Technology

21st -22nd November, 2013

Acoustics 2013 — Technologies for a Quieter India, 10th - 15th November, 2013

CSIR Foundation Day Celebrations

26th September, 2013

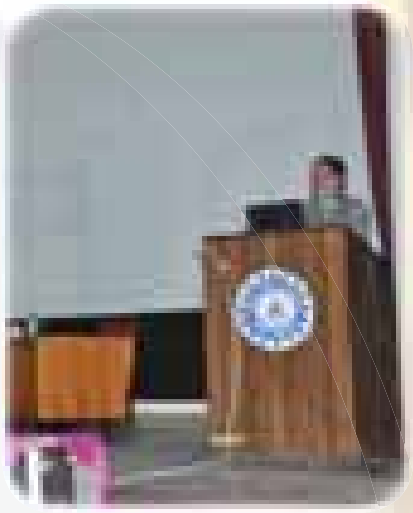

CSIR-NPL Open Day Celebration

27th September, 2013










National Science Day

28th February, 2014

INSA Lecture by Dr. R. A. Mashelkar

24th December, 2013

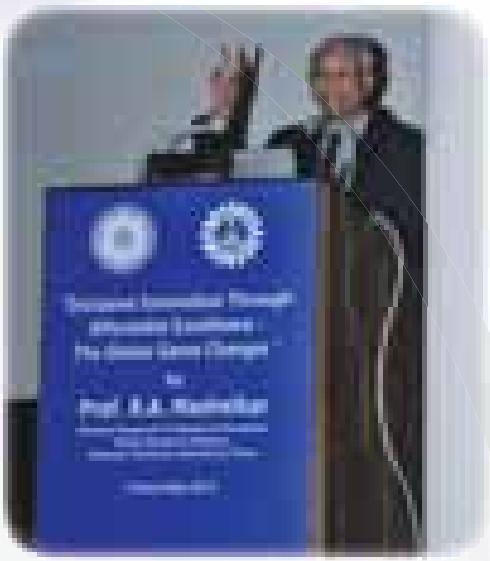

Training Programme on Calibration & Uncertainty Evaluation in Dimension

14th - 15th May, 2013

Training Programme on Mass Metrology, 20th - 22nd August, 2013

Training Programme on Force Torque & Hardness

4th - 6th September, 2013

Residential Training Programme for Legal Metrology Officers on Mass, Volume, Density & Length , Blood Pressure Measurement & Clinical Thermometers

18th- 22nd November, 2013

Workshop on Coordinate metrology

17th - 18th December 2013

Residential Training Programme for Legal Metrology Officers on Laboratory Quality Management System

28th - 31st January 2014

Independence Day Celebrations

15th August, 2013

Hindi Pakhwara Celebrations, 17th September 2013

45th SSB Memorial Tournament, 22nd - 24th October 2013

Vigilance Awareness Week

28th - 2nd November, 2013

Address by the Director, 1st January, 2014

NPL Club Annual Sports

Mini Marathon, 14th March, 2014

Volleyball Match, 20th February, 2014

Participation of CSIR-NPL in Annual Pusa Horticulture Show

1st - 2nd March, 2014

Dr G C Jain Memorial Prize to Dr Sonal

(MRSI the Best PhD Thesis Award in Materials Science 2014)

Title of the PhD Thesis:
"Group II-VI Semiconductor Nano-crystals for Photo- and Electroluminescence Applications"

Supervisors:
Dr D Haranath (CSIR-NPL) and Prof Mushahid Husain (JMI

MRSI-ICSC Prize to Dr V P S Awana

प्रभागीय गतिविधियाँ

Divisional Activities

राजभाषा कार्यान्वयन

राजभाषा यूनिट

राजभाषा यूनिट दिन-प्रति-दिन के सरकारी कार्यों में राजभाषा हिन्दी के प्रगामी प्रयोग को बढ़ाने का कार्य करती है। राजभाषा यूनिट का मुख्य उत्तरदायित्व संघ सरकार की राजभाषा नीति, राजभाषा अधिनियम के उपबंधों तथा आदेशों से प्रयोगशाला के वैज्ञानिकों/अधिकारियों/कर्मचारियों को अवगत कराना, अनुपालन कराना एवं अनुपालन हेतु सहायता प्रदान करना है।

राजभाषा यूनिट के उत्तरदायित्व

1. कार्यान्वयन

- संघ सरकार की राजभाषा नीति, राजभाषा अधिनियम के उपबन्धों तथा आदेशों से प्रयोगशाला के वैज्ञानिकों/अधिकारियों/कर्मचारियों को अवगत कराना, अनुपालन कराना एवं अनुपालन हेतु सहायता प्रदान करना।
- प्रत्येक तिमाही में निदेशक, एन पी एल की अध्यक्षता में राजभाषा कार्यान्वयन समिति की बैठक का आयोजन, कार्य सूची एवं कार्यवृत्त तैयार करना। बैठक में लिए गए निर्णयों पर अनुवर्ती कार्रवाई करना।
- प्रयोगशाला की राजभाषा कार्यान्वयन प्रगति सम्बन्धी तिमाही प्रगति रिपोर्ट तैयार कर सी एस आई आर मुख्यालय भेजना।
- हिन्दी दिवस/हिन्दी सप्ताह/हिन्दी पखवाड़ा/हिन्दी मास मनाना।
- प्रत्येक तिमाही में हिन्दी कार्यशालाओं/व्याख्यानों का आयोजन करना।
- राजभाषा विभाग, गृह मंत्रालय, भारत सरकार से प्राप्त वार्षिक कार्यक्रम में निर्धारित लक्ष्यों को प्राप्त करने हेतु उचित कार्रवाई करना।
- संसदीय राजभाषा समिति के निरीक्षण सम्बन्धी कार्य तथा समिति को दिए गए आश्वासनों को पूरा करने हेतु कार्रवाई करना।
- प्रत्येक वर्ष विज्ञान विषयों पर हिन्दी में दो दिवसीय राष्ट्रीय संगोष्ठी का आयोजन।

2. प्रशिक्षण एवं प्रकाशन

- हिन्दी प्रशिक्षण (प्रबोध, प्रवीण एवं प्राज्ञ पाठ्यक्रम)।
- हिन्दी टंकण/आशुलिपि एवं कम्प्यूटर पर हिन्दी में कार्य करने का प्रशिक्षण दिलाना।
- प्रत्येक छ:माही में हिन्दी समीक्षा पत्रिका का प्रकाशन।
- प्रयोगशाला की वार्षिक रिपोर्ट तथा अन्य महत्त्वपूर्ण प्रकाशनों में हिन्दी अंश का संपादन।

3. अनुवाद

- प्रयोगशाला में प्रयुक्त सभी प्रपत्रों (फार्मों), मानक मसौदों का द्विभाषीकरण।
- अंग्रेजी से हिन्दी और हिन्दी से अंग्रेजी में अनुवाद कार्य।
- राष्ट्रीय भौतिक प्रयोगशाला के वार्षिक प्रतिवेदन के महत्त्वपूर्ण अंशों का हिन्दी अनुवाद।
- प्रयोगशाला की वेबसाइट का हिन्दी अनुवाद।

कार्मिक

1.	मंजु	हिन्दी अधिकारी
2.	जय नारायण उपाध्याय	हिन्दी अधिकारी
3.	विजय सिंह	वरिष्ठ आशुलिपिक (हिन्दी)

व्याख्यान

सरकारी कार्यालयों में हिन्दी का प्रयोग – कठिनाइयां व समाधान

राष्ट्रीय भौतिक प्रयोगशाला राजभाषा हिन्दी के प्रयोग को बढ़ावा देने के लिए सतत् प्रयत्नशील है, जिसके अंतर्गत प्रयोगशाला के वैज्ञानिकों/कर्मचारियों के लिए प्रत्येक

श्री वी के कौशिक, प्रशासन नियंत्रक, दिनांक 27 जून, 2013 को आयोजित राजभाषा कार्यशाला में व्याख्यान देते हुए

तिमाही में उपयोगी विषयों पर आधारित व्याख्यान/कार्यशाला का आयोजन किया जाता है। प्रयोगशाला के राजभाषा नीति के प्रभावी कार्यान्वयन हेतु दिनांक 27 जून, 2013 को प्रशासन के अधिकारियों/कर्मचारियों के लिए **'सरकारी कार्यालयों में हिन्दी का प्रयोग – कठिनाइयां एव समाधान'** विषय पर एक कार्यशाला का आयोजन किया गया, जिसमें श्री विजय कुमार कौशिक, प्रशासन नियंत्रक ने दैनिक सरकारी कामकाज में राजभाषा हिन्दी के प्रयोग में आने वाली कठिनाइयों पर अपने विचार व्यक्त किए और उनका समाधान भी प्रस्तुत किया। श्री कौशिक ने उपस्थित सदस्यों से व्यक्तिगत स्तर पर चर्चा की व उन्हें हिन्दी में अधिक से अधिक कार्य करने के लिए प्रेरित व प्रोत्साहित किया। साथ ही, उनकी शंकाओं का निवारण भी किया। इस प्रकार यह कार्यशाला अपने उद्देश्य में सफल रही।

बायो–मैडिकल विज्ञान एवं प्रौद्योगिकी पर राष्ट्रीय सम्मेलन

21–22 नवम्बर, 2013

विज्ञान एवं प्रौद्योगिकी किसी भी समाज की समृद्धि और विकास का घोतक है। भारतवर्ष में विज्ञान एवं प्रौद्योगिकी से जुड़ी जानकारी और विचारों का आदान–प्रदान करने में यदि राजभाषा हिन्दी का प्रयोग करें तो यह समाज के विकास और समृद्धि की दिशा में अधिक उपयोगी होगा साथ ही यह भारतीय विज्ञान के लिए गौरव एवं स्वाभिमान की भी बात होगी। इसी संदर्भ में राष्ट्रीय भौतिक प्रयोगशाला, नई दिल्ली प्रत्येक वर्ष वैज्ञानिक एवं प्रौद्योगिकी के किसी भी ज्वलंत विषय पर एक राष्ट्रीय संगोष्ठी या सम्मेलन हिन्दी भाषा में आयोजित करती रही है। जहां सभी प्रस्तुति एवं चर्चा का माध्यम हिन्दी भाषा होती है।

इस वर्ष राष्ट्रीय भौतिक प्रयोगशाला, नई दिल्ली में ''बायो–मैडिकल विज्ञान एवं प्रौद्योगिकी'' विषय पर दिनांक 21–22 नवम्बर, 2013 को दो दिवसीय राष्ट्रीय सम्मेलन का आयोजन किया गया। इस सम्मेलन में ''बायो–मैडिकल विज्ञान एवं प्रौद्योगिकी'' पर परिचर्चा करने हेतु देश के विभिन्न भागों से वैज्ञानिक, प्राध्यापक एवं शोध छात्र–छात्राओं को आमंत्रित किया गया। इस सम्मेलन में मुख्य अतिथि डा. राजेश एस. गोखले, निदेशक, सी एस आई आर–जीनोमिकी और समवेत जीव विज्ञान संस्थान, दिल्ली थे।

सम्मेलन का शुभारंभ प्रो. रमेशचन्द्र बुधानी, निदेशक, एन पी एल के स्वागत भाषण से हुआ। निदेशक महोदय ने मुख्य अतिथि डा. राजेश एस. गोखले एवं सभागार में उपस्थित वैज्ञानिक समुदाय, प्राध्यापकों एवं शोध छात्र–छात्राओं का अभिनन्दन करते हुए एन पी एल में जैव चिकित्सा विज्ञान एवं प्रौद्योगिकी के क्षेत्र में हो रहे शोध कार्यों के बारे में बताया। तत्पश्चात् मुख्य अतिथि डा. राजेश एस गोखले ने ''**त्वचा में होमो स्टेटिक**

राष्ट्रीय सम्मेलन में उपस्थित वैज्ञानिक समुदाय को सम्बोधित करते हुए प्रो. आर.सी. बुधानी, निदेशक, एन.पी.एल.

तंत्र: रंजकता रियो स्टेट की ट्यूनिंग'' शीर्षक पर मुख्य अभिभाषण दिया। श्री टी वी जोशुवा, प्रशासन नियंत्रक ने एन पी एल में राजभाषा गतिविधियों का संक्षिप्त उल्लेख किया। डा. ए. एम. बिरादर ने सम्मेलन के बारे में बताया व डा. रंजना मेहरोत्रा ने धन्यवाद प्रस्ताव प्रस्तुत किया।

इस सम्मेलन में 6 तकनीकी सत्र थे जिनमें 5 आरंभिक व्याख्यान और 27 आमंत्रित वार्ताएं और 33 पेपर प्रस्तुतीकरण थे। इन वार्ताओं में जैव चिकित्सा विज्ञान एवं प्रौद्योगिकी से सम्बन्धित विभिन्न विषयों जैसे त्वचा में होमोस्टेटिक तंत्र, हृदय बायोमार्कर, डी एन ए ट्रिप्लेक्स बनाने वाले ओलईगोन्युक्लियोटाईड्स का कैंसर चिकित्सा में अनुप्रयोग, वहन योग्य चिकित्सा उपकरणों का विकास, नवीन विद्युत पदार्थों का संवेदक एवं जैव संवेदकों में अनुप्रयोग आदि पर व्याख्यान प्रस्तुत किए गए।

राष्ट्रीय सम्मेलन में मुख्य अतिथि डा. राजेश गोखले, निदेशक, आई जी आई बी मुख्य अभिभाषण देते हुए

सम्मेलन के समापन समारोह की अध्यक्षता डा. ए सेन गुप्ता द्वारा की गयी। इस प्रकार राजभाषा हिन्दी में आयोजित यह दो दिवसीय राष्ट्रीय सम्मेलन **बायो-मैडिकल विज्ञान एवं प्रौद्योगिकी** से जुड़े विभिन्न पक्षों के लिए अत्यन्त प्रासंगिक रहा।

हिन्दी पखवाड़ा रिपोर्ट

राजभाषा विभाग, गृह मंत्रालय, भारत सरकार की हिन्दी पखवाड़ा सम्बन्धी व्यवस्थाओं को ध्यान में रखते हुए प्रयोगशाला में दिनांक 01 सितम्बर, 2013 से

हिन्दी दिवस समारोह में उपस्थित जनसमुदाय को सम्बोधित करते हुए डा. ए सेन गुप्ता, आऊट स्टैडिंग वैज्ञानिक

17 सितम्बर, 2013 तक हिन्दी पखवाड़ा मनाया गया। प्रयोगशाला में स्टाफ सदस्यों को हिन्दी में अधिक से अधिक कार्य करने के लिए प्रोत्साहित एवं प्रेरित करने के उद्देश्य से हिन्दी पखवाड़ा मनाए जाने से पूर्व एवं पखवाड़ा के दौरान विभिन्न प्रतियोगिताओं का आयोजन किया गया। प्रत्येक वर्ष की भाँति इस वर्ष भी जो प्रतियोगिताएं आयोजित की गयी वे इस प्रकार से हैं :-

इन सभी प्रतियोगिताओं में प्रयोगशाला के स्टाफ सदस्यों ने उत्साहपूर्वक भाग लिया व अत्यधिक रूचि प्रदर्शित की। प्रयोगशाला के सभागार में दिनांक 17.09.2013 को मुख्य समारोह आयोजित किया गया। डा. ए. सेन गुप्ता, आउटस्टैडिंग साइंटिस्ट ने कार्यक्रम का शुभारंभ किया। इस अवसर पर उन्होंने प्रयोगशाला के स्टाफ सदस्यों को हिन्दी में अधिक से अधिक कार्य करने के लिए प्रेरित एवं प्रोत्साहित करते हुए अपना संदेश

हिन्दी दिवस समारोह में विजेता प्रतिभागियों को पुरस्कार प्रदान करते हुए डा. ए सेन गुप्ता, आऊटस्टैडिंग वैज्ञानिक

क्रम सं.	प्रतियोगिताएं	दिनांक
1.	शब्दावली एवं अनुवाद प्रतियोगिता	12 अगस्त, 2013
2.	टंकण प्रतियोगिता	19 अगस्त, 2013
3.	साइंस क्विज़ प्रतियोगिता	22 अगस्त, 2013
4.	निबन्ध प्रतियोगिता	26 अगस्त, 2013
5.	हिन्दी टिप्पण एवं आलेखन प्रतियोगिता (डेस्क प्रतियोगिता)	30 अगस्त, 2013
6.	वर्ष के दौरान हिन्दी में किया गया अधिकतम कार्य एवं हिन्दी डिक्टेशन	02 सितम्बर, 2013
7.	काव्य पाठ प्रतियोगिता	06 सितम्बर, 2013

दिया। समारोह के अंत में हिन्दी पखवाड़ा मनाए जाने के दौरान आयोजित की गयी प्रतियोगिताओं में भाग लेने वाले विजेता प्रतिभागियों को पुरस्कार प्रदान किए गए।

कार्यशाला

राजभाषा विभाग, गृह मंत्रालय भारत सरकार द्वारा हिन्दी के लिए जारी वार्षिक कार्यक्रम में राजभाषा नीति संबंधी निदेशों का अनुपालन सुनिश्चित करते हुए दिनांक 6 मार्च, 2014 को प्रशासन के अधिकारियों/कर्मचारियों के लिए एक कार्यशाला का आयोजन किया गया। कार्यशाला में व्याख्यान देने के लिए डा. पूरन पाल, वरि. हिन्दी अधिकारी, सी एस आई आर को आमंत्रित किया गया। डा. पूरनपाल ने **'प्रयोगशाला में राजभाषा कार्यान्वयन तथा महत्त्व'** विषय पर व्याख्यान देते हुए कहा कि प्रयोगशाला में सरकारी काम-काज में हिन्दी के प्रयोग में वृद्धि हुई है लेकिन आज भी लक्ष्य प्राप्त नहीं किए जा सके हैं। कार्यालय में हिन्दी का प्रयोग बढ़ा है किन्तु अभी भी बहुत सा काम अंग्रेजी में हो रहा है। जबकि केन्द्रीय सरकार सरकारी काम-काज में इस्तेमाल की जाने वाली हिन्दी के स्वरूप के बारे में अपनी नीति कई बार स्पष्ट कर चुकी है। इसके बावजूद इस संबंध में भ्रम दूर नहीं हो पाया है और लोगों के मन में यह विचार है कि सरकारी हिन्दी कोई अलग किस्म की हिन्दी होती है। इसी कारण

राजभाषा कार्यशाला में व्याख्यान देते हुए डा. पूरन पाल

वे अपने काम-काज में हिन्दी का इस्तेमाल करने से हिचकिचाते हैं।

डा. पूरन पाल ने आगे बताया कि लिखते वक्त हिन्दी लिखने की कोशिश करें। अंग्रेजी में मसौदा तैयार करके उसका हिन्दी में अनुवाद करने के बजाए बेहतर यही होगा कि मसौदा मूल रूप से हिन्दी में तैयार किया जाए। लक्ष्य यह है कि सरकारी काम-काज में मूलत: हिन्दी का प्रयोग हो इस कार्यशाला में प्रशासन के लगभग 45 अधिकारियों/कर्मचारियों ने भाग लिया और अपनी रूचि प्रदर्शित करते हुए अधिक से अधिक कार्य हिन्दी में किए जाने का आश्वासन दिया। इस प्रकार यह कार्यशाला अपने उद्देश्य में सफल रहीं।

आगन्तुक पुस्तिका से ...

From the visitors book ...

प्रभागीय अधिदेश

ऊर्जा संचयन भौतिकी प्रभाग

ऊर्जा संचयन भौतिकी (पीईएच) प्रभाग का प्राथमिक कार्य सी एस आई आर मेगा ऊर्जा मिशन पहल अर्थात् सी एस आई आर – टैपसन (नेटवर्क के माध्यम से सौर ऊर्जा के उपयोग हेतु प्रौद्योगिकी तथा उत्पाद) कार्यक्रम के तहत नवोन्नत वैज्ञानिक तथा प्रौद्योगिकीय अनुसंधान तथा विकास कार्य करना है। सी एस आई आर टैपसन प्रायोजित परियोजनाओं के अंतर्गत विभिन्न क्षेत्रों जैसे ऑर्गेनिक फोटोवोल्टीय (NWP-54), क्रिस्टलीय तथा पॉलीक्रिस्टलीय सिलिकन सोलर सेल (NWP-55), अक्रिस्टलीय/माइक्रो/ नैनोक्रिस्टलीय Si तथा CIGS सोलर सेल (एम एन आई ई प्रायोजित परियोजना HAP113532) तथा अजैविक एवं जैविक प्रकाश उत्सर्जी उपकरण (NWP-55) में अनुसंधान तथा विकास कार्य किया गया।

इसके अतिरिक्त, ओ एल पी–120132 के अंतर्गत कुछ अधिक महत्त्वपूर्ण गतिविधियों में अनुसंधान तथा विकास कार्य किया गया; जिसमें ताप–वैद्युत–बल्क नैनो तथा तनु फिल्में, पॉलीमॉरफिक कार्बन तनु फिल्में तथा प्रकाशिक तनु फिल्में सम्मिलित हैं। इसके अलावा संयुक्त भारत–यू.के. ऊर्जा पहल के तहत "एक्सिटॉनिक सौर सेल की कुशलता तथा उत्पादन क्षमता का विकास (एपैक्स)" शीर्षक वाली संयुक्त परियोजना पर अनुसंधान तथा विकास कार्य प्रगति पर है जिसमें दो देशों से लगभग 10 प्रमुख संस्थान भाग ले रहे हैं तथा सी एस आई आर – एन पी एल अग्रणी प्रयोगशाला है।

PT B7 : PC 70 BM पर आधारित इनवर्टिड सौर सेल, जो PCE > 7% का प्रदर्शन करता है, का विकास पॉलीमर सौर सेल (पीईसी) में एक अभिनव योगदान है। उपकरणों के जीवन–काल के संबंध में, उपकरण को प्रावृत्त (Encapsulation) करने के साथ–साथ विस्तृत Ca इंटरफेस परत को समाविष्ट करने का अभिनव विचार >100 hrs तक स्थिर रहने योग्य पाया गया। यह आविष्कार पेटेंट प्रक्रिया के अधीन है। सिलिकन सौर सेल के क्षेत्र में, परमाण्विक परत निक्षेपण (ALD) तकनीक का उपयोग कर निक्षेपित की गयी तापीय तथा प्लाज्मा Al_2O_3 फिल्म के उपयोग द्वारा नवोन्नत सतह पुनर्संयोजन वेग (SRV) मूल्यों (<10cm/S) का प्रापण किया गया। सिलिकन सतह पैसिवेशन के कारण यह महत्त्वपूर्ण है तथा सिलिकन सौर सेल पर इनके अनुप्रयोग से उपकरण की क्षमता विशेषत: तनु सिलिकन वैफर आधारित सौर सेल में सुधार होगा। सिल्वर सहायता प्राप्त एकल चरण रसायन नक्काशी द्वारा लम्बवत् सिलिकन नैनो तार (SiNW) के वृहद् क्षेत्र संविरचना के संरूपण बलगति विज्ञान की जाँच की गयी। (पिछले कुछ समय में एन पी एल में एक प्रक्रिया विकसित की गयी)। SiNW व्यूह के अत्यधिक निम्न परावर्तक सतहें नवीन फोटोवोल्टिक आर्किटेक्चर में प्रभावी प्रकाश अवशोषी पदार्थ के रूप में उल्लेखनीय क्षमता रखती है। A-Si तथा CIGS परियोजनाओं में मादित तथा अमादित अक्रिस्टलीय/ माइक्रोक्रिस्टलीय सिलिकन तनु फिल्में को हाल ही में नवीकृत बहु–चैम्बर PECVD प्रणाली का उपयोग कर p-i-n सौर सेल हेतु 4 इंच x 4 इंच सबस्ट्रेट पर निक्षेपित किया गया। CIGSe तथा C2TS में, फिल्मों का सौर सेल की संविरचना हेतु प्रक्रिया इष्टतमीकरण के लिए कोलाइडली मार्ग तथा उनके अभिलक्षणन द्वारा संश्लेषित किया गया। इसके अतिरिक्त, (I) पारदर्शी चालकत्व तथा एफईटी उपकरणों के लिए FCVA तकनीक द्वारा ग्रेफिन, (ii) क्षेत्र – उत्सर्जन के लिए MWPECVD तकनीक द्वारा CNT – ग्रेफिन जैसे हाइब्रिड फिल्मों का संश्लेषण किया गया। अत्यधिक मादित n-टाईप सिलिकन सबस्ट्रेट तथा लम्बवत ओ एल ई टी (VOLET) पर P13/टेट्रासीन का उपयोग कर एम्बीपोलर क्षेत्र प्रभाव ट्रांजिस्टर की संविरचना की गयी है। इसके साथ ही, अवरक्त थर्मोग्राफी के उपयोग कर तापमान मापन द्वारा जूल तापन का मात्रात्मक विश्लेषण तथा आर्गेनिक प्रकाश उत्सर्जी डायोड (OLEDs) का ताप आकलन तथा उपकरण जीवन काल के साथ उनका सह–संबंध स्थापित किया गया है। विभिन्न सबस्ट्रेट तापमानों तथा आर एफ शक्ति पर सम तथा विषम ऐपीटेक्सीय GaN फिल्मों की वृद्धि आर एफ प्लाज्मा एम बी ई के उपयोग द्वारा हुई है।

इस प्रभाग में कुछ नई सुविधाओं का सृजन भी किया गया है, जिनमें ओ पी वी उपकरणों के अभिलक्षणन

हेतु सौर अनुकारी, ओ एल ई डी अभिलक्षणन सैट-अप, क्षणिक प्रकाश चालकता सैट-अप आदि सम्मिलित हैं।

पदार्थ भौतिकी तथा अभियांत्रिकी प्रभाग

यह प्रभाग चयनित क्षेत्रों में सहक्रियात्मक अनुसंधान तथा विकास प्रयासों के माध्यम से औद्योगिक तथा सामरिक क्षेत्रों हेतु नवोन्नत पदार्थों, प्रक्रियाओं एवं प्रौद्योगिकियों के विकास के प्रति समर्पित है। इस प्रभाग का विकासात्मक परियोजनाओं अथवा उच्च शैक्षणिक कार्यक्रमों के माध्यम से विभिन्न अनुसंधान तथा विकास संगठनों जैसे सी एस आई आर प्रयोगशालाएँ, डी एस टी, आई आई टी, दिल्ली विश्वविद्यालय (DU) आदि के साथ सक्रिय सहयोग है।

नम्य एवं बहुलक पदार्थ अनुभाग बहुलकों, नम्य पदार्थों तथा द्रव क्रिस्टल के मूलभूत तथा प्रायोगिक विज्ञान में अनुसंधान के प्रति समर्पित है। हाल ही के वर्षों में द्रव क्रिस्टल के अनुसंधान में महत्त्वपूर्ण वृद्धि हुई है। इन मध्य चरणों को क्रम में लगाने पर क्रॉसित ध्रुवकों के अंतर्गत प्रकाश-संचरण होता है। एन पी एल विभिन्न प्रकार के नैनो पदार्थों जैसे धातु और धातु ऑक्साइड नैनो कणों, क्वांटम डॉट्स, कार्बन नैनोट्यूब और ग्रेफिन आदि के साथ मादित कर लौह-विद्युत द्रव क्रिस्टल के वैद्युत प्रकाशिक गुणधर्मों की ट्यूनिंग पर ध्यान केन्द्रित कर रहा है। हाल ही में, यह समूह द्रव क्रिस्टल के क्षेत्र में, गैर-प्रदर्शन अनुप्रयोगों जैसे द्रव क्रिस्टल पर आधारित जैव-संवेदकों का विकास, विभिन्न अमिश्रणीय तरल आदि के साथ द्रव क्रिस्टल इंटरफेस की गतिकी के अध्ययन में भी विविधता लाया है। इसके अलावा, यह समूह बेरियम स्ट्रोनशियम टाइटनेट (बी एस टी) और पॉलीएनीलीन (PANI) में विस्तृत ग्रेफाइट (EG) के संपुटीकरण के माध्यम से रडार अवशोषण अनुप्रयोग हेतु उच्च प्रदर्शन माइक्रोवेव अवशोषण पदार्थ का विकास कर रहा है। पॉलीएनीलीन (PANI) कोर में कम ग्रेफीन ऑक्साइड (rGO)/γ-Fe_2O_3 युक्त नलीदार कोर-शैल आकारिकी को उच्च परीक्षा प्रभाविता/ई एम आई अवशोष्य पदार्थ के रूप में विकसित किया है। हृदय संबंधी रोगों (CVD) के निदान हेतु कॉर्डियक बायोमार्कर के लेबल मुक्त संसूचन के लिए SWNTs/ग्रेफाइट नैनोप्लेट (GNPs) हाइब्रिड आधारित क्षेत्र प्रभाव ट्रांजिस्टर (FET) उपकरण के संविरचन का प्रदर्शन किया जाता है।

कार्बन तथा भौतिकी अनुभाग ने नवीन 'इलेक्ट्रोस्पिनिंग' तकनीक का उपयोग कर PAN तथा PVA बहुलकों से निम्न लागत उच्च प्राप्ति निरंतर कार्बन नैनो तंतुओं को संश्लेषित किया है। Fe_3O_4 तथा ZnO नैनोकणों से सुसज्जित हल्के वजन वाले कार्बन फोम (C Foams) का विकास किया गया है जिन्होंने उत्कृष्ट ई एम आई परिरक्षण प्रतिक्रिया का प्रदर्शन किया है। सी एस आई आर - टैपसन परियोजना (NWP-56) के तहत, नैनो आकार के SnO_2 निगमित लम्बी लम्बाई के MWCNT का उपयोग मुक्त स्टैंडिंग बांइडर सैस कंडक्टिंग पेपर के विकास के लिए किया गया, जिसका सी ई सी आर आई, कराईकुडी में ऐनोड इन-लिथियम (Li)-आयन बैटरी के रूप में सफलतापूर्वक प्रदर्शन किया गया। MWCNT समर्थित प्लेटिनम को भी कीमत प्रतियोगी पी ई एम ईंधन सेल के विकास हेतु उत्प्रेरक के रूप में संश्लेषित किया गया।

संदीप्तिशील पदार्थ तथा उपकरण अनुभाग ने सौर सेल अनुप्रयोग हेतु अत्यधिक क्षमतावान आतिथेय YVO_4 में लैंथेनाइड आयन Er^{3+}, Yb^{3+}, Eu^{3+} के युगपत मापन द्वारा द्वि-उत्तेजन, द्वि-उत्सर्जन फॉस्फर की संविरचना की है। यह प्रदर्शित किया गया कि सिल्वर नैनोप्रिज़्म (Ag NP) निकट क्षेत्र उत्पन्न करता है तथा बहुध्रुवीय नैनो-एंटीना की तरह कार्य करता है। एक नवीन लाल-उत्सर्जी $Gd_2CaZnO_5:Eu^{3+}$ (GCZO:Eu^{3+}) नैनो फॉस्फर प्रणाली विकसित की गयी। अगली पीढ़ी के सिलकन सौर सेल हेतु विस्तृत स्पेक्ट्रमी परिवर्तक (UV-IR) के रूप में $Gd_2(MoO_4)_3$:RE (Eu, Er, Yb) नैनो फॉस्फर के विकास हेतु प्रयास किए जा रहे हैं।

बहु-लौह विज्ञान तथा चुंबक अंशांकन की क्षमता का विकास कर लिया है और सिजियम मैग्नेटोमीटर को प्राथमिक मानक के रूप में सफलतापूर्वक संस्थापित किया है। विद्युत-चंबुकीय विकिरण तथा ई एल एफ/ई एम एफ मीटर के अंशांकन हेतु ऑनलाइन सर्वे आरंभ किया गया। स्पंदित लेसर निक्षेपण तकनीक द्वारा मैग्नेशियम फेराइट की तनु फिल्मों, सिरिया युक्त मैग्नेशियम फेराइट

की तनु फिल्मों, सिरिया युक्त मैग्नेशियम फेराइट 0. % Cr (Cr:BTO) पर 0.1 से मादित $BaTiO_3$ का विकास किया गया। प्रचक्रण पंपन प्रेरित प्रचक्रण हॉल प्रभाव की RF स्पटर्ड Co/Pt द्विस्तरीय तनु फिल्म स्पिनट्रॉनिक्स अनुप्रयोग हेतु जाँच की गयी।

बायोमेडिकल उपकरण अनुभाग द्वारा जैव–आण्विक इलेक्ट्रॉनिक्स हेतु डी एस टी केन्द्र की सफलतापूर्वक स्थापना की गयी है। कुल कोलेस्ट्रोल का पता लगाने के लिए दो आदि प्ररूप उपकरण विकसित किए गए। डी एन ए जैव–संवेदक के विकास के लिए आयरन ऑक्साइड नैनोकणों को प्रवृत करने वाले स्थिर कैटिआनिक पोली (लैक्टिक–को–ग्लाइकोलिक एसिड) (PLGA) माइक्रोस्फियर को संश्लेषित किया गया। विद्युत–सक्रिय स्वर्ण नैनोकणों (AuNP) का नियंत्रित संश्लेषण किया गया तथा जैव–संवेदी प्रदर्शन की जांच की गयी। जैव–आण्विक अंतरक्रिया की जांच करने के लिए एक लेबल–मुक्त CysCdS-Au जैवे–संवेदक प्लेटफार्म/उपकरण का विकास किया गया।

धातु तथा मिश्र धातु समूह ने ताप–वैद्युत उपकरणों के विकास के लिए मूलत: अतिनिम्न जालक तापीय चालकता के साथ Cu_3SbSe_3 ताप–वैद्युत पदार्थों को संश्लेषित किया है। संवर्धित ताप–वैद्युत प्रदर्शन युक्त एक नवीन अर्ध हाइसलर व्युत्पन्न $Zr_9Ni_7Sn_8$ बल्क नैनोकम्पोजिट का विकास किया गया। दुर्लभ मिट्टी रहित स्थायी चुंबकीय पदार्थों जैसे MnAl, Mn-Bi-Fe, मैंगनीज एण्टामोनाइड आदि का विकास कार्य गलित प्रचक्रण तकनीक द्वारा किया जा रहा है। हल्के वजन एवं उच्च शक्ति वाले एल्यूमीनियम कार्बन नैनोट्यूब कम्पोजिट का विकास भी क्रायोमीलिंग तथा तप्त निष्कासन द्वारा किया जा रहा है।

रेडियो तथा वायुमण्डलीय विज्ञान

एन पी एल का रेडियो तथा वायुमण्डलीय विज्ञान प्रभाग रेडियो विज्ञान तथा अनुप्रयोग, अंतरिक्ष मौसम तथा आयन मंडल, पृथ्वी के वायुमण्डल का रसायन तथा भौतिकी, वायुमण्डलीय प्रदूषण तथा जलवायु परिवर्तन आदि क्षेत्रों में राष्ट्र की वैज्ञानिक आवश्यकताओं की पूर्ति करता है। मुख्य अनुसंधान क्षेत्र : (1) रेडियो विज्ञान तथा (2) वायुमण्डलीय विज्ञान। वायुमण्डलीय विज्ञान में वायुमण्डलीय रसायन, वायुमण्डलीय स्पेक्ट्रम विज्ञान, वायुमण्डलीय भौतिकी हेतु अनुरूपण तथा प्रतिरूपण का अध्ययन सम्मिलित है।

रेडियो विज्ञान

यह भारत में एक अद्वितीय समूह है जो रेडियो संचार, संचालन तथा अन्य उन्नत अनुप्रयोगों की बेहतरी के उद्देश्य से रेडियो तरंग संचरण का प्रयोग करते हुए आयनित, अनायनित, ट्रांसफेरिक मीडिया तथा पृथ्वी के निकट रेडियो पर्यावरण के अभिलक्षण निर्धारण में संलग्न है। इसमें स्थिर और मोबाइल संचार के लिए रेडियो चैनल मापन और प्रतिरूपण, वीएचएफ और यूएचएफ आवृत्ति बैंड्स में नवीन आंकड़ा सैट्स (समूह) का सृजन करना, भारत के विभिन्न क्षेत्रों के ऊपर प्रतिरूपों का विकास करना तथा विभिन्न प्रयोक्ता अभिकरणों के साथ पारस्परिक संपर्क सम्मिलित है। भारत तथा ध्रुवीय क्षेत्रों के ऊपर जीपीएस, टॉमोग्रफिक अभिग्राहक, आयन सोंद आदि सहित उपग्रह तथा भू–आधारित पद्धति का प्रयोग करते हुए आयनमण्डलीय/क्षोभमण्डलीय प्राचल/मापदंडों संबंधित निगरानी एवं प्रतिरूपण भी किया जा रहा है। हम अपने अंतरिक्ष मौसम क्षेत्रीय चेतावनी केन्द्र (आरडब्ल्यूसी–एनपीएल–भारत) के माध्यम से विश्वभर में फैले प्रयोक्ताओं को आयनमण्डलीय पूर्वानुमान/अद्यतन अनुमान भी प्रदान करते हैं तथा प्रेक्षित आंकड़ों के साथ प्रतिरूप तुलना के माध्यम से अन्तरराष्ट्रीय संदर्भ आयनमण्डल (आई आर आई) प्रतिरूप को लगातार सुधारते रहते हैं। अटार्कटिक वैज्ञानिक खोज यात्राओं के द्वारा ध्रुवीय आयनमण्डल का अध्ययन करने के लिए भू–'आधारित प्रौद्योगिकयों जैसे आयनोसोंडें, जीपीएस–अभिग्राहकों का उपयोग किया जा रहा है।

वायुमण्डलीय विज्ञान

वायुमण्डलीय रसायन समूह विभिन्न स्रोतों से ग्रीनहाउस गैसों के उत्सर्जन के संबंध में जानकारी हासिल करने, हमारे देश के ग्रामीण क्षेत्रों में प्रयोग में लाए जा रहे बायोमास ईंधनों से निकलने वाले कणिकामय पदार्थों और सूक्ष्ममात्रिक गैसों (सल्फर डाईआक्सॅाइड, नाइट्रोजन ऑक्साइड और नाइट्रोजन डाईऑक्साइड) तथा कचरा भराव स्थलों और खेतों में लगी गेंहू एवं धान के फसलों से होने वाले उत्सर्जनों की मात्रा का आकलन करता है।

इसके साथ ही हम नवोन्नत प्रौद्योगिकी का उपयोग करते हुए रासायनिक अभिलक्षणन, विविक्त सामग्री का स्रोत प्रभाजन तथा आस–पास के महासागरों, हिमालय तथा ध्रुवों सहित देश के विभिन्न क्षेत्रों पर पूर्वगामी पूर्वानुमान भी करते हैं। यह समूह विभिन्न प्रतिरूपों तथा प्रेक्षणों का प्रयोग करते हुए वायुमण्डलीय ओजोन, इसके रसायनिक संगठन तथा गतिकी का भी अध्ययन करता है।

पराबैंगनी दृश्यमान तथा एनआईआर–आई आर क्षेत्र में वायुमण्डलीय का स्पेक्ट्रमदर्शी मापन करते हुए वायुमण्डलीय ऐरोसॉल्स, अनुरेख गैसों सौर विकिरण तथा उनकी पारस्परिक क्रिया के विषय में वृहद् जानकारी एकत्रित की जाती है। यह वायुमण्डलीय ऐरोसॉल के प्रकाशिक तथा भौतिक अभिलक्षणन निर्धारण में समर्थ बनाता है तथा गैस नमूनों और वायुमण्डलीय स्तम्भ/कॉलम में अनुरेख रासायनिक गुणांकों को पहचानने में मदद करता है। उच्च विभेदन ओपन–पाथ एफटीआईआर, सूक्ष्म–स्पंद एलआईडीएआर नवीनतम आधुनिक उपकरण हैं जो ऐरासॉल प्रकाशिक गहराई ऐरोसॉल की उर्ध्वाधर परिच्छेदिका, ऐरोसॉल आकार वितरण, ऐरोसॉल्स के प्रकीर्णन और अवशोषण गुणाकों, एकल प्रकीर्णन एल्बिडो (एसएसए), प्रकाशिक गुणधर्मों पर ऐरोसॉल की आकृति एवं आकार के प्रभाव, रासायनिक अभिलक्षणन आदि के अध्ययन के संपूरक हैं। मापन की अनुमार्गणीयता तथा अन्य उद्देश्यों से इस प्रभाग में ओजोन मानक को जोड़ा गया है।

गणितीय प्रतिरूपण इस प्रभाग की समस्त गतिविधि समूहों का अभिन्न एवं अनिवार्य अंग है तथा इसका उद्देश्य वायुमण्डलीय प्रक्रियाओं को युगपत तथा प्रतिरूपित करने के लिए इस प्रभाग में अथवा अन्यत्र एकत्रित किए गए विभिन्न आंकड़ा समूहों को आत्मसात् करना है।

समय और फ्रीक्वेंसी

अधिदेश और मिशन

समय तथा फ्रीक्वेंसी प्रभाग द्वारा निम्नलिखित क्षेत्रों में शोध कार्य किए जा रहे हैं :–

* अति स्थिर परमाणु फ्रीक्वेंसी स्रोत
  - सीज़ियम फाउंटेन-I तथा सीजियम फाउंटेन-II
  - अतंरिक्ष अनुप्रयोग हेतु रूबिडियम परमाणु घड़ी
  - एकल प्राप्त इटर्बियम आयन ऑप्टिकल फ्रीक्वेंसी मानक
  - इंस्ट्रूमेंटेशन
* परिशुद्ध समय मापन प्रणालियाँ
  - भारत मानक समय (आई एस टी) का अनुरक्षण
  - समय हस्तांतरण लिंक
  - समय का प्रसार
  - अंशांकन सेवाएँ

सीजियम फाउंटेन एक प्राथमिक मानक है और यह दोहरी विभक्त ग्राउण्ड स्टेट के अति सूक्ष्म विखण्डन का अत्यन्त परिशुद्ध और सटीक मापन उपलब्ध कराता है तथा समय के SI यूनिट को परिभाषित करता है। इस प्रकार के परिशुद्ध मापन डिवाइस को विकसित करने के लिए लेज़र्स, वेक्यूम प्रौद्योगिकी, मैग्नेटिक शील्डिंग और स्वदेश में विकसित इलैक्ट्रॉनिक, मैकेनिकल और आप्टिकल प्रणालियों में प्रौद्योगिकीय नवोन्मेषी के विशिष्ट संयोजन की आवश्यकता होती है। पूरे विश्व में केवल लगभग 10 सीजियम फाउंटेन चालू (वर्किंग) हैं। भारत में प्रथम सीजियम फाउंटेन फ्रीक्वेंसी मानक सी एस आई

आर – एन पी एल (एन पी एल आई) में पूर्ण रूप से स्वेदशी विकसित किया गया है और जो अब पूरी तरह से प्रचालन सक्षम है तथा एन्हांस्ड परिशुद्धता सहित दूसरे सीजियम फाउंटेन को हाल ही में विकसित किया गया है।

यह प्रभाग, भारतीय सैटेलाइटस् में लगाने के लिए परमाणु घड़ियों को विकसित करके भारत के सामरिक महत्त्व के अतंरिक्ष कार्यक्रम में भी अपना योगदान दे रहा है। प्रभाग द्वारा विकसित रूबिडियम (Rb) परमाणु घड़ी के फिजिक्स (भौतिक) पैकेज को भारतीय अतंरिक्ष अनुसंधान संगठन (इसरो) को हस्तांतरित किया गया है। काँच के बल्ब और सैल्स में Rb को भरने की विवेचनात्मक (Critical) प्रौद्योगिकी भी इस प्रभाग द्वारा स्वदेशी रूप में विकसित की गयी है।

हाल ही में एकल प्राप्त इटर्बियम (Yb) आयन पर आधारित आप्टिकल फ्रीक्वेंसी मानकों पर शोध कार्य आरंभ किया गया है। इस प्रकार की घड़ी को विकसित करना एक उच्च कोटि का शोध कार्य है जिसमें लेजर्स, आप्टिक्स, वैक्यूम प्रणलियाँ, पदार्थों, मैकेनिकल डिजाइन, साफ्टवेयर और स्वदेशी विकसित इलेक्ट्रॉनिक्स में कई नवोन्नत प्रौद्योगिकियाँ शामिल हैं। भारत में इस क्षेत्र में अनुसंधान एन पी एल आई के लिए विशिष्ट है।

व्यापक आर एण्ड डी के अलावा हमारा प्रभाग भारत में उच्चतर स्तर के समय तथा फ्रीक्वेंसी मापिकी के लिए उत्तरदायी है। यह प्रभाग का अधिदेश भारतीय मानक समय (आई एस टी) का अनुरक्षण, इसका प्रसार और अति – परिशुद्ध उपग्रह लिंकों का प्रयोग करके इसे अन्तरराष्ट्रीय बाट तथा मापन ब्यूरो (बी आई पी एम) के अनुसार राष्ट्र का टाइम–प्रोवाइडर (समय प्रबन्धक) है। इसके अतिरिक्त यह प्रभाग विभिन्न घड़ियों तथा फ्रीक्वेंसी स्रोतों के लिए अंशांकन सेवाएँ भी उपलब्ध कराता है।

शीर्ष स्तरीय मानक एवं औद्योगिक मापिकी (ALSIM)

सारांश

सी एस आई आर – एन पी एल का शीर्ष स्तरीय मानक एवं औद्योगिक मापिकी प्रभाग राष्ट्रीय मानकों को स्थापित करने, अनुरक्षण तथा उन्नयन एवं भौतिक – यांत्रिक, इलेक्ट्रिकल और इलेक्ट्रॉनिक्स मानकों के क्षेत्र में अन्य मान्यता प्राप्त प्रयोगशालाओं को अनुमार्गणीयता प्रदान करने के लिए उत्तरदायी है। इसमें 12 उप–प्रभाग शामिल हैं; इनकी 'अंशांकन एवं मापन क्षमताओं का अंतरराष्ट्रीय स्तर पर मापन एवं अंशांकन में समतुल्यता के अनुरक्षण हेतु नियमित अंतराल पर सम–समूहों द्वारा पुनरीक्षण किया जाता है। इस प्रभाग (ALSIM) की गतिविधियों को 'विज्ञान एवं प्रौद्योगिकी में मापन नवाचार' (MIST) नामक सी एस आई आर नेटवर्क परियोजना के तहत निधि उपलब्ध करायी जाती है। गत वर्ष अनेक गतिविधियां शुरू की गयीं। संक्षेप में निम्नवत् हैं :–

(i) सी एस आई आर – एन पी एल ने वाट संतुलन हेतु प्रारंभिक शोध कार्य शुरू कर दिया है।

(ii) भारत में, उच्च क्षमता वाले वजन की मापिकी अभिलक्षणन के निर्धारण हेतु सुविधा केवल सी एस आई आर – एन पी एल, नई दिल्ली में उपलब्ध है। हम 100 कि.ग्रा., 200 कि.ग्रा. और 2000 कि.ग्रा. तक की उच्च वजन क्षमताओं के लिए अंशांकन सुविधा प्रदान करते हैं।

(iii) इसी प्रकार, 1000 लीटर व 2000 लीटर के अति उच्च क्षमता वाले वाल्यूमेट्रिक वैसेल्स को अंशांकित किया गया, जिससे उच्च परिशुद्धता के वाल्यूमेट्रिक वैसेल्स के निर्माण व विकास में निर्माताओं को मदद मिलती है।

(iv) ब्रिनेल, रॉकवेल (सतही रॉकवेल सहित), विकर्स एवं माइक्रों–विकर्स कठोरता के द्वितीयक कठोरता मानकीकरण मशीनों की स्थापना हुई।

(v) एक शीर्ष से शीर्ष वोल्टता मापन माड्यूल का सफलतापूर्वक डिजाइन किया गया तथा पराश्रव्य शक्ति मूल्यांकन में वोल्टता मापन में त्रुटियों के न्यूनीकरण को ध्यान में रखते हुए इसकी क्रियाशीलता को प्राप्त किया गया।

(vi) एन पी एल में स्वदेश विकसित धारा टी ई ई का उपयोग कर AC-DC धारा ट्रांसफर मापन सुविधा के वर्तमान परास को 20A से 80A तक विस्तारित

किया गया। अब, सी एस आई आर – एन पी एल उपयोगकर्त्ता संगठनों को 30A, 50A तथा 80A के AC-DC धारा शंटों के अंशांकन हेतु अनुमार्गणीयता प्रदान करने में सक्षम है।

(vii) विकरित शक्ति घनत्व मानक के लिए क्रॉफोर्ड संकल्पना पर आधारित स्वदेशी तकनीक पर आधारित एक GTEM को विकसित किया है। यह प्रस्तावित GTEM 0.7-2.5 GHz के आवृत्ति परास के लिए उपयोगी है।

(viii) 100KV/2000Amp तक ट्रांसफॉर्मर क्षय मापन प्रणाली (TLMS) के अंशांकन हेतु एक नई सुविधा स्थापित की गयी है तथा बिजली निगमों एवं उत्पादकों को अंशांकन सुविधा के साथ–साथ अनुमार्गणीयता प्रदान की जा रही है।

इसके अतिरिक्त, ALSIM प्रभाग निम्नलिखित अंतरतुलना गतिविधियों में शामिल है :–

(i) 100 किग्रा., 20 ग्रा. एवं 1 कि. ग्रा. के नाममात्र मूल्यों के तीन मानक वजनों के साथ द्रव्यमान प्राचलों पर एक अंतर प्रयोगशाला तुलना की गयी। इसमें सार्क एन एम आई (बी एस टी आई, बांग्लादेश, एन पी एस एल, पाकिस्तान, एन बी एस एन, नेपाल एवं एम यू एस एस डी, श्रीलंका) ने भाग लिया। सी एस आई आर – राष्ट्रीय भौतिक प्रयोगशाला, भारत (एन पी एल आई) इस कार्यक्रम में पथ–प्रदर्शक प्रयोगशाला थी।

(ii) अंतरराष्ट्रीय अंतर–तुलना (लंबाई प्राचल हेतु मुख्य प्रयोगशाला एन पी एल आई) में बी एस टी आई – बांग्लादेश, एम यू एस एस डी – श्रीलंका एवं एन पी एस एल – पाकिस्तान के साथ भाग लिया।

(iii) ए पी एम पी – टी – एस 7 : कोबाल्ट – कार्बन (Co-C) गलनक्रांति नियत बिन्दु (1324C) पर Pt/Pd थर्मोपल की तुलना की गयी, जो कि प्रयोगशाला में विकसित की गयी।

(iv) ए पी एम पी – टी एस–8 : ए पी एस पी टी सी टी/डी ई सी : उच्च परिशुद्धता अल्कोहल, जल व तेल बाथ का उपयोग कर -41°C से 250°C के परास में एस पी आर टी के विरूद्ध लिक्विड–इन–ग्लास थर्मोमीटर की तुलना की गयी। माप परिणामों को विश्लेषण के बाद एस आई आर आई एम, मलेशिया को प्रस्तुत किया जाएगा।

(v) हमारे समूह द्वारा चार सार्क देशों बांग्लादेश, नेपाल, श्रीलंका और पाकिस्तान के एन एम आई के बीच एल आई जी टी (LIGT) (O°C-100°C) एवं टाइप–एस थर्मोकपल (0-1000°C) में एक अंतर प्रयोगशाला तुलना आयोजित की गयी।

(vi) ज्योति तीव्रता (ए पी एम पी. पी आर – के 3. ए) के ए पी एम पी मुख्य तुलना में भाग लिया एवं मापन सम्पन्न किया। एन एम आई, जापान – पायलट प्रयोगशाला को अंतिम रिपोर्ट सौंप दी गयी।

(vii) ए पी एम पी. एन. पी – K13 (एन एम आई, जापान द्वारा नियंत्रित) मसौदा तैयार किया जा रहा है। मसौदा – ए की प्रति सभी भाग लेने वाले प्रयोगशालाओं में परिचालित की गयी है। इस मुख्य तुलना का प्रधान उद्देश्य सभी प्रतिभागी संस्थानों के हाइड्रोलिक दाब मानकों का गेज मोड में 50 Mpa से 500 Mpa तक के दाब परास में निष्पादन की तुलना करना था।

(viii) बी आई पी एम तथा एन पी एल आई के मध्य 10KΩ एवं 1Ω की द्विपक्षीय तुलना की गयी। मापन परिणामों का विश्लेषण कार्य जारी है।

(ix) ए पी एम पी के तहत 6.5 डिजिट मल्टीमीटर (DMM) की अंतर–तुलना के लिए एन पी एल पायलट लैब तथा समन्वयक है, जिसमें 16 देश भाग ले रहे हैं।

एन ए बी एल दक्षता जांच कार्यक्रम में सक्रिय भागीदारी निम्नवत् है :–

(i) एन पी एल – एन ए बी एल – पी टी – कार्यक्रम, टाइप–एस थर्मो–कपल के लिए 0-1200°C के

परास में एन ए बी एल–टी–टेम्प–006 सम्पन्न हुआ। इस कार्यक्रम में 12 अंशांकन प्रयोगशालाओं ने भाग लिया।

(ii) एन पी एल – एन ए बी एल – पी टी – कार्यक्रम के तहत् 1μF (एन ए बी एल–ई– कैपिसिटेंस–003) एवं 10pF तथा 100pF (एन ए बी एल – ई – कैपिसिटेंस–004) परास में संधारिता मापन हेतु दो दक्षता जांच (PJ) कार्यक्रमों का आयोजन किया गया।

ए एल एस आई एम प्रभाग द्वारा विभिन्न प्राचलों में सार्क देशों, उद्योगों, विधिक मापिकी अधिकारियों के लिए बड़ी संख्या में प्रशिक्षण कार्यक्रम का आयोजन किया जाता है।

क्वांटम परिघटना एवं अनुप्रयोग

एफ आई बी समूह का मुख्य फोकस प्लासमोनिक के नैनोरिंगों तथा ग्रैफीन के एकल सतह तत्काल धात्विक सम्पर्क हेतु नैनो उपकरणों, नैनो संरचनाओं एवं एंटीना के विनिर्माण पर केन्द्रित था। इसके अतिरिक्त, Au विच्छेद संधि (~2nm गैप) उपकरणों का निर्माण, एकल अणुओं एवं नैनोकणों के अध्ययन हेतु इलेक्ट्रोमाइग्रेशन का प्रयोग कर किया गया।

तनु प्रशीतक (डी आर) की एक अद्वितीय सुविधा के रूप में स्थापना एवं परीक्षण किया गया है जो कि 10mK के न्यूनतम तापमान के साथ 14 टेसला तक के अति उच्च चुम्बकीय क्षेत्र के साथ नोबल एवं मूलभूत क्वांटम परिघटना को पकड़ने में सहायक/क्रियाशील है।

बल्क पदार्थों में अतिचालकता की निरंतर क्रियाशील गतिविधियों ने रोचक परिणाम दिए हैं। उदाहरण के लिए, Sr_{o}. $5La_{o}$.$5FBiS_{2}$ निकाय के अतिचालक संक्रमण तापमान में पांच गुणा वृद्धि, 2K से 10K की हुई। साथ ही, 1GPa से ऊपर के अनुप्रयुक्त हाइड्रोस्टैटिक दाब के अंतर्गत अर्द्ध–धात्विक से धात्विक सामान्य अवस्था ताप चालन को देखा गया।

पल्स्ड लेजर निक्षेपण तकनीक का उपयोग करके विभिन्न समूहों के कृत्रिम अभियंत्रित ऑक्साइड विषय संरचनाओं की वृद्धि की गयी तथा उनके बहुफलनात्मक गुणों यथा, मल्टिफेरोसिटी, अतिचालकता, चुम्बकत्व एवं फोटोचालकता आदि का अध्ययन किया गया। घनत्व फलन सिद्धांत (DFT) का उपयोग करके संक्रमण धातु अंतराफलकों की इलेक्ट्रॉनिक अवस्था तथा विभिन्न गुणों के साथ उनकी इंटरप्ले की सैद्धांतिक गणना पर ध्यान केंद्रित किया गया।

प्रोग्रामनीय जोसेफसन वोल्टता मानक, अंतरराष्ट्रीय स्तर के समतुल्य 'यूनिट' वोल्ट के प्रसार में प्रयुक्त, को अतिस्थायी मार्जिन एवं फ्लैटस्पॉट्स को प्राप्त करने के लिए और अनुकूल बनाया गया। निम्न तापक्रम (1.6K तक) के लिए एक नवीन द्रव हिलियम क्रायोस्टैट तथा माइक्रोवेव मापन (40GHz तक) के लिए चुम्बकीय क्षेत्र (130 गॉस तक) की स्थापना की गयी है। ज्योति तीव्रता एवं अन्य प्रकाशमिति प्राचलों के वर्तमान मानकों को पुनर्परिभाषित करने के लिए परिमाण के न्यूनतम दो क्रमों तक अनिश्चितता को कम करने के लिए संसूचक आधारित प्राथमिक मानक के तौर पर क्रायोजेनिक रेडियो मीटर को स्थापित किया गया है। स्वत: प्रवर्तित प्राचलिक डाऊन परिवर्तन (SPDC) को 355 nm पर 25 पल्स के विड्थ उत्सर्जन के Nd-YAG लेसर को प्रदर्शित किया गया। विभिन्न स्पेक्ट्रोस्कोपिक तकनीकों का उपयोग करके वर्तमान बायोमोलेकूलर अनुसंधान के तहत कैंसररोधी औषधि DNA अन्योन्यक्रिया का विश्लेषण कर लाभ उठाया जा रहा है। औषधि – DNA अन्योन्यक्रिया को समझने के लिए, विभिन्न औषधि – DNA में सतह उन्नयित रामन स्पेक्ट्रोस्कोपी द्वारा मोलर अनुपातों का अध्ययन किया गया। एलिसिन की कैंसररोधी क्रियाओं को तलाशने के लिए एलिसिन की न्यूक्लियिक अम्ल बंधन क्षमता का अध्ययन किया गया।

परिष्कृत और विश्लेषणात्मक उपकरण

सभी आधुनिक प्रौद्योगिकी से युक्त बिल्डिंग ब्लॉकों तथा सामग्री पर किए गए शोध के साथ–साथ अनुप्रयोगों हेतु उन्हें सख्त मानकों के अनुरूप बनाए रखना है। शुद्ध संरचना और क्रिस्टलोग्राफिक पूर्णता का संयोजन पदार्थ गुणों को नियंत्रित करने वाली मूल सामग्री अभिलक्षणों

में है। कैरेक्टराइजेशन सभी तीन मुख्य प्रावस्थाओं ठोस, तरल और गैस से सम्बन्धित है। इन कार्यों को आगे बढ़ाने के लिए बहुत ही उन्नत प्रकार की विशेषज्ञता की जरूरत होती है और अत्यंत परिष्कृत सुविधाओं की आवश्यकता है।

एन पी एल के परिष्कृत और विश्लेषणात्मक उपकरण प्रभाग में आवृत्ति विज्ञान के लिए पदार्थों के अभिलक्षणन, रासायनिक संरचना, शुद्धता, संरचना (दोषों सहित क्रिस्टलोग्राफिक पूर्णता और ठोस सतह पतली फिल्मों और इंटरफेस के अध्ययन के लिए उच्च गुणवत्ता सुविधाएं मौजूद हैं। प्रयोगशाला के लिए यह एक केन्द्रीय सुविधा है। यहां यह उल्लेख करना श्रेयस्कर होगा कि ऐसी सुविधाओं के रख-रखाव और विकास में शामिल वैज्ञानिक न केवल संगठन के अन्य समूहों के लिए कैरेक्टराइजेशन सुविधाएँ प्रदान कर रहे हैं बल्कि बहुत ही सक्रिय रूप से उन्नत क्षेत्रों में अपने स्वयं के अनुसंधान कार्यक्रम में लगे हुए हैं और इस प्रकार वे इस क्षेत्र के नवीनतम विकास के करीब रहने और ज्ञान बढ़ाने में ग्रुप को सक्षम कर रहे हैं।

प्रभाग में, ऐसे समर्पित समूह हैं जो एक्स-रे विश्लेषण, इलेक्ट्रॉन और आयन माइक्रोस्कोपी EPR और IR स्पैक्ट्रोस्कोपी और विश्लेषणात्मक रसायन विज्ञान के क्षेत्र में काम कर रहे हैं।

आगन्तुक पुस्तका से ...

From the visitors book ...

ऊर्जा संचयन भौतिकी

Physics of Energy Harvesting

Dr Suresh Chand
Chief Scientist
Email: schand@nplindia.org

D 01.01 Silicon Solar Cells

Dr Parakram Kumar Singh
Dr Abdul Mobin
Sh C M S Rauthan
Dr (Ms) Vandana
Dr Sanjay Kumar Srivastava
Dr P Prathap
Sh Mukul Sharma

D 01.02 Polymorphic Carbon Thin Films

Dr Omvir Singh Panwar
Dr Sreekumar Chockalingam
Sh Jagdish Chand

D 01.03 Organic and Hybrid Solar Cells

Dr Suresh Chand
Dr (Ms) Kiran Jain
Dr Asit Patra
Dr Vinay Gupta
Dr Chandra Kant Suman
Dr Rajiv Kr. Singh
Dr. J P Tiwari
Dr Gauri Datt Sharma
Dr Rachana Kumar

D 01.04 Thermoelectrics-Bulk, Nano and Thin Films

Dr T D Senguttuvan
Dr Praveen Kumar Siwach
Dr V K Hans

D 01.05 Organic and Inorganic LEDs

Dr Suresh Chand
Dr S T Lakshmikumar
Dr S M Shivaprasad
Dr Amish G Joshi
Dr Govind
Dr (Ms) Ritu Srivastava
Dr Senthil Kumar
Dr Mahesh Kumar
Dr Prabir Pal
Dr Sunil Singh Kushvaha
Dr Ajay Kumar Shukla
Sh Murari Lal Sharma
Dr Shrinivasa Rao Ragam
Dr Mukesh Jewariya

D 01.06 Optical Thin Films & Ceramics

Dr K M K Srivatsa
Dr Preetam Singh

D 01.07 Silicon Thin Film Photovoltaic

Dr Sushil Kumar
Sh Kamlesh Patel
Dr S Sudhakar
Ms Kalpna Lodhi

D 01.08 Chemical Route for Compound Semiconductor PV

Dr Shailesh Narayan Sharma
Dr Jeya Kumar Ramanujam

Physics of Energy Harvesting

The primary mandate of Physics of Energy Harvesting (PEH) Division is to carry out cutting edge scientific and technological R&D under the CSIR Mega Solar Energy Mission Initiative viz. - the CSIR TAPSUN (Technologies and Products for Solar energy utilization through Networks) Program. Under CSIR TAPSUN funded projects, R&D was carried out in various areas such as organic photovoltaic (NWP-54), crystalline and poly crystalline Si solar cells (NWP-55), amorphous/ micro/noncrystalline Si and CIGS solar cells (MNRE funded project GAP113532) and inorganic and organic light emitting devices (NWP-55).
Besides this, R&D work was carried out in some more important activities under OLP-120132 which included thermoelectric-bulk, nano and thin films, polymorphic carbon thin films and optical thin films. Also under the joint Indo-UK energy initiative a joint project entitled "Advancing the efficiency and production potential of excitonic solar cells (APEX)" R&D remained in progress where about 10 leading institutes from the two countries are participating and CSIR-NPL is the lead laboratory.

During the year, drawing on the excellent fundamental and applied research in these areas several papers have been published in journals with high impact factor as well as some national and international patents have been filed on important inventions. For example, there has been a significant progress on the development of Polymer Solar Cells (PSCs). One of the innovative contribution in PSCs is the development of a modified PTB7:PC60BM light absorbing active layer which has the potential of giving cost effective, efficient, flexible and stable polymer solar cells. Using this modified material, power conversion efficiency (PCE) ~ 6.2% has been achieved which has been certified by independent measurements made in the Prof Heeger's Laboratory in USA. The invention is in the process of patenting. There has also been significant progress in the area of Si solar cells which includes, aluminium oxide films for silicon surface passivation, alternative anti-reflection coatings and development of a simple process for producing black surface for silicon solar cells. Besides this important contributions have been made in other area such as synthesis of graphene from a-C films deposited by FCVA technique, obtaining ZT value of 1.1 at 470K for Bi_2Te_3 +BiTe (8mol %) sample, fabrication of unipolar OFET on optimized SiO_2 dielectric materials using unipolar semiconducting material DH4T, growth of epitaxial GaN on sapphire by Ultra High Vacuum Pulsed Laser Deposition (UHV-PLD) System, defect related studies using DLTS technique, amorphous & micro-crystalline silicon thin film deposition for solar cells using VHF PECVD and improved quality CIGS absorber layer by both vacuum and non-vacuum techniques, respectively.

Some new facilities were also created in the division which includes, polymer solar cell device fabrication facility using glove box integrated with evaporator and encapsulation system, atomic layer deposition system, ultrafast femto- second laser spectroscopy, ultra high vacuum pulsed laser deposition (UHV-PLD) system, etc.

Silicon Solar Cells

1. Passivation schemes to reduce surface recombination velocity

Al_2O_3 thin films are grown in a thermal ALD reactor (M/s Picosunoy, Finland) using trimethylaluminum [TMA, $Al(CH_3)_3$)] and H_2O as the precursors for aluminum and oxygen, respectively, at a substrate temperature of 300°C. The films are grown on p-and n-type, FZ, Si (100), 325µm thick substrate. Samples of different thickness are prepared (Table 1.1). All the films are sintered at 400°C in nitrogen ambient for 10 min using RTP annealing system.

Lifetime was measured using Sinton lifetime tester and calculated recombination velocity values (SRV) are shown in Fig. 1.1 Films uniformity was confirmed using AFM and SEM. We are able to achieve low SRV values for both p-and n-Si surfaces. Samples S1-S3 shows good surface passivation for as deposited films as is shown by low SRV values as compared to bare samples. But sintering leads to degradation in passivation, which is shown in increased SRV values.

Recently, for a thickness of 30nm film (n-Si) deposited using thermal ALD, we are able to realize SRV values close to the state of the art values reported in literature (1-10cm/s) by optimizing sintering time (T_{sint}). Fig.1.2 shows average effective lifetime (τ_{eff}) as a function of injection level (Δn). SRV values are compiled in Table 1.2.

Metal-insulator-semiconductor (MIS) structure is being investigated with the help of capacitance-voltage (C-V) measurements to understand the effect of fixed charges activation and interface defect density.

Table 1.1

Sample	Film thickness (nm)
Bare	-
S1	93
S2	48
S3	30
S4	11

Table 1.2

T_{sint} (s)	SRV (cm/s)
0	23.6
90	9.58
105	7.87
120	8.76

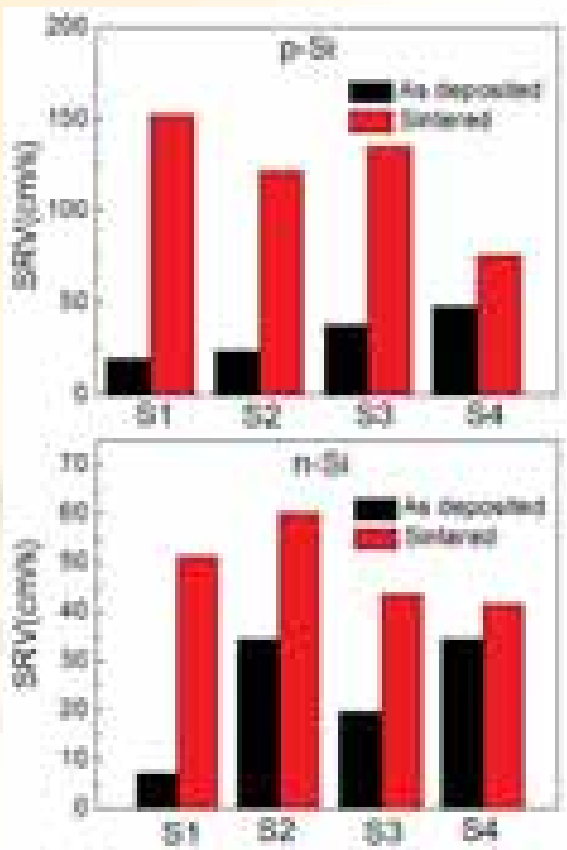

Fig. 1.1: SRV values for as diposited and sintered samples in p-si and n-Si

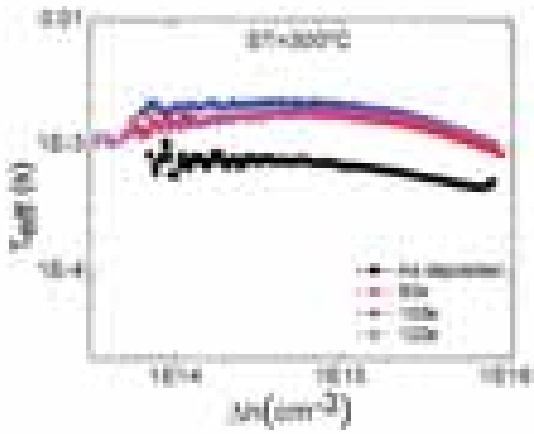

Fig. 1.2: SRV for as deposited and sintered samples p-Si and n-Si

2. Large area fabrication of vertical silicon nanowire arrays by silver assisted single-step chemical etching and their formation kinetics

Vertically aligned silicon nanowire (SiNW) arrays have been fabricated over large area using a silver assisted single-step electroless wet chemical etching (EWCE) method, which involves etching of silicon wafers in aqueous hydrofluoric acid (HF) and silver nitrate ($AgNO_3$) solution. A comprehensive systematic investigation on the influence of different parameters such as etching time (up to 15 h), solution temperature (10-80°C), $AgNO_3$ (5-200 mM) and HF (2-22 M) concentrations on multi-crystalline silicon (mc-Si) wafers, is presented to establish a relationship of these parameters with silicon nanowires (SiNWs) morphology. A linear dependency of nanowires length on etch time is obtained even at higher temperature (10-50^{0}C). Activation energy for the formation of SiNWs on Si (100) has been found equal to ~0.51 eV. It has been shown for the first time that surface area of the Si wafer exposed to etching solution is an important parameter in determining the etching kinetics in the single-step process. Our results establish that single-step EWCE offers a wide range of parameters to produce high quality vertical SiNWs in a very simple and controlled manner.

A mechanism to explain the influence of various parameters on the evolution of nanowire structure is also proposed. Furthermore, the SiNW arrays have extremely low reflectance (<3% for Si (100) NWs and <12% for mc-Si NWs) compared to ~35% in the polished surface in 350-1000 nm wavelength range. The remarkably low reflecting surfaces of SiNW arrays have great potential as an effective light absorber material in novel photovoltaic architectures, other optoelectronic and photonic devices.

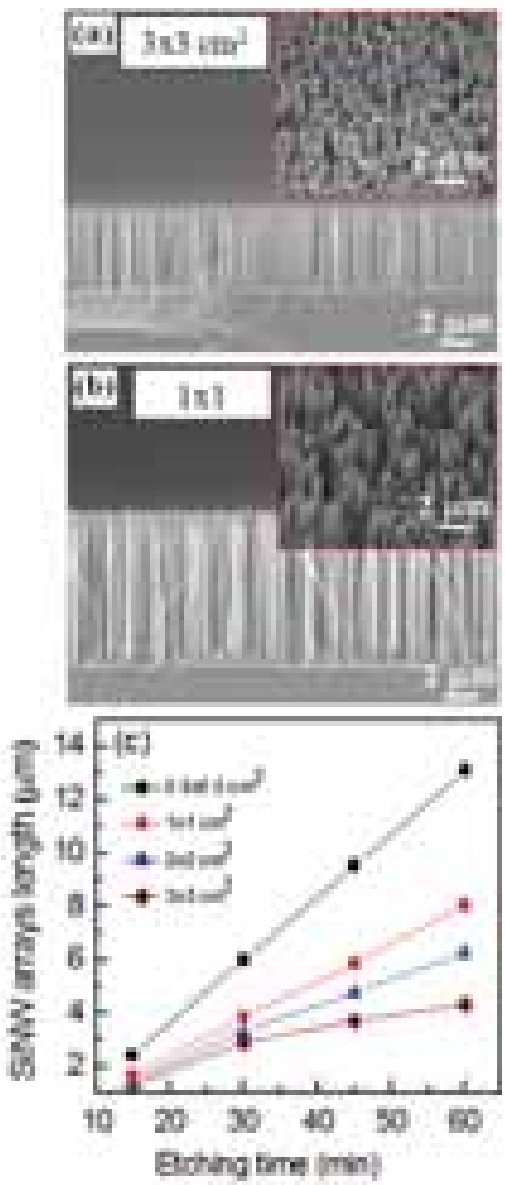

Fig. 1.3: Cross sectional SEM image comparing the length of SINWs prepared on (a) 3x3 cm^2 and (b) 1x1 cm^2 wafer area under identical etching conditions. (c) SiNW arrays length with etching time for different size of the Si wafers prepared

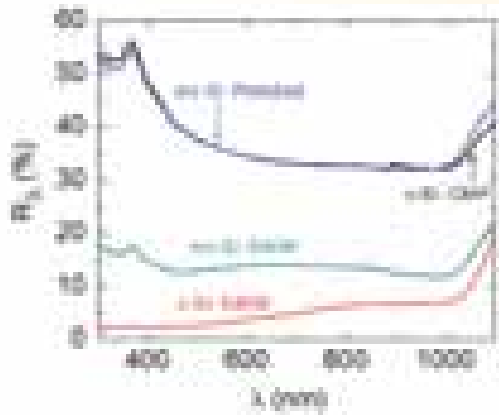

Fig. 1.4: Hemispherical reflectances (R_λ) of SiNW arrays made on c-Si (100) and mc-Si wafers for 30 min. For comparison, R_λ of polished c-Si (100) and mc-Si surface are also shown in the figure

Polymorphic Carbon Thin Films

(i) R&D on nitrogenated amorphous carbon thin films having embedded nanocrystallites deposited by filtered anodic jet carbon arc (FAJCA) technique

Nitrogenated amorphous carbon films having embedded nanocrystallites (a-C: N: nc) deposited using FAJCA technique have been characterized by XRD, HRTEM, SEM, EDAX, Raman, electrical conductivity, optical band gap, nanoindentation, field emission and ammonia gas sensing measurements. XRD confirmed the amorphous nature of the films. An ultrafine nanograined microstructures with average grain size between 8 to 10 nm were observed throughout the HRTEM image and the majority of grains were single crystallites. The conductivity (σ_D), activation energy (ΔE), optical band gap (E_g), residual stress (S), hardness (H), elastic modulus (E), plastic index parameter (H/E), percentage elastic recovery (% ER), emission threshold (E_T) and emission current density (J_{max}) of a-C: N: nc films evaluated were found to be strongly dependent on the applied negative substrate bias. Maximum values of H = 42.7 GPa, E = 330.4 GPa, H/E = 0.129, %ER = 74.4 at 3 mN load have been obtained for a-C: N: nc films deposited at - 60 V substrate bias. The lowest value of E_T = 4.9 V/μm (corresponding to 1μA/cm^2 current density) accompanied with J_{max} = 1 mA/cm^2 at 20 V/μm electric field and field enhancement factor (β) = 1805.6 have been obtained for a-C: N: nc film deposited at -60 V substrate bias. The ammonia gas sensing behavior has also been observed in these films at room temperature with fast response and recovery time as 29 and 66.9 s, respectively. The typical sensing and field emission characteristics of the a-C: N: nc films are shown in Fig. 1.5.

(ii) R & D on phosphorous doped amorphous/nanocrystalline silicon carbon films deposited by filtered cathodic vacuum arc (FCVA) technique

The crystalline size evaluated from XRD measurements, residual stress and average roughness of phosphorous doped amorphous / nanocrystalline silicon carbon films deposited using FCVA technique are found to be 28 to 32 nm, 0.5 to 3.3 GPa and 0.8 to 2.8 nm, respectively, at different arc currents from 30 to 100 A. We have used phosphorous doped silicon ingot as cathode material in the gas environment of C_2H_2. The advantage of this process is that no hazardous and toxic gases like PH_3 and SiH_4 have been used and this is a high deposition rate process. Capacitance-Voltage measurement on Al/a-SiC: P/c-Si (MIS) structure has

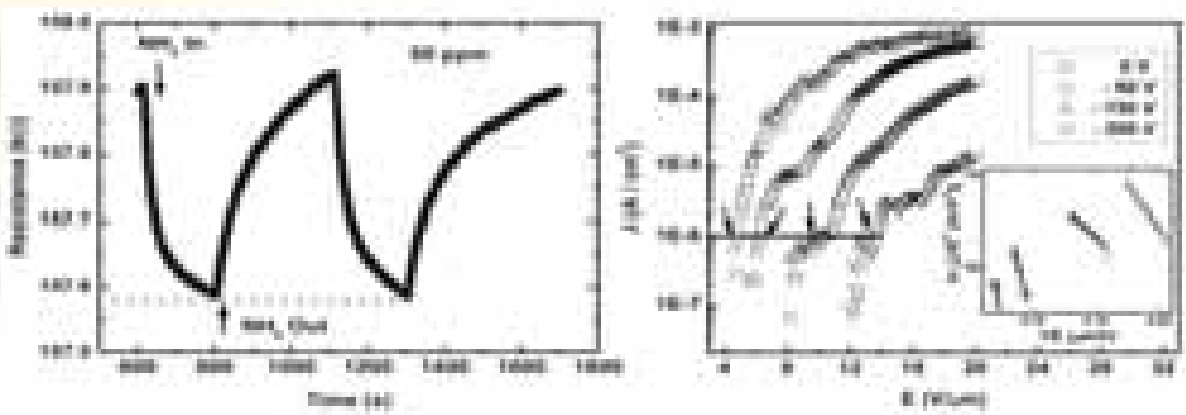

Fig. 1.5: (a) Ammonia gas sensing behavior and
(b) field emission characterics of the a-C: N: nc films

been carried out. The density of states (DOS), evaluated in the transition region between accumulation and depletion region, are found to be in the range $9.6x10^{16}$- $4.8x10^{17}$ cm^{-3} at different arc currents. These values are consistent with the values obtained in P doped amorphous / microcrystalline SiC: H films deposited by the conventional PECVD technique using SiH_4, PH_3 and CH_4 gas mixtures.

(iii) R & D on boron doped amorphous/nanocrystalline silicon films deposited by filtered cathodic vacuum arc (FCVA) technique

FCVA technique has also been used to deposit boron doped amorphous / nanocrystalline silicon films using boron doped silicon ingot as cathode material with and without hydrogen gas. Various process parameters such as substrate temperature and substrate bias have been attempted. The advantage of this process is that no hazardous and toxic gases like B_2H_6 and SiH_4 have been used and this is a high deposition rate process. A growth rate of ~5A°/s has been achieved using 100 A arc current in boron doped amorphous/microcrystalline silicon films. Various characterization of electrical conductivity (σ_D), activation energy, (ΔE) optical band gap (E_g), XRD, EDAX and SEM, Raman, FTIR etc. are in progress .

(iv) Synthesis of graphene from a-C films deposited by FCVA technique for transparent conducting and FET device

A low cost and scalable technique of filtered cathodic vacuum arc (FCVA) is presented for the synthesis of graphene using solid carbon source. FCVA technique has been utilized to deposit a-C films of thickness of 3 and 6 nm on $Ni/SiO_2/Si$ substrate and subsequently annealed at 750 and 800^{0}C in vacuum and cooled to room temperature for transforming a-C films into graphene. The number of layers is controlled by varying the parameters like the thickness of a-C films and the annealing conditions. High transmittance (~89.3%) and a low sheet resistance (~540Ω/square cm) have been obtained in graphene derived from 3 nm thick a-C film. It is a good transparent conducting material for a large variety of applications in the near future. The calculated mobility of the FET device fabricated is ~725 $cm^2V^{-1}s^{-1}$. In future, lowering the thickness of a-C films for single and bilayer graphene for variety of applications such as photodetector, shottky diode etc. will be attempted. The fabrication steps in synthesizing graphene, transmittance curve, and output and transfer characteristics of the FET device made are shown in Fig. 1.6.

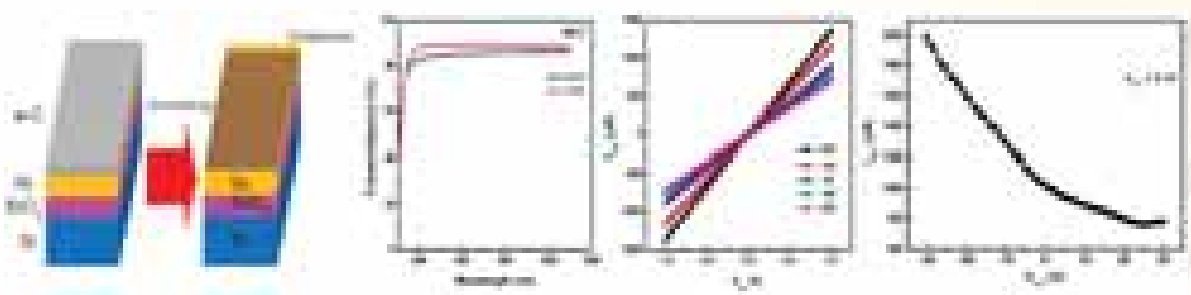

Fig. 1.6: (a) Fabrication steps for synthesizing few layer graphene
(b) Transmiitance curve, (c, d) Output and transfer characteristics of FET device

(v) Synthesis of carbon nanotube-graphene hybrid films on nickel substrates by microwave plasma enhanced chemical vapor deposition (MW PECVD) technique.

Recently, multi-walled carbon nanotube (MWCNT)-graphene hybrid films have attracted the attention of many researchers worldwide due to its potential to reduce agglomeration and thereby enhance the electrical properties which otherwise could not be realized using CNT or graphene alone. Our group was successful in depositing MWCNT-graphene hybrid films on nickel substrates using a 2.45 GHz MW PECVD system. The effect of hydrogen partial pressure on the growth of MWCNT-graphene hybrid films and their field emission properties were investigated. The presence of graphene was confirmed by high resolution transmission electron microscope (HRTEM) and Raman spectrometer. The HRTEM images showed both MWCNT and sheet like graphene structures. Raman spectra showed 2D, G, D and D+G peaks at approximately 2690, 1590, 1350 and 2930 cm^{-1} respectively. The minimum threshold field for electron emission was found to be 3.6 V/µm (corresponding to 1µA/cm^2 current density) for the hybrid films deposited at 20 Torr pressure whereas the maximum current density of 0.12 mA/cm^2 and field enhancement factor of ~3356 was obtained for the sample deposited at 5 Torr pressure. The typical HRTEM image, Raman spectra and field emission characteristics of MWCNT-graphene film are shown in Fig. 1.7.

Organic and Hybrid Solar Cells

R&D work was carried out at CSIR- NPL on the development of OPV devices using the existing and modifying donor/acceptor materials for improved power conversion efficiency and lifetime.

R&D of our group concentrate on the development of organic bulk hetrojunction solar cells based on (i) existing internationally available donor:acceptor materials, (ii) modifying suitably these existing materials, (iii) developing new donor :acceptor materials, (iv) hybrid polymer inorganic nano-structure, quantum dots and small molecule semiconductors, etc. It also undertakes (v) studies on hole transport layer (HTL), electron transport layer (ETL), photovoltaics, nanoscale characterization, Impedance spectroscopy and optimization of buffer layer etc. for the development of efficient stable solar cell.

(i) R&D towards the development of High efficiency Inverted Polymer Solar Cell

In tune with the objectives of CSIR TAPSUN project (NWP-54) we carried out R&D towards the improvement in efficiency and life time of PV devices. Starting from the PEDOT: PSS based devices, we worked on MoO_3 based inverted solar cells as well as conventional organic solar devices. After optimising the process of device fabrication we achieved power conversion efficiency (PCE)~ 7.6 % for device having configuration ITO/PFN/PTB-7:PC_{71}BM/Al (Fig.1.8). The PCE in OPV devices depends strongly on the properties of donor:acceptor

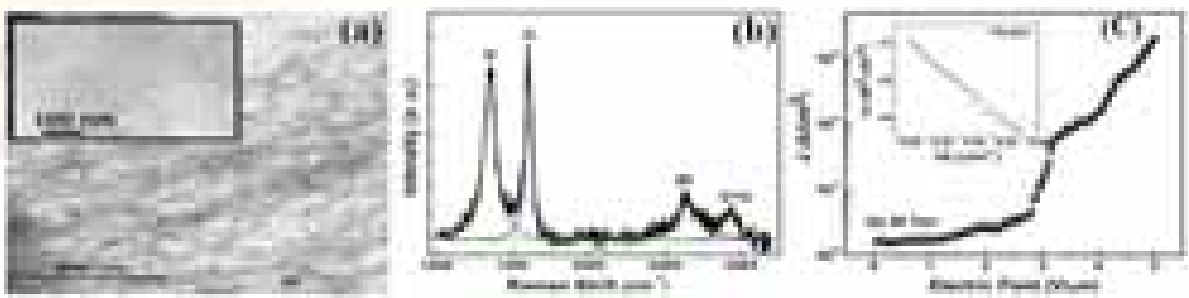

Fig. 1.7: (a) HRTEM image, (b) Raman spectra, (c) Field emission properties of MWCNT-graphene

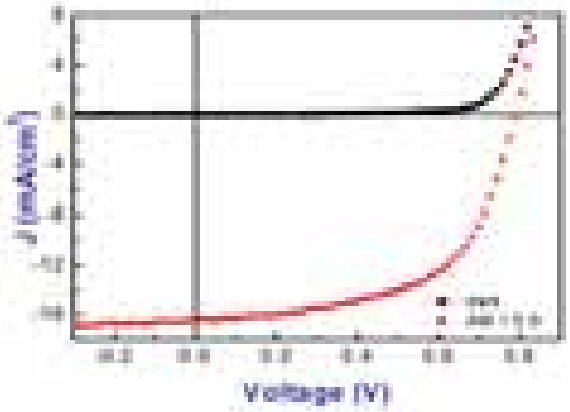

Fig. 1.8: J-V characteristics of Polymer Solar Cell with PCE ~ 7.6%

materials which vary due to degradation (self life of the material) or change of batch of PTB-7. Through current R&D We are addressing this aspect to achieve consistency and reproducibility for high PCE in these polymer solar cells.

(ii) R&D towards the improvement in life time of Polymer Solar Cells

Further during the optimization, we developed a process of an extended Ca layer deposition in the device structure ITO/MoO_3/P3HT: PCBM/Ca/Al, and got success in improving the life time of the conventional device from 80 hrs to 400 hrs (Fig. 1.9). Moreover, with the encapsulation of the device ITO/MoO_3/P3HT: PCBM/Ca/Al improves the life time up to~1000 hrs. This life time improvement work is under patenting (00943DEL 2014, dated first April 2014).Further R&D on this concept is in progress.

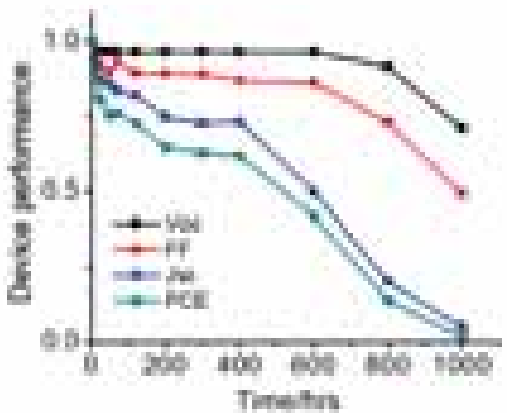

Fig. 1.9: Showing the Life time of ~ 500 hrs in Polymer solar Cells

(iii) R&D towards the concept of modified interface layer for Polymer Solar Cells

Inverted polymer Solar Cells of the classical poly (3-hexylthiophene) (P3HT):(6,6)-phenyl-C_{61}butyric acid methyl ester ($PC_{61}BM$) blend on indium tin oxide substrates were fabricated, which shows improved device performance, by using a facile solution–processed ZnO-polyelectrolytes [poly (diallyldimethylammonium chloride) (PDADMAC), Poly (acrylic acidsodium salt) (PAS), poly (4-styrenesulfonic acid) (PSS), and Polyvinylpyrrolidone (PVP)]nanocomposite as a cathode interface layer compared to devices using pristine ZnO as cathode buffer layer in ambient conditions. The devices with different combinations ofpolyelectrolyte with ZnO show different improvements in the device efficiency. The combinations of ZnO with PVP and PDADMAC show highest amount of improvements in the efficiency by a factor of <17–19. The improvement of the efficiency may be due to various phenomena, such as the passivation of ZnO surface as well as bulk traps, work function modification, improved energy level alignment, improved electronic coupling of the inorganic/organic interface, improved light harvesting, and decrease of surface as well as bulk charge recombination in the device. The introduction of polyelectrolyte into ZnO inhibits the aggregation

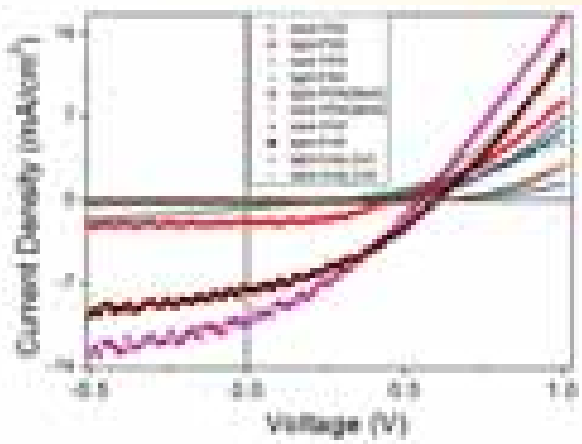

Fig. 1.10: J-V plot for devices- ITO|ZnO|P3HT:PC_{61}BM|MoO_3|Al, ITO|ZnO-PAS|P3HT:PC_{61}BM|MoO_3|Al, ITO|ZnO-PSS|P3HT:PC_{61}BM|MoO_3|Al, ITO|ZnO-PVP|P3HT:PC_{61}BM|MoO_3|Al, and ITO|ZnO-PDADMAC|P3HT:PC_{61}BM|MoO_3|Al

of ZnO nanoparticles yielding the large area ZnO nanoclusters; and hence, forming the uniform film of ZnO resulting in the modifications of morphology as well as electronic structure of ZnO-polyelectrolyte nano-composite favouring better electronic coupling between cathode and active layer and hence enhancing the current and, consequently, the efficiency. This simple low temperature ZnO-polyelectrolyte nanocomposite based protocol proposed for cathode interface layer modification may be very much useful for roll to roll industrial manufacturing of organic solar cells.

(iv) R&D on Efficient Solution - Processed Small Molecule: Cadmium Selenide Quantum Dot bulk heterojunction solar cells

For the first time, bulk heterojunction (BHJ) solar cells based on blends of solution- processed small molecule [7,72-(4,4-bis(2-ethylhexyl)-4H-silolo[3,2-b:4,5-b2]dithiophene-2,6-diyl)bis(6-fluoro-4-(52-hexyl-[2,22-bithiophen]-5yl)benzo[c] [1,2,5] thiadiazole)] p-DTS(FBTTh$_2$)$_2$: Cadmium Selenide (CdSe) (70:30, 60:40, 50:50 and 40:60) are prepared in the device configuration: Indium Tin Oxide (ITO)/ poly(3,4-ethylenedioxythiophene): poly(styrenesulfonate) (PEDOT:PSS)/p-DTS(FBTTh$_2$)$_2$: CdSe/Ca/Al. CdSe QDs were synthesized as follows. In brief, a mixture of CdO (cadmium oxide, 0.8mmol), OA (oleic acid, 2.5mmol) and ODE (1-octadecene, 20 mL) was taken in a three-neck flask and kept under vacuum with a constant stirring and maintained at 100 °C. Afterwards, the mixture was heated at 300 °C under nitrogen flow until a clear colorless solution was obtained. Selenium precursor (ODE-Se, 6.4mL, 0.25M) was injected to the clear cadmium solution. The reaction was stopped by cooling down the mixture to room temperature followed by a cleaning procedure with polar solvents. For replacing the thick ligand shells (obtained via the synthesis) with a thinner shell, that enables an efficient charge transfer at the polymer/nanoparticle interface; particles were precipitated with acetone and re-dissolved in 10mL of pyridine. After heating the solution to 65 °C for 3h it was left for overnight

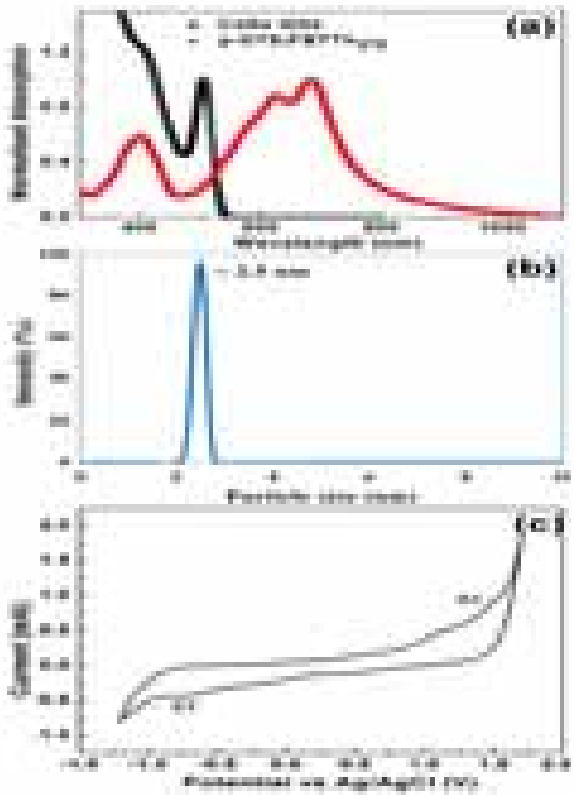

Fig. 1.11: (a) UV-vis spectra of p-DTS(FBTTh 2) 2 and CdSe QDs. (b) DLS analysis diagram of CdSe QDs. (c) Cyclic voltammogram record of CdSe QDs film at 10 mVs $^{-1}$ in 0.1M TBATFB in acetronitrile in a three electrode configuration

stirring. Ease in precipitation of the particles in hexane ensures a successful ligand exchange. Finally CdSe QDs were dissolved in cholorbenzene (CB) for the solar cell device fabrication.

To evaluate band gap values of donor-acceptor materials, UV-Vis absorption spectroscopy studies were carried out in thin films of p-DTS(FBTTh$_2$)$_2$ and CdSe QDs on the quartz glass. The films were prepared from 10mg/ml solutions of p-DTS(FBTTh$_2$)$_2$ and CdSe QDs in CB spin casted at 2000 rpm. Figure 1.11(a) shows the normalized UV-Vis spectra of p-DTS(FBTTh$_2$)$_2$ and CdSe QDs films. The p-DTS(FBTTh$_2$)$_2$ films exhibits broad low energy transitions at 625 and 680 nm. The absorption spectrum of CdSe QDs gives a well-defined and sharp exciton peak at 505 nm indicating narrow size distribution. The diameter of CdSe QDs was found to be ~2.5 nm from dynamic light scattering (DLS, DynaPro NanoStar light scatterer) analysis

(Fig 1.11(b)). The band gap (E_g) of CdSe QD as calculated from the absorption edge of the UV spectrum is ~2.34 eV. Due to quantum confinement of charges in QDs, the electron transfer is mediated through conduction band edge and the valence band edge rather than the onset of reduction and oxidation potential. Therefore in QDs, the cathodic and anodic peaks of cyclic voltammogram determine the HOMO and LUMO energy levels as shown in Fig. 1.11(c). In this figure the cathodic (C1) and anodic peaks (A1) are at 1.55 and -0.75 V, respectively, which are the positions of LUMO and the HOMO. As such the potential difference of 2.30 V is in good agreement with the band gap (2.34 eV) obtained from UV-Vis spectrum (Fig 1.11a). The calculated HOMO/LUMO for CdSe QDs are -5.95/ -3.65 and HOMO/LUMO of p-DTS(FBTTh$_2$)$_2$ are -5.12/ -3.34.

Figure 1.12(a) shows the molecular structure of SM viz. p-DTS(FBTTh$_2$)$_2$ whereas the fabricated device structure of the BHJ solar cell is illustrated in Fig. 1.12(b). The SM-BHJ solar cells were prepared in the following configuration: ITO/PEDOT:PSS/ p-DTS(FBTTh$_2$)$_2$:CdSe/Ca/Al. The p-DTS(FBTTh$_2$)$_2$: CdSe (donor: acceptor) blend solution was prepared in different weight ratios of 70:30, 60:40, 50:50 and 40:60, respectively having a total conc. of 35mg/ml in cholorbenzene with 0.4 v % of 1, 8-diiodooctane (DIO) as a processing additive. The energy levels and work functions of the components of the BHJ device are illustrated in Fig. 1.12(c). Due to the energy level offset between the p-DTS(FBTTh$_2$)$_2$ and CdSe QDs, p-DTS(FBTTh$_2$)$_2$ acts as an electron donor and CdSe acts as an electron acceptor. Fig. 1.12(d, e) shows a high resolution

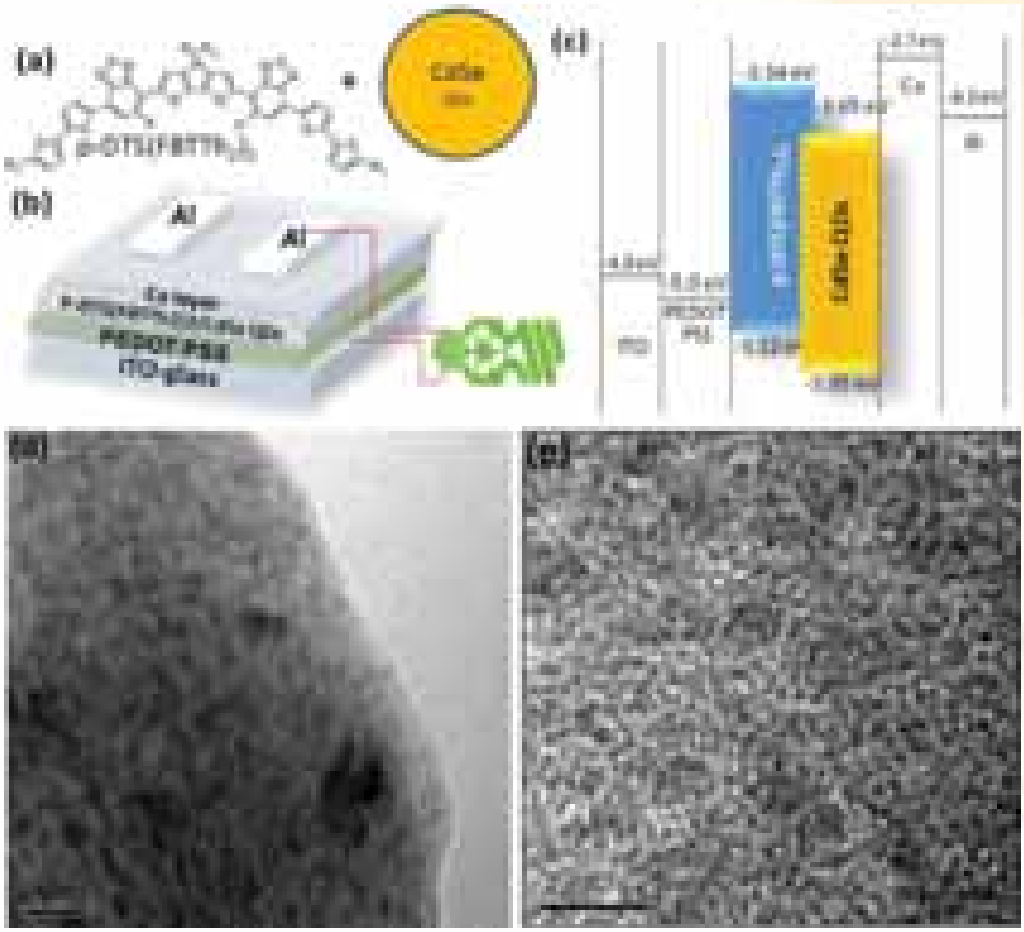

Fig. 1.12: (a) The molecular structures of p-DTS(FBTTh 2) 2. (b) The device structure of the p-DTS(FBTTh 2) 2:CdSe QDs solar cell. (c) Energy level diagram of SM-BHJ solar cells with sequential layers of ITO/PEDOT:PSS/p-DTS(FBTTh 2) CdSe BHJ/Ba layer/Al cathode. (d, e) HRTEM images of the p-DTS(FBTTh 2) 2:CdSe::60:40 blend

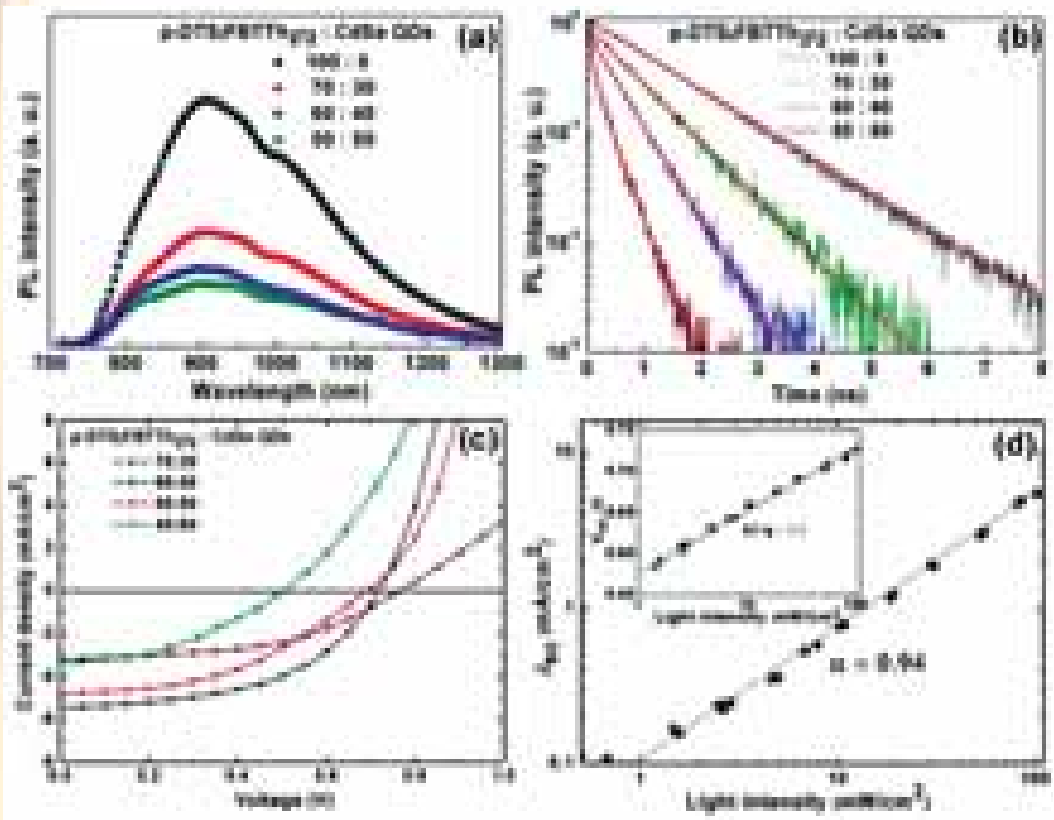

Fig. 1.13: (a) PL spectra and (b) PL decays of of p-DTS(FBTTh 2) 2 and after the addition of CdSe QDs in different ratios. (c) J-V characteristics of the p-DTS(FBTTh 2) 2/CdSe QDs BHJ solar cells in various ratios under AM 1.5G irradiation at 100 mW/cm ^{2}. (d) p-DTS(FBTTh2)2:CdSe (6:4) solar cell with measured Jsc of (symbols) on a logarithmic scale as a function of illumination intensity (symbols). Fitting a power law to these data yields á. The inset shows measured Voc as a function of illumination intensity (symbols), together with linear fits to the data

transmission electron microscopy (HRTEM) image of CdSe QDs dispersed in a host p-DTS(FBTTh$_2$)$_2$ matrix viz. p-DTS(FBTTh$_2$)$_2$:CdSe QDs::60:40 by weight. The TEM image quite explicitly reveals a uniform distribution of CdSe QDs in p-DTS(FBTTh$_2$)$_2$ matrix having CdSe QDs of size ~2.5 nm.

Photoluminescence (PL) is a powerful tool for evaluating the charge transfer from the donor to acceptor. Figure 1.13(a) shows the PL spectra of pristine p-DTS(FBTTh$_2$)$_2$ film and the blends of p-DTS(FBTTh$_2$)$_2$:CdSe QDs, respectively. The quenching effect is abundantly clear as the PL intensity of p-DTS(FBTTh$_2$)$_2$ has been significantly reduced after blending with CdSe QDs. Significant reduction/ quenching in PL intensity of the blends relative to the pristine p-DTS(FBTTh$_2$)$_2$ indicates the donor-acceptor charge transfer process via p-p interaction between SM and CdSe QD. This would enable the charge separation at the interface, wherein the hole would transport through p-DTS(FBTTh$_2$)$_2$ and electron would transport through CdSe QD with their subsequent collection at the respective electrode thus resulting into the flow of current and an efficient generation of electricity. This efficient quenching/ charge transfer process is revealed at a picosecond scale, as shown in Fig. 1.13(b). PL decay time of the p-DTS(FBTTh$_2$)$_2$ is significantly reduced after CdSe QDs incorporation due to a charge transfer. For data analysis we describe PL decays in thin films of p-DTS(FBTTh$_2$)$_2$ with a bi-exponential function {PL(t) = $a_1e^{-t/t}{}_1 + a_2e^{-t/t}{}_2$, $a_1 + a_2 = 1$}. The values of a_1, a_2, t_1 and t_2 are listed in Table 1.3 for reference. The decay constant (t) of pristine p-DTS(FBTTh$_2$)$_2$ film (1.38 ns) get significantly reduced after the incorporation of CdSe QDs, due to the charge transfer from p-DTS(FBTTh$_2$)$_2$ to CdSe QDs.

Table-1.3 Photovoltaic properties and parameters of the two-exponential approximation of the PL decays

Having established the efficient charge transfer process between the donor and the acceptor, we fabricated the BHJ solar cells. Fig. 1.13c shows the current density versus voltage (*J-V*) characteristics of the BHJ devices ITO/PEDOT:PSS/ p-DTS(FBTTh$_2$)$_2$:CdSe-QDs/Ca/Al with p-DTS(FBTTh$_2$)$_2$:CdSe QDs in the weight ratios of 70:30, 60:40, 50:50 and 40:60, respectively. It is important to mention here that in these measurements, the Al deposition area and the mask area were 10.5 mm^2 and 10 mm^2, respectively. The device parameters evaluated from these characteristics are summarized in Table-1.3. It is seen from Fig. 1.13(c) and Table-1.3 that the device with 70:30 weight ratio results in a PCE = 1.18% with device parameters being J_{sc} = 3.17 mA/cm^2, V_{oc} = 0.764 V, and a FF = 49%, respectively. However, for 60:40 weight ratio, the device performance improves to J_{sc} = 5.45 mA/cm^2, V_{oc} = 0.727 V, and FF = 51% with corresponding PCE = 2.02%. With the further increase in the concentration of CdSe QDs in p-DTS(FBTTh$_2$)$_2$, i.e. for 50:50 and 40:60 ratios, the PCE decreases to 1.45% and 0.65%, respectively for which the device parameters are shown in Table-1.3. This reduction in PCE can be explained in terms of excess QDs agglomerating or providing an extended pathway that can connect anode to the cathode, which leads to current leakage, reduction in V_{oc} and FF. It establishes that p-DTS(FBTTh$_2$)$_2$:CdSe QDs in 60:40 ratio provides the optimum ratio for obtaining the best PCE. The high J_{sc} value in the optimized device is attributed to the high mobility of hole in p-DTS(FBTTh$_2$)$_2$. On the other hand the low FF might be due to the insufficient percolation of CdSe QDs in the small molecule's matrix. Further, smaller particles have found to yield a lower fill factor, compensating for the gain in V_{oc}.

To gain an insight into the type of dominating charge recombination processes, we studied the variation of J_{sc} as a proportional function of illumination intensity using a power law dependence of J_{sc} upon light intensity, In Fig. 1.13d, the data for the optimized device viz. p-DTS(FBTTh$_2$)$_2$:CdSe QDs::60:40 wt. ratios, is plotted on a log-log scale and fit to a power law using equation 1. The fitting of the data yields á = 0.94, which is close to unity with a nearly linear dependence of J_{sc}, indicating that the charge transport is dominated by the monomolecular recombination, which can either be germinate recombination or due to the presence of traps. The recombination mechanisms can also be extracted by studying the V_{oc} as a function of illumination intensity. At V_{oc} the photocurrent is zero and all photogenerated carriers recombine within the cell. In the case of bimolecular (Langevin) recombination being the sole loss mechanism, it has been shown that the V_{oc} of a BHJ solar cell is given by,

$$\delta V_{oc} = \left(\frac{kT}{q}\right)\ln[J] + \text{const.} \quad \ldots\ldots\ldots\ldots 1$$

where I is the incident light intensity, This implies that the slope of V_{oc} versus ln(I) is equal to kT/e for bimolecular recombination and $2kT/e$ for monomolecular SRH recombination. The result is shown in the inset of Fig. 1.13d, where the slope is 1.3 kT/q imply that recombination at open circuit in these devices is a combination of monomolecular (trap assisted) and bimolecular processes. Finally BHJ hybrid solar cells based on solution- processed SM with CdSe QD have a great potential. The BHJ solar cell with p-DTS(FBTTh$_2$)$_2$:CdSe QDs in 60:40 ratio exhibited the highest PCE of ~2%. In these devices, the recombination mechanism is governed by a combination of both monomolecular and bimolecular recombination. Further optimization is going on by the suitable modification of the morphology/interface layers etc. in these BHJ solar cells.

(v) R&D on Indigenous Development of donor/Acceptor materials for OPV devices.

Polymer synthesis: Present a new method for tuning the HOMO/LUMO energy level and band gap control in BDT-based copolymers by introduces hereocycles for solar cell applications. Our method takes advantage of the different aromaticity of the furan, thiophene and selenophene ring with effect of extended conjugation to enable band gap tuning in the range of 0.1-0.4 eV. We also present an efficient synthetic method, characterization, and comparative DFT calculations for new copolymers,

In order to study the effect of heteroatom on BDT-based copolymers on OPV performance we synthesized three new copolymers **P3a-c** is depicted in Scheme 1. The copolymers **P3a-c** were prepared by Stille coupling polymerization of distannylated compound **1** with dibromo-compound **2a-c** respectively using catalytic amount of Pd(PPh$_3$)$_4$ in toluene. To examine the effect of extended conjugation and solubility on OPV performance, we also synthesized copolymer **P5** by Stille coupling polymerization between **1** and **4**.

Photovoltaic Properties. Photovoltaic properties of the polymers **P3b-c** were investigated in solar cell structures of ITO/MoO_3/P3HT:PCBM/Al (Table 1.4). The polymeric active layers were spin-coated from a dichlorobenzene solution. Figure 1.14 shows the photo *J-V* curves of the polymer solar cells under AM 1.5 condition at 100 mW/cm^2.

Table 1.4. Summarized OPV performance of P3b and P3c (ITO/MoO_3/P3HT:PC71BM/Al)

New Polymers	Jsc (MA/cm^2)	Voc (V)	FF	PCE(%)[1]
P3c	4.38	0.818	37	1.32
P3b	2.96	0.63	45	0.84

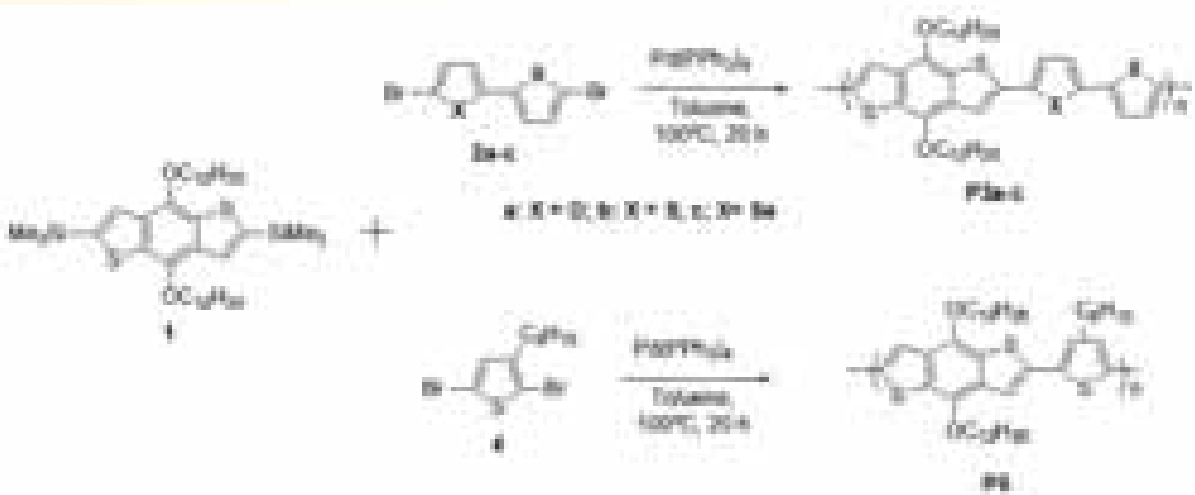

Scheme-1: Synthesis of copolymers **P3a-c** and **P5** via Stille cross-coupling polymerization

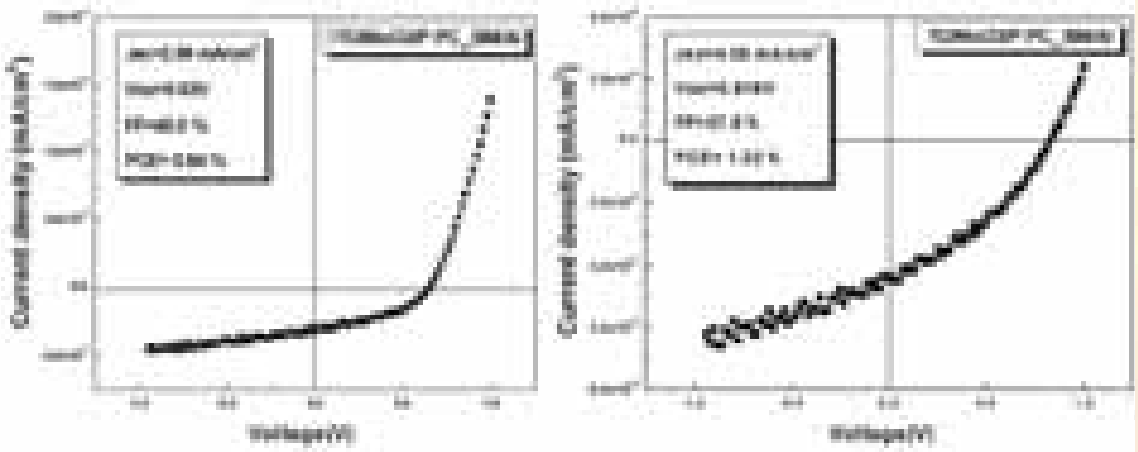

Fig. 1.14: Current density versus voltage (J-V) curves of polymers **P3b-c**

We are working on synthesis of existing, modified and new materials synthesis for application as acceptor in organic photovoltaics. We are also modifying the synthesis process for the greener approach for existing material in order to reduce the production cost on bulk scale production.

We have demonstrated a cost effective and eco-friendly process for *one-pot* synthesis of **existing material** PC61BM under aerobic conditions where, the key step of diazomethane intermediate preparation is modified. Instead of using pyridine and sodium methoxide under inert atmosphere, we used triethyl amine and dichloromethane under aerobic conditions as shown in scheme 2. This process is envisaged as a green chemistry and will open channels for the large scale synthesis of PC61BM and its derivatives for solar cells applications without bothering for controlled environment conditions. Thus synthesized PC61NB shows comparable device property commercial PC61BM (Figure 1.15).

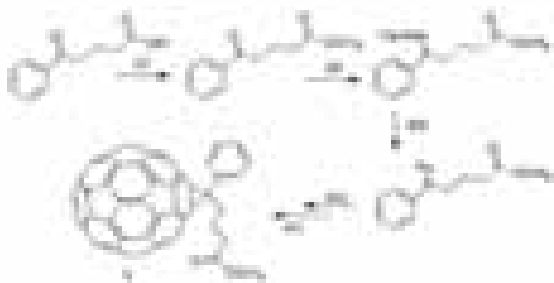

Scheme 2: (i) MeOH, CH_3COOH, reflux; (ii) *p*-toluene sulfonyl hydrazide, MeOH, reflux; (iii) triethyl amine, dichloromethane, 0°C; (iv) C_{60} in o-DCB followed by column purification to isolate [5,6] adduct; (v) refluxed in o-DCB.

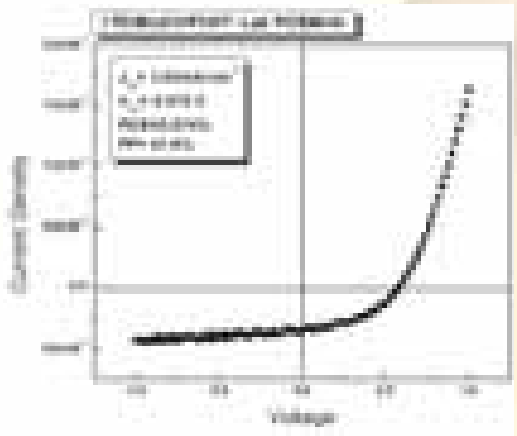

Fig. 1.15: Device properties for synthesized PC61BM

This green approach of methanofullerene production has been used to synthesis modified materials which have shown better power conversion efficiency 1.2% in organic photovoltaics compared to PC61BM due to higher reduction potential (figure 1.15 & 1.16).

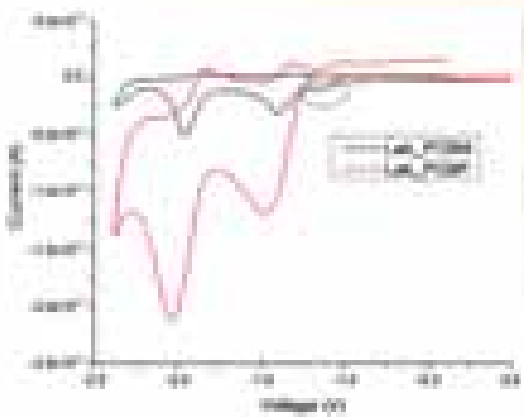

Fig. 1.15a: Cyclic voltammogram of modified PCBM

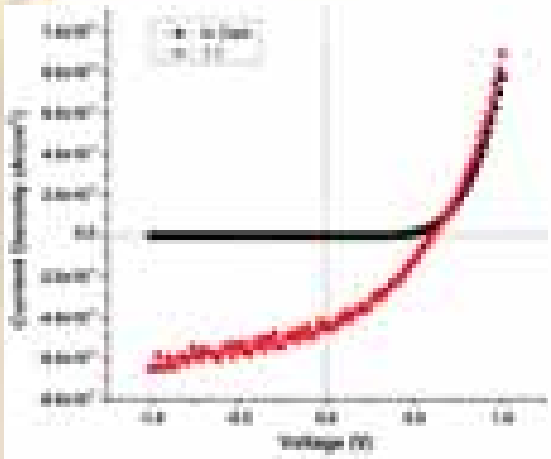

Fig. 1.16: Device properties for modified PCBM

New Acceptor Material Synthesis. In order to tune the energy levels of acceptor materials, different types of functional groups (electron withdrawing and donating type) have been attached exohedrally on fullerene[60] ball to synthesize acceptor molecules 1-3. Cyclic voltammetry clearly shows the fine tuning of HOMO and LUMO energy levels of these materials.

(1) (2) (3)

Materials are showing good absorption along with high quenching of P3HT donor polymer fluorescence peaks on mixing ascertaining high charge transfer between donor and acceptor molecules (Fig. 1.17 & 1.18).

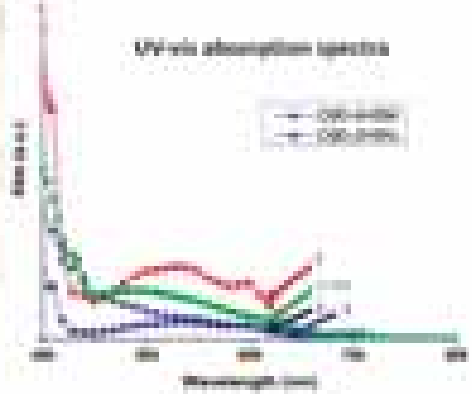

Fig. 1.17: UV-vis absorption of 1-3 and PCBM

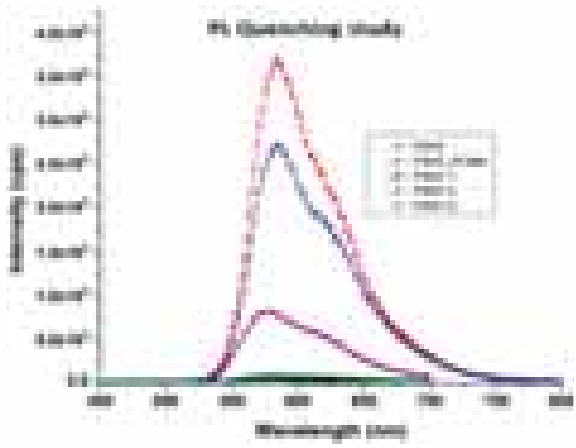

Fig. 1.18: PL quenching study on mixing with P3HT

Photovoltaic Properties. Photovoltaic properties of 1 was investigated in solar cell structures of ITO/MoO_3/P3HT:1/Al under ambient. The polymer active layers were spin-coated from a dichlorobenzene solution. Figure 1.19 shows the photo *J-V* curves of the polymer solar cells under AM 1.5 condition at 100 mW/cm^2 (Table 1.5).

Table 1.5. Summarizeds OPV performance of

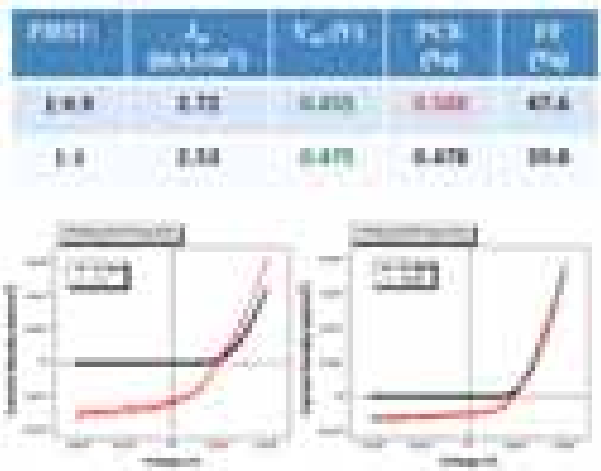

Fig. 1.19: Current density versus voltage (J"V) plots of acceptor 1 with P3HT.

device

Thermoelectrics-Bulk, Nano and Thin Films

Synthesis of Chalcogenides with enhanced thermoelectric properties

Antimony telluride (Sb_2Te_3) has been

synthesized by solvothermal route using different solvents, and its thermoelectric properties were measured. The data is compared with two reported literature. Jin et.al- prepared Sb_2Te_3 by Solvothermal synthesis identical to our route. Dong et.al- prepared Sb_2Te_3 by Microwave assisted solvothermal synthesis and reports highest ZT for this compound. The electrical conductivity (σ) of our sample is found to be much higher than the reported work. Seebeck coefficient (S) was found to be in between of the two reported data. This is attributed to the dependence of S on the particle size. In our case, the average particle size is 100-150nm while Dong et.al report particle size of 50-70nm and that of Jin et.al is 600nm. So, larger S was achieved for smaller particle size. Therefore, the resultant power factor ($S^2\sigma$) was much higher for our sample. This poses as-synthesized sample, with higher power factor, to

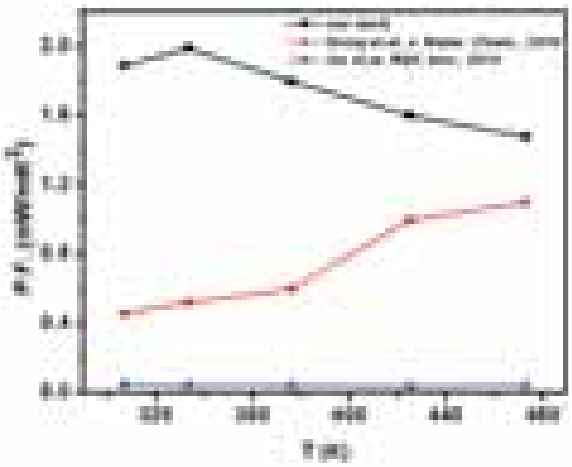

Fig. 1.20: Power factor as a function of Temperature

be efficient for thermoelectric applications.

Copper anstimony telluride (Cu_3SbSe_3) has attained great attention for thermoelectric applications. The thermal conductivity of Cu_3SbSe_3 is anomalously low and nearly temperature independent. It is due to the anharmonicity of trivalent Sb in this compound. This relatively low thermal conductivity results in enhanced thermoelectric performance. We also have investigated solvothermally synthesized Cu_3SbSe_3. The as-synthesized powder was compacted into a pellet by Spark plasma sintering (SPS) technique and investigated the thermal conductivity (κ) in the

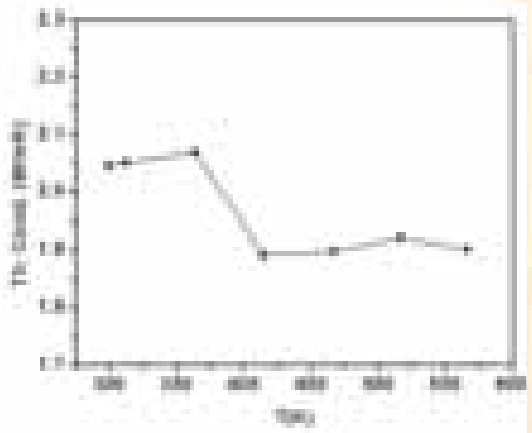

Fig. 1.21: Thermal conductivity as a function of Temp.

temperature range 300 to 600K.

κ ~2.04 W/smK at room temperature and remains in the range 2.05-1.9 W/mK in the specified temperature range. The data shows that thermal conductivity increases only slightly with decreasing temperature, thus is almost temperature independent in agreement with reported literature. The low value of ê is due to the increased bond anharmonicity associated with Sb^{3+} state in Cu_3SbSe_3 [Skoug et.al, App. Phys. Lett., 2010]. The observed trend of thermal conductivity for Cu_3SbSe_3 poses it to be an efficient thermoelectric material.

Organic and Inorganic light emitting diodes

Organic: (i) Development of Ambipolar field effect transistor

Ambipolar field effect transistor in the configuration Si/SiO_2/Tetracene/P13/Au has been fabricated on heavily doped *n*-type silicon substrate with 230-nm-thick thermal grown SiO_2 as insulator. The tetracene layer is grown at a rate of 0.1-0.2 Å/s with layer thickness 20nm. The P13 (N,N'-ditridecylperylene-3,4,9,10-tetracarboxylicdiimide) layer is also grown at a rate of 0.1-0.2 Å/s with the substrate at room temperature and layer thickness is 20nm. The output and transfer characteristics were obtained from 20 micron channel length. The OFET device parameters like threshold voltages and on/off ratio etc. have been calculated. The calculated value of μ_h = 1.28 x $10^{-4}cm^2$/V-sec

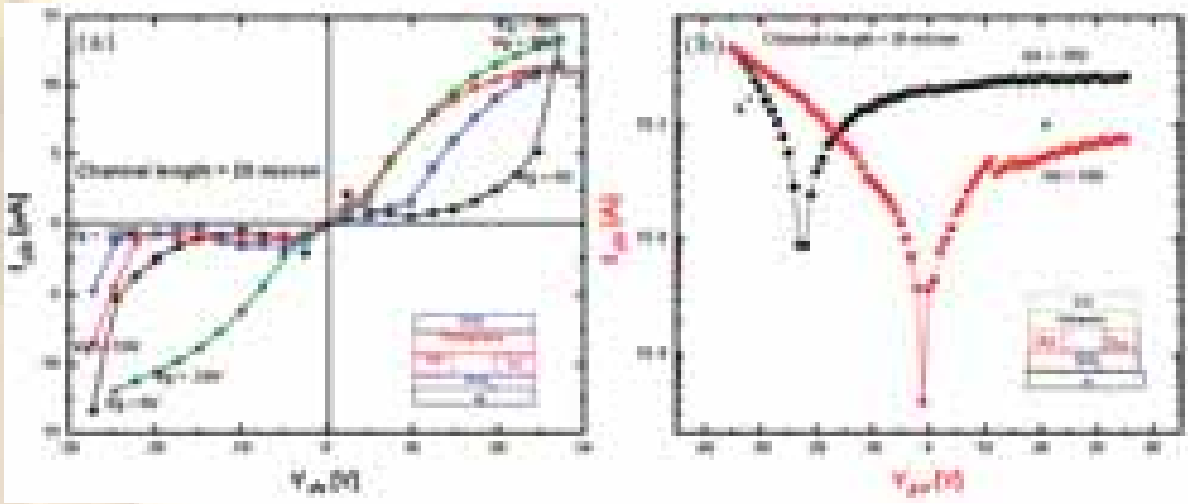

(a) (b)

Fig. 1.22: (a&b)Output and Transfer characteristics of ambipolar organic field effect transistor (AOFET)

(tetracene) and μ_e = 5.90 x 10^{-5} cm^2/V-sec(P13).

Also, The hole mobility of thermally stable 2, 7-bis [N, N-bis (4-methoxy-phenyl) amino]-9, 9-spirobifluorene (Spiro Meo TPD) thin films has been investigated by using top contact organic field effect transistor (OFET) characteristics. OFET in the top contact configuration was fabricated using the thermal evaporation method. A heavily doped n^{++} type Si wafer with an oxide layer of 270nm thickness was used as a substrate and was cleaned using solvents. Organic layer and gold electrodes were deposited at room temperature. The geometry factors of the fabricated OFET devices were: the Length (L) = 30 micron and width (W) = 2mm with the aspect ratio of order of 100. Transistor characteristics of fabricated OFET device were performed by Keithley 4200 interface with cascade probe station. The electrical characteristics of the OFETs show that the drain current I_{ds} increases as the negative gate voltage V_g values are increased. The sign of the field enhanced current (I_{ds} < 0 with V_g < 0) is consistent with the p type behaviour of Spiro MeO TPD in the accumulation regime of operation of the device. The threshold voltage was found to be -13.5 V. The following conventional relation for mobility applied in inorganic FETs has been used in the present case:

$$I_{ds} = \left(\frac{W}{2L}\right)\mu C_i \left(V_g - V_o\right)^2 \quad (5)$$

Where I_{ds} is the drain-source current in the saturation region, μ is the field-effect mobility, L and W are the channel length and width, respectively, V_g and V_o are the gate voltage and threshold voltage, respectively. C_i is the capacitance of the insulating layer per unit area. The field-effect mobility in the saturation region, using this equation, has been estimated to be 1.93 x 10^{-3} cm^2/Vs. An on/off ratio was estimated to be 1.98x10^1 for V_{ds} =-5V.

(ii) Development of Vertical OLET

Vertical OLET(VOLET) has been fabricated in the configuration ITO/PEDOT:PSS/PFO/Al/LiF/Al. When capacitor cell is under bias; thin, rough and partially oxidized middle source electrode modulates the charge injection in OLED cell. The output and transfer characteristics were obtained for this VOLET configuration (Fig 1.23(a)) using semiconductor characterization system Keithley 4200 .

(iii) Joule Heating Studies of OLEDs and Its Implications on Life Time

A quantitative analysis of Joule heating by temperature measurements using infrared thermography and heat estimation of organic light emitting diodes (OLEDs) and their correlation with device life time have been done. Schematic setup

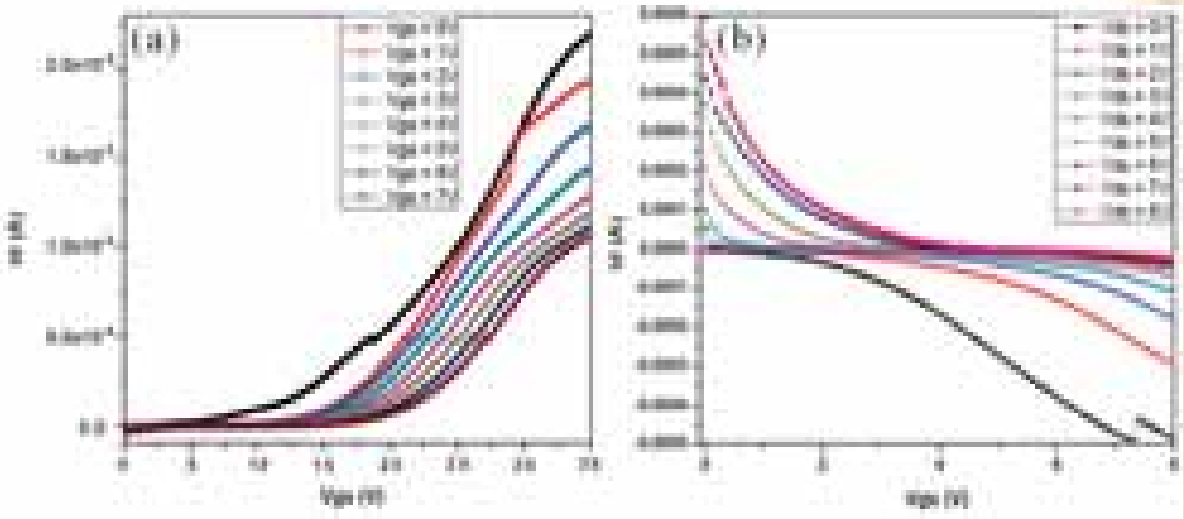

(a) (b)

Fig. 1.23: (a&b) Output and transfer characteristics of the PFO based VOLET.

In this VOLET device, the electron current is very low when the gate bias is 0V, because of the high injection barrier height between the source electrode (Al) and the LUMO of the LEP. By applying the gate bias, the energy level alignment between source electrode and organic material changes, and the electron injection barrier is lowered. Thus, higher and balanced electron-hole injection is achieved even at low source-drain bias. As a result, excitons are formed more efficiently in the LEP and stronger light emission can be observed at higher gate bias and Electron injection barrier of VOLET is lowered by gate modulation. Gate bias controls the threshold voltages of Light Emitting Cell, current flow and the light intensity. Light emission was observed from emissive layer when Vg ≥ 2V

used for the temperature measurements of OLEDs is shown in Fig.1.24. These temperature measurements were performed at 10, 20, 30, 40, and 50 mA/cm^2 current densities and studied with operational time. The temperature rise of the device has increased from 9.8 to 16.6 °C within 168 h at an operating current density of 40 mA/cm^2. This has been ascribed as due to the external contamination by water, oxygen, and dust particles as well as by internal heat generation. Encapsulation of the device avoids external degradation of OLEDs by preventing the destruction caused by these external contaminations. In this way, encapsulation has led to the decreased temperature rise of 12.4 °C within the duration of 168 h, which reflects the improved stability of the device. The temperature measured has been used to calculate the heat generated inside the device by solving the heat conduction equation using a transverse matrix approach. It has been found by these calculations that about 97%–98% of the power supplied to the device are converted into the heat for un-encapsulated device and results in

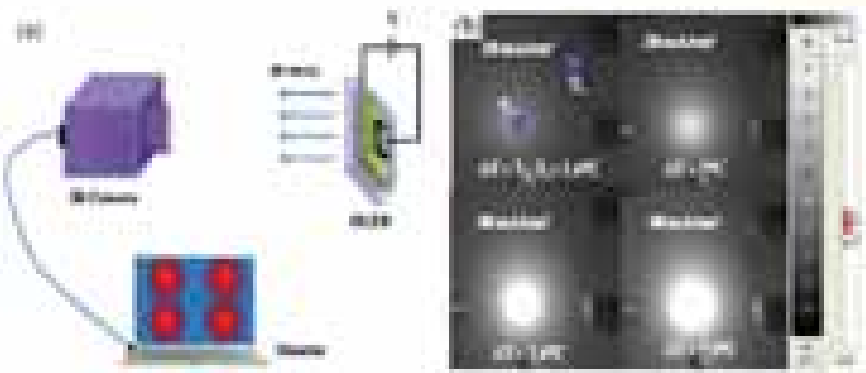

Fig. 1.24: (a) Schematic setup used for the temperature measurements of OLEDs. (b) IR thermograph for OLED operating at a current density of 10, 20, 30 and 40 mA/cm^2

rapid degradation of device with time, which in turns leads to the increase in operating voltage and decrease in luminous intensity with operational time. Proper encapsulation has reduced the heat generated inside the device by about 3%–4%, thereby, increasing the life time of the device. However, the glass encapsulation reduces the possibilities of the device cooling by heat convection to the atmosphere and prohibited the maximum utilization of encapsulation.

(iv) Exciton quenching by diffusion of 2,3,5,6-tetrafluoro-7,7',8,8'-tetra cyano quino dimethane and its consequences on joule heating and lifetime of organic light-emitting diodes

The effect of F_4-TCNQ insertion at the anode/hole transport layer (HTL) interface was studied on joule heating and the lifetime of organic light-emitting diodes (OLEDs).These parameters were found to be severely affected by the diffusion of F_4-TCNQ. F_4-TCNQ causes the luminescence quenching in emissive layer. To study the quenching mechanism and F_4-TCNQ diffusion using photoluminescence (PL) spectroscopy, we have selected tris (8-hydroxyquinoline) aluminum (Alq_3) as emissive layer and fabricated samples having a structure glass/ F_4-TCNQ (x nm)/á-NPD (y nm)/Alq_3 (10 nm), where x and y has been varied. In the samples having y = 0 nm, the PL intensity of Alq_3 was found to reduce drastically upon increase of x from 0 nm (i.e. without F_4-TCNQ layer) to 0.5 nm. The PL intensity was found to decrease continuously with the increase of x until x = 2.5 nm. In these samples, we have also observed that the quenching by F_4-TCNQ also changed the excited state life time of Alq_3, which indicates towards a dynamic quenching mechanism. Further, the diffusion of F_4-TCNQ has been observed by increasing the value of y and was found that as y increases, the PL intensity has started to increase before being saturated at a certain value of y (> 15 nm for all samples with different values of x). This indicates that F_4-TCNQ diffuses through α-NPD and leads to the quenching of Alq_3. The data of PL intensity has been used to estimate the diffusion length and this length has been found to increase with the increase in thickness of F_4-TCNQ. Further, the effect of the F_4-TCNQ interface layer has been studied on the joule heating and lifetime of OLED. Joule heating was found to reduce significantly (pixel temperature decrease by about 10°C at a current density of 40 mAγcm^2) by this insertion. However, the lifetime was found to reduce significantly with a 1 nm thick F_4-TCNQ layer, and it improved by increasing the thickness of this layer. Thermal diffusion of F_4-TCNQ into HTL leads to F_4-TCNQ ionization by charge transfer, and drift of these molecules into the emissive layer caused faster degradation of the OLEDs. This drift was found to reduce with an increase in the thickness of F_4-TCNQ.

(v) Multilayer thin film encapsulation for organic light emitting diodes

The study of a transparent and effective hybrid thin film encapsulation (TFE) with alternate multilayer structure made up of two organic materials with entirely different morphological properties has been done. This work reports on alternate multilayer structure composed of two organic materials belonging to the same family of organic compounds yet exhibiting entirely different morphological properties(Fig.1.25). N, N'-diphenyl-N, N'-bis-3-methylphenyl (1, 1'-biphenyl) (TPD) is well known to have a very low glass transition temperature imparting poor thermal stability to the material. Thin films of TPD are readily crystallized as soon as the thicker TPD films are deposited which is remarkable since the material tends to form crystals that are expected to result in different permeation pathways along the grain boundaries. Another organic film from the same family of TPD with a Spiro structure (2, 7-bis [N,N-bis(4-methoxy-phenyl)amino]-9,9-spirobifluorene) (Spiro Meo-TPD) exhibits a relatively high glass transition temperature thus imparting very high thermal stability to the material. Thin films of Spiro Meo-TPD are relatively dense and amorphous with substantially reduced density of the defects. These thin films act as

planarization layers. The alternate stacks of these layers provide efficient decoupling of the defects leading to considerably slower diffusion of water vapour and oxygen into the device. To avoid the direct contact of these sensitive films with ambient atmosphere, MgF_2 films are used. Therefore, this alternate system is further protected by barrier coatings of normal and GLAD deposited MgF_2 which is in direct contact with the ambient atmosphere. Glancing angle of 85^0 was chosen because significant morphological changes, resulting in columnar structures, are observed at such high angles of incident vapor flux w.r.t the substrate normal. Note that a neat MgF_2 layer acts as substantial barrier coating. However, neither a neat MgF_2 layer nor the simple organic alternate multilayer structure can reach the high quality barrier characteristics. A dramatic reduction in water and oxygen permeation was obtained by employing this multilayered geometry which leads to a longer tortuous diffusion path and hence significantly enhanced lifetime of the OLEDs.

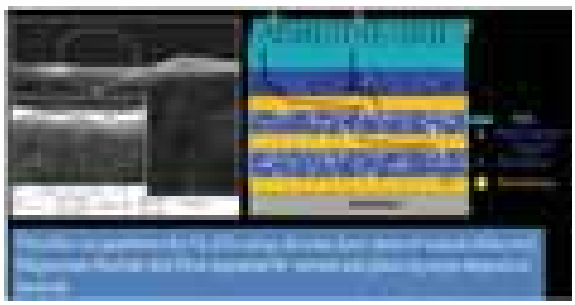

Fig. 1.25

Inorganic: (i) Steady State Photoconductivity Laboratory

The set up was developed for Photoconductivity measurements in modulated current regimes using lock-in technique and in DC regimes using source measure unit. The set up allows us to perform,

Photocurrent as a function of Photon energy (Current vs. wavelength)

Spectral dependence measurements both in DC and in modulated regimes

Measurements with variable frequency from 20 Hz – 10 KHz in modulated regimes

Stationary state measurement (Persistent Photocurrent) in DC mode

Photocurrent as a function of temperature (10 K – 300 K)

The modulated current regimes eliminates the effect of any stray light, dark current or any other unmodulated signal or any signal modulated at any other frequency. A lock-in amplifier is used for measuring photocurrent signals. A Source-Measure unit is used for measuring photocurrent signal in DC mode with continuous light. The available equipments are:-

Light sources: Dual light source (Xenon lamp and Quartz Halogen lamp)

Spectral range : 250 - 1800 nm with Xenon Lamp and Quartz Halogen Lamp

Operation temperature range: 10 - 300 K with closed cycle cryostat (ARS)

Sensitivity: In modulated current regime $2x10^{-11}$ A with a Lock-in amplifier with sensitivity of 10 μV and R_{load} of 470 KW.

Monochromator average resolution: 0.01 nm

A source-measure unit

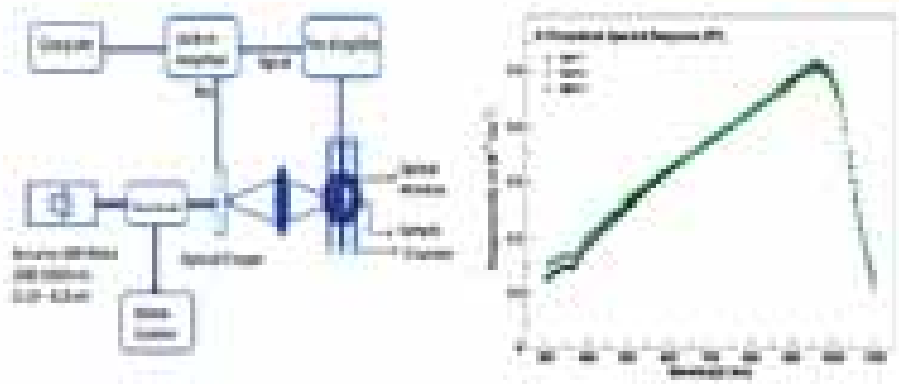

Fig. 1.26 Photoconductivity measurement set up and the photodiode spectral response (RT) for spot 1, 2 and 3

Existing facility:

(ii) Growth and characterization of PAMBE Grown GaN films at Different Plasma Powers

We are working on Plasma Assisted Molecular Beam Epitaxial (PAMBE) growth of III-nitride materials. III-nitride consists of the binary materials like Gallium Nitride (GaN), Indium Nitride (InN) & Aluminum Nitride (AlN) and ternary materials such as Indium Gallium Nitride (InGaN), Aluminum Gallium Nitride (AlGaN) and Aluminum Indium Nitride (AlInN). III-nitrides exhibit direct band-gaps over the entire visible spectrum and are the preferred materials for visible optoelectronics viz. LEDs and diode LASERs are finding new applications in power electronics, blue-UV LASERs, intersubband optoelectronics, photocatalysis and photovoltaics.

GaN, a direct, wideband gap semiconductor is an attractive material for high temperature and power devices. Major efforts have been made to grow a fine quality GaN but it is quite challenging as the growth conditions such as growth temperature and III-V flux ratio significantly affect the growth mechanism of GaN and resulting surface morphology.

In the present work we have studied the effect of Plasma power on the growth and quality of GaN. Keeping all the other growth parameters nearly identical, the two samples were grown at different RF Plasma powers. GaN growth took place in a highly controlled Ultra-High-Vacuum (UHV) environment in RIBER Compact 21 PAMBE. The system is equipped with Ga Knudsen cells and ADDON RF Plasma source for nitrogen. Thick GaN layers were grown on a 3.5μm MOCVD GaN template on c-plane sapphire (0001) as the substrate. The growth was carried out at a pressure of $1x10^{-5}$ Torr with similar growth parameters such as constant Ga & N fluxes, etc. at substrate temperature of 760°C under Ga-rich conditions. The only difference was that for one sample Plasma power was 250W and for another it was 400W. In-situ RHEED was used for continuous monitoring.

Surface morphology of the epitaxial GaN films was characterized using STM and AFM techniques. Fig. 1.27(a) represents the large area AFM image of GaN film grown at a plasma power of 425 W. We found very large flat islands with root-mean-square (rms) roughness value of 7.68 nm. With further change in growth condition, as the plasma power is decreased to 250 W, smooth GaN film was obtained with rms roughness of 0.62 nm as shown in Fig. 1.27(b). The surface pits have lateral size 20-30 nm with depth of 4-6 nm. From small area STM image, we obtained that the GaN film consisting of arrays of narrow (width 50-100 nm) terraces with step heights ~ 3 Å close to one monolayer (2.6 Å) thick GaN(0001) and surface pits were mostly found at the junction of several steps.

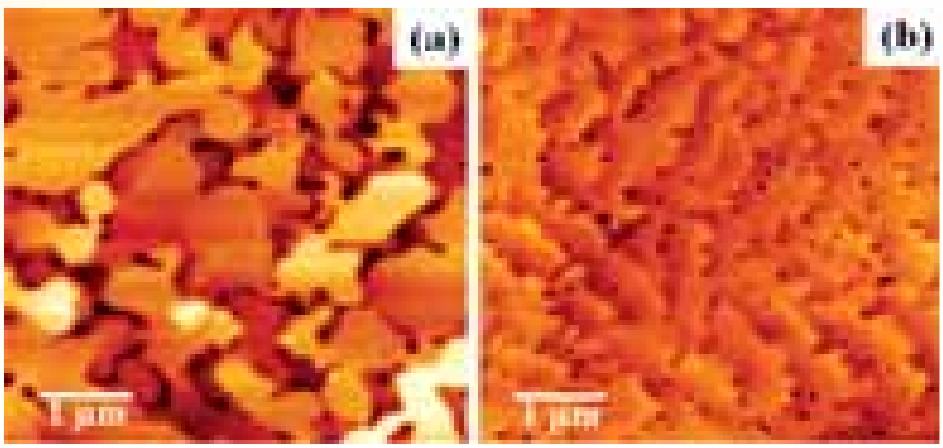

Fig. 1.27: AFM images of PAMBE grown GaN films grown on 3.5 mm epilayer GaN template on c-sapphire at different plasma power: 425 W (b) 250 W. Scan area: 5 *m*m × 5 *m*m

Similar trend was seen with the HR-XRD rocking curve ω-scan. It indicates a decrease in the full width at half maximum (FWHM) value of the film grown at a lower plasma power. Symmetric (002) and asymmetric (102) ω-scan of the two GaN films have been acquired. FWHM value for the ω-scan for sample with a plasma power of 425W is 239 arc-sec and 396 arc-sec for (002) and (102) planes respectively. As the plasma power is decreased to 250 W, the FWHM value decreases to 237 arc-sec and 356 arc-sec for (002) and (102) planes respectively.

(iii) Growth and Characterization of High Quality Single crystalline Homoepitaxial GaN films grown by RF-Molecular Beam Epitaxy

High quality single crystalline homoepitaxial GaN films were grown using RF plasma assisted Molecular Beam Epitaxy (RF-MBE) on MOCVD grown GaN/Sapphire template. In order to grow high quality single crystalline GaN films, the growth parameters such as flux, substrate temperature, RF- power etc have been optimized. GaN films were grown under different substrate temperature (730 and 745°C) at RF power 500W. The AFM image shows that the surface consists of array of terraces (width 500 nm) separated by bunch of atomic steps (~45 Å) for sample "a" while a very smooth surface morphology with step flow growth (step height of 4-5 Å and r.m.s roughness ~ 0.3 nm for 1x1 mm^2 area) is observed for sample "b". FESEM images supported the AFM results. HR-XRD rocking curve (Figure 1.28(c)) shows the high quality single crystalline homo-epitaxial GaN films with FWHM 169 arcsec & 179 arcsec for sample "a" and "b" respectively. The photoluminescence spectra of both the samples show a very sharp band-to-band emission at 363nm. A small peak corresponds to yellow band emission (560nm) is observed for sample "a" while no such emission is observed for sample "b". These results are comparable with the internationally reported values for GaN films. In summary, high quality epitaxial GaN films were grown by using RF-MBE with competitive results.

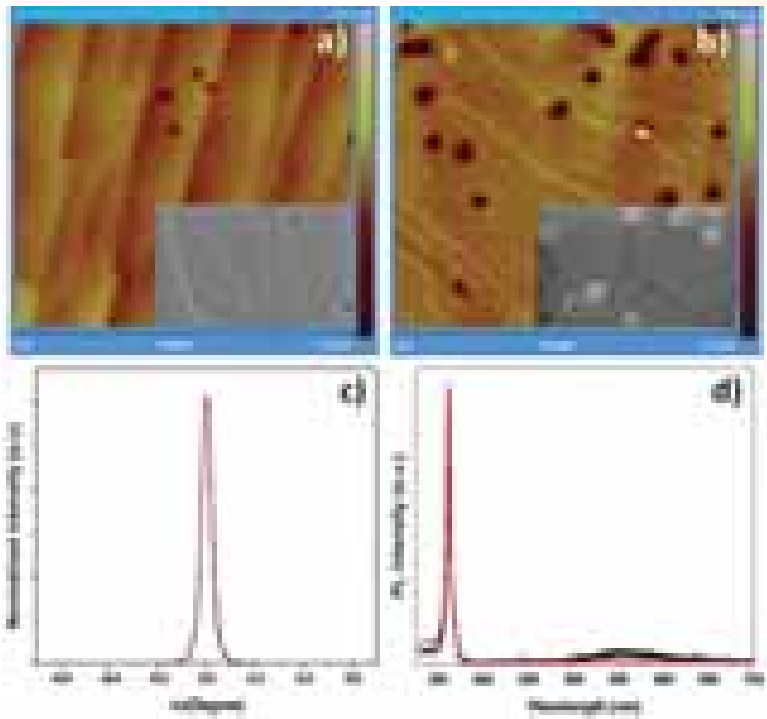

Fig. 1.28: a) and b) shows the AFM images of GaN surface grown at 730 and 745°C respectively (inset shows the corresponding FE-SEM image). c) HR-XRD data of both the samples and d) PL spectra of GaN films

(iv) A New Approach to Clean GaN Surfaces

III-nitrides are well established materials having key importance in the field of solid state lighting, sensors and photovoltaic devices. The fabrication and preparation of these GaN based devices require processing in different ambient and causes surface contamination and it is very essential to prepare clean surface for fabrication of any efficiently working device as the contamination significantly affects the electronic structure, quality of metal contacts and hence the overall device performance. The pervious reported cleaning procedures lack their commercialization because of their complex and time consuming nature. A new, quick and simple approach is adopted which demonstrate the effectiveness to clean GaN surfaces. The method involve ex-situ chemical etch followed by in-situ thermal annealing, which can be used at commercial level. X-Ray and Ultra-violet photoelectron spectroscopic analysis revealed significant changes in elemental composition, electronic structure, band alignment and surface chemistry after cleaning of the films. The cleaning resulted in drastic reduction in surface contaminations by achieving a surface with no Carbon as well as minimal remnant Oxygen species. The stoichiometry, n_O/n_N ratio, electron affinity and ionization energy of the cleaned GaN film were also calculated.

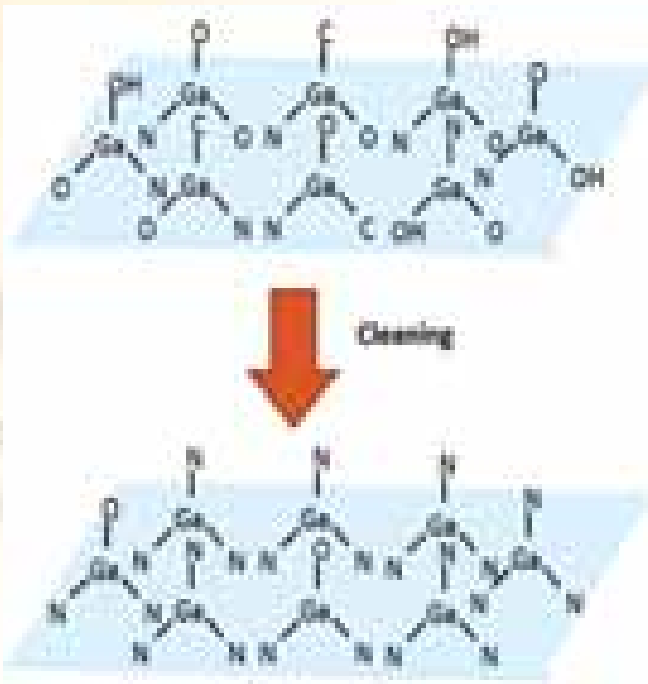

Fig. 1.29: Schematic for new approach to clean epitaxially grown GaN surfaces

(iv) Growth and Rutherford backscattering spectroscopy of GaN epitaxial layers grown on sapphire (0001) by ultra high vacuum pulsed laser deposition technique

GaN epitaxial layers have been grown hetero-epitaxially on c-plane sapphire substrate using an ultra high vacuum pulsed laser deposition (UHV-PLD) technique. Different targets such as liquid gallium metal and bulk GaN polycrystal were ablated for the GaN growth in the presence of r.f. nitrogen plasma. The grown GaN layers were characterized for their structural properties by high resolution x-ray diffraction (HRXRD) and Rutherford back scattering (RBS) spectroscopy. From HRXRD, the GaN layers grown under r.f. nitrogen plasma were found to grow epitaxially on sapphire (0001) substrates with good crystalline quality. The (0002) plane x-ray rocking curve measurements revealed the full width at half maximum of 110 and 245 arc sec for the GaN layers grown using solid HVPE grown GaN solid and Ga liquid targets, respectively. The quantitative analysis of crystalline quality near interface and film region of the grown GaN layer has been examined using Rutherford backscattering geometry (RBS) in channeling condition. A well-collimated (divergence ~ 0.05°) He^{++} ion beam of energy 3 MeV from 1.7 MV Pelletron accelerator was used for the RBS/channeling measurements. The backscattered particles were detected using a surface barrier Si detector at an angle of 165° with respect to the incident beam. The RBS spectra of the GaN layers grown using two different targets are presented in Fig. 1.30. In all cases, the signal from Ga, Al, O and N are clearly seen in the RBS spectra. The channeling is poor with large yield at the GaN/sapphire interface region due to the formation of high density of TDs and low angle grain boundaries.

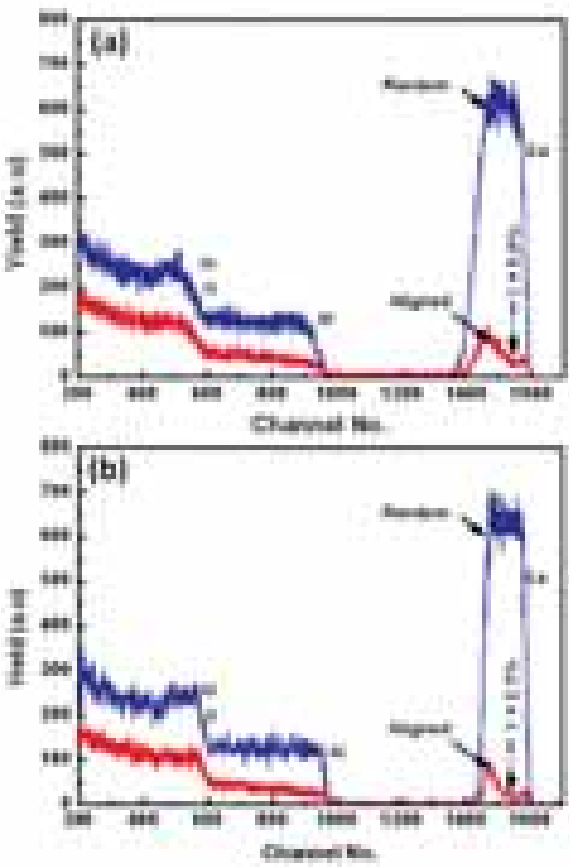

Fig. 1.30: Rutherford backscattering spectrum of GaN epitxial layers grown on sapphire (0001) substrate by UHV-PLD technique using (a) liquid galium and (b) HVPE grown GaN solid targets

However, in the film region, the ion channeling yield (Y) (the ratio of the backscattering yield of aligned direction to that from the random direction in the near surface region) is very low, i.e. ~5.9 % for the GaN layer grown using liquid gallium target and ~2.3 % for the layer grown out of bulk GaN target. The low RBS yield in the aligned direction is an indication of the high crystalline quality of the grown GaN layers. The GaN layers are also found to be highly stoichiometric. The GaN layers grown using HVPE grown bulk GaN target has the superior crystalline quality.

Optical Thin Films

R&D work was carried on the characterization of a variety of samples such as GaN, oxides etc using the DLTS technique.

Silicon Thin Film Photovoltaic

Amorphous & micro/nano crystalline silicon thin films for solar cell application

R & D Activities:

During this period, we continued further to work for optimization of process condition for deposition of amorphous & microcrystalline silicon thin films using recently refurbished multi-chamber PECVD system. Doped and undoped films were grown as a function of various process conditions such as pressure, frequency, power and hydrogen & Argon dilution. Under optimized process condition p-i-n solar cells were made. Subsequently process was scaled up for the area of 4 inch x 4 inch.

Optimized p-i-n layers were deposited in separate chambers having dark and photo conductivities values as $1.0x10^{-5}$, $2.4x10^{-10}$, $3.9x10^{-3}$ and $1.2x10^{-5}$, $1.5x10^{-5}$, $5.0x10^{-3}$ $\Omega^{-1}cm^{-1}$ respectively. These layers were deposited on various size of substrates from 1 inch x 1 inch to 4 inch x 4 inch. Using these p-i-n layers single junction solar cells was made and the efficiency (η) of these cells were measured at 100 mW/cm^2 on 1 inch x 1 inch & 4 inch x 4 inch p-i-n layers deposited on TCO as front contact and Al as back contact (various size defined as cell): smallest size: 1mm dots (η: 8.45% max., 5.46% average) & biggest size: 80 mm x 8 mm (η: 0.76%). Further optimization of doped and undoped layers of amorphous & microcrystalline silicon layers is in progress to get uniform efficiency over 4 inch x 4 inch area. The isolation of devices is in progress to reduce the leakage current.

During this period simulation work was also carried out for understanding & improvement of the efficiency of single junction microcrystalline p-i-n silicon solar cells by computer aided one-dimensional AFORS-HET software. The optimized values of band gap of p-, i- and n-layers of μc-Si:H were found to be 1.5 eV, 1.4 eV and 1.5 eV and their thicknesses were found to be 5 nm, 2000 nm and 20 nm, respectively. The optimization of values of N_a (acceptor concentration) and N_d (donar

concentration) were also performed and highest efficiency of 17% for μc-Si:H is realized at N_a and N_d of 10^{20} cm^{-3}. This study will be useful to solve the issues associated with existing μc-Si:H solar cell technology and may help in fabricating high efficiency micromorph solar cells.

Chemical Route for Compound Semiconductor PV

CIGS Activity

(i) CIGSe&CZTSe films were synthesized by colloidal route (aqueous free) and without resorting to post-selenization treatments at high temperatures. Successive purification steps lead to effective removal of insulating barrier of TOP/TOPO capping ligands from the surface of CIGSe nanocrystals which improves the charge transport properties considerably.

(ii) CZT films were deposited by pulsed laser deposition (PLD) technique using a composite target made of Cu2ZnSn (CZT). Deposited CZT thin films were found to consist of Cu:Zn:Sn in atomic ratio of 38:51:11.

पदार्थ भौतिकी एवं इंजीनियरिंग

Materials Physics and Engineering

Dr Ashok M. Biradar
Chief Scientist Email : abirador@nplindia.org

D02.01 Polymer & Soft Materials

Dr Ashok Manikrao Biradar
Dr Krishan Kumar Saini
Dr S K Dhawan
Dr Rajesh
Dr Nirmalya Kumar
Dr Pankaj Kumar
Sh Parveen Saini
Sh Chander Kant
Sh Vinod Kumar Tanwar

D 02.02 Physics & Engineering of Carbon

Dr Rakesh Behari Mathur
Dr Sanjay Rangnate Dhakate
Dr Bhanu Pratap Singh
Dr (Ms) Priyanka Heda Maheshwari
Dr (Ms) Saroj Kumari
Sh Pinaki Ranjan Sen Gupta
Sh Rajesh Kumar Seth

D 02.03 Luminescent Materials and Devices

Dr (Ms) Santa Chawla
Dr Divi Haranath
Dr Bipin Kumar Gupta

D 02.04 Multiferroics and Magnetics

Dr R K Kotnala

D 02.05 Biomedical Instrumentation

Dr Ashok Manikrao Biradar
Dr (Ms) Gajala Sumana
Dr Ved Varun Agrawal
Sh Manoj Kumar Pandey

D 02.06 Metals & Alloys

Dr Ajay Dhar
Dr Vipin Jain
Dr Dinesh Kumar Misra
Dr (Ms) Nidhi Singh
Sh Bathula Sivaiah
Sh M Saravanan
Sh Rajiv Sikand

Materials Physics and Engineering Division

This division has been dedicated to develop state of the art materials, processes and technologies for Industrial and Strategic sectors through synergistic R&D efforts in the chosen areas. The division has active collaborations with different R&D organizations, such as, CSIR laboratories, DST, IITs, Delhi University (DU), etc. through developmental projects or higher educational programs.

The *Soft and Polymeric Materials section* is dedicated to research in fundamental and applied science of polymers, soft materials and liquid crystals. Research in liquid crystal has substantially grown in recent years. Ordering in these mesophases results in light transmission under crossed polarizers. NPL is focusing on the tuning of electro-optical properties of ferroelectric liquid crystals by doping with various types of nanomaterials like metal and metal oxide nanoparticles, quantum dots, carbon nanotubes and graphene etc. Recently the group has started diversification in the field of liquid crystals into non-display applications also, such as development of biosensors based on liquid crystals, studying the dynamics of liquid crystal interface with various immiscible fluids *etc.*. Also, the group has been developing high performance microwave absorption material for the radar absorbing application through encapsulation of barium strontium titanate (BST) and expanded graphite (EG) in polyaniline (PANI). A tubular core-shell morphology having reduced graphene oxide (rGO)/γ-Fe_2O_3 in polyaniline (PANI) core is developed as high shielding effectiveness/EMI absorbable material. The fabrication of SWNTs/graphite nanoplates(GNPs) hybrids based field-effect transistor (FET) deviceis demonstrated for the label free detection of cardiac biomarkers for the diagnosis of cardiovascular diseases (CVD).

The *Physics and Engineering of Carbon* section has synthesized low cost high yield continuous carbon nanofibers from PAN and PVA polymers using a novel "Electrospinning" technique. Lightweight carbon foams (CFoams) decorated by Fe_3O_4 and ZnO nanoparticles are developed that have demonstrated excellent EMI shielding response. Under a CSIR-TAPSUN project (NWP-56), nanosized SnO_2 incorporated long length MWCNTs are used to develop free standing binder less conducting paper, which is successfully demonstrated as anode inlithium (Li)-ion battery at CECRI-Karaikudi. MWCNTs supported platinum is also synthesized as catalyst for the development of cost competitive PEM fuel cell.

The *Luminescent Materials and Devices* section has fabricated a dual excitation, dual emission phosphor by simultaneously doping of lanthanide ions Er^{3+}, Yb^{3+}, Eu^{3+} in a highly efficient host YVO_4 for solar cell application. It is demonstrated that silver nanoprism (Ag NP) generates near field and act as multipolar nano-antenna. A novel red-emitting $Gd_2CaZnO_5:Eu^{3+}$ (GCZO:Eu^{3+}) nanophosphor system is developed. Further efforts are underway to develop $Gd_2(MoO_4)_3$:RE (Eu, Er, Yb) nanophophor as a Broad Spectral converter (UV-IR) for promising Next Generation silicon solar cells.

The *Multiferroics and Magnetics* section has developed capability for the precise calibration of NMR Teslameter and successfully installed Cesium Magnetometer as a primary standard. Onsite survey for electromagnetic radiation and calibration of ELF/EMF meters is initiated. Thin films of Magnesium ferrite, ceria added magnesium ferrite and $BaTiO_3$ doped with 0.1 at% Cr (Cr:BTO) are developed by the pulsed laser deposition technique. Spin pumping induced spin-Hall effect is investigated in RF sputtered Co/Pt bilayer thin lm forspintronics application.

The *Biomedical Instrumentation* section has successfully established a DST center for biomolecular electronics. Two prototype devices for the detection of total cholesterol are developed. Stable cationic poly (lactic-co-glycolic acid) (PLGA) microspheres encapsulating the iron oxide nanoparticles are synthesized for the development of a DNA biosensor. Controlled synthesis of electroactive gold nanoparticles (AuNP) is conducted and biosensing performance is investigated. A label-free CysCdS-Au biosensor platform/ device is developed to investigate the biomolecular interactions.

The *Metals & Alloys Group* has synthesized Cu_3SbSe_3 thermoelectric material with intrinsically ultralow lattice thermal conductivity for the development of thermoelectric devices. A new half-Heusler Derivative $Zr_9Ni_7Sn_8$ Bulk Nanocomposite with enhanced thermoelectric performance is developed. The development of novel Rare-Earth Free Permanent Magnetic Materials, e.g.,MnAl, Mn-Bi-Fe, manganese antimonide,etc is under progress using the melt spinning technique. Lightweight and high strength Aluminum-carbon nanotube composites are also under development using cryomilling and hot extrusion.

Polymer and Soft Materials

Faster display devices with improved contrast based on MgO nanoparticles/ ferroelectric liquid crystal composites

We have studied and reported that by dispersing magnesium oxide nanoparticles (MgO NPs) into the host ferroelectric liquid crystal (FLC) W301, MgO NPs/FLC composite showed significantly faster response and improved optical tilt angle. The fastening of response time in MgO NPs/FLC composite has been attributed to the decrease in rotational viscosity and increase in surface anchoring energy. Due to the enhanced surface interaction of MgO NPs having surface defects with mesogens, a strong surface anchoring is experienced on the FLC molecules that not only fastened the response but also improved the optical tilt angle of the MgO NPs/ FLC composites, which ultimately resulted in improved contrast. A systematic approach has been followed to elucidate an idea of designing faster display devices with improved contrast based on MgO NPs/FLC composites. Nanosized particles of MgO were synthesized *via.* hydrothermal method from magnesium nitrate ($MgNO_3.6H_2O$), sodium hydroxide (NaOH) and de-ionized water (H_2O) as precursors in appropriate amount. From electron microscopic investigation, it has been seen that the size of these NPs ranged between 30 to 60 nm with an average size of about 50 nm. The MgO NPs/ FLC composite was prepared by adding various concentrations (wt.%) of nanopowder of MgO NPs with the FLC material. The mixture was then ultrasonicated for about 40 min. in the isotropic phase of the FLC material to ensure the homogeneous dispersion of MgO NPs in the FLC host material. The pure and MgO NPs doped W301 material were then introduced into the LC sample cells by means of capillary action at temperature just above the isotropic transition temperature.

Faster electro-optic response of MgO NPs/ FLC composites

The electro-optic response time at room temperature (25 °C) for various concentrations of

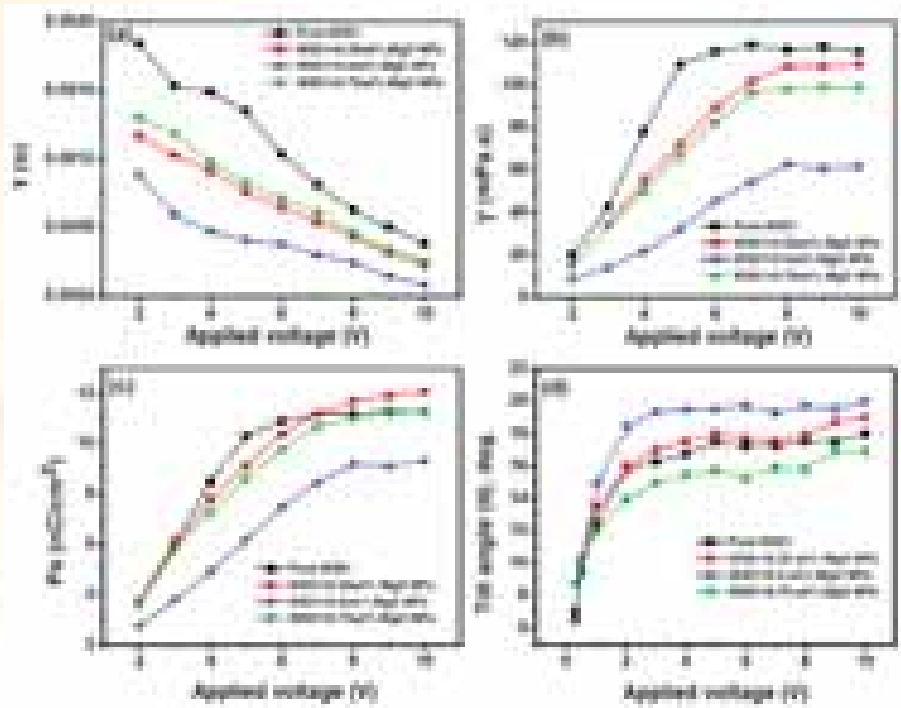

Fig.2.1: Behaviour of (a) response time (τ), (b) rotational viscosity (γ), (c) spontaneous polarization (Ps), and (d) optical tilt angle (θ) of pure and different concentrations of MgO NPs doped FLC material W301 at room temperature

MgO NPs doped FLC material, W301 as a function of applied voltage and a comparison with pure W301 is shown in Fig. 2.1(a). It is clearly seen from the Fig. 2.1(a) that the MgO NPs/FLC composites respond faster than pure W301 and the response time shows a strong dependence on MgO NPs concentration. On the systematic assessment of the response time of composites with different concentration of MgO NPs, 0.5 wt.% showed the fastest response and it had fastened the response time by ~50% than the pure FLC. From Fig. 2.1(a), it is seen that the value of response time of pure W301 is 1.6 ms at an applied voltage of 4 V whereas, 0.5 wt.% MgO NPs doped W301 showed its electro-optic response in 0.8 ms.

The rotational viscosity of LC material is directly related to its response time as follows;

$$\tau = \frac{\gamma}{P_S E} \quad \text{.....(1)}$$

where τ is response time, γ is the rotational viscosity, Ps is the spontaneous polarization, and E is the applied electric field respectively. It is seen from Fig. 2.1(b) that the rotational viscosity of the FLC material W301 is decreased on doping with MgO NPs, which is in good agreement with the above mentioned relation. The reduction in rotational viscosity is attributed mainly due to two reasons. Firstly, due to the non-trivial dielectric anisotropic properties of the MgO NPs and FLC material, both experience a torque on the application of electric field and hence rotational viscosity is decreased. Secondly, perturbations in order parameters such as spontaneous polarization and optical tilt angle of FLC material on doping with MgO NPs reduce the rotational viscosity of FLC, which is illustrated in Fig. 2.1(c) and Fig. 2.1(d). Surface anchoring energy and cell gap of LC also play a key role in LC response time. The relation between response time and anchoring energy for strong anchoring is as follows;

.....(2)

where τ is the response time, γ is the rotational viscosity, K_{33} is the bent elastic constant, d is the cell gap and W is the anchoring energy strength coefficient respectively. It is clear from the above mentioned equation that response time is reduced on increase of anchoring energy strength.

Enhancement in optical tilt angle and contrast of MgO NPs/ FLC composites

As seen in Fig. 2.1(d), the optical tilt angle is enhanced on doping with MgO NPs and it is having a strong dependence on MgO NPs concentrations. Here, on doping with 0.5wt% of MgO NPs the value of tilt angle showed an increment of ~2.5° in all applied voltages above 1 V. The MgO NPs used in this study is having a non-zero dipole moment along (111) plane (ref.: JCPDS file no. 870652, lattice parameter: a = 0.4211 nm). Thus the MgO NPs having inherent dipole moment interact with the dipolar mesogens, which results in the improvement of optical tilt angle. Improvement in optical tilt ultimately leads to the improvement of contrast of LC displays.

Fig. 2.2 exhibits a schematic diagram of the interaction of MgO NPs with mesogen. Due to the dipole-dipole interaction between the FLC molecules and NPs a strong intrinsic field inside the sample is created.

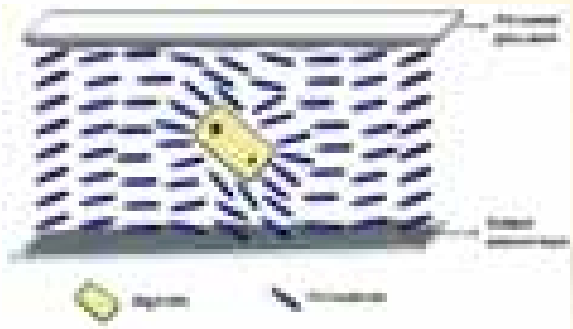

Fig. 2.2: Schematic representation of MgO NPs doped W301 material filled cell

The optical micrographs indicating the dark and bright states of pure (Fig. 2.3(a) and (b)) and doped samples (Fig. 2.3(c) and (d)) are shown. From this figure it is seen that the molecular alignment of FLC material, W301 is improved on doping with MgO NPs. The light leakage in the dark state of doped samples (Fig. 2.3(c)) is also reduced, giving an improved darkness due to the dipole-dipole

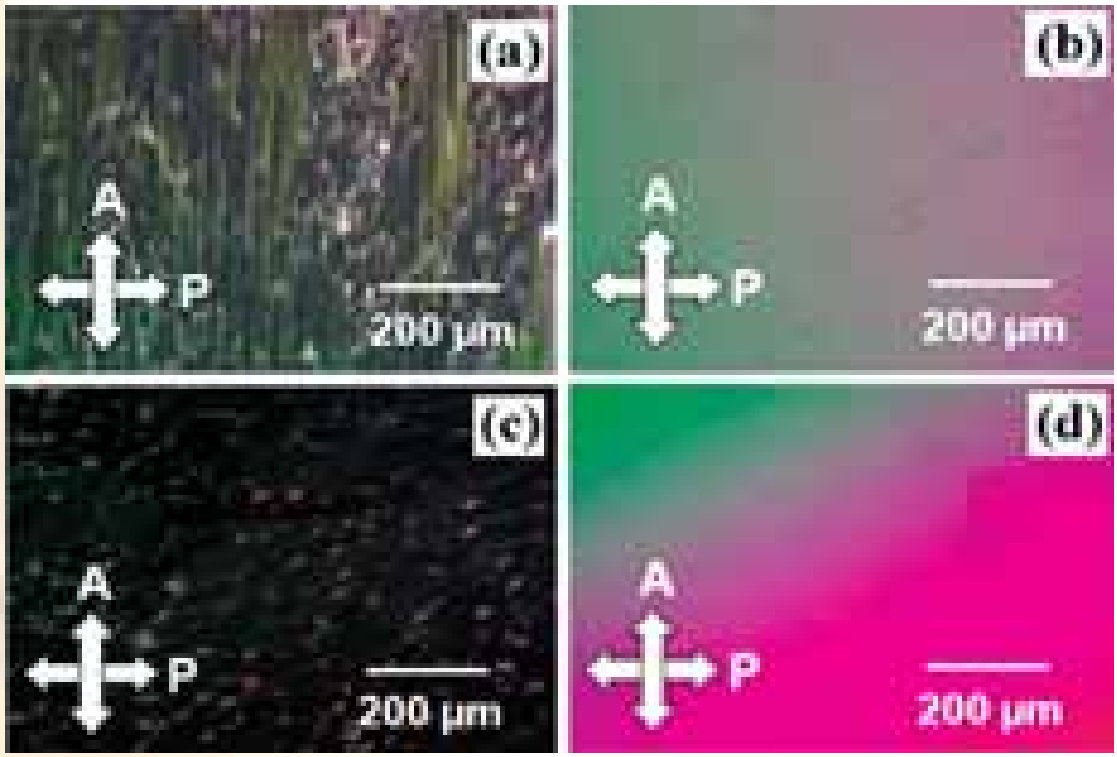

Fig. 2.3: Polarizing optical micrographs showing (a) dark and (b) bright states of pure W301 material and (c) dark and (d) bright state of MgO NPs doped W301 material filled cell

interaction and increase of surface anchoring strength of FLC with NPs. The bright state (Fig.2.3 (d)) also shows an improved texture than pure W301 (Fig. 2.3(b)).

For quantifying this, we had taken the characteristics of optical spectrum intensity with wavelength of pure and doped samples. Fig. 2.4 shows the fitted data of the optical spectrum intensity versus wavelength from spectrum analyzer of the pure and doped samples at dark state (Fig. 2.4(a)) and bright state (Fig.2.4(b)).

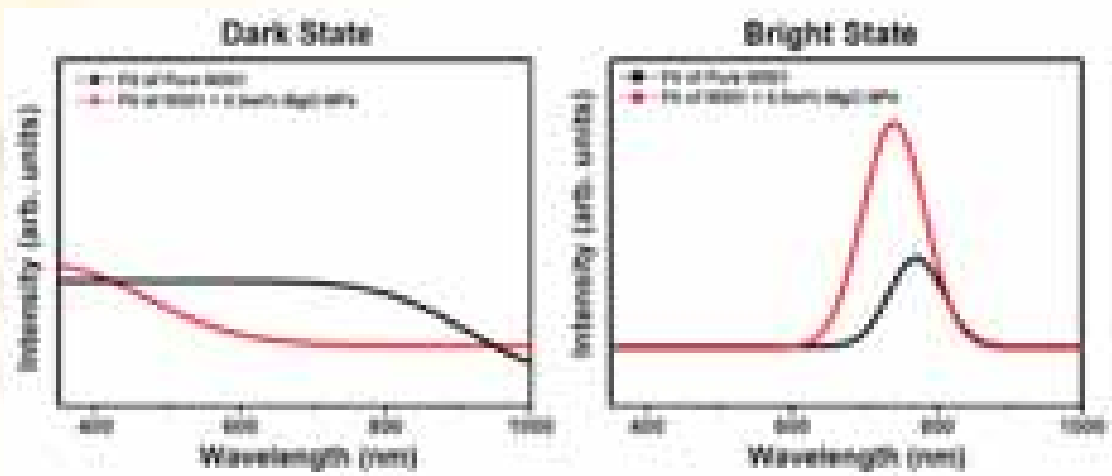

Fig. 2.4: The fitted data for the optical spectrum intensity versus wavelength from spectrum analyzer of the pure W301 and MgO NPs doped sample at (a) dark state and (b) bright state

It is clearly seen from the Fig. 2.4(a) that the intensity of dark state is less for the doped sample while the intensity of bright state is almost doubled (Fig. 2.4(b)) than the pure W301. A clear confirmation of improvement of contrast is obtained from this, where the dark state of the sample became darker and the bright state became brighter on doping with MgO NPs.

This report systematically presented the feasibility of fabricating MgO NPs/FLC composites having faster response time with improved contrast for future display applications and other electro-optic applications, such as beam steering or polarization shutters.

Self assembled monolayer based liquid crystal biosensor for free cholesterol detection

A unique cholesterol oxidase (ChOx) liquid crystal (LC) biosensor, based on the disruption of orientation in LCs, is developed for cholesterol detection. A self-assembled monolayer (SAM) of Dimethyloctadecyl [3-(trimethoxysilyl)propyl] ammonium chloride (DMOAP) and (3-Aminopropyl) trimethoxy-silane (APTMS) is prepared on a glass plate by adsorption. The enzyme (ChOx) is immobilized on SAM surface for 12 h before utilizing the film for biosensing purpose. LC based biosensing study is conducted on SAM/ChOx/LC (5CB) cells for cholesterol concentrations ranging from 10 mg/dl to 250 mg/dl. The sensing mechanism has been verified through polarizing optical microscopy, scanning electron microscopy, and spectrometric techniques.

The schematic of whole procedure is shown in Fig. 2.5, which highlights the design of the current LC based biosensor. It is well known that alignment of LC is highly dependent on the surface effects. A slight change on the surface leads to change in the alignment of LC molecules, which can be detected through a polarizing optical microscope (POM). This notion is used in the present study. For this purpose, a reference cell is used to achieve the homeotropic alignment of 5CB using above mentioned SAM. In this configuration, no light is passed through the LC cell. The presence of cholesterol can be detected in terms of non-zero transmitted light intensity through the LC cell containing cholesterol solution.

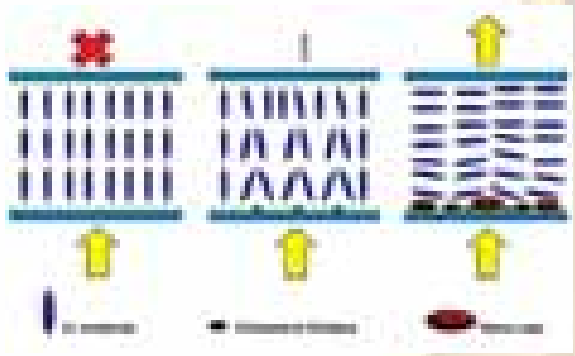

Fig. 2.5: Schematic showing idea and working of proposed liquid crystal based cholesterol biosensor. (a) No light transmission in case of homeotropic alignment (b) Slight transmission of light due to the presence of ChOx (c) Maximum light transmission in case of homogeneous alignment caused due to the presence of cholesterol

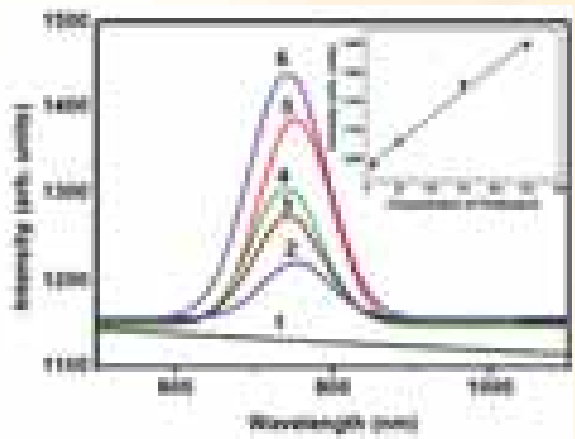

Fig. 2.6: Intensity of transmitted light through liquid crystal cells as a function of wavelength recorded using a spectrometer for (a) reference cell (b) enzyme cell (c) biosensing cell with cholesterol concentration as 10 mg/dl (d) 50 mg/dl (e) 150 mg/dl and (f) 250 mg/dl

Here, the intensity of transmitted light through different surface treated LC cells is measured with a spectrometer and plotted as a function of wavelength. The various plots are shown in Fig. 2.6. It can be inferred that the intensity increases with an increase in cholesterol concentration. The homeotropic alignment resulting from the reference cell shows the lowest intensity, which acts as a reference and shown as 1. However, immobilization of ChOx enzyme itself

brings change in the alignment and thus shows higher intensity relative to reference, which is shown as 2. The various cholesterol concentrations show regular increment in intensity (3, 4, 5 and 6), which is the basis of cholesterol sensing. The intensity versus concentration of cholesterol is plotted and shown as inset of Fig. 2.6. Figure 2.6 simply summarizes the understanding and the working idea of LC based cholesterol biosensor.

Tailored polyaniline/barium strontium titanate/expanded graphite multiphase composite for efficient microwave absorption

Designing of high performance microwave absorbing material using a simple, cost-effective and scalable method by encapsulating barium strontium titanate (BST) and expanded graphite (EG) in polyaniline (PANI) matrix in the presence of dodecylbenzene sulfonic acid (dopant) in aqueous medium by chemical oxidative polymerization is reported. Different formulations have been prepared to study the effect of dielectric constituent on the electrical and dielectric properties of polyaniline composite. The optimum dielectric properties due to incorporation of BST and moderate conductivity due to embedded EG in PANI matrix collectively contribute in designing an absorption based shield. One of the formulation shows shielding effectiveness due to absorption more than 50 dB (>99.9999 % attenuation) while reflection loss less than 1 dB in Ku-band (12.4-18 GHz) frequency range. Since, observed attenuation of this absorption dominated shielding is greater than the recommended limit (30 to 40 dB) of commercial application therefore these are potentially applicable as radar absorbing material. The morphologies of BST, EG, PANI and PANI composites were investigated using SEM Fig. 2.7 (a) illustrate the BST nanoparticles derived from citric precursor method. In general, chemically derived BST nanoparticles results agglomeration similar to previous observations.

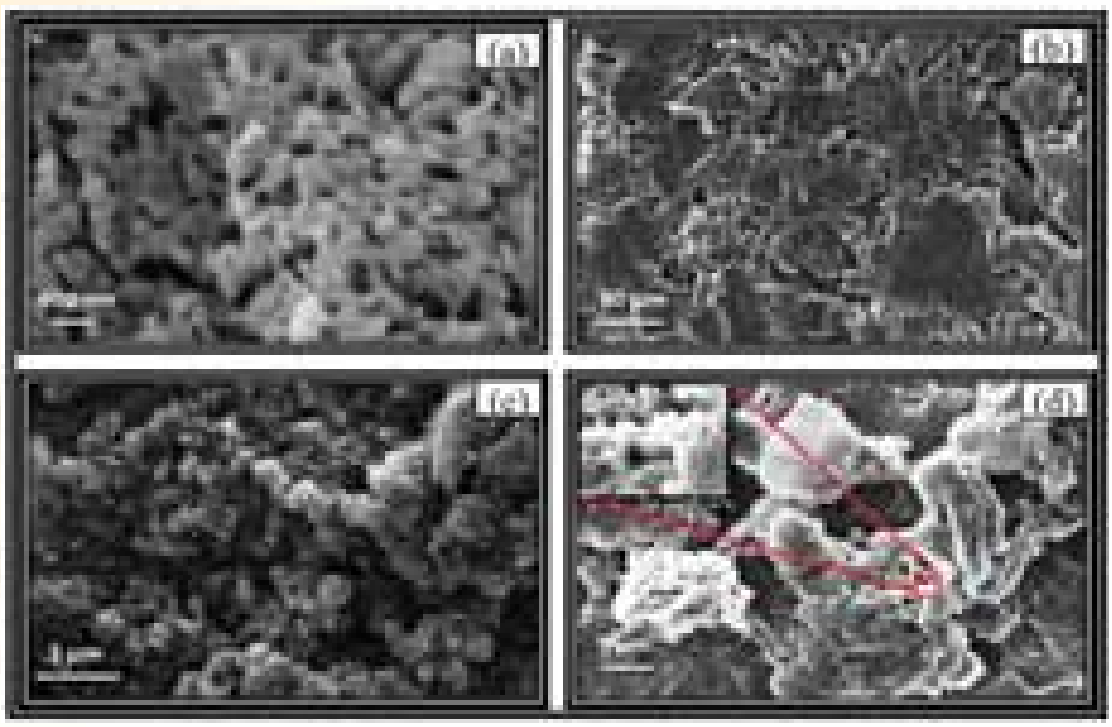

Fig. 2.7: SEM image (a) BST (b) EG (c) DBSA doped PANI and (d) PANI Composite

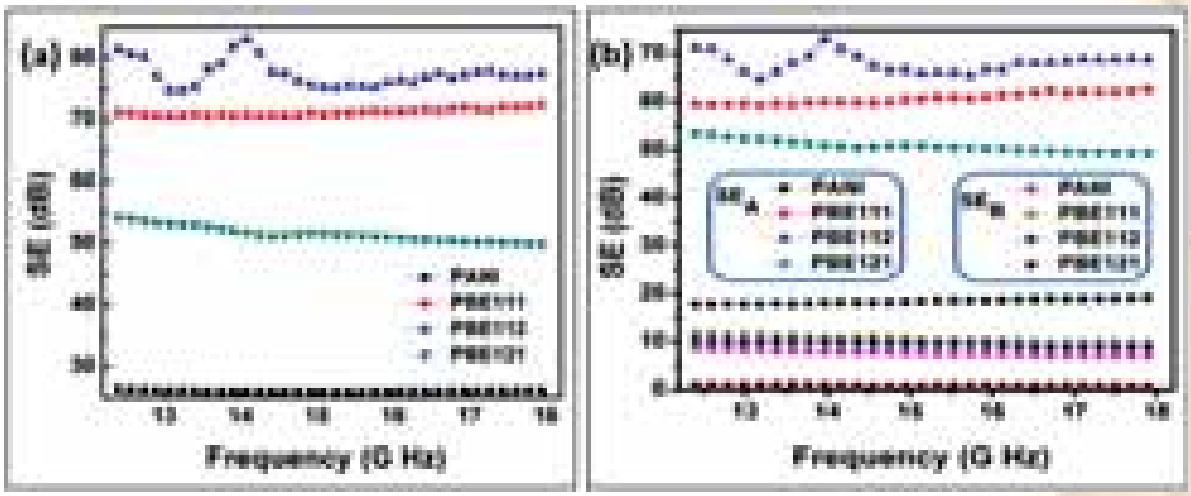

Fig. 2.8 (a) EMI SE (b) SE_A and SE_R of PANI and its composites in Ku band

The EG consisted folded and wrinkled sheets that were randomly aggregated and their sizes are up to a few micrometers as seen in Fig. 2.7 (b). Fig. 2.7 (c) shows the SEM image of DBSA doped PANI. The resulting PANI powder was homogeneous and form agglomerates with different sizes rock shapes. SEM micrograph of PBE121 composites revealed the presence of BST particles and EG sheets. BST particles are appearing as bright dots due to their nanostructure and EG appear as sheets (Fig. 2.7d).

Fig. 2.8 (a) shows the total SE while Fig 2.8 (b) illustrates the SE_A and SE_R of PANI and its composites. The SE value of 26, 71, 81, and 54 dB is achieved for PANI, PBE111, PBE112 and PBE121, respectively. Composite PBE121 gives very interesting SE result with SE_A more than 50 dB and SE_R less than 1 dB in entire frequency range. From the detailed shielding analysis, it has been observed that at 15.0 GHz, SE_A value increases with increase in EG content while SE_R have no significant change. Moreover SE_A and SE_R decreases with increasing content of BST in PANI-EG matrix. When the BST content reaches 9 wt% in PANI-EG matrix the SE_R values obtained less than 1 dB which is minimum value of reflection achieved so far with retaining optimum microwave absorption. EMI shielding using highly conducting materials such as metals is governed by reflection rather than absorption. On the other hand, hybrid conducting composite provide EMI shielding 'predominantly due to absorption, owing to the presence of electric dipoles.

Encapsulation of γ-Fe_2O_3 decorated reduced graphene oxide in polyaniline core-shell tubes as an exceptional tracker for electromagnetic environmental pollution

The ultimate goal of development of a new material γ-Fe_2O_3 decorated reduced graphene oxide (rGO):Polyaniline (PANI) core-shell tubes has been done for absorbing electromagnetic interference (EMI) pollution. Herein, we report the synthesis and characterization of a PANI tubes consisting of rGO decorated with iron oxide nanoparticles (RF). The intercalated RF was synthesized by thermal decomposition of ferric acetyl acetonate in reducing atmosphere. Furthermore, RF was further encapsulated through the oxidative polymerization of aniline in the presence of β–Naphthalene sulphonic acid which results in RF/PANI core-shell morphology. Scanning electron microscopy results confirm the formation of tubular core-shell morphology having 5-15 μm length and 1-5 μm diameter (Fig. 2.9). The presence of rGO/ γ-Fe_2O_3 in PANI core enhances the interfacial polarization and the effective anisotropy energy of the composite which contributes to more scattering and leads to the high shielding effectiveness

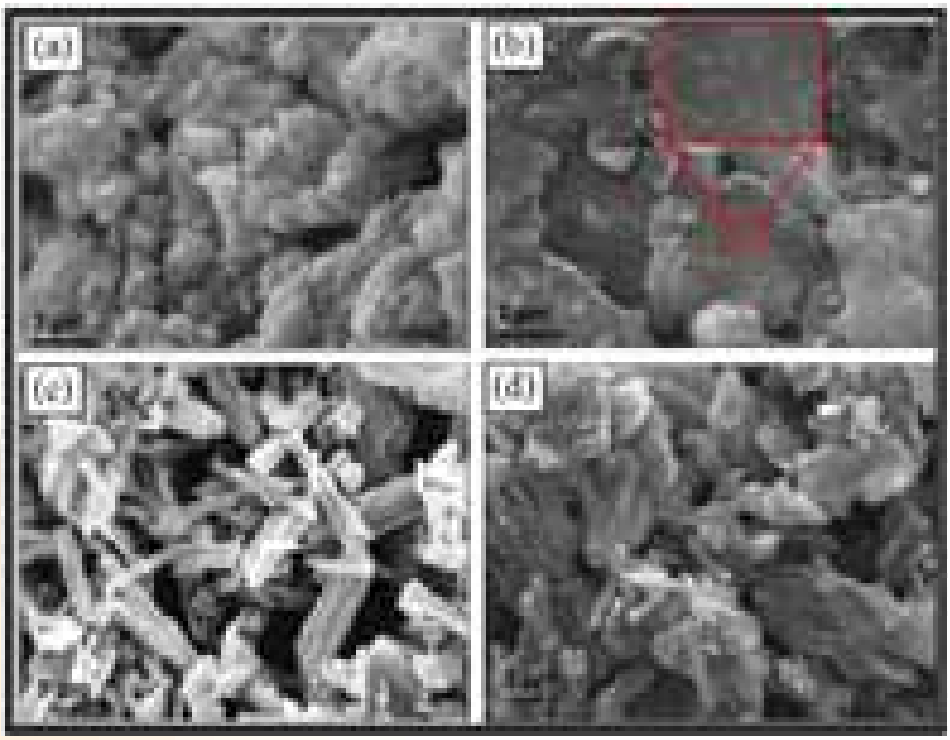

Fig. 2.9: SEM images of (a) iron oxide nanoparticles derived from $Fe(acac)_3$ by thermal decomposition at 186°C, (b) reduced graphene oxide sheets decorated with ã-Fe_2O_3 nanoparticles, (c) PRF10 and (d) PRF13, showing the formation of tube like structure with RF particles inside the tubes

(SE_T~51dB) at a critical thickness of 2.5 mm. Additionally, the effective complex permeability and permittivity parameters of composites have been evaluated from experimental scattering parameters (S11 & S21) using theoretical calculations given in Nicholson"Ross and Weir algorithms.

Synthesis of ferrofluid based nanoarchitectured polypyrrole composites and its application for electromagnetic shielding

The monodispersion of magnetic nanoparticles in conducting polymer is the

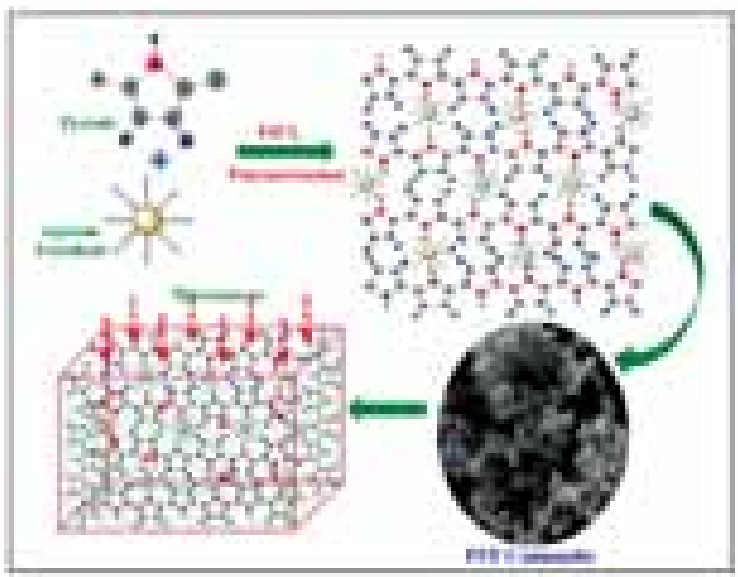

Fig. 2.10: Schematic representation for the synthesis of polypyyrole-ferrofluid nanocomposites

prerequisite to make a high quality composite for tunable electromagnetic interference (EMI) shielding. To meet this challenge, we have designed and synthesized ferrofluid based nanoarchitectured polypyrrole composites containing Fe_3O_4 (8-12 nm) via in situ oxidative polymerization as shown in Fig. 2.10. To tune the microwave signals, polypyrrole composites (PFF) with different monomer/ferrofluid weight ratios have been prepared and characterized in microwave frequency domain. A maximum shielding effectiveness value of SE_A(max) ~ 20.4 dB (~99% attenuation) due to the absorption of microwave has been observed in the frequency range of 12.4-18 GHz and attenuation level varied with ferrofluid loading. The electrical conductivity of PFF composite is of the order of 10^{-2} S cm^{-1} order and having superparamagnetic nature with saturation magnetization (Ms) of 5.5 emu g^{-1}. The lightweight PFF composites with high attenuations can provide full control over the atomic structure and are favorable for the practical EMI shielding application for commercial electronic appliances.

The variation of the SEA and SER with frequency for PPy and PFF composites in 12.4-18.0 GHz (Ku-band) is shown in Fig. 2.11. From the figure, it has been revealed that PFF composites show absorption dominated SE rather than reflection. In polypyrrole composite sheets with matching thickness of ~ 2.0 mm, maximum SE due to absorption (SE_A(max) has been ca. 20.4, 18.6 and 18.1 dB for PFF13, PFF12, and PFF11 samples at 18.0 GHz, respectively whereas the SEA(max) value of 17.6 dB has been observed for Py. For the reflection part, SE_R has been ca. 3.1, 2.9, 2.5 and 5.2 dB for PFF13, PFF12, PFF11 and PPy samples at 18.0 GHz, respectively. The results demonstrate that the absorption of microwave and overall shielding effectiveness (SE = SE_A + SE_R) up to 23.5 dB (~ 99.5% attenuation) for PFF13, increases with the concentration of the ferrofluid in the composite. The increase in the absorption with the addition of ferrofluid in PFF samples may be attributed to the higher dielectric and magnetic losses induced by Fe_3O_4 nanoparticles present in ferrofluid. In case of PPy, absorption is still the dominating factor but the reflection part is on the higher side, which makes it less favorable as microwave absorbing material.

Designing of green chitosan-polymer composite coatings for corrosion protection of mild steel in saline conditions

Chitosan-polypyrrole-SiO_2 composites were synthesized by chemical oxidative polymerization of pyrrole in chitosan solution using $FeCl_3$ as an oxidant. The synthesized composites were loaded

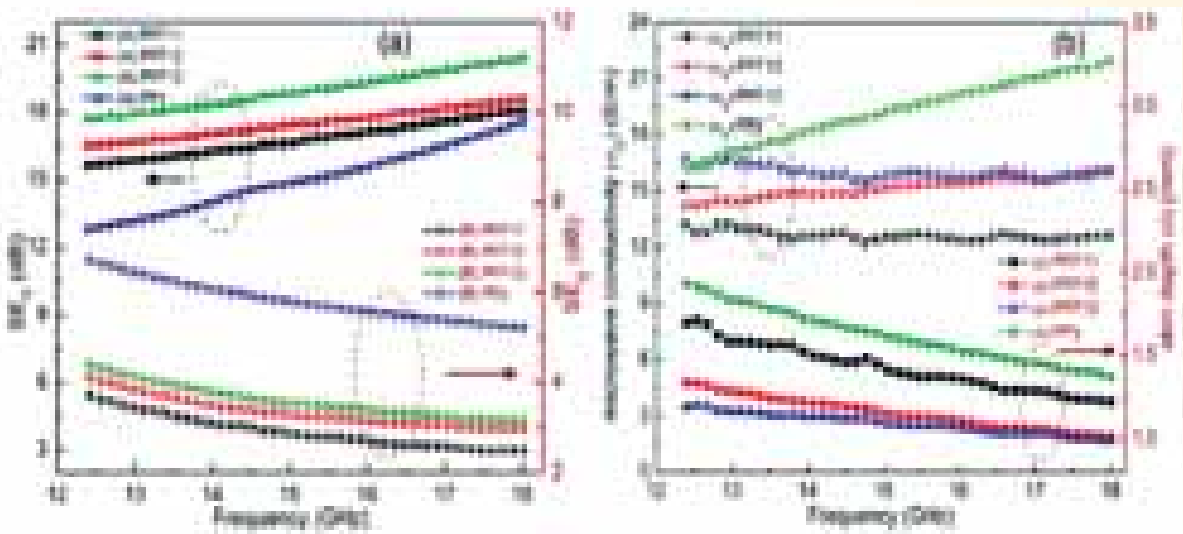

Fig. 2.11: (a) Dependence of shielding effectiveness (SE_A and SE_R) of PPy and PFF composites as a function of frequency (b) Variation of microwave conductivity with skin depth of PPy and PFF composites as a function of frequency

Table 2.1: Different electrochemical parameters obtained by Tafel extrapolation in 3.5% NaCl solution

Sample name	Loading of composite	Ecorr (mV)	Icorr (nA/cm^2)	Rp (KΩ)	Protection Efficiency (% P.E)
EC	-	-582.49	8.45x102	31.87	-
CsPC1	1.0 wt.%	36.46	0.51	105580	99.96
CsPC2	2.0 wt.%	20.75	0.24	156200	99.97
CsPC3	3.0 wt.%	-46.68	3.79	22632	99.85
CsPC4	4.0 wt.%	95.43	3.91	21068	99.84
CP	1.0 wt.%	-42.80	3.27	20580	99.83

in epoxy resin and subsequently coated on mild steel substrates using powder coating technique. XRD and FTIR analyses show a synergistic interaction between chitosan and polypyrrole. Microstructural analyses reveal the formation of polymer particles with distinct spherical morphology. SiO_2 particles embedded in the polymer matrix are clearly noticed from the FE-SEM micrographs. TGA thermograms show a better thermal stability of chitosan-polypyrrole-SiO_2 composite as compared to polypyrrole-SiO_2 composite (without chitosan). DSC curves reveal a high cross linking density for epoxy coatings loaded with chitosan composite. Tafel plots exhibits a significantly low value of corrosion current density (icorr) for epoxy coatings with 2 wt% loading of chitosan-polymer composite.

The corrosion protection efficiency (% P.E.) is measured to be maximum (99.97 %) for the epoxy coatings with 2 wt% loading of chitosan-polymer composite as given in Table 2.1. The weight loss measurements and salt spray test results clearly exhibit a significantly high corrosion resistance of chitosan-polymer composite coated mild steel substrates. Photographs of epoxy coated mild steel samples and polymer incorporated into epoxy powder coated on mild steel panels after 65 days under salt spray conditions is shown in Fig. 2.12.

Label free detection of cardiac biomarkers for the diagnosis of cardiovascular diseases

Cardiovascular disease (CVD) is the leading cause of morbidity and mortality worldwide and accounts for approximately half of all the deaths within the western world. Coronary ischemia is the root cause of acute myocardial infarction (AMI). As MI causes irreversible damage to the heart, a

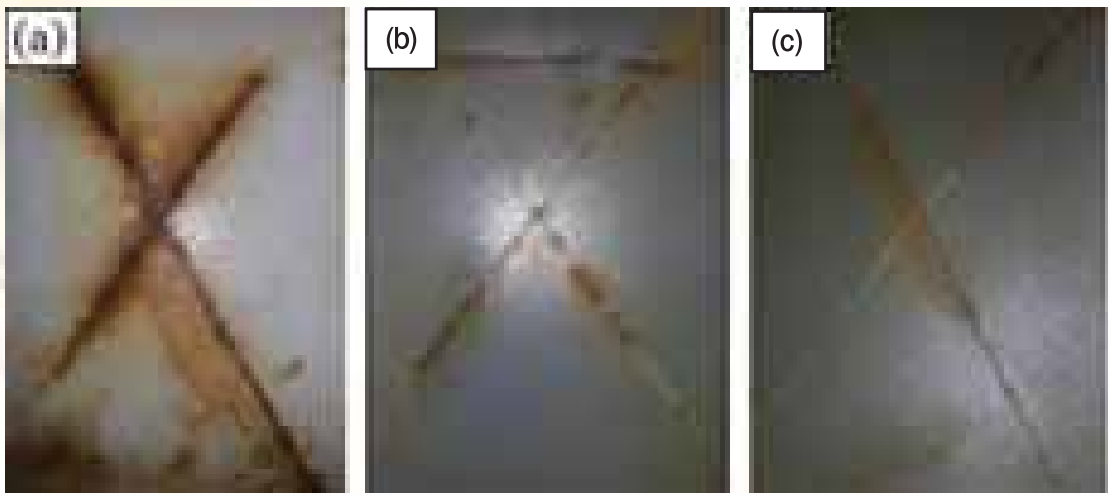

Fig. 2.12: Photographs of (a) epoxy coated and epoxy with (b) 1.0 wt%, (c) 2.0 wt% loading of chitosan-polypyrrole-SiO_2 composite (CsPC) coated mild steel specimens exposed to salt spray fog after 65 days

patient suspected of MI must be diagnosed quickly, efficiently, and comprehensively based on the information obtained from the measurement of cardiac specific biomarkers within the patient's blood. Hence, cardiac markers continue to play a major role in the diagnosis and management of patients suspected of having myocardial damage or AMI. Previously, the commonly used biomarkers for early detection of CVD included the MB isoenzyme of creatine kinase (CK-MB) and myoglobin. However, in the recent years, CK-MB has been replaced by cardiac troponin I (cTnI), a more specific biomarker. Based on literature data and clinical assessments, cTnI levels greater than 1.2 ng mL^{-1} is taken as the definition of AMI, making a cut off value of 0.1 ng/ml of cTnI to identify patients at higher risk for very early adverse outcomes.

We demonstrate the fabrication of single walled carbon nanotubes (SWNTs)/graphite nanoplates (GNPs) hybrids based nanoelectronic chemiresistive/FET device for the quantitative detection of cTnI (schematic shown in Fig. 2.13). The GNPs capped with 3-mercaptopropionic acid (MPA) are attached to SWNT through an organic molecular bilinker 1-pyrenemethylamine. The highly specific cTnI antibody was covalently immobilized on GNPs through capping agent using carbodiimide coupling reaction. The cTnI interaction to its corresponding complementary antibody was studied with respect to changes in conductance in SWNTs channel, and a detailed field-effect transistor characteristic (FET) was delineated.

The fabrication of the device at each step of surface modification of the aligned SWNTs was monitored by recording the current-voltage (I-V) characteristics from -0.5V to + 0.5V (Fig. 2.14a). Fig. 2.14b shows the dependence of the source-drain current, I_{sd}, on the back gate voltage, V_g, of the SWNTs FET after each surface modification steps in the range -40 to +40 V, at a drain voltage (V_d) of 0.1V.

It has been found that the charge transfer characteristic in SWNT hybrid device upon biomolecular functionalization is governed by the electrostatic gating effect without showing much change in the charge mobility. To investigate the sensitivity of the hybrid device, it was exposed to varying concentrations of target antigen cTnI in PBS (pH 7.4). Fig. 2.15 shows the normalized response of the cTnI-GNP/SWNTs hybrid $[(R-R_0)/R_0$, where R_0 and R is the resistance of the device measured before and after exposure to cTnI, as a function of cTnI concentration in PBS. The device exhibited a

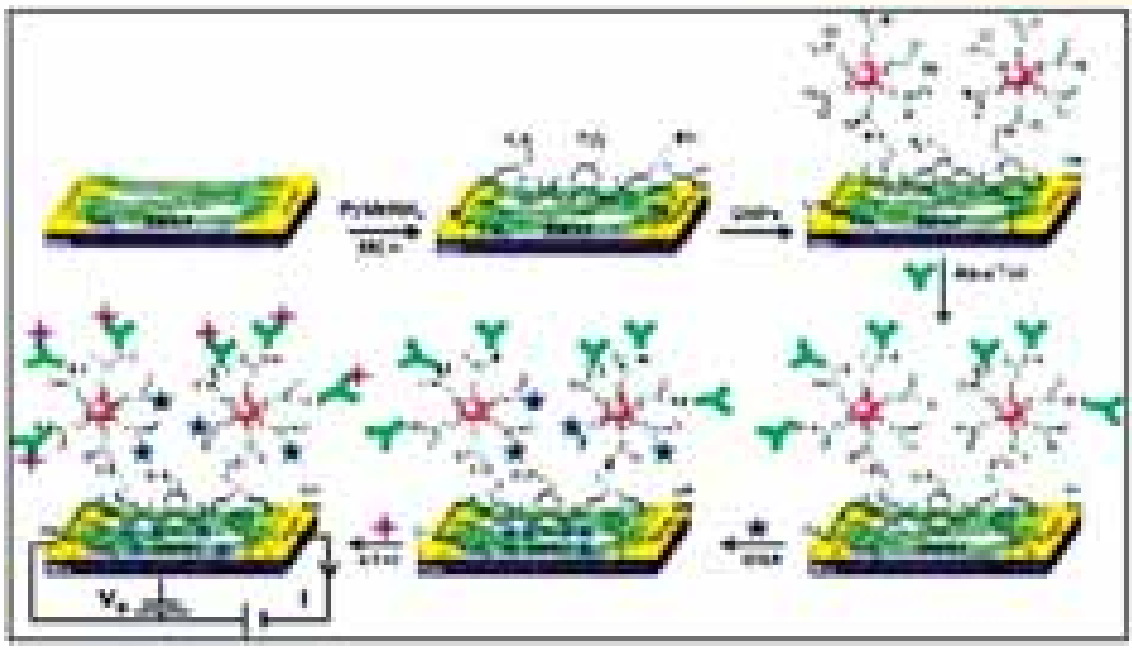

Fig. 2.13: Schematic illustration of the different stages of device fabrication

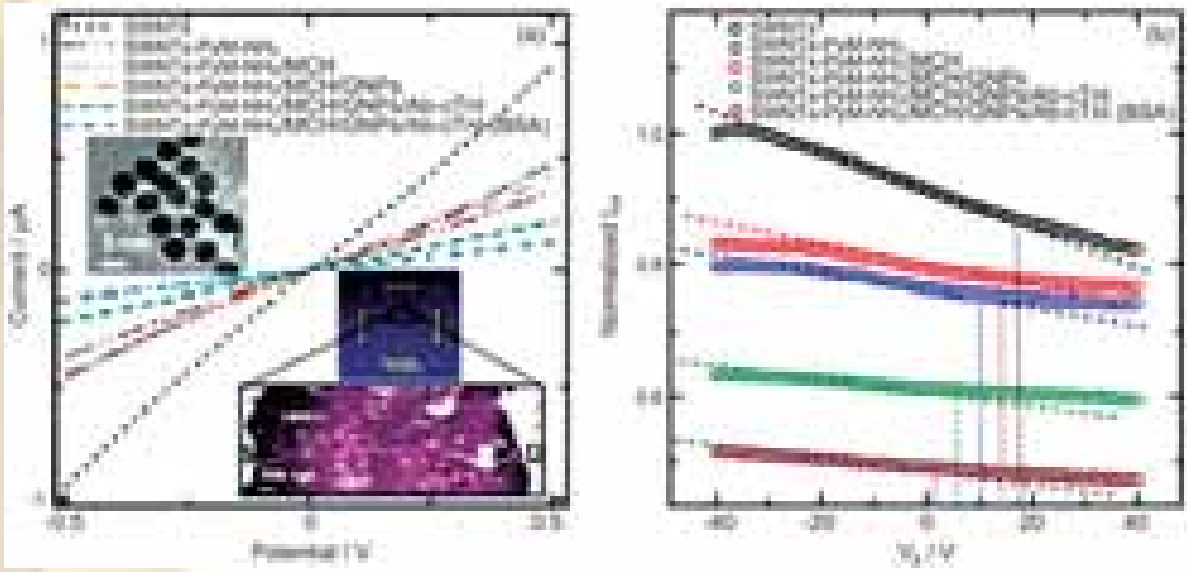

Fig. 2.14: (a) Current versus voltage (I-V) curves and (b) typical gate voltage dependence of the normalized source-drain current (I_{sd}) at V_d of 0.1V of SWNTs chemiresistive device at different stages of fabrication

linear response to cTnI from 0.01 to 10 ng mL^{-1} with a sensitivity of about 20% per decade ng mL^{-1} cTnI.

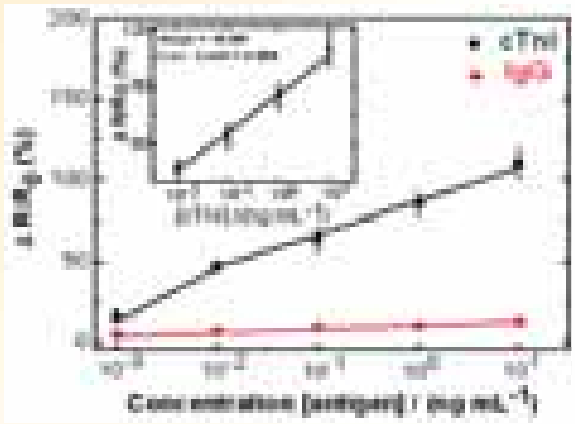

Fig. 2.15: Calibration curve of cTnI and mouse IgG detection on cTnI-GNP/SWNTs chemiresistive biosensor

We also demonstrates a facile strategy to synthesize a ZnS-RGO nanocomposite consisting of 3-mercaptopropionic acid (MPA) capped ZnS nanocrystals, ZnS(MPA), anchored on RGO sheets through a linker and deposited onto silane modified indium-tin-oxide (ITO) glass plate for the fabrication of a bioelectrode. In this work, we have utilized large surface ZnS (MPA) nanocrystals, where the surrounding carboxyl functional groups provided a high loading of protein antibody, Ab-cMb, molecules through strong carbodiimide linkage. The stepwise construction of the prototype assembly is represented in Fig. 2.16.

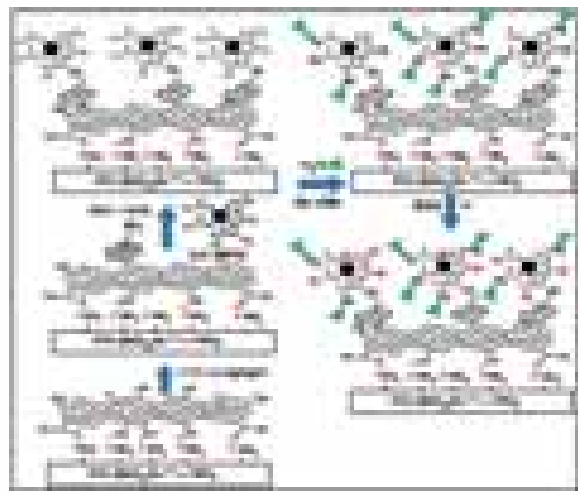

Fig. 2.16: Schematic representation of the stepwise fabrication of the bioelectrode

To study the chemical homogeneity of ZnS in the matrix of GO nano-sheets, spectroscopy (EDXS attached with TEM) was performed (Fig. 2.17). Fig. 2.17a is a bright field micrograph of a nanocomposite of GO with ZnS. The EDXS spectrum exhibits the presence of the peaks corresponding to energy levels of C (0.277 keV; Ka), Zn (1.011 keV; La and 8.631 keV; Ka), S (2.30 keV; Ka) and Cu (0.929 keV; La and 8.0431 keV; Ka),

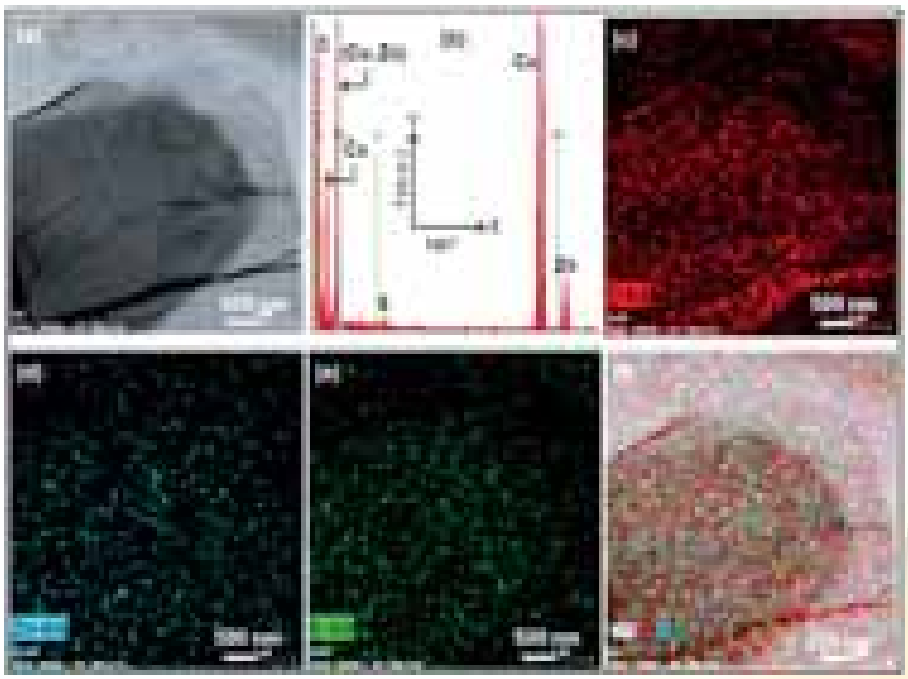

Fig. 2.17: HR-TEM image and corresponding EDXS chemical measurements; showing (a) composite microstructure of nano-sheets of graphene oxide (GO) with nanoparticles of ZnS, (b) corresponding EDXS spectrum with X-axis: 0 to 10 keV, (c) elemental map of C, (d) elemental map of Zn, (e) elemental map of S and (f) overlapped elemental maps of C, Zn and S

as displayed in Fig. 2.17b. The elemental distribution of C, Zn and S is shown in Fig. 2.17c, d and e, respectively. The overlapped elemental mapping of all three elements (C, Zn, S) is shown in Fig. 2.17f, suggesting a uniform distribution of ZnS NPs throughout the GO nanosheets.

A detailed electrochemical immunosensing study has been carried out on the bioelectrode towards the detection of target cardiac specific biomarker antigen myoglobin, Ag-cMb. The optimal fitted equivalent circuit model that matches the impedance response has been studied to delineate the biocompatibility, sensitivity and selectivity of the bioelectrode. The bioelectrode exhibited a linear electrochemical impedance response to Ag-cMb in a range of 10 ng to 1 μg mL^{-1} in PBS with a sensitivity of 177.56 &! cm^2 per decade. The impedimetric sensing performance of the bioelectrode with ZnS–RGO nanocomposite towards the quantitative detection of target protein antigen, Ag-cMb, in PBS was studied and compared with that of native RGO sheets without ZnS nanoparticles, to highlight the contribution of the ZnS nanoparticles in the overall enhanced immunosensing performance.

Physics and Engineering of Carbon

Development of continuous Carbon nanofibers by Electrospun

In this project the continuous carbon nanofibers are synthesized by electrospinning technique from PAN and PVA polymer. The carbon nanofibers synthesis from the PVA is a challenging task because it gets degraded during heat treatment. Therefore in the present project, the high yield carbon nanofibers are developed from polyvinyl alcohol by applying a special technique. Fig. 2.18 shows the SEM image of PVA nanofibers (2.18a) and carbon nanofibers (2.18b). The diameter of electrospun PVA nanofiber is in the range of 300-350 nm while that of carbon nanofibers is 200-250 nm. These low cost carbon nanofiber can be used for low cost filtration, super capacitor, anode materials for batteries and medical applications.

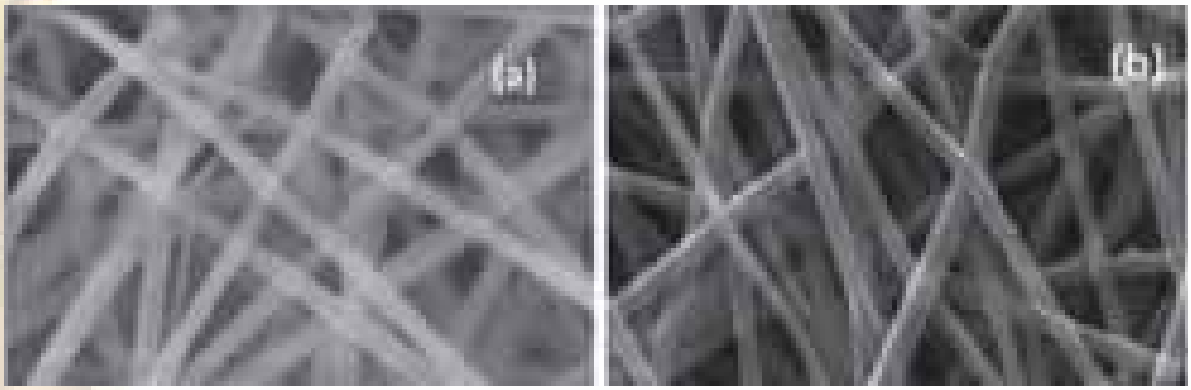

Fig. 2.18: (a) PVA nanofiber and (b) Carbon nanofibers derived from PVA

Carbon foam decorated with magnetic and dielectric nanoparticles to improve microwave absorption

Carbon foams (CFoams) are sponge-like high performance light weight engineering materials possess excellent electrical and mechanical properties as well as thermal stability. In CFoam, pore walls i.e., ligaments, are interconnected to each other, that are responsible for the conduction path and hence contribute to high electrical conductivity due to mobile charge carrier (delocalized π electron).The high value of electrical conductivity causes the CFoam as an electromagnetic radiation reflector rather than absorber. While in certain application shielding materials have mandatory to absorb maximum electromagnetic radiation. Therefore, to improve the absorptivity of electromagnetic radiation in light weight CFoam, the CFoams are decorated by Fe_3O_4 and ZnO nanoparticles (Fig. 2.19a). Inset of the figure shows the Fe_3O_4 nanoparticles and evolution of ZnO nanorods. It is observed that Fe_3O_4 and ZnO nanoparticles coating not only improved the absorption losses but also enhanced the compressive strength of CFoam by 100%. The CFoam demonstrate excellent shielding response in the frequency range 8.2 to 12.4 GHz in which total shielding effectiveness(SE) dominated by absorption losses. The total shielding effectiveness is -48.5 dB and it is governed by absorption losses -41.5 dB (Fig. 2.19b).

Synthesis and development of graphene based polymer composite: Its application in polymer electrolyte membrane fuel cells (DST project)

In this project, we are synthesizing high quality graphene by chemical vapor deposition (CVD) technique by indigenously fabricated CVD setup in the Laboratory. The single layer graphene

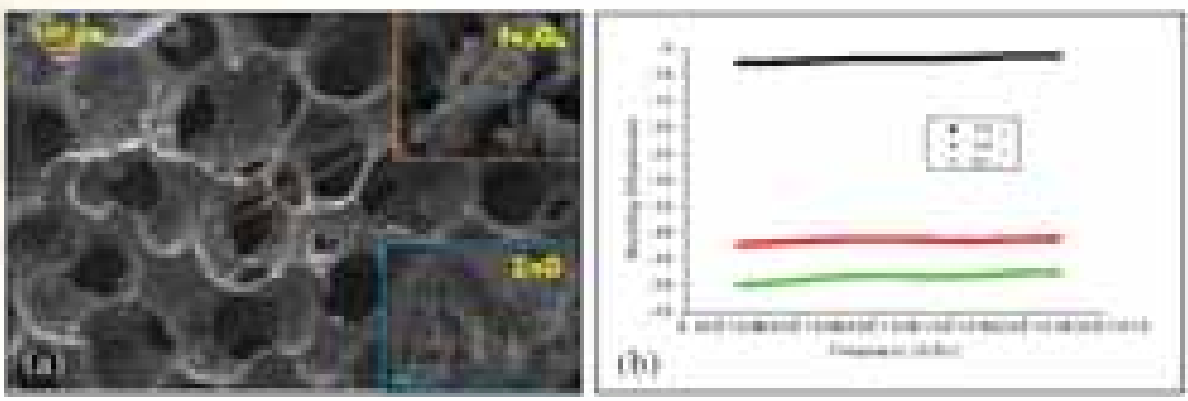

Fig. 2.19: (a)SEM micrograph of Carbon foam coated with Fe_3O_4 and ZnO nanoparticles and (b) Shielding effectiveness of Fe_3O_4-ZnO coated carbon foam

Fig. 2.20: (a) SEM micrograph of SLG (b) Optical micrograph of SLG on SiO2/Si Substrate and (c) Raman Spectra of SLG

(SLG) synthesized on the high purity copper substrate and transferred on the Silicon substrate. Fig. 2.20a shows the SEM micrograph of graphene sheet on the copper substrate. The graphene is transferred from copper substrate to SiO_2/Si by etching copper by chemical method. Fig. 2.20b shows the graphene sheet in which some portion is folded. Fig. 2.20c shows Raman spectra of single layer graphene in which intensity ratio of 2D/G is more than three.

Development of carbon based anode for Li-ion Battery (under CSIR-TAPSUN project NWP-56)

a) Under the CSIR-TAPSUN project, using a novel technique nanosize SnO_2 incorporated in house grown long length multiwalled carbon nanotubes are used to make free standing binder less conducting paper of size 20 cm × 20cm (Fig. 2.21a). The SnO_2 particles were uniformly attached on the surface of MWCNTs as shown in the FESEM image (Fig. 2.21b). These electrodes showed a discharge capacity of 496 mAh/g for more than 100 cycles at C/5 rate (Fig. 2.21c). This anode was used in a Li-ion battery at CECRI, Karaikudi to successfully demonstrate for lighting a solar lantern up to 6h (Fig. 2.21d). A patent has already been filed on this process and few industries are interested in this product.

b) Mesocarbon microbeads (MCMB) were prepared from heat treatment of coal tar pitch and petroleum pitch under reduced pressure in a

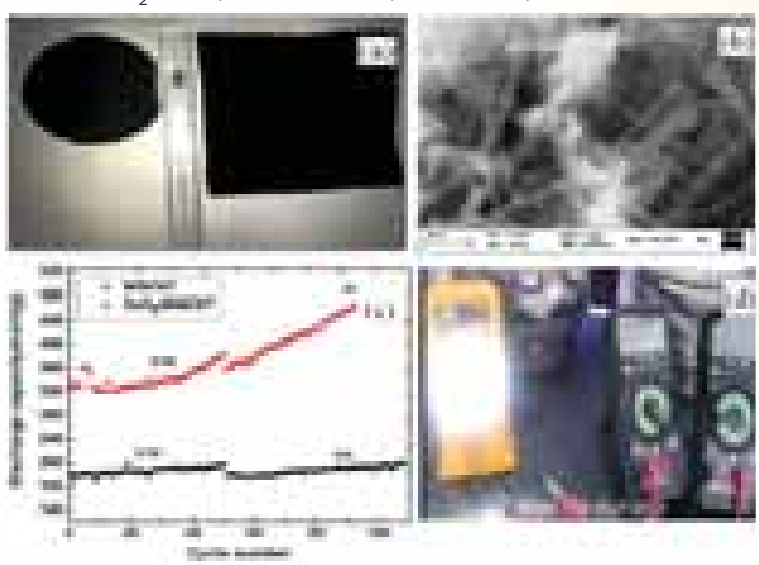

Fig. 2.21: (a) Optical image of free standing SnO_2/MWCNT composite anode of size 20cm´20cm, (b) FESEM image of SnO_2/MWCNT composite (c) discharge capacity of MWCNT and SnO_2/MWCNT composite anode and (d) demonstration of lighting of solar lantern using SnO_2/MWCNTs anode based Li-ion battery

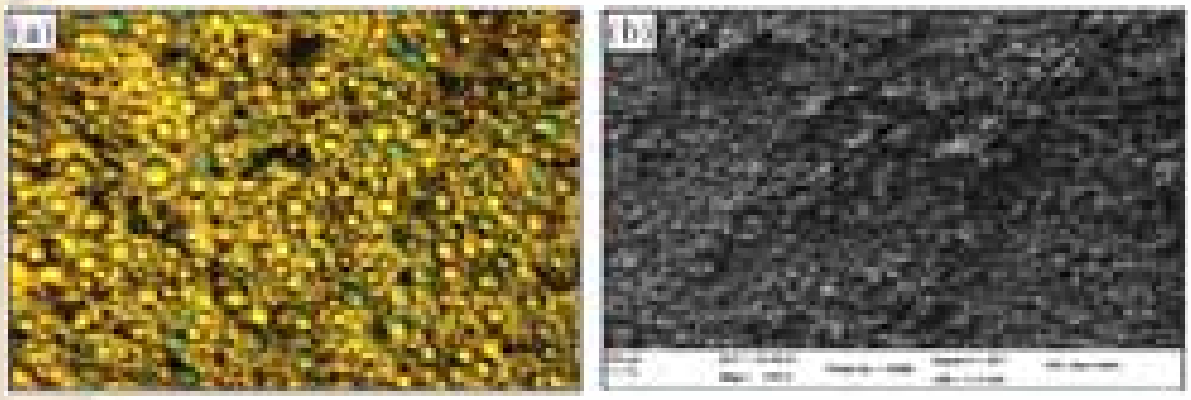

Fig. 2.22: (a) Optical micrograph of pitches heat treated at 390°C,
(b) Scanning electron micrographs of mesocarbon microbeads

distillation assembly. These pitches were again heated in furnace at 390 °C in an inert atmosphere. In optical texture, small mesophase spherules of size varying from 45 to 65 µm embedded in pitch were clearly seen (Fig. 2.22a). These spherules were then extracted with tar oil and quinoline to separate MCMB from pitch. Scanning electron micrograph of extracted MCMB is shown in Fig. 2.22b. Microstructure of the MCMB looks spherical bead like structure with average particle size of 50 µm.

Further modifications of MCMB with some metal oxides are continued and then the samples will be sent to CSIR-CECRI, Karaikudi for electrochemical study for electrochemical characterization (charging/discharging capacity) and suitability for anode of Li ion battery.

Development of Carbon Nanotube supported Platinum as Catalyst for PEM Fuel Cell

Conventionally carbon black supported Platinum is being used as Fuel cell catalyst that gives a PEM fuel cell power density of nearly 700 – 800 mW/cm^2 with a platinum loading of 0.5 mg/ cm^2 on both the electrodes (Fig. 2.23a). Studies have been carried out whereby multiwalled Carbon Nanotube (MWCNTs) supported Platinum has been developed as Catalyst for PEM Fuel Cell. The high surface area of MWCNTs can lead to better utilization of the available catalyst. Hence similar PEMFC performance has been achieved with 0.25 mW/ cm^2 of Pt loading as shown in Fig. 2.23b. Thus by reducing the amount of Platinum to 50 % the technology can go a long way in developing cost competitive fuel cells.

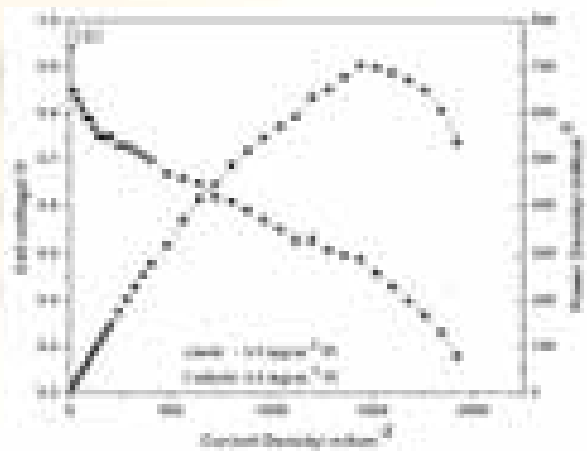

Fig. 2.23a: PEMFC performance with 0.5 mg/cm^2 of Pt loading on both electrodes

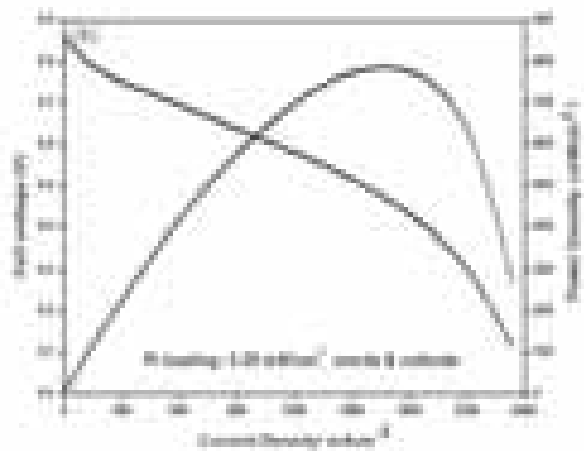

Fig. 2.23b: PEMFC performance with 0.25 mw/cm^2 of Pt loading on both electrodes

Development of advanced carbon materials and products for very high power MW Tubes

The high density graphite samples were prepared by using semi-coke (SC) powder obtained from heat treatment of coal tar pitch by mixing with additives such as natural graphite (NG), synthetic graphite (SG) and carbon black (CB) through ball milling. The mixed powders of different carbonaceous materials were moulded into blocks using cold isostatic press and carbonized to 1000°C and higher up to 2200°C in an inert atmosphere to obtain high density graphite sample. Iso-moulds of high density graphite of size dia. 30 mm and height 70 mm ware machinable and possess density of 1.76 g/cm^3, bending strength 68 MPa and electrical resistivity 2.0 mΩcm.

Samples of copper reinforced graphite were prepared by mixing different carbonaceous powders such as coal tar pitch (CTP), SC, NG, SG, CNT with copper (Cu) using powder metallurgy method. The mixed powders were moulded into blocks using hydraulic press of size dia. 55 mm and height 23 mm and then carbonized upto 1000 °C in an inert atmosphere. The properties were measured after heat treatment to 1000 °C and found to be density of 2.49 g/cm^3, bending strength of 49 MPa and electrical resistivity of 1.7 mΩcm.

Luminescent Materials and Devices Group

Fabrication of dual excitation dual emission phosphor with plasmonic enhancement of fluorescence for simultaneous conversion of solar UV and IR to visible radiation

A dual excitation, dual emission phosphor has been fabricated by simultaneous doping of lanthanide ions Er^{3+}, Yb^{3+}, Eu^{3+} in a highly efficient host YVO_4 which is simultaneously excitable by UV and IR radiation and dual emission i.e., fluorescence in bright red under UV excitation and intense green under IR excitation (Fig. 2.24). A direct assembly of Ag nanoparticles (NPs) and YVO_4: Er^{3+}, Yb^{3+}, Eu^{3+} on a suitable substrate showed enhancement of fluorescence of Eu^{3+} red emission under UV excitation. Such studies indicate that two dimensional conformal transparent layer of Ag NP-phosphor combine on a silicon solar cell may be used as DC and UC solar spectrum converter from UV/IR to visible region where spectral response of Si is high.

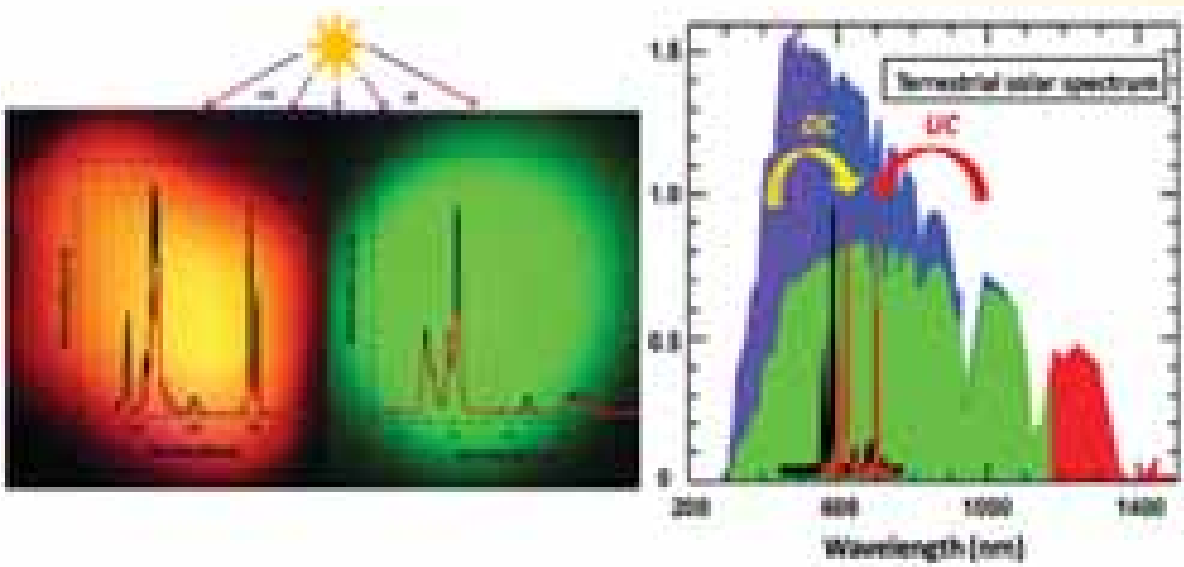

Fig. 2.24: Dual excitation phosphor with simultaneous conversion capability of solar UV and IR radiation to red and green light

Silver Nanoprisms Acting as Multipolar Nano Antennas under Low Intensity Infrared Optical Field Excites Fluorescence from Eu^{3+}

Silver nanoprism (Ag NP) generates near field due to multipolar surface plasmon resonance (SPR) and lightening rod effect and act as multipolar nano antenna. The ability of Ag NPs to create such effect even under infra red (IR) optical field far off resonance from the SPR frequency is demonstrated through Finite difference time domain simulations of exact Ag NP and hybrids. The conclusive experimental proof of such near field around Ag NPs under low intensity (2mW) IR (980nm) light came when it could excite fluorescence from $YVO_4:Eu^{3+}$ nanoparticles which otherwise do not fluoresce under IR. The results (Fig. 2.25) open up new vistas for exclusive plasmonic excitation of fluorescence through metal NP hybrids/ensembles.

Silver nanoprism enhanced fluorescence in $YVO_4:Eu^{3+}$ nanoparticles

Silver nanoprisms of different sizes influence fluorescence enhancement in $YVO_4:Eu^{3+}$ nanoparticles to various degrees under excitation of green light (532 nm). Local field generated by silver nanoprism and their dimers is simulated through FDTD method and a direct correlation with fluorescence enhancement is established.

Hot electron injection in carbon nanotube doped phosphor nanocomposite for ultra-bright electroluminescence

The effective doping of multi-walled carbon nanotube (CNT) in the ZnS:Cu phosphor nanocomposite and thereafter improvement in the optical performance of electroluminescent (EL) device due to increased local eld effects has been studied in detail. To facilitate doping of CNTs into the phosphor and decrease the operating voltage of the EL device, CNTs were shortened by milling and incorporated effectively using a flux assisted solid-state annealing reaction. Interestingly shorter the length of CNTs used; greater was the local field enhancement, improvement in brightness and efficiencies observed for the EL devices. When the field is applied, adequate charge carriers are tunneled into the ZnS:Cu system through the tips of the CNTs by forming high energy hot spots thus enhancing the local field. The improved device characteristics are due to field enhancement and effective transfer of energy from hot spots to copper activator by impact ionization. The detailed electrical characterization of the novel EL device

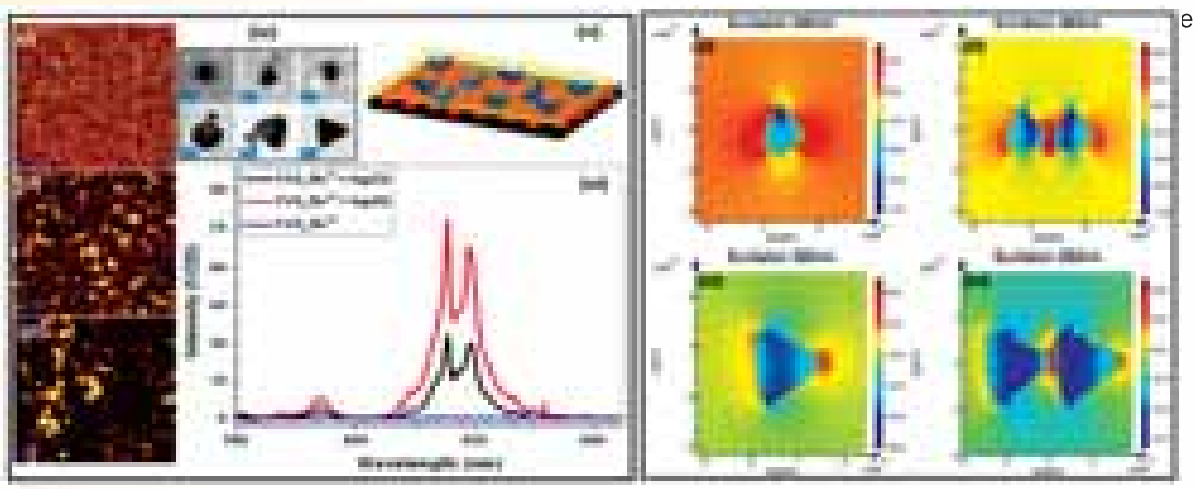

Fig. 2.25: Confocal fluorescence image of thin films of (i) $YVO_4:Eu$ (ii) $YVO4:Eu^{3+}$ + 22nm Ag nanoprism combine (iii) $YVO_4:Eu^{3+}$ + 45nm Ag nanoprism combine (iv) TEM images of Ag nanoprisms (v) schematic of arrangements of $YVO_4:Eu^{3+}$ NPs (red spheres), PVA layer (yellow transparent layer) and Ag NPs (blue prisms) in thin films used for study, (vi) integrated fluorescence spectra of the samples under 980nm laser excitation taken by Confocal fluorescence measurements. Simulated near field images of single Ag nanoprisms (22 nm and 45 nm) and dimers calculated by FDTD method, by importing exact TEM image of Ag NP

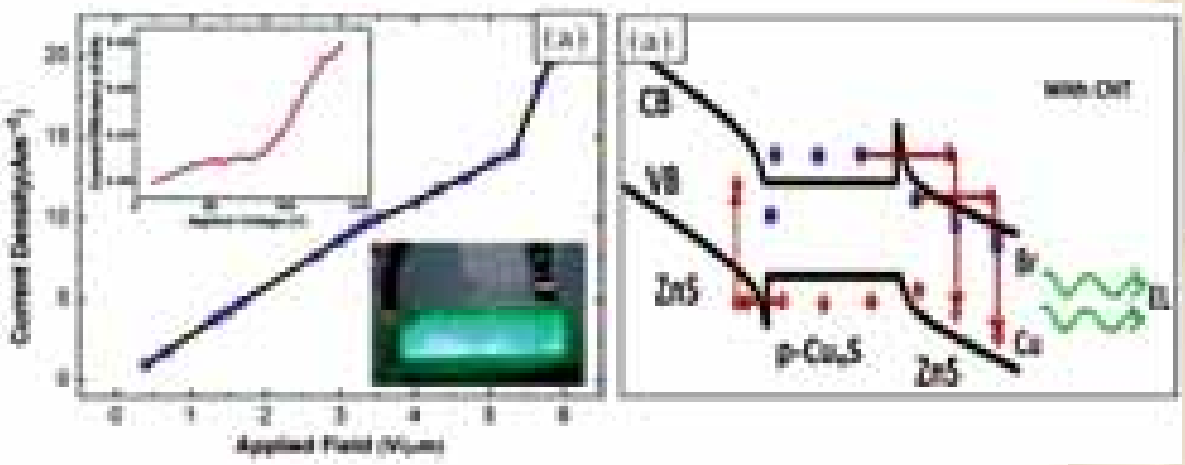

Fig. 2.26 (a): Variation of current density (J) as a function of applied field (E) for the AC driven EL device; first inset shows change in the current efficiency of the EL device as a function of applied voltage; second inset shows the photograph of the working device at an operating voltage of 100 V_{AC} and 2.5 kHz. (b) Scheme showing band bending model due to incorporation of CNTs

presented (Fig. 2.26) by considering the hot electron injection model.

Multifold blue absorption of a new red-emitting nanophosphor for LEDs

There has been a stringent demand for blue (~450 to 470 nm) absorbing and red (~611 nm) emitting material systems in phosphor converted white light emitting diodes (WLEDs) available in the market. The conventionally used red-emitting Y_2O_3:Eu^{3+} phosphor has negligible absorption for blue light produced by GaInN based LED chips. To address this issue, a new red-emitting Gd_2CaZnO_5:Eu^{3+} (GCZO:Eu^{3+}) nanophosphor system having exceptionally strong absorption for blue (~465 nm) and signicant red (~611 nm) photoluminescence is presented (Fig. 2.27). This is attributed to a dominant f–f transition ($^5D_0/^7F_2$) of Eu^{3+} ions, arising due to an ecient energy transfer from the Gd sites of the host lattice to Eu^{3+} ions. The external quantum yield (QY) measured at 465 nm absorption and 611 nm emission revealed that

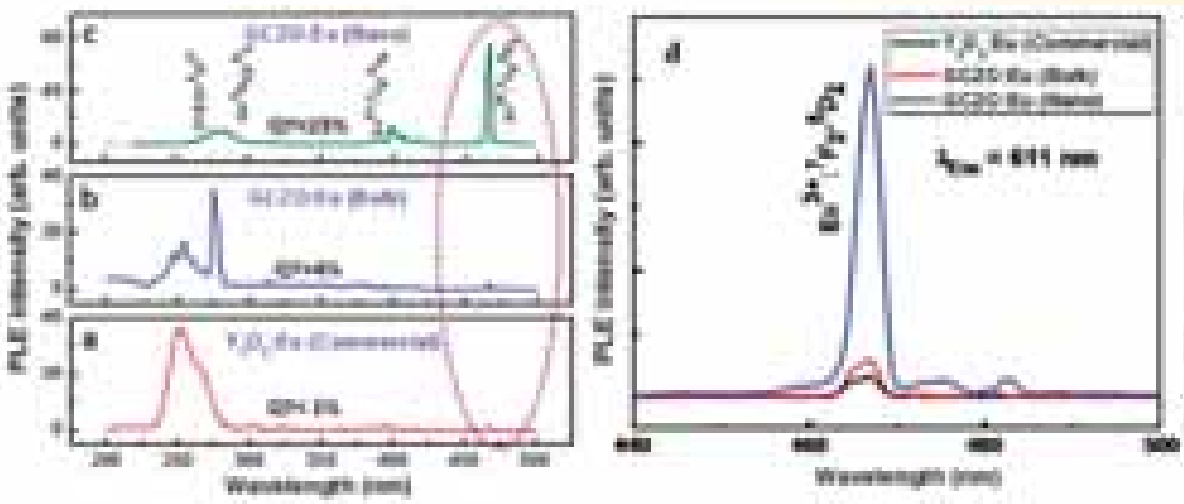

Fig. 2.27: Photoluminescence excitation (PLE) of (a) commercial Y_2O_3:Eu^{3+} phosphor, (b) GCZO:Eu^{3+} microcrystalline bulk phosphor, (c) GCZO:Eu^{3+} nanophosphor monitored at ~611 nm emission. The dotted region depicts the multifold blue light absorption at ~465 nm for GCZO:Eu^{3+} and (d) magnified version of the same, useful for improving color rendering in WLEDs

the GCZO:Eu^{3+} nanophosphor has better QY of 23% as compared to commercial Y_2O_3:Eu^{3+}, which is <1%. X-ray diffraction and microscopy observations showed the nanocrystalline nature and slightly elongated morphology of the sample, respectively. While the energy dispersive X-ray analysis identied the chemical constituents of the GCZO:Eu^{3+} nanophosphor, the color overlay imaging confirmed the substitution of Eu^{3+} for Gd^{3+} ions. As seen from the QY statistics it is highly anticipated that the multifold absorption at ~465 nm would certainly improve the color rendering properties of existing WLEDs.

Probing on lanthanide doped nanophosphor as a broad spectral converter (UV-IR) for promising next generation Si-solar cell

Recent thrust in the research activity of lanthanide doped nanomaterials have been largely attributed to its fascinating properties and its vast potential applications in display technology, optoelectronics, bio-imaging, and for security applications. The current focus in this field is to develop efficient luminescent materials for enhancing the efficiency of Si-solar cells via modification of the solar spectrum response. Lanthanide ions are the primary entities to achieve efficient spectral conversion. Because of their rich energy level structure and lanthanide can accomplish both down-shifting (DS) and up-conversion (UC) processes which may allow for facile photon management. Our main objective is to make an attempt to synthesize nanophosphors which can absorb UV-IR region and may be modify as well as convert the solar spectrum into beneficial energy with high efficiency.

We have successfully demonstrated the synthesis of highly luminescent DS and UC $Gd_2(MoO_4)_3$:RE nanophosphor by solid state reaction which can be scale up in pilot plant. The as-synthesized luminescent DS $Gd_2(MoO_4)_3$:Eu^{3+}

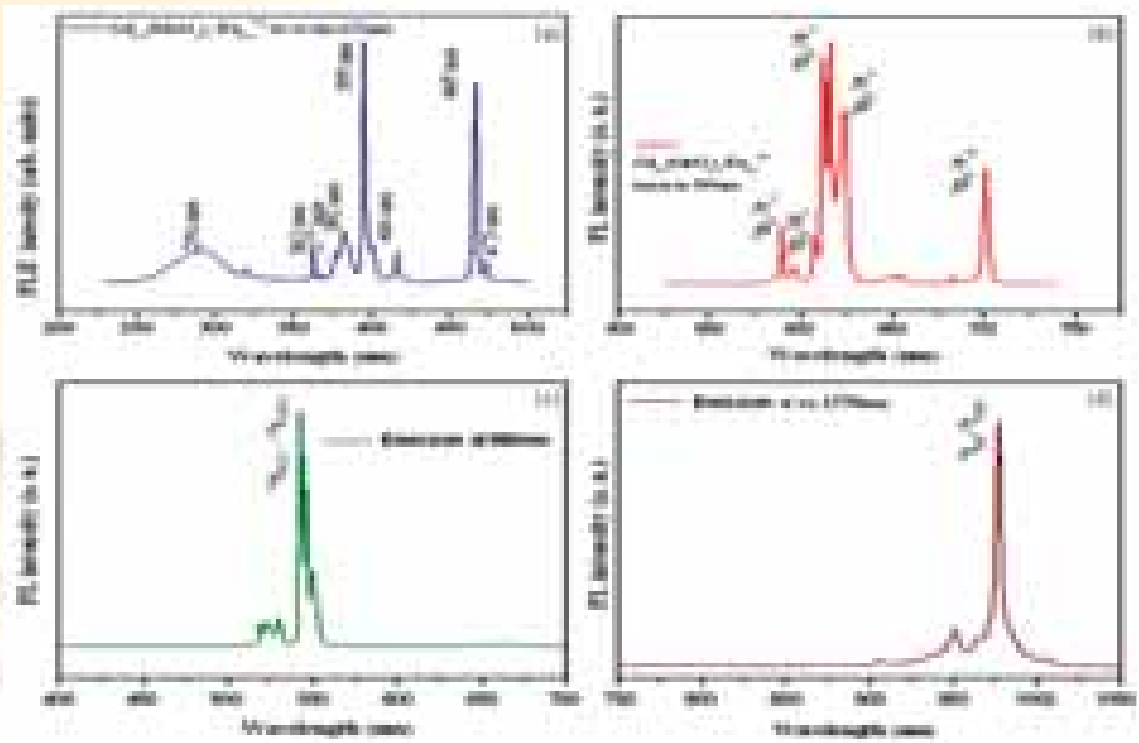

Fig. 2.28: photoluminescence excitation spectrum of $Gd_2(MoO_4)_3$:Eu^{3+} DS nanophosphor at émission 623nm émission wavelength, (b) photoluminescence émission spectrum of $Gd_2(MoO_4)_3$:Eu^{3+} DS nanophosphor at émission 395nm excitation wavelength, (c) photoluminescence emission spectrum at excitation 980nm and (d) photoluminescence emission spectrum of UP $Gd_2(MoO_4)_3$:RE (Er^{3+},Yb^{3+}) phosphor at excitation 1550 nm

nanophosphor exhibits excitable at 291, 362, 377, 385, 416, and 465nm with strong red emission peaking at 623nm wavelength as shown in Figure 2.28 (a &b). The as-synthesized luminescent UC $Gd_2(MoO_4)_3$:Er^{3+},Yb^{3+} nanophosphor exhibits excitable at 980 and 1550nm with emission peaks at 542 and 977 nm wavelength as shown in Figure 2.28 (c & d). The obtained Photoluminescent results confirms the full utility of $Gd_2(MoO_4)_3$:RE (Eu, Er, Yb) nanophophor as a Broad Spectral converter (UV-IR) for promising Next Generation Si-Solar Cell.

Multiferroics and Magnetics

Magnetic Metrology

Calibration and Test activities for R&D institutions & industrial instruments have been undertaken and 61 calibration/test reports were issued, this led to Rs.7.8 Lakh of ECF earning.

A calibration methodology for precise NMR Teslameter by using High Resolution Frequency counter has been developed and achieved uncertainty of 35 μT/T in the measurement range of 0.043T-1.0T.

As an special initiative we have successfully installed our Cesium Magnetometer (as Primary standard for low magnetic field measurement facility) with an uncertainty of 10nT/T for 20,000 nT-1,00,000 nT magnetic field range. Lot of efforts have been put to improve uncertainty for low magnetic field measurement ranges.

For the first time an onsite survey has been successfully initiated for electromagnetic radiation measurement, calibration of ELF/EMF Meters.

The best possible efforts are being tried out to improve further uncertainty of measurement to provide best calibration/test results with minimum probable error. Our group provides solution to industrial problems.

Colossal Humido Resistance, CHR, in ceria added magnesium ferrite thin film by pulsed laser deposition

First time, magnesium ferrite and ceria added magnesium ferrite thin films have been prepared by Pulsed laser deposition technique. Pure magnesium ferrite showed decrease in resistance from 230 GOhm at 10%RH to 184 MOhm at 95%RH. While 1 wt% Ce:MgF thin film resistance was 1.8 TOhm at 10% RH which deceased to 754 KOhm at 95 %RH exhibiting approximately a seven-order decrease in the resistance (Fig. 2.29). The DC resistance of pure magnesium ferrite film was 256 GOhm at 0 %RH

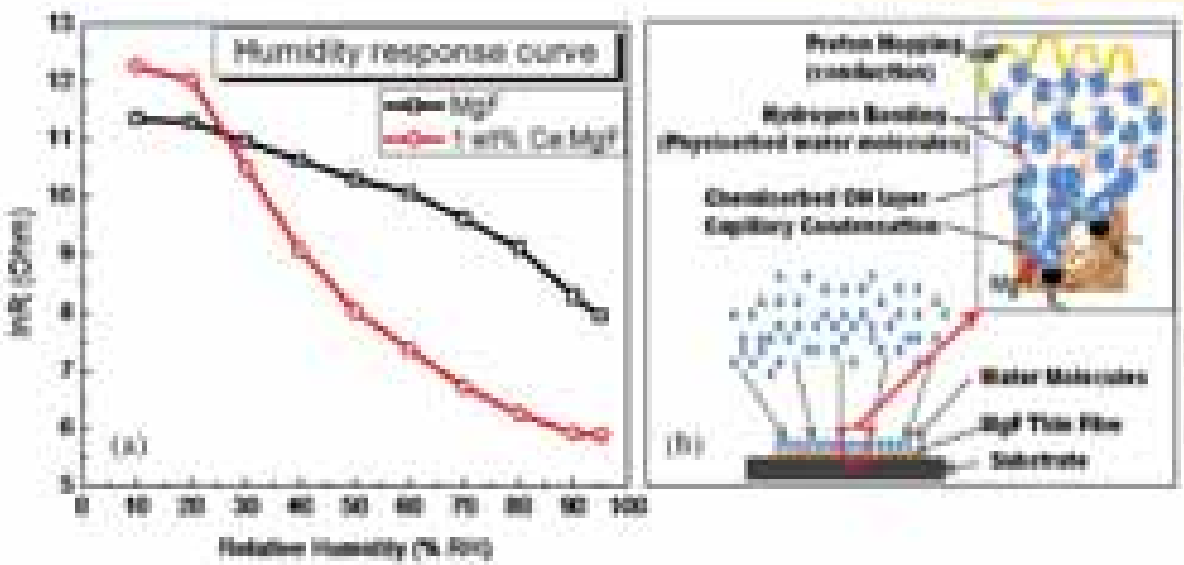

Fig. 2.29: (a) lnR vs. % relative humidity plot for thin lms showing change in resistance with humidity and (b) humidity sensing mechanism by film.

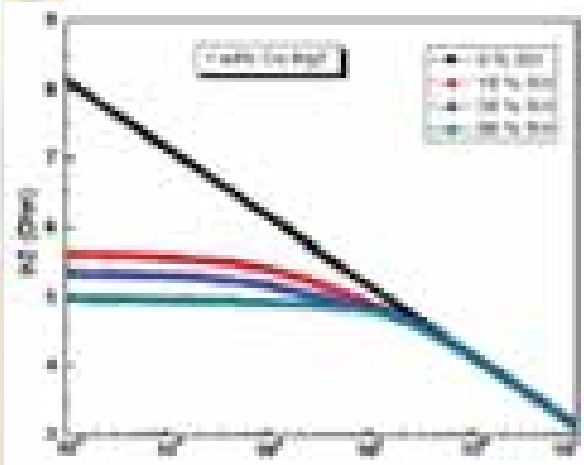

Fig. 2.30: ln Z vs. log of frequency for1 wt% Ce:MgF at 0%RH, 10%RH, 50%RH and 90%RH

and it increased to 2.3 TOhm by ceria addition. Such a colossal change in resistance of thin film with humidity (natural source) can be best exploited for new type of energy conservative colossal humidoresistance based devices contrary to colossal magnetoresistance (CMR) devices operated by externally applied magnetic field. A comparison between GMR & CHR is shown below in Table 2.2. It is evident from the impedance plots that in dry atmosphere (0%RH) lnZ of the films decreased linearly with increasing frequency exhibiting material transport characteristics (Fig. 2.30). When films exposed to humidity, initial drastic decrease in impedance of films by humidity is due to conduction of H_3O^+ and H^+ ions in physisorbed water molecules via hydrogen bonding at low frequency on the surface of films. The constant region extended at higher 90% RH compared to lower 10%RH due to increased H_3O^+ ions concentration at higher humidity. This exhibits conduction contribution is due to very low concentration of free H_3O^+ ions.

Table 2.2

GMR (giant magneto-resistance)	CHR (colossal humido-resistance)
Multilayer is required	Single layer is required
Thickness of each layer is critical	Thickness is not below 60 nm
Very High External Magnetic Field is Needed	Natural Source relative Humidity is Needed
Change in %MR is 0.7-1/Oe	Change in resistance is 0.1 Mohm/1%RH

Spin pumping induced Spin Hall Effect on Co/Pt bilayer thin film

Spin pumping induced spin-Hall effect has been investigated in RF sputtered Co/Pt bilayer thin film for its application in the field of spintronics. Microwave power has been applied in presence of a magnetic field and measured the FMR voltage spectra across the film. Schematic illustrations of flow of spin current J_s and charge current J_c in Co/Pt bilayer thin lm on Si substrate is shown in Fig 2.31.

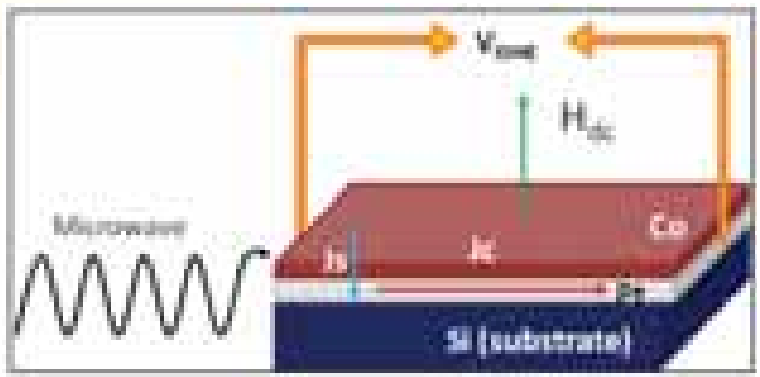

Fig. 2.31: Schematic illustrations of flow of spin current J_s and charge current J_c in Co/Pt bilayer thin lm on Si substrate

The saturation magnetization of the Co/Pt bilayer thin film was measured as 0.55 x 10^3 emu/cm^3 when the applied magnetic field was kept perpendicular and 0.32 x 10^3 emu/cm^3 for parallel magnetic field with respect to film plane. It exhibits film is perpendicularly anisotropic (Fig. 2.32). The FMR signal was excited by a microwave signal, while applying sweeping dc magnetic field along and perpendicular to the film plane separately. The maximum dc voltage measured was 5.78 V at 0.1GHz in perpendicular applied magnetic field on the bilayer (Fig. 2.33).

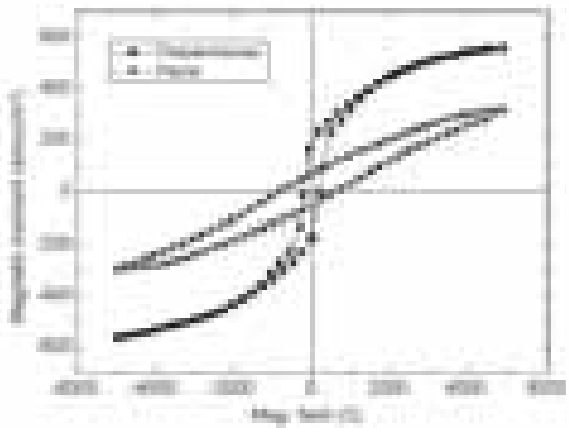

Fig. 2.32: Schematic illustrations of flow of spin current J_s and charge current J_c in Co/Pt bilayer thin lm on Si substrate

Induced magnetism and magnetoelectric coupling in ferroelectric $BaTiO_3$ by Cr-doping synthesized by facile chemical route

Phase pure barium titanate (BTO) and Cr doped BTO have been synthesized by a facile single-step metal-organic decomposition (MOD) method. Ferroelectric transition temperature value for pure BTO is decreased to 108 °C by 1.5 Cr doping in BTO due to tetragonal to distorted cubic structural change (Fig. 2.34). Diamagnetism of BTO transformed into ferromagnetic behaviour by Cr-doping on the expense of decrease in polarization. The ME coupling coefficient of 1.5 Cr:BTO at room temperature maximum value of 'α' obtained 13 mV $cm^{-1}Oe^{-1}$ for 2800 Oe (Fig. 2.35).

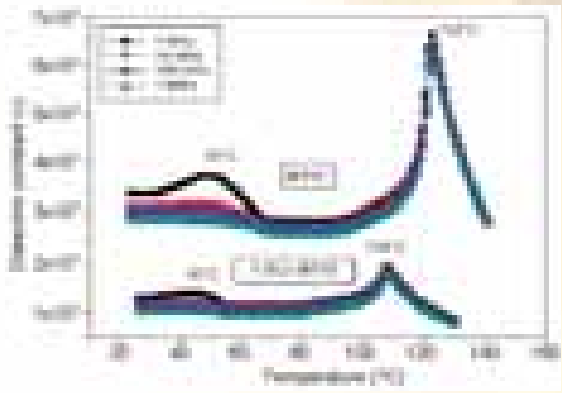

Fig. 2.34: Ferroelectric transition temperature of pure BTO and 1.5Cr:BTO at different frequencies

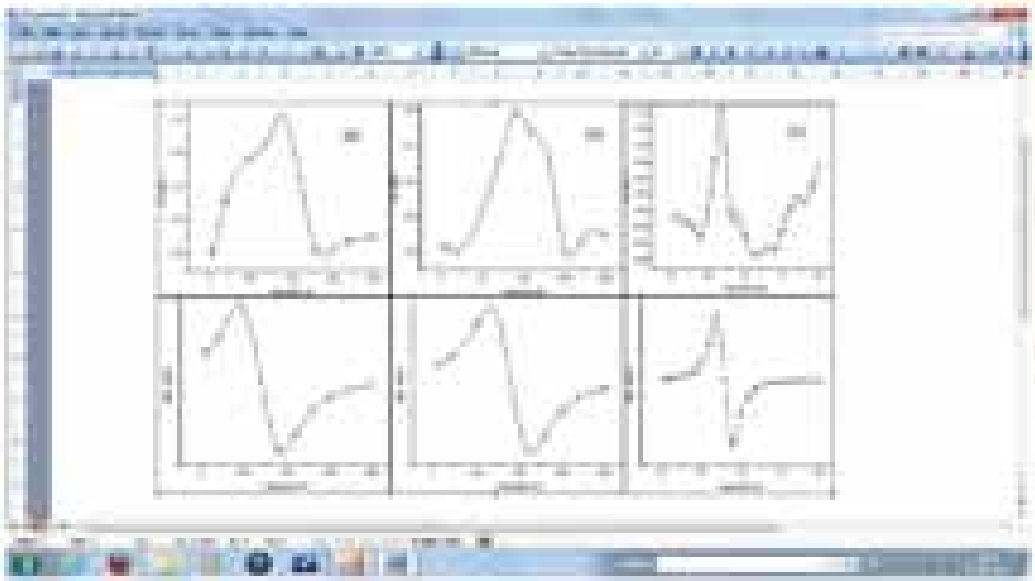

Fig. 2.33: Maximum dc voltage generated is 5.78 V at 0.1 GHz

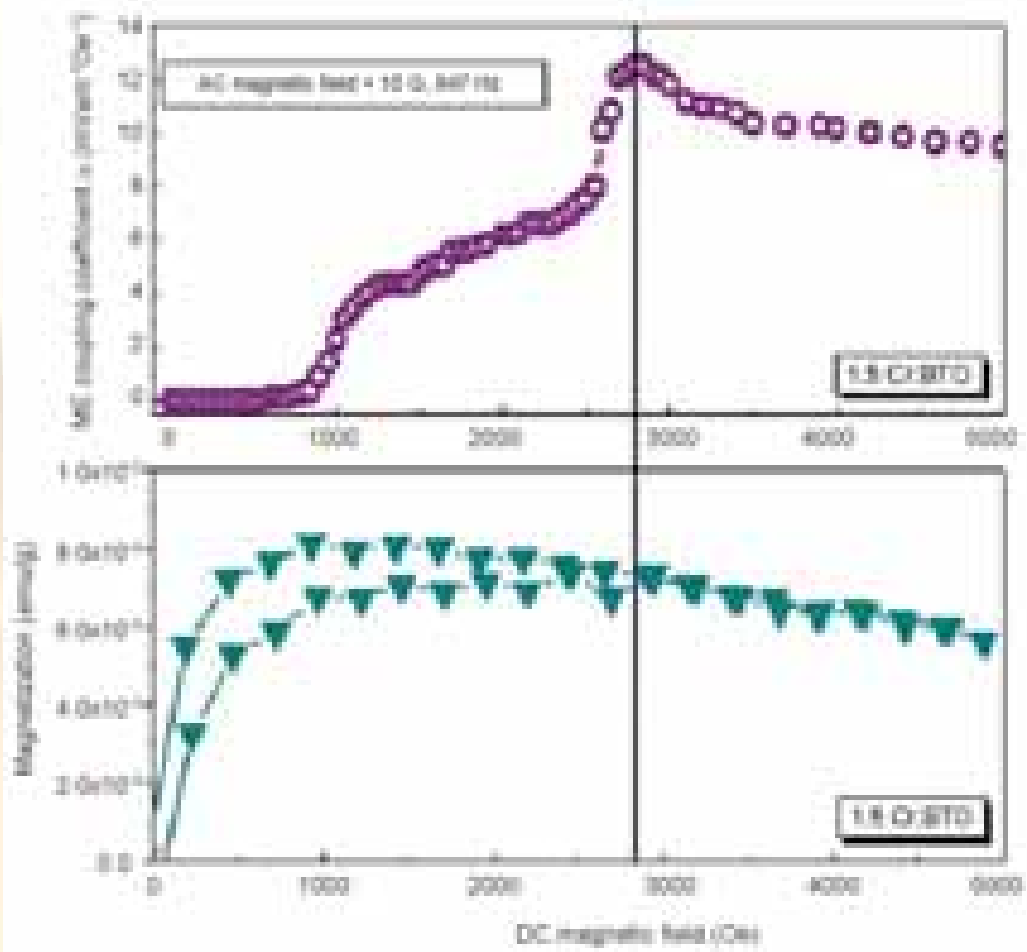

Fig. 2.35: Room temperature measurement of Linear magnetoelectric coupling coefficient vs. DC magnetic field plot for 1.5 Cr:BTO merged with room temperature magnetization curve indicating highest ME coupling at externally applied DC magnetic field

Magnetoelectric Coupling of Multiferroic Chromium Doped Barium Titanate Thin Film Probed by Magneto-Impedance Spectroscopy

Thin film of $BaTiO_3$ doped with 0.1 at% Cr (Cr:BTO) has been prepared by Pulsed laser deposition technique for the first time. A smooth platform of uniform color of film reveals smooth growth of thin film. The magnetic domains recorded in the MFM image are clearly visible in the form of alternating dark and bright contrast fringes, exhibiting strong and weak magnetic force on MFM tip. The size of the domain in this is about 1-2 μm in width. MFM images qualitatively further supports the quantitative magnetization of ferroelectric film obtained by MH loop (Fig. 2.36). Theoretical impedance equation fitted to experimental data in Cole-Cole plot for thin film (Fig. 2.37) in presence of transverse magnetic field resolved the increase in grain capacitance from 4.58×10^{-12} to 5.4×10^{-11} F. Ten times higher ME coupling coefficient 137 mV/cm than bulk value of 13 mV/cm has been obtained even at lower applied magnetic field 1000 Oe (Fig. 2.38).

Magnetoelectric coupling-induced anisotropy in multiferroic nanocomposite (1-x) $BiFeO_3$–x$BaTiO_3$

Nanocomposite (1 –*x*)$BiFeO_3$–x$BaTiO_3$ for *x* = 0.1, 0.2 and 0.3 has been investigated for magnetoelectric (ME) coupling at atomic scale mixing of the two phases. XRD results revealed

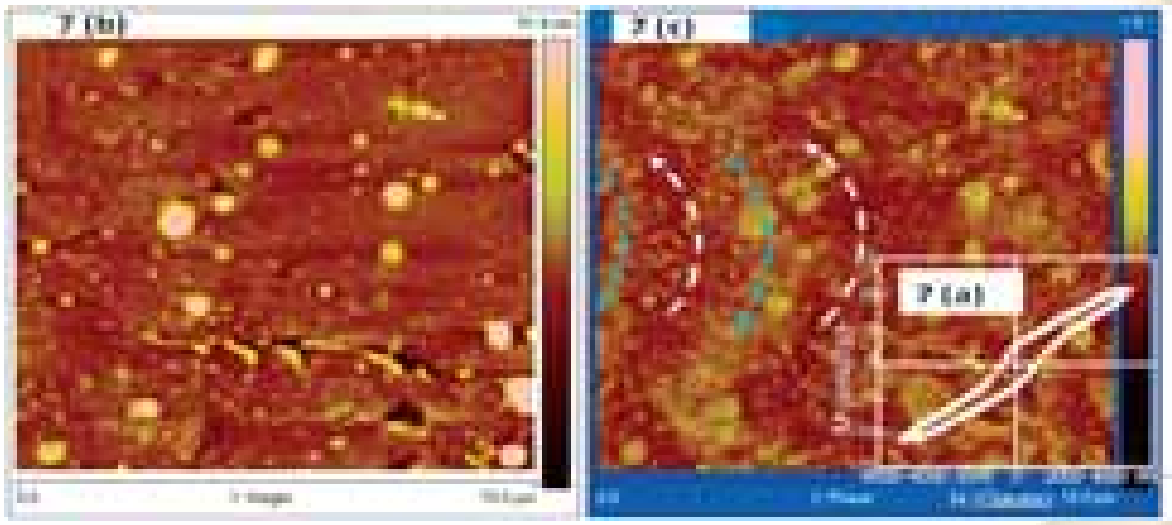

Fig. 2.36: (a) M (Magnetic moment) vs. H (Magnetic field) loop for Cr:BTO thin film, (b) Room temperature AFM image and (c) the corresponding MFM image of the Cr:BTO film taken on the scale of 15 μm

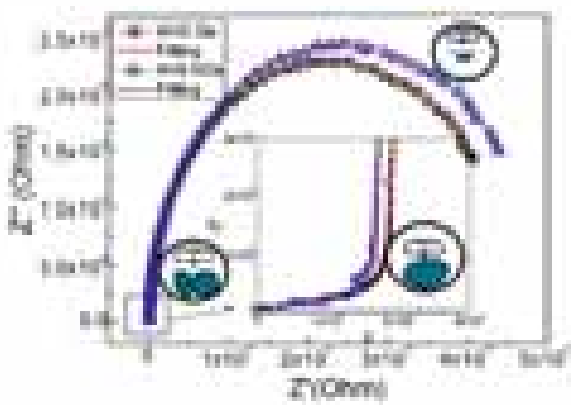

Fig. 2.37: Impedance spectroscopy plot Z" vs. Z' at zero and 5 KOe magnetic field and theoretical plot fitting to experimentally observed curves, inset shows close view fitting of theoretical plot on two curves

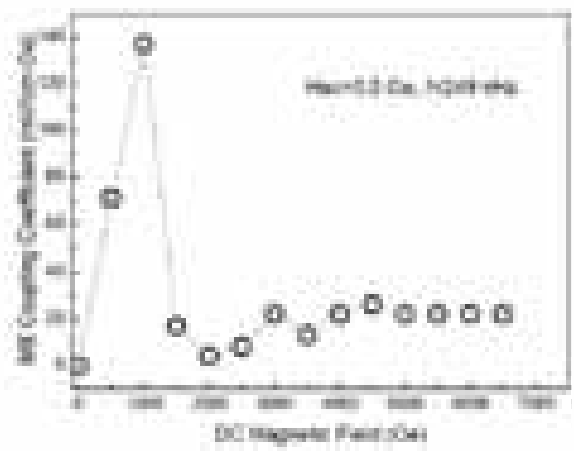

Fig. 2.38: Induced voltage per unit AC field and film thickness with applied DC bias magnetic field

rhombohedral phase for x= 0.1 composition while cubic phase was observed for x= 0.2 and 0.3 composition (Fig. 2.39). Correlated magnetic and dielectric transition temperatures were determined as an evidence of ME coupling in the material. The computed value of magnetic anisotropy constant 4.8×10^3 erg/cm^3 was found to be maximum for *x* = 0.1 composition. A frequency-dependent

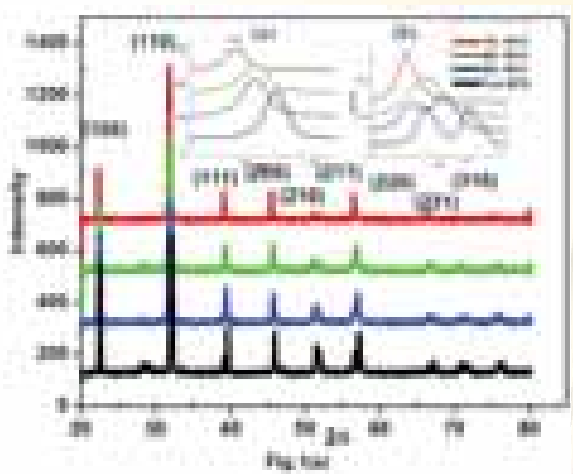

Fig. 2.39: Comparison of XRD results of nanocomposite (1-x) $BiFeO_3$–x$BaTiO_3$ for x = 0, 0.1, 0.2 and 0.3, inset (a) shows (100) peak shifting towards lower anglea representing increasing lattice parameter and inset (b) shows disappearance of splitting of (110) peak representing phase transition from rhombohedral to cubic structure

dielectric maximum was found to be at 395°C for 10 kHz for x= 0.1 (Fig. 2.40) which shifted to 450°C at 1 MHz. Dielectric maximum ME coupling coefficient (α) was maximum 2.74 mV/cmOe for x = 0.1.

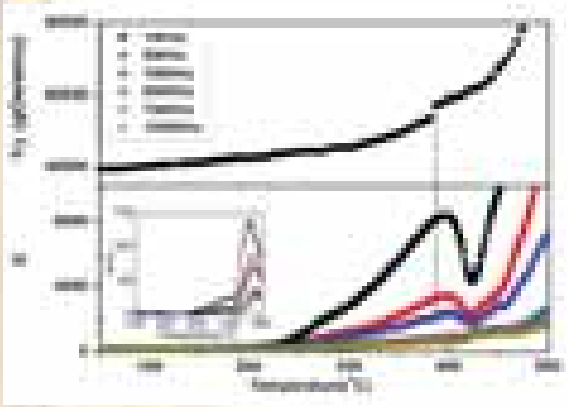

Fig. 2.40: Presence of magnetic anomaly at dielectric transition temperature for nanocomposite $0.9BiFeO_3$–$0.1BaTiO_3$

Biomedical Instrumentation

The Biomedical Instrumentation section has successfully established a DST center for biomolecular electronics under a DST funded project. The section has also established two prototype devices for detection of total cholesterol. This section is dedicated to research in both pure and applied science and integrated research field involving the principles of Physics, Chemistry, Biotechnology and Instrumentation with the following objectives:

- To focus on R & D in controlled target- drug delivery, diagnostics and therapeutics based on smart inorganic and organic materials, conducting polymers, nanomaterials and biocompatible materials for bioelectronics devices, biomedical sensors and innovative technologies
- Developing, identifying and building new information and knowledge based strategies for generating new materials for molecular electronic applications such as conducting polymers, self-assembled monolayers, nanophosphors, sol-gel films, Langmuir Blodgett monolayer films etc
- Fabricate on-line, in-situ and ultimately non-invasive tools of diagnostic devices
- Highly specific, sensitive and selective polymeric multivariate biosensor, whole cell biosensor for pesticides/heavy metal detection etc
- Nucleic acid hybridization biosensors for microbial detection
- Technological development of novel devices, processes and methodologies, and transfer of technical expertise for pilot production of biomedical sensors
- To generate and supplement technical manpower in the area of biosensors and bio-molecular and molecular electronics
- Generate high quality research papers and patents
- Transfer of technical know-how on molecular electronics devices to pertinent industries

The group has also undertaken the integrated M. Tech.-Ph.D./ Ph.D. programme on biosensors under Academy of Scientific and Innovative Research (AcSIR) and other collaborative academic institutes.

Some of the research highlights for detection of Escherichia coli, Cholesterol and LDL, using various non conventional approaches, such as, liquid crystals cell and microfludics cells have been used for detection of cholesterol also novel material such as Cationic poly (lactic-co-glycolic acid) iron oxide nanosphere as nucleic acid sensors.

Cationic poly (lactic-co-glycolic acid) iron oxide microspheres for nucleic acid detection

Herein, we envisage the possibility of preparing stable cationic poly (lactic-co-glycolic acid) (PLGA) microspheres encapsulating the iron oxide nanoparticles (IONPs; 8–12 nm). The IONPs are incorporated into PLGA in organic phase followed by microsphere formation and chitosan coating in aqueous medium via nano-emulsion technique. The average size of the microspheres, as determined by dynamic light scattering are about 310 nm, while the zeta potential for the composite

remains near 35 mV at pH 4.0. These microspheres are electrophoretically deposited on to indium tin oxide (ITO)-coated glass substrate used as cathode and parallel platinum plate as the counter electrode. This platform is utilized to fabricate a DNA biosensor, by immobilizing a probe sequence specific to Escherichia coli. The bioelectrode shows a surface-controlled electrode reaction with the electron transfer coefficient (α) of 0.64 and charge transfer rate constant (ks) of 61.73 s^{-1}. Under the optimal conditions, this biosensor shows a detection limit of 8.7×10^{-14} M and is found to retain about 81% of the initial activity after 9 cycles of use.

Electrochemically Assembled Gold Nanostructures Platform: Electrochemistry, Kinetic Analysis, and Biomedical Application

A novel one-step electrochemical method for controlled synthesis of electroactive gold nanoparticles (Au NPs) in an organic medium using an organometallic precursor $Au(PPh_3)Cl$ [Ph = phenyl] has been proposed. The hierarchical assembly of Au nanostructures has been tuned on indium tin oxide (ITO) surface during electrochemical reduction of $Au(PPh_3)Cl$ using cysteamine. The Au NPs act as building blocks to form secondary structures of Au that has been confirmed using transmission electron microscopic studies. The presence of triphenylphosphine in Au film enhances the electrocatalytic activity, resulting in higher charge transfer kinetics. The cholesterol oxidase (ChOx) as a model enzyme has been immobilized on various fabricated nanostructured Au films. Direct electron transfer properties of nanostructured Au films result in third-generation cholesterol biosensor. We have investigated the biosensing performance of different Au nanostructures toward cholesterol estimation at low operating potential (+0.3 V). The high sensitivity of 4.22 AM^{-1} cm^{-2} and low detection limit of 5.49 μM of this biosensor (ChOx-Glu/Cys-Au/ITO) is due to higher current resulting from monodisperse Au NPs. In addition, this bioelectrode shows charge transfer rate constant as 247.27 s^{-1} and low Km^{app} value as 0.57 mM. The biosensor shows good reproducibility, stability, and selectivity and thus can be utilized for health care diagnostics application.

Protein–Conjugated Quantum Dots Interface: Binding Kinetics and Label-Free Lipid Detection

We propose a label-free biosensor platform to investigate the binding kinetics using antigen–antibody interaction via electrochemical and surface plasmon resonance (SPR) techniques. The l-cysteine in situ capped cadmium sulfide (CdS; size < 7 nm) quantum dots (QDs) self-assembled on gold (Au) coated glass electrode have been covalently functionalized with apolipoprotein B-100 antibodies (AAB). This protein conjugated QDs-based electrode (AAB/CysCdS/Au) has been used to detect lipid (low density lipoprotein, LDL) biomolecules. The electrochemical impedimetric response of the AAB/CysCdS/Au biosensor shows higher sensitivity (32.8 $k\Omega\ \mu M^{-1}/cm^2$) in the detection range, 5–120 mg/dL. Besides this, efforts have been made to investigate the kinetics of antigen–antibody interactions at the CysCdS surface. The label-free SPR response of AAB/CysCdS/Au biosensor exhibits highly specific interaction to protein (LDL) with association constant of 33.4 kM^{-1} s^{-1} indicating higher affinity toward LDL biomolecules and a dissociation constant of 0.896 ms^{-1}. The results of these studies prove the efficacy of the CysCdS-Au platform as a high throughput compact biosensing device for investigating biomolecular interactions.

Metals & Alloys

Thermoelectric material Cu_3SbSe_3 with intrinsically ultralow lattice thermal conductivity

This is the first comprehensive study on the synthesis, characterization and thermoelectric property evaluation of Cu_3SbSe_3, synthesized using a single-step process employing a solid-state reaction in vacuum. The synthesized material was

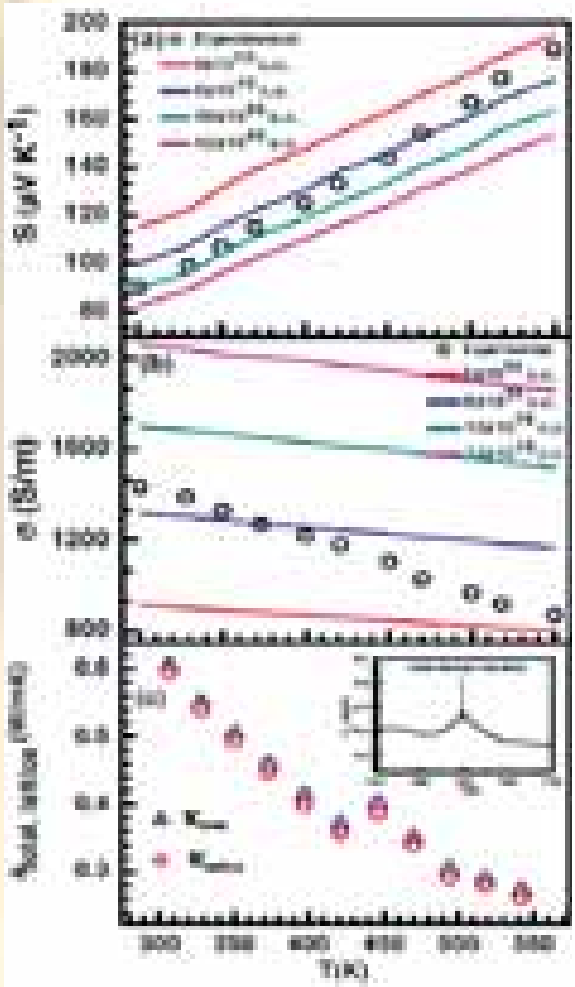

Fig. 2.41: Temperature dependence of transport properties of Cu_3SbSe_3. The open circles represent the experimental points and the coloured lines depict the theoretically predicted curves, for different carrier concentration. (a) Seebeck coefficient. (b) electrical conductivity (c) total thermal conductivity. The inset shows the temperature dependence of specific heat

characterized for its structure and composition employing X-ray diffraction (XRD), field emission scanning electron microscopy (FESEM), transmission electron microscopy (TEM), energy dispersive X-ray spectroscopy (EDXS) X-ray photoemission spectroscopy (XPS) and differential scanning calorimeter (DSC). These detailed characterization results clearly confirmed the formation Cu_3SbSe_3 in a single phase.

The electrical transport measurement results (Fig. 2.41) indicated that, contrary to the earlier theoretical prediction, Cu_3SbSe_3 exhibits a p-type behavior in the measured temperature range of 300-550 K and exhibits a order-disorder transition at ~ 450 K, which has also been reported earlier. Electronic band structure of Cu_3SbSe_3 has been evaluated using first-principle density functional theory (DFT) calculations and the electrical transport properties were theoretically evaluated using Boltzmann transport theory (Fig. 2.42). These theoretical predicted values of thermopower (S) and electrical conductivity (σ) were found to be in reasonable agreement with the experimental results. The measured thermal conductivity (κ) was found to be 0.26 $Wm^{-1}K^{-1}$ (550 K), which is the lowest value reported for this material thus far and is among the lowest for thermoelectric materials. However, despite a ultralow κ and moderate S, the calculated thermoelectric figure-of-merit was abysmally low, which is due to very low σ. Thus, it has been experimentally established for the first time that pristine Cu_3SbSe_3 is not a good thermoelectric material, which is contrary to the previously reported proposition. Nevertheless, it is suggested that this material could be a good potential thermoelectric material owing to its ultralow κ coupled with a reasonable value of α, as σ can be tailored favorably by employing suitable metallic doping.

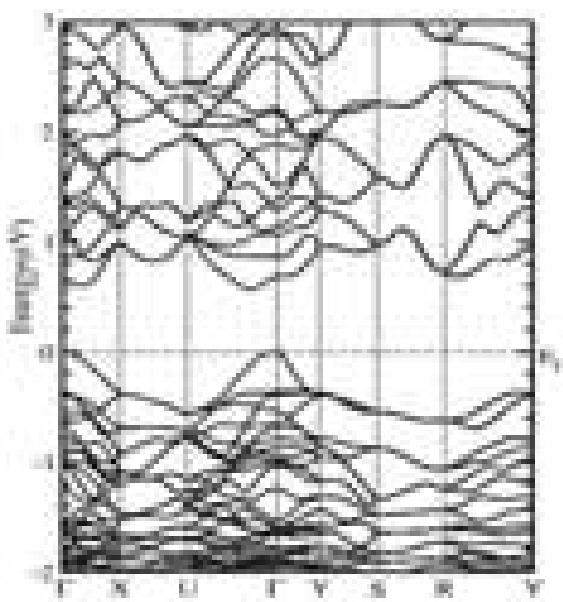

Fig 2.42: DFT results for Band Structure of Cu_3SbSe_3

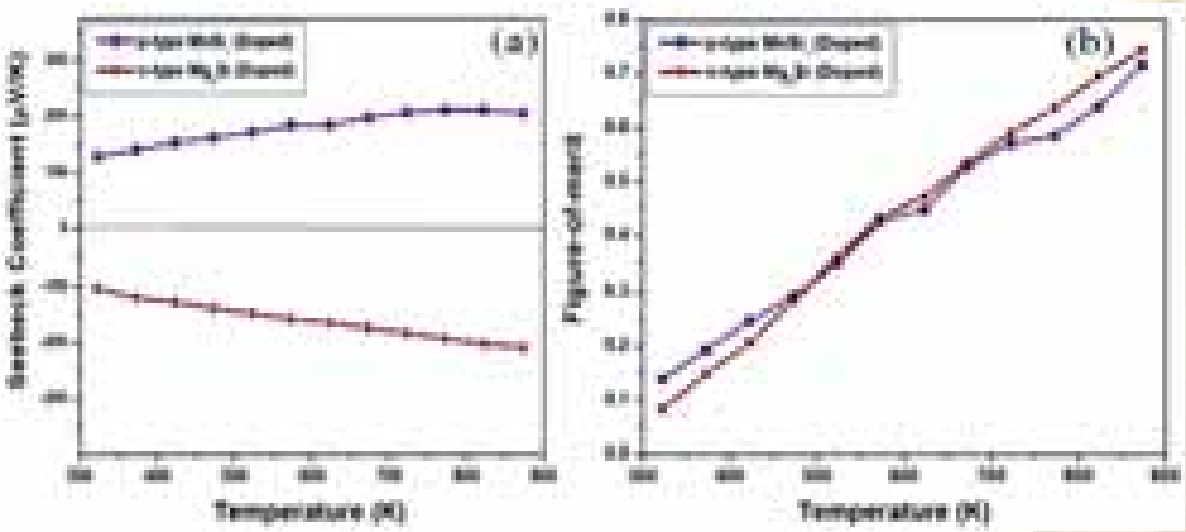

Fig. 2.43: Seeback coefficient of figure-of-merit of (a) n-type Mg_2Si and (b) p-type $MnSi_\gamma$

Development of cost effective Mg_2Si Based thermoelectric material

Silicides are being considered as potential TE materials and have been the focus of research for the past about five years. Silicides are one of the cheapest elements compared to constituent elements of conventional thermoelectric materials. We have synthesized both n-type Mg_2Si and p-type $MnSi_\gamma$ successfully, via milling using high energy ball milling followed by reaction sintering employing spark plasma sintering (SPS). Fig. 2.43 shows the Seebeck coefficient and figure-of-merit compatibility of these synthesized p & n-type materials.

Enhanced Thermoelectric Performance of a new half-Heusler Derivative $Zr_9Ni_7Sn_8$ Bulk Nanocomposite

Varying valence electron concentration per unit cell (VEC) in half-Heusler (HH) derives a large number of structures and substructures which can be exploited to improve the thermoelectric performance of HH. Herein, we report $Zr_9Ni_7Sn_8$ having VEC of 17.25 per formula unit which is off-stoichiometric HH ZrNiSn for thermoelectric applications. The structural analysis employing XRD, SEM and TEM (Fig. 2.44) confirms the resulting material to be a composite of HH and Ni_3Sn_4-type phases. Rietveld analysis estimates the

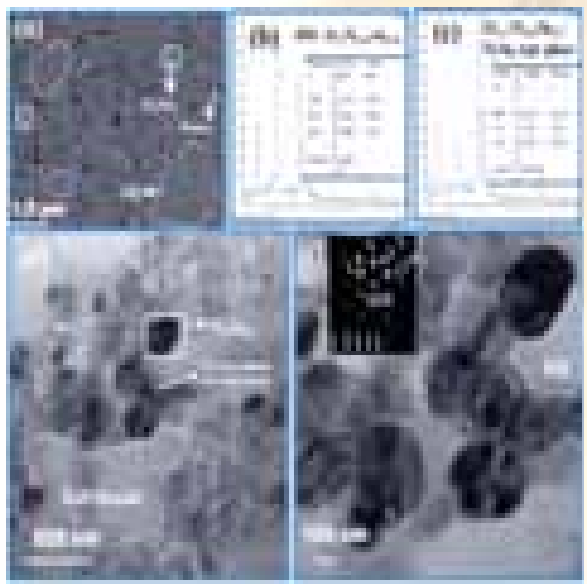

Fig. 2.44: (a) SEM morphology of BC $Zr_9Ni_7Sn_8$ showing a composite consisting two phases of HH (dotted circle), Ni_3Sn_4 (Square box) and small pores. (b) EDAX-SEM recorded from the dotted portion (fig.a), shows the presence of all the elements and quantification shows a phase very close to the HH. (c) EDAX-SEM obtained from the region marked as square box (fig. a) shows the presence of Ni, Sn & Zr elements and quantification shows a phase very close to Ni_3Sn_4-type phase with Zr surrounding the grain boundaries of Ni_3Sn_4 phase (d) Bright field TEM image also shows two contrasts in the sample which confirm the presence of two phases. (e) High magnification TEM image clearly shows two phases. The inset, shows SAED pattern corresponding to dotted region, reveal HH phase with zone axis [11]

volume fraction of HH to be 75.6±1.2% and 24.6± 0.8% for Ni_3Sn_4 phase. Interestingly, the present composite results in substantial increase in electrical conductivity (σ) by ~75% and a drastic reduction in thermal conductivity (κ) by ~56%, leading to a thermoelectric figure of merit (ZT) of 0.38 at 773K, which is ~87% higher than in normal HH ZrNiSn (Fig. 2.45). Further, the nanostructuring of the composite, employed by inechanical milling, derives to a significantly reduced κ (i.e. from 4.56W/mK to 3.36W/mK, at 323K), yielding to a ZT of 0.90 at 773K, which is >300% enhancement over the normal HH. The experimental results have been compared with the Bergman and Fel model for calculating effective thermoelectric parameters in composites. The results obtained in the present work motivate to design *in-situ* bulk composite consisting of HH and metallic inclusions Ni_3Sn_4 in an off-stiochiometric HH composite with VEC smaller than 18 for drastic reduction in κ and simultaneous improvement in the electrical transport.

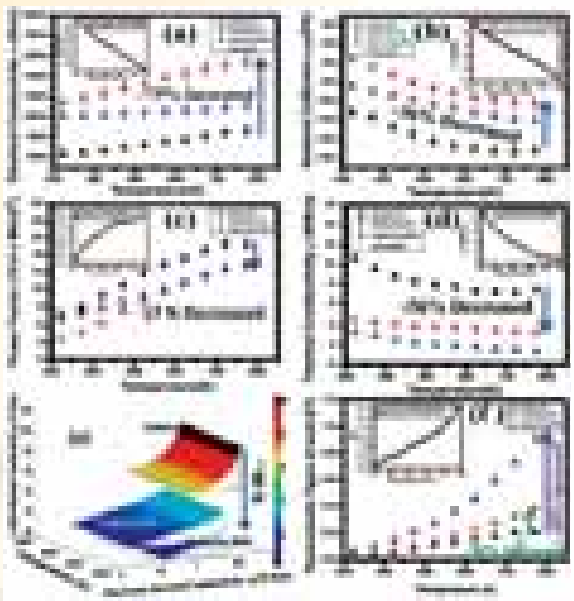

Fig. 2.45: Temperature dependence of thermoelectric properties of ZrNiSn normal HH, $Zr_9Ni_7Sn_8$ bulk composite (BC), $Zr_9Ni_7Sn_8$ bulk nanocomposite (BNC), Ni_3Sn_4 [in inset] and calculated effective thermoelectric parameters for composite using Bergmen & Fel model (a) electrical conductivity (b) Seebeck coefficient (c) power factor (d) total thermal conductivity (e) lattice and electronic thermal conductivity (f) calculated thermoelectric figure of merit

Role of nanoscale features in enhancing the thermoelectric performance of spark plasma sintered nanostructured p-type SiGe alloy

Nanostructured *p-type* $Si_{80}Ge_{20}$ alloy synthesized employing high energy ball milling followed by spark plasma sintering (SPS) after optimizing the process parameters. X-ray diffraction pattern of the ball milled powder showed the crystallite size was ~14 nm and further coarsened up to ~22 nm after spark plasma sintering (SPS). The rapid-heating rates associated with SPS resulted in a densification of 97.3%, while retaining the nanostructured features, which was obtained after ball-milling. Thermal conductivity of nanostructured $Si_{80}Ge_{20}$ alloy after SPS has been measured to be 2 W/mK at 900°C which is 22% less than the best reported value so far. The reduced thermal conductivity was mainly due to the increased interfaces consisting of randomly distributed high angle grain boundaries with atomic defects or disorders (TEM in Fig. 2.46). Also, the FESEM analysis of sintered alloy confirmed the

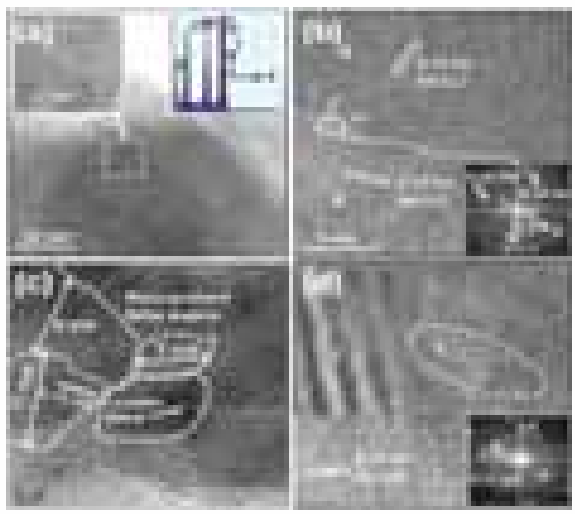

Fig. 2.46: Temperature dependence of thermoelectric properties of ZrNiSn normal HH, $Zr_9Ni_7Sn_8$ bulk composite (BC), $Zr_9Ni_7Sn_8$ bulk nanocomposite (BNC), Ni_3Sn_4 [in inset] and calculated effective thermoelectric parameters for composite using Bergmen & Fel model (a) electrical conductivity (b) Seebeck coefficient (c) power factor (d) total thermal conductivity (e) lattice and electronic thermal conductivity (f) calculated thermoelectric figure of merit

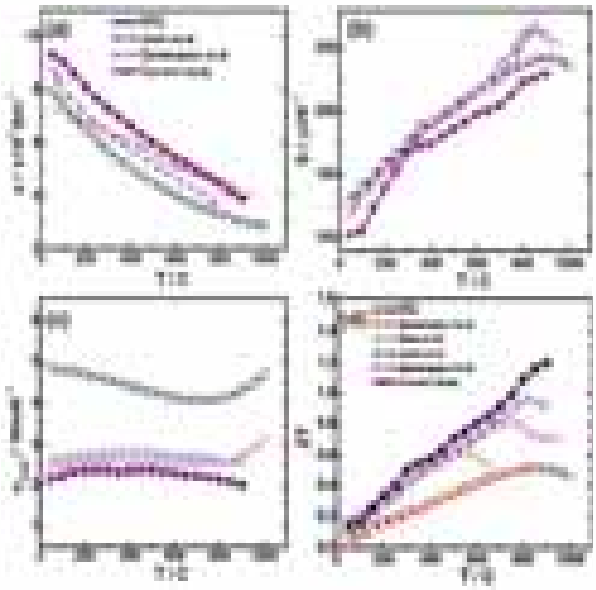

Fig. 2.47 : Temperature dependence of thermoelectric properties of sintered p-type $Si_{80}Ge_{20}$ nanostructured alloys (a) Electrical conductivity (b) Seebeck coefficient (c) Total thermal conductivities (d) Lattice thermal conductivity comparison with other SiGe alloys available in literature(d) figure-of-merit and its comparison with those reported in literature

heterogeneous distribution of nano-sized pores of size 25 to 150 nm within the matrix. Further, high HRTEM observations confirmed the post sintering nanoscale features with large density of interfaces. Finally, the significant reduction in thermal conductivity without scarifying the electrical conductivity resulted in considerable enhancement of ZT about ~1.2 at 900 °C (Fig. 2.47), which is a 26% higher value to that of best reported for p-type $Si_{80}Ge_{20}$ alloys.

Synthesis of Rare Earth free Permanent Magnetic Materials

The main objective of this activity is to synthesis Rare-Earth Free Permanent Magnetic Material e.g. MnAl, Mn-Bi-Fe, manganese antimonide etc. employing arc melting, Melt spinning, conventional melting, high energy ball milling and spark plasma sintering techniques. Efforts have been made to synthesize single-phase MnBiFe alloy essentially using melt spinning technique and annealing. As melt spun MnBiFe alloy gives better properties than as arc melted alloy. Optimization of annealing parameter by controlling annealing temperature and time resulted in a BHmax around 2MGOe (Fig. 2.48).

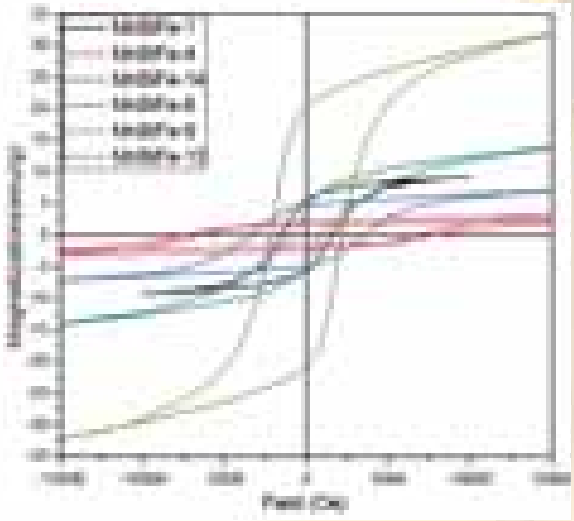

Fig. 2.48: M-H curves of MnBiFe with synthesized using different processing methods and annealing conditions

Development of Aluminum alloy-Carbon Nanotubes (Al-CNTs) composites employing Cryomilling and hot extrusion

One of the major challenges towards the development of Al-CNTs and similar metal matrix composites is achieving a uniform dispersion of CNTs in the metal matrix, since Vander Wall forces cause agglomeration of CNTs during mechanical alloying with metal powder. The research on the development of high strength-light weight Al-CNTs composites has been initiated with the support of CSIR-NPL. In this activity, the powder mix of pure Al alloy and MWCNTs (0.5 wt.%) was obtained by solution dispersion method, which was milled in liquid N_2 using a cryomilling attritor. Different parameters, such as ball to powder ratio and milling time were varied keeping milling speed as fixed as 240 rpm. For the balls to powder weight ratio of 20:1 and milling time of 2 h, a uniform dispersion of CNTs in the Al matrix was obtained (shown in Fig 2.49a). The cryomilled pure Al-CNTs powder was consolidated by (i) cold pressing at ~400 MPa followed by sintering under vacuum at ~550 °C and

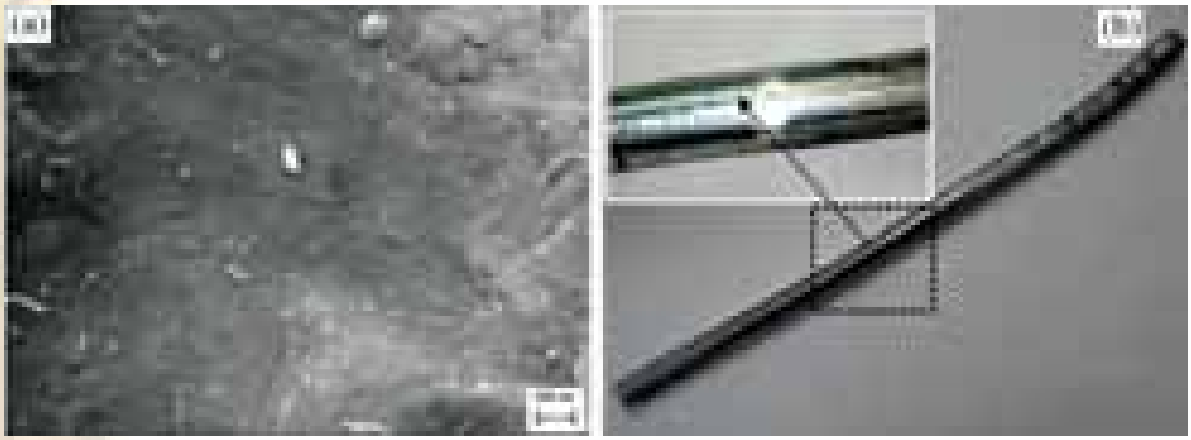

Fig. 2.49: (a) SEM micrograph of cryomilled Al-MWCNTs (0.5 wt%) composite powder showing a uniform dispersion of CNTs in the aluminum matrix and (b) Photograph of the hot extruded Al-0.5 wt% MWCNTs rod [close-up view in (b) shown in inset represents defect-free lustrous surface]

(ii) pre-compacted followed by hot extrusion at 400°C at an extr usion ratio of 15 so as to develop rods of 12 mm dia (Fig. 2.49b). The pure Al-0.5% CNTs composite powder has delivered tensile strength and Vickers microhardness of ~35 MPa and 32 HV_{200}, respectively, which has been enhanced to >200 MPa and 72 HV_{200}, respectively after hot extrusion.

रेडियो एवं वायुमंडलीय विज्ञान प्रभाग

Radio and Atmospheric Sciences

Dr M.V.S.N. Prasad
Chief Scientist, Email : myprasad@nplindia.org

D 03.01 Radio Science

Dr M V S N Prasad
Dr Arun Kumar Upadhayaya
Dr Rupesh M Das
Ms Beena Gupta
Sh Man Mohan Gupta
Ms Smriti Tiwari Singh

D 03.02 Atmospheric Science

Dr Bhuwan Chandra Arya
Dr Meena Jain
Dr Chhamendra Sharma
Dr Tuhin Kumar Mandal
Dr Sachchidanand Singh
Dr (Ms) Monika Jain Kulshreshta
Sh Ashish Ranjan
Dr. Sumit Kumar Mishra
Dr Sudhir Kumar Sharma
Dr Rajesh Agnihotri
Dr. Radhakrishnan S.R
Sh Arun Kumar Ghoghar
Sh. Shambhu Nath
Ms Shiv Kumari Bhatia
Sh Vinod Kumar Sharma
Sh Alok Mukherjee

Radio and Atmospheric Sciences

The Radio and Atmospheric Sciences Division (RASD) of NPL caters to the scientific needs of the nation in the areas of radio science and applications, space weather and ionosphere, chemistry and physics of the earth atmosphere, atmospheric pollution and climate change etc. The major research areas are: (i) Radio Science, and (ii) Atmospheric sciences. Atmsopheric science involves study of Atmospheric chemistry, Spectroscopy of Atmosphere, simulation and modeling for atmospheric physics.

Radio Science

RASD has unique group in India which is involved in the characterization of the ionized, non ionized tropospheric media and the near earth radio environment using radio wave propagation for the purpose of betterment of radio communications, navigation and other advanced applications. This consists of radio channel measurements and modeling for fixed and mobile communications, generating new data sets in VHF and UHF frequency bands, development of models over various regions of India and interaction with various user agencies. Monitoring and modeling related to ionospheric / tropospheric parameters using satellites and ground based systems including GPS, Tomographic Receivers, Ionosonde, etc., are also being carried out. Division also provides ionospheric forecasting/nowcasting to users worldwide through space weather Regional Warning Center (RWC, NPL-India) and have consistently improved the International Reference Ionosphere (IRI) model through model comparisons with observed data. Ground based techniques like ionosonde, GPS receivers are being utilized to study polar ionosphere through Antarctic scientific expeditions.

Atmospheric Sciences

The atmospheric science group of RASD is engaged in developing the Greenhouse gas (GHG) inventory from different sources, emission estimates of particulate matter (PM) and trace gases (SO_2, NO and NO_2) from biomass fuels consumed in rural sector of our country, emissions from land fills and wheat and rice crop fields etc. At the same time group also carry out chemical characterization using state-of-the-art techniques and source apportionment of particulate matter (PM) and precursors for different regions in the country, including the surrounding oceans, Himalayas and poles. This group also studies the atmospheric ozone, its chemistry and dynamics using various models and observations.

A wide range of information about the atmospheric aerosols, trace gases, solar radiation and their interactions is generated by conducting spectroscopic measurements of the atmosphere in the UV, Visible and NIR-IR spectral range. It enables the optical and physical characterization of the atmospheric aerosols and help in identifying the trace chemical constituents in the gas samples or in the atmospheric column. The high resolution Open-Path FTIR, micro-pulse LIDAR are the recent modern equipments that supplement the study of aerosol optical depth, vertical profile of aerosols, aerosol size distribution, scattering and absorption coefficients of aerosols, single scattering albedo (SSA), effect of aerosol shape and size on optical properties, chemical characterization, etc. A ozone standard has been added in the division for traceability of measurement and other purposes. Mathematical modeling is an integral part of all the activity groups in the division, and the objective of this is to assimilate the various data sets generated in the division and elsewhere to simulate and model the atmospheric processes.

3.1 Radio Science

3.1.1 New data set generation for verification of electromagnetic macro model for path loss prediction in cellular communication systems

Cellular operators providing services in GSM bands of 900 &1800 MHz extensively use radio planning tools for the design of cellular systems.The reason that the 0.8 to 2.1 GHz cellular band was chosen for mobile broadband is that the reflection from buildings is negligible, and yet the signals can penetrate buildings and terrain and do not significantly bounce inside the rooms.In order to investigate the variation of path loss exponent/path loss in the near and far field regions of GSM base stations extensive experimental investigations utilizing 36 base stations have been conducted in the Maharashtra and Goa regions of Western India.In Goa region experiments were conducted in Panjim city (5 base stations) and in the Maharashtra region measurements were conducted in the cities of Aurangabad (5 base stations), Pune (15 base stations), Nagpur (6 base stations), Kolhapur (5 base stations).Out of the total 36 base stations used in the study 10 stations operated on 1872 MHz and the remaining 26 operated on 900 MHz.

The transmitting power of all base station is 40dBm and transmitting gain is 8dBi for all base stations. The gain of the receiving antenna is 0 dB and the height is 1.5m.Near field distance increases with frequency and with base station antenna height. The receiver is standard Nokia equipment used in drive in tools for field trials. The position of the mobile is determined from the GPS receiver and this information with the co-ordinates of the base station was utilized to deduce the distance traveled by the mobile from the base station. The signal strength information recorded in dBm was converted into path loss values utilizing the gains of the antenna.

The observed path loss values were utilized to deduce path loss exponents for each base station as a function of distance. The variation of path loss exponent has been studied in the near and far fields of base station. The general trend observed in the case of base stations with large values of h_b ranging from 35-60m is the fall of exponent from high values of 8 at distances close to transmitter to values slightly below 3, fluctuates and settles to a value of 3 and increases to a value of 4 after some intermediate distances. In the case of base stations with low h_b values more or similar trend is observed, but the difference comes in the slightly higher value of settled exponent. In all the cases exponent falls to a value of 3 at distances of 200-250m. A typical variation of path loss exponent in the case of Panjim city is shown in fig 3.1 which follows the above description. The increase in path loss exponent values is observed after some intermediate distances of 1500-2500 m. It is advisable to go for smaller base station antenna heights to reduce the near field zones.

In this study, it is shown that a physics based electromagnetic macro model can provide accurate data for the path loss exponent in a cellular network using electromagnetic simulation tools that depend only on some physical parameters of the macro model. The deployment of electromagnetic macro model has been carried out in collaboration with Syracuse University, USA. In a macro model, one needs to include only the electrical parameters of the environment without including the clutter effect factors such as buildings, trees and so on. Figure

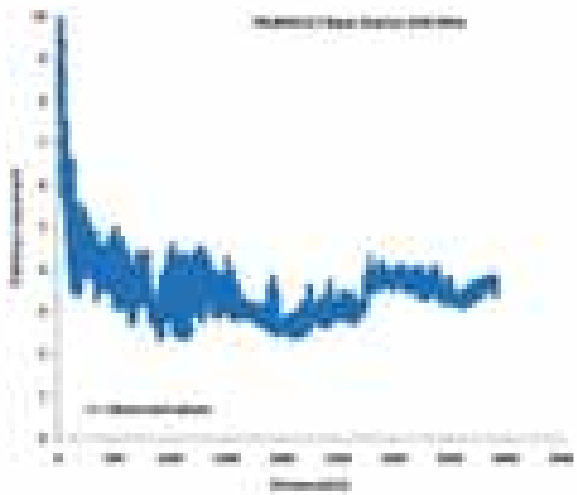

Fig. 3.1: Variation of path loss exponent as a function of distance for Panjim base station

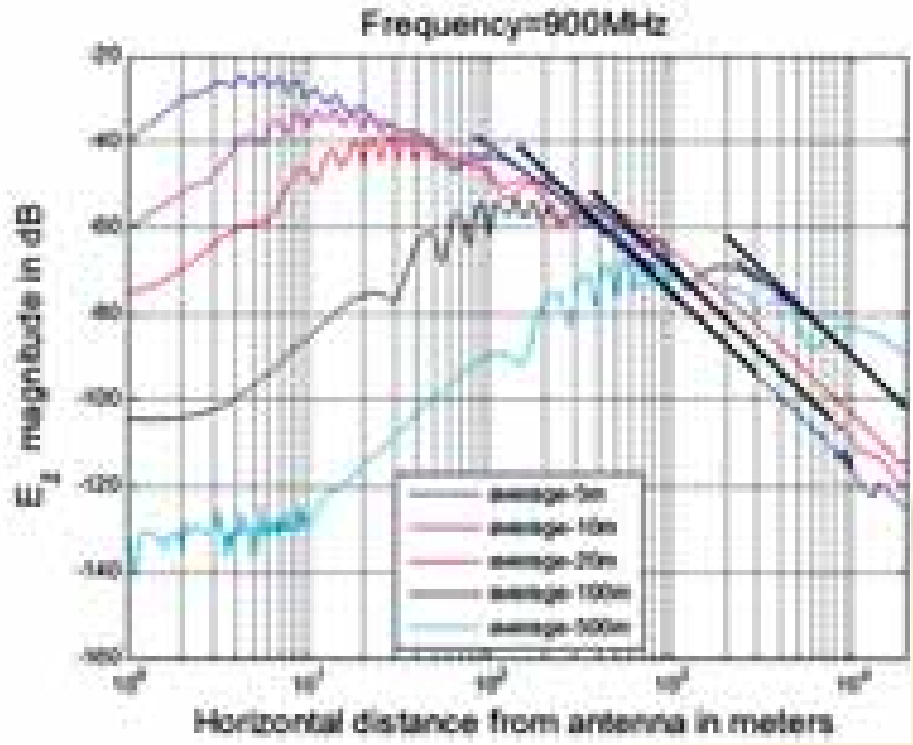

Fig. 3.2: Variation of electric field as a function of distance using electromagnetic model for various heights of base station antenna at 900 MHz

3.2 plots the field strength as a function of the radial distance for different height of the antenna above the ground. In this figure, it is seen that near the transmitting antenna there is an interference between the direct space wave and the field from the image produced by the imperfect ground, providing variation of the total field strength. This is often labeled as fading. There is a height gain in the far field of the antenna but in the near field which is of importance in cellular communication there is actually a height loss. Hence, it is proposed that a better solution will then be to deploy the transmitting antenna closer to the ground. In that case the region of the variation in the field strength would be quite small and the field strength will decay monotonically inside the remainder of the cell minimizing fading.

3.1.2. Ionsopheric Studies

3.1.2.1 A statistical analysis of occurrence characteristics of Spread-F irregularities over Indian region

We have investigated the regularities of a change in spread F probability during day-to-day, under varying solar variability, latitudinal behavior and their response to geomagnetic storm in equatorial and low-mid latitude stations. The occurrence characteristics of Spread-F irregularities, is obtained from daily hourly ionosonde data from a low-mid latitude station, Delhi (28.6°N, 77.2°E), for more than half a solar cycle (2001 to 2007). The latitudinal behavior of Spread-F is studied using ionosonde data from anomaly crest station, Ahmedabad (23.01°N, 72.36°E) and equatorial station, Kodaikanal (10.2° N, 77.5°E) for low, moderate and high solar activity periods. The maximum percentage occurrences of Spread-F were observed during the low solar activity year 2007, we believe, the low plasma and neutral density during 23/24 solar cycle minimum could be an important factor leading to the generation and propagation of TIDs and gravity waves. Figure 3.3 shows the local time behavior of percentage occurrence of spread-F during different seasons at Delhi station.

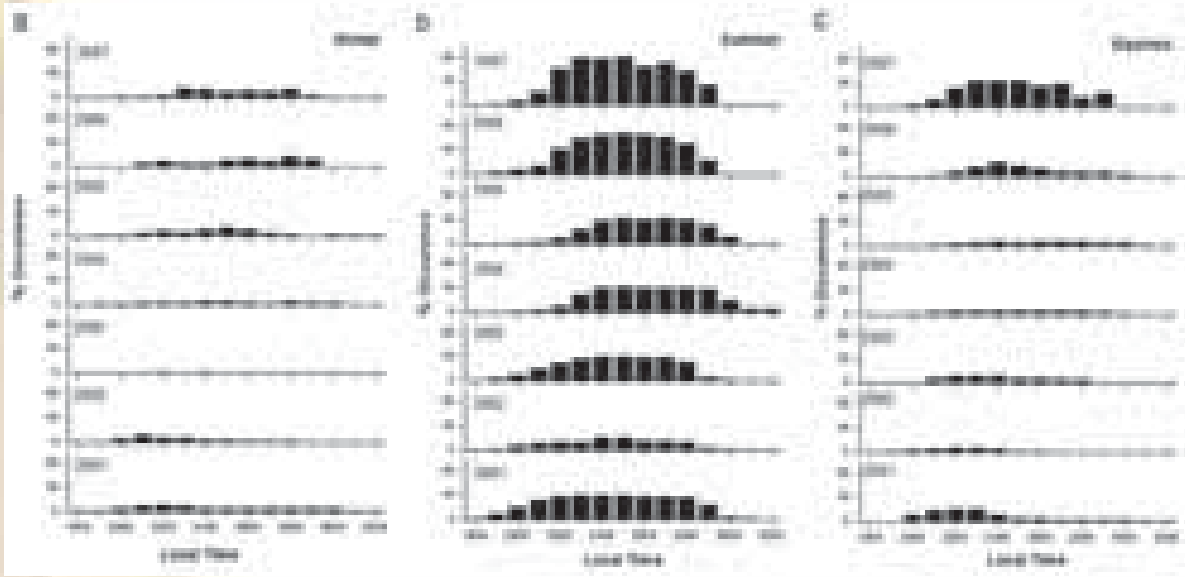

Fig. 3.3: (a), (b) and (c) show local time behavior of percentage occurrence of spread- Fduring different seasons of year 2001 to 2007 at low latitude station Delhi

3.1.2.2 Ionospheric F2- region: Variability and sudden stratospheric warmings

The possibility of links between the meteorological phenomena and the upper atmosphere have been discussed very profoundly during the last two decades.We therefore investigate the extent of ionospheric changes following SSWs of 2007, 2008 and 2009 using ionosonde data from six different stations in the Asian zone thus covering a broad latitudinal range from 23.2°N to 45.1°N . We find that ionospheric F2-region shows some significant perturbations soon after the start of the warming. However characteristics of these perturbations vary from event to event and from station to station. We also examine the data on equatorial electrojet strength (EEJ) during these warmings and find there are significant changes in the EEJ strength during the SSW events. The following conclusions are drawn from the analysis.

1. There are perceptible ionospheric perturbations which can be linked to warmings.
2. These perturbations are in the form of enhancements and depressions in foF2 resulting in peak electron density variations which could be larger than 200% when compared with the normal magnetically quiet time ionosphere.
3. The low latitude station Okinawa (26.6^{0}N ,121.8^{0}E) showed semidiurnal ionospheric perturbations during the SSW event of 2009, a feature previously reported from the total electron content measurements. This feature was not found during the SSW event of 2008. On the other hand the "EIA Crest" station Bhopal (23.29°N, 77.46°E), showed some evidence of 6-hour periodicity in ionospheric changes during the SSW event of 2007.

3.1.2.3 Systematic study of latitudinal ionospheric response to the geomagnetic storm occured during 7th and 9th March 2012.

Global Ionospheric responses to the geomagnetic storms are not homogeneous. The present work is an attempt to explore the spatial and temporal behaviour of earth's ionized media over the southern hemispheric region during the geomagnetic storm events observed on 7th and 9th March 2012. The Ionospheric Total Electron Content (ITEC) observed with the help of South American GPS network has been utilized. The

geophysical conditions reveals that the first storm commenced on 7th March 2012 at around 0100 UT having which was lower in magnitude with respect to the second storm observed on 9th March 2012 at 1200 UT. The recorded maximum negative excursion in Dst-index is -74nT and -131nT respectively for 7th March and on 9th March 2012. However, enhanced AuroralElectrojet (AE) confirms the electro-dynamic disturbances at auroral zone during the above said period.

The analysed TEC results shown in Fig 3.4 confirm that the expansion of Equatorial ionsopheric anomaly(EIA) along with state of ion density over mid latitude region was not only affected by equatorial electrojet (EEJ) strength but also by the direction of neutral wind. On the basis of different combinations of equatorial and high latitude dynamics, the results are classified and explained in two different parts.

The first part covers the process involved on 7th March 2012, when the EEJ strength is slightly lesser than that of the normal day and the AE- index is at moderate level. The combined effect of weaker EEJ and moderate AE- index leads to become favourable for equator-ward transportation of plasma which limits latitudinal expansion of EIA as compare to normal day. The consequences are clearly observed in analysed ITEC parameter over equatorial to high latitude region. The spatial and temporal behaviour of ITEC shows positive effect at equatorial and near equatorial region with simultaneous depletion at low-mid latitudes. On the other hand, elevated AE is responsible for day time equator-ward neutral wind and drives the transport of plasma from higher latitude to low latitude region along with the slope of geomagnetic field lines. Furthermore, the slope of mid-latitude geomagnetic field lines uplifts the plasma at higher altitudes

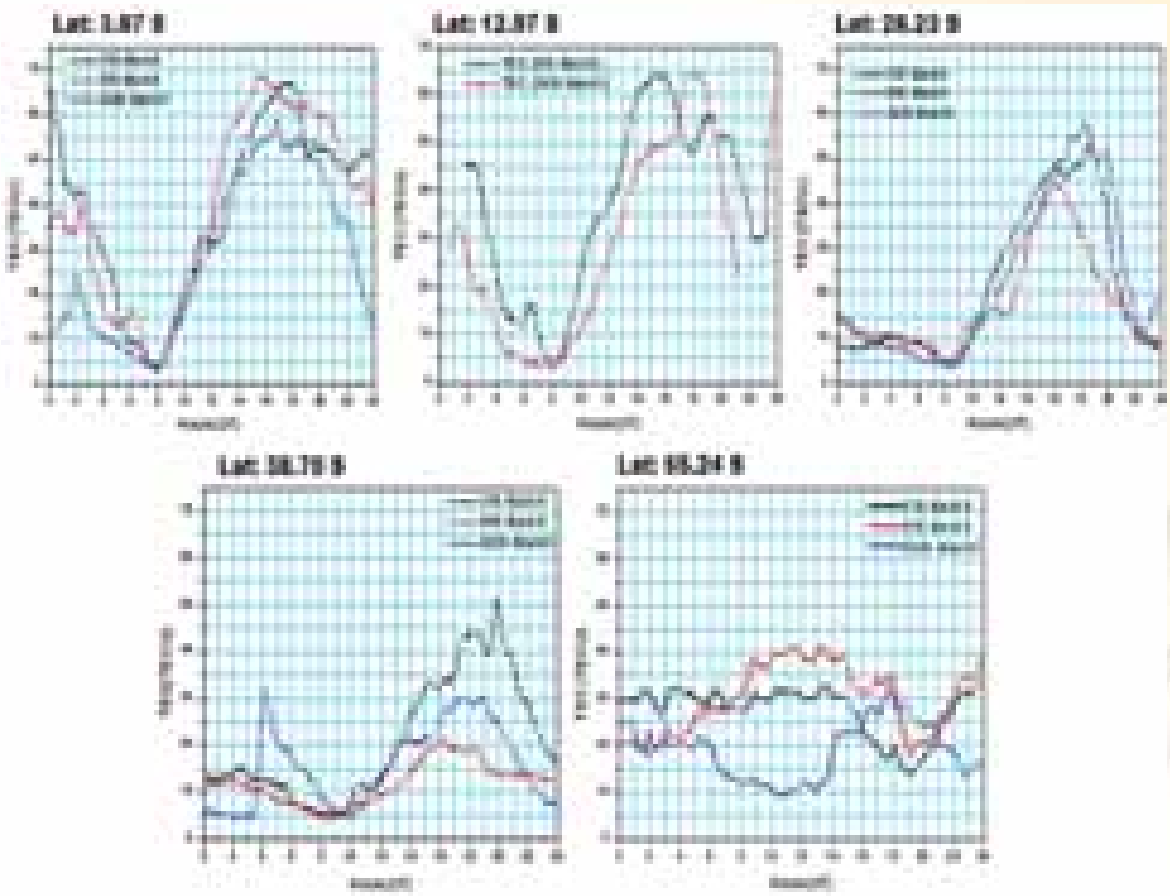

Fig. 3.4: Storm days along with control day Ionospheric total electron content variation over different geographic locations

where the recombination rate is very low and cause to enhance the ITEC value over mid latitude region. The observed enhanced ITEC at high latitudes followed by depletion supports the above explanation.

The second part shows the modified ionospheric spatial and temporal variation under storm modified equatorial and high latitude electrical conditions. Reversal of EEJ or occurrence of Counter electrojet (CEJ) over equatorial region along with significantly higher AE-index has been registered on 9th March 2012. This combination provided a unique opportunity to study the latitudinal behaviour of earth's ionosphere when an unusual negative force is acting over the equator. Presence of CEJ prevented the formation EIA and shows enhanced ITEC value at equatorial region coincides with time of ion diplition over low and low mid-latitude region. Finally, the work confirms that the geomagnetic storms are responsible to perturb equatorial and high latitude dynamics in various ways and modifies the normal spatial and temporal behaviour of Ionosphere.

3.1.3 Research Activities at Antarctica:

CSIR-National Physical Laboratory has been participating regularly in the Indian Antarctica Expedition to conduct scientific research in the area of Upper and Lower atmosphere. During the year 2013-14, two Research Proposals were accepted from the CSIR-NPL, to participate in the 33rd Indian Scientific Expedition to Antarctica (33-ISEA). The titles of the proposals are: (1) Impact on Space-weather events on Polar Region Ionosphere, and (2) To study the Aerosol radiation forcing over the Antarctic region by measuring Aerosol properties and Radiation. The main aim of the proposed study are: (1) morphological study of Polar region Ionosphere i.e. day to day behavior of different ionospheric parameters like bottom side ionospheric plasma density, variation of critical frequency and height of different ionospheric layers, (2) investigation of solar wind – thermospheric - magnetospheric-ionospheric coupling over polar region during high solar activity period with special emphasis on adverse space weather conditions, (3) collection data for Aerosol Optical Depth, radiation flux in the UV and broad band and absorbing aerosol (BC) and (4) to obtain Aerosol Radiative properties including radiative forcing at Antarctica.

3.2 Atmospheric Sciences

3.2.1 CSIR Network Project "Probing the Changing Atmosphere and its Impacts in Indo-Gangetic Plains (IGP) and Himalayan Regions [AIM – IGPHim]"

The CSIR Network Project "AIM_IGPHim" (PSC-0112) is being pursued by the network partner laboratories namely CSIR (CMMACS, CRRI, IHBT, IMMT, NBRI, NEERI & NEIST) with CSIR-NPL is functioning as the nodal laboratory. This project has been initiated by the network partner laboratories to understand the causes of atmospheric changes and the impacts of changing atmosphere on agriculture, human health and bio-diversity in the Indo-Gangetic Plains (IGP) and Himalayan regions which have significant socio-economic bearings for country as a whole. In particular, the project envisages addressing following questions:

- How the atmosphere in IGP and Himalayan regions is changing and what are the major reasons for that?
- What is the magnitude and mechanism of impact of carbonaceous aerosols and dust in modifying atmospheric processes over this region?
- How will the atmospheric processes respond to future anthropogenic perturbations in the region?
- What is the impact of changing atmosphere on crops, flora and human health in IGP and Himalayan regions?

During the year 2013-14, the project activities have started picking up steam to meet the envisaged outcomes of the project. In this direction, a number of activities have been undertaken by the network partners, some of which are listed below:

- NPL teams has visited a number of sites for assessing the feasibility of establishing background monitoring station in Western Himalayan region and has short-listed 'Purara' (N 29054.511', E 79037.549', height 3856 feet) in 'Bageshwar' District of Uttrakhand and Palampur (H.P.) as the potential sites. A final decision has been taken to establish the station at IHBT campus, Palampur (H.P.).
- Patterns of long-distance transport of pollutants have been investigated through back trajectory and forward trajectory analyses for potential background monitoring sites as well Delhi and Bhubaneswar using models like HYSPLIT and TRAJSTAT (Fig 3.5)
- Continuous Ambient Air Monitoring System (CAAMS) and Lidar equipment for background atmospheric monitoring have been ordered for installation at proposed background monitoring site.
- Campaign based atmospheric measurements have been carried out in Himachal Pradesh and Thar desert areas along with regular measurements at Delhi.
- Greenhouse gas (GHG) emission inventories have been created for IGP states for transport, energy and waste sectors.
- Weather Monitoring Systems have been installed at Itanagar & Imphal besides sampling of gases and aerosols from coke oven plant site in North-East India have been started.
- T63 atmospheric transport model, MOZART has been setup for modeling of carbon fluxes

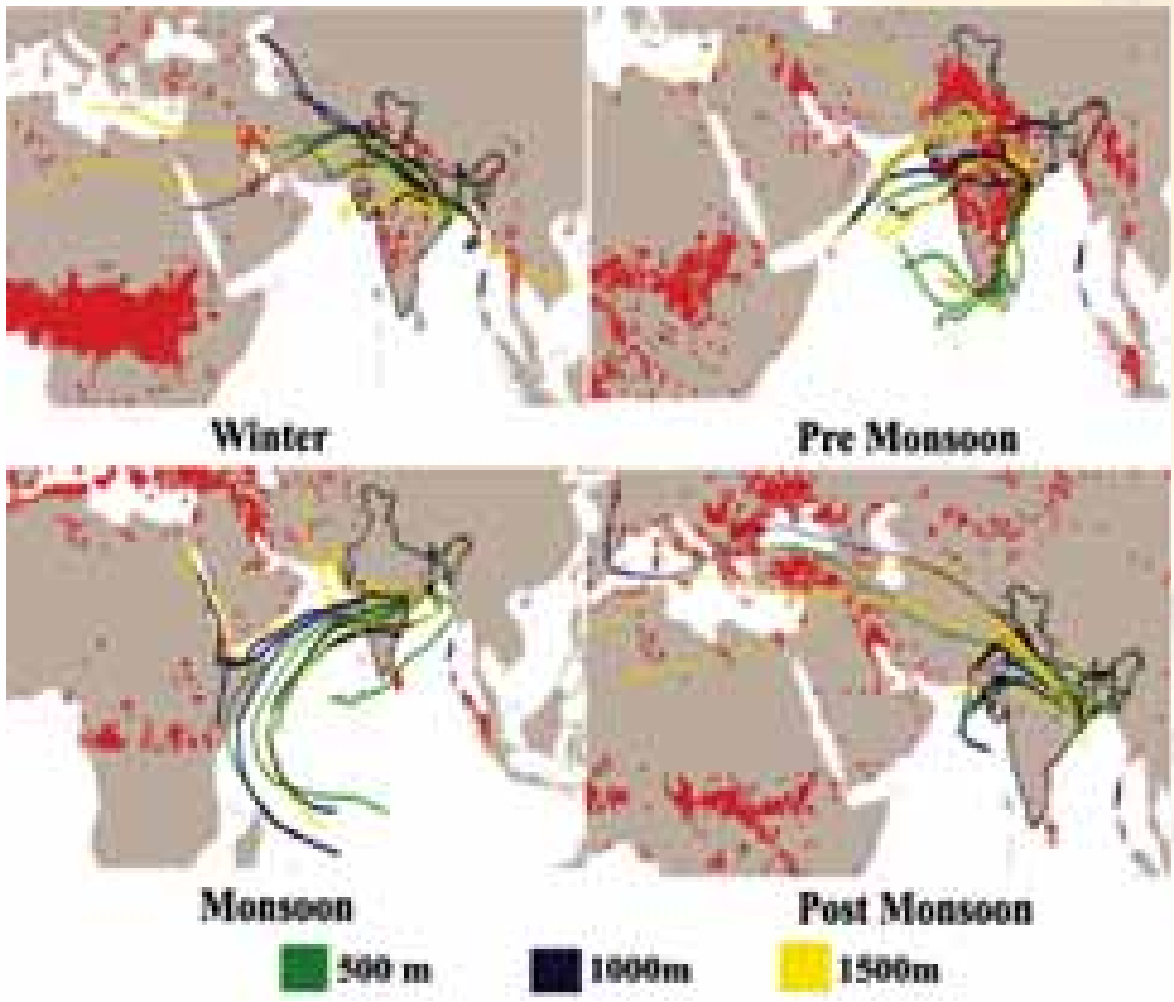

Fig. 3.5: Backward trajectory Analysis for pollutants' transport patterns of Bhubaneswar during different seasons

which would be validated using the measured CO_2 values.

- Initial results of the Free-Carbon dioxide Enrichment Experiment (FACE) suggest that wheat crop will perform better under future climate change scenario with respect to elevated CO_2.
- Phyto-sociological sampling have been performed to record tree density and basal area in trans-Himalayan region (3658 m amsl) in the District of Lahaul&Spiti (H.P.) for assessment of impact of changing atmosphere on bio-diversity.

3.2.2 Estimation of emissions of Carbon dioxide and other Air Pollutants from Diesel Consumption in Cellular Base Stations in India

At present, India is the second largest global telecom market after China. The telecom industry has attracted 8% of the cumulative foreign direct investment over the last two years in India. Indian telecom companies are now starting to make a major impression globally. Indian mobile telecom industry had 584.3 million subscribers in 2010-2011 with an annual growth rate of 49%. However, this growth has bearing on climate due to the $CO_2$and other air pollutants' emissions associated with the diesel fuel used in this sector to provide power which is also a dominant cost component for telecom companies. Climate change and air quality are serious concerns caused due to the increasing emissions of Greenhouse gases (GHGs) and other air pollutants. Mobile communication network in India is becoming a significant source of emission in India. This sector had 400,000 Base Transceiver Stations (BTS) during 2010-2011 whose 40% power requirements was met by grid electricity while remaining 60% was met by diesel generators which consumed 4.9% of the total diesel sold in India and emit GHGs. Using the IPCC 2006 and USEPA AP-42 methodology emissions from diesel consumption in this sector have been computed. The results showed that this sector contribute 10308 Gg of CO_2, 1.4 Gg of CH_4 and 0.08 Gg of N_2O in 2010-11. Another estimate showed that only 1.93% of total diesel sold in India was consumed in this sector which has been estimated to emit 4010 Gg of CO_2, 0.54 Gg of CH_4 and 0.03 Gg of N_2O. This leads to a sectoral carbon foot print range of 1.101-2.831 million ton carbons. Estimations from BTS revealed that diesel consumption is also responsible for 22-56 Gg CO, 102-264 Gg NO_x, 6.7-17 Gg SO_x, and 7-18.5 Gg PM_{10}. District wise mobile tower data for the 24 states of India have also been collected which have been used to generate district-wise emission inventory of CO_2 for these states of India shown in following figure 3.6. However, as district-wise tower data for remaining eight Indian states could not be obtained by authors, the district wise emission inventory for these states could not be prepared, although the emissions from diesel fuel consumed in BTS in these eight states are also included in the total CO_2 emission inventory.

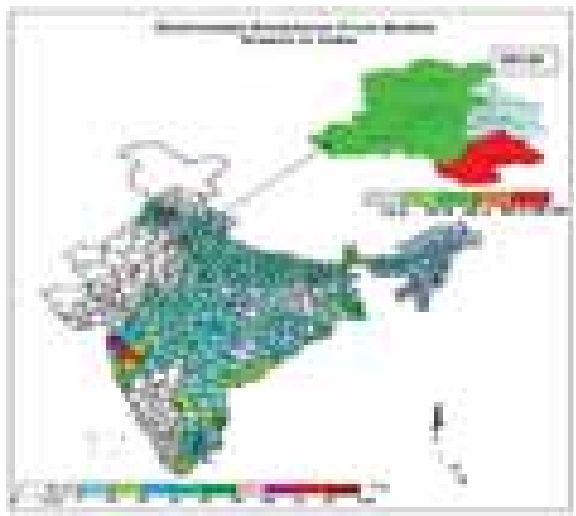

Fig. 3.6: District wise CO_2 Emission from mobile towers in India (Inset figure shows CO_2 emissions from mobile towers in different districts of Delhi)

3.2.3 Consultancy project on Preparation of the Third National Communication and other new information to the UNFCCC:

The Ministry of Environment, Forests Climate change (MoEF&CC) has undertaken the "Preparation of the Third National Communication

(TNC) and other new information to the United Nations Framework Convention (UNFCCC) on climate change as part of fulfillment of India's obligation to UNFCCC. In this context , the MoEF has initiated the process of preparation of "Biennial Update report (BUR) and awarded the above consultancy project to NPL for estimation of N_2O, and integrate the measured emission factors to estimate the CH_4 emission from solid waste dumping in managed landfills and open dumping sites at national scale for the period 2008 to 2010.

3.2.4 Characteristics of ambient ammonia over Delhi

Characteristics of ambient ammonia were evaluated along with other trace gases (NH_3, NO, NO_2, SO_2 and CO) and particulates ($PM_{2.5}$ and PM_{10}) over Delhi during December 2011 to June 2012. The average mixing ratios of ambient NH_3, NO, NO_2, SO_2 and CO were recorded as 21.2 ± 5.4 ppb, 19.5 ± 4.9 ppb, 17.4 ± 1.4 ppb, 1.7 ± 0.5 ppb and 1.6 ± 0.7 ppm respectively during winter, whereas the average mixing ratios of ambient NH_3, NO, NO_2, SO_2 and CO were recorded as 20.8 ± 4.7 ppb, 21.7 ± 6.3 ppb, 16.8 ± 3.1 ppb, 2.2 ± 0.8 ppb and 1.8 ± 0.9 ppm respectively during summer. The average monthly NH_3/NH_4^+ ratios varied from 0.28 to 2.56 with an average value of 1.46 in winter. The higher NH_3/NH_4^+ ratio (3.5) was observed in summer indicates the abundance of NH_3 in the atmosphere during summer. The higher fraction of particulate NH_4^+ observed in winter than summer attributes to conversion of gaseous NH_3 into NH_4^+. The results emphasized that the traffic could be one of the significant sources of ambient NH_3 at the urban site of Delhi as illustrated by positive correlations of NH_3 with traffic related pollutants (NO_x and CO) (Fig 3.7). Surface wind analysis and wind directions also support the road side traffic and agricultural activities at the nearby areas indicating possible major sources of ambient NH_3 at the study site.

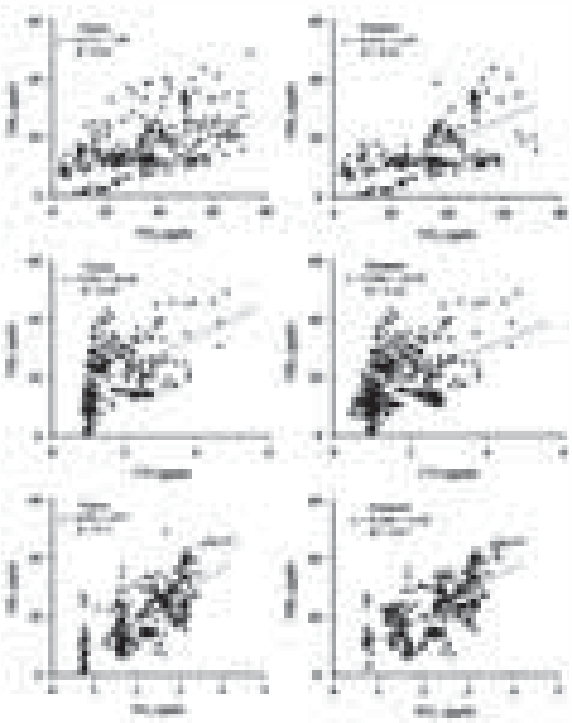

Fig. 3.7: Scatter plots of NH_3 versus NO_x, NH_3 versus CO and NH_3 versus SO_2 in different seasons during December 2011 to June 2012 at Delhi

3.2.5 Source apportionment of PM_{10} and $PM_{2.5}$ over Delhi using receptor model

Positive Matrix Factorization (PMF, a receptor model) was used to quantify the contribution of different types of sources of PM_{10} and $PM_{2.5}$ over Delhi during January to December 2013. Concentrations of PM_{10} (186.9 ± 51.9 μg m^{-3}) & $PM_{2.5}$ (153.8 ± 38.2 μg m^{-3}) and its chemical compositions i.e., organic carbon (OC: 26.5 μg m^{-3} of PM_{10}& 27.7 μg m^{-3} of $PM_{2.5}$), elemental carbon (EC: 10.7 μg m^{-3} of PM_{10}& 10.7 μg m^{-3} of $PM_{2.5}$), water soluble inorganic ionic components (WSIC) and major & trace elements of were used for source apportionment. The application of PMF analysis helped to identify the emission sources for 80% of the total PM_{10} mass and 87% of total $PM_{2.5}$ mass at the observational site of Delhi.

3.2.6 Study on trace gases and particulate matter ($PM_{2.5}$) over the northwestern Himalayan region of India

Ambient trace gases (NH_3, NO, NO_2 and SO_2) and black carbon (BC) were measured along with

particulate matter ($PM_{2.5}$) over the northwestern Himalayan region (Palampur, Kullu, Shimla, Solan and Nahan) of Himachal Pradesh (HP), India in a campaign mode during 12-22 March 2013 to evaluate the ambient air quality of the region. The average mixing ratio of ambient NH_3, NO, NO_2 and SO_2 were recorded as 7.1±2.6, 3.1±1.3, 3.9±1.4 and 1.7 ± 0.7 ppb respectively over the northwestern Himalayan region. The average concentration of BC was estimated as 2.2 ± 0.5 µg m^{-3} over the region whereas average concentrations of $PM_{2.5}$ mass was estimated as 41.8 ± 7.9 µg m^{-3}. The spatial variation of ambient trace gases (NH_3, NO, NO_2 and SO_2), BC and particulate matter ($PM_{2.5}$) over the northwestern Himalayan region, India reveals that the region is mainly influenced by local activities i.e, tourism activities, agricultural activities, biomass burning and vehicular emissions (Fig.3.8). A significant positive linear correlation of NH_3 and NH_4^+ with SO_4^{2-}, NO_3^- and Cl^- (NH_4^+ vs. SO_4^{2-}, r^2= 0.652; NH_4^+ vs. NO_3^-, r^2= 0.701; and NH_4^+ vs. Cl^-, r^2= 0.627)of the particulate ($PM_{2.5}$) indicating the possible formation of $(NH_4)_2SO_4$, NH_4NO_3 and NH_4Cl aerosols over the region.

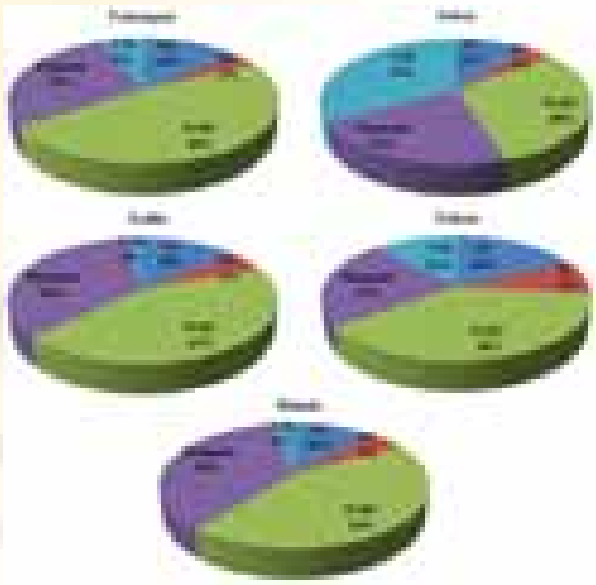

Fig. 3.8: Percentage distribution of OC, EC, WSIC, major and minor elements and UM (unidentified mass) of $PM_{2.5}$ mass at different locations of northwestern Himalayan region of India

3.2.7Role of convection in hydration of tropical UTLS: Implication of AURA MLS long-term observations

Water vapor distribution at different levels of tropical region namely Asian monsoon region, African Monsoon region and American monsoon region has been studied. Figure 3.9 presents temporal variation of water vapor mixing ratio (WVMR) over the Asian monsoon region from 3 years of observations by AURA-MLS. An examination of WVMR at various pressure levels indicate that water vapor transport is rather fast up to a level of 147-121 hPa whereas it is relatively slow above this level. Seasonal variation in water vapor is observed and noted to be closely associated with seasonal northward movement of ITCZ.

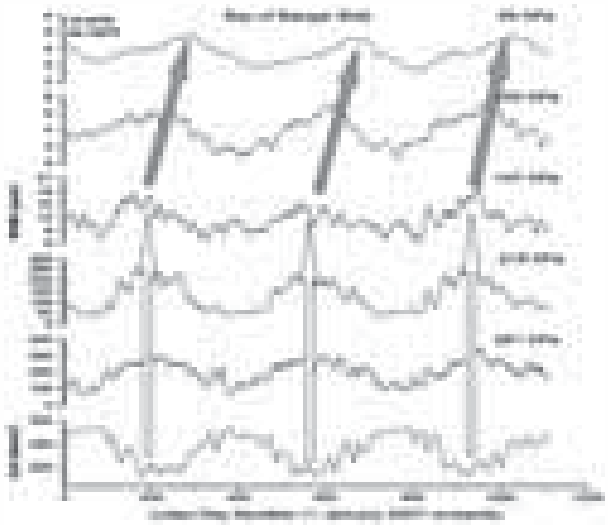

Fig. 3.9: Time series of WVMR at 261, 215, 147, 100 and 68 hPa level along with the time series of daily mean OLR for the period of 1 January 2007–31 March 2010 over Bay of Bengal region. Arrows indicate that minimum in OLR is almost simultaneous to maximum in WVMR261 to WVMR147. Filled arrows show correspondence between occurrence of low OLR and WVMR100

3.2.8 Abundance of Atmospheric Organic Aerosols in $PM_{2.5}$ in Delhi region

Polycyclic Aromatic Hydrocarbons (PAHs) are generally contributed by the incomplete combustion of biomass, coal, oil and petroleum etc.Most of PAHs are considered as carcinogenic in nature.

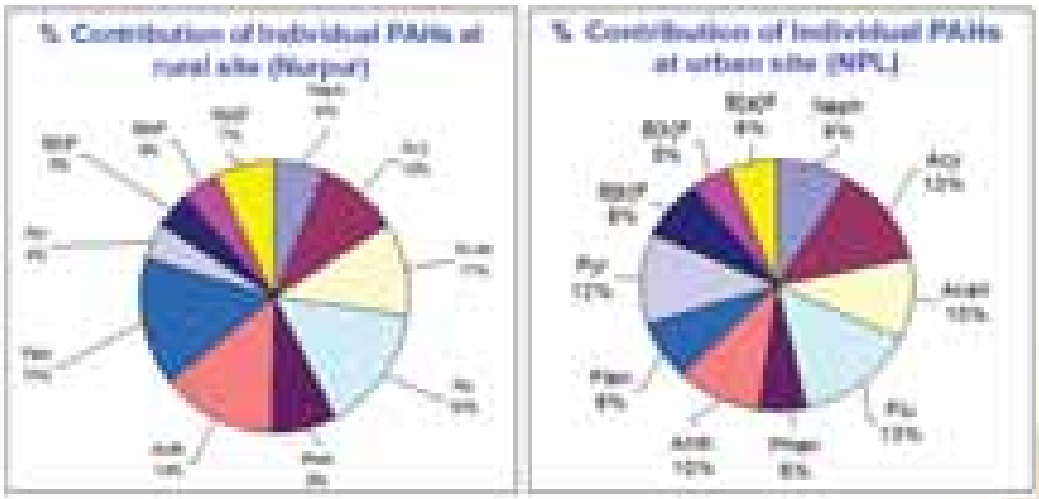

Fig. 3.10: Percent contribution of individual PAHs at rural and urban sites in Delhi region

Long term exposure to PAHs can lead to serious health effects such as mutation, cancers of lung and respiratory tract etc. A total of 11 PAHs i.e.,Naphthalene, Acenaphthylene, Acenaphthene, Fluorene, Phenanthrene, Anthracene, Fluoranthene, Pyrene, Benzo(b)fluoranthene, Benzo(k)fluoranthene, benzo(a)pyrenehave been identified and quantified in the ambient air at Nurpur (rural site) and NPL (urban site)in Delhi region. Abundance of almost all the PAHs has been noticed higher at urban site than at rural site. PAHs such as Acy, Flu, Acen and Pyrhave been noticed as dominating species at urban site while at rural site, Flu, Flan and Anthspecies dominated. These findings indicated that fossil fuel combustion is the major source of PAHs at urban site while biomass burning is the major contributor of PAHs at rural site. The percent contribution of individual PAH to the total PAHs at both the sites has been shown in Fig. 3.10.

n-Alkanes are stable non-polar as well as reasonably refractive, aliphatic hydrocarbons originated from biogenic sources and motor vehicle exhaust etc. Fifteen individual species of n-Alkanes (C21-C35) have been identified and quantified in the ambient air at both rural and urban sites. The percent contribution of n-Alkanes at both the sites has been shown in Fig. 3.11.

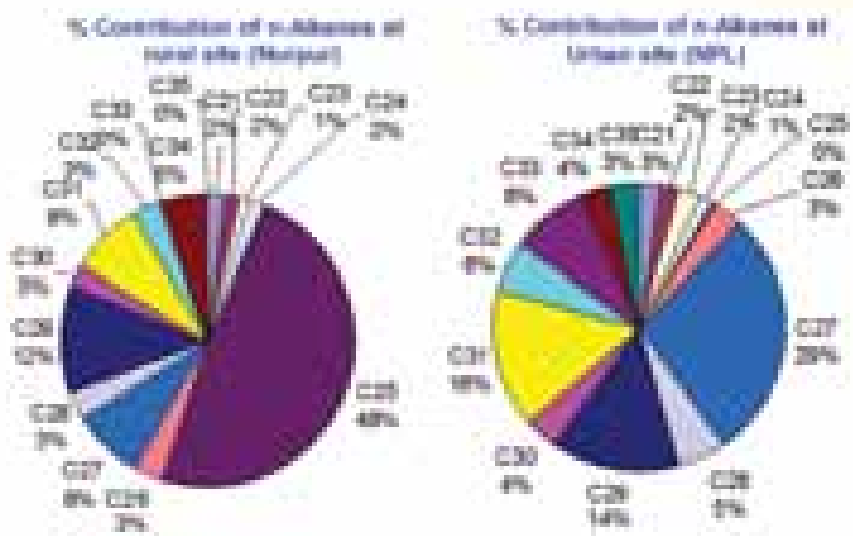

Fig. 3.11: Percent contribution of individual n-Alkanes at rural and urban sites in Delhi region

The percent contribution of n-Alkanes has shown a significant difference in their atmospheric abundance at urban and rural sites. This is probably due to the difference in source types. At urban site, the petrogenic n-Alkanes dominated over biogenic species whereas biogenic n-Alkanes dominated over petrogenic species at rural.

3.2.9 Experimental setup and standardization of a continuous flow stable isotope mass spectrometer for measuring stable isotopes of Carbon, Nitrogen and Sulfur in Environmental samples

Standardization of a newly acquired stable isotope ratio mass-spectrometer (*Isoprime 100,*Isoprime® UK) coupled with elemental analyzer (*Pyrocube,*Elementar®-Germany) in a continuous flow mode (CF-IRMS) was carried out for making accurate and precise measurements of C, N and S isotopes in a variety of natural as well as synthetic organics and sulfur containing solid samples. Instrument was calibrated using a suite of certified international standards supplied by *International Atomic Energy Agency Vienna* and cross-checked against several *in-house* laboratory standards used by other institutions of international repute. A synthetic organic compound *Sulfanilamide* was continuously used along with international standards to develop an *in-house* internal laboratory standard for the accurate and precise isotopic measurements. Overall estimated uncertainties of C, N and S isotopic measurements are better than 0.2, 0.2 and 0.3 ‰, respectively; which are well within the recommended limits of aforementioned isotopic data. After successful installation and setting up standardized protocols chemical and C, N, S isotopic analyses of atmospheric aerosols collected from differing environments of India and surface soil samples are currently underway.

3.2.10 High Ozone observed during summer and autumn months of the years 2012 and 2013

Surface ozone is a harmful pollutant that can negatively impact the human health. The World Health Organization (WHO), based on the epidemiological time-series studies and field studies have set a new air quality standard of ozone concentration of 50 ppb (daily maximum 8 hourly mean) in 2006. The ambient air quality and cleaner air for Europe (CAFE) have set eight hourly mean not to be exceeded 60ppb for the protection of human health. High concentrations of surface ozone have harmful effects on vegetation and crops. The severity of ozone on crops, vegetation and forest depends on the concentration and duration of exposure.

Ozone forms in the atmosphere from the chemical reaction of volatile organic compound (VOCs) and nitrogen oxides (NOx) in the presence of sun light. Its concentration is dependent on temperature and amount of sunshine. The main source of VOCs is motor vehicles, industrial processes, petroleum industries, pesticides application, fuel combustion and bio-mass burning. NOx are mostly from motor vehicle and fuel combustion from electric utilities and other industrial processes.

The 8 hourly mean of day time ozone (10 A.M to 5 P.M) in the summer month of April, May, June and Autumn months of September, October and November for year 2013 is shown in figure 3.12. The ozone concentration during the observation period exceeds WHO standard of 50ppb. Most of the summer and autumn days, it is observed to be in the range of 60 ppb to 130 ppb.

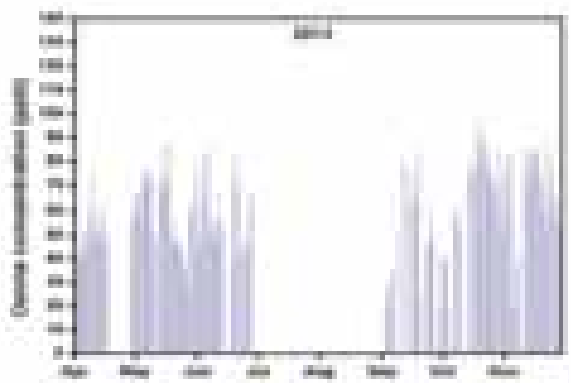

Fig. 3.12: Eight hourly mean (10:00 A.M to 05:00 P.M) value of ozone concentration during April-May- June (summer) and September-October-November (Autumn) months of the year 2013

In the month of October and November, most of the days the 8 hourly average exceed even the value observed during summer days. It may be due to excessive bio-mass burning in this season.

3.2.11 High NOx observed in foggy days

High concentrations of NOx were observed during foggy conditions as compared to clear days over the observational site at NPL, New Delhi. One of the typical diurnal variation of NOx on foggy (17th and 18th of December 2013) and clear day (19th December 2013) is shown in Figure 3.13. It has been observed that in foggy days nearly four-fold of NOx concentration were observed as compared to clear day. Fog contains small water droplets and aqueous phase chemistry became active as a result of scavenging of HOx radical by fog droplets which suppress the usual gas phase reaction HO_2+ NO→ OH+NO_2 present in the clear day. In foggy condition the sink for NO reduces and also the consumption of Ozone took place by the reaction $O_2^- + O_3 \xrightarrow{H_2O} H_2O_3 + OH^-$. It implied that in urban areas more gaseous pollutants may present in the atmosphere.

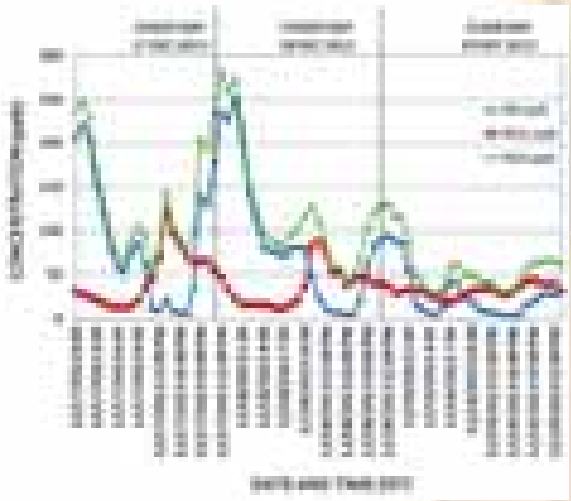

Fig. 3.13: NOx concentrations during foggy days in December 2013 in Delhi

3.2.12: Role of cloud condensation nuclei and turbulence on the precipitation characteristic of clouds

Cloud turbulence and aerosols (act as cloud condensation nuclei, CCN) play an important role in the formation, maintenance and precipitation characteristics of the clouds. In order to understand the role of turbulence and aerosol particle below the cloud on cloud precipitation the data obtained from the UV LIDAR (Light Detection And Ranging) system installed at NPL, New Delhi is used. A rain cloud appeared on a particular day of the monsoon season in 2009 (from 10:00 to 10:22 hrs, IST) is selected for the study. To study the importance of the region below the cloud (sub-cloud region) on the growth (thickness) of cloud, the quantity called cloud-to-sub cloud ratio (CSR) is calculated and is shown in figure 3.14.

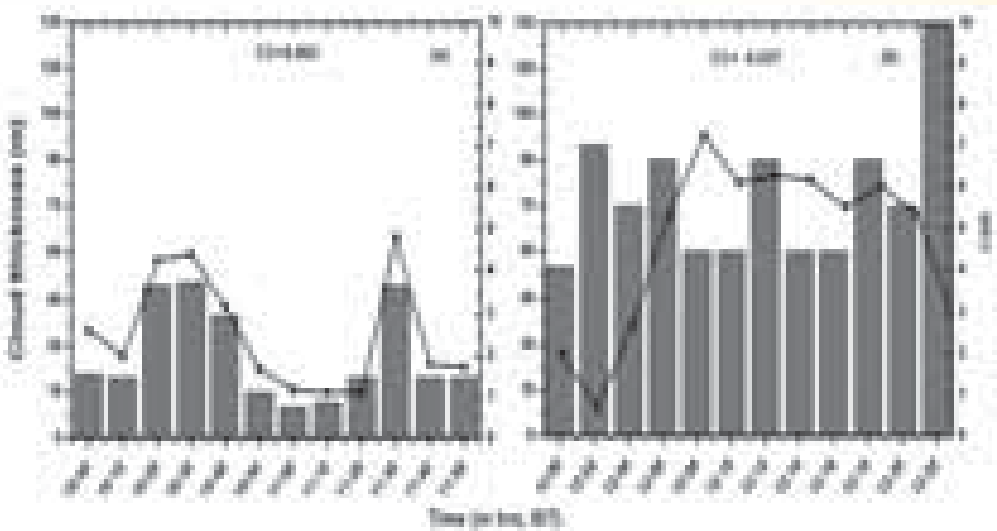

Fig. 3.14: Cloud to sub-cloud (CSR) versus cloud thickness obtained on a particular day of the monsoon season in 2009 (from 10:00 to 12:22 hrs, IST)

3.2.13 Variability in radiative properties of major aerosol types over Delhi:

Aerosol measurements over an urban site at Delhi in the western Ganga basin, northern India, were carried out during 2009 using a ground-based automatic sun/sky radiometer to identify their different types and to understand their possible radiative implications. Differentiation of aerosol types over the station was made using the appropriate thresholds for size-distribution of aerosols (i.e. fine-mode fraction, FMF at 500 nm) and radiation absorptivity (i.e. single scattering albedo, SSA at 440 nm). Four different aerosol types were identified (Figure 3.15), viz., polluted dust (PD), polluted continent (PC), mostly black carbon (MBC) and mostly organic carbon (MOC), which contributed ~48%, 32%, 11% and 9%, respectively to the total aerosols. Interestingly, the optical properties for these aerosol types differed considerably, which were further used, for the first time, to quantify their radiative implications over this station. The highest atmospheric forcing was observed for PC aerosol type (about +40 W m^{-2}, along with the corresponding atmospheric heating rate of 1.10 K day^{-1}); whereas the lowest was for MBC aerosol type (about +25 W m^{-2}, along with the corresponding atmospheric heating rate of 0.69 K day^{-1})

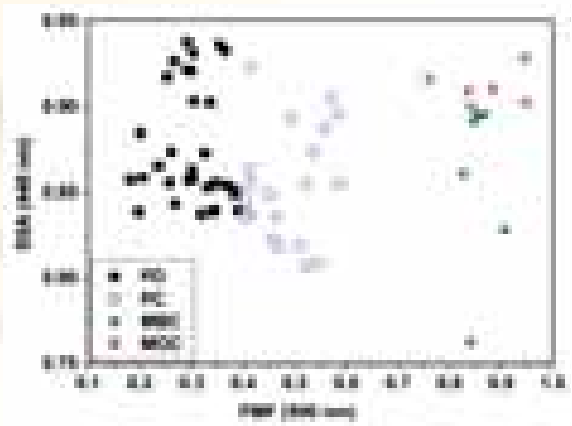

Fig 3.15: Density plot of sun/sky radiometer derived SSA (at 440 nm) versus FMF (at 500 nm) for different aerosol types over Delhi during 2009

3.2.14 Radiative Impact of Fireworks at Varanasi: A Case Study

Weeklong intensive observational campaign for aerosol study was carried out at a representative urban location in the eastern Indo-Gangetic Plain (IGP), Varanasi during the Diwali festival (October 29 to November 04, 2005, Diwali on November 01, 2005), to investigate changes in aerosol properties and radiative forcing between firework affected and nonaffected periods. Results show a substantial increase (~27%) in aerosol optical depth, aerosol absorption coefficients, and aerosol scattering coefficients during affected period as compared to non-affected periods. Magnitudes of radiative forcing at top of atmosphere during affected and non-affected periods are found to be 10 ± 1 and 12±1Wm^{-2}, respectively, which are “31 ±7 and “17 ±5Wm^{-2}, respectively, at surface. It suggests an additional cooling of ~20% at top of atmosphere, ~45% cooling at surface, and additional atmospheric heating of 0.23Kday^{-1} during fireworks affected period, which is 30% higher than the normal.

3.2.15 Morphological, mineralogical characterization of mineral dust over the Indian Desert and nearby: Implications to Dust Optics

The aerosols are known to play an important role in the terrestrial climate system through their direct and indirect influences on the radiation budget while the magnitude and sign of both effects remain highly uncertain. Amongst various aerosol species, mineral aerosols are radiatively most important aerosol types in the atmosphere due to their widespread distribution . Mineral dust scatters and absorbs not only solar radiation but also absorbs and emits outgoing long wave radiation. The magnitude and even the sign of the direct radiative forcing by mineral dust is highly uncertain. In common modeling practice, radiative transfer simulations and remote sensing implementations, shape of dust particles is assumed to be homogenous sphere so that the classical Lorenz-Mie theory can be used. However, based on the

measurement and modeling studies, the optical properties of real dust particles have been found to be quite different compared to that of volume-equivalent spheres.This emphasized the need of regional database on particle morphology, mineralogy and mixing states.

To generate the database on dust morphology originated from the Thar Desert and nearby regions, a series of field campaign have been organized over the Thar Desert and nearby semi-arid zones (local source of mineral dust) under CSIR XII Five Year Plan Network Project. The field observation conducted in a semi-arid region (in vicinity of the Thar Desert, Jaipur, Rajasthan) during late winter, 2012 revealed the predominance of "Layered", "Angular" and "Flattened" particles in the background atmosphere. The morphological parameters, aspect ratio (AR) and circularity parameter (CIR) which give information on extent of particle nonsphericity, were reported to be 1.4 and 0.8, respectively based on frequency distribution of total 235 dust particles collected from the study site. The sensitivity study depicted in Figure 3.16 at 550 nm wavelength reveals that the equivalent sphere model may underestimate Single Scattering Albedo (SSA) for the dust with low hematite content while both underestimation/ overestimation are probable in case of dust with high hematite content. The effect of AR on the dust scattering is significant in case of dust with high hematite content compared to that of low hematite. Therefore, a statistical representative database of regional dust morphology is imperative especially for the dust particles rich in hematite.

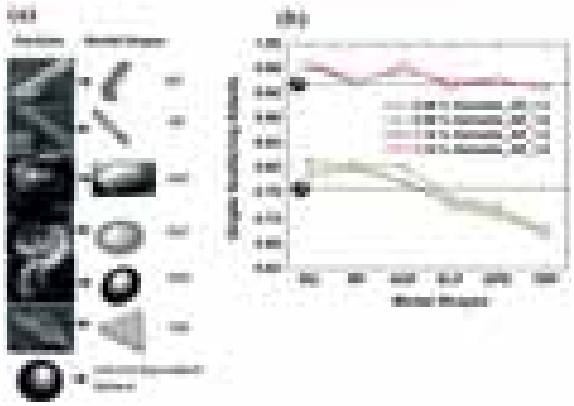

Fig. 3.16: (a) Images of individual particles and their equivalent model shapes (Rectangular Grain, RG; Rectangular Plate, RP; Hexagon Plate, HXP; Ellipsoid, ELP; Spheroid, SPD; and Triangular Plate, TRP) together with their volume equivalent sphere (b) numerically estimated Single Scattering Albedo, SSA (at 0.55 μm wavelength) for the model shapes (shown in (a)) with AR values 1.5 and 1.6 for given VER 1.2 μm and minimum (1.10%) and maximum (5.68%) hematite content in mineral dust

The optical/radiative simulation of pure mineral dust becomes further more complicated when the long range transported mineral dust form a heterogeneous mixture with the carbonaceous species. Keeping this in mind, a field campaign has also been organized at IIT,Kanpur in collaboration with Dept. of Civil Eng., IITK. The analysis reveals the predominance of complex agglomerates of dust and carbonaceous species.

3.2.16 Morphological and mixing state characterization of atmospheric particles within Atmospheric Boundary Layer over New Delhi:

To study the morphology and mixing state of atmospheric particles (within Atmospheric Boundary Layer) together with vertical profiles of met parameters (temperature, pressure and humidity), a tethered balloon observation has been conducted from 21-28 Feb, 2014 (7 PM-3.30 AM) at NPL in collaboration with TIFR Balloon facility under CSIR XII Five Year Plan Network Project. The morphological analysis reveals the predominance of carbon onion structures agglomerated with complex carbon nano structures at 700 m altitude while sub and super-micron size carbon fractals were observed at the surface level. The detailed analysis of particles collected at different altitude is underway.

समय और फ्रीक्वेंसी मानक

Time and frequency Standards

Dr Amitava Sengupta
Outstanding Scientis
Email : sengupta@nplindia.org

D 04.01 Ultrastable Atomic Frequency Sources

Dr Amitava Sengupta
Dr Ashish Agarwal
Dr Subhasis Panja
Dr Poonam Arora
Dr. Subhadeep De
Mrs. Suchi Yadav

D 04.02 Precise Timing Systems

Dr Amitava Sengupta
Mrs. Arundhati Chatterjee
Mrs. Pranalee Thorat
Mr. Anil Kumar Suri
Mrs. Preeti Kandpal
Mr. Mahavir Prasad Olaniya

Time and Frequency Standards

Mandate and Mission

Time and Frequency division is presently working in the following areas:

- ❖ Ultrastable Atomic Frequency Sources
  - *Cesium Fountain-I and Fountain-II*
  - *Rubidium Atomic Clock for Space Applications*
  - *Single Trapped* Ytterbium *Ion Optical Frequency Standard*
  - *Instrumentation*
- ❖ Precise Timing Systems
  - *Maintenance of Indian Standard Time (IST)*
  - *Time Transfer Links*
  - *Time Dissemination*
  - *Calibration Services*

A Cs fountain is a primary standard and provides most precise and accurate measurements of the hyperfine splitting of its doubly splitted ground state, which defines SI unit of time. The development of such a precision measurement device requires a remarkable combination of technological innovations in lasers, vacuum technology, magnetic shielding and indigenously developed electronic, mechanical and optical systems.There are only about ten working Cs fountains around the world. In India, the first Cs fountain frequency standard, exclusively and indigenously developed at CSIR-NPL (NPLI), is now fully operational and a second Cs fountain with enhanced accuracy is currently being developed.

The division is also contributing to India's strategic space program by developing atomic clocks to be put on Indian Satellites. The Physics package of Rubidium (Rb) atomic clock, developed by the division, has been transferred to Indian Space Research Organization (ISRO). The critical technology for filling Rb in glass bulbs and cells has also been indigenously developed in the division.

Recently, the research on optical frequency standards based on single trapped Ytterbium (Yb) ion has been initiated. Developing such a clock is a high-end research which includes several state-of-the-art technologies in lasers, optics, vacuum systems, materials, mechanical design, software and indigenously developed electronics. Within India, research in this field is also exclusive to NPLI.

Apart from extensive R & D, our division is responsible for the highest level of time and frequency metrology in India. The mandate of the division is maintenance of IST, its dissemination and keeping it traceable to the International Bureau of Weights and Measures (BIPM) using ultra-precise satellite links. NPLI is the time-provider to the nation as per parliamentary act of India. In addition, the division also provides calibration services for various clocks and frequency sources.

Ultrastable Atomic Frequency Sources

1.1 Cesium Atomic Fountain Clocks

The definition of one second in SI unit is based on the microwave transition between two hyperfine ground states of a Cs atom. A Cs fountain frequency standard realizes this definition most precisely and hence it operates as a primary standard. In a fountain, Cs atoms are cooled to ~ μK and launched against gravity through a microwave cavity. The atoms interact with the microwaves on the way up and down and their probability of transition to the other state, as a function of the microwave frequency, is probed in the detection region. Worldwide, only 10 such fountains are operational at the leading National Metrology Institutes (NMIs) at USA, UK, France, Germany, Italy and Japan. Some other countries such as India, Russia, China and Korea are also currently developing Cs fountain primary standards. International atomic timescale (TAI) is a weighted average of time kept by atomic clocks all over the world. The increasing number of operational fountain frequency standards has contributed to the maintenance of TAI at an unprecedented level of accuracy, with fractional uncertainty of the time interval below 10^{-15}. India's first Cs fountain frequency standard (India-CsF1), as shown in Fig. 4.1, is now fully operational. The fountain is being evaluated for its frequency stability and accuracy.

Recently, the division started to design and build a second Cs fountain with special design features that enable us to carefully investigate the systematic errors in order to enhance the accuracy of our frequency standard to a few parts in 10^{16}.

Fig. 4.1: Physics package and the optical set-up of the first Cs fountain clock (India-CsF1)

1.1.1 First Cs Fountain: India CsF1

India-CsF1 is currently being evaluated for its frequency stability and accuracy due to both statistical and systematic shifts. The fountain is being operated almost continuously. In each evaluation (lasting 10-20 days), major systematic shifts due to blackbody radiation (BBR), 2nd order Zeeman, shift gravitational potential and collisional shift are calculated and corrected.

During an evaluation, the fountain frequency is compared with the Hydrogen MASER (H-MASER) which is contributing to the universal coordinated time (UTC) and hence fountain is evaluated with respect to the UTC following the traceability chain as shown in Fig. 4.2. The Allan deviation of the frequency difference between the fountain and the H-Maser shows that fountain frequency is stable to few parts in 10^{15} at less than one day of averaging.

Recently, an international inter-comparison campaign was conducted where six Cs fountain clocks from NIM (China), NPLI (India), PTB (Germany) and SU (Russia) were compared by two way satellite time and frequency transfer (TWSTFT)

Fig. 4.2: Traceability chain of India-CsF1 to UTC

and GPS Carrier Phase (GPSCP) technologies, with PTB and SU having 2 PFSs respectively. A TWSTFT link between Asia and Europe has been established in 2005, to contribute to the calculation of TAI and to enable comparison between primary frequency standards. Since 2010, the geostationary satellite AM2 which belongs to RUSSIA Intersputnik was used in Europe-Asia link. At present, the participant laboratories of this link include NICT, NIM, NPLI, NTSC, PTB, SU and TL. The set-up used by each participating laboratory for the international inter-comparison of the fountains is depicted in Fig. 4.3. The UTC (k) was used as references for both TWSTFT station and GPS receiver, the pair of UTC (k) was compared directly by TWSTFT and GPS CP links. The phase difference between the UTC (k) and the H-maser was measured by the phase comparator, and the frequency of the H-Maser was measured by the fountain clock.

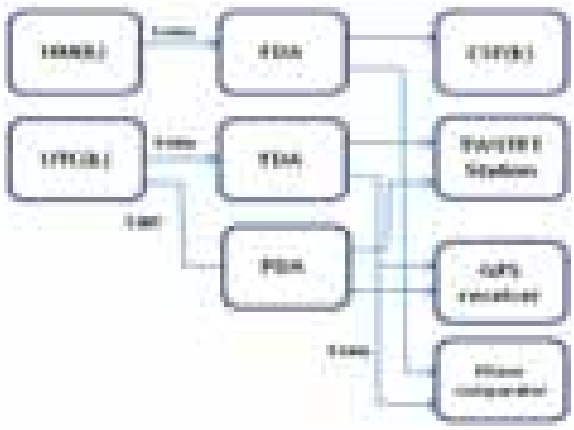

Fig. 4.3: Comparison Setup: (HM: Hydrogen Maser, FDA: Frequency Distribution Amplifier, CSF: CesiumFountain clock, k: lab code)

The intercomparison campaign was conducted in May 2013 and lasted 21 days. During this period, the fountain was operated almost continuously. The frequency differences and the comparison uncertainties between the compared fountain pairs were evaluated. The comparison uncertainty (u) results from combining the uncertainties of the two compared fountain clocks and the uncertainty introduced by the comparison link. The uncertainty of the fountains evaluated and provided by each lab is shown in Tab. 4.1, including statistical and systematic uncertainties, u_A and u_B, respectively. Statistical uncertainties for 21d and 13d are represented by u_A(21d) and u_A(13d), respectively.

Table 4.1: Results of the international inter-comparison: the uncertainties of the fountains (in 10^{-15})

Fountains	u_A(21 d)	u_A(13 d)	uB
CSF(NIM)	/	0.59	2.0
CSF(NPLI)	0.53	0.50	2.42
CSF1(PTB)	0.13	0.16	0.73
CSF2(PTB)	0.17	0.20	0.33
CSF1(SU)	0.85	1.13	1.5
CSF2(SU)	0.29	0.36	0.5

The result of frequency difference between our fountain and fountains of PTB and SU is shown in Fig. 4.4.The final results showed that all the frequency differences between the fountains

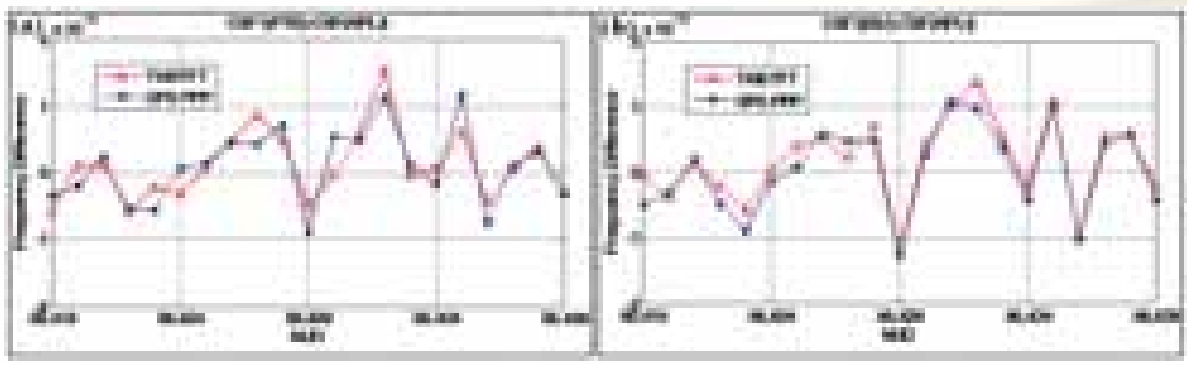

Fig. 4.4: Frequency difference between India's fountain NPLI-CsF1 with (a) Germany's fountain PTB-CsF1 and (b) Russia's Cs fountain SU-CsF2

agreed within the 1-sigma uncertainty in the low 10^{-15} level. After the successful international inter-comparison, the fountain is being periodically evaluated with respect to TAI.

1.1.2 Second Cs Fountain

A 2nd Cs fountain is being designed and developed in the division. Special design features will be incorporated in this fountain in order to have better accuracy and stability. Novel technique of optical pumping will be used to increase the S/N ratio in this fountain. The cavity design has been improved to reduce distributed cavity phase shifts and the MOT geometry of (1, 1, 1) has been chosen to reduce light shifts. With these improvements, it is expected that the 2nd fountain clock will be an order of magnitude more accurate than India-CsF1. Most of the planning and design of crucial components has been completed for this fountain. The electronics subsystems have been indigenously developed. The assembly of the fountain is planned in the upcoming Apex Metrology Laboratory at NPLI. In the last one year, most of the work has been to estimate the increase in the atomic population in the desired clock state using two laser pumping scheme. The term optical pumping (OP) refers to the redistribution of atoms among their fine or hyperfine structure levels by means of light.

In a Cs fountain, the atoms are state-selected, just before Ramsey interaction, by applying a microwave ð-pulse that transfers the selected atoms (10%) to the F', m_f=0 state. The remaining non-selected atoms (90%) are removed from the sample by a radiation pressure pulse. Thus nearly 90% of the potential clock signal is lost.The S/N ratio can be increased by converting at least some of lost atoms to useful atoms. This is done by shining a light beam on the atoms before state selection which pumps the atoms to the desired clock state. With proper selection of transition, polarization, interaction time, intensity and linewidth, theoretically all the atoms can be pumped to the desired clock state. This fact makes this novel technique really useful for Cs fountain for effectively increasing the S/N ratio and hence the stability and accuracy of the fountain.

In order to use OP in the 2nd fountain, rigorous theoretical calculations have been done to find out the wavelength, polarization, interaction time, intensities and detuning of the lasers which will be used for OP. Density Matrix approach was used in order to solve 25 coupled differential equations for the Cs atom and the populations of the all different sublevels were calculated. The results are summarized in Fig. 4.5 and it can be seen that if an OP laser intensity of 3mW/cm^2, repump laser

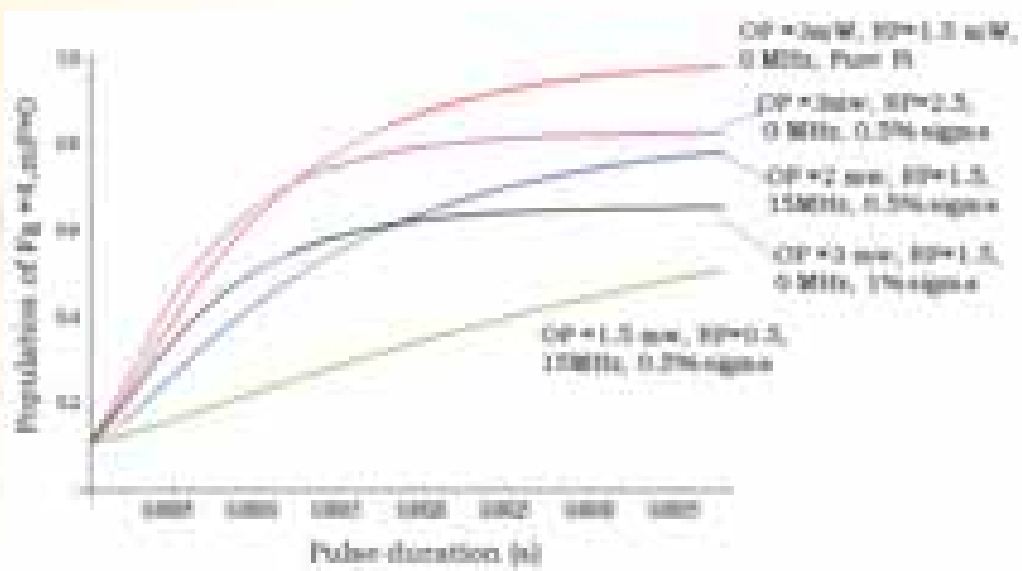

Fig. 4.5: Normalized population in the desired clock state as a function of the OP pulse duration

of intensity of 1.5mW/cm^2 tuned to resonace with pure pi polarisation is shined on the atoms for 350 μs we can have 98% population in the desired clock state.

1.2 Rubidium Atomic Clock for Space

The division also develops Rb Atomic Clocks. This strategic technology is currently available only with US, Europe, Russia and China. From India's perspective, it needs to be indigenized as ISRO has started to launch satellites with onboard Rb Atomic Clocks in the space for building the Indian navigation system. For this purpose, NPLI has already developed an atomic clock using imported Rb bulbs and cells. Recently the Rb filling technology has been developed in order to produce Rb Bulbs and Cells within the country. This year, bulbs were filled with isotopically enriched ^{87}Rb, which will increase performance of the clock. Further, the repeatability of Rb filling facility was improved by using heat pipes for producing a cold spot for Rb collection, as shown in Fig. 4.6.

1.3 Single Trapped Ytterbium (Yb) Ion Optical Frequency Standard

We are developing an atomic clock based on an optical transition of a single trapped $^{171}Yb^+$ ion. Accuracy of such a clock is enhanced by two orders of magnitude than the microwave (Cs fountain) clock, since the operational frequency of the clock is about 10,000 times larger than that in cesium. Optical frequency standards with a single trapped ion provide long term stability since they are free from Coulomb and inter atomic interactions and eliminate collisional shifts. There are several ions such as $^{199}Hg^+$, $^{88}Sr^+$, $^{40}Ca^+$, $^{171}Yb^+$, $^{115}In^+$ and $^{27}Al^+$ which are being used worldwide for building the trapped ion optical frequency standards. Among them $^{27}Al^+$ operates with the highest fractional accuracy $\Delta\nu/\nu = 8.6\times10^{-18}$, however it requires stupendous effort for cooling the ion sympathetically and developing the clock laser at deep ultra-violet wavelength. In $^{171}Yb^+$, $m_F = 0$ energy levels associated to the clock transitions are insensitive to the first order Zeeman shifts. The state associated to the E^{3-} transition has sensitivity of -5.95 for measuring the temporal constancy of fine structure constant, which is three orders of magnitude higher than in $^{27}Al^+$. In this report, short descriptions about the design of our ion trap, resonator cavity for delivering rf and optical setups for 369.5 nm laser are given.

1.3.1. Design of ion trap and ultra-high vacuum chamber

Ytterbium-ion will be trapped in a Paul trap of end-cap design since it provides maximum optical access at the trap center, which is one of the critical criteria for our experiment. Ideally the quadrupole potential generated by the ion trap should not have any admixture of the higher order multipoles, however in practice the higher order

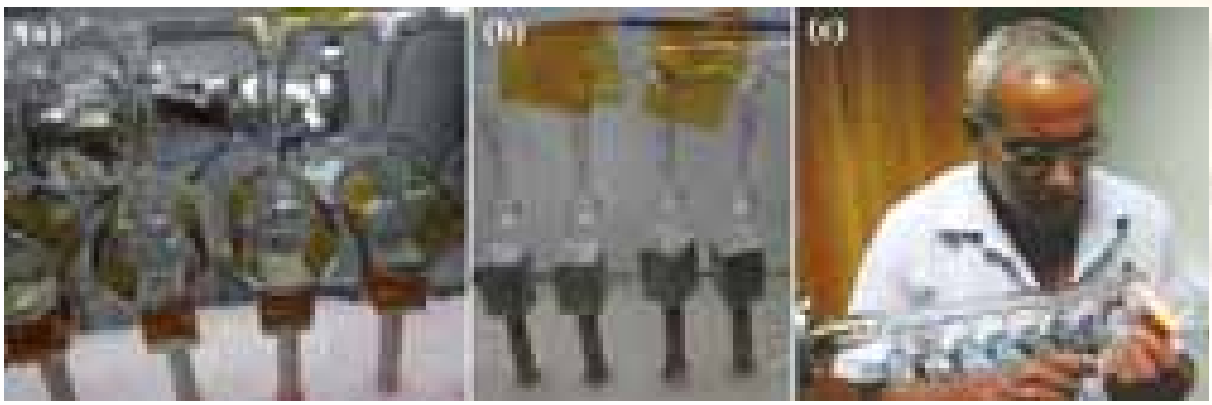

Fig. 4.6: (a) Use of heat pipe to create a cold spot for collection of Rb in cells; (b) collection of Isotopic Rb in bulbs; (c) pinching off of cells from manifold

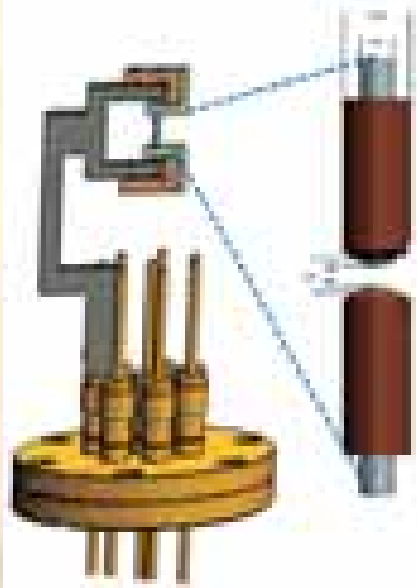

Fig. 4.7: Design of the end cap trap mounted on an electrical feed-through along with enlarged view of the trap electrodes. All dimensions are given in mm

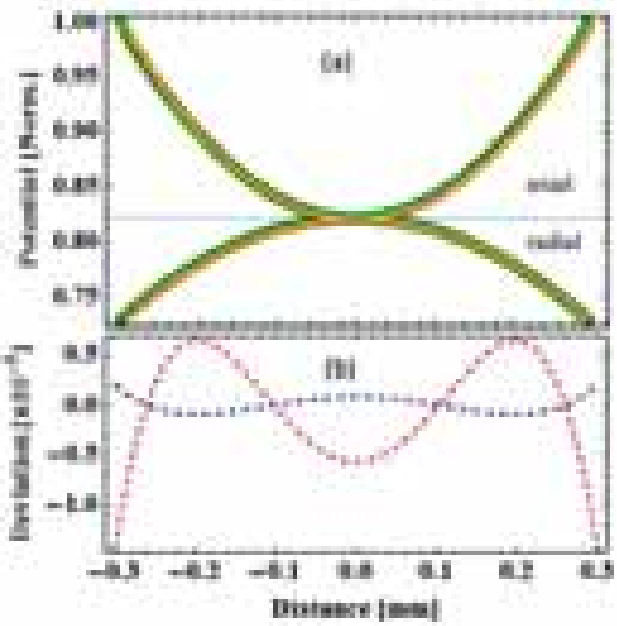

Fig. 4.8: (a) Normalized trapping potentials along the radial and axial directions: numerically simulated (green); harmonic fit (red) and anharmonic fit (yellow). (b) Deviation of the harmonic potential from the anharmonic potential along axial (blue) and radial (red) directions

multipoles usually arise due to imperfect machining and misalignment of the electrodes.

We have numerically simulated electric field lines with various electrode geometries using a commercial software 3D Charged Particle Optics program (CPO-3D), CPO Ltd., USA to identify the most efficient trap geometry with negligible anharmonic contribution in it. The calculated potentials along radial and axial directions are shown in the Fig. 4.8. We have finalized the design of the endcap type quadrupole ion trap in which the electrodes are made out of tantalum due to the inert nature of tantalum. The end cap electrodes are made of 1 mm diameter rod and the concentric shielding electrodes are built from tubes of inner and outer diameters 1.4 mm and 2 mm, respectively, as shown in Fig. 4.7. In our optimized geometry tip of the end caps and shielding electrodes will be separated by a 0.6 mm and 1 mm respectively. Collision between the trapped ion and the background gas will introduce shift in the energy levels of the ion and finally affect the accuracy of the clock. In order to avoid collision between background gas and the trapped ion, the whole experiment will be performed within ultrahigh vacuum condition. We have designed an UHV chamber with optimum volume and possibility of probing the ion along three mutually orthogonal directions as shown in Fig. 4.9. The trap chamber has a re-entrant view port for placing the objective lens very close to the single trapped ion for the enhancement of light collection efficiency from it.

Fig. 4.9: Design of the prototype UHV chamber for trapping $^{171}Yb^{+}$ ions

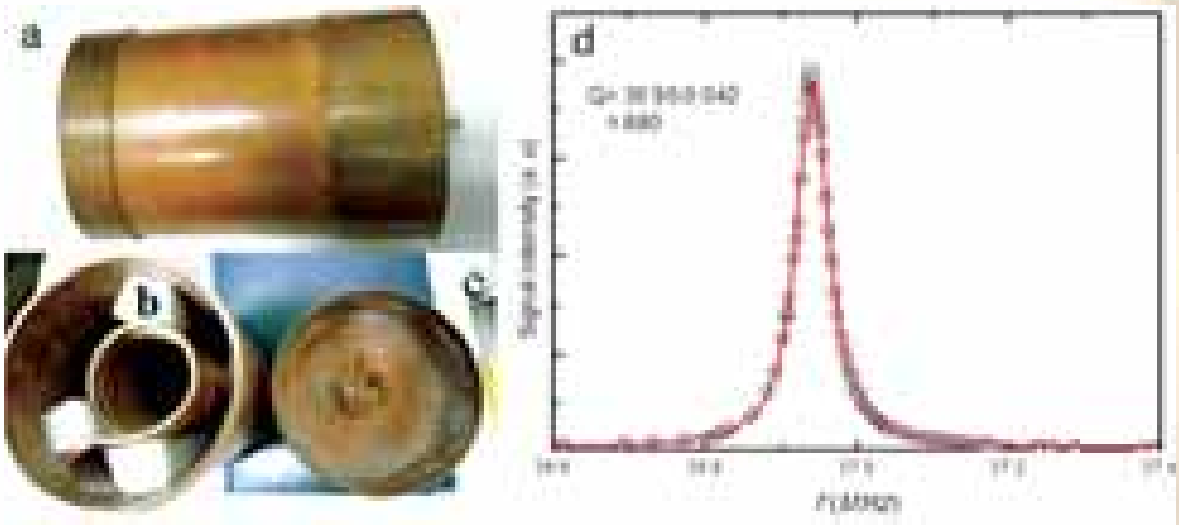

Fig. 4.10: Photograph of the resonator (a), helical coil with shield (b) and primary antenna coil (c). Frequency response of the unloaded resonator (d)

1.3.2. Helical resonator for delivering low bandwidth high voltage RF:

In order to trap ions, narrow bandwidth at large amplitude ~1 kV peak-to-peak radio frequency (RF) voltage need to be applied at the electrodes. Wide frequency bandwidth results in unstable trapping and unwanted heating of the ions and direct delivery of high voltage RF to a trap may damage the source due to impedance mismatch between source and the trap electrodes. A helical resonator allows impedance matching between an RF source and an ion trap, enabling high voltages while reducing the noise injected into the system. In order to maximize the filtering of this noise, the resonator must have a high *Q* factor, and hence a narrow bandwidth. We have built a helical resonator, where the rf signal is inductively coupled by a small antenna placed just before the helical coil (Fig. 4.10).

The unloaded resonant frequency of the resonator f = 37 (±0.5) *MHz* with very high quality factor Q = 900 (±50). Both resonant frequency and Q will change when it will be connected with the trap because of the capacitive loads of trap and connectors.

1.3.3 Optical setup for 369.5 nm laser

The optical arrangements for production of $^{171}Yb^{+}$ by photoionization and laser cooling have been designed. The two step photoionization process first excites an electron from the $^{1}S_{0}$ level to the $^{1}P_{1}$ level of the neutral Yb with a 399 nm light from a commercial extended cavity diode laser (ECDL) system and then another radiation at 369.5 nm will supply energy to bring it to the continuum and ionizes the atom into a $^{171}Yb^{+}$ ion. A commercial frequency doubled ECDL system will produce the 369.5 nm light (TA-SHG Pro, Toptica Photonics AG) for laser cooling and an intense part of it will be used for photoionization. A large fraction of the laser beam passes through a 200 MHz acousto optic modulator (AOM) as shown in Fig. 4.11. The 0^{th}-order will be used for photoinozation and the double passed 1^{st}-order will be used for fluorescence detection. A 14.7 GHz blue detuned sideband will be generated from rest of 369.5 nm light by taking the 2^{nd}-order sideband of a 7.37 GHz electro optic modulator (EOM). For fine tuning of the frequency and controlling the optical power, EOM output will be double passed through a 200 MHz AOM. Remaining light will be used for the state selection which will be produced by using a combination of 2.1 GHz EOM and double passing through 200 MHz.

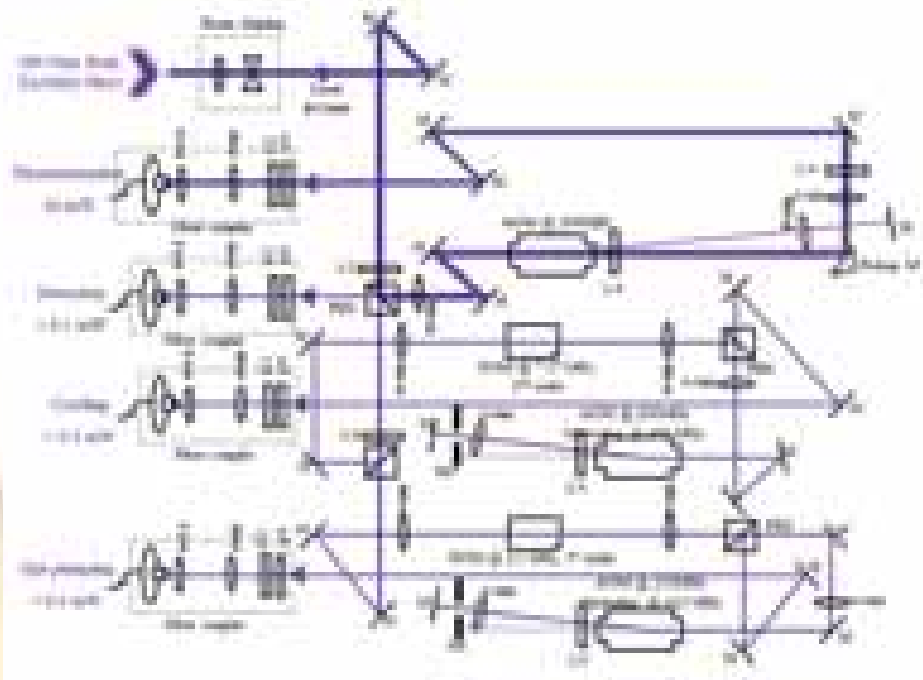

Fig. 4.11: Layout of the 369.5 nm optics set up

1.4 Instrumentation

The ongoing research activities of the division in the field frequency standards with Cesium fountain, trapped Ytterbium ion and Rubidium atoms stored in bulbs and cells, require in-house development of the electronic instruments. For building such state-of-the-art experiments, a lot of instrumentation in the field of machine design, vacuum technology, lasers & optics, computer networking & data acquisition and electronics is required. In this section, a glimpse of our recent in-house instrumentation is given. We shall describe universal driver circuit for driving home made mechanical shutters; fountain sequence controller, dc power supply, photodiode readout, camera tuner, temperature controller for Cesium oven and current source for magnetic field.

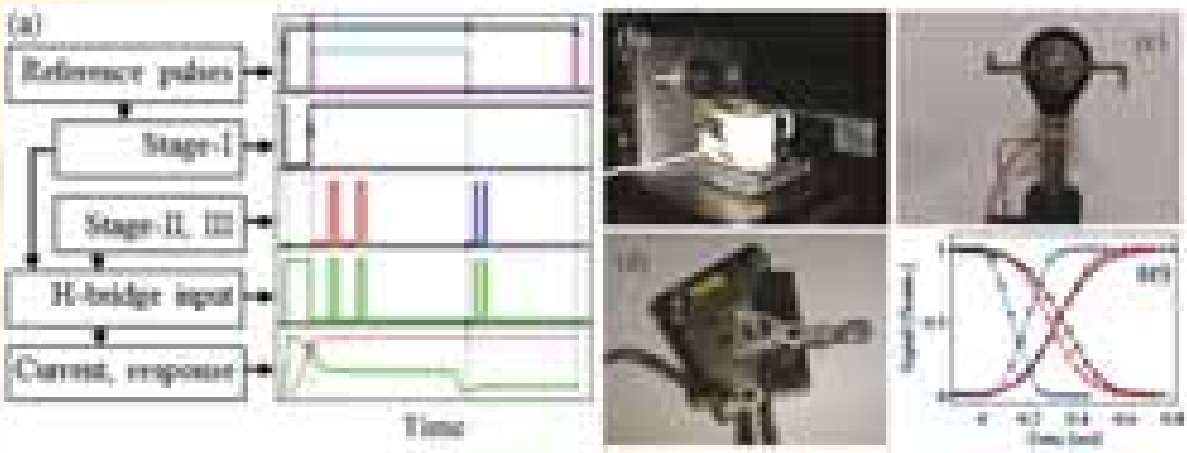

Fig. 4.12: (a) TTL (grey), triggers (magenta), duration of stage-II (cyan), pulses in stage II & III (red & blue), resultant pulse trains in the PWM output for producing the three stages of currents (green), and relative response of the relay shutter (red). The vertical axes are draws in arbitrary units. Photographs of (b) relay, (c) DCM, (d) HDD shutters and (d) their response characteristics as relay (red), DCM (black) and HDD (blue) while blocking and unblocking a laser beam of diameter 1 mm at 10 Hz TTL

Shutter driver: Blocking and unblocking of laser lights synchronized to an experimental sequence is an important requirement in the atomic frequency standards experiment. AOMs are usually used for fast switching; however mechanical shutters are additionally required for complete blocking of the lights. Many times experimentalists build low cost shutters, for example, by modifying piezoelectric transducers, voice coil of a loudspeaker, electromagnetic relay, voice coil actuator of a hard disc drive (HDD) and stepper motor. Vibrations and acoustic noise produced by these mechanical shutters are the main drawbacks for operating them in a laser lab. We have designed a universal driver for low noise operation of the shutters based on electromagnetic relay, dc motor (DCM) and laptop HDD (Fig. 4.12 b-d). The driver puts out high (stage-I), medium (stage-II) and low (stage-III) currents using the pulse width modulation technique (see Fig. 4.12a), which are used for overcoming the inertia, fast sweeping and soft landing of the shutters, respectively. The shutters operate symmetrically in both ways and their measured response times are 600(20) ìs, 650(20) ìs and 360(25) ìs for the relay, DCM and HDD based shutters, respectively for blocking-unblocking a laser beam of diameter 1 mm (Fig. 4.12e).

Fountain sequence controller: An electronic module for sequential control of the associated experimental building blocks, *e.g.*, currents for producing magnetic fields, mechanical shutters and AOMs for operating the Cesium fountain has been designed (Fig. 4.13a). A microcontroller receives user defined working parameters and timing information from a control computer and sends out the synchronized control signals to the relevant modules. This module also contains a direct digital synthesis (DDS) chip, which receives signal from the microcontroller and generates rf at desired frequencies and amplifies them for driving the AOMs. There are several AOMs controlled by this module for the purpose of producing lasers beams at different frequencies for magneto optical trapping, polarization gradient cooling, blowing atoms in the undesired states and fluorescence detection at controlled intensities which are required at different stages of fountain operation.

DC power supply: Many subsystems in our experiments require regulated linear dc voltages. We have standardized a dc power distributor which have eight outputs through XLR connectors as shown in Fig. 4.13b, where each of these XLR outputs contain + 24 V, - 24 V and + 5 V. These voltages are further regulated down to required values on-board in the subsystems. The module contains a dc power supply as well as they are connected to uninterrupted power supply (UPS), since our experiments are designed to operate over long duration without any interruption.

Figure 4.13: Electronic modules for (a) fountain sequence controller, (b) dc power supply, (c) photodiode readout, and (d) multiple camera tuners, (e) caesium source temperature controller, (f) c-field constant current source

Photodiode readout: Multiple lasers at several different frequencies are used in our experiments, for example, optical frequency standard with single trapped ion will require simultaneous operation of five lasers and each of them at multiple frequencies. Malfunctioning of any of the laser beams will fail the experiment. Hence we intend to monitor and log laser power at different stages within this huge optical setup. For this purpose, we have designed photodiode amplifier circuit and readout system as shown in Fig 4.13c. We use ethernet connectors and network cables for biasing the photodiodes by supplying voltages from the

readout modules and get the signals back there. Each module can acquire data from four photodiodes and display their signals. These signals can also be sent to the data-logger.

Camera tuners: We frequently use cameras for monitoring fluorescence from the trapped atoms, infrared light and other weak laser beams. Monitoring laser beams using camera are very helpful during precision alignment, for example, mode matching of laser light to a Fabry-Perot cavity. We use black and white bullet cameras for these purposes which are sensitive at the infrared wavelengths and watch the signals on television screens. We have developed 6-by-2 multiplexing switch, as shown in Fig. 4.13d, so that a pair of cameras can be viewed at a time. In this module we also use Ethernet connectors and network cables for biasing the cameras and reading out their signals.

Cesium source temperature controller: Cs source is the heart of the Cs fountain frequency standard. Cs source is integrated with octagonal cooling chamber and the amount of Cs diffusing to the chamber is controlled by controlling the temperature of the Cs ampoule. This electronic module, as shown in Fig. 4.13e, is designed to serve this purpose, maintaining the temperature from 10°c to 80°c. It is based on lock in amplifier and proportional-Integral-derivative (PID) techniques for precise control of temperature. We use thermo-electric coolers (TECs) for cooling and heating the Cs ampoule.

C-field constant current source: This highly stable constant current source system has been developed for reduction of the magnetic sensitivity of an atomic clock against the non-uniformity and variations of the C-field. These current sources as shown in Fig. 4.13f are based on embedded system, consists of a constant-current source circuit, a micro-controller control unit and D/A converter circuit as well as the power supply component. These are designed for different ranges between 10 μA to 300 mA.

Precise Timing Symstems

NPLI is the time keeper of the country and is responsible for highest level of time and frequency metrology in India as per the international standards. The major activities are maintenance of IST, Time transfer using satellite links, time dissemination and calibration services.

2.1 Maintenance of Indian Standard Time (IST)

NPLI is maintaining IST (UTC+05:30) within ±10ns, as shown in Fig. 4.14, with the help of five Cs atomic clocks and one H-Maser in environment controlled chamber with uninterrupted power supply. The UTC (NPLI) is inter-compared with international time scale using precise time transfer links. This has been facilitated by introducing dual frequency GPS receivers and two way satellites time and frequency transfer (TWSTFT) by uploading data to BIPM on daily basis. BIPM publishes two results: circular-T (monthly) and UTC-Rapid (weekly).

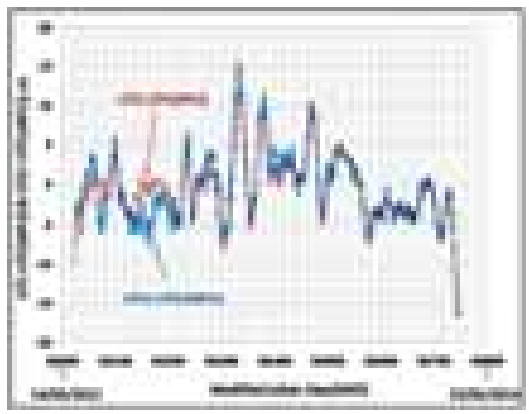

Fig. 4.14: Behavior of UTC (NPLI) and UTCr (NPLI) from April, 2012 to March, 2014

2.1.1. NPL Clock Rates and Weights

Five Cs clocks and a H-maser are contributing to TAI from November 2012. BIPM calculates TAI by assigning weights to more than 600 clocks from 65 laboratories, located at different places around the globe, including those at NPLI. The weight assigned is decided by stability (rate) of a clock. The clock rates and weights are shown in Fig. 4.15. One of the five Cs clocks has

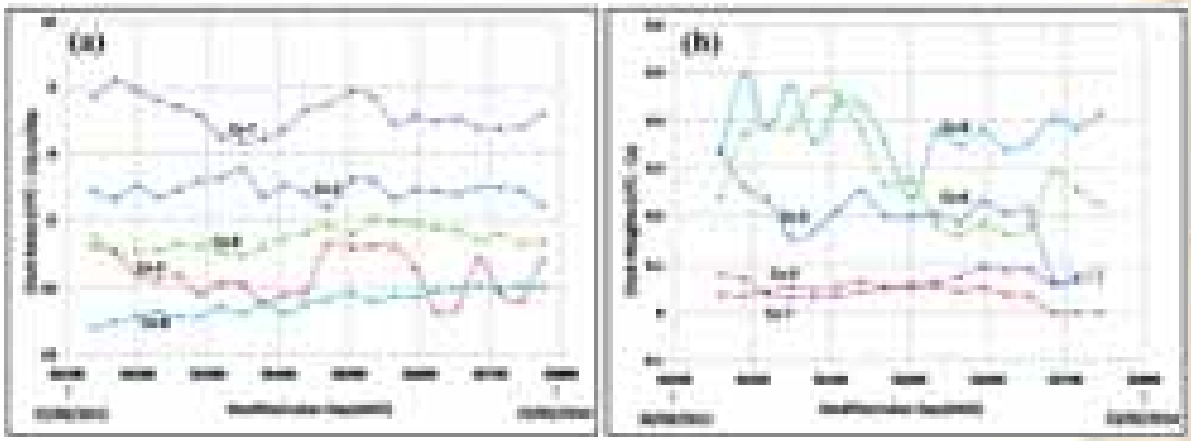

Fig. 4.15: (a) Clock rates for Cs-2, Cs-3[-25 ns/d], Cs-6[-5ns/d], Cs-7[-90 ns/d], Cs-8[+15 ns/d]; (b) Clock weights for Cs clocks at CSIR-NPL

recently started getting zero weight because its stability (clock rate) has deteriorated due to aging.

2.2. Time Transfer Links

Time transfer links established by NPL are used to contribute UTC (NPLI) to International Time Scale and for fountain frequency evaluation.

2.2.1. Two Way Satellite Time & Frequency Transfer system (TWSTFT)

This system is already installed and fully operational. There are seven participating timing labs in the Eu-Asia network namely PTB (Germany), NICT (Japan), NTSC (China), TL (Taiwan), SU (Russia), NIM (China) and NPLI (India). There are total twelve sessions of measurements recorded every day by inter-comparison with all the participating laboratories and then a formatted data measurement in the form of International Telecommunication Union-ITU format file is

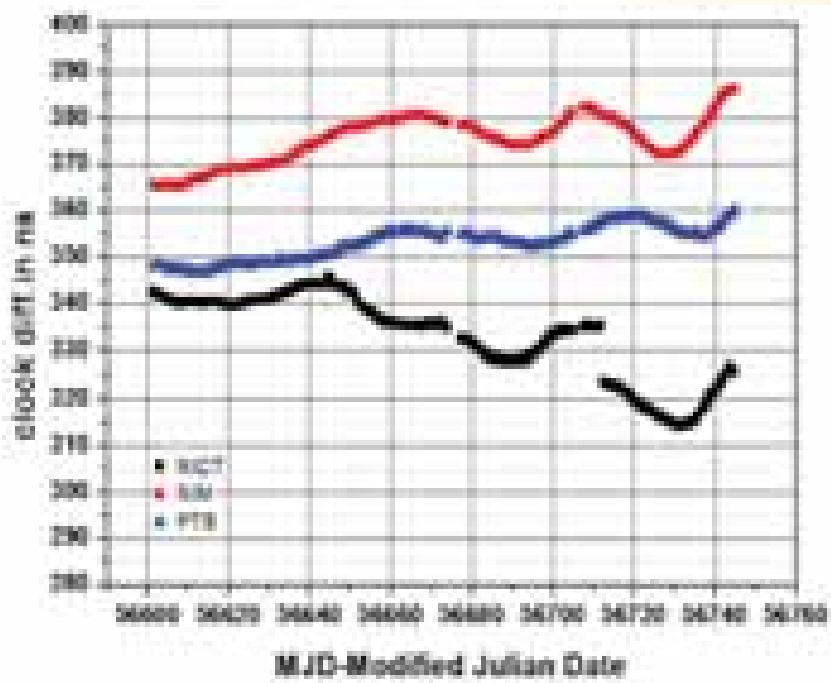

Fig. 4.16: Variation of UTC (NPLI) with respect to the timescales of NICT, NIM and PTB using TWSTFT (data: November 2013 to March 2014)

generated. The whole process had been automated by indigenously developed software. This ITU formatted data is uploaded on the BIPM ftp server ftp.bipm.org on daily basis for doing algorithmic calculations at BIPM end. Results of these calculations are published by BIPM in Cir-T every month which shows the stability of UTC (NPLI). The variation of the UTC (NPLI) with respect to timescales of NCT, NIM and PTB using TWSTFT data over one year is shown in Fig. 4.16.

2.2.2. GPS -Precise Point Positioning (PPP) Technique

This technique allows precise comparison of atomic clocks. Two popularly known software solution packages which give precision at the level of a hundred picoseconds are - 1) NrCan- Natural Resources Canada(link:www.nrcan.gc.ca) and 2) Atomium - Royal Observatory of Belgium (link: http://gnss.be/atomium).We have compared the results from these two PPP solutions for two dual-frequency co-located GPS receivers at NPL: GPS1 (Septentrio) and GPS2(TTS4). Both the softwares give accuracy within ± 1 ns as shown in Fig. 4.17.

2.3 TIME DISSEMINATION

2.3.1. Teleclock service

NPLI has been providing a moderate accuracy time synchronization service, known as teleclock, over the telephone network for several years. This service can be accessed by using the teleclock receiver which has been developed by NPLI. These receivers utilize landline telephone or mobile network depending on the type of receivers. This service can be used to synchronize the real time clock (RTC) of a computer also. Know-how for the teleclock receiver has been transferred to four Indian industries that manufacture and market these to domestic users - such as, railways, airports, stock exchange etc.

During last one year, few consultancy projects have been carried out to provide teleclock based time synchronization service to several agencies of national importance. These are, Controller of Certifying Authorities (CCA) and six other Certifying Authorities (CAs): NIC, IDRBT, TCS, EMUDRA, nCode and Sify. The CCA and CAs issue digital signatures that incorporate time stamping traceable to IST for banks, financial institutions and individuals.

2.3.2 Network Time Protocol (NTP) Service

NTP service over the internet is operational under the URL: *time.nplindia.org* by which any computer can be synchronized to IST with an accuracy of few tens of ms. During the last one year, new users of NTP services are Stock Holding Corporation of India (SHCIL) and State Bank of India (SBI) who use it to synchronize their back end software.

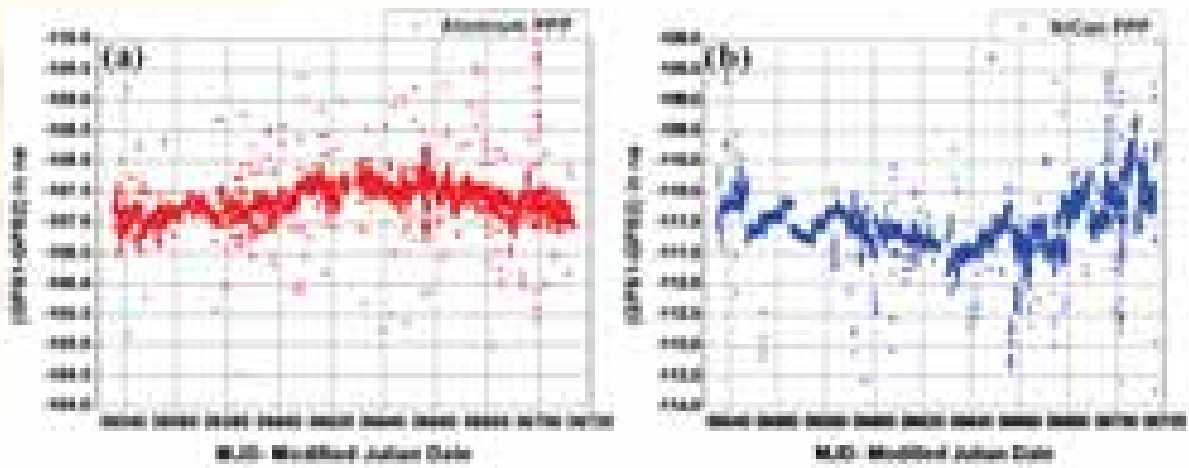

Fig. 4.17: PPP results using a) Atomium and b) NrCan (data: August 2013 to February 2014)

Table 4.2: List of calibrations done in the year 2013-14.

S.no.	Calibration equipment	No. of calibration certificates issued	Clients
1	Rb Frequency standard	5	Airforce, Palam, ERTL (North), BEL Bengaluru, M/S Accord software Josephson voltage Standard, NPL
2	Stop watch	6	Central Institute of plastic Engineering,Lucknow Hindustan Petroleum,Delhi National council for Cement and building materials, Ballabgarh Fluid flow Standard, NPL, Mass Standard, NPL
3	Frequency counter	3	Pressure and Vaccum. Std, NPL LF, HF Impedence and DC Standards, NPL Magnetic Standards, NPL
4	Teleclock	5	M/S N code solutions, M/S Jubilant Clinical system, Noida M/S eMudra services T&F division, NPL
5	Quartz Oscillator	1	Josephson voltage Standard, NPL
6	Timer	3	M/S Transcal Eng.(P) Ltd. Bengaluru M/S Electrical Research and Development,Vadodara Capital Power System, Noida
7	GPS Receiver	1	M/S Signal and System, Chennai

2.4 CALIBRATION SERVICES

2.4.1. Calibrations Record

The division carries out calibration services for different institutes, industries as well as for different divisions within NPL. The detailed list of equipment calibrated in the year 2013-14 along with clients is given in Table 4.2. Total earning from calibrations in the last one year is about Rs. 5.5 Lakhs.

2.4.2. Calibration and Measurement Capabilities (CMCs)

The list of CMCs available with the division is summarized in Table 4.3. These CMCs are certified by BIPM and their details are available in Appendix C of BIPM website.

Table 4.3 : List of CMCs of T & F Division.

S. No.	Quantity	Instrument or Artifact	Instrument Type or Method	Values, Units	Uncertainties
1	Frequency	General Frequency Source	Time Interval Measurements	1, Hz	9.0 E-14 Hz/Hz
2	Frequency	General Frequency Source	Time Interval Measurements	0.1, MHz	9.0 E-14 Hz/Hz
3	Frequency	General Frequency Source	Time Interval Measurements	1, MHz	9.0 E-14 Hz/Hz
4	Frequency	General Frequency Source	Time Interval Measurements	5, MHz	9.0 E-14 Hz/Hz
5	Frequency	General Frequency Source	Time Interval Measurements	10, MHz	9.0 E-14 Hz/Hz
6	Frequency	General Frequency Source	Direct Frequency Measurements	1, MHz	6.4E-12 Hz/Hz
7	Frequency	General Frequency Source	Direct Frequency Measurements	5, MHz	6.4E-12 Hz/Hz
8	Frequency	General Frequency Source	Direct Frequency Measurements	10, MHz	6.4E-12 Hz/Hz
9	Time Scale Difference	Local clock Vs UTC(NPLI)	Time Interval Measurements	-0.5 to 0.5, s	2 ns
10	Time Scale Difference	Local clock Vs UTC	Time Interval Measurements	-0.5 to 0.5, s	38 ns
11	Time Interval	Time Difference Meter	Time Interval Measurements	1 to 1740, s	1.4E+02 ms

2.4.3. Remote Calibration

Recently, we have added a facility of remote calibration in the division. Brief description of the setup and procedure is given in this section along with specific results from the remote calibration of Rb standard at Bharat Electronics Ltd. (BEL).

The experiment uses either the GPS common view method or the all-in-view method. In the first method, as shown in Fig. 4.18, CGGTTS(CCTF Group on GNSS Time Transfer Standards) data at the master site is taken from the GPS Receiver (GPS common view) which receives 10MHz and 1pps from the reference standard UTC (NPLI). A similar setup is present at the remote site where the 10 MHz and 1pps are obtained from the local reference (device under calibration). The comparison data is logged in the local computer. After completion of the experiment, the data collected at the remote

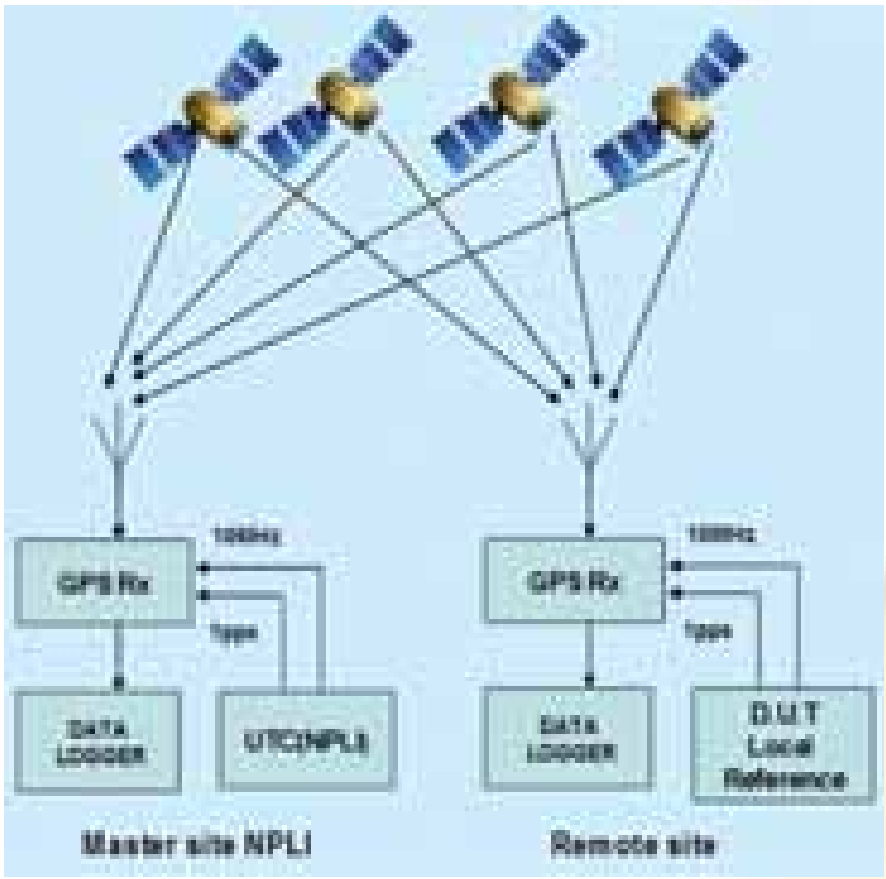

Fig. 4.18: Remote calibration set-up using GPS common view method

site is sent to the master site. Data can be treated in two ways. One way is to take data from the same satellite at two sites and the difference is recorded. Hence, the behavior of the device under calibration is obtained with respect to the reference UTC (NPLI). As shown in Fig. 4.19a, we can see the behavior of the Rb standard with respect to NPLI. Its variation is not exactly linear. The data is further used to calculate stability of Rb for different time periods, as shown in Fig. 4.19b.

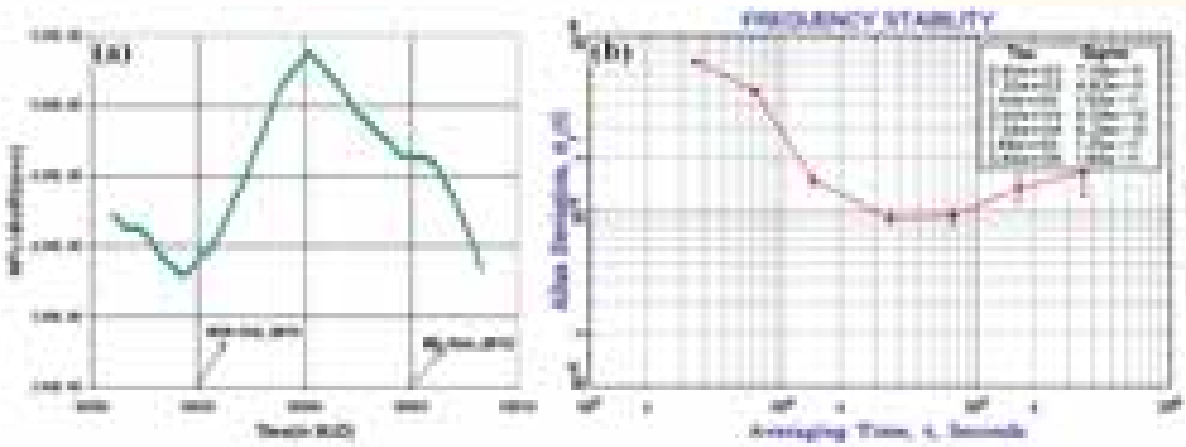

Fig. 4.19: (a) Behavior of BEL Rb standard with NPLI; (b) Frequency stability of the BEL Rb with NPLI

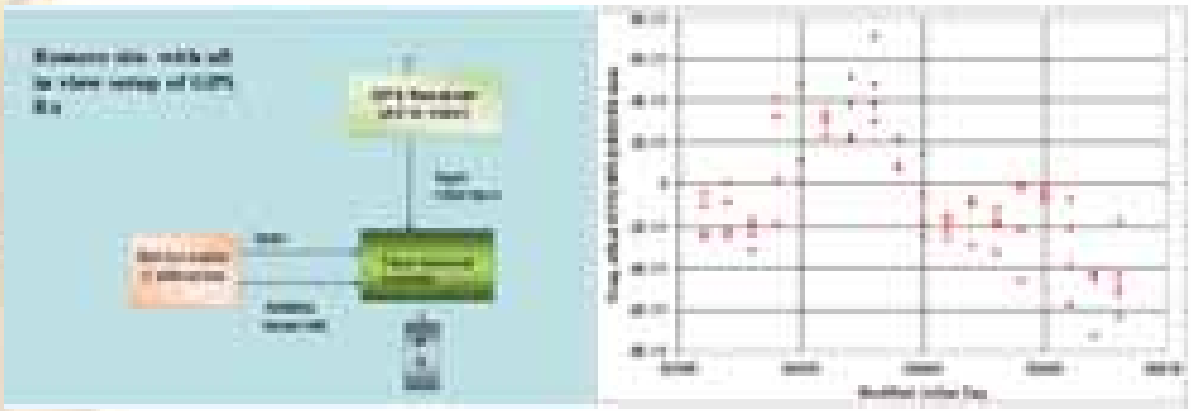

Fig. 4.20: (a) Remote calibration set-up at the remote side using the GPS all-in-view method; (b) frequency offset between UTC (NPLI) and BEL Rb standard frequency

In the second method, as shown in Fig. 4.20a, the GPS receiveris used in all-in-view mode. In this case, a GPS receiver is set up at the remote site which provides an average 1pps output. The phase difference between this 1pps with the local 1pps from Rb standard is measured using a counter and logged in a computer. Similarly, the data is measured using a counter and saved in computer at the master site. The frequency offset data obtained using this method is shown in Fig. 4.20b. Once the experiment is over, the data is transferred from the remote site via internet and analyzed to obtain the frequency difference between the reference source and the device under calibration.

शीर्ष स्तरीय मानक एवं औद्योगिक मापिकी

Apex level Standards and Industrial Metrology

Dr Ashis Kumar Bandyopadhyay
Chief Scientist
Email : akband@nplindia.org

D 05.01 Mass Standards

Sh Anil Kumar
Sh Harish Kumar
Sh Gautam Mandal
Sh Mahargha Baran Das

D 05.02 Standards of Dimension

Dr K P Chaudhary
Sh Arif Sanjid
Sh Vinod Kumar
Sh Sandeep Kumar
Sh Abhishek Singh
Sh Virendra Babu
Sh Ravi Khanna
Sh Mukesh Kumar

D 05.03 Temperature and Humidity Standards

Dr Yesh Pal Singh
Dr Dilip Dhondiram Shivagan
Sh Jagannath Prasad
Sh Rasik Behari Sibal

D 05.04 Optical Radiation Standard

Dr H C Kandpal
Dr (Ms) Ranjana Mehrotra
Sh Virendra Kumar Jaiswal
Dr Parag Sharma
Sh K N Basavaraju
Sh Sudama
Dr Bharat Kumar Yadav

D 05.05 Force and Hardness Standards

Dr Sushil Kumar Jain
Dr S Seela Kumar Titus
Sh Rajesh Kumar
Sh Harish Kumar
Sh Vikram

D 05.06 Pressure and Vaccum Standards

Dr Ashis Kumar Bandyopadhyay
Sh D Arun Vijayakumar
Dr Sanjay Yadav
Dr (Ms) Nita Dilawar
Sh Om Prakash
Sh Harish Kumar
Sh Virendra Kumar Gupta

D 05.07 Acoustics, Ultrasonic, & Vibration Standards

Dr Ashok Kumar
Dr Mahavir Singh
Sh Naveen Garg
Dr P.K. Dubey
Dr Kirti Soni
Sh Gurbir Singh
Ms Reeta Gupta
Dr Yudhisther Kumar Yadav

D 05.08 Fluid Flow Measurement Standards

Sh Shiv Kumar Jaiswal
Sh Ishwar Singh Taak

D 05.09 LF & HF Impedance & DC Standards

Sh Anil Kishore Saxena
Dr Sher Singh Rajput
Sh Ajeet Singh
Sh Rajbeer Singh
Sh M A Ansari
Sh Satish
Sh Kul Bhushan Ravat
Sh Mohammad Saleem
Sh Avdhesh Kumar Goel

D 05.10 LF & HF Voltage, Current & Microwave Standards

Sh Anil Kumar Govil
Sh Pramendra Singh Negi
Sh Saood Ahmed
Sh Bijendra Pal

D 05.11 AC High Voltage and AC High Current Standards

Sh Mukesh Kumar Mittal
Sh Sridhar Lingam

D 05.12 AC Power & Energy Standards

Sh Mukesh Kumar Mittal
Sh Joges Chandra Biswas
Sh Anoop Singh Yadav

Apex Level Standards and Industrial Metrology

Apex Level Standards and Industrial Metrology (ALSIM) division of CSIR-NPL is responsible for establishing, maintaining and upgrading the national standards and providing traceability to other accredited laboratories in the field of physico-mechanical and electrical and electronics standards. It comprises of twelve sub-divisions, their 'Calibration and Measurement Capabilities (CMCs) are peer reviewed at regular intervals, to maintain equivalence in measurements and calibrations at the international levels. The activities of the ALSIM are funded by CSIR-Network project entitled: Measurement Innovations in Science and Technology (MIST).

During this period many new activities have been undertaken, in brief, these are as follow:

(i). CSIR–NPL also has started preliminary investigations for development of a Watt Balance.

(ii). In India, facility for determination of metrological characterization of high capacity weights is only available at CSIR–NPL, New Delhi. The group provides calibration facilities at the apex level for high capacity weights like 100 kgs, 200 kgs and up to 2000 kgs. The characterization work has been carried out for ISRO, Sriharikota for their research and development related activities.

(iii). Similarly, very high capacity volumetric vessels of 1000 l and 2000 l are calibrated for M/s Rockwin Flow Meters Pvt. Ltd., Faridabad. The metrological investigations help the manufacturer to fabricate and develop high precision volumetric vessels for further traceability of volumetric measurements in higher range.

(iv). Secondary hardness standardizing machines of Brinell, Rockwell (including superficial Rockwell), Vickers and micro-Vickers hardness were established. This enables us to provide traceability in hardness measurement including a newly introduced micro-Vickers scale.

(v). A peak to peak measurement module has been successfully designed and its functionality realized with a view to minimize the error in voltage measurement in the ultrasonic power evaluation. It has been found to be better and more accurate than measuring the rf voltage directly.

(vi). The range of AC-DC current transfer measurement facility at NPL has been extended from existing 20A to 80A using ingeniously developed current TEE. Now CSIR-NPL is capable of providing traceability to user organizations by calibrating the AC-DC current shunts of 30A, 50A, and 80A along with the thermal current converters or thermal transfer standard in the frequency range 40 Hz - 10 kHz.

(vii). To establish Standards for Radiated Power Density, a GTEM have been indigenously developed based on Crawford concept. The proposed GTEM is applicable for frequency range 0.7 - 2.5 GHz.

(viii). A new facility for the calibration of Transformer Loss Measuring System (TLMS) up to 100kV/ 2000Amps has been established and calibration services as well as traceability is provided to power corporations and manufacturers.

Besides, ALSIM division is actively involved in the intercomparison activities namely:

(i). An inter-laboratory comparison has been conducted on mass parameter with three standard weights of nominal values of 100 mg, 20 g and 1 kg. The inter-laboratory comparison has been aimed to evaluate the competence and the compatibility of the measurement results reported by the SAARC NMIs (BSTI, Bangladesh; NPSL, Pakistan; NBSM, Nepal and MUSSD, Sri Lanka). CSIR – National Physical Laboratory, India (NPLI) was the pilot laboratory of this program.

(ii). Participating in international inter-comparison (NPLI as pilot laboratory in length, parameters) with BSTI- Bangladesh, MUSSD-Sri Lanka and NPSL-Pakistan.

(iii). APMP-T-S7: Comparison of Pt/Pd thermocouple at Cobalt-carbon (Co-C) eutectic fixed point (1324 °C), which has been developed in the laboratory.

(iv). APMP-T-S8: APMP TCT/DEC: Comparison of Liquid-in-glass thermometers against SPRTs covering a range from -41 °C to 250 °C using high precision alcohol, water and oil baths. The measurement results after analysis shall be submitted to SIRIM, Malaysia.

(v). An Inter-laboratory comparison in LIGT (0-100 °C) and Type-S thermocouple (0-1000 °C) was organized by our group among the NMIs of four SAARC countries namely Bangladesh, Nepal, Sri Lanka and Pakistan.

(vi). Participated in the APMP Key Comparison of Luminous Intensity (APMP. PR-K3.a) and have finished the measurements. Final report of the measurements was submitted to NMI, Japan- the Pilot Laboratory in March 2014.

(vii). APMP.M.P-K13 (piloted by NMIJ, Japan) is under draft stage, draft A is being circulated to the participating laboratories. The main objective of this key comparison is to compare the performance of hydraulic pressure standards of participating institutes, in the pressure range 50 MPa to 500 MPa in gauge mode to essentially support the objective evidence for high pressure CMCs of the participating institutes.

(viii). A bilateral comparison of 10 k &! & 1&! between BIPM and NPLI was carried out. Measurement analysis is in progress.

(ix). NPL is a Pilot Lab and coordinating the inter-comparison (P1-APMP.EM-S8) of 6½ Digit Multimeter (DMM) under Asia Pacific Metrology Programme (APMP), in which 16 countries are participating.

The results are communicated to NMI-Australia for consultation. The individual results will be communicated to participating labs for their comments, etc. Thereafter it will be submitted as draft A report to APMP.

Also taking active part in the NABL proficiency testing programme as follow:

(i). NPL-NABL-PT-Program, NABL-T-Temp-006 has been completed for Type-S thermocouple in the range from 0 to1200 °C. 12-Calibration laboratories participated in the program.

(ii). Under NPL-NABL-PT-Program, two Proficiency Testing (PT) Programmes for Capacitance Measurements are being carried out:

(a) 1 µF (NABL – E – Capacitance - 003)

(b) 10 pF & 100 pF (NABL – E – Capacitance - 004)

The ALSIM division is conducting large numbers of training programme, in various parameters, for industries, legal metrology officers and for SAARC countries.

Mass Standards

Mass Standard has been mandated to provide apex level traceability and dissemination of standards to the calibration laboratories and user industries in the area of mass, volume, density and viscosity. Except viscosity, volume and density are the derived units from mass. Mass plays very vital role and the National Prototype Kilogram No. 57 (NPK-57) is the primary standard of mass in India. NPK-57 is used to calibrate the transfer mass standards and these transfer mass standards are further used in maintaining the unbroken chain of traceability.

Development of model of Watt Balance principle

CSIR–NPL also has started preliminary investigations for development of a Watt Balance. The investigations are done for static and dynamic phases of the Watt Balance. An experimental set up has been established. A wheel of diameter 300 mm, and thickness 10 mm has been fabricated, which is made of Aluminum. The wheel is fitted with knife edge made of gun metal and placed over the suitably flattened aluminum plate fixed to wooden base. The wheel is provided with two pans of diameter 40 mm attached to each other by a string.

Fig .5.1: Experimental setup for Watt Balance Principle Demonstration

Metrological characterization of high capacity weights (100 kg, 200 kg, 500 kg, 1000 kg & 2000 kg) of Indian Space Research Organization, Sriharikota

In India, facility for determination of metrological characterization of high capacity weights is only available at CSIR–NPL, New Delhi. The group provides calibration facilities at the apex level for high capacity weights like 100 kgs, 200 kgs and up to 2000 kgs. The characterization work has been carried out for ISRO, Sriharikota for their research and development related activities.

Fig. 5.2: High Capacity Weights of ISRO, Sriharikota

Metrological investigations of high capacity volumetric vessels of Rockwin Flow Meters.

Similarly, very high capacity volumetric vessels of 1000 l and 2000 l are calibrated for M/s Rockwin Flow Meters Pvt. Ltd., Faridabad. The metrological investigations help the manufacturer to fabricate and develop high precision volumetric vessels for further traceability of volumetric measurements in higher range.

Fig. 5.3: A Typical High Capacity Volumetric Vessel

Metrological characterization of balance of 1.5 t of Shankar Wires, Deoghar

Though the balances of varying capacity up to 100 kg may be calibrated by some of NABL accredited laboratories, but in higher capacity, only

CSIR–NPL has the facilities. A 1.5 t balance of M/s Shankar Wires Pvt. Ltd, Deoghar has been recently investigated for its metrological capability at site and the report has been prepared.

Fig. 5.4: 1.5 t Balance of M/s Shankar Wires Pvt. Ltd. at Deoghar

Metrological investigations of Reference Grade Hydrometers

The reference grade hydrometers play a very vital role in maintaining the traceability of density from the primary solid density standard to the working hydrometers. The reference grade hydrometers are used to calibrate the laboratory grade hydrometers or secondary reference grade hydrometers, which in turn calibrates working hydrometers. The working hydrometers are used for density measurement of the liquids directly. Hence, correction of the reference grade hydrometers is very important.

The observations of the investigations have been published in International Journal of Modern Physics: Conference Series, Vol. 24, 2013.

CSIR NPLI – PTB – SAARC Program

Under CSIR NPLI – PTB – SAARC program, the following activities took place:

a. Attended the Second Co-ordination meeting on Regional Cooperation Metrology at Islamabad, Pakistan during April 22-25, 2013.
b. A two days on site training program (April 26-27, 2013) was conducted at NPSL, Pakistan for better understanding of the mass measurement, uncertainty of measurement and calibration of balances etc.
c. Assistance in assessment through NABL to NBSM, Nepal & SQCA, Bhutan accreditation in mass parameter by CSIR – NPL assessors.
d. Helped SLSI, Sri Lanka & NBSM, Nepal for inter – laboratory comparison in mass parameter.
e. An inter-laboratory comparison has been conducted on mass parameter with three standard weights of nominal values of 100 mg, 20 g and 1 kg. The inter-laboratory comparison has been aimed to evaluate the competence and the compatibility of the measurement results reported by the SAARC NMIs (BSTI, Bangladesh; NPSL, Pakistan; NBSM, Nepal and MUSSD, Sri Lanka). CSIR – National Physical Laboratory, India (NPLI) was the pilot laboratory of this program.

Fig. 5.5: Preliminary Results of SAARC-PTB Inter-laboratory comparison for 1000 g

Density measurement of special alloy developed by Heavy Alloy Penetration Plant, Trichy.

Some special purpose materials have been developed and fabricated by Heavy Alloy Penetration Plant, Tiruchirappalli under Ministry of Defense for their specific requirement. The density of such samples has been measured very precisely.

Metrological characterization of Dead weights for Dead Weight Tester, Dead Weight Force Machine & Fluid Flow Standards.

Dead weights from in-house activities as well as from calibration laboratories and organizations like ERTL are regularly received for calibration of their dead weights in N. The calibration of such

dead weights is very pivotal in maintaining traceability of pressure, force, torque, fluid flow etc. from apex level to user industries as well as in CSIR–NPL too.

STANDARDS OF DIMENSION

Participating in international inter-comparison (NPLI as pilot laboratory in length, parameters) with BSTI- Bangladesh, MUSSD-Sri Lanka and NPSL-Pakistan.

1. Procurement of 3D Coordinate Measuring Machine (Make: Mitutoyo):

Fig. 5.6: Experimental setup for electronic level calibration

2. Improving uncertainty of measurement in the calibration of electronic level by minimising various systematic errors:

Engineering levels with typical resolutions of 1µm/m are very often used for inspecting flatness of surface plates, straightness of machine guides and inclinations of machine parts, surfaces etc. Measurement laboratories calibrate these engineering levels using small angle generating instruments viz. sine bar, tilting table. For the engineering level and small angle generators many national measurement institutes have their best calibration capability of an uncertainty in the range of ±1µm/m to ±4µm/m at a 95% confidence level. At NPL-India, an experimental setup is established to investigate various systematic errors. The imperfections are a) misalignment of line of measurement b) flatness, levelling of working platform c) force balancing/weight distribution along the cantilever d) pivoting of tilting table. These imperfections are minimized to improve the repeatability. Further, Laser interferometer is used to calibrate the engineering levels on a tilting table. Uncertainty of measurement for each experiment improved up to ±0.8 µm/m.

TEMPARATURE AND HUMIDITY STANDARDS

Temperature standards at NPL are established in accordance with the International Temperature Scale of 1990 (ITS-90) by realizing and maintaining the equilibrium states called fixed points of high purity substances. Ar, Hg, H_2O, Ga, In, Sn, Zn, Al and Ag measured by the platinum resistance thermometers covering the range from 84K to 1234K and realizing Ag and Cu points in blackbody cavities by spectral photoelectric radiation pyrometer, LP4 and thus extends the temperature range from 1234 K to 3500 K.

The **humidity standard** is maintained through a temperature-pressure humidity generator, Thunder Scientific, USA made, and capable of generating humidity in the range from 10%Rh to 95% RH with a precision of 0.1% RH. The temperature and pressure indicators used in the Chamber are traceable to NPL.

This Section is providing **apex level calibration** to a large number of NABL accredited laboratories, govt. departments and user industries for all types of temperature measuring standards and instruments in the range from -200 °C to 3000 °C and humidity measuring instruments in the range from 10%RH to 95%RH. A significant amount of ECF was generated through these calibration services.

APMP key comparisons

This year the Group has completed two major APMP comparisons.

APMP-T-S7: Comparison of Pt/Pd thermocouple at Cobalt-carbon (Co-C) eutectic fixed point (1324 °C), which has been developed in the laboratory. The results submitted to NMI, Korea.

APMP-T-S8: APMP TCT/DEC: Comparison of Liquid-in-glass thermometers against SPRTs covering a range from -41 °C to 250 °C using high precision alcohol, water and oil baths. The measurement results after analysis shall be submitted to NIMT Thailand.

Temperature & Humidity Standards Group has initiated an innovative project on Boltzmann constant entitled "Determination and realization of thermodynamic temperature by acoustic gas thermometry" for redefinition of unit, kelvin. Work is in progress on the preliminary experimental

requirements.

Fixed point of silver with new set-up installed this year has been utilized to calibrate HTPRTs. The results on experimental runs taken on the fixed point have improved the precision and uncertainty in the measurement of the Ag-point. The facility has been utilized for calibration of SPRTs and HTPRTs of in-house and international standards. One such calibration requirement has been received from Sri Lanka Standards Institution (SLSI), Sri Lanka.

National & International Collaboration

NPL-NABL-PT-Program, NABL-T-Temp-006 has been completed for Type-S thermocouple in the range from 0 to1200 C. 12-Calibration laboratories participated in the program.

Expertise was provided to NABL for Core Accreditation Committee decisions and in the assessment of calibration laboratories in the field of thermal calibration.

The Group is associated as one of the teams in the NPL-PTB SAARC project. An Inter-laboratory comparison in LIGT (0-100 °C) and Type-S thermocouple (0-1000 °C) was organized by our group among the NMIs of four SAARC countries namely Bangladesh, Nepal, Sri Lanka and Pakistan. The Group provided expertise for peer review of calibration laboratory namely Shri Lanka Standards Institution (SLSI), under the Sri Lanka Accreditation Board (SLAB) during 20-24 Jan, 2013.

OPTICAL RADIATION STANDARDS

Dissemination and maintenance of the units of optical radiation of standards have direct impact on societal needs as lighting is one of the largest industrial sectors in the country. We have participated in the APMP Key Comparison of Luminous Intensity (APMP. PR-K3.a) and have finished the measurements. Final report of the measurements was submitted to NMI, Japan- the Pilot Laboratory in March 2014. The report of the Key Comparison is expected after all the measurements at other NMIs are finished. This will help continuation of the CMCs of the Optical Radiation Standards section of NPLI. Measurements of luminous intensity were performed on three intensity lamps for preparing artifacts for APMP Key Comparison for Luminous Intensity.

Measurement results of APMP Key Comparison for Luminous Intensity (APMP. PR-K3.a)

Table 5.1 1st Round Measurement (2013)

Lamp No.	Current(A)	Voltage(V)	Distribution Temperature or CCT (K)	Luminous Intensity (cd)
OSRAM Wi41/G: 60	5.862	30.42	2856±20	280.8
OSRAM Wi41/G: 67	5.856	30.36	2856±20	276.3
OSRAM Wi41/G: 87	5.880	30.41	2856±20	276.6

Table 5.2 2nd Round Measurement (2014)

Lamp No.	Current(A)	Voltage(V)	Distribution Temperature or CCT (K)	Luminous Intensity (cd)
OSRAM Wi41/G: 60	5.862	30.42	2856±20	280.4
OSRAM Wi41/G: 67	5.856	30.36	2856±20	276.6
OSRAM Wi41/G: 87	5.880	30.41	2856±20	276.3

The final report of key comparison will be published soon by the Pilot laboratory after compilation of results obtained from all the participating laboratories.

Calibration and Testing services: A good amount (about 80 lakhs) of ECF was generated in the year 2013-14 through the initiative taken for calibration of new generation energy saving lamps.

FORCE AND HARDNESS STANDARDS

Force, torque and hardness measurements play a vital role in several industries and research in stress measurement and analysis of materials, products and processes for safety, reliability, stability, efficiency, etc. This group has been engaged in establishing primary standards in all these areas for providing the necessary traceability to the user industries across the county. This group is constantly involved in research and developmental activity for augmenting and upgrading the standards at par with other leading National Metrology Institutes (NMIs) to establish equivalence to the international system of measurements.

Recently, static piezoelectric actuation has been deployed in low force measurement as it exhibits a good stiffness compared to other actuators. An attempt has been made to investigate the feasibility of developing a piezoelectric actuator to exert a desired force on a load cell and to study the observed force versus displacement characteristics. A piezoelectric stack is developed comprising of 14 units of PZT-4 piezo ceramic elements each having a thickness of about 5mm. They are joined together with alternative polarity and the elements are electically connected in parallel. The stack is appropriately mounted inside the diamond shaped frame using a proper stopper and bolt arrangement as dipicted in fig 5.7. Hence the stack is pre-stressed in tension. On the application of the external excitation voltage to the stack elements, they undergo either contraction or expansion depending upon the polarity of the applied voltage. The corresponding transvers or longitudial displacement of the piezoactuator can be utilized for futher application on any desired module as applicable.

Fig. 5.7: Experimental Set-up

The Figure 5.8 shows a typical behaiour of the 1000N force transducer with the increase in the applied voltage, indicating that a force of about 1N is attained in the range of the measurements performed. The Repeatability of the measurement is found to be within 1% which indicates that such piezo actuators can be used for the realization, generation and measurement of small forces.

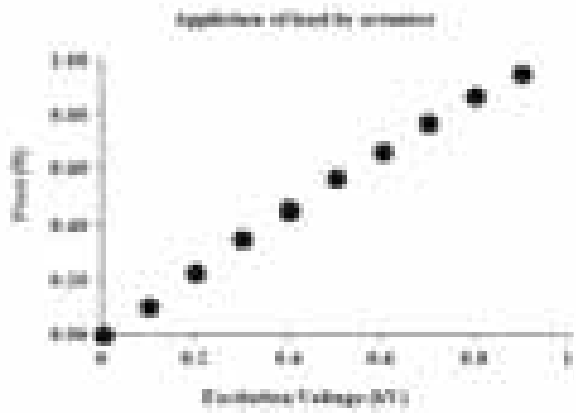

Fig. 5.8: The variation of measured force on the 1000N force transducer output with Excitation Voltage

The Calibration Measurement capability (CMC) of a torque generating system in the range of 1Nm to 20Nm, using a simple circular pulley as schematically illustrated in Fig.5.9, is reaffirmed.

A fine metallic strip is properly attached at the periphery of the circular section as shown in the figure to support a loading hanger. The circular disc is separately calibrated from the NPL dimension standard for its diameter (radial arm), also the masses used are calibrated from the NPL Mass standard and the calibration and measurement capability (CMC) of this system was theoretically estimated by considering the uncertainty associated with them. A precision flange type torque transducer of capacity 20Nm was used as torque transfer standard to reaffirm the calibration and measurement capability of this system. The CMC of the torque generating system was determined considering the contributions of various uncertainty components including the uncertainty associated with the mean values obtained from the primary machine using the standard procedure. In this way the CMC of the torque machine in the 1-20Nm was reaffirmed and this gives us confidence about the performance of the machine.

Fig. 5.9: Torque generating system in the 1-20 Nm range

Secondary hardness standardizing machines of Brinell, Rockwell (including superficial Rockwell), Vickers and micro-Vickers hardness were established. These machines were calibrated for the applied forces for the different hardness scales possible in the machine. The evaluated forces were found to conform to the requirement of the international standards ISO 6506/7/8 and the calibration measurement capability of the machines were also evaluated. By using these facilities, hardness blocks calibration are provided for the user industries and other calibration laboratories. This enables us to provide traceability in hardness measurement including a newly introduced micro-vickers scale which is shown in Figure 5.10.

Fig. 5.10: Micro Vickers Hardness Machine

The group is actively involved in large scale dissemination of the standards of Force, Torque and Hardness to the user industries and calibration laboratories by providing the necessary measurement traceability for these parameters. About 700 calibration reports were issued to the customers all over the county in force, hardness and torque parameters during the last year and the ECF realized in this process was approximately Rs 75 lakh. The group also provides training to the metrologists working in different sectors like NABL accredited laboratories, legal metrology divisions, industries, etc.

VACUUM AND PRESSURE STANDARDS

The Pressure Standards group has the mandate to establish, maintain and upgrade the national pressure standards and provide national traceability via apex level calibration and consultancy services for reference and pressure measuring instruments received from industries and other users in the pressure range starting from atmospheric pressure to 1.0 GPa.

The pneumatic pressure section primarily establishes, maintains and upgrades the standards for pneumatic pressures in the pressure range 0.04

to 40 MPa. The primary as well as the secondary standards are dead weight testers which are characterized against each other as well as are traceable through a continuous chain of overlapping pressures to the ultrasonic interferometer manometer. The measurements made are world class and traceable to the international standards.

In addition to the above mentioned activities, the group is also engaged in basic research which includes investigation of materials under high pressure as well phonon behavior at liquid N_2 temperatures using state of the art Raman spectrometer. The group also collaborates with researchers within and outside NPL for Raman characterization of strategic materials, temperature dependent Raman studies and assists in the analysis of the data. The results have been published in reputed international journals.

PRESSURE STANDARDS

Raman studies

In continuation of our research on high pressure behavior of rare earth oxides, data analysis was completed for PrO_2 and Ho_2O_3 and results of phase progression of lanthanide dioxides (CeO_2 and PrO_2) have been published. The detailed analysis of results of Er_2O_3, Tb_4O_7 is underway.

At ambient, Raman spectra were recorded for a number of samples in collaboration with various groups of NPL as well as other organizations e.g. Delhi University, DTU etc. These include samples like CZTS, ZnO, Fe_2O_3, Bi_2Te_3, GaN, Graphene, Cu_2SbSe_3, $LaInO_3$, TiO_2, Ir_2O_3, GeTe, FeCNT etc. etc.

High Pressure Raman study of Lanthanide dioxides (CeO_2 & PrO_2)

The phase progression in nano-crystalline oxides PrO_2 and CeO_2 up to pressures of 49 GPa and 35 GPa, respectively, were investigated via in situ Raman spectroscopy at room temperature. With an increase in applied pressure the Raman modes due to the cubic phase were seen to steadily shift to higher wavenumbers for both the samples. However, we observed the appearance of a number of new peaks around a pressure of about 34.7 GPa in CeO_2 and 33 GPa in PrO_2 which were characteristic of an orthorhombic α-$PbCl_2$ type structure. The mode Gruneisen parameters for both the phases were obtained from the pressure

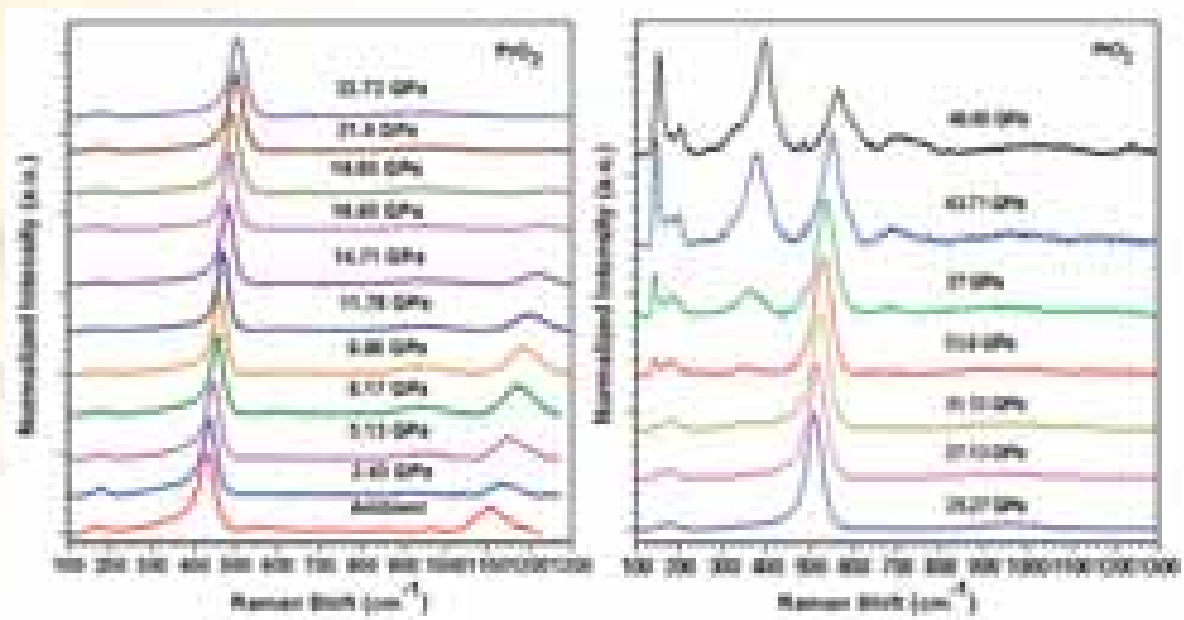

Fig. 5.11: High pressure Raman spectra of PrO_2

dependence of frequency shifts. On decompression, the high pressure phase existed down to a total release of pressure. Although the high pressure Raman data for PrO_2 has not been reported so far, nevertheless, the Gruneisen parameters for the orthorhombic modes obtained after extrapolation to the atmospheric pressure gave values comparable to those of CeO_2.

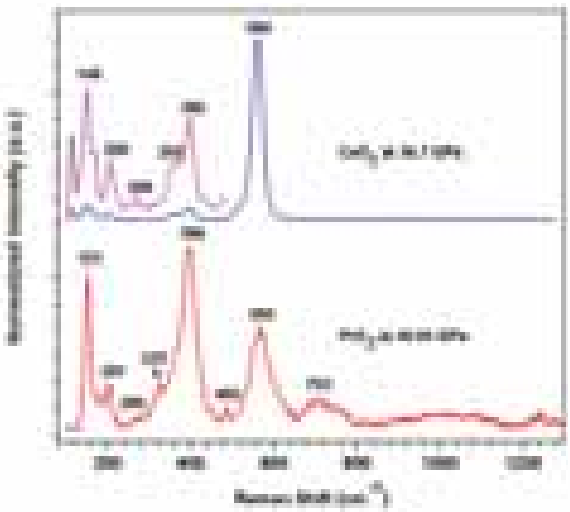

Fig. 5.12: A comparison of the high pressure orthorhombic phase Raman peaks of CeO_2 at 34.7 GPa and PrO_2 at 49.95 GPa

Draft A Results of APMP KEY COMPARISON (APMP. M.P.K13)

The *Draft A* report of this comparison, identified as APMP.M.P-K13, piloted by NMIJ, Japan is received. The main objective of the key comparison is to compare the performance of hydraulic pressure standards of participating institutes, in the pressure range 50 MPa to 500 MPa in gauge mode to essentially support the objective evidence for high pressure CMCs of the participating institutes. The total participating institutes were 10 including NMIJ/AIST, Japan; NPLI, India; NMC/A*STAR, Singapore; NIM, Thailand; NMIA, Australia; NIM, China; CMS/ITRI, Chinese Taipei; KIM-LIPI, Indonesia; KazInMetr, Kazakhstan and KRISS, Korea. In this comparison, a set of pressure balance utilizing 3 piston-cylinder assemblies of 2 mm^2 nominal effective area was circulated as the transfer standard (TS). As per draft report, NPLI results are in excellent agreement with pilot laboratory (having relative deviations better than 9 ppm) and also with other participating institutes as shown in the Fig. 5.13. In the *Draft A* report, the results of the respective participating institutes are compared in terms of the deviations from the pilot institute's result. The results of this comparison will be linked to the corresponding CCM key comparison, CCM.P-K13 in which NPLI was also a successful participating institute.

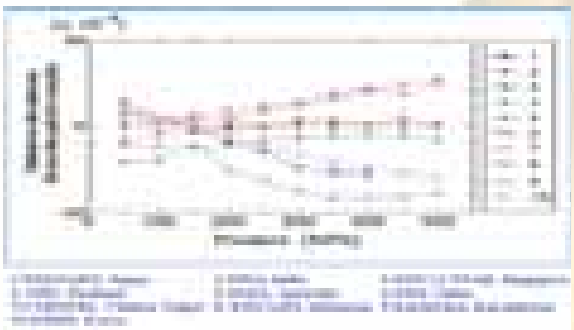

Fig. 5.13: Relative deviations of the participating institutes' results from the pilot institute's results

Comparison of National and Industrial Hydraulic Pressure Standards in the Pressure Range up to 500 MPa

An in-house comparison of several pressure standards maintained by NPL and some other Indian pressure measurement laboratories was carried out using a transfer standard (TS), designated as NPL500MPN, in the pressure range 50-500 MPa, having nominal effective [A'_p] as 1.96 mm^2. The objective of the comparison is to determine the values of the A'_p of TS and their uncertainties at specified pressures. The comparison was carried out at pressure points of 50, 100, 150, 200, 250, 300, 350, 400, 450 and 500 MPa. The TS was cross-floated against the NPL secondary and primary pressure standards, (NPL500MPA and NPL-H1) and 2 industrial pressure standards (CMERI and YANTRIKA). The comparison data thus obtained are analyzed in terms of A'_p(mm^2) as a function pressure p (MPa). The values of the A'_p and λ thus obtained are also compared with the values of the TS deduced from

recently completed CCM intercomparison exercise. Finally, the consistency of the results in the whole pressure range (50 to 500) MPa is compared with median of A'_p(mm^2) values against all laboratory standards (LSs) and found that the results are compatible, uniform and traceable to each other (Fig. 5.14). The degree of equivalence has also been estimated and it is observed that all the standards agree well within the standard measurement uncertainty of the respective LS.

Fig. 5.14: Relative deviation of A_p from median values

VACUUM STANDARDS

- **Barometric Pressure Standards activity**

Ultrasonic Interferometer Manometer (UIM), Force Balanced Piston Gauge (FPG) and AIR Piston Gauge (APG), all primary pressure standards are being maintained in good working condition. The measurement uncertainty of UIM and APG in both absolute and gauge pressure regions are twice notified in BIPM KCDB as Calibration Measurement Capabilities (CMC) of NPL, India, during 2004 and 2009 through Peer Review conducted in every 5 year duration.

Table 5.3. Measurement uncertainity of Pressure Standard

STANDARD	RANGE	EXPANDED UNCERTAINTY (at k = 2)	DATE OF COMMISSION
UIM	1.0 Pa to 130.0 kPa (abs)	Q(0.0092 Pa , 0.00072% of rdg)	1982
	1.0 Pa to 130.0 kPa (gauge)	Q(0.0092 Pa , 0.00072% of rdg)	
APG	20.0 kPa to 360.0 kPa (g)	± 0.0012% of rdg	2001
	6.5 kPa to 360.0 kPa (abs)	Q(0.14 Pa , 0.0012% of rdg)	
FPG	1.0 Pa to 15.0 kPa (abs)	Q(0.012 Pa, 0.0025 % of rdg)	2010
	1.0 Pa to 15.0 kPa (gauge)	Q(0.012 Pa, 0.0025 % of rdg)	

STANDARD	RANGE	EXPANDED UNCERTAINTY (at k = 2)	YEAR OF COMMISSION
DPI 145 (01)	0.01 hPa to 1000.0 hPa (abs)	Q(0.006 hPa, 0.012% of rdg)	
	35.0 hPa to 1300.0 hPa (abs)	Q(0.006 hPa, 0.01% of rdg)	1997
	-1000.0 hPa to 0 to +4000.0 hPa (g)	Q(0.006 hPa, 0.014% of rdg)	
DPI 145 (02)	0.0 hPa to 2600.0 hPa (abs)	Q(0.006 hPa, 0.015% of rdg)	
	-200.0 hPa to 0 to +200.0 hPa (g)	Q(0.006 hPa, 0.6% of rdg)	2011

Several secondary pressure standards are also being maintained in good condition for R&D and calibration work. Traceability of all these secondary standards is maintained through calibration of the same against the National Primary Pressure Standards. The measurement uncertainty details of these standards are given in the above table 5.3.

	-1000.0 hPa to 0 to +1000.0 hPa (g)	Q(0.006 hPa, 0.03% of rdg)	
CDG	0.0 Pa to 133.0 Pa (abs)	Q(0.01 Pa, + 0.22% of rdg)	2001
CDG	0.0 Pa to 13.3 kPa (abs)	Q(0.011 Pa, + 0.11% of rdg)	1995
CDG	-1.33 kPa to 0 to + 1.33 kPa (g)	Q(0.012 Pa, + 0.3% of rdg)	
RSG (01)	-1.0 kPa to 0 to +1.0 kPa (g)	Q(0.014 Pa, + 0.8% of rdg)	2001
RSG (02)	-10.0 kPa to 0 to +10.0 kPa (g)	Q(0.059 Pa, + 0.1% of rdg)	2012

Vacuum Standards activity

CMCs :

Static Expansion System ~ Range: 10 Pa to 0.05 Pa (Exp Uncertainty: ± 4.0E-03 Pa, coverage factor ~2, confidence level ~ 95%

Continuous Expansion (Dynamic Expansion) System ~ Range: 10^{-1} Pa to 10^{-6} Pa (Exp Uncertainty: ± 2.0E-02 Pa, coverage factor ~2, confidence level ~ 95%

ACOUSTICS, ULTRASONIC AND VIBRATION STANDARDS

The Acoustics and Vibration standard of NPLI is at present maintaining the standards of sound pressure and vibration amplitude in compliance with ISO 17025 & relevant IEC Standards with measurement uncertainties at par with other NMIs. The traceability to regional laboratories and public sector undertakings is provided by the calibrations of electro-acoustic equipments traceable to the national standards. The division is focusing on reducing the measurement uncertainties to an extent at par with some of the reputed NMIs and extension of sound and vibration facilities to shock calibration and free field calibration of microphones. The division is also focused on upgradation of sound transmission loss and sound absorption measurement facility with an objective of reducing measurement uncertainty in sound transmission loss and sound absorption and development of acoustical materials for noise control and abatement. The division is focused to upgrade the measurement standards not only to establish a strong traceability chain throughout the country, but also to help public sector and govt. undertakings, industries and society for noise and vibration abatement and control. The Ultrasonic standard of NPL, India is focused on realizing the primary standard of Ultrasonic power and provides calibration and testing services in the area of ultrasonic metrology, thus providing traceability to both the industrial and public sector undertakings. The division is responsible for upgradation and maintenance of primary standard of ultrasonic power with an objective of reducing the measurement uncertainty primarily due to rf voltage measurements. A new differential peak to peak measurement approach to reduce the ac voltage measurement error has been investigated.

Maintenance and up-gradation of National standards of sound, pressure and vibration amplitude

The Acoustics and Vibration Standard are responsible for maintenance and upgradation of two primary standards viz., Standard of Sound Pressure and Standard of Vibration Amplitude. The division is responsible to establish, maintain and continually upgrade the national standards of measurements of sound and vibration and disseminates the standards by providing the apex level calibration services to the industry and institutions of the country. The primary standard of sound pressure is maintained through absolute calibration of standard condenser microphones in the coupler cavity by the reciprocity technique in the frequency range 31.5 Hz to 25 kHz. The primary standard of vibration amplitude is maintained through absolute calibration of standard reference

accelerometers using the Laser interferometer in the range 5 Hz to 10 kHz. The accuracy of primary standards is verified periodically through participation in key comparison exercises with with leading NMIS of the world.

The division is focused on reducing the measurement uncertainties in realizing the primary standards of sound and vibration. The measurement uncertainty calculated in calibration of reference accelerometer is calculated to be 0.3% at 160 Hz at par with other NMIs in APMP region, while for the extended frequency range it varies between 0.3 to 1.25 % (k=2, 95 % confidence level). Efforts are in progress to reduce the measurement uncertainties in the low frequency range (0.1 Hz to 5 Hz) and high frequency range (≥ 10 Hz).

Fig. 5.15: National Primary Standard of vibration realized at CSIR-NPL, India

Continuous efforts are targeted towards reducing the measurement uncertainties in realization of primary standard of sound pressure using the well known reciprocity method. The dimensional characterization of microphones has lead to reaffirmation of measurement uncertainty in pressure sensitivity determination to 0.04 to 0.15 dB in the frequency range 31.5 Hz to 25 kHz. The use of the optical method for measuring the front cavity volume has refined the measurement methodology followed by adaptation of a self reliant, traceable and systematic measurement procedure in comparison to the earlier use of nominal values for the sensitivity fitting exercise.

Study of Atmospheric Boundary Layer (ABL) for Air pollution application.

SODAR (Sonic Detection And Ranging) is an acoustic remote sensing technique for monitoring the dynamics of the lower atmospheric boundary layer (ABL) thermal structures in real time. SODAR has capabilities to provide a direct pictorial view of the prevailing meteorological processes such as onset/dissipation of free convection, inversion, fumigation is considered a useful aid for air quality assessment studies. Use of site specific SODAR data pertaining to inversion/mixing height is often recommended for environment protection agencies for environment impact assessment (EIA) and planning strategies for disaster management under the accidental release of pollutants.

Fig. 5.16: Echograms of Atmospheric Boundary layer height observed for Delhi in December, 2013

National Physical Laboratory, New Delhi has designed, developed & fabricated a mono-static SODAR. The SODAR system is capable of monitoring the ABL up to a height of 1 km. High power acoustic burst, of 100 ms duration, at 2 KHz is repeatedly transmitted vertically, every 6 sec. using an acoustic antenna. The antenna comprises of 4' parabolic dish with a transducer placed at its focus. The backscattered signals from atmospheric turbulent regions occurring along the propagation path are received by the same antenna and processed to produce echogram of the prevailing meteorological phenomenon

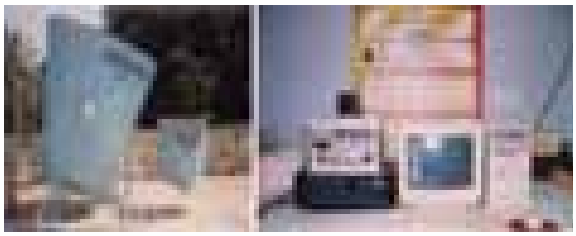

Fig. 5.17: (a) & (b) Indigenous SODAR facility design and developed by CSIR-NPL, India

- Upgradation of present C-Scan system for immersion NDT

Ultrasonics Standard section upgraded the present C-Scan system and developed a new C-Scan system for immersion NDT. C-scan system provides a pictorial information at a depth inside the sample immersed into water and is useful in bulk material characterization. It is of utmost importance for the characterization of ultrasonic transducers and development of measurement technique.

Fig. 5.18: Schematic of the developed C-scan System

Fig. 5.19: C-Scan system for immersion NDT

Automated system of total acoustic power measurement

A peak to peak measurement module has been successfully designed and its functionality realized with a view to minimize the error in voltage measurement in the ultrasonic power evaluation. It has been found to be better and more accurate than measuring the rf voltage directly. As the circuit employs a very fast diode and peak detector, it has fast dynamic response. It holds the dc voltage within one complete input rf cycle. Such fast technique is necessarily needed too the automation. The dc output obtained from the developed module needs to be measured with higher accuracy. This ultimately increases the measurement accuracy of rf voltage.

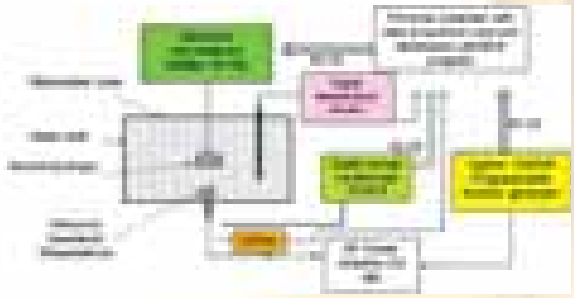

Fig. 5.20: Block diagram showing the parts of radiation force balance setup at NPL, India used to measure total ultrasonic power of a transducer

FLUID FLOW MEASUREMENTS STANDARDS

The Fluid Flow Measurement Standards group has the mandate to provide apex level testing and calibration services for the different types of domestic and industrial water flowmeters. The group has a Water Flow Calibration Facility (i.e. Primary Standard of Flow) for calibration of different types of water flowmeters as per ISO 4185 standard. Since the present facility is obsolete now, therefore, its upgradation using latest instrumentation and controls was planned. For this purpose, Rs. 1.65 Crores has been sanctioned in XII-Five Year Plan (2012-17) under MIST project.

The group also has a Water Meter Testing Facility (i.e. Secondary Standard of Flow), for testing of domestic/ industrial water meters of sizes 15 mm to 50 mm as per IS 779, IS 6784 and ISO 4064 standards.

The Gas Flow Calibration System in the flow range 10 sccm to 1000 slm with expanded uncertainty of 0.2% (at k=2) is being installed. This system would be used for calibration of mass flow controllers, mass flow meters and rotameters.

An automatic Water Flow Calibration Standard (i.e. Primary Standard of Flow) of size

DN100 was developed in technical collaboration with M/s Bharti Automation Pvt. Ltd., New Delhi. The traceability of this system was established using various standards instruments traceable to national standards. The uncertainty of this system for volume flow rate is 0.03% (at κ=2) for collected mass of 2000 kg (Table 5.4).

Table 5.4 : Uncertainty of New Water Flow Calibration System of size DN100

Sources of uncertainty for volume flow rate	Standard uncertainty	
	At 2000 kg	At 1000 kg
Collected Mass in Weighing Tank	0.01%	0.02%
Collection Time (including diverter timing error)	0.01%	0.01%
Water Density	0.05%	0.005%
Combined uncertainty (μ_c)	0.015%	0.023%
Expanded uncertainty (U) at κ=2	0.03%	0.05%

LF, HF IMPEDENCE AND DC STANDARDS

This activity is maintaining the LF & HF impedance standards, DC standards and DC High Voltage standards.

LF & HF Impedance Standard: This activity is maintaining the primary standards of capacitance, inductance and ac resistance. Value to the 10 pF capacitor is assigned through primary standard, a calculable cross capacitor, with an uncertainty of 0.6 ppm using precision ac bridges. Scale of capacitance is built up from 10 pF to 1 F using transformer ratio arm bridges. The unit of ac resistance, Ohm, is also realized from capacitance standard, using Quadrature Bridge and other precision ac bridges at 1kΩ. The scale of resistance from 1 Ω to 1 MΩ builds up with Kelvin double arm ac bridge. The unit of inductance, Henry, is realized from capacitance and resistance using Maxwell-Wien bridge. Value to 100 µH to 10 H is assigned through this bridge.

The Precision Coaxial air-lines are taken as the primary standard of HF capacitance standard, traceable to length standards. The capacitance values of these air lines at high frequencies have been evaluated from their dimensions by using the transmission line theory and taking into account the distributive effects associated with the coaxial lines. A set of seven air-lines of different lengths from 3 cm to 30 cm exhibit capacitance values which vary from 2 pF to 20 pF respectively and has been employed in the frequency range of 10 kHz to 100 MHz. Transfer standards of capacitance at high frequency include a set of four coaxial capacitors (1 pF to 20 pF) and four 4-TP (Terminal Pair) air dielectric capacitors (1 pF to 1000 pF) which are calibrated against the primary standard. These transfer standards are then used to calibrate the LCR meters and Impedance analyzer in the range of 1 pF to 1000 pF from 10 kHz to 10 MHz and 1 pF to 20 pF from 10 MHz to 100 MHz respectively.

DC standards: This activity is maintaining National Standards of DC voltage, DC current and DC resistance. The apex level calibration facilities have been provided to the ERTLs, ETDCs, Defence and other government organizations for dissemination of traceability.

DC High Voltage Standards: This group is providing calibration facility for High Voltage DC equipments ie. DC High Voltage probe, DC High Voltage divider, DC High Voltage Power Supplies and DC Volt meter, upto 100 kV. Primary standard of DC High Voltage is the Resistive Divider, which is traceble to Josephson voltage standard.

Bilateral comparison of 10 kΩ & 1Ω Standards between NPLI & BIPM (BIPM.EM-K13.a and b)

A bilateral comparison of 10 k Ω & 1Ω between BIPM and NPLI was carried out.

The traveling standards were kept at 23°C for about two weeks to recover the temporal behavior following transportation. Then the measurements were taken for over 2-3 weeks. The measurements were carried out using DCC bridge with a 50 mA dc current for 1 Ω resistors and 100mA for 10 kΩ resistors. After measurements in this group and QHR Group, the standards were returned to the BIPM. Measurement analysis is in progress.

Re-establishment of High Value Capacitor calibration facility (100 mF to 1F)

This Facility was established at NPL in year 1986. However this facility was discontinued in Year 2008 due to no demand from the customers. Now many organizations are demanding calibration of capacitors from value 100 mF to 1 F.

Hence, this has now been re-established for calibration of 100 mF and 1 F at a frequency of 60 Hz

APMP Comparison of 6½ Digit Multimeter (DMM)

NPL is a Pilot Lab and coordinating the inter-comparison *(P1-APMP.EM-S8)* of 6½ Digit Multimeter (DMM) under Asia Pacific Metrology Programme (APMP), in which 16 countries are participating. The participating countries are Australia, Hong Kong, Sri Lanka, Kazakhstan, Egypt, South Africa, Thailand, New Papua Guinea, Vietnam, Jordan, Mangolia, Philippines, Malaysia, Indonesia, Syria and India (Pilot Lab).

The circulation of artifact completed in April 2013.

The DC measurements are carried by our group and ac measurement by D#5.10. Measurements, data consolidation and analysis were carried out. The results are communicated to NMI-Australia for consultation. The individual results will be communicated to participating labs for their comments, etc. Thereafter it will be submitted as draft A report to APMP.

To Conduct Inter-Laboratory Proficiency Testing amongst the NABL Accredited Laboratories in India (CLP 003732)

Under this Project, our group is co-ordinating two Proficiency Testing (PT) Programmes for Capacitance Measurements:

(i) 1 µF (NABL – E – Capacitance - 003)

(ii) 10 pF & 100 pF (NABL – E – Capacitance - 004)

The first circulation loop completed in the month of July 2012. The eight participating labs in first loop are ERTL (N), ETDC – Mohali, C & I Systems- Rajasthan, ETDC - Jaipur, IDEMI – Mumbai, EQDC - Vadodara, EQDC - Gandhinagar, NCQC – Ahmedabad.

The second circulation loop started from Sep. 2012 and completed in Jan 2013. This circulation scheme includes nine participating labs viz. PMMPL - Noida, ECIL -Hyderabad, BDL - Hyderabad, BEL - Bangalore, Transcal - Bangalore, ETDC-Bangalore, ERTL (E), ERTL (S) and Karandikar Lab-Mumbai.

Interim report submitted to NABL in May 2013. NABL communicated the En values to the respective labs. Final report is under preparation.

Evaluation of Four-Terminal-Pair Air Capacitance Standards

At low frequency, the most precise standard of capacitance is a three terminal capacitor popularly known as cross calculable capacitor. The reference standards of capacitance at high frequency include the set of four-terminal-pair (4TP) capacitance standards with nominal values of 1 pF, 10 pF, 100 pF and 1000 pF. Recently CSIR-NPL has initiated the process for the establishment of traceability of high frequency capacitance standards. The evaluation of 4TP capacitance standard consists of three parts; measurement of reference capacitance and capacitive components at 1 kHz, determination of inductive components using resonance technique and computation of capacitance of 4TP standard (C_{4TP}) using extrapolation.

The concept of 4TP has been introduced by Cutkosky in 1964 and he defined 4TP standards as the most precision admittance and impedance standards. Cutkosky expressed the impedance of 4TP linear network as

$$Z_{4TP} = \frac{Z_{11}Z_{22} - Z_{12}Z_{21}}{Z_{11}} \qquad (1)$$

Jones extrapolates the 4TP capacitance standard from 1 kHz to higher frequencies using resonance technique. 4TP standards of Agilent 16380A set can be represented as an electrical equivalent circuit model (EECM) described by Yonekura and Wakasugi, consisting of low value inductors and resistors, leakage capacitances and common mode inductance shown in Fig. 5.21. Suzuki evaluated 4TP capacitance standard using single port RF network analyzer and computed its Z_{4TP} mathematically. But single port measurements cannot be sufficiently accurate for a calculation of Z_{4TP} at each frequency of interest. To overcome the limitations of Suzuki method, a method based on four-port scattering matrix, S is proposed by Callegaro and Durbiano using EECM. The s-parameters of 4TP impedance standards could be measured using two-port-network analyzer by connecting two terminal pair at a time and

terminating other two with characteristic impedance.

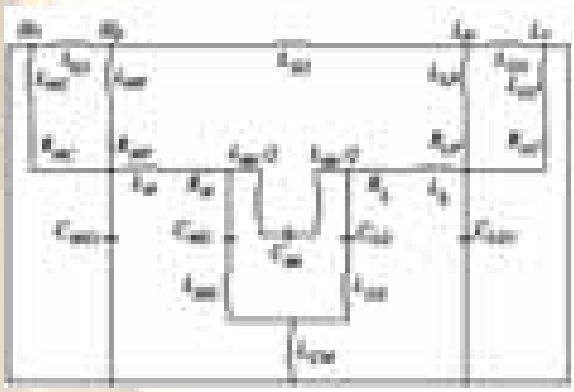

Fig. 5.21. Electrical Equivalent Circuit Model (EECM) of Agilent 16380A set air capacitance standard

Measurement Procedure

The technique proposed for the evaluation of 4TP capacitance standard involves the use of the relation between S and Z given as

(2)

Where U is unit matrix [4 X 4] and Z_0 is the characteristic impedance, 50 Ω.

The s-parameters are measured using two-port vector network analyzer with impedance analysis option (Agilent E5061B). The nine s-parameters (s_{12}, s_{22}, s_{32}, s_{24}, s_{31}, s_{34}, s_{41}, s_{42} & s_{44}) are measured from 10 MHz to 500 MHz for each value of 1 pF, 10 pF, 100 pF and 1000 pF and then converted into impedance parameters using (2).

A. Determination of Series and Parallel Resonance Frequencies

The parallel resonance frequency (fp) of capacitance standard is determined from zero crossing of imaginary part of 4TP impedance ($Im(Z_{4TP})$) versus frequency graph. The series resonance frequency (fs) of capacitance standard is determined from the zero crossing obtained from imaginary part of 4TP admittance ($Im(Y_{4TP})$) versus frequency graph. Table 5.5 shows fp and fs thus obtained for each nominal value of capacitance standard.

Table 5.5: fs and fp for 4TP capacitance standards

	1 pF	10 pF	100 pF	1000 pF
fs, MHz	393.12	327.88	180.58	61.75
fp, MHz	89.62	244.89	262.96	251.02

B. Measurement of Capacitive and Inductive Components of Electrical Equivalent Circuit Model *(EECM)*

To evaluate 4TP capacitance standards, it is required to determine the capacitive and inductive components of EECM. The reference capacitance (C_{oo}) at 1 kHz is measured using AH2700 ultra precision capacitance bridge from Andeen Hagerling while high-to-ground (C_{HG}) and low-to-ground leakage capacitances (C_{LG}) are measured using GR 1615 capacitance bridge from General Radio. Table 5.6 shows the capacitive components measured using capacitance bridge at 1 kHz.

Table 5.6: C_{oo}, C_{HG} & C_{LG}

EECM components	1 pF	10 pF	100 pF	1000 pF
C_{oo}, pF	0.9999	9.998	99.99	1000.74
C_{HG}, pF	17.4	25.5	31.2	33.5
C_{LG}, pF	49.2	29.5	32.4	35.3

The fs and fp are used to compute the inductive components of the equivalent model. In the reported technique L_{CM}, L_H and L_L are computed by solving (3) for the resonance conditions.

(3)

C. Computation of Four-Terminal-Pair Capacitance

C_{4TP} has been computed using (3) for 4TP air dielectric capacitance standards from 1 kHz to 30 MHz as shown in Table 5.7. The sensitivity coefficients have been determined using the partial differentiation to compute the expanded uncertainty (Ue) of capacitance standards with the help of measurement automation program. The

measurement uncertainty due to capacitance bridge, network analyzer and resonance frequency have been included in the uncertainty budget.

Summary and Results

The C_{4TP} and Ue have been computed for 1 pF, 10 pF, 100 pF and 1000 pF up to 30 MHz. The computed capacitance and expanded uncertainty are comparable with the results reported by other NMIs. The results are further compared and validated with the high frequency LCR Meter (Agilent 4285A). The accuracy of the network analyzer has less effect on the uncertainty budget because it provides only series and parallel resonance frequencies. The measurement automation programs have been developed to ease the process of measurement and for the computation of resonance frequencies & measurement uncertainty.

Table 5.7: Computed C_{4TP} and Ue

Frequency, MHz	1 pF		10 pF	
	C_{4TP}, pF	Ue, %	C_{4TP}, pF	Ue, %
0.001	1.000	± 0.50	9.998	± 0.10
0.01	1.000	± 0.50	9.998	± 0.10
0.1	1.000	± 0.50	9.998	± 0.10
1	1.000	± 0.50	9.998	± 0.10
10	0.988	± 0.57	9.990	± 0.14
30	0.895	± 1.44	9.924	± 0.48
Frequency, MHz	100 pF		1000 pF	
	C_{4TP}, pF	Ue, %	C_{4TP}, pF	Ue, %
0.001	100.0	± 0.05	1001	± 0.05
0.01	100.0	± 0.05	1001	± 0.05
0.1	100.0	± 0.05	1001	± 0.05
1	100.0	± 0.05	1001	± 0.06
10	100.4	± 0.16	1028	± 0.63
30	103.7	± 1.09	1319	± 6.89

Charge Measurement:

To provide calibration and traceability for low level electrical charge down to 200 pC:

Several modifications have been made in the previous design of the charge generation and measurement set up using the constant voltage method which resulted in achieving measurement of charges down to 100 pC with very good accuracy. The lowest measurement range achieved improves upon the targeted value of 200 pC. The operation of the set up has been automated with GPIB control using software developed in LabVIEW for instrument control and data acquisition. Table 5.8 illustrates the measurement results.

Table 5.8: Measurement Results

Charge Range	Uncertainty Achieved
100 nC – 1 nC	0.1% to 0.5%
1 nC – 100pC	0.5%

Automation of Calibration

The dc parameter calibrations of reference DMM and multifunction calibrator have been automated with PC control using calibration automation software developed in LabVIEW. The calibration automation software performs all necessary instrument controls as well as acquisition, processing, recording, reporting and storage of the test and calibration data. Separate software modules have been created for voltage, current and resistance calibrations. Calibration of any one parameter can be done for a complete range of values in a single run of the program with the calibration result saved in an excel file at the end. Automation reduces considerably the calibration time and avoids possible mistakes in recording the measured data and calculations. Automation programs for other commonly used instruments are also under development.

LF &HF VOLTAGE, CURRENT AND MICROWAVE STANDARDS

CSIR-NPL has the responsibility to upgrade the present apex level calibration facility and to provide traceability to user organizations. We are providing national traceability in the LF voltage,

current, HF voltage and Microwave attenuation, impedance, power parameters through apex level calibration to *ISRO, DRDO, Naval Dockyard, Air Force, BEL*, STQC labs, regional laboratories and the other user organizations.

Traceability of National microwave power standard has been re-established from 10 MHz to 18 GHz with an uncertainty ranging from 0.2 % to 0.8 %. Dissemination of transfer standards for maintaining the traceability of measurements is under progress. The established VNA traceability has been used in assigning VSWR/ reflection coefficient mismatch uncertainty for the coaxial thermistor mount, primary standard of microwave power. At present, NPLI has a coaxial micro-calorimeter in 7 mm line working upto 18 GHz. With the advancement in metrology most of the NMIs of the world have the calibration facility upto 50 GHz. Development of NPLI 2.4 mm coaxial microcalorimeter is under progress at LNE France, which will help in fulfilling the demand of high frequency and microwave power calibration to keep pace with international level.

We have participated in an international APMP key comparison (July-August 2013) **APMP.EM.RF-K8.CL** "*Microwave Power in 50 ohm coaxial line; frequency 10 MHz to 18 GHz*" to establish a close degree of equivalence in measurements among the participating NMIs. In this Key Comparison **NMI-Japan** is the Pilot laboratory along with thirteen participating laboratories of APMP including NPL India. The travelling standards consist of two thermocouple power sensors and a power meter.

Fig. 5.22. Direct Comparison Technique used in APMP Intercomparison

Thermal current converters (TCC) or thermal transfer standard (TTS) with AC-DC current shunts are used as reference standards for LF current in the frequency range from 40 Hz to 10 kHz. These standards provide accurate and precision measurement for LF current. The range of AC-DC current transfer measurement facility at NPL has been extended from existing 20A to 80A using indigenously developed current TEE. Now CSIR-NPL is capable of providing traceability to user organizations by calibrating the AC-DC current shunts of 30A, 50A, and 80A along with the thermal current converters or thermal transfer standard in the frequency range 40 Hz - 10 kHz.

Fig. 5.23. AC-DC current transfer measurement facility upto 80A

Progress under the establishment of Standards for Radiated Power Density:

A handheld spectrum analyzer (FSH8, R&S Germany) alongwith two isotropic probes have been procured. To calibrate the procured probe inside a GTEM cell, a GTEM cell have been indigenously developed based on Crawford concept. The proposed GTEM is applicable for frequency range 0.7 - 2.5 GHz.

Fig. 5.24. Setup for E-field probe calibration and measured VSWR

Utilizing the BSNL base station situated at New Rajinder Nagar (28°37'42.5"N 77°10'25.0"E), radiated power density at 1.8 GHz and 2.4 GHz frequencies was measured at distances varying from 1 to 30 m. The radiated power density measurements were repeated using the VSNL tower located at Dasghara (28°37'29.4"N 77°09'48.6"E) for the same frequency points and varying distances. An E-Field probe along with Spectrum Analyzer is used as receiver to measure the signal strength, electric field strength and radiated power density. Radiated power density measurements (W/m^2) at above two locations were performed with the help of E- field probe and spectrum analyzer with embedded software for different frequencies. Equipment used for these measurements are traceable to Microwave Attenuation, Impedance, Power Standards and Dimensional Metrology at CSIR- NPL, India.

Fig. 5.25. Radiated power density measurement with results (1.8 GHz and 2.4 GHz)

AC HIGH VOLTAGE AND HIGH CURRENT STANDARDS

This activity is maintaining National Standards for AC High Voltage and High Current Ratios at power frequencies (50Hz) by using Reference Standard High Voltage Ratio Measuring System (HVRMS) and Reference Standard Current Transformers and also maintaining the National Standards for the calibration and measurement of AC High Voltage Capacitance and Tan δ upto 200kV at 50Hz by using Reference Std. Capacitors & High Precision C,L & Tan δ Measuring System.

This activity is providing traceability and calibration services for Current Transformers, Current Transformer Testing Sets, AC High Current Sources, Clamp Meters, Current Probes, Current Shunts, CT Burdens, Voltage Transformers, Voltage Transformers Test Sets. HV Probes, Electrostatic Voltmeters (ESVM), HV Break Down Test Sets, Voltage Transformer Burdens, AC High Voltage Sources, HV dividers, κV Meters, Capacitance & Tan Delta Bridges, insulation level of test objects like Transformers, Bushings, insulators, Cables, etc.

Established a new facility for the calibration of Transformer Loss Measuring System (TLMS) with the existing facilities. By this facility accurate measurement of the transformer losses is possible. High Stakeholder like BHEL, NTPC and other transformer manufacturers and bulk power users will be benefited largely.

AC POWER AND ENERGY STANDARDS

The activity is maintaining the primary standard of AC Power & Energy (PPCS) traceable to voltage, resistance and time. Working range is 10V to 480V/10mA to 100A/ PF:1 to 0.01(lag/ lead) at frequency range 40 Hz to 400 Hz.

The single phase and three phase reference standards are calibrated against this PPCS and then used in our calibration benches for providing traceability to all power sector organizations, other laboratories and energy meter manufacturers in India and in SAARC countries.

Calibration of three phase class 0.01 and single phase class 0.005 reference standards are now being done in NPL which were earlier being sent to other NMIs.

The new CMCs of AC Power & Energy Standard has been uploaded on BIPM website in March 2014. The best uncertainties in active power are ± 0.005% in reactive power ± 0.009% and in apparent power ± 0.008%.

The Isoltaion transformer has been calibrated using two comparators.

By conventional method we could calibrate from 120A to 1 A at UPF and at 0.8 lag PF only but

by this new method we could calibrate the Isolation Transformer from 12oA to 0.01A and at every power factor, i.e., 1 – 0.01(i/c).

Primary Power Calibration System (PPCS) is set up and is being used for disseminating traceabillity in India and in SAARC countries and the results of Isoltaion transformer will be traceble to PPCS through the current values and phase between voltage and currents.

क्वान्टम परिघटना एवं अनुप्रयोग

Quantum Phenomena and Applications

Dr Hem Chandra Kandpal

Chief Scientist
Email : hckandpal@nplindia.org

D 06.01 Josephson Junctions and Single Electron Tunneling Physics

Dr Vijay Narain Ojha
Dr Veerpal Singh Awana
Ms Sandhya Malikar Patel

D 06.02 Quantum Transport in Thin Film Heterostructures

Prof R C Budhani
Dr Vijay Kumar Gumber
Dr Hari Krishna Singh
Dr (Ms) Anjana Dogra
Dr Parveen Siwach

D 06.03 Nanoscale Measurements

Dr (Ms) Rina Sharma
Dr Vijay Kr. Toutam
Dr Ashok Kumar

D 06.04 Quantum Optics and Photon Physics

Dr Hem Chandra Kandpal
Dr Ranjana Mehrotra
Sh Virendra Kumar Jaiswal
Dr Parag Sharma

D 06.05 Superconductivity : Materials and Dissipation Physics

Prof R C Budhani
Dr (Ms) P L Upadhyay
Dr Anurag Gupta
Sh Rajendra Singh Meena
Dr Sudhir Husale
Dr Rajib Kr. Rakshit

D 06.06 Electronics & Instrumentation Cell

Dr Tushya Kumar Saxena
Ms Manju Singh
Ms Priyanka Jain
Ms Poonam Sethi Bist

Quantum Phenomena and Applications

FIB group's main focus was on fabrication of nanodevices, nanostructures and plasmonic antennas, for instance metal contacts on single layers of grapheme and nanorings of permalloy. In addition, Au break junctions (~ 2nm gap) devices using electromigration have been fabricated to study single molecules and nanoparticles.

Dilution Refrigerator (DR) was installed and tested as a unique facility, which is functional with temperatures reaching as low as 10 mK along with very high magnetic fields upto 14 Tesla, to capture novel and fundamental quantum phenomena.

Continued activity of superconductivity in bulk materials produced interesting results. For instance, five-fold increase in superconducting transition temperature of $Sr_{0.5}La_{0.5}FBiS_2$ system from 2 K to above 10 K, accompanied with semi-metallic to metallic normal state conduction is seen under applied hydrostatic pressure of just above 1GPa.

Artificially engineered oxide heterostructures of various families have been grown using pulsed laser deposition (PLD) technique and their multifunctional properties namely, multiferroicity, superconductivity, magnetism and photoconductivity have been studied. Focus is also given on the theoretical calculations of electronic states and its interplay with various properties of transition metal interfaces using Density Function Theory (DFT).

Programmable Josephson Voltage Standard, used to disseminate 'Unit' Volt at par to the international level, has been further optimized to get very stable margins and flatspots. Also a new liquid helium cryostat for low temperature (up to 1.6 K) and magnetic field (up to 130 gauss) for microwave measurements (up to 40 GHz) has been established.

To redefine the existing scale of luminous intensity and other photometric parameters, cryogenic radiometer has been installed as detector based primary standard to reduce uncertainties by at least two orders of magnitude. Spontaneous parametric down conversion (SPDC) has been demonstrated with a Nd-YAG laser of 25ps pulse width emitting at 355nm.

Current biomolecular research exploits the analysis of anticancer drug–DNA interaction using various spectroscopic techniques. Understanding drug-DNA interaction, surface enhanced Raman spectroscopy in different drug/DNA molar ratios are studied. Nucleic acid binding ability of allicin has also been studied to explore the anti-cancer activity of allicin.

Jesephson Junctions and Single Electron Tunneling Physics

1. Programmable Josephson Voltage Standard

The Programmable Josephson Voltage Standard, used to disseminate 'Unit' Volt at par to international level, has been further optimized to

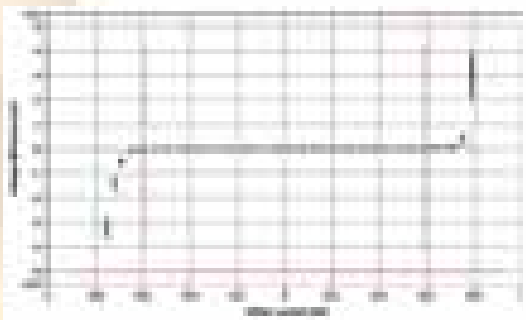

Fig. 6.1: Step flatness test at 18.645387894 GHz and "0 dBm. The array configuration is 'nnnnnnn nnnnnnnnpppppppp' starting from subarray 1 and ending at subarray 23. '0' represents the zero step, 'n' the negative step and 'p' the positive step. The total array output is 0.23 mV, measured by the system nanovoltmeter on the 1mV range

get very stable margins and flatspots. Figure 6.1 shows the better and uniform margin around the 0 mA dither current which indicate the consistent functioning of the system.

The Bank of Zeners (National Standards for voltage) of LF, HF and DC standard group at NPL were calibrated and certificates were issued to maintain the traceability. The uncertainty reported were ± 350 nV at 10 V and ± 200 nV at 1.018 V, inclusive of the noise of the Zeners.

2. CRYOSTAT SYSTEM

Cryostat system for the low temperature, low magnetic and microwave measurements of superconducting thin films and devices.

The facility of Liquid Helium Cryostat for low temperature, low magnetic field and microwave measurement upto 40 GHz has been established. A cryostat system had been designed and set up in the sub-division with an idea to lower the

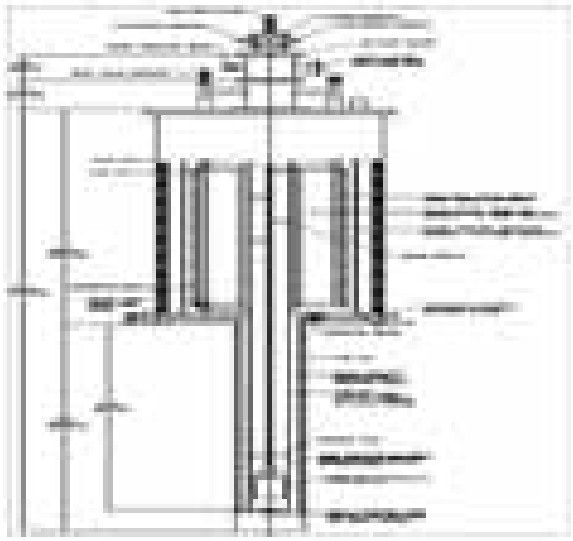

Fig. 6.2: Schematic of Crystal System

temperature to 1.6 K by pumping the bath using rotary pump and study the transport characteristics of superconducting films, nanowires, nano devices with and without low magnetic field and microwave power. Also superconducting micowave anntenas, striplines, resonatores and filters etc.

3. AUTOMATION

The in-house LabVIEW program for R-T measurement, I-V measurement, Differential I-V measurement etc. had been developed to study the transport characteristics of superconducting films, nano devices etc. at very low temperature (1.6 K)in the newly established cryostat system.

The program for temperature sensor calibration had also been developed to calibrate

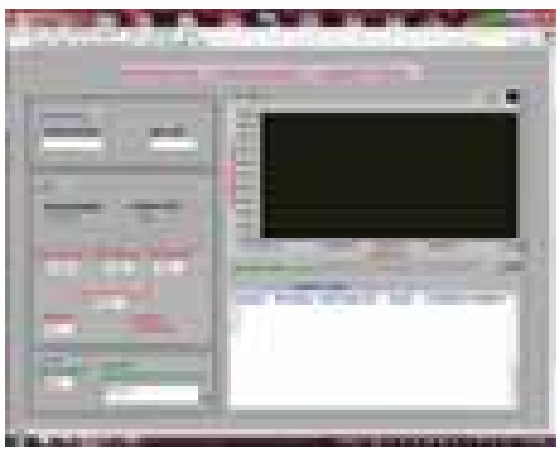

Front Panel of R-T measurement showing R-T characteristics of YBCO

the uncalibrated cernox sensor from calibrated cernox censor thereby reducing the cost and foreign exchange involved in the purchasing of calibrated sensor.

An electromagnet had been designed to study the sample under various magnetic field conditions (Range upto 130 gauss) by varying the current. This process is also automated using Lab VIEW.

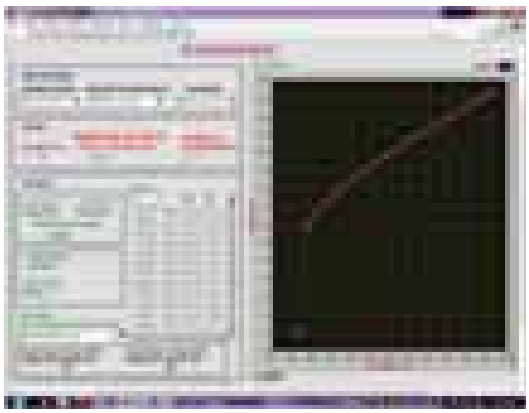

Front Panel of dI/dV measurement with magnetic field

Quantum Transport in Thin Film Hetrostructures

1. Fabrication of graphene based field effect transistor (GFET) at NPL:

Graphene is a 2-D carbon-based material with unique properties, has attracted a lot of attention due to high carrier mobilities that holds promise for electronic applications. Researcher's speculated that graphene could be used as transistors with scaling limits and operating speeds beyond those of conventional transistors.

Here we show transfer electronic properties of graphene field effect transistors and investigate further novel transport characteristics of graphene in the superconducting regime such as specular Andreev reflections, the relativistic Josephson effect, pseudo-diffusive dynamics of ballistic electrons, etc.. To study these new phenomenon's experimentally is very challenging due to the complex procedure of sample fabrication. We plan to use the state of art nanofabrication facilities such as Focused ion beam microscope (FIB), ebeam lithography to fabricate superconductor graphene superconductor junctions. We use simple method of mechanical exfoliation to deposit nanolayers of graphene and superconducting tungsten nanowire graphene junctions will be made to study the supercurrent in graphene induced by the superconducting contacts through proximity effects.

Fig. 6.3: A-C show GFET fabricated at CSIR_NPL for the first time, and its electronic transfer properties and gate dependence are presented in Fig 1D and 1E respectively. Mobility was found around 6144 $cm^2 V^{-1} S^{-1}$

2. Implementation of digital pattern milling control for the fabrication of plasmonic metamaterial nanostructures:

Plasmonic metamaterials (PMs) are engineered nanostructured fabricated either by FIB or ebeam lithography with rationally designed, building blocks which provides a platform for developing optical devices with unconventional properties for responses to light, acoustic waves, heat flows that are unattainable with naturally available materials. Implementation of FIB milling control by digital pattern generation gave access

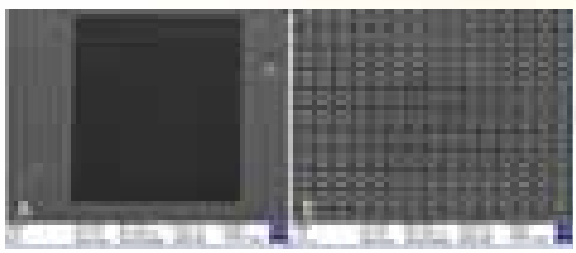

Fig. 6.4: A&B show FESEM images of split hexagon rings fabricated by FIB milling

to fabricate metamaterials with high accuracy. The PMs show some extraordinary properties such as a negative refractive index, imaging with the nanometerscale resolution, invisibility cloaks, efficient light concentrators, nano-optics and quantum information applications.

3. Non-interacting NiFe Nanoring Lattices: Scaled Magnetization

Magnetic films patterned into nanosized elements have opened a new field for developing MRAMs with enhanced storage density. However, scaling down the size of magnetic elements to realize high storage capacity poses fundamental challenges of stability of magnetization due to spin wave excitation in confined geometries. Here we fabricate and study the detailed investigations of permalloy ring structures through magnetization measurements by specifically addressing the two

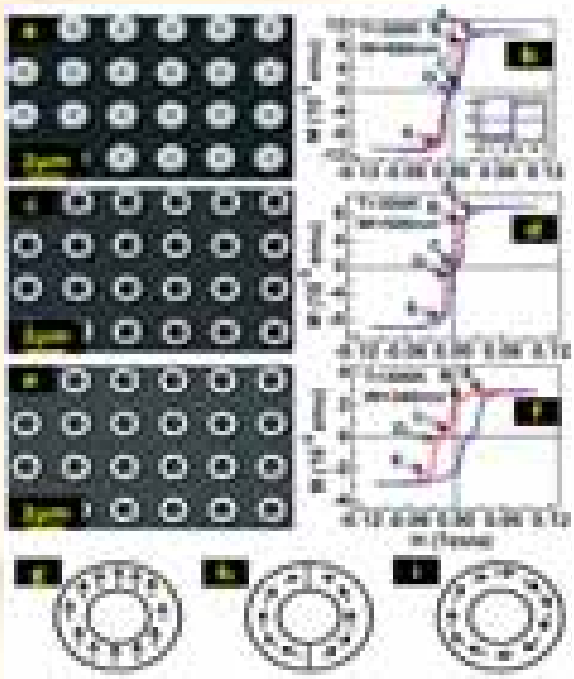

Fig. 6.5: (a, c and e) show the SEM micrographs of 660, 500 and 340nm NiFe ring sample respectively. The M(H) loops of all the samples measured at 300 K for in-plane field are shown in Fig.3(b, d and f). Inset of Fig.3(b) shows M(H) loop of the plain $Ni_{80}Fe_{20}$ thin film sample. The points marked as A to E indicate pronounced change of slope in the M(H) curves. Schematic of various magnetic states: (g) single domain (SD), (h) onion state (OS) and (i) vortex state (VS)

step OS (onion state) to VS (vortex state) transition, where the first step seems to evolve due to the nucleation, growth and depinning of the vortex domain walls in the OS. The second step is characterized by a rapid movement of the diametrically opposite VDWs, and their subsequent annihilation, resulting in the formation of the VS. The key feature of this study is how the stability of various magnetic states of the rings are affected over a temperature scale of 3 to 300 K, and over time as the magnetizing field is turned off.

Quantum Optics and Photon Physics

1. Cryogenic Radiometer Facility Established

To redefine the uncertainty in estimating the uncertainty in the measurement of existing scale of luminous intensity by at least two orders of magnitude from its present value of 0.72% at coverage factor k=2, and other photometric parameters with reduced uncertainties, cryogenic radiometer facility was established. Initial results show that the facility is working fine and has been used to calibrate the responsivity of the trap detectors (with quantum efficiency =1) which would be used to estimate the uncertainty in the luminous intensity scale presently established by NPL. Stride towards quantum candela and low absorption measurements in nonlinear absorbers are on.

2. SPDC with Pulsed Laser to Produce High Photon Flux

We have established recently a facility of spontaneous parametric down conversion (SPDC) with pump beam at 355nm from a Nd-YAG picosecond laser generating two degenerate beams at 710nm. Since the peak power of this laser is several kilowatts the photon flux produced is expected to be very high. The power of the photon flux would be measured by using the calibrated trap detectors (calibrated against the cryogenic radiometer) at this preliminary stage. With more sophistication in the system, namely increasing the thickness of the crystal and cooling the crystal, the no. could be enhanced. This work will further be extended to do experiments on indistinguishablity of photons.

3. Sub-wavelength Interference in the Field Assisted by Surface Plasmons

Theoretical study on the optical transmission from a thin metallic double slit to study the effect of surface plasmons and behavior of surface plasmons under different double slit conditions was made. The second-order correlation function as a function of the displacement of the detectors for different values of slit separation was studied. It was shown that surface plasmons excited at one slit and propagating to the other slit modulate the coincidence counts with the variation of slit separation. Sub-wavelength interference effect was also observed for the field assisted by surface plasmons. It was also shown that the second order interference-diffraction pattern changes with slit separation and at some particular value of slit separation it changes into the Hanbury Brown and Twiss (HBT) effect.

4. Experimental Study on Modulation of Stokes Parameters on Propagation of a Gaussian Schell model Beam in Free Space

The effect on the Stokes parameters of a Gaussian Schell model beam on propagation in free space was studied experimentally and results were matched with the theory that in general the degree of polarization of a Gaussian Schell model beam doesn't change on propagation if the three spectral correlation widths ∴ . are equal and also the beam width parameters · ∴. It was experimentally shown that all the four Stokes parameters at the centre of the beam decrease on propagation while the magnitude of the normalized Stokes parameters and the spectral degree of polarization at the centre of the beam remain constant for different propagation distances.

5. Effect of coherence and polarization on the polychromatic partially coherent dark hollow beam

An experimental study was carried out to investigate the effect of coherence and polarization on the polychromatic partially coherent dark hollow beam (PCDHB). The experimental results show that the spatial coherence and source polarization affect the dark region of the generated hollow beam. The study shows that by varying the source degree of polarization (DOP) we get a tunable dark region. We find that longer the spatial coherence length of the input beam, larger the central dark size of the resultant PCDHB. Further it is shown that polychromatic PCDHB with low spatial coherence travel longer distance without being distorted than the beam with high initial spatial coherence. This kind of polychromatic beams may find potential application in the field of polychromatic light based free-space optical (FSO) communications.

6. A structural insight into binding mechanism of nitrosourea derivatives (anticancer agents) with DNA

Cancer is the uncontrolled growth of abnormal cells in the body. DNA, the genetic material inside the malignant cells replicates very fast hence it becomes prime target for the action of antitumor agents. Our current research work involves the analysis of anticancer drug –DNA interaction using various spectroscopic techniques. Attenuated total reflection- Fourier transform infrared spectroscopy (ATR-FTIR) was used to determine binding sites of drug on DNA. Circular dichroism (CD) spectroscopy was used to confirm conformational variations in DNA molecule upon drug-DNA interaction. Thermodynamic parameters of drug-DNA reaction were calculated by isothermal titration calorimetry (ITC). These spectral techniques provide information on all the heterogeneous conformations of biomolecules present in the sample. In particular, present work includes the interaction exploration between double stranded DNA and nitrosourea derivatives, a class of highly toxic anticancer agents widely used in the treatment of various types of cancer. Knowledge about the structural and conformational effects on DNA due to its interaction with nitrosourea derivatives is almost lacking. Biological importance of drug-DNA interaction studies forces to focus the

attention on understanding of nitrosourea derivatives binding with DNA to delineate its mechanism at molecular level. Results of the present study demonstrate that nitrosourea derivative is not a simple alkylating agent rather it causes major grove-directed-alkylation. Spectral outcome are suggestive of base binding and local conformational changes in DNA upon drug interaction. Investigation of drug-DNA interaction is an essential part of rational drug designing that also provides information about the drug's action at molecular level. Results, demonstrated here, may contribute in the development of new nitrosourea therapeutics with better efficacy and lesser side effects.

7. Application of surface enhanced Raman spectroscopy in understanding drug-DNA interaction

In order to get more insight to the mechanism of action of anticancer drug, a recent and highly sensitive technique related to Raman spectroscopy i.e. surface enhanced Raman spectroscopy (SERS) is employed. This ultrasensitive technique allows the detection and characterization (monitoring structural changes) of drug's interaction with even single molecule (like one of the nitrogenous bases of DNA). Advances in the application of SERS combines modern laser spectroscopy with nanotechnology. It results in strongly enhanced Raman signals when molecules (drug-DNA complexes) are attached to SERS- active substrate. We synthesized silver and gold nanoparticles (~50nm) in the form of colloidal solution. Free DNA and drug-DNA complexes was added to this solution and incubated at room temperature for varying degree of time. Thin layer of the prepared solution are deposited on glass surface and subsequently analyzed using SERS. Different drug/DNA molar ratios are studied to determine the binding sites and binding mode of anticancer drugs with DNA.

8. Analysis of nucleic acid interacting properties and anti-cancer activity of allicin

This study was designed to examine the cytotoxic potential and nucleic acid binding ability of allicin. MTT assay was used to assess the cell viability of A549 lung cancer cells against allicin. It was observed that allicin inhibits the proliferation of cancer cells in a concentration dependent manner. In further studies, the binding of allicin to DNA and RNA was studied in vitro by spectroscopic techniques. Fourier transform infrared spectroscopy exhibited that allicin binds preferentially to minor groove of DNA double helix via thymine base. Analysis of tRNA-allicin complex has also revealed that allicin binds primarily through nitrogenous bases. Some amount of external binding with phosphate backbone was also observed for both DNA and RNA. UV-visible absorption spectra of both DNA-allicin and RNA allicin complexes showed hypochromic shift with an estimated binding constant of $1.2 \times 10^4\ M^{-1}$ for DNA and $1.06 \times 10^3\ M^{-1}$ for RNA binding. No major transition from the B-form of DNA and A-form of RNA is observed after their interaction with allicin.

Superconductivity: Materials and Dissipation Physics

1. Transport and Megnetic properties

In bilayers (B) of fully spin polarized ferromagnet (F) Co_2FeSi and superconductor (S) NbN, proximity coupling and magnetic switching dynamics were shown to be correlated. The upper critical field derived from resistivity measurements shows a dimensional crossover with a reduced effective thickness of the S layer. At temperatures (T) << superconducting T_c, the measured M-H loops show two step switching; one at T-independent value ~ 7 Oe and other at strongly T-dependent value becoming very large ~ 1 kOe at 2 K. These results reveal induced ferromagnetism in S-layer at the S/F interface with vortex pinning influenced dynamics.

Interesting results on dynamics of magnetization (M) reversal and relaxation as a function of temperature (T) were obtained in three non-interacting NiFe ring arrays having fixed ring outer diameter and varying widths. The M(H) loops show a double step transition from onion state (OS) to vortex state (VS) at all temperatures (T = 3 to

300 K) and angles (è = 0 to 90°). The critical reversal fields HC1 (OS to VS) and HC2 (VS to OS) show a pronounced dependence on T, ring width and è. Estimation of the transverse and vortex domain wall energies reveal that the latter is favored in the OS. The OS was also the remanent state in the smallest rings and decay with the effective energy scale (U/T) of 50 and 32 meV/K at 10 and 300 K, respectively. The robust in-plane anisotropy of magnetization of ring assemblies was established by scaling the M(H) with è.

Comprehensive study of inter-grain connectivity (A_F), pinning, percolation threshold (P_c) and anisotropy (g) in in-situ processed samples of MgB_2 samples with stochiometric composition, excess Mg (5 wt.%) and further 3 wt.% addition of various non-Carbon based additives like nano-Ag, nano-Ni and YBCO. The superconducting transitions stay nearly unchanged in all samples. The major findings based on quantitative analysis of resistive r(T,B) trasnistions and magnetic critical current density J_c(B,T) data in all the samples are: (1) along with previously studied ex-situ samples, the J-$_c$(A_F) shows a significant increase at A_F~7%; (2) the irreversibility lines lie lower than the characteristic T_{c0}(B) lines in the B-T phase diagram; (3) a universal core pinning (dI- and/or dT_c- type) mechanism is revealed in the entire T range 5–30 K; and (4) typical values of P_c ~ 0.57±0.04 is indicative of weak link networks.

The activity on search for new superconductors is continued. A novel phenomenon related to semi-metallic to metallic transformation along with fivefold increase in superconducting transition temperature of BiS_2 based superconductor $LaSr_{1/2}F_{1/2}BiS_2$ under moderate hydrostatic pressure of 1GPa was seen (Fig. 6.6).

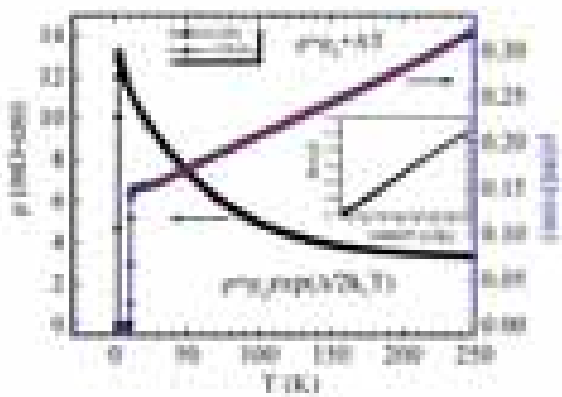

Fig.6.6: Resistivity versus temperature of $LaSr_{1/2}F_{1/2}BiS_2$ with and without pressure

S&T services & facilities (up to six for each category): Installation and Test of HP (0-3GPa) pressure cell (Fig. 6.7) on existing PPMS, can work down to 2K and up to 14 Tesla field for electrical transport measurements.

2. Pulsed Laser deposited Oxide heterostructures:

Artificially engineered oxide heterostructures of various families are of interest because of the multifunctional properties they exhibit like multiferroicity, superconductivity, magnetism, photoconductivity and so on. For engineering of such oxide heterostructures/interfaces pulsed laser deposition (PLD) technique is known worldwide since it allows growth of uniform, stoichiometric and high quality thin films. Our group in CSIR-NPL has good expertise in the deposition of thin films/heterostructures of various types of oxide thin films using PLD. Moreover, reflection

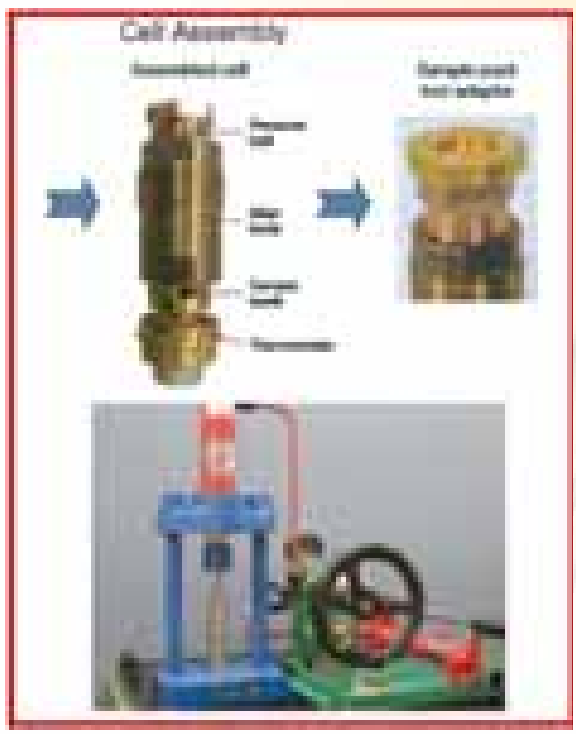

Fig. 6.7: New pressure cell for existing PPMS

high-energy electron diffraction (RHEED) gun equipped with NPL-PLD oxide chamber enables us to do the controlled layer-by-layer growth of thin films with the additional information about growth mode. At present we are dealing with a versatile group of the materials like multiferroics, superconductor, and two dimensional (2D) electron gas systems.

(i) Multiferroics:

The multiferroic materials exhibit coexistence of ferromagnetic (FM) and ferroelectric (FE) orders. In these materials, the FM domains can be controlled by the application of electric field and vice versa, which provides an additional degree of freedom in tuning the functionality of device.These materials find attractive applications in non-volatile RAM (NvRAM), actuators, transducers etc. Due to incompatible mechanism of FE and FM, very few multiferroic materials exist in single phase and possess low magnetoelectric (ME) coupling. Therefore, there is a need of artificial multiferroic systems like composites, bilayers and superlattices, where the strongest coupling is present due to precise control of strain and crystallographic orientation. We are working on the growth of bilayers and superlattices of LCMO/BTO perovskite structures on Nb-STO substrate by PLD. The combination of ferromagnetic LCMO and ferroelectric BTO has probability to exhibit multiferroic characteristics. Here our study focuses on the ME coupling in these systems via the measurements of temperature dependent ferroelectric (polarization loop) properties and conduction mechanism (IV) in presence of magnetic field. The magneto-transport properties have already been reported by various groups; but the effect of magnetic field on ferroelectric properties remains unexplored.

(ii) Superconductivity:

Another area of research is the growth of thin films of $BaBiO_3$ and $BaPbO_3$ as well as their doped systems. The $BaBiO_3$ is the parent compound of superconducting compound $Ba_{1-x}K_xBiO_3$ which has a superconducting transition temperature of 30K. Our motive is to optimize the deposition conditions so as to discover superconductivity in the engineered interfaces of $BaPbO_3/BaBiO_3$.

(iii) Two dimensional electron gas at oxide interfaces:

The interface of two band insulators $LaAlO_3/SrTiO_3$ has been a subject of rigorous experimentation because of the unusual properties exhibited by it. Apart from the much debated generation of a quasi 2 Dimensional Electron Gas, the interface also exhibits superconductivity, ferromagnetism and giant Persistent Photoconductivity. We are involved in studying the nature of the 2- Dimensional Electron Gas with Cr doping at Al site in $LaAlO_3/SrTiO_3$ (LAO/STO)

Fig. 6.8: Observed RHEED images before and after deposition of LAO/STO. Also shown the RHEED oscillations obtained for 20uc LAO/STO

Fig. 6.9: Observed RHEED images before and after deposition of $LCrO_3$/STO

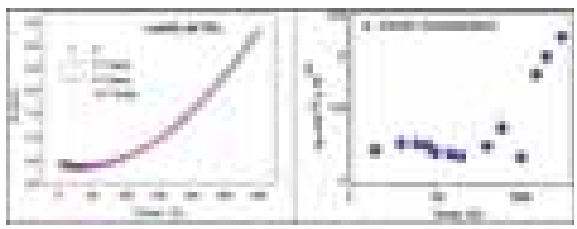

Fig. 6.10: Variation of resistance with temperature (with and without field) for LAO/STO Observed RHEED images before and after deposition of LAO/STO. Graph on right side represents the carrier concentration of the LAO/STO film with temperature

interface. We have successfully deposited grown good quality ultra thin unit cell $LaAl_{1-x}Cr_xO_3/SrTiO_3$ with x = 0.0, of samples. Figure 6.8 shows the observed RHEED images before and after deposition for LAO/STO. The clean streaks for the deposited film assure the 2D, clean growth of the material. Also shown the RHEED oscillations obtained for 20uc LAO/STO. Similar RHEED images are being obtained for all the deposited doped films as well except the pure $LaCrO_3$/STO where we see the 3D growth of the sample. Shown 3D (spotty pattern) growth of the $LaCrO_3$/STO sample in Fig. 6.9.

Further the effect of Cr doping on the interface conductivity, magneto- transport, superconducting transition and photoconductivity is being investigated. Figure 6.10 shows the metallic character of the LAO/STO with and without field.. Focus is also on the theoretical calculations of electronic states and its interplay with various properties of transition metal interfaces using Density Function Theory (DFT).

3. Magnetic thin films, multilayers and devices

Perpendicular anisotropic magnetic materials such as CoFeB, FePt, CoPt due to their high thermal stability and low critical current for current-induced magnetization switching and half-metallic heusler alloys such as Co_2FeSi, Co_2MnSi for their large spin-polarization, high Curie temperature and high magnetic moment are promising candidates for next-generation high-density non-volatile memory, logic chip etc. Research activities in this direction are in progress which would essentially lead to the development of various magnetic devices namely, magnetic tunnel junctions (MTJ) using magnetic alloys such as Co_2MnSi, Co_2FeSi, CoFeB and also elemental ferromagnets such as Co, Fe etc.

4. Ferromagnet/superconductor heterostructures

Studies of the repercussion of mutual coexistence of superconductivity and ferromagnetism in a ferromagnet-superconductor system led to the several fundamental and technological issues such as ð-phase superconductivity, pair breaking, triplet pairing, flux pinning, domain wall superconductivity, field-enhanced superconductivity etc. Great advances in material processing techniques in recent years have allowed creation of novel ferromagnet-superconductor hybrids.

Broad outline of the scope for the proposed work includes:

- Spin polarized transport through a FM-SC-FM layers system in heusler alloy and CoFeB based ferromagnet and nitride based superconducting system.
- The possibility of ð-phase coupling and its practical implementation in SC-FM-SC structures.
- Exchange bias effect in spin valve structures such a CrN/CMS/NbN/CMS, CrN/CMS/NbN/CoFeB etc.

5. Superconducting nanowire single photon detectors (SNSPDs)

SNSPDs are expected to play major role in quantum optical information processing technology, compared to avalanche photodiodes (APDs), which have limitation in single photon detection due to their spectral responses in those wavelengths.

The broad objectives of this project are to fabricate superconducting nanowire arrays using e-beam lithography, focused ion beam milling techniques, and to characterize their quantum optical response.

6. Dilution Refrigerator facility with 14 Tesla magnet

The R&D Activities of the DR lab is focused on to the studies of electronic/magnetic and superconducting properties of ultra-small scale systems at extremely low temperatures and very high magnetic fields. The search for novel and exotic phenomena such as Kondo effect, proximity coupled tunneling phenomena; Andreev Reflection, spin polarized tunneling, fractional quantum Hall effect etc. are envisaged.

The measurements to unravel these novel phenomena will be carried out using a state of the art Dilution Refrigerator facility equipped with a 14 Tesla superconducting magnet. Systems of interest for the above mentioned phenomena are listed below:

i. Superconductor-ferromagnet-superconductor junctions and its variants like superconductor-insulator-superconductor, or ferromagnet-superconductor-ferromagnet junctions,
ii. 2DEG systems,
iii. Quantum dots and 1D systems

The Dilution Refrigerator facility has been installed at CSIR-NPL to augment the research areas in condensed matter Physics at the mK temperature range. With this facility the exciting and exotic quantum phenomena occurring at temperatures as close as 10 mK can be captured. Also the facility has been equipped with a magnetic field of 14 Tesla (uni-axial). This is a cryofree system, with 'zero' consumption of liquid helium. Initial cooling is done using the pulse tube refrigerator and heat exchangers. The 'dilution' process starts at temperatures of the order of less than 1 K. To facilitate the dc transport and low frequency measurements the sample stage is been provided with 48 wires (12 twisted pairs of constantan wires in one set and 12 twisted pairs of Nb-Ti in the other set) terminated at room temperature connectors with thermal anchoring at different stages. Additionally the system can support microwave measurements up to a frequency range of 40 GHz. The base temperature of the system is read by a generic 'ruthenium oxide' temperature sensor.

The salient features of this facility are given below:

i. Cryo-free operation based on pulse tube refrigerator
ii. Controlled temperature range: 10 mK -30 K(in different steps)
iii. Cooling power : 3 ìW at 20 mK, 200 ìW at 100 mK, 300 ìW at 120 mK
iv. Top loading sample mechanism with a sample exchange time of 8-10 hours
v. 14 Tesla magnetic field(uni-axial)
vi. In-built options for performing microwave absorption/irradiation experiments at mK range
vii. Cooling time to the base temperature is nearly 40 hours

The DR system at CSIR-NPL has got installed in the month of December 2013, Figure 6.11 shows the photograph of the Dilution Refrigerator system along with the inside views and the mixing chamber plate. After successful installation several trial runs were conducted with standard superconducting samples. Figure. 6.12(A) shows the typical cooling process of the DR starting from the room temperature. It is to be noted that the base temperature of 10 mK has been reached by continuous cooling process of about 36 hours.

As part of the system configuration for dc and low frequency measurements, a sample holder has been designed using the OFHC copper plate and test samples of known superconducting

Fig. 6.11: (A) the Dilution Refrigerator, Triton-200(Oxford Instruments), (B) the inside view of the dilution fridge, where in different plates associated with the dry DR, heat exchangers and the mixing chamber are visible, (C) the mixing chamber of the DR (heart of the DR unit) onto which the mixing plate is anchored. This is the experimental stage of the DR, in magnet systems the sample stage will be anchored onto this mixing plate with proper thermal contact; the rod hanging from the mixing plate in Fig.1 (B)

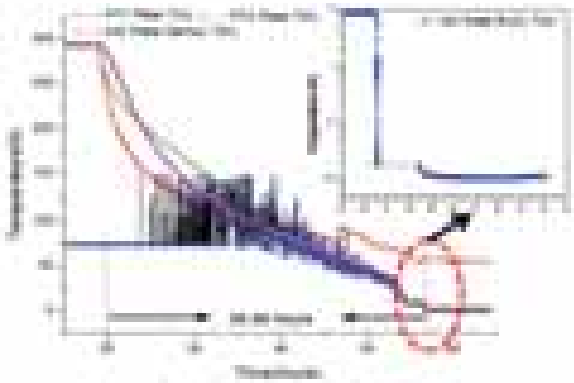

Fig. 6.12: Typical cooling process of the DR, wherein the temperature variation of the different plates as function of time is recorded. It takes nearly 36 hours to reach the base temperature, assuming that the cooling starts from the room temperature. The inset (magnified view of encircled portion) shows the temperature variation of the mixing plate during the condensation process. The mixing plate temperature is read using a generic ruthenium oxide sensor

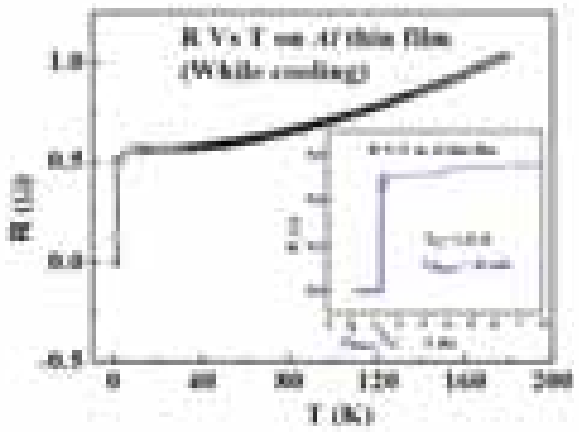

Fig. 6.13: shows the resistance-temperature plot of an Aluminium film. The T_C of the film is 1.22 K, agreeing with the values reported for the Al film

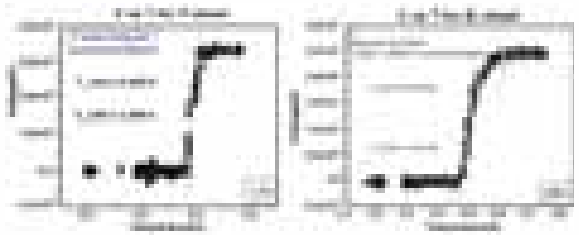

Fig. 6.14(A): Variation of voltage vs. temperature for Ti sheet, Tc(onset) is 0.41 K, figure3(B), Variation of voltage vs temperature for Zr sheet , the Tc(onset) is 0.61 K, these values agrees well with the reported Tc values for these metals

transition temperatures were loaded for initial runs. We have tested Al, Zr and Ti to and recorded its variation of resistance as a function of temperature. Figure 6.13 shows the measurement result for the Al thin film. The T_C is around 1.22 K. In Figures 6.14(A) and 4(B) are the results for Zr and Ti thin sheets done in separate run. The T_C values of Zr and Ti respectively are 610 mK and 410 mK. These measurement results well agrees with the reported T_C values of these metals and shows that there is no thermal lag between the mixing chamber temperature and the sample.

In conclusion CSIR-NPL has now equipped with a facility to capture novel and fundamental phenomena occurring at temperatures as close as 10 mK and with high magnetic field of 14 Tesla. Emerging and novel phenomena such as proximity coupled tunneling through superconductor-ferromagnet-superconductor junctions, studies on fractional quantum hall effect on quantum dots and 2D electron gas systems, superconducting and magnetic properties of vast variety of hetero junctions, superconducting properties of 1 D systems etc. can be studied using this facility. With the DR got installed, CSIR-NPL is the coldest temperature point in Delhi.

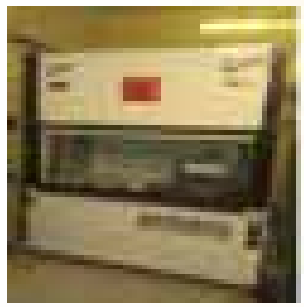

Fig. 6.15 UV-Photo lithography and Argon Ion Milling

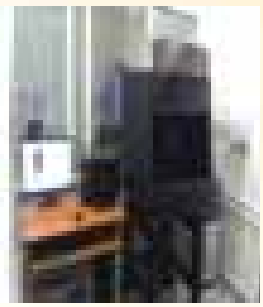

Fig. 6.16 Surface Profilometer

आगन्तुक पुस्तिका से ...

From the visitors book ...

परिष्कृत एवं विश्लेषात्मक उपकरण

Sophisticated and Analytical Instruments

Prof R C Budhani
Director
Email : dnpl@nplindia.org

D 07.01 Crystal Growth and X-ray Analysis

Dr Godavarthi Bhagavannarayana
Dr (Ms) Rashmi
Dr Kamlesh Kumar Maurya
Dr Narayanaswamy Vijayan

D 07.02 Electron & Ion Microscopy

Dr Sukhvir Singh
Dr Avanish K Srivastava
Ms Santosh Singh
Dr Surendra Pal Singh
Dr Vidya Nand Singh
Dr Manas Kumar Dala
Sh K.N. Sood
Sh Dinesh Singh
Sh Jai Sankar Tawale
Sh Praveen Tanwar
Sh Sandeep Singh
Sh Stalin K.
Ms. Geetanjali Sehgal

D 07.03 EPR & Magnetic Fluid

Dr Rajendra Prasad Pant
Dr Abdul Basheed Gounda
Sh Sumit Mohan

D 07.04 Analytical Chemistry

Sh Prabhat Kumar Gupta
Dr Nahar Singh
Dr (Ms) Prabha Johri
Dr Shankar Gopala Aggarwal
Dr Sushree Swarupa Tripathy
Dr (Ms) Daya Soni
Sh Niranjan Singh
Sh Rajiv Kumar Saxena
Dr Khem Singh
Ms Jyoti Pokhariya
Ms Sulakshina Bhat
Ms Sunita Raina

Sophisticated and Analytical Instruments

Materials, the building blocks of all modern technologies for research as well as for applications have to conform to strict specifications. Basic material characteristics which control material properties are composition, purity, structure and crystalline perfection. Characterization is concerned with all the three phases mainly solid, liquid and gases. The expertise needed to carry out these tasks is very advanced and the facilities required are very sophisticated.

The Sophisticated and Analytical Instruments Division at NPL houses high quality facilities for characterization of materials for morphology, chemical composition, purity, structure (including defects), crystallographic perfection and the study of solid surface thin films and interfaces. This is the central facility for the laboratory. It is worth mentioning that scientist involved in the maintenance and development of such facilities are not only providing these characterization facilities to other groups of the organization but are very actively engaged in their own research program in advanced areas thus enabling the group to remain close to the latest development in the field and to contribute towards generation of knowledge.

The division comprises of dedicated groups working in the field of X-Ray Analysis, Electron and Ion Microscopy, EPR and IR Spectroscopy and Analytical Chemistry. The division also as major forms in metrology in chemistry (Mic) and certified reference materials.

Crystal Growth and X-ray Analysis

Crystal Growth and X-ray Characterization of advanced materials

Single crystals and recently realized nano-crystals are the building blocks for the modern technology. CSIR-NPL has variety of crystal growth systems like Czochralski (CZ) and Vertical Bridgman Technique (VBT) for melt growth and slow evaporation solution technique (SEST), temperature lowering technique and Sankaranarayanan-Ramasamy (SR) methods for solution growth. For the synthesis of nano-crystals, we have the facilities like microwave furnace to grow nano-crystals with microwave irradiation process and bomb cell for hydrothermal synthesis. Due to stringent properties of modern devices, the composition, purity, crystal structure, and crystalline perfection including defects and interfaces of these materials are to be evaluated very accurately. X-ray methods have been well proven for these studies because of their accurate, non-destructive and convenient nature. The X-ray analysis group at NPL has variety of sophisticated X-ray analysis techniques namely: (i) X-ray florescence spectrometer for the elemental analysis for wide variety of elements with atomic numbers ranging from 4 to 92 either in liquid or solid form, (ii) Powder X-ray diffractometer for structural and phase analysis of crystalline materials either in the form of polycrystals or thin films, (iii) a double crystal X-ray diffractometer specially meant for X-ray topography to see pictorially the macroscopic deviation of the structure for large size single crystals/wafers/thin films, (iv) a high-resolution X-ray diffractometer cum reflectometer specially established for characterization of nano-epitaxial or amorphous films, quantum structures and their devices like light emitting devices etc. for determination of various parameters like composition, thickness, roughness of surfaces and interfaces and (v) an in-house developed state-of-the art level multicrystal X-ray diffractometer for high-resolution XRD, diffuse X-ray scattering, crystallographic orientation, curvature measurements to get the full understanding about the structural perfection at microscopic level in a non-destructive way. This group is having vast experience in the growth of variety of technologically important single crystals like LN, BGO, BSO, KDP, ADP, BMZ, ZTS, ZTC, LA, LAP, LAM, GG, GP etc. The current major activities are to grow topological and multiferroic single crystals for energy conversion/ saving and sensor applications. In addition to the characterization of bulk single crystals and nano-crystals, this group is involved in the characterization of various crystalline/amorphous thin films and device structures like GaN based LEDs.

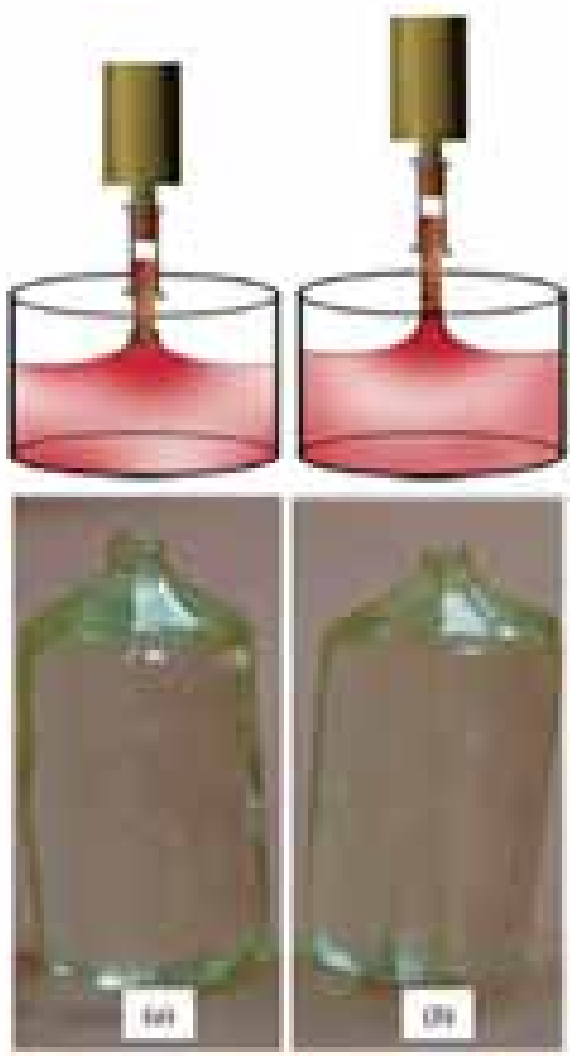

Fig. 7.1: Good quality Mg-doped LN crystals [(a) 2 mol% and (b) 4 mol%] were grown by maintaining the Solid/Liquid interface at a level above the molten charge

In this financial year along with Ph.D. students and collaborators, this group has been achieved a remarkable R&D output, which is published in 44 SCI journals with high impact factors (Three papers have IF > 4). As per the News letter of Indian Association for Crystal Growth, Feb. 2014 (issue 26), the head of this activity was reported as the 2nd top scientist in the area of crystal growth in terms of publications with 245 SCI publications in international journals. A few of the significant published investigations in the current financial year by this group are described briefly in the following.

- Effect of Seeding on crystalline perfection and optical properties on Mg doped congruent Czochralski (CZ) grown $LiNbO_3$ (LN) was studied by maintaining the Solid/Liquid interface at a level above the molten charge. In this way Mg-doping up to 6 mol% could be succeeded without formation of any cracks or boundaries which are otherwise common. Mg doping lead to increase the energy difference between bands. The high-resolution X-ray diffraction (HRXRD) and conoscopic analysis reveals that the crystalline perfection and optical homogeneity of the grown crystals are excellent and does not contain any residual strain. Ref.: J. Appl. Cryst.46 (2013) , IF=5.15.

- A novel comparative study of crystalline perfection and optical homogeneity in Nd:GGG crystals grown by CZ technique with different crystal/melt interface shapes (convex/flat/concave) controlled by seed rotation was carried out. This investigation lead to optimize the best crystal growth conditions (seed rotation) to get a optically homogeneous crystal with a spectacular correlation between optical homogeneity, crystalline perfection and crystal/melt interface shape governed by the seed rotation. By maintaining a slightly concave solid/liquid interface, excellent quality (as evaluated by the observed low FWHM values of rocking curves) was achieved for the grown crystals suited for laser applications.

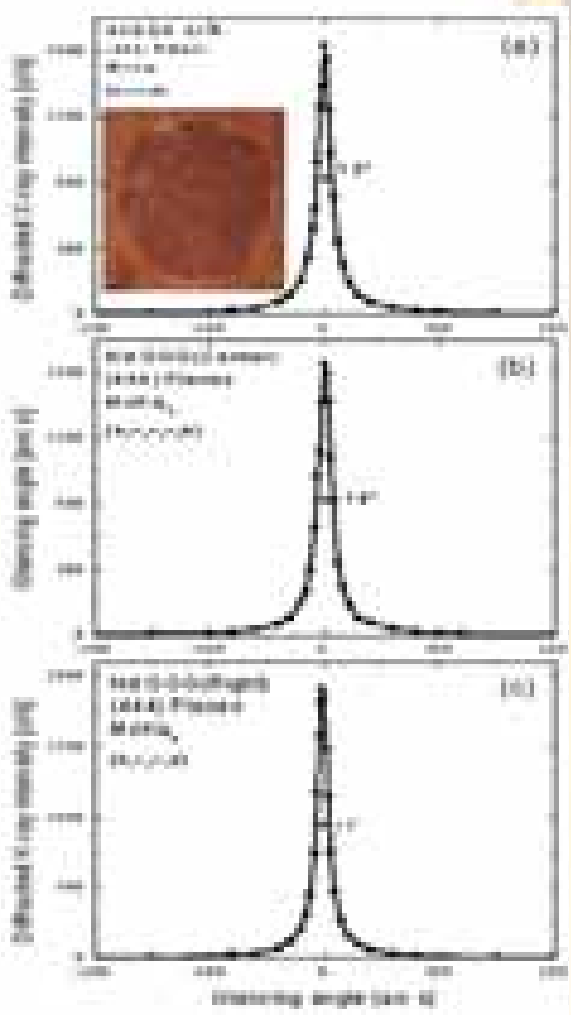

Fig. 7.2: HRXRD rocking curves recorded at different places of the crystal by keeping a slightly concave solid/liquid interface. Inset shows the optically homogeneous crystal with well developed facets

- In a view to reduce the unwanted antisitic defects in Fe:LN, Zr is co-doped and Zr, Fe co-doped congruent LN single crystals were grown by CZ-method suitable for photorefractive and photonic applications and characterized by HRXRD, Powder XRD, XRF, Prism coupler, UV-Vis. and thermal

diffusivity studies. HRXRD studies reveal the absence of structural grain boundaries even with co-doping. However, the crystal is under tensile strain of ~ -1.19x10^{-3}. Birefringence was found to be 0.0822 for 532 nm and 0.705 for 1064 nm. Thermal conductivity was found to be lesser than the undoped equivalent. **J. Appl. Cryst.** 46 (2013) 601-609. IF=5.15.

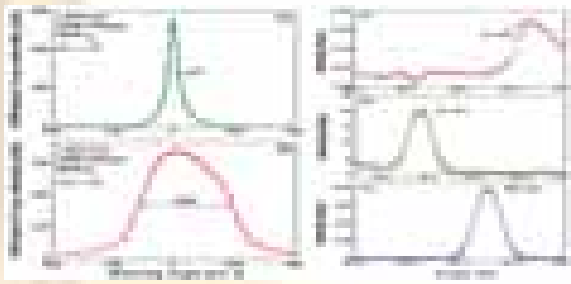

Fig. 7.3a: High-resolution diffraction curves recorded for pure and Zr,Fe-codoped $LiNbO_3$ single crystals

Fig. 7.3b: X-ray fluorescence spectra of the doped LN single crystals with dopants: (a) Fe, (b) Zr and (c) Nb

- Diethylammonium p-hydroxybenzoate (DEPH) nonlinear optical single crystals were grown successfully by slow evaporation solution growth technique. Crystalline perfection, third order nonlinear refractive index (n_2), nonlinear absorption coefficient ($\hat{a}$) and susceptibility ($\div^3$) parameters and laser damage threshold were estimated. Applied Physics A 112(2013)711-717

- Bismuth Silicon Oxide (BSO) is an efficient material for piezo-electric and electro-optic applications. BSO single crystal were grown by CZ method by a home-made system and its detailed mechanical characterization was carried out by Vickers microhardness. Fracture toughness, crack propagation, brittleness index and yield strength have been reported. The experimentally studied mechanical behavior of the crystal is explained using various theoretical models. The anisotropic nature of the crystals is studied using Knoop indentation technique.

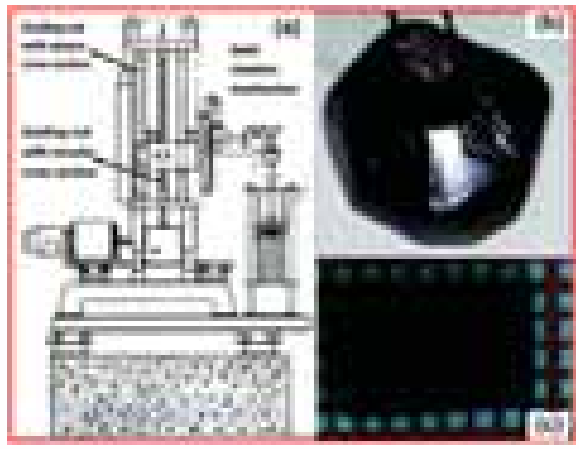

Fig. 7.4: (a) Schematic of the home-made Czochralski crystal puller, (b) as grown BSO single crystal and (c) cut and polished rectangular piece of the grown crystal

- The relative second harmonic generation (SHG) efficiency, optical transmittance and mechanical strength was found to be increased by glycine doping in KDP crystals [Spectrochimica Acta - Part A: Molecular and Biomolecular Spectroscopy 103(2013) 199 – 204].

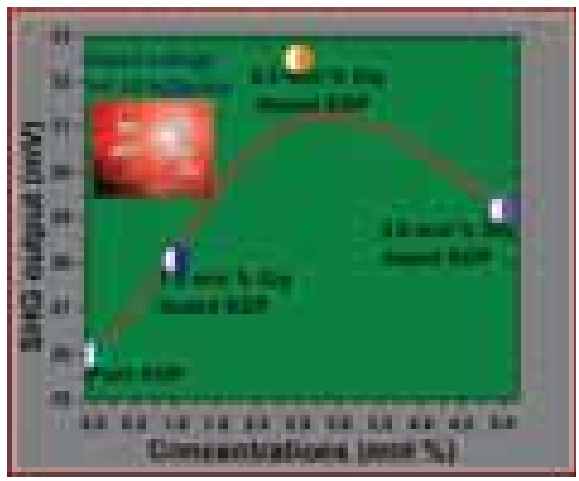

Fig. 7.5: Relative SHG efficiency versus glycine concentration in KDP crystals

- A good quality single crystal of ninhydrin has been grown by unidirec-tional SR method and studied for its structural and optical properties. [CrystEngComm, 15 (2013), 2127-2132].

- We have grown Bi_2Se_3 and Bi_2Te_3 Single crystals by vertical Bridgman technique (VBT) for thermoelectric applications and examined its figure of merit.

AcSIR

The Division is also actively involved in AcSIR. A Course entitled "Advanced Materials Characterization Techniques" for the third Batch of PGRPE/Ph.D. on Advanced Materials Physics & Engineering is successfully taught with six practicals. The theme of the course is "An advanced level introduction on characterization techniques for the analysis of composition, purity and structure including defects, surface and interface analysis." The course contains twelve X-ray related techniques, five spectroscopic and 7 microscopic techniques along with their basic theory and analysis of the results.

Scientific Support and R&D Collaborations: This group is actively involved in providing scientific support to various groups of NPL and various outside laboratories through R&D collaborations by characterizing variety of samples by in-house developed multicrystal X-ray diffractometer, Bruker AXS D8 Advance Powder X-ray Diffractometer and the recently established XRF and HRXRD cum XRR systems. Variety of samples have been characterized for purity including phase analysis, structure and perfection for various projects at NPL including the CSIR network projects NWP-025 and NWP-045 on materials development/metrology. Many thin films of different materials like HfO_2, $LaCrO_3$, $LaAlCrO_3$, FePt, PSMO, LAO, V_2O_5, NbGe, GaN, NBN, CFS etc. have been characterized by HRXRD technique. Some multilayer LED structures of AlGaN/InGaN/GaN films made by CEERI have also been characterized. No. of samples characterized to various NPL groups and collaborators: (i) by multicrystal HRXRD: ~ 150, MRD system ~ 365, Powder XRD: ~575, XRF~75

Major important technical achievements

A newly procured Vertical Bridgeman Crystal Growth system has been installed successfully to grow bulk single crystals.

ELECTRON & ION MICROSCOPY

Electron & Ion microscopy facilities are being utilized at NPL as the central facility for the characterization of materials. This group is equipped with state of the art and most modern equipments such as TOF-SIMS, SEM, AFM/STM, TEM and high resolution TEM with EDS and STEM attachements. Different types of samples in the form of thin films, powders, and composites prepared by various techniques have been received from different groups of NPL working on the development of new and advanced materials. These samples have been characterized for their particles shape, size, distribution of particles, phase identification and crystallographic structure etc., using these facilities. Scientists of electron & ion microscopy group are actively engaged in the synthesis and characterization of thermoelectric materials under the TAPSUN project and contributed significantly.

Responsibilities included maintenance, up gradation and operation of the microscopes together with carrying out studies and investigations of new trends in the field of nano-materials have been the major work of the group. Electron & Ion microscopy group is doing basic research towards shape and size control of nanostructures as well as their synthesis using different methods: chemical as well as physical routes. Collaboration with some very prominent groups in the field of nano-science in NPL, user industries and other research institutions has been another activity of the group.

Many industrial units and other scientific organizations also made use of this facility for different type of materials characterization and testing for quality improvement of their products, which has resulted in generation of considerable ECF to the laboratory. Recently this group has carried out the failure analysis of the lithium ferrite based phase shifter failure in X-Band frequency received from M/s Central Electronics Limited

Sahibabad and identified the cause of failure of their samples on the basis of the microstructural investigations using scanning electron microscope (SEM). During the microstrutural investigations a large no. of defects in the form of deep pits, cracks, micro-cracks, micro-holes and debris have been found throughout their material as shown in Fig. 7.6.

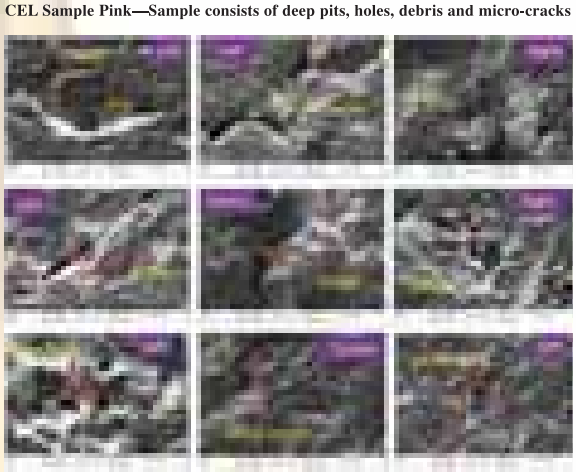

Fig. 7.6: SEM images of the CEL samples showing various defects in the material

Synthesis of Gold nanoparticles and Gold nanorods have been done by using chemical route. Gold nanoparticles synthesis will be optimized to obtain uniform size distribution of GNPs Size dependent toxicity will be assessed and compared with the nanoparticles obtained from NIST and gold nanoparticle drug conjugate will be tested for cancer cell lines to assess the therapeutic efficacy. This work is being carried out under the project Nano-SHE. About 300 samples have been characterized by using HRTEM facility.

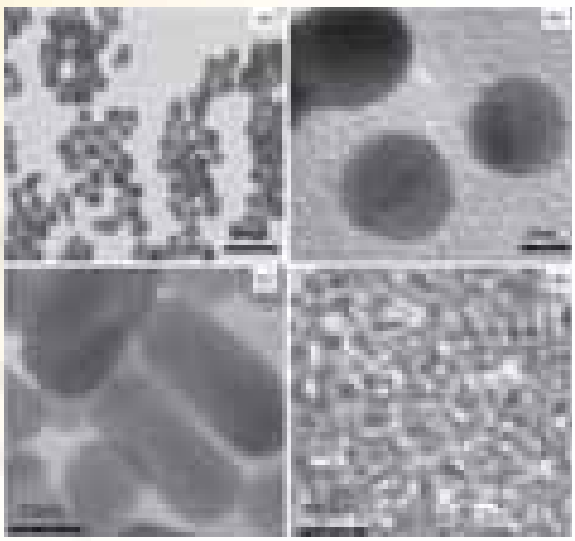

Fig. 7.7: TEM and HRTEM images of as synthesized gold nanoparticles showing uniform distribution of gold particles having different shapes

Scanning Electron Microscopy and Energy Dispersive Spectroscopy is another central facility of the laboratory which is extensively used by various R & D groups of NPL, other scientific R & D institutes and Industrial organizations for characterization of materials for surface microstructure and chemical compositional measurement. More than 1500 samples were received from various R&D groups of NPL as well as from industries have been examined by SEM and EDS for surface microstructure and compositional analysis. Thermally evaporated Sn for 5hrs showed the formation SnO_2 nanoparticles shown in Fig.7.8 revealing **facetted spherical morphology.** An amount of Rs. 2.25 lakhs was realized as test charges for SEM/EDS characterization work for industries.

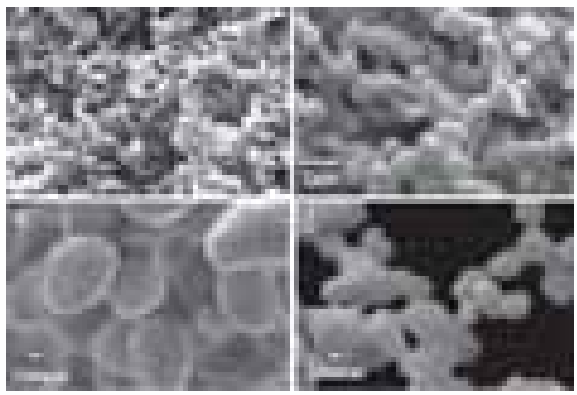

Fig. 7.8: SEM images of SnO_2 nanostructures with evaporation time 5hr at different magnification (a,b,c,d) reveals facetted spherical morphology

Scanning probe microscopy (SPM) is another central facility in CSIR-NPL and is extensively used by different R & D groups. CSIR NPL has Multimode-V (NS-V) which includes AFM, STM and other advanced mode techniques i.e. Magnetic Force

Microscopy (MFM) (used for measuring spatial variation of magnetic forces over the sample), Electric Force Microscopy (EFM) (used for measuring electric field gradient above the sample) & Nanolithography (one of the nanoscale technology for the fabrication of nanometer scale structures and devices).

Material science is at frontier of the technological development these days and in the age of miniaturization of devices, thin films play a significant role. It is important to understand the growth mechanism and quality of thin film to be used for technological development. Scanning Probe Microscope (SPM) which includes Atomic force Microscope (AFM) and Scanning Tunneling Microscope (STM) and various other advanced techniques for electrical and magnetic characterization is one of the powerful and fast growing tool for the characterization of thin films. Figure 7.9 (a) shows the AFM image of $Pr_{0.58}Sr_{0.42}MnO_3$(PSMO) thin film deposited on LaAlO3 (LAO) (001) substrate using dc sputtering. Clear granular morphology can be seen with rms roughness ~ 0.681 nm and average grain size around 30-50 nm. Figure 7.9(b) shows the AFM image of same sample after annealing at 900 ˚C for 12 hrs in flowing oxygen atmosphere. The annealing effect, i.e. terrace like morphology is clearly visible in AFM image with average terrace height ~ 1.7 nm.

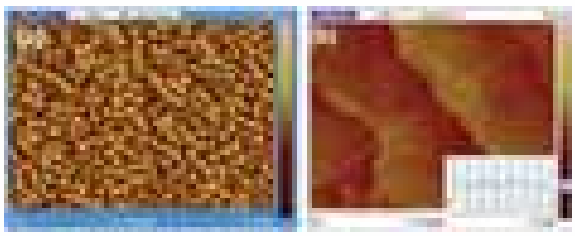

Fig. 7.9: AFM images of PSMO (a) as grown and (B) annealed at 900°C in Oxygen atmosphere on $LaAlO_3$ (001) substrate by DC sputtering

About 450 samples were characterized using SPM for the study of morphological effects like particle size, roughness and other magnetic & electrical properties of variety of materials like manganites,polymers and their composites, CNTs, ZnO, TiO_2 nanoparticles, graphene oxide, graphene sheets and magnetic material thin films etc.

TOF-SIMS available at NPL is a surface analytical technique which uses a pulsed beam of primary ions focus onto a sample surface, producing secondary ions in a sputtering process. These secondary ions are then accelerated into a "flight tube" and their mass is determined by measuring the exact time at which they reach the detector (i.e. time-of-flight). High mass resolution, excellent detection limit (in ppm/ppb), high lateral resolution and depth resolution makes it an important technique for various organic as well as inorganic applications. Detection of all elemental and molecular ions along with their isotopes is the unique property of TOF-SIMS. Interface analysis in the order of few nanometers is possible using this surface technique. Quantification of the sample can also be done with the help of a standard reference material. TOF-SIMS present in NPL is shown in Fig: 7.10.

Many samples from NPL as well as outside NPL were tested and studied which includes both organic and inorganic samples. Few results can be seen below: Depth profiling of Irganox-3114 nanoscale delta layers in a matrix of Irganox-1010 using conventional Cs^+ and O_2^+ ion beams.

In this work, we showed that though the conventional ions like Cs^+ or O_2^+ do not give large molecule based information like in the case of bombardment of cluster ions, but if there are unique elements or isotopes in the analyte (in this

Fig. 7.10: (a) Structure of Irganox, (b) Cs^+ depth profile (c) 3-D image showing the delta layers at four different depths

case, nitrogen) then so far as the depth resolution and its related parameters are concerned, the data shown by these mono or di-atomic ions are comparable or some times better than the data shown by cluster ion bombardment for depth profiling.

Many other technologically important device materials were characterized using TOFSIMS facility which are listed below:

Utilization of residual $CdCl_2$ in CBD-CdS to realize grain growth in CdTe: A novel route. CdTe films were deposited by thermal evaporation onto chemical bath deposited CdS (CBD- CdS) films. The composite films were subjected to rapid thermal annealing to observe simultaneous grain growth in both the CdS and CdTe layers. TOF-SIMS measurements were done to observe the compositional uniformity in the film and to measure the interfacial mixing behavior.

Inclusion of nano-Ag plasmonic layer in enhancing the performance of p-Si/CdS and InP/CdS solar cells.

Introduction of plasmonic layer in p-Si/CdS solar cell indicated an enhancement of short circuit current which improved the overall increase in efficiency. Location of the plasmonic layer in the above cell structure and its effect on overall performance of the cell has been critically studied using TOFSIMS depth profiling besides the morphology, particle size distribution, optical absorption, I-V & C-V characteristics and lifetime of the photo generated carriers.

EPR & Magnetic Fluids

Ferrofluids are new class of technologically advanced magnetic materials, which combine both fluid and magnetic properties comparable to those of solid magnet. The rare combination of fluidity and the compatibility of interacting with a magnetic field are achieved in ferrofluids. These fluids have been used in liquid seals, dampers, drug delivery agents, to sink float systems for separation of materials. They are also used in micro and nanoelectromechanical (MEMS & NEMS) systems and also in cancer treatment. The DST has a National Network Programme on ferrofluid of NPL has a major role to play in this project. We have prepared ferrolfuids of mixed ferrites nanoparticles doped with rare earth elements (Gd,Pr). They are investigated for their structural, morphological, rheological, magnetic and spin dynamical behaviour by various sophisticated analytical instruments. The investigations have helped us in developing stable and suitable ferrofluids for energy conversion devices. The research group has sophisticated equipments like X & Q band EPR spectrometer which has been used to characterize the paramagnetic and ferromagnetic characteristics like damping constant, magnetic anisotropy, flux density, spin waves, Spin glass transmission, superparamagnetic behavior, spin concentration, stiffness constant in thin films and magnetic fluid samples. The other equipments in the group are Powder XRD, Magnetorheometer with Rheomicroscopy and particle size analyzer. Some of the results of our investigations are as follows:

I. Synthesis and Characterization of Carbon nanotube based (CNT) hybrid Ferrofluids:

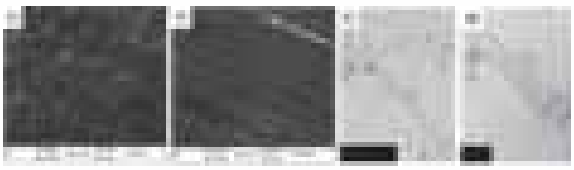

Fig. 7.11: SEM micrographs of (a) Fe_3O_4 / MWCNT nanocomposite (H = 0 G), (b) Fe_3O_4 / MWCNT nanocomposite (H = 3 kG) Yellow arrow indicates the direction of magnetic field. (c) & (d) TEM micrographs of Fe_3O_4 / MWCNT nanocomposite at different magnifications

A stable water based fluid is prepared having both magnetic nanoparticles and MWCNTs in a well dispersed state. The method for the preparation is very simple and does not require initial mixing of the two components. The hybrid fluid exhibits good magnetic and sedimentation stability.

The MWCNTs were purified and functionalized by acid treatment. In second stage, a water based ferrofluid is prepared by chemical coprecipitation method. The dispersions of MWCNTs and ferrofluid were mixed in different volume ratios viz. 1:1, 1:2, 1:3 etc. to obtain Fe_3O_4 - MWCNT hybrid composites in well dispersed liquid

state. The analysis of XRD patterns confirm the desired crystalline phases of nanoparticles and nanotubes. The effect of magnetic field on alignment of MWCNTs is observed with varying concentrations of this hybrid fluid. For 1:1 ratio, it is shown in figure 7.11 (a – b). Fig 7.12. Shows the schematic diagram of ion dipole interaction of Fe_3O_4 - MWCNT hybrid ferrofluid.

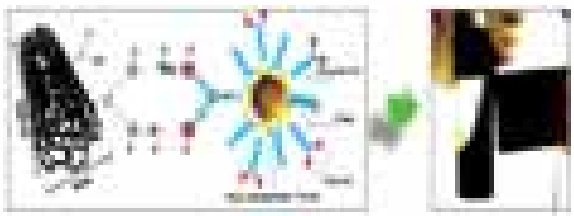

Fig. 7.12: Schematic illustration of weak ion-dipole interaction existing in Fe_3O_4 - MWCNT hybrid fluid

The peak positions in FTIR spectra of Fe_3O_4 / MWCNTs are quite similar to the functionalized MWCNTs except few notable differences (Figure 13). The intensity of C-H vibrations (2850 – 3000 cm^{-1}) is quite enhanced and easily visible in the last two spectra due to contribution by oleic acid and sodium oleate surfactants. A decrease in relative intensity is probably accompanied by the interaction between outer functional groups of nanotubes and nanoparticles. The C=O vibrations, characterized by peak at ~ 1705 cm^{-1} is sharper in Fe_3O_4 / MWCNTs as compared to ferolfuid. Moreover, its increased value from 1702 to 1706 cm^{-1} after adsorption of particles onto tube further supports the existing chemical interactions between the two components.

Fig. 7.13: FTIR spectra of hybrid fluid

The sedimentation stability of hybrid fluids were visually assessed by leaving it for a long period of time. The dispersions were found to be stable for several months respectively. The stability of Fe_3O_4 - MWCNT hybrid fluid decreases with increasing MWCNTs content which is clearly understood if one takes into account the stability of individual components. The dominating weak ion-dipole interactions are the main cause of sedimentation and magnetic stability of the hybrid fluid.

II. Exchange bias effect in $CoFe_2O_4$

The $CoFe_2O_4$ samples were synthesized by coprecipitation method at four temperatures 20°C, 40°C, 60°C and 80°C. The particles size thus obtained were found to be of 8 nm, 17 nm, 29 nm, and 45 nm (S_1-S_4). The particles size was confirmed

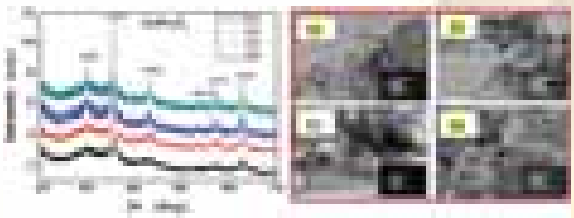

Fig. 7.14: XRD patterns of $CoFe_2O_4$ samples and HRTEM micrograpahs

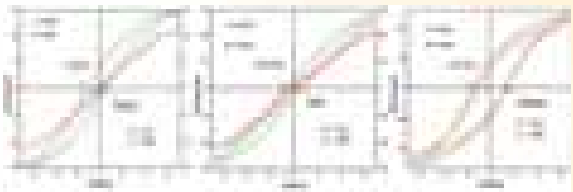

Fig. 7.15: M-H curves of $CoFe_2O_4$ samples

by taking X-ray diffraction (XRD) patterns and TEM micrographs. X-ray diffraction patterns and TEM micrographs of $CoFe_2O_4$ samples are shown in Fig.7.14. The structural, morphological and magnetic properties of these particles were analyzed using XRD, HRTEM and SQUID.

Fig.7.1 6: (a). Variation of Coercive and Exchange bias field of $CoFe_2O_4$ samples (b) Estimation of Exchange bias field in $CoFe_2O_4$

The magnetic measurements of $CoFe_2O_4$ measured at 100 K are shown in Fig. 7.15.. The sample with a larger particle size has a larger magnetization and larger coercivity, which suggests the enhanced Ferromagnetic (FM) ordering as the particle size increasing. For a sufficiently small particle size, though the anisotropy of the Antiferromagnetic (AFM) becomes smaller, more disordered uncompensated spins appear which result in decrease in coercivity. It is observe that when size increases towards single domain, the coercivity increases and then reaches to a maximum value of 3023.67 Oe for D = 29 nm, which further decreases with the succeeding increase of average particle size. This is due to the fact, as particles are larger than the single domain size, the motion of domain walls becomes predominant and the coercivity decrease.

To have a deep insight of coreshell structure the exchange bias has been done. Figure 7.16 shows the M(H) loops for all the samples measured at 100 K zero-field-cooled (ZFC) and field cooled (FC) process from 300 K in a magnetic field of 7 kOe. It is evident that the ZFC hysteresis loop keeps good central symmetry, and the magnetization behavior of all samples is consistent with all the samples measured at 300 K. While, field cooled M (H) loops displays a horizontal shift as well as vertical shift in bilayer system where an antiferromagnetic layer with strong anisotropy is deposited on a top of a ferrimagnetic layer and the horizontal shift have been termed as exchange field H_{EB}. The EB field $H_{EB} = (H_1 - H_2)/2$, where H_1 and H_2 are the positive and negative coercive fields, respectively. The EB interaction is responsible for shifting of magnetic loops towards both field directions. When the temperature is lowered through the Neel temperature of the AFM layer its spins align with respect to each other and may also couple with the FM spins depending upon the interfacial exchange coupling between the two layers. This generates a uniaxial anisotropy parallel to the cooling field direction. A large anisotropy of AFM layer prevents the AFM spin rotation in AFM layer and this in turn prevents the FM spins in turning away from the cooling direction. Furthermore, it has been shown that the hysteresis loop also shows a vertical shift of the magnetization that is related to the presence of pinned interfacial spins. A positive (upward) shift is attributed to a ferromagnetic interface coupling and a negative shift for an antiferromagnetic interface coupling. The results show that the size 17 nm is critical in minimizing coercivity and exchange bias field as shown in Fig 7.16.

III. Rheomicroscopic investigation of chain formation in MR fluids:

MR fluids were prepared using micron sized (<5mm) Fe_3O_4 powder acquired from Sigma-Aldrich. The particles were ball milled for two hours to reduce the size by keeping the weight to ball ratio 1:10 in a Retsch co. Ball mill in the presence of kerosene and binder. The particles were homogenized and ultrasonicated by adding oleic acid and kerosene. Then, the ground particles were investigated for crystalline phase and morphological studies using XRD, HRTEM. A rheomicroscopy set up has been used to monitor the formation and deformation of chain like structures in varying strain amplitude and magnetic field.

Fig. 7.17 shows the schematic chain formation and deformation with increasing shear rate under a constant magnetic field 1 Tesla conditions. The easiest approach to consider the structures of magnetic interparticle interaction, a microscopic model of chain formation is to be taken in to consideration. Thermal energy and viscous stresses try to randomize particles and rupture the chains.

Fig. 7.17: Schematic showing chain formation and deformation at increasing shear rates

It is seen that at lower shear rate, the magnetic field effectively induces dipole-dipole

interaction to lead the chain formation and consequently lengthening the chains (Fig. 7.18). At this stage the thermal energy is lower than the interaction energy and so is the shear viscous energy leading to the formation and further lengthening of the chains. At higher shear rates,

Fig. 7.18: Variation in average chain length with shear rate at different magnetic field

the viscous forces lead the Dipole-dipole interaction and the breaking of the chains sets in leading to the rupture of the chain like structures.

It is observed that upon the application of magnetic field a collinear with the vorticity of micron sized Fe_3O_4 particles in rotational flow with oscillatory strain in a parallel plate system, chain like structures is formed along the direction of the magnetic field. In situ recorded videos of the system

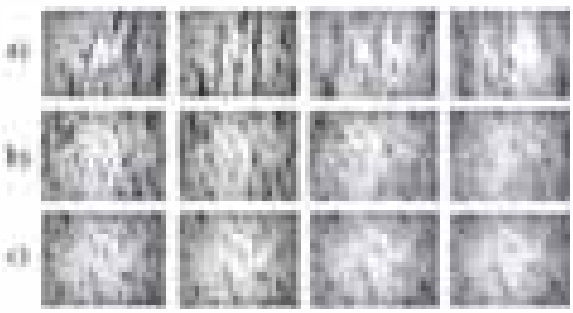

Fig. 7.19: Microscopic images at different shear rates at a) 467.5G b) 217G c) 120G magnetic fields

were converted into a sequence of images using ImageJ software. Then Images at a constant interval of time were taken out and processed as shown in Fig 7.19 (a-c). The lengths of chainlike structures were calculated in each of these frames. Average length of chains in a frame increases initially with increase in shear rate (~ 90 m) and reaches a maximum to gradually decay down to that in initial field and shear conditions (5-20m).

IV. FMR investigation in $La_{0.67}Ca_{0.33}MnO_3$ thin films

Ultra high thin films various thickness 5, 20, 100, 200 nm were fabricated on SrTiO3 substrate using pulsed laser technique to study the thickness depended magnetic properties using FMR technique. From Fig. 7.20 (a) it can be seen that as we move from RT to lower temperature, up to 280 K a single paramagnetic resonance peak with almost consistent resonance field ~3400 G is observed. After this, film shows phase transition from para to ferro having Curie temperature ~275 K which is in correspondence with magnetization data.

Below this transition peak splitting begins. After 275 K we can clearly see the shifting of one peak towards higher resonance field side other one towards lower. Similar trend was also observed for film with thickness 100. From temperature 260-220 K an additional spin wave kind of behaviour was also observed for 200 nm.

This behavior shows that the film is

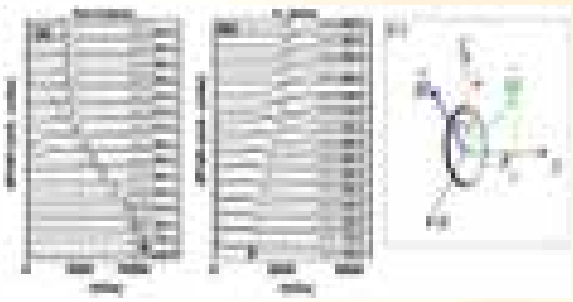

Fig. 7.20: (a) FMR spectra of LCMO 200nm thin film at different temperatures for field applied (a) perpendicular and (b) parallel to the film plane (c) schematic co-ordinate system for FMR measurements

homogenous in thickness. Fig. 7.20 (b) shows that with lowering temperature resonance field shifts towards lower field side. In Fig. 7.21.Variation of resonance field for LCMO films with thickness 100 and 200 nm were shown. From the Fig. 7.21 we found the resonance field diverges at temperatures 255 K and 270 K which are the Curie temperatures for 100 and 200 nm LCMO films respectively. Furthermore to investigate anisotropy the angular variation has been done (schematic Fig. 7.20 (c)).

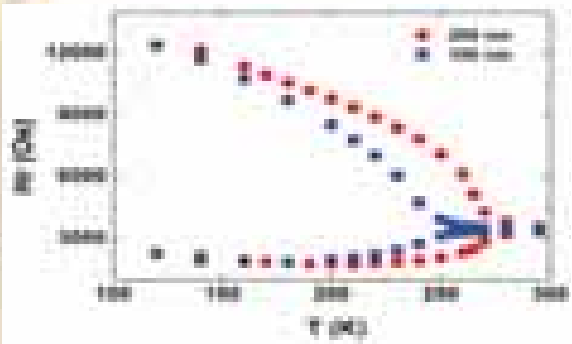

Fig. 7.21: Temperature dependence of the resonance field (Hr) for 200 nm and 100 nm LCMO films in both parallel and perpendicular orientation

ANALYTICAL CHEMISTRY

The Analytical Chemistry group has been providing support for chemical characterization of materials for their chemical composition, purity/ impurity assessment and conformity requirements needs in NPL/ stakeholders and in the MiC & CRM activities, including R&D for method development for challenging problems in water and air quality. The activities in the metrology in chemistry (MiC) and certified reference materials (CRM) realize SI mole. These activities are to help provide SI traceability at apex level in chemical measurements through a network of MiC expert partners, under the CSIR network project, 'measurement for innovation in science & technology (MIST)', in various sectors impacting quality of life and international trade. At NPL the group's focus under MiC is to prepare standard gas mixtures & inorganic elemental solutions standards for services related to air/ water quality and climate change GHG standards issues. With PTB Germany the group has MiC cooperation project 'Strengthening the quality infrastructure in environmental analytics-CEMI. The group has carried out R&D in method development, purity/ impurity analysis, aerosol metrology and proficiency testing (PT) schemes for iron ore/ coal with NML Jamshedpur and pesticide solutions with IITR Lucknow. The group has advance instrumental techniques like ICP-HR-MS, F&GF-AAS, GC with FID/ TCD/ ECD & PDHID, IC, UFLC, SMPS, gas analyzers and the high precision balances. Gravimetric preparation, validation, certification and dissemination of reference materials in the field of aqueous elemental/ ionic solutions for water quality and standard gas mixtures are done. During this period under gas metrology activities, efforts were made for cylinder preparation/ processing for gravimetric preparation of ~2000 µmol/ mol CH_4 gas standard mixture in N_2 for APMP.QM-S7 international comparison. The group carryout consultancy and R&D for societal issues viz. for purification of water for toxic contaminants like pesticides, arsenic, chromium, cyanide, mercury, poly-aromatic hydrocarbon, microbes etc using nano-materials etc. A process for improving water quality contaminated by pesticides has been developed and filed for patent.

R & D Activities

Atmospheric aerosol studies require R&D in particle growth information due to individual process for climate modeling and other purposes. A simplified approach has been developed, based on particle number size distribution measured by scanning mobility particle sizer (SMPS), to calculate particle growth due to self-coagulation, coagulation scavenging and condensation processes. Three particle growth event days were classified during November – December 2013 for 10 days SMPS measurements conducted in particle size range from 9 – 425 nm, at CSIR-National Physical Laboratory, New Delhi. The study led to derive formulae which addresses growth rate due to self-coagulation (GR_{scoag}), coagulation scavenging (GR_{scav}) and condensation (GR_{cond}). A growth event day, November 4 and a non-event day, December 16 have been selected for an example (Fig. 7.22). Total growth rate (GR_{total}) was calculated based on the regression fit of the plot between geometric mean diameter (GMD) and local time of the number size distribution measured on November 4. From the regression equation, GR_{total} calculated to be 15.4±11 nm h^{-1}. Using the formulae derived in this study, GR_{scoag} and GR_{scav} were calculated to be 3.8±0.4 and 8.0±6 nm h^{-1}, respectively. The estimated total growth rate, which is a sum of GR_{scoag}, GR_{scav} and GR_{cond}, $GR_{cond,}$ was 3.6 nm h^{-1}. This approach is simple, and growth by individual

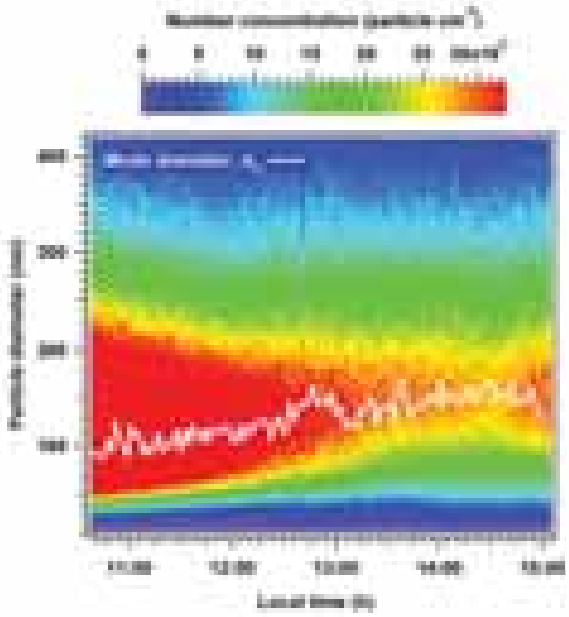

Fig. 7.22: Time series of size-resolved particle number concentration on November 4 (i.e., a growth event day as an example). The white line represents the particle mode peak diameter

processes can be calculated without knowing several other parameters which include vapor concentration of atmospheric constituents, heterogeneous processes, complex modeling procedures, etc.(Sarangi B., Aggarwal S.G. and Gupta P.K., AAQR, In press, 2014)

Gravimetric preparation of standard gas mixtures

Five gas mixtures of CH_4 (conc. range ~ 1600 µmol/mol to 2000 µmol/mol) in nitrogen has been gravimetrically prepared and verified/ analyzed by GC using TCD detector, and the mixtures have been compared with the gravimetric composition value against its analytical measurement value (verification value) using equation

$$\left|x_{i,prep} - x_{i,ver}\right| \leq 2\sqrt{u_{i,prep}^2 + u_{i,ver}^2}$$

where $x_{i,ver}$ and $u_{i,ver}$ are the measurement result from verification and it's standard uncertainty, respectively. These efforts were utilized for participation in APMP.QM-S7 international supplementary comparison of 2000 µmol/ mol CH_4 in N_2 gas mixture. Equivalences results are shown in Fig. 7.23.

Group has also participated in other international comparisons viz. APMP.QM-K19: pH of borate buffer using glass electrode; and APMP.QM-P21: determination of arsenic species, total arsenic and cadmium in brown rice flour. In addition to these comparisons, the group has taken initiative for PT schemes like pesticide purity (with IARI Delhi), elements in Quartz (with NCCCM-BARC Hyd), metals in road dust (with CRRI) and metals in lube oil/ viscosity in oil (with IIP Dehradun). Another batch of As, Hg, Ni and NO_3 elemental solutions preparations of ~100 mg/kg concentrations have been completed and are ready for release.

The group has completed consultancy

Fig. 7.23: Degree of equivalence for the APMP.QM-S7 (k = 2)

projects of ~Rs 9.0 lakhs from M/s Emerald Jewel Industry India Ltd, Coimbatore, Tamil Nadu for recovery of gold and silver and from M/s Mysore Paints & Varnish Limited, Mysore for recovery of silver from process waste (Fig. 7.24).

Group has done notable work in application of zinc peroxide nano-particles for water purification contaminated by inorganic and organic

Fig. 7.24: Recovery of silver (~99.9%) from process waste

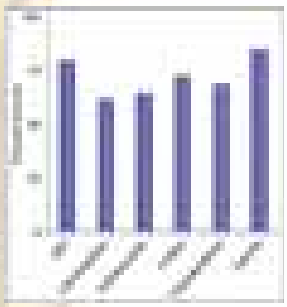

Fig. 7.25: % removal of pesticides

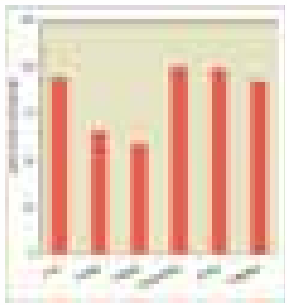

Fig. 7.26: % removal of microbes

(pesticides, microbes) contaminants. The focus was on various pesticides for removal studies like lindane, chloropyriphos, pp-DDT, pp-DDE, α-endosulfan, and α-endosulfan (Fig, 7.25). As a result of further studies on this material group has filed another patent on process in paints for antimicrobial agent and preparation thereof. We have purified the water contaminated by microbes (Fig. 7.26). The same zinc peroxide nano-particle material can also be used in several items, like paint, cement, wall putty, cosmetics etc. to control microbial growth.

वैज्ञानिक एवं प्रशासनिक सहायक सेवाएं

Scientific and Administrative Support Services

Centre For Calibration & Testing (CFCT)
Dr Rakesh Kumar Garg
Dr V K Gumber
Dr R G Mathur

Planning, Monitoring and Evaluation Group (PME)
Sh T Raghavendra
Sh V D Arora
Sh Ashok Kumar
Ms Anita Sharma

Industrial Liaison Group (ILG)
Dr (Ms.) Jyoti Lata Pandey

HUMAN RESOURCE DEVELOPMENT GROUP
Dr Rajeev Chopra

International Science and Technology Affairs Group (ISTAG)
Dr V. K. Gumber
Sh Ashwini Kumar Suri

Knowledge Resource Centre (KRC)
Sh N K Wadhawa
Sh Abhishek Sharma
Sh Jagdish Prasad
Sh rajpal Zamaji Walke
Ms Neetu Chandra

Central Workshop
Dr R K Kotnala
Sh Ravi Khanna
Sh P Srinivasan
Sh Jai Pal Singh
Sh Amar Singh

Computation & Network Facility
Dr Ravi Mehrotra
Dr Ashish Ranjan
Ms Deepti Chaddha
Mr Nitin Sharma
Ms Anjali Sharma
Mr Trilok Bhardwaj
Mr Kanwaljit Singh
Mr Vijay Sharma

Quality Management System
Dr Rakesh Kumar Garg

Scientific and Administrative Support Services

Centre For Callbration & Testing (CFCT)

Centre For Calibration & Testing (CFCT) has been established to promote Calibration & Testing Services of the laboratory. It acts as an interface between all the calibrating and testing groups of the CSIR-NPL and nearly 2000 customers from industries, various laboratories and government organizations from all over the country and abroad. Based upon the requirements of the customer the CFCT services are tuned up for customer satisfaction.

Most of the information required by the customers are kept online such as Calibration & Testing Charges, Calibration & Testing Request Form, Important Information, Site Calibration and FAQ.

Planning, Monitoring and Evaluation Group (PME)

Contract R & D Projects, as Sponsored, Collaborative and Grant-in-Aid Projects are undertaken by the Laboratory with funding from External Agencies. Before submission of the project proposals to the outside agencies they are evaluated by the Group based on various criteria and conditions. Monitoring and developing of complete database for report generation on projects are done and project files are created and maintained. Similarly Major Laboratory Projects and other In-house Projects funded by CSIR & NPL, undertaken in NPL, are also monitored. Fund allocation and processing of indents is an important activity undertaken by this group. The report on completed projects and refund of unspent balance to the funding agencies at the end of project are made by the group.

PME prepares Annual Plan and Five Year Plan for NPL. It organizes Research Council meetings and coordinates the Management Council meetings, organized by administration. Time to time PME disseminates information on projects, performance reports and ECF reports to CSIR. PME is also involved in monitoring of Networking Projects and XII five year plan projects. PME developed manpower data and maintains staff positions and disseminates the information to various authorities. The group also maintains and regulates the appointments of project staff under various externally funded projects.

PME has the additional responsibility of getting feedback on degree of customer satisfaction in a prescribed format from funding agencies who are funding the different contract research projects in NPL. The process is done at the end of each project. This function has been initiated by CSIR under the supervision of Customer Satisfaction Evaluation Unit (CSEU) at CSIR Headquarter, Rafi Marg, New Delhi – 110 001. The feedback received from the funding agencies are sent to CSEU, CSIR.

PME prepares many types of reports on Manpower in different formats as required from time-to-time and also does different type of Analysis for manpower planning of the laboratory.

Industrial Liaison Group (ILG)

The Industrial Liaison Group (ILG) is responsible for the commercialization of research and knowledge developed by the NPL scientists and researchers. Our focus is to foster and develop collaborative work environments between researchers, industry partners and funding agencies. We want to ensure that the relationships created through the commercialization of a technology continue to add value for all partners; leading to ongoing research projects for the inventor and the industry partner and to the commercialization of complementary technologies. In addition, this group also undertakes consultancy, technical services and dissemination of science and knowledge base. This group is responsible for all matters connected with business development. It also helps in organizing “Technology Day” and “World Metrology Day” function where all licensees are invited to interact and deliberate with scientists concerned with development of the technology. It also helps in organizing “Open Day” function,

wherein few thousand school and college students with their teachers are invited to see the various scientific and technical activities at NPL. This group further carries out the dissemination of science through publication in CSIR News, CSIR Annual report, business and industrial magazines and their websites and through advertisements in newspapers, conferences, symposiums, various other events and their souvenirs and also through participation in exhibitions. Processing of applications for the awards pertaining to technology or consultancy services is rendered. This group also undertakes distribution of royalty, premia and intellectual fee pertaining to consultancy, technical services and technology know transferred. It further updates industries, licensees and scientists for any CSIR/DST entrepreneurship/funding schemes for applying for awards/ projects. It updates scientists about scientific and technical exhibition, events. It acts as bridge in resolving scientific and technical issues raised by industries/clients for providing them solution through technical and consultancy services. This group also takes care of the management of S & T outputs with other funding agencies viz. DST, CSIR, NRDC, CDC, FICCI, etc. This group interacts with FICCI and loads technology inventions at their website for wider exposure, collaborative work, market search and entrepreneurship demand. During the year, the group disseminated Knowledgebase / Technology during India-Africa Exhibition held in Vigyan Bhawan, Taj Palace and at 100th Indian Science held during January 3 -7 2013 at Kolkata. It also extended support to M/s NISCAIR, New Delhi who made documentary film on CSIR-NPL. This group initiated its efforts for possible knowledge alliance with Sensor Technology Pvt. Ltd., Prabhatam Radisafe Limited, New Delhi, Reinste Nano Ventures Pvt. Ltd, Noida, Jyoti Cero Composite, Jamshedpur, GTC Technologies, Houston USA in the area of carbon composite, energy, sensor electronics, solar energy biological instrumentation water purification, EMI shielding, radiation safety etc. A registration certificate for setting-up of NPL Technology Innovation Center (NTIC) under Sec-25 company act was received on 22th May 2012 (2012-13). This group coordinated with CSIR HQs for Scientific Enterprise scheme in the area of ECG-plug-In device. This group resolved the issue of silver recovery from inedible ink waste which was accumulated/ generated by M/s Mysore Paints & Varnish Ltd, Mysore over the years and this may be taken up as consultancy project in future.

HUMAN RESOURCE DEVELOPMENT GROUP

The HRD Group represents the central group of the laboratory providing several activities in various areas of core competence of the lab and also related to research scholars/students. The basic objective behind all these activities is to make the Human Resource better informed, knowledgeable and highly skilled & trained so that it can prove to be more competitive, productive and useful to the society. All these eventually lead to the generation of trained S&T manpower in the country.

The group is involved in various activities, such as, Organisation of Industrial Training in Metrology/Standards, help & support to Research Scholars, Students' Training for M.Tech./MCA/ M.Sc. and other equivalent degree courses, Institutional Visits, Deputation of NPL staff members to attend conferences, AcSIR related activities (Ph.D.& M.Tech.) etc,.

International Science and Technology Affairs Group (ISTAG)

International Scientific Collaborations help the scientists to share their innovative ideas for developing cutting edge technologies & provide the opportunities to carry out research in emerging fields of science and technology. ISTAG group facilitates the overseas visits of scientific and technical personnel of the laboratory to get acquaintance of latest research & learn new techniques. It assists the scientists to participate in International conferences, seminars, technical

meetings and summer schools. It helps the scientists to get prestigious international fellowships. This group advises the scientists to avail the overseas visits under bilateral exchange programmes. It organizes the visits of foreign delegations at NPL. International experts are invited to give talks and lectures at NPL. Arranging visits for international candidates attending training programmes is also the job of this group. International collaborative projects, bilateral exchange programme and MOU with foreign institutions are also handled by this group.

Knowledge Resource Centre (KRC)

CSIR-NPL Knowledge Resource Center (KRC) has been providing library and information support to researchers for R & D pursuits.

Over the years, it has developed a rich collection of scholarly books and journals for the purpose, especially in the field of physics and related sciences. During the current year, KRC subscribed numerous scholarly journals and added variety of books both in English and Hindi languages to enrich its textual collection. Regarding the services offered, KRC serves the NPL community with services like Reprographic service, Electronic Document Delivery service, Inter Library Loan service, Reference service, Literature Search service etc.

CSIR-NPL-KRC offers online access to more than 6000+ **full text journals under the e-consortium** project of NKRC (CSIR+DST). The project facilitates access to electronic content from various publishers such as, ACS (American Chemical Society), AGU (American Geophysical Union), AIP (American Institute of Physics), APS (American Physical Society), IOP (Institute of Physics), OSA (Optical Society of America), Oxford University Press, RSC (Royal Society of Chemistry), Springer, Wiley - Blackwell etc.

KRC is also providing access to internet edition of **Indian Standards.**

The shift in technology achieved with the installation of improved routers helped in attracting the R & D personnel in large number to make use of NPL-KRC and leads to optimize the use of the subscribed/ entitled e-resource as well as internet resources.

On continuous basis, KRC maintains its site on the NPL intranet to provide latest information on its activities such as additions to its collection, current subscribed journals, new journals received during the week, links to electronic libraries, publishing houses, and papers published by NPL researchers.

NPL-KRC also maintains NPL website (http://www.nplindia.org) on Internet to inform others about the activities of NPL such as its role towards the society, thrust area of research, facilities, services and achievements.

To improve the quality, speed and effectiveness of services, KRC has completed the retro-conversion of books available in Hindi language. With this, end users of KRC would avail the value added services associated with the NPL-KRC Information System (NKIS). Further, to serve the users with the online database of resources held in the KRC, three dedicated computer has been installed in the NPL-KRC, entirely for OPAC service.

In the direction of providing free worldwide access to the intellectual outputs of NPL in form of journals articles, research papers, conference papers, technical reports, preprints, and other scholarly communication and also to support the concept of open access initiative, NPL-KRC has established the Institutional Repository (IR@NPL) http://npl.csircentral.net/ and till date, around 990 records has been added.

Under Information Sciences Cluster of National Laboratories scheme of CSIR, project entitled "CSIR Knowledge Gateway & Open Source Private Cloud Infrastructure (KNOWGATE)" have been planned. Main aims of the project are (i) bridge gap between CSIR laboratories by promoting sharing of information resources; (ii) facilitate CSIR KRCs Integrated Library Management Solution using open source software; (iii) to enhance the capacity and capability of CSIR computing power

through CSIR private cloud infrastructure and Open Source Software Technology Solution Cell (OSSTSC). Towards, achieving the predefined objectives of the project, NPL-KRC is contributing actively its maneuvers.

Publication of Annual Report is another important activity of **Knowledge Resource Centre** (KRC). On receiving inputs from various Divisions & other concerned groups, Text and Appendices of Annual Report are compiled, corrected and published in the form of Annual Report since last year.

Central Workshop

Central Workshop of the CSIR-NPL has started in the year 1950. To become a premier research organization in the area of physical sciences and also known as the National Metrology Institute of India. The central mechanical workshop of the lab is playing a vital role in the designing and development of highly precision and sophisticated instruments, components and parts using in the nano science and other research labs of the NPL. A large number of components are fabricated in the workshop such as Laser Beam Expander, Transverse Electro Magnetic shell, Micro Precision shadow Masks, specimen of Watt Balance, High-precision OFHC copper block for ultra-low temperature measurements, etc. Beside this our workshop helps in the maintenance of Apex level standards and establishing the new facility in the laboratory in several manners. The central workshop facility also involves in the fabrications/ manufacturing of the accessories and spares using for calibration and testing of the different instruments and notional earning of approximately is about 1.0 Crore. We have completed total no. of 568 jobs from Central Workshop and 75 no. of jobs from Glass Technology Units during the year 2013-14.

To facilitate this, the central workshop equipped with a state-of-the-art facility that comprises of Precision Lathe Machine, CNC Deckle Milling Machine, Micro Milling Machine, Tool and Cutter Grinder, Precision Surface Grinder, Sheet Metal Shop, Welding Shop

Mechanical Design and Fabrication Workshop

This Division provides mechanical engineering support to all on-going project activities in terms of mechanical design, fabrication, quality control, integration / assembly and installation of various electronic & microwave components / subsystems / systems. The division has qualified and experienced manpower and a mix of conventional and CNC machines tools for mechanical fabrication and CAD facilities. The division also has chemical plating facility which contributes to various on-going projects in terms of precision cleaning, electro-polishing and electroplating of critical Microwave components.

Computation & Network Facility (CNF)

The Computation & Network Facility (CNF) caters to the specialized computing and communication needs of the laboratory. It configures, administers and maintains various servers, a campus LAN and internet connectivity as required. Most of the solutions are integrated in house and deployed on linux based servers.

Major facilities include email, web hosting on intranet and internet, webcast, database, security solutions and high performance computing. A completely new and efficient email solution has been integrated and deployed in this year using a host of open source packages.

In the area of research and education, CNF staff teaches Advanced Computational Physics to M.Tech. students under the AcSIR programme. Under a DST sponsored project "Innovative Product Development Centre", low cost medical instrumentation is being developed.

The CSIR-ERP implementation activities steered in the laboratory. A 20TB SAN and database and application servers have been installed in the Data Centre to connect to the CSIR-ERP network. CSIR-NPL stood second in terms of Finance & HR activities across all CSIR laboratories and awarded

Institutional Award for Enterprise Resource Planning (ERP). Ms Anjali Sharma, Scientist at CNF was awarded with Outstanding Achievement Award from DG, CSIR on 26th September 2013, for her contributions in implementing ERP at CSIR-NPL.

Quality Management System

This group maintains Quality System in NPL, based on the international standard IS/ISO/IEC 17025:2005, in the area of Test and Calibration. All the test/calibration areas of NPLI are periodically audited to confirm the continued compliance to the international standard.

The Quality Manual was revised time to time, depending upon reorganization of the different activities.

A delegation from NPL participated in APMP General Assembly and related meetings held in Taiwan. Laboratory Report of NPL was prepared and submitted to APMP in its General Body meeting. The QMS annual report was also submitted in APMP QS TC meeting.

This group is also organizing a special training course on "Quality Management System – Laboratory Management, Need for Calibration / Accreditation as per IS/ISO/IEC-17025". Special training course was also conducted for the staff of Department of Legal Metrology on their demand.

Seven scientist and technical persons attended the assessor course based on IS/ISO/IEC 17025:2005 organized by National Board of Accreditation for Test and Calibration Laboratories (NABL).

परिशिष्ट

Appendices

Appendix 1

Papers Published by NPL Researchers in SCI Indexed Journals during April 2013 to March 2014

- Abdullah, M. M.; Singh, P.; Hasmuddin, M.; Bhagavannarayana, G.; and Wahab, M. A. "In situ growth and ab initio optical characterizations of amorphous Ga_3Se_4 thin film: A new chalcogenide compound semiconductor thin film." Scripta Materialia 69 (Sep 2013): 381-384.
- Agarwal, A.; Khasa, S.; Seth, V. P.; and Arora, M. "Study of EPR, optical properties and dc conductivity of VO^{2+} ion doped TiO_2 center dot R_2O center dot B_2O_3 (R = Li and K) glasses." Journal of Alloys and Compounds 568 (Aug 2013): 112-117.
- Agarwal, A.; Khasa, S.; Seth, V. P.; Sanghi, S.; and Arora, M. "Effect of MoO_3 on electron paramagnetic resonance spectra, optical spectra and dc conductivity of vanadyl ion doped alkali molybdo-borate glasses." Journal of Molecular Structure 1060 (Feb 2014): 182-190.
- Agarwal, R.; Awasthi, A.; Mital, S. K.; Singh, N.; and Gupta, P. K. "Statistical Model to Study the Effect of Agriculture Crop Residue Burning on Healthy Subjects." Mapan-Journal of Metrology Society of India 29 (Mar 2014): 57-65.
- Agarwal, R.; Awasthi, A.; Singh, N.; Mittal, S. K.; and Gupta, P. K. "Epidemiological study on healthy subjects affected by agriculture crop-residue burning episodes and its relation with their pulmonary function tests." International Journal of Environmental Health Research 23 (Aug 2013): 281-295.
- Agarwal, S.; Jangir, D. K.; Singh, P.; and Mehrotra, R. "Spectroscopic analysis of the interaction of lomustine with calf thymus DNA." Journal of Photochemistry and Photobiology B-Biology 130 (Jan 2014): 281-286.
- Aggarwal, S. G.; Kumar, S.; Mandal, P.; Sarangi, B.; Singh, K.; Pokhariyal, J.; Mishra, S. K.; Agarwal, S.; Sinha, D.; Singh, S.; Sharma, C.; and Gupta, P. K. "Traceability Issue in PM 2.5 and PM10 Measurements." Mapan-Journal of Metrology Society of India 28 (Sep 2013): 153-166.
- Agrawal, V.; Jain, K.; Arora, L.; and Chand, S. "Synthesis of CdS nanocrystals in poly(3-hexylthiophene) polymer matrix: optical and structural studies." Journal of Nanoparticle Research 15 (Jun 2013): 14.
- Ahmad, R.; Arora, V.; Srivastava, R.; Sapra, S.; and Kamalasanan, M. N. "Enhanced performance of organic photovoltaic devices by incorporation of tetrapod-shaped CdSe nanocrystals in polymer-fullerene systems." Physica Status Solidi A-Applications and Materials Science 210 (Apr 2013): 785-790.
- Ahmad, S., and Negi, P. S. "Coaxial microcalorimeter - National standard for microwave power up to 18 GHz at NPLI." Indian Journal of Pure & Applied Physics 52 (Mar 2014): 170-174.
- Ahmad, S.; Pal, B.; Negi, P. S.; and Bandyopadhyay, A. K. "Assigning RF/DC Transfer Difference to High Frequency Voltage Primary Standard up to 1 GHz at NPLI." Mapan-Journal of Metrology Society of India 28 (Jun 2013): 113-117.
- Ahmad, S.; Shah, J.; Puri, N. K.; Negi, P. S.; and Kotnala, R. K. "Influence on ferromagnetic resonance signal of perpendicular magnetic anisotropic Co/Pt bilayer thin film due to microwave induced spin-Hall effect." Applied Physics Letters 103 (Jul 2013): 5.
- Alen, S.; Sajan, D.; Vijayan, N.; Chaitanya, K.; Nemec, I.; and Jothy, V. B. "Growth, electronic absorption and vibrational spectral analysis of semiorganic nonlinear optical material potassium acid phthalate: A scaled quantum mechanical force field study." Journal of Molecular Structure 1040 (May 2013): 155-163.
- Ali, M. A.; Srivastava, S.; Pandey, M. K.; Agrawal, V. V.; John, R.; and Malhotra, B. D. "Protein-

Conjugated Quantum Dots Interface: Binding Kinetics and Label-Free Lipid Detection." Analytical Chemistry 86 (Feb 2014): 1710-1718.

- Ali, M. A.; Srivastava, S.; Solanki, P. R.; Reddy, V.; Agrawal, V. V.; Kim, C.; John, R.; and Malhotra, B. D. "Highly Efficient Bienzyme Functionalized Nanocomposite-Based Microfluidics Biosensor Platform for Biomedical Application." Scientific Reports 3 (Sep 2013): 9.
- Aloysius, R. P.; Dhankhar, M.; and Kotnala, R. K. "Enhanced low field magnetoresistance in Sr_2Fe_{1-x} AgxMoO_6 double perovskite system." Journal of Alloys and Compounds 574 (Oct 2013): 335-339.
- Anandan, P.; Arivanandhan, M.; Hayakawa, Y.; Babu, D. R.; Jayavel, R.; Ravi, G.; and Bhagavannarayana, G. "Investigations on the growth aspects and characterization of semiorganic nonlinear optical single crystals of L-histidine and its hydrochloride derivative." Spectrochimica Acta Part A-Molecular and Biomolecular Spectroscopy 121 (Mar 2014): 508-513.
- Ansari, I. A.; Shahabuddin, M.; Alzayed, N. S.; Ziq, K. A.; Salem, A. F.; Awana, V. P. S.; and Kishan, H. "Enhancement of critical current density for nano (n)-ZnO doped MgB_2 superconductor." Physica C-Superconductivity and Its Applications 495 (Dec 2013): 208-212.
- Anshul, A.; Kotnala, R. K.; Aloysius, R. P.; Gupta, A.; and Basheed, G. A. "Magnetodielectric coupling in epitaxial Nd_2CoMnO_6 thin films with double perovskite structure." Journal of Applied Physics 115 (Feb 2014): 4.
- Anshul, A.; Kumar, A.; Gupta, B. K.; Kotnala, R. K.; Scott, J. F.; and Katiyar, R. S. "Photoluminescence and time-resolved spectroscopy in multiferroic $BiFeO_3$: Effects of electric fields and sample aging." Applied Physics Letters 102 (Jun 2013): 5.
- Arora, M., and Saini, P. "Overall expanded uncertainty estimation in polaron concentration of p-toluene sulfonic acid doped polyaniline by EPR spectroscopy." Indian Journal of Pure & Applied Physics 51 (Nov 2013): 758-764.
- Arora, P.; Awasthi, A.; Bharath, V.; Acharya, A.; Yadav, S.; Agarwal, A.; and Sen Gupta, A. "Atomic clocks: A brief history and current status of research in India." Pramana-Journal of Physics 82 (Feb 2014): 173-183.
- Arora, P.; Purnapatra, S. B.; Acharya, A.; Agarwal, A.; Yadav, S.; Pant, K.; and Sen Gupta, A. "NPLI Cesium Atomic Fountain Frequency Standard: Preliminary Results." Ieee Transactions on Instrumentation and Measurement 62 (Jul 2013): 2037-2042.
- Arya, G. S.; Kotnala, R. K.; and Negi, N. S. "Enhanced magnetic and magnetoelectric properties of In and Co codoped $BiFeO_3$ nanoparticles at room temperature." Journal of Nanoparticle Research 16 (Dec 2013): 11.
- Ashokkumar, M.; Narayanan, N. T.; Gupta, B. K.; Reddy, A. L. M.; Singh, A. P.; Dhawan, S. K.; Chandrasekaran, B.; Rawat, D.; Talapatra, S.; Ajayan, P. M.; and Thanikaivelan, P. "Conversion of Industrial Bio-Waste into Useful Nanomaterials." Acs Sustainable Chemistry & Engineering 1 (Jun 2013): 619-626.
- Awasthi, A. M.; Bhardwaj, S.; Awana, V. P. S.; Albisetti, A. F.; Giunchi, G.; and Narlikar, A. V. "Carrier transport in magnesium diboride: Role of nano-inclusions." Applied Physics Letters 103 (Sep 2013): 5.
- Babita; Satish; Singh, A.; and Saxena, A. K. "Determination and Validation of Average Value of National Standard of DC Voltage Using Different Methods at CSIR-NPLI." Mapan-Journal of Metrology Society of India 28 (Jun 2013): 99-104.
- Babita; Sharma, D. K.; Satish; Ansari, M. A.; and Saxena, A. K. "A versatile automation program using LabVIEW for low de current measurement." Journal of Scientific & Industrial Research 73 (Feb 2014): 91-94.
- Babu, V.; Pasha, S. K.; Gupta, G.; Majumdar, C. B.; and Choudhury, B. "Enzymatic Surface Modification of Polyacrylonitrile and Its Copolymers: Effects of Polymer Surface Area and Protein Adsorption." Fibers and Polymers 15 (Jan 2014): 24-29.
- Bamzai, K. K.; Kour, G.; Kaur, B.; Arora, M.; and Pant, R. P. "Infrared spectroscopic and electron paramagnetic resonance studies on Dy substituted magnesium ferrite." Journal of Magnetism and Magnetic Materials 345 (Nov 2013): 255-260.

- Bano, T.; Singh, S.; Gupta, N. C.; and John, T. "Solar global ultraviolet and broadband global radiant fluxes and their relationships with aerosol optical depth at New Delhi." International Journal of Climatology 33 (May 2013): 1551-1562.
- Bansal, S.; Pandya, D. K.; Kashyap, S. C.; and Haranath, D. "Growth ambient dependence of defects, structural disorder and photolumine scence in SnO_2 films deposited by reactive magnetron sputtering." Journal of Alloys and Compounds 583 (Jan 2014): 186-190.
- Barala, S. K.; Arora, M.; Puri, C.; Saini, K. K.; Kotnala, R. K.; and Saini, P. K. "Ferrofluid/ Activated Carbon Composites for Water Purification and EMI Shielding Applications." Magnetohydrodynamics 49 (Jul-Dec 2013): 277-281.
- Barrionuevo, D.; Ortega, N.; Kumar, A.; Chatterjee, R.; Scott, J. F.; and Katiyar, R. S. "Thickness dependent functional properties of $PbZ_{0.52}Ti_{0.48}O_3/La_{0.67}S_{0.33}Mn_{03}$ heterostructures." Journal of Applied Physics 114 (Dec 2013): 10.
- Batra, N.; Kumar, V. P.; Srivastava, S. K.; and Singh, P. K. "X-ray photoelectron spectroscopic study of silicon surface passivation in alcoholic iodine and bromine solutions." Journal of Renewable and Sustainable Energy 6 (Jan 2014): 10.
- Bhatia, R.; Gaur, J.; Jain, S.; Lal, A.; Tripathi, B.; Attri, P.; and Kaushik, N. K. "Synthetic Strategies for Free & Stable N-Heterocyclic Carbenes and Their Precursors." Mini-Reviews in Organic Chemistry 10 (May 2013): 180-197.
- Bhatt, R. C.; Singh, S. K.; Srivastava, P. C.; Agarwal, S. K.; and Awana, V. P. S. "Impact of sintering temperature on room temperature magneto-resistive and magneto-caloric properties of $Pr_{2/3}Sr_{1/3}Mn_{03}$." Journal of Alloys and Compounds 580 (Dec 2013): 377-381.
- Bhushan, R.; Dutta, K.; Agnihotri, R.; Rengarajan, R.; and Singh, S. P. "Decadal Variations in Oceanic Properties of the Arabian Sea Arabian Sea Water Column Since Geosecs." Radiocarbon 56 (2014): 313-325.
- Biscaras, J.; Bergeal, N.; Hurand, S.; Feuillet-Palma, C.; Rastogi, A.; Budhani, R. C.; Grilli, M.; Caprara, S.; and Lesueur, J. "Multiple quantum criticality in a two-dimensional superconductor." Nature Materials 12 (Jun 2013): 542-548.
- Bisht, A.; Chockalingam, S.; Tripathi, R. K.; Dwivedi, N.; Dayal, S.; Kumar, S.; Panwar, O. S.; Chand, J.; Singh, S.; and Kesarwani, A. "Improved surface properties of beta-SiAlON by diamond-like carbon coatings." Diamond and Related Materials 36 (Jun 2013): 44-50.
- Boopathi, K.; Ramasamy, P.; and Bhagavannarayana, G. "Growth and characterization of Cu (II) doped negatively soluble lithium sulfate monohydrate crystals." Journal of Crystal Growth 386 (Jan 2014): 32-37.
- Buch, Z.; Kumar, V.; Mamgain, H.; and Chawla, S. "Silver Nanoprisms Acting as Multipolar Nanoantennas under a Low-Intensity Infrared Optical Field Exciting Fluorescence from Eu^{3+}." Journal of Physical Chemistry Letters 4 (Nov 2013): 3834-3838.
- Caprara, S.; Biscaras, J.; Bergeal, N.; Bucheli, D.; Hurand, S.; Feuillet-Palma, C.; Rastogi, A.; Budhani, R. C.; Lesueur, J.; and Grilli, M. "Multiband superconductivity and nanoscale inhomogeneity at oxide interfaces." Physical Review B 88 (Jul 2013): 5.
- Chakraborty, B. R.; Shard, A. G.; Dalai, M. K.; and Sehgal, G. "Depth profiling of Irganox-3114 nanoscale delta layers in a matrix of Irganox-1010 using conventional Cs^+ and $O^{-2}(+)$ ion beams." Surface and Interface Analysis 46 (Jan 2014): 36-41.
- Chakraborty, M.; Sharma, C.; Pandey, J.; and Gupta, P. K. "Assessment of energy generation potentials of MSW in Delhi under different technological options." Energy Conversion and Management 75 (Nov 2013): 249-255.
- Chand, M.; Kumar, S.; Shankar, A.; Sonia; Jain, K.; Singh, S.; and Pant, R. P. "The Effect of size Distribution on Viscoelastic Properties of ferrofluid." Magnetohydrodynamics 49 (Jul-Dec 2013): 489-494.
- Chandran, A.; Prakash, J.; Naik, K. K.; Srivastava, A. K.; Dabrowski, R.; Czerwinski, M.; and Biradar, A. M. "Preparation and characterization of MgO nanoparticles/ ferroelectric liquid crystal composites for faster

display devices with improved contrast." Journal of Materials Chemistry C 2 (2014): 1844-1853.

- Charak, S., and Mehrotra, R. "Structural investigation of idarubicin-DNA interaction: Spectroscopic and molecular docking study." International Journal of Biological Macromolecules 60 (Sep 2013): 213-218.
- Chauhan, S.; Kumar, M.; Chhoker, S.; Katyal, S. C.; and Awana, V. P. S. "Structural, vibrational, optical and magnetic properties of sol-gel derived Nd doped ZnO nanoparticles." Journal of Materials Science-Materials in Electronics 24 (Dec 2013): 5102-5110.
- Chawla, S.; Saroha, M.; and Kotnala, R. K. "White Light Emitting Magnetic ZnO:Sm Nanoparticles Prepared by Inclusive Co-Precipitation Synthesis." Electronic Materials Letters 10 (Jan 2014): 73-80.
- Chawla, S.; Sharma, S.; and Kotnala, R. K. "Tailoring magnetic and photoluminescence properties in ZnS/ZnO core/shell nanostructures through Cr doping." Applied Surface Science 284 (Nov 2013): 33-39.
- Chawla, S.; Sharma, S.; and Shah, J. "Fabrication of ZnS:Cr nanoparticles with superparamagnetism and fluorescence properties." Materials Letters 108 (Oct 2013): 189-192.
- Christopher, N. R.; Singh, N.; Singh, S. K.; Gahtori, B.; Mishra, S. K.; Dhar, A.; and Awana, V. P. S. "Appreciable Magnetic Moment and Energy Density in Single-Step Normal Route Synthesized MnBi." Journal of Superconductivity and Novel Magnetism 26 (Nov 2013): 3161-3165.
- Dagar, J.; Yadav, V.; Tyagi, P.; Singh, R. K.; Suman, C. K.; and Srivastava, R. "Effect of reduction of trap charge carrier density in organic field effect transistors by surface treatment of dielectric layer." Journal of Applied Physics 114 (Dec 2013): 5.
- Daivajna, M. D.; Kumar, N.; Awana, V. P. S.; Gahtori, B.; Christopher, J. B.; Manjunath, S. O.; Syu, K. Z.; Kuo, Y. K.; and Rao, A. "Electrical, magnetic and thermal properties of $Pr_{0.6-x}Bi_xSr_{0.4}Mn_{0.3}$ manganites." Journal of Alloys and Compounds 588 (Mar 2014): 406-412.
- Datta, A.; Smith, P.; and Lal, R. "Effects of long-term tillage and drainage treatments on greenhouse gas fluxes from a corn field during the fallow period." Agriculture Ecosystems & Environment 171 (May 2013): 112-123.
- Dayal, S.; Kumar, S.; Dwivedi, N.; Chockalingam, S.; Rauthan, C. M. S.; and Panwar, O. S. "Structural and nano-mechanical properties of nanostructured diamond-like carbon thin films." Metals and Materials International 19 (May 2013): 405-410.
- Dey, K. K.; Kumar, P.; Yadav, R. R.; Dhar, A.; and Srivastava, A. K. "CuO nanoellipsoids for superior physicochemical response of biodegradable PVA." RSC Advances 4 (2014): 10123-10132.
- Dhiman, P.; Batoo, K. M.; Kotnala, R. K.; Chand, J.; and Singh, M. "Room temperature ferromagnetism and structural characterization of Fe,Ni co-doped ZnO nanocrystals." Applied Surface Science 287 (Dec 2013): 287-292.
- Dhiman, P.; Chand, J.; Kumar, A.; Kotnala, R. K.; Batoo, K. M.; and Singh, M. "Synthesis and characterization of novel Fe@ZnO nanosystem." Journal of Alloys and Compounds 578 (Nov 2013): 235-241.
- Dogra, A.; Chowdhury, P.; Ghosh, S. K.; Gupta, S. K.; and Ravikumar, G. "Planar Hall effect in electrodeposited CoCu/Cu multilayer." Applied Physics a-Materials Science & Processing 111 (Apr 2013): 323-328.
- Dogra, S.; Singh, J.; Sharma, N. D.; Samanta, K.; Poswal, H. K.; Sharma, S. M.; and Bandyopadhyay, A. K. "Phase progression via phonon modes in lanthanide dioxides under pressure." Vibrational Spectroscopy 70 (Jan 2014): 193-199.
- Dwivedi, N.; Kumar, S.; Carey, J. D.; Tripathi, R. K.; Malik, H. K.; and Dalai, M. K. "Influence of Silver Incorporation on the Structural and Electrical Properties of Diamond-Like Carbon Thin Films." ACS Applied Materials & Interfaces 5 (Apr 2013): 2725-2732.
- Dwivedi, N.; Kumar, S.; and Malik, H. K. "Role of base pressure on the structural and nano-mechanical properties of metal/diamond-like carbon bilayers." Applied Surface Science 274 (Jun 2013): 282-287.

- Evans, D. M.; Schilling, A.; Kumar, A.; Sanchez, D.; Ortega, N.; Katiyar, R. S.; Scott, J. F.; and Gregg, J. M. "Switching ferroelectric domain configurations using both electric and magnetic fields in Pb(Zr,Ti)O3-Pb(Fe,Ta)O3 single-crystal lamellae." Philosophical Transactions of the Royal Society A-Mathematical Physical and Engineering Sciences 372 (Feb 2014): 7.
- Ganguly, P.; Kumar, A.; Tripathi, S.; Haranath, D.; and Biradar, A. M. "Faster and highly luminescent ferroelectric liquid crystal doped with ferroelectric $BaTiO_3$ nanoparticles." Applied Physics Letters 102 (Jun 2013): 4.
- Gangwar, J.; Dey, K. K.; Tripathi, S. K.; Wan, M.; Yadav, R. R.; Singh, R. K.; Samta; and Srivastava, A. K. "NiO-based nanostructures with efficient optical and electrochemical properties for high-performance nanofluids." Nanotechnology 24 (Oct 2013): 15.
- Garg, N.; Kumar, A.; and Maji, S. "Parametric sensitivity analysis of factors affecting sound insulation of double glazing using Taguchi method." Applied Acoustics 74 (Dec 2013): 1406-1413.
- Garg, N.; Kumar, A.; and Maji, S. "Significance and implications of airborne sound insulation criteria in building elements for traffic noise abatement." Applied Acoustics 74 (Dec 2013): 1429-1435.
- Garg, N., and Maji, S. "Vibration induced due to Acoustic Excitation in Diffuse field conditions." Acoustics Australia 41 (Dec 2013): 219-224.
- Gaur, N.; Kumar, A.; Sanjid, M.A.; Chaudhary, K.P.; and Maji, S. "Reaffirmation of measurement incertainity in pressure sensitivity determinatiion of LS2P microphones by reciprocity method", Measurement 51)May 2014); 281-288.
- Gaur, A., and Kumar, P. "Effect of degradation on electronic properties of polymer solar cells." Polymers for Advanced Technologies 24 (Jul 2013): 630-637.
- Gaur, A., and Kumar, P. "Studies on stability of bi-functional P3HT:PCBM:rubrene optoelectronic devices." Applied Physics A-Materials Science & Processing 111 (Jun 2013): 877-886.
- Gaur, J.; Jain, S.; Bhatia, R.; Lal, A.; and Kaushik, N. K. "Synthesis and characterization of a novel copolymer of glyoxal dihydrazone and glyoxal dihydrazone bis(dithiocarbamate) and application in heavy metal ion removal from water." Journal of Thermal Analysis and Calorimetry 112 (May 2013): 1137-1143.
- Ghosh, B.; Ghosh, D.; Hussain, S.; Chakraborty, B. R.; Dalai, M. K.; Sehgal, G.; Bhara, R.; and Pal, A. K. "Utilization of residual $CdCl_2$ in CBD-CdS to realize grain growth in CdTe: A novel route." Materials Research Bulletin 48 (Nov 2013): 4711-4717.
- Goel, P.; Arora, M.; and Biradar, A. M. "Electro-optic switching in iron oxide nanoparticle embedded paramagnetic chiral liquid crystal via magneto-electric coupling." Journal of Applied Physics 115 (Mar 2014): 6.
- Goel, P.; Arora, M.; and Biradar, A. M. "Evolution of excitation wavelength dependent photoluminescence in nano-CeO_2 dispersed ferroelectric liquid crystals." RSC Advances 4 (2014): 11351-11356.
- Goel, P., and Biradar, A. M. "Atypical dielectric behavior in sol-gel derived fine grain PZT/CeO_2 nanocomposites." Journal of Physics and Chemistry of Solids 74 (Jun 2013): 854-861.
- Gope, J.; Kumar, S.; Sudhakar, S.; Lodhi, K.; Rauthan, C. M. S.; and Srivastava, P. C. "Influence of argon dilution on the growth of amorphous to ultra nanocrystalline silicon films using VHF PECVD process." Journal of Alloys and Compounds 577 (Nov 2013): 710-716.
- Gope, J.; Kumar, S.; Sudhakar, S.; Rauthan, C. M. S.; and Srivastava, P. C. "Effect of silane flow rate on structural, electrical and optical properties of silicon thin films grown by VHF PECVD technique." Materials Chemistry and Physics 141 (Aug 2013): 89-94.
- Grover, R.; Srivastava, R.; Kamalasanan, M. N.; and Mehta, D. S. "Light outcoupling efficiency enhancement in organic light emitting diodes using an organic scattering layer." Physica Status Solidi-Rapid Research Letters 8 (Jan 2014): 81-85.
- Grover, R.; Srivastava, R.; Kamalasanan, M. N.; and Mehta, D. S. "Multilayer thin film encapsulation for organic light emitting diodes." RSC Advances 4 (2014): 10808-10814.
- Grover, R.; Srivastava, R.; Kamalasanan, M. N.; and Mehta, D. S. "Novel organic electron

injection layer for efficient and stable organic light emitting diodes." Journal of Luminescence 146 (Feb 2014): 53-56.

- Gupta, A.; Singh, G.; Kumar, D.; Kishan, H.; and Budhani, R. C. "Giant coercivity enhancement and dimensional crossover of superconductivity in Co_2FeSi-NbN nanoscale bilayers." Applied Physics Letters 103 (Oct 2013): 5.
- Gupta, M.; Kotnala, R. K.; Khan, W.; Azam, A.; and Naqvi, A. H. "Magnetic, transport and magnetoresistance behavior of Ni doped $La_{0.67}Sr_{0.33}Mn_{1-x}Ni_xO_3$ (0.00 <= x <= 0.09) system." Journal of Solid State Chemistry 204 (Aug 2013): 205-212.
- Gupta, R.; Shah, J.; Chaudhary, S.; Singh, S.; and Kotnala, R. K. "Magnetoelectric coupling-induced anisotropy in multiferroic nanocomposite (1-x)$BiFeO_{3-x}BaTi_{03}$." Journal of Nanoparticle Research 15 (Sep 2013): 9.
- Gupta, R.; Singh, B. P.; Singh, V. N.; Gupta, T. K.; and Mathur, R. B. "Origin of radial breathing mode in multiwall carbon nanotubes synthesized by catalytic chemical vapor deposition." Carbon 66 (Jan 2014): 724-726.
- Gupta, T. K.; Singh, B. P.; Mathur, R. B.; and Dhakate, S. R. "Multi-walled carbon nanotube-graphene-polyaniline multiphase nanocomposite with superior electromagnetic shielding effectiveness." Nanoscale 6 (2014): 842-851.
- Gupta, T. K.; Singh, B. P.; Singh, V. N.; Teotia, S.; Singh, A. P.; Elizabeth, I.; Dhakate, S. R.; Dhawan, S. K.; and Mathur, R. B. "MnO_2 decorated graphene nanoribbons with superior permittivity and excellent microwave shielding properties." Journal of Materials Chemistry A 2 (2014): 4256-4263.
- Gupta, T. K.; Singh, B. P.; Teotia, S.; Katyal, V.; Dhakate, S. R.; and Mathur, R. B. "Designing of multiwalled carbon nanotubes reinforced polyurethane composites as electromagnetic interference shielding materials." Journal of Polymer Research 20 (Jun 2013): 7.
- Gupta, V.; Kyaw, A. K. K.; Wang, D. H.; Chand, S.; Bazan, G. C.; and Heeger, A. J. "Barium: An Efficient Cathode Layer for Bulk-heterojunction Solar Cells." Scientific Reports 3 (Jun 2013): 6.
- Gupta, V.; Upreti, T.; and Chand, S. "Efficient solution-processed small molecule: Cadmium selenide quantum dot bulk heterojunction solar cells." Applied Physics Letters 103 (Dec 2013): 5.
- Hashim, M.; Alimuddin; Kumar, S.; Shirsath, S. E.; Kotnala, R. K.; Shah, J.; and Kumar, R. "Synthesis and characterizations of Ni^{2+} substituted cobalt ferrite nanoparticles." Materials Chemistry and Physics 139 (May 2013): 364-374.
- Hashim, M.; Alimuddin; Shirsath, S. E.; Kotnala, R. K.; Meena, S. S.; Kumar, S.; Roy, A.; Jotania, R. B.; Bhatt, P.; and Kumar, R. "Influence of $Ni2^+$ substitution on the structural, dielectric and magnetic properties of Cu-Cd ferrite nanoparticles." Journal of Alloys and Compounds 573 (Oct 2013): 198-204.
- Hashim, M.; Alimuddin; Shirsath, S. E.; Meena, S. S.; Kotnala, R. K.; Kumar, S.; Bhatt, P.; Jotania, R. B.; and Kumar, R. "Study of structural and magnetic properties of (Co-Cu)Fe_2O_4/PANI composites." Materials Chemistry and Physics 141 (Aug 2013): 406-415.
- Hashim, M.; Alimuddin; Shirsath, S. E.; Meena, S. S.; Kotnala, R. K.; Parveen, A.; Roy, A. S.; Kumar, S.; Bhatt, P.; and Kumar, R. "Investigation of structural, dielectric, magnetic and antibacterial activity of Cu-Cd-Ni-FeO_4 nanoparticles." Journal of Magnetism and Magnetic Materials 341 (Sep 2013): 148-157.
- Hirtz, M.; Kumar, N.; and Chi, L. F. "Simulation Modeling of Supported Lipid Membranes - A Review." Current Topics in Medicinal Chemistry 14 (Mar 2014): 617-623.
- Jain, S. K.; Titus, S. S. K.; Kumar, R.; and Jain, K. K. "Design, development and fabrication of 50 kN force standard machines to provide national traceability in force measurement to the industries." Journal of Scientific & Industrial Research 72 (Jun 2013): 333-339.
- Jangir, D. K.; Kundu, S.; and Mehrotra, R. "Role of Minor Groove Width and Hydration Pattern on Amsacrine Interaction with DNA." Plos One 8 (Jul 2013): 9.
- Jayanthi, K.; Manorama, S. V.; and Chawla, S. "Observation of Nd^{3+} visible line emission in ZnO: Nd^{3+} prepared by a controlled reaction in

the solid state." Journal of Physics D-Applied Physics 46 (Aug 2013): 7.

- Jha, P. K.; Jha, P. A.; Srivastava, G.; Jha, A. K.; Kotnala, R. K.; and Dwivedi, R. K. "Analytical comparison of magnetic and electrical properties using modified Landau theory in bismuth ferrite: Effect of milling." Journal of Magnetism and Magnetic Materials 349 (Jan 2014): 95-99.
- Jha, R., and Awana, V. P. S. "Effect of Se doping in recently discovered layered $Bi_4O_4S_3$ superconductor." Physica C-Superconductivity and Its Applications 498 (Mar 2014): 45-49.
- Jha, R., and Awana, V. P. S. "Superconductivity in Layered $CeO_{0.5}F_{0.5}BiS_2$." Journal of Superconductivity and Novel Magnetism 27 (Jan 2014): 1-4.
- Jha, R.; Jyoti, J.; and Awana, V. P. S. "Impact of Gd Doping on Morphology and Superconductivity of NbN Sputtered Thin Films." Journal of Superconductivity and Novel Magnetism 26 (Oct 2013): 3069-3074.
- Jha, R.; Kishan, H.; and Awana, V. P. S. "Superconducting and magneto-transport properties of BiS_2 based superconductor $PrO_{1-x}F_xBiS_2$ (x=0 to 0.9)." Journal of Applied Physics 115 (Jan 2014): 6.
- Jha, R.; Rani, P.; and Awana, V. P. S. "Revisiting Heat Capacity of Bulk Polycrystalline $YBa_2Cu_3O_7$-delta." Journal of Superconductivity and Novel Magnetism 27 (Feb 2014): 287-291.
- Jones, A. P.; Crain, J.; Cipcigan, F. S.; Sokhan, V. P.; Modani, M.; and Martyna, G. J. "Electronically coarse-grained moleculer dynamics using quantum Drude oscillators." Molecular Physics 111 (Dec 2013): 3465-3477.
- Joshi, D.; Gupta, R.; Kumar, A.; Kumar, Y.; and Yadav, S. "A Precision Ultrasonic Phase Velocity Measurement Technique for Liquids." Mapan-Journal of Metrology Society of India 29 (Mar 2014): 9-17.
- Joshi, D.; Kumar, A.; Gupta, R.; and Yadav, S. "Sensitivity Enhancement of Concurrent Technique of Acoustic Impedance Measurement." Mapan-Journal of Metrology Society of India 28 (Jun 2013): 79-83.
- Joshi, T.; Ganguly, P.; Haranath, D.; Singh, S.; and Biradar, A. M. "Tuning the photoluminescence of ferroelectric liquid crystal by controlling the size of dopant ZnO quantum dots." Materials Letters 114 (Jan 2014): 156-158.
- Joshi, T.; Singh, S.; Choudhary, A.; Pant, R. P.; and Biradar, A. M. "Mechanism of homeotropic alignment of ferroelectric liquid crystals doped with ferro-fluid and applications." Applied Physics Letters 103 (Jul 2013): 5.
- Kala, S.; Theissmann, R.; and Kruis, F. E. "Generation of AuGe nanocomposites by co-sparking technique and their photo-luminescence properties." Journal of Nanoparticle Research 15 (Sep 2013): 12.
- Kalaiselvi, P.; Raj, S. A. C.; Vijayan, N.; and Haranath, D. "Growth structural, spectral, optical and mechanical studies of gamma bis glycinium oxalate ($GBGO_x$) new NLO single crystal by SEST method." Optik 125 (2014): 1825-1828.
- Katna, A. K.; Kotnala, R. K.; and Negi, N. S. "Acceptor dependent structural, micro-structural and dielectric properties of $PbTiO_3$ nano-particles." Physica B-Condensed Matter 425 (Sep 2013): 95-99.
- Kaur, A.; Saharan, R.; and Dhawan, S. K. "Investigation of charge transport properties in conducting copolymers of aniline with 3-aminobenzenesulfonic acid for their applications as antistatic encapsulation materials blended with low-density polyethylene." Polymer International 63 (Feb 2014): 252-257.
- Kaur, D.; Chaudhary, S.; Pandya, D. K.; Gupta, R.; and Kotnala, R. K. "Magnetization reversal studies in structurally tailored cobalt nanowires." Journal of Magnetism and Magnetic Materials 344 (Oct 2013): 72-78.
- Kedawat, G.; Srivastava, S.; Jain, V. K.; Kumar, P.; Kataria, V.; Agrawal, Y.; Gupta, B. K.; and Vijay, Y. K. "Fabrication of Artificially Stacked Ultrathin ZnS/MgF_2 Multilayer Dielectric Optical Filters." ACS Applied Materials & Interfaces 5 (Jun 2013): 4872-4877.
- Kefi, S.; Guttal, V.; Brock, W. A.; Carpenter, S. R.; Ellison, A. M.; Livina, V. N.; Seekell, D. A.; Scheffer, M.; van Nes, E. H.; and Dakos, V. "Early Warning Signals of Ecological Transitions:

Methods for Spatial Patterns." Plos One 9 (Mar 2014): 13.

- Khan, F.; Baek, S. H.; Mobin, A.; and Kim, J. H. "Enhanced performance of silicon solar cells by application of low-cost sol-gel-derived Al-rich ZnO film." Solar Energy 101 (Mar 2014): 265-271.
- Khan, F.; Baek, S. H.; Singh, S. N.; Singh, P. K.; and Kim, J. H. "Effective passivation of silicon surface by AZO films: Application in bifacial solar cells." Solar Energy 97 (Nov 2013): 474-483.
- Kharkwal, A.; Sharma, S. N.; Jain, K.; Arora, L.; Chawla, P.; Singh, A. K.; and Chand, S. "Polymeric stabilization of hybrid nanocomposites: a comparison between in situ and ex situ-grown $CuInS_2$ in poly(3-hexylthiophene) polymer." Colloid and Polymer Science 291 (Nov 2013): 2607-2617.
- Kotnala, R. K.; Shah, J.; and Gupta, R. "Colossal humidoresistance in ceria added magnesium ferrite thin film by pulsed laser deposition." Sensors and Actuators B-Chemical 181 (May 2013): 402-409.
- Krishna, A.; Vijayan, N.; Riscob, B.; Gour, B. S.; Haranath, D.; Philip, J.; Verma, S.; Jayalakshmy, M. S.; Bhagavannarayana, G.; and Halder, S. K. "Phase matching, X-Ray topography, optical and thermal analysis of L-alanine cadmium chloride monohydrate: a nonlinear optical material." Applied Physics A-Materials Science & Processing 114 (Mar 2014): 1257-1265.
- Krishnakumar, V.; Satyanarayana, M.; Radhakrishnan, S. R.; Dhaman, R. K.; Jayeshlal, G. S.; Motty, G. N. S.; Pillai, V. P. M.; Raghunath, K.; Ratnam, M. V.; Rao, D. R.; and Sudhakar, P. "Lidar investigations on the optical and dynamical properties of cirrus clouds in the upper troposphere and lower stratosphere regions at a tropical station, Gadanki, India (13.5 degrees N, 79.2 degrees E)." Journal of Applied Remote Sensing 8 (Mar 2014): 21.
- Krishnan, P.; Gayathri, K.; Bhagavannarayana, G.; Jayaramakrishnan, V.; Gunasekaran, S.; and Anbalagan, G. "Growth, spectral, thermal, dielectric, mechanical, linear and nonlinear optical, birefringence, laser damage threshold studies of semi-organic crystal: Dibrucinium sulfate heptahydrate." Spectrochimica Acta Part A-Molecular and Biomolecular Spectroscopy 112 (Aug 2013): 152-160.
- Kumar, A.; Scott, J. F.; and Katiyar, R. S. "Dynamic nanocrystal response and high temperature growth of carbon nanotube-ferroelectric hybrid nanostructure." Nanoscale 6 (2014): 1064-1070.
- Kumar, A.; Singh, R. K.; Agarwal, K.; Singh, H. K.; Srivastava, P.; and Singh, R. "Effect of p-toluenesulfonate on inhibition of overoxidation of polypyrrole." Journal of Applied Polymer Science 130 (Oct 2013): 434-442.
- Kumar, A.; Singh, R. K.; Singh, H. K.; Srivastava, P.; and Singh, R. "Enhanced capacitance and stability of p-toluenesulfonate doped polypyrrole/carbon composite for electrode application in electrochemical capacitors." Journal of Power Sources 246 (Jan 2014): 800-807.
- Kumar, A.; Singh, R. K.; Singh, H. K.; Srivastava, P.; and Singh, R. "Mechanism of direct current electrical charge conduction in p-toluenesulfonate doped polypyrrole/carbon composites." Journal of Applied Physics 115 (Mar 2014): 9.
- Kumar, A.; Srivastava, R.; Nishal, V.; Kadyan, P. S.; Kamalasanan, M. N.; and Singh, I. "Ternary zinc complexes as electron transport and electroluminescent materials." Journal of Organometallic Chemistry 740 (Sep 2013): 116-122.
- Kumar, A.; Tandon, R. P.; and Awana, V. P. S. "Spin dynamics, short-range order and superparamagnetism in superconducting ferromagnet $RuSr_2Gd_{1.4}Ce_{0.6}Cu_2O_{10}$ $^{-delta}$." Journal of Magnetism and Magnetic Materials 349 (Jan 2014): 224-231.
- Kumar, A.; Tripathi, S.; Deshmukh, A. D.; Haranath, D.; Singh, P.; and Biradar, A. M. "Time evolution photoluminescence studies of quantum dot doped ferroelectric liquid crystals." Journal of Physics D-Applied Physics 46 (May 2013): 7.
- Kumar, A.; Tyagi, P.; Reddy, M. A.; Mallesham, G.; Bhanuprakash, K.; Rao, V. J.; Kamalasanan, M. N.; and Srivastava, R. "Chemical structure dependent electron transport in 9,10-bis(2-phenyl-1,3,4-oxadiazole) derivatives of

anthracene." RSC Advances 4 (2014): 12206-12215.

- Kumar, A.; Tyagi, P.; Srivastava, R.; Mehta, D. S.; and Kamalasanan, M. N. "Energy transfer process between exciton and surface plasmon: Complete transition from Forster to surface energy transfer." Applied Physics Letters 102 (May 2013): 5.
- Kumar, D.; Joshi, P. C.; Hossain, Z.; and Budhani, R. C. "Spin polarized carrier injection from full Heusler alloy Co_2MnSi into superconduting NbN (vol 102, pg 112409, 2013)." Applied Physics Letters 103 (Oct 2013): 1.
- Kumar, G.; Sharma, S.; Kotnala, R. K.; Shah, J.; Shirsath, S. E.; Batoo, K. M.; and Singh, M. "Electric, dielectric and ac electrical conductivity study of nanocrystalline cobalt substituted Mg-Mn ferrites synthesized via solution combustion technique." Journal of Molecular Structure 1051 (Nov 2013): 336-344.
- Kumar, H., and Kumar, A. "Metrological performance evaluation of force standard machines using intercomparison as a measure at National Physical Laboratory, India." Current Science 105 (Oct 2013): 1138-1143.
- Kumar, H., and Sharma, C. "Experimental investigations of different force measuring systems." Indian Journal of Pure & Applied Physics 51 (Jun 2013): 393-398.
- Kumar, H.; Sharma, C.; and Kumar, A. "The development and characterization of a square ring shaped force transducer." Measurement Science & Technology 24 (Sep 2013): 9.
- Kumar, J.; Sharma, D.; Ahluwalia, P. K.; and Awana, V. P. S. "Enhanced superconducting performance of melt quenched $Bi_2Sr_2CaCu_2O_8$ (Bi-2212) superconductor." Materials Chemistry and Physics 139 (May 2013): 681-688.
- Kumar, M. K.; Sudhahar, S.; Pandi, P.; Bhagavannarayana, G.; and Kumar, R. M. "Studies of the structural and third-order nonlinear optical properties of solution grown 4-hydroxy-3-methoxy-4 '-N '-methylstilbazolium tosylate monohydrate crystals." Optical Materials 36 (Mar 2014): 988-995.
- Kumar, M.; Pasha, S. K.; and Govind. "Kinetically controlled growth of gallium on stepped Si (553) surface." Applied Surface Science 283 (Oct 2013): 1071-1075.
- Kumar, M.; Shankar, S.; Kotnala, R. K.; and Parkash, O. "Evidences of magneto-electric coupling in BFO-BT solid solutions." Journal of Alloys and Compounds 577 (Nov 2013): 222-227.
- Kumar, M.; Singh, K.; Dhawan, S. K.; Tharanikkarasu, K.; Chung, J. S.; Kong, B. S.; Kim, E. J.; and Hur, S. H. "Synthesis and characterization of covalently-grafted graphene-polyaniline nanocomposites and its use in a supercapacitor." Chemical Engineering Journal 231 (Sep 2013): 397-405.
- Kumar, N.; Aloysius, R. P.; Gaur, A.; and Kotnala, R. K. "Study of ferromagnetic-metal type Sr_2FeMoO_6 + xAg (x=0-10 wt%) composites." Journal of Alloys and Compounds 559 (May 2013): 64-68.
- Kumar, N.; Khurana, G.; Gaur, A.; and Kotnala, R. K. "Room temperature low field magnetoresistance in $Sr_2FeMoO_6/Zn_xFe1_{-x}Fe_2O_4$ composites." Journal of Applied Physics 114 (Aug 2013): 5.
- Kumar, N.; Misra, P.; Kotnala, R. K.; Gaur, A.; and Katiyar, R. S. "Room temperature magnetoresistance in $Sr_2FeMoO_6/SrTiO_3/Sr_2FeMoO_6$ trilayer devices." Journal of Physics D-Applied Physics 47 (Feb 2014): 5.
- Kumar, N.; Misra, P.; Kotnala, R. K.; Gaur, A.; Rawat, R.; Choudhary, R. J.; and Katiyar, R. S. "Polycrystalline Sr_2FeMoO_6 thin films on Si substrate by pulsed laser deposition for magnetoresistive applications." Materials Letters 118 (Mar 2014): 200-203.
- Kumar, N.; Srivastava, A. K.; Nath, R.; Gupta, B. K.; and Varma, G. D. "Probing the highly efficient room temperature ammonia gas sensing properties of a luminescent ZnO nanowire array prepared via an AAO-assisted template route." Dalton Transactions 43 (2014): 5713-5720.
- Kumar, P.; Dogra, A.; and Toutam, V. "Pinhole mediated electrical transport across $LaTiO_3/SrTiO_3$ and $LaAlO_3/SrTiO_3$ oxide hetero-structures." Applied Physics Letters 103 (Nov 2013): 4.
- Kumar, P.; Gupta, A.; Dhakate, S. R.; Mathur, R. B.; Nagar, S.; and Gupta, V. K. "Covalent

immobilization of xylanase produced from Bacillus pumilus SV-85S on electrospun polymethyl methacrylate nanofiber membrane." Biotechnology and Applied Biochemistry 60 (Mar-Apr 2013): 162-169.

- Kumar, P.; Kumar, M.; and Shivaprasad, S. M. "Residual thermal desorption studies of Ga adatoms on trenched Si(5512) surface." Applied Surface Science 282 (Oct 2013): 348-350.
- Kumar, P.; Sharma, A.; and Singh, D. P. "Effect of voltage sweep direction on the performance evaluation of P3HT:PCBM solar cells." Progress in Photovoltaics 21 (Aug 2013): 950-959.
- Kumar, R.; Dhakate, S. R.; and Mathur, R. B. "The role of ferrocene on the enhancement of the mechanical and electrochemical properties of coal tar pitch-based carbon foams." Journal of Materials Science 48 (Oct 2013): 7071-7080.
- Kumar, R.; Kumar, A.; Singh, S.; and Pandey, O. P. "Reduction of WO_3 to WC nanoparticles by the reflux reaction." Materials Science 49 (Jul 2013): 102-109.
- Kumar, R.; Shanker, R.; Kotnala, R. K.; and Chawla, S. "Luminomagnetic $K_2Gd_{1-x}Zr(PO_4)_3$: xTb^{3+} phosphor with intense green fluorescence and paramagnetism." Physica Status Solidi A-Applications and Materials Science 210 (Sep 2013): 1933-1937.
- Kumar, S. A.; Bhandari, H.; Sharma, C.; Khatoon, F.; and Dhawan, S. K. "A new smart coating of polyaniline-SiO_2 composite for protection of mild steel against corrosion in strong acidic medium." Polymer International 62 (Aug 2013): 1192-1201.
- Kumar, S.; Ali, M. A.; Anand, P.; Agrawal, V. V.; John, R.; Maji, S.; and Malhotra, B. D. "Microfluidic-integrated biosensors: Prospects for point-of-care diagnostics." Biotechnology Journal 8 (Nov 2013): 1267-1279.
- Kumar, S., and Kumar, H. "Development and Testing of Ring Shaped Force Transducers." Journal of Scientific & Industrial Research 73 (Feb 2014): 103-106.
- Kumar, S.; Vandana; Rauthan, C. M. S.; Kaul, V. K.; Singh, S. N.; and Singh, P. K. "Spectral and Injection Level Dependence of Recombination Lifetimes in Silicon Measured by Impedance Spectroscopy." IEEE Journal of Photovoltaics 4 (Jan 2014): 380-386.
- Kumar, V.; Gaur, A.; and Kotnala, R. K. "Comparative study of room temperature and low temperature magnetization and magnetoelectric coupling behavior of Ti and Pr doped $BiFeO_3$." Superlattices and Microstructures 67 (Mar 2014): 233-241.
- Kumar, V.; Gaur, A.; Sharma, N.; Shah, J.; and Kotnala, R. K. "High temperature dielectric and magnetic response of Ti and Pr doped $BiFeO_3$ ceramics." Ceramics International 39 (Sep 2013): 8113-8121.
- Kumar, V.; Khan, A. F.; and Chawla, S. "Intense red-emitting multi-rare-earth doped nanoparticles of YVO_4 for spectrum conversion towards improved energy harvesting by solar cells." Journal of Physics D-Applied Physics 46 (Sep 2013): 9.
- Kumar, V.; Singh, S.; Kotnala, R. K.; and Chawla, S. "$GdPO_4$:Eu^{3+} nanoparticles with intense orange red emission suitable for solar spectrum conversion and their multifunctionality." Journal of Luminescence 146 (Feb 2014): 486-491.
- Kumar, V.; Srivastava, S.; Umrao, S.; Kumar, R.; Nath, G.; Sumana, G.; Saxena, P. S.; and Srivastava, A. "Nanostructured palladium-reduced graphene oxide platform for high sensitive, label free detection of a cancer biomarker." RSC Advances 4 (2014): 2267-2273.
- Kushvaha, S. S.; Kumar, M. S.; Maurya, K. K.; Dalai, M. K.; and Sharma, N. D. "Highly c-axis oriented growth of GaN film on sapphire (0001) by laser molecular beam epitaxy using HVPE grown GaN bulk target." AIP Advances 3 (Sep 2013): 10.
- Kushvaha, S. S.; Pal, P.; Shukla, A. K.; Joshi, A. G.; Gupta, G.; Kumar, M.; Singh, S.; Gupta, B. K.; and Haranath, D. "Effect of growth temperature on defects in epitaxial GaN film grown by plasma assisted molecular beam epitaxy." AIP Advances 4 (Feb 2014): 9.
- Kyaw, A. K. K.; Wang, D. H.; Gupta, V.; Zhang, J.; Chand, S.; Bazan, G. C.; and Heeger, A. J. "Efficient Solution-Processed Small-Molecule Solar Cells with Inverted Structure." Advanced Materials 25 (May 2013): 2397-2402.

- Love, J. A.; Nagao, I.; Huang, Y.; Kuik, M.; Gupta, V.; Takacs, C. J.; Coughlin, J. E.; Qi, L.; van der Poll, T. S.; Kramer, E. J.; Heeger, A. J.; Nguyen, T. Q.; and Bazan, G. C. "Silaindacenodithiophene-Based Molecular Donor: Morphological Features and Use in the Fabrication of Compositionally Tolerant, High-Efficiency Bulk Heterojunction Solar Cells." Journal of the American Chemical Society 136 (Mar 2014): 3597-3606.
- Majumder, M.; Ghoshray, K.; Ghoshray, A.; Pal, A.; and Awana, V. P. S. "Local electromagnetic properties of magnetic pnictides: a comparative study probed by NMR measurements." Journal of Physics-Condensed Matter 25 (May 2013): 10.
- Mallesham, G.; Balaiah, S.; Reddy, M. A.; Sridhar, B.; Singh, P.; Srivastava, R.; Bhanuprakash, K.; and Rao, V. J. "Design and synthesis of novel anthracene derivatives as n-type emitters for electroluminescent devices: a combined experimental and DFT study." Photochemical & Photobiological Sciences 13 (2014): 342-357.
- Mathur, S.; Vyas, R.; Jain, R.; Kumar, P.; Sachdev, K.; and Sharma, S. K. "Comment on Electrochemical behavior of different structural states of the alloy Ti_6ONi_4O and related works Response." Journal of Non-Crystalline Solids 376 (Sep 2013): 235-236.
- Mathur, S.; Vyas, R.; Jain, R.; Kumar, P.; Sachdev, K.; and Sharma, S. K. "Effect of ion beam irradiation on the corrosion behavior of the melt spun ribbon Ti_6ONi_4O." Journal of Non-Crystalline Solids 376 (Sep 2013): 238-238.
- Maurya, D.; Kumar, A.; Petkov, V.; Mahaney, J. E.; Katiyar, R. S.; and Priya, S. "Local structure and piezoelectric instability in lead-free (1-x) $BaTiO_{3-x}$ $A(Cu_{1/3}Nb_{2/3})O^{-3}$ (A = Sr, Ca, Ba) solid solutions." RSC Advances 4 (2014): 1283-1292.
- Meena, R. S.; Pal, A.; Kumar, S.; Rao, K. V. R.; and Awana, V. P. S. "Magneto-transport and Magnetic Susceptibility of $SmFeAsO_{1-x}F_x$ (x=0.0 and 0.20)." Journal of Superconductivity and Novel Magnetism 26 (Jul 2013): 2383-2389.
- Meena, R. S.; Pal, A.; Rao, K. V. R.; Kishan, H.; and Awana, V. P. S. "Electrical and Magnetic Behaviour of $PrFeAsO_{0.8}F_{0.2}$ Superconductor." Journal of Superconductivity and Novel Magnetism 27 (Mar 2014): 687-691.
- Mehrotra, R.; Jangir, D. K.; Agarwal, S.; Ray, B.; Singh, P.; and Srivastava, A. K. "Interaction Studies of Anticancer Drug Lomustine with Calf Thymus DNA using Surface Enhanced Raman Spectroscopy." Mapan-Journal of Metrology Society of India 28 (Dec 2013): 273-277.
- Mehta, A.; Sharma, S. N.; Chawla, P.; and Chand, S. "Constraints in post-synthesis ligand exchange for hybrid organic (MEH-PPV)-inorganic (CdSe) nanocomposites." Colloid and Polymer Science 292 (Feb 2014): 301-315.
- Mehta, D. S.; Inam, M.; Prakash, J.; and Biradar, A. M. "Liquid-crystal phase-shifting lateral shearing interferometer with improved fringe contrast for 3D surface profilometry." Applied Optics 52 (Sep 2013): 6119-6125.
- Mishra, M.; Singh, A. P.; and Dhawan, S. K. "Expanded graphite-nanoferrite-fly ash composites for shielding of electromagnetic pollution." Journal of Alloys and Compounds 557 (Apr 2013): 244-251.
- Mondal, K.; Ali, M. A.; Agrawal, V. V.; Malhotra, B. D.; and Sharma, A. "Highly Sensitive Biofunctionalized Mesoporous Electrospun TiO_2 Nanofiber Based Interface for Biosensing." ACS Applied Materials & Interfaces 6 (Feb 2014): 2512-2523.
- Moorthy, K. K.; Beegum, S. N.; Srivastava, N.; Satheesh, S. K.; Chin, M.; Blond, N.; Babu, S. S.; and Singh, S. "Performance evaluation of chemistry transport models over India." Atmospheric Environment 71 (Jun 2013): 210-225.
- Morales, A. I.; Benzoni, G.; Gottardo, A.; Valiente-Dobon, J. J.; Blasi, N.; Bracco, A.; Camera, F.; Crespi, F. C. L.; Corsi, A.; Leoni, S.; Million, B.; Nicolini, R.; Wieland, O.; Gadea, A.; Lunardi, S.; Gorska, M.; Regan, P. H.; Podolyak, Z.; Pfutzner, M.; Pietri, S.; Boutachkov, P.; Weick, H.; Grebosz, J.; Bruce, A. M.; Nunez, J. A.; Algora, A.; Al-Dahan, N.; Ayyad, Y.; Alkhomashi, N.; Allegro, P. R. P.; Bazzacco, D.; Benlliure, J.; Bowry, M.; Bunce, M.; Casarejos, E.; Cortes, M. L.; Bacelar, A. M. D.; Deo, A. Y.; de Angelis, G.; Domingo-Pardo, C.; Doncel, M.; Dombradi, Z.; Engert, T.; Eppinger, K.; Farrelly, G. F.; Farinon, F.; Farnea, E.; Geissel, H.; Gerl, J.; Goel, N.; Gregor, E.; Habermann, T.; Hoischen, R.; Janik, R.; Klupp, S.; Kojouharov, I.; Kurz, N.; Mandal, S.;

Menegazzo, R.; Mengoni, D.; Napoli, D. R.; Naqvi, F.; Nociforo, C.; Prochazka, A.; Prokopowicz, W.; Recchia, F.; Ribas, R. V.; Reed, M. W.; Rudolph, D.; Sahin, E.; Schaffner, H.; Sharma, A.; Sitar, B.; Siwal, D.; Steiger, K.; Strmen, P.; Swan, T. P. D.; Szarka, I.; Ur, C. A.; Walker, P. M.; and Wollersheim, H. J. "beta-decay studies of neutron-rich Tl, Pb, and Bi isotopes." Physical Review C 89 (Jan 2014): 13.

- Mukherjee, S.; Roy, A.; Auluck, S.; Prasad, R.; Gupta, R.; and Garg, A. "Room Temperature Nanoscale Ferroelectricity in Magnetoelectric $GaFeO_3$ Epitaxial Thin Films." Physical Review Letters 111 (Aug 2013): 5.
- Murali, M. G.; Dalimba, U.; Yadav, V.; and Srivastava, R. "New thiophene-based donoracceptor conjugated polymers carrying fluorene or cyanovinylene units: Synthesis, characterization, and electroluminescent properties." Polymer Engineering and Science 53 (Jun 2013): 1161-1170.
- Muthiah, S.; Pulikkotil, J.; Srivastava, A. K.; Kumar, A.; Pathak, B. D.; Dhar, A.; and Budhani, R. C. "Conducting grain boundaries enhancing thermoelectric performance in doped Mg_2Si." Applied Physics Letters 103 (Jul 2013): 5.
- Muthu, K.; Bhagavannarayana, G.; Mahadevan, C. K.; and Meenakshisundaram, S. P. "Growth and characterization of hexaaquacobalt(II) dipotassium tetrahydrogen tetra-o-phthalate tetrahydrate crystals." Materials Chemistry and Physics 139 (May 2013): 623-628.
- Narayana, T.; Subbaiah, Y. P. V.; Prathap, P.; Reddy, Y. B. K.; and Reddy, K. T. R. "Influence of sulfurization temperature on physical properties of Cu_2ZnSnS_4 thin films." Journal of Renewable and Sustainable Energy 5 (May 2013): 7.
- Narayanan, R.; Das, A.; Deepa, M.; and Srivastava, A. K. "Energy Relay from an Unconventional Yellow Dye to CdS/CdSe Quantum Dots for Enhanced Solar Cell Performance." Chemphyschem 14 (Dec 2013): 4010-4021.
- Narayanan, R.; Deepa, M.; Friebel, F.; and Srivastava, A. K. "A CdS/Bi_2S_3 bilayer and a poly(3,4-ethylenedioxythiophene)/S2- interface control quantum dot solar cell performance." Electrochimica Acta 105 (Aug 2013): 599-611.
- Nicolaidis, N.; Vaughan, B.; Mulligan, C. J.; Bryant, G.; Zillger, T.; Trnovec, B.; Hubler, A. C.; Holmes, N.; Cooling, N. A.; Griffith, M. J.; Bilen, C.; Kumar, P.; Feron, K.; Zhou, X. J.; Elkington, D.; Belcher, W. J.; and Dastoor, P. C. "Solution processable interface materials for nanoparticulate organic photovoltaic devices." Applied Physics Letters 104 (Jan 2014): 4.
- Nishal, V.; Kumar, A.; Kadyan, P. S.; Singh, D.; Srivastava, R.; Singh, I.; and Kamalasanan, M. N. "Synthesis, Characterization, and Electroluminescent Characteristics of Mixed-Ligand Zinc(II) Complexes." Journal of Electronic Materials 42 (Jun 2013): 973-978.
- Oksanen, E.; Pandey, V.; Pandey, A. K.; Keski-Saari, S.; Kontunen-Soppela, S.; and Sharma, C. "Impacts of increasing ozone on Indian plants." Environmental Pollution 177 (Jun 2013): 189-200.
- Ortega, N.; Kumar, A.; Resto, O.; Maslova, O. A.; Yuzyuk, Y. I.; Scott, J. F.; and Katiyar, R. S. "Compositional engineering of $BaTiO_3$/$(Ba,Sr)TiO_3$ ferroelectric superlattices." Journal of Applied Physics 114 (Sep 2013): 9.
- Palai, A. K.; Kumar, A.; Shashidhara, K.; and Mishra, S. P. "Polyalkylthiophene-containing electron donor and acceptor heteroaromatic bicycles: synthesis, photo-physical, and electroluminescent properties." Journal of Materials Science 49 (Mar 2014): 2456-2464.
- Pande, S.; Chaudhary, A.; Patel, D.; Singh, B. P.; and Mathur, R. B. "Mechanical and electrical properties of multiwall carbon nanotube/polycarbonate composites for electrostatic discharge and electromagnetic interference shielding applications." RSC Advances 4 (2014): 13839-13849.
- Pandey, B. K.; Shahi, A. K.; Shah, J.; Kotnala, R. K.; and Gopal, R. "Optical and magnetic properties of Fe_2O_3 nanoparticles synthesized by laser ablation/fragmentation technique in different liquid media." Applied Surface Science 289 (Jan 2014): 462-471.
- Pandey, H., and Budhani, R. C. "Structural ordering driven anisotropic magnetoresistance, anomalous Hall resistance, and its topological overtones in full-Heusler Co_2MnSi thin films." Journal of Applied Physics 113 (May 2013): 9.
- Pandey, H.; Rout, P. K.; Anupam; Joshi, P. C.; Hossain, Z.; and Budhani, R. C. "Magnetoelastic

coupling induced magnetic anisotropy in Co_2(Fe/Mn)Si thin films." Applied Physics Letters 104 (Jan 2014): 5.

- Pandey, M.; Mishra, P.; Saha, D.; Sengupta, K.; Jain, K.; and Islam, S. S. "Nanoporous alumina (gamma- and alpha-phase) gel cast thick film for the development of trace moisture sensor." Journal of Sol-Gel Science and Technology 68 (Nov 2013): 317-323.
- Pandey, S. D.; Samanta, K.; Singh, J.; Sharma, N. D.; and Bandyopadhyay, A. K. "Anharmonic behavior and structural phase transition in Yb_2O_3." AIP Advances 3 (Dec 2013): 11.
- Pandi, P.; Peramaiyan, G.; Kumar, R. M.; Bhagavannarayana, G.; and Jayavel, R. "Studies of structural, third order nonlinear optical and laser damage threshold properties of diethylammonium p-hydroxybenzoate single crystal." Applied Physics A-Materials Science & Processing 112 (Sep 2013): 711-717.
- Panwar, O. S.; Kesarwani, A. K.; Dhakate, S. R.; Singh, B. P.; Rakshit, R. K.; Bisht, A.; and Chockalingam, S. "Few layer graphene synthesized by filtered cathodic vacuum arc technique." Journal of Vacuum Science & Technology B 31 (Jul 2013): 5.
- Patel, M. K.; Ali, M. A.; Agrawal, V. V.; Ansari, Z. A.; Ansari, S. G.; and Malhotra, B. D. "Nanostructured magnesium oxide biosensing platform for cholera detection." Applied Physics Letters 102 (Apr 2013): 5.
- Patel, M. K.; Ali, M. A.; Srivastava, S.; Agrawal, V. V.; Ansari, S. G.; and Malhotra, B. D. "Magnesium oxide grafted carbon nanotubes based impedimetric genosensor for biomedical application." Biosensors & Bioelectronics 50 (Dec 2013): 406-413.
- Patel, M. K.; Ali, M. A.; Zafaryab, M.; Agrawal, V. V.; Rizvi, M. M. A.; Ansari, Z. A.; Ansari, S. G.; and Malhotra, B. D. "Biocompatible nanostructured magnesium oxide-chitosan platform for genosensing application." Biosensors & Bioelectronics 45 (Jul 2013): 181-188.
- Pavunny, S. P.; Kumar, A.; Misra, P.; Scott, J. F.; and Katiyar, R. S. "Properties of the new electronic device material $LaGdO_3$." Physica Status Solidi B-Basic Solid State Physics 251 (Jan 2014): 131-139.
- Pavunny, S. P.; Misra, P.; Thomas, R.; Kumar, A.; Schubert, J.; Scott, J. F.; and Katiyar, R. S. "Advanced high-k gate dielectric amorphous $LaGdO_3$ gated metal-oxide-semiconductor devices with sub-nanometer equivalent oxide thickness." Applied Physics Letters 102 (May 2013): 5.
- Peramaiyan, G.; Pandi, P.; Vijayan, N.; Bhagavannarayana, G.; and Kumar, R. M. "Crystal growth, structural, thermal, optical and laser damage threshold studies of 8-hydroxyquinolinium hydrogen maleate single crystals." Journal of Crystal Growth 375 (Jul 2013): 6-9.
- Prasad, Mvsn; Sharma, C.; Arya, B. C.; Mandal, T. K.; Singh, S.; Kulshrestha, M. J.; Agnihotri, R.; Mishra, S. K.; and Sharma, S. K. "Experimental Facilities to Monitor Various Types of Atmospheric Parameters in the Radio and Atmospheric Sciences Division (RASD) of CSIR-National Physical Laboratory." Mapan-Journal of Metrology Society of India 28 (Sep 2013): 193-203.
- Prathap, P.; Bartringer, J.; and Slaoui, A. "Selective emitter formation by laser doping of spin-on sources." Applied Surface Science 278 (Aug 2013): 173-179.
- Puri, N.; Mishra, S. K.; Niazi, A.; Biradar, A. M.; and Rajesh. "Structural and impedance spectroscopic studies on biofunctionalized poly(pyrrole-co-pyrrolepropylic acid) film." Synthetic Metals 169 (Apr 2013): 18-24.
- Purnapatra, S. B.; Arora, P.; Yadav, S.; Agarwal, A.; and Sen Gupta, A. "Characterization of laser beams for cesium atomic fountain experiment." Indian Journal of Pure & Applied Physics 51 (Sep 2013): 615-620.
- Putra, A.; Campbell, D. L.; Price, R. M.; De, S.; and Spielman, I. B. "Optimally focused cold atom systems obtained using density-density correlations." Review of Scientific Instruments 85 (Jan 2014): 6.
- Rajesh; Puri, N.; Mishra, S. K.; Laskar, M. J.; and Srivastava, A. K. "Microstructural and Potential Dependence Studies of Urease-Immobilized Gold Nanoparticles-Polypyrrole Composite Film for Urea Detection." Applied Biochemistry and Biotechnology 172 (Jan 2014): 1055-1069.

- Rajesh; Sharma, V.; Puri, N. K.; Singh, R. K.; Biradar, A. M.; and Mulchanadani, A. "Label-free detection of cardiac troponin-I using gold nanoparticles functionalized single-walled carbon nanotubes based chemiresistive biosensor." Applied Physics Letters 103 (Nov 2013): 4.
- Rajeswari, R.; Jyothi, L.; Jayasankar, C. K.; Babu, S. S.; Vijayan, N.; and Haranath, D. "Synthesis, Structural and Luminescent Properties of Novel Eu^{3+}:Y_2CaZnO_5 Nanophosphor for White Light-Emitting Diodes." Science of Advanced Materials 5 (Nov 2013): 1539-1545.
- Ramanujam, J., and Verma, A. "High-efficiency, low cost Si solar cells." Abstracts of Papers of the American Chemical Society 245 (Apr 2013): 1.
- Rani, A., and Singh, Y. P. "Comparison of Transfer Standard Industrial Lamps against PTB-assigned Radiance Temperature of Vacuum and Gas Filled Tungsten Strip Lamps." Mapan-Journal of Metrology Society of India 28 (Jun 2013): 129-140.
- Rani, A.; Upadhyay, R. S.; and Singh, Y. P. "Investigating Temperature Distribution of Two Different Types of Blackbody Sources Using Infrared Pyrometry Techniques." Mapan-Journal of Metrology Society of India 28 (Jun 2013): 91-98.
- Rani, N.; Vijayan, N.; Jat, S. K.; Maurya, K. K.; Kumar, P.; Prakash, A. P. G.; Bhagavannarayana, G.; and Wahab, M. A. "Effect of 100 keV N^+ion irradiation on the organic single crystal of hippuric acid for nonlinear optical applications." Radiation Effects and Defects in Solids 168 (Sep 2013): 705-716.
- Rani, P.; Jha, R.; and Awana, V. P. S. "AC Susceptibility Study of Superconducting $YBa_2Cu_3O_7$:Ag_x Bulk Composites (x=0.0-0.20): The Role of Intra and Intergranular Coupling." Journal of Superconductivity and Novel Magnetism 26 (Jul 2013): 2347-2352.
- Rani, P.; Pal, A.; and Awana, V. P. S. "High field magneto-transport study of $YBa_2Cu_3O_7$:Ag^x (x=0.00-0.20)." Physica C-Superconductivity and Its Applications 497 (Feb 2014): 19-23.
- Rao, G. K.; Kumar, A.; Singh, M. P.; Biradar, A. M.; and Singh, A. K. "Influence of pendent alkyl chains on Heck and Sonogashira C-C coupling catalyzed with palladium(II) complexes of selenated Schiff bases having liquid crystalline properties." Journal of Organometallic Chemistry 753 (Mar 2014): 42-47.
- Rastogi, A.; Pulikkotil, J. J.; and Budhani, R. C. "Enhanced persistent photoconductivity in delta-doped $LaAlO_3/SrTiO_3$ heterostructures." Physical Review B 89 (Mar 2014): 8.
- Reddy, B. N.; Deepa, M.; and Joshi, A. G. "Highly conductive poly(3,4-ethylenedioxypyrrole) and poly(3,4-ethylenedioxythiophene) enwrapped Sb_2S_3 nanorods for flexible supercapacitors." Physical Chemistry Chemical Physics 16 (2014): 2062-2071.
- Reddy, B. N.; Pathania, A.; Rana, S.; Srivastava, A. K.; and Deepa, M. "Plasmonic and conductive Cu fibers in poly (3,4-ethylenedioxythiophene)/ Cu hybrid films: Enhanced electroactivity and electrochromism." Solar Energy Materials and Solar Cells 121 (Feb 2014): 69-79.
- Reshak, A. H.; Chen, X. A.; Auluck, S.; Kamarudin, H.; Chysky, J.; Wojciechowski, A.; and Kityk, I. V. "Linear and Nonlinear Optical Susceptibilities and the Hyperpolarizability of Borate $LiBaB_9O_{15}$ Single-Crystal: Theory and Experiment." Journal of Physical Chemistry B 117 (Nov 2013): 14141-14150.
- Reshak, A. H.; Kamarudin, H.; and Auluck, S. "Electronic structure, density of electronic states, and the chemical bonding properties of 2,4-dihydroxyl hydrazone crystals (C13H11N304)." Journal of Materials Science 48 (May 2013): 3805-3811.
- Reshak, A. H.; Kamarudin, H.; Kityk, I. V.; and Auluck, S. "Electronic structure, charge density, and chemical bonding properties of C11H8N2O o-methoxydicyanovinylbenzene (DIVA) single crystal." Journal of Materials Science 48 (Aug 2013): 5157-5162.
- Reshak, A. H.; Khan, S. A.; and Auluck, S. "Electronic band structure and specific features of AA- and AB-stacking of carbon nitride (C3N4): DFT calculation." RSC Advances 4 (2014): 6957-6964.
- Reshak, A. H.; Khan, S. A.; and Auluck, S. "Linear and nonlinear optical properties for AA and AB stacking of carbon nitride polymorph (C_3N_4)." RSC Advances 4 (2014): 11967-11974.

- Reshak, A. H.; Khan, S. A.; and Auluck, S. "Thermoelectric properties of a single graphene sheet and its derivatives." Journal of Materials Chemistry C 2 (2014): 2346-2352.
- Reshak, A. H.; Khyzhun, O. Y.; Kityk, I. V.; Fedorchuk, A. O.; Kamarudin, H.; Auluck, S.; and Parasyuk, O. V. "Electronic Structure of Quaternary Chalcogenide $Ag_2In_2Ge(Si)S$-6 Single Crystals and the Influence of Replacing Ge by Si: Experimental X-Ray Photoelectron Spectroscopy and X-Ray Diffraction Studies and Theoretical Calculations." Science of Advanced Materials 5 (Apr 2013): 316-327.
- Reshak, A. H.; Lakshminarayana, G.; Ebothe, J.; Fedorchuk, A. O.; Fedyna, M. F.; Kamarudin, H.; Mandracci, P.; and Auluck, S. "Band structure, density of states, and crystal chemistry of $ZrGa_2$ and $ZrGa_3$ single crystals." Journal of Alloys and Compounds 556 (Apr 2013): 259-265.
- Reshak, A. H.; Nouneh, K.; Kityk, I. V.; Bila, J.; Auluck, S.; Kamarudin, H.; and Sekkat, Z. "Structural, Electronic and Optical Properties in Earth-Abundant Photovsoltaic Absorber of Cu_2ZnSnS_4 and $Cu_2ZnSnSe_4$ from DFT calculations." International Journal of Electrochemical Science 9 (Feb 2014): 955-974.
- Reshak, A. H.; Parasyuk, O. V.; Fedorchuk, A. O.; Kamarudin, H.; Auluck, S.; and Chysky, J. "Optical Spectra and Band Structure of $Ag_xGa_xGe_{1-x}Se_2$ (x=0.333, 0.250, 0.200, 0.167) Single Crystals: Experiment and Theory." Journal of Physical Chemistry B 117 (Dec 2013): 15220-15231.
- Riscob, B.; Bhatt, R.; Vijayan, N.; Bhaumik, I.; Ganesamoorthy, S.; Wahab, M. A.; Rashmi; and Bhagavannarayana, G. "Structural, optical and thermal properties of Zr-Fe co-doped congruent $LiNbO_3$ single crystals." Journal of Applied Crystallography 46 (Jun 2013): 601-609.
- Riscob, B.; Bhaumik, I.; Ganesamoorthy, S.; Bhatt, R.; Vijayan, N.; Karnal, A. K.; Wahab, M. A.; and Bhagavannarayana, G. "Effect of Mg doping on the growth aspects, crystalline perfection, and optical and thermal properties of congruent $LiNbO_3$ single crystals." Journal of Applied Crystallography 46 (Dec 2013): 1854-1862.
- Riscob, B.; Shkir, M.; Ganesh, V.; Vijayan, N.; Maurya, K. K.; Rao, K. K.; and Bhagavannarayana, G. "Synthesis, crystal growth and mechanical properties of Bismuth Silicon Oxide (BSO) single crystal." Journal of Alloys and Compounds 588 (Mar 2014): 242-247.
- Rout, P. K.; Pandey, H.; Wu, L. J.; Anupam; Joshi, P. C.; Hossain, Z.; Zhu, Y. M.; and Budhani, R. C. "Two-dimensional electron-gas-like charge transport at the interface between a magnetic Heusler alloy and $SrTiO_3$." Physical Review B 89 (Jan 2014): 5.
- Roy, A.; Prasad, R.; Auluck, S.; and Garg, A. "Engineering polarization rotation in ferroelectric bismuth titanate." Applied Physics Letters 102 (May 2013): 5.
- Sachdev, D., and Dubey, A. "Mesoporous silica/polyphosphoric ascid (SBA-15/PPA) nanocomposites for acylation of naphthalene." Catalysis Communications 39 (Sep 2013): 39-43.
- Saini, P.; Arora, M.; Arya, S. K.; and Tawale, J. S. "Effect of controlled doping on electrical properties and permittivity of PTSA doped polyanilines and their EMI shielding performance." Indian Journal of Pure & Applied Physics 52 (Mar 2014): 175-182.
- Saini, P., and Choudhary, V. "Conducting polymer coated textile based multilayered shields for suppression of microwave radiations in 8.2-12.4 GHz range." Journal of Applied Polymer Science 129 (Sep 2013): 2832-2839.
- Sajan, D.; Vijayan, N.; Safakath, K.; Philip, R.; and Karabacak, M. "Multi-photon absorption effect and intra-molecular charge transfer of donor-pi-acceptor chromophore ethyl p-amino benzoate." Spectrochimica Acta Part A-Molecular and Biomolecular Spectroscopy 108 (May 2013): 197-210.
- Sambyal, P.; Singh, A. P.; Verma, M.; Farukh, M.; Singh, B. P.; and Dhawan, S. K. "Tailored polyaniline/barium strontium titanate/expanded graphite multiphase composite for efficient radar absorption." RSC Advances 4 (2014): 12614-12624.
- Satish; Ansari, M. A.; and Saxena, A. K. "Determination and Comparison of

Temperature Coefficient of Standard Inductors by Measuring Change in Inductance and Resistances." Mapan-Journal of Metrology Society of India 29 (Mar 2014): 73-76.

- Saud, T.; Saxena, M.; Singh, D. P.; Saraswati; Dahiya, M.; Sharma, S. K.; Datta, A.; Gadi, R.; and Mandal, T. K. "Spatial variation of chemical constituents from the burning of commonly used biomass fuels in rural areas of the Indo-Gangetic Plain (IGP), India." Atmospheric Environment 71 (Jun 2013): 158-169.
- Selvan, G. K.; Kanagaraj, M.; Muthu, S. E.; Jha, R.; Awana, V. P. S.; and Arumugam, S. "Hydrostatic pressure effect on T-c of new BiS_2-based $Bi_4O_4S_3$ and $NdO_{0.5}F_{0.5}BiS_2$ layered superconductors." Physica Status Solidi-Rapid Research Letters 7 (Jul 2013): 510-513.
- Selvapandiyan, M.; Arumugam, J.; Sundaramoorthi, P.; and Sudhakar, S. "Effect of sodium chloride on the properties of ZTS single crystals." Journal of Alloys and Compounds 558 (May 2013): 34-38.
- Selvapandiyan, M.; Arumugam, J.; Sundaramoorthi, P.; and Sudhakar, S. "Influence of $MgSO_4$ doping on the properties of zinc tris-thiourea sulphate (ZTS) single crystals." Journal of Alloys and Compounds 580 (Dec 2013): 270-275.
- Sengar, S. K.; Mehta, B. R.; and Govind. "Size and alloying induced shift in core and valence bands of Pd-Ag and Pd-Cu nanoparticles." Journal of Applied Physics 115 (Mar 2014): 8.
- Shahane, G. S.; Zipare, K. V.; and Pant, R. P. "Synthesis and Characterization of Superparamagnetic Fe_3O_4 Nanoparticles for Ferrofluid Application." Magnetohydrodynamics 49 (Jul-Dec 2013): 317-321.
- Shankar, A.; Chand, M.; Kumar, S.; Singh, V. N.; Basheed, G. A.; Thakur, S.; and Pant, R. P. "Spin Resonance Investigations on water based Magnetite Ferrofluid." Magnetohydrodynamics 49 (Jul-Dec 2013): 310-316.
- Shanker, R.; Khan, A. F.; Kumar, R.; Chander, H.; Shanker, V.; and Chawla, S. "Understanding and arresting degradation in highly efficient blue emitting $BaMgAl_{10}O_{17}:Eu^{2+}$ phosphor-A longstanding technological problem." Journal of Luminescence 143 (Nov 2013): 173-180.
- Sharma, A.; Kotnala, R. K.; and Negi, N. S. "Structural, dielectric, magnetic and ferroelectric properties of $(PbTiO_3)_{0.5}$-$(Co_{0.5}Zn_{0.5}Fe_2O_4)_{0.5}$ composite." Physica B-Condensed Matter 415 (Apr 2013): 97-101.
- Sharma, A.; Kotnala, R. K.; and Negi, N. S. "Observation of multiferroic properties and magnetoelectric effect in (x) $CoFe_2O_4$ -(1-x) $Pb_{0.7}Ca_{0.3}Ti_{0.3}$ composites." Journal of Alloys and Compounds 582 (Jan 2014): 628-634.
- Sharma, A.; Sumana, G.; Sapra, S.; and Malhotra, B. D. "Quantum Dots Self Assembly Based Interface for Blood Cancer Detection." Langmuir 29 (Jul 2013): 8753-8762.
- Sharma, I. D.; Saini, P. K.; and Sharma, V. K. "Structural, optical, morphological and electrical characteristics of polyaniline for device applications." Indian Journal of Engineering and Materials Sciences 20 (Apr 2013): 145-149.
- Sharma, N.; Gaur, A.; Kumar, V.; and Kotnala, R. K. "Multiferroicity and magnetoelectric coupling in doped ZnO." Superlattices and Microstructures 65 (Jan 2014): 299-308.
- Sharma, R.; Ali, M. A.; Selvi, N. R.; Singh, V. N.; Sinha, R. K.; and Agrawal, V. V. "Electrochemically Assembled Gold Nanostructures Platform: Electrochemistry, Kinetic Analysis, and Biomedical Application." Journal of Physical Chemistry C 118 (Mar 2014): 6261-6271.
- Sharma, S. N.; Mehta, A.; Kumar, U.; and Chand, S. "Role of surface passivating ligand and growth temperature on the size quantization effects of colloidal hybrid (MEH-PPV/P3HT:PbSe) nanocomposites." Physica E-Low-Dimensional Systems & Nanostructures 57 (Mar 2014): 103-112.
- Sharma, S., and Chawla, S. "Enhanced UV emission in ZnO/ZnS core shell nanoparticles prepared by epitaxial growth in solution." Electronic Materials Letters 9 (May 2013): 267-271.
- Sharma, S.; Shah, J.; Kotnala, R. K.; and Chawla, S. "Red upconversion luminescence and paramagnetism in Er/Yb doped SnO_2." Electronic Materials Letters 9 (Sep 2013): 615-620.
- Sharma, V.; Kumar, A.; Ganguly, P.; and Biradar, A. M. "Highly sensitive bovine serum albumin

biosensor based on liquid crystal." Applied Physics Letters 104 (Jan 2014): 4.

- Shkir, M.; Riscob, B.; Ganesh, V.; Vijayan, N.; Gupta, R.; Plaza, J. L.; Dieguez, E.; and Bhagavannarayana, G. "Crystal growth, structural, crystalline perfection, optical and mechanical properties of Nd^{3+} doped sulfamic acid (SA) single crystals." Journal of Crystal Growth 380 (Oct 2013): 228-235.
- Shkir, M.; Riscob, B.; Hasmuddin, M.; Singh, P.; Ganesh, V.; Wahab, M. A.; Dieguez, E.; and Bhagavannarayana, G. "Optical spectroscopy, crystalline perfection, etching and mechanical studies on P-nitroaniline (PNA) single crystals." Optical Materials 36 (Jan 2014): 675-681.
- Singh, A. K.; Singh, S. K.; Kumar, P.; Gupta, B. K.; Prakash, R.; and Rai, S. B. "Lanthanide Doped Dual-Mode Nanophosphor as a Spectral Converter for Promising Next Generation Solar Cells." Science of Advanced Materials 6 (Feb 2014): 405-412.
- Singh, A. P.; Gupta, B. K.; Mishra, M.; Govind; Chandra, A.; Mathur, R. B.; and Dhawan, S. K. "Multiwalled carbon nanotube/cement composites with exceptional electromagnetic interference shielding properties." Carbon 56 (May 2013): 86-96.
- Singh, A. P.; Mishra, M.; Sambyal, P.; Gupta, B. K.; Singh, B. P.; Chandra, A.; and Dhawan, S. K. "Encapsulation of gamma-Fe_2O_3 decorated reduced graphene oxide in polyaniline core-shell tubes as an exceptional tracker for electromagnetic environmental pollution." Journal of Materials Chemistry A 2 (2014): 3581-3593.
- Singh, A.; Sinsinbar, G.; Choudhary, M.; Kumar, V.; Pasricha, R.; Verma, H. N.; Singh, S. P.; and Arora, K. "Graphene oxide-chitosan nanocomposite based electrochemical DNA biosensor for detection of typhoid." Sensors and Actuators B-Chemical 185 (Aug 2013): 675-684.
- Singh, B. P.; Prasanta; Choudhary, V.; Saini, P.; Pande, S.; Singh, V. N.; and Mathur, R. B. "Enhanced microwave shielding and mechanical properties of high loading MWCNT-epoxy composites." Journal of Nanoparticle Research 15 (Apr 2013): 12.
- Singh, B. P.; Saini, K.; Choudhary, V.; Teotia, S.; Pande, S.; Saini, P.; and Mathur, R. B. "Effect of length of carbon nanotubes on electromagnetic interference shielding and mechanical properties of their reinforced epoxy composites." Journal of Nanoparticle Research 16 (Dec 2013): 11.
- Singh, B. P.; Srivastava, A. K.; Tiwari, S.; Singh, S.; Singh, R. K.; Bisht, D. S.; Lal, D. M.; Singh, A. K.; Mall, R. K.; and Srivastava, M. K. "Radiative Impact of Fireworks at a Tropical Indian Location: A Case Study." Advances in Meteorology (2014): 8.
- Singh, B.; Mehta, B. R.; Varandani, D.; Govind; Narita, A.; Feng, X.; and Mullen, K. "Bipolar resistive switching properties of Ti-CuO/(hexafluoro-hexa-peri-hexabenzocoronene)-Cu hybrid interface device: Influence of electronic nature of organic layer." Journal of Applied Physics 113 (May 2013): 7.
- Singh, C.; Srivastava, S.; Ali, M. A.; Gupta, T. K.; Sumana, G.; Srivastava, A.; Mathur, R. B.; and Malhotra, B. D. "Carboxylated multiwalled carbon nanotubes based biosensor for aflatoxin detection." Sensors and Actuators B-Chemical 185 (Aug 2013): 258-264.
- Singh, G.; Joshi, P. C.; Hossain, Z.; and Budhani, R. C. "Reentrant superconductivity in $HoNi_5$-NbN-HoNi5 nanostructures." EPL 103 (Aug 2013): 6.
- Singh, G.; Verma, A.; and Jeyakumar, R. "Fabrication of c-Si solar cells using boric acid as a spin-on dopant for back surface field." RSC Advances 4 (2014): 4225-4229.
- Singh, J.; Roychoudhury, A.; Srivastava, M.; Chaudhary, V.; Prasanna, R.; Lee, D. W.; Lee, S. H.; and Malhotra, B. D. "Highly Efficient Bienzyme Functionalized Biocompatible Nanostructured Nickel Ferrite-Chitosan Nanocomposite Platform for Biomedical Application." Journal of Physical Chemistry C 117 (Apr 2013): 8491-8502.
- Singh, J.; Roychoudhury, A.; Srivastava, M.; Solanki, P. R.; Lee, D. W.; Lee, S. H.; and Malhotra, B. D. "A dual enzyme functionalized nanostructured thulium oxide based interface for biomedical application." Nanoscale 6 (2014): 1195-1208.

- Singh, J.; Srivastava, M.; Roychoudhury, A.; Lee, D. W.; Lee, S. H.; and Malhotra, B. D. "Optical and electro-catalytic studies of nanostructured thulium oxide for vitamin C detection." Journal of Alloys and Compounds 578 (Nov 2013): 405-412.
- Singh, K.; Tiwari, S.; Jha, A. K.; Aggarwal, S. G.; Bisht, D. S.; Murty, B. P.; Khan, Z. H.; and Gupta, P. K. "Mass-size distribution of PM10 and its characterization of ionic species in fine (PM2.5) and coarse (PM10-2.5) mode, New Delhi, India." Natural Hazards 68 (Sep 2013): 775-789.
- Singh, N.; Singh, S. P.; Gupta, V.; Yadav, H. K.; Ahuja, T.; Tripathy, S. S.; and Rashmi. "A Process for the Selective Removal of Arsenic from Contaminated Water Using Acetate Functionalized Zinc Oxide Nanomaterials." Environmental Progress & Sustainable Energy 32 (Dec 2013): 1023-1029.
- Singh, N.; Srivastava, A. K.; Sood, K. N.; and Dhar, A. "High density aligned Si nanowires synthesised using electroless etching." Materials Technology 28 (Jul 2013): 199-204.
- Singh, N.; Tripathy, S. S.; Soni, D.; Singh, K.; and Gupta, P. K. "Evaluation of purity with its uncertainty value in high purity lead stick by conventional and electro-gravimetric methods." Chemistry Central Journal 7 (Jun 2013): 10.
- Singh, P.; Bala, A.; Nautiyal, T.; and Auluck, S. "An insight into evolution of electronic, magnetic, optical, and vibrational properties of ultrathin Pd nanowires." Journal of Nanoparticle Research 15 (Jul 2013): 15.
- Singh, P.; Hasmuddin, M.; Shakir, M.; Vijayan, N.; Abdullah, M. M.; Ganesh, V.; and Wahab, M. A. "Investigation on structural, optical, thermal, mechanical and dielectric properties of L-proline cadmium chloride monohydrate single crystals: An efficient NLO material." Materials Chemistry and Physics 142 (Oct 2013): 154-164.
- Singh, P.; Sinha, O. P.; Srivastava, R.; Srivastava, A. K.; Thomas, S. V.; Sood, K. N.; and Kamalasanan, M. N. "Surface modified ZnO nanoparticles: structure, photophysics, and its optoelectronic application." Journal of Nanoparticle Research 15 (Jul 2013): 9.
- Singh, S. J.; Prakash, J.; Pal, A.; Patnaik, S.; Awana, V. P. S.; and Ganguli, A. K. "Study of Ni and Zn doped CeOFeAs: Effect on the structural transition and specific heat capacity." Physica C-Superconductivity and Its Applications 490 (Jul 2013): 49-54.
- Singh, S., and Beegum, S. N. "Direct radiative effects of an unseasonal dust storm at a western Indo Gangetic Plain station Delhi in ultraviolet, shortwave, and longwave regions." Geophysical Research Letters 40 (May 2013): 2444-2449.
- Singh, V. N.; Partheepan, G.; Kumar, B.; and Khare, A. "Growth of indium nitride nanopetal structures on indium oxide buffer layer." Materials Express 3 (Dec 2013): 360-364.
- Singh, V.; Sharma, S.; Dwivedi, R. K.; Kumar, M.; and Kotnala, R. K. "Multiferroic and optical properties of Pr-substituted bismuth ferrite ceramics." Physica Status Solidi a-Applications and Materials Science 210 (Jul 2013): 1442-1447.
- Singh, V.; Sharma, S.; Kumar, M.; Kotnala, R. K.; and Dwivedi, R. K. "Structural transition, magnetic and optical properties of Pr and Ti co-doped $BiFeO_3$ ceramics." Journal of Magnetism and Magnetic Materials 349 (Jan 2014): 264-267.
- Singhal, R.; Pivin, J. C.; Chandra, R.; and Avasthi, D. K. "Ion irradiation studies of silver/amorphous carbon nanocomposite thin film." Surface & Coatings Technology 229 (Aug 2013): 50-54.
- Singhal, S. K.; Kumar, V.; Stalin, K.; Choudhary, A.; Teotia, S.; Reddy, G. B.; Mathur, R. B.; Singh, S. P.; and Pasricha, R. "Gold-Nanoparticle-Decorated Boron Nitride Nanosheets: Structure and Optical Properties." Particle & Particle Systems Characterization 30 (May 2013): 445-452.
- Sivakumar, N.; Kanagathara, N.; Varghese, B.; Bhagavannarayana, G.; Gunasekaran, S.; and Anbalagan, G. "Structure, crystal growth, optical and mechanical studies of poly bis (thiourea) silver (I) nitrate single crystal: A new semi organic NLO material." Spectrochimica Acta Part A-Molecular and Biomolecular Spectroscopy 118 (Jan 2014): 603-613.
- Soni, K.; Kapoor, S.; and Parmar, K. S. "Long-term Aerosol Characteristics over Eastern,

Southeastern, and South Coalfield Regions in India." Water Air and Soil Pollution 225 (Jan 2014): 12.

- Srivastava, A. K. "Role of NPL-India in Nanotechnology and Nanometrology." Mapan-Journal of Metrology Society of India 28 (Dec 2013): 263-272.
- Srivastava, A. K.; Yadav, V.; Pathak, V.; Singh, S.; Tiwari, S.; Bisht, D. S.; and Goloub, P. "Variability in radiative properties of major aerosol types: A year-long study over Delhi An urban station in Indo-Gangetic Basin." Science of the Total Environment 473 (Mar 2014): 659-666.
- Srivastava, A.; Pal, A.; Singh, S.; Shekhar, C.; Singh, H. K.; Awana, V. P. S.; and Srivastava, O. N. "Magnetotransport and thermal properties characterization of 55 K superconductor $SmFeAsO_{0.85}F_{0.15}$." AIP Advances 3 (Sep 2013): 13.
- Srivastava, M. K.; Singh, S.; Siwach, P. K.; Kaur, A.; Awana, V. P. S.; Maurya, K. K.; and Singh, H. K. "Comparative study of magnetic and magnetotransport properties of $Sm_{0.55}Sr_{0.45}MnO_3$ thin films grown on different substrates." AIP Advances 3 (May 2013): 13.
- Srivastava, P.; Kumar, A.; Mishra, A.; Meena, N. K.; Tripathi, J. K.; Sundriyal, Y. P.; Agnihotri, R.; and Gupta, A. K. "Early Holocene monsoonal fluctuations in the Garhwal higher Himalaya as inferred from multi-proxy data from the Malari paleolake." Quaternary Research 80 (Nov 2013): 447-458.
- Swamy, G. V.; Pandey, H.; Srivastava, A. K.; Dalai, M. K.; Maurya, K. K.; Rashmi; and Rakshit, R. K. "Effect of thermal annealing on Boron diffusion, micro-structural, electrical and magnetic properties of laser ablated CoFeB thin films." AIP Advances 3 (Jul 2013): 8.
- Swati, G.; Mishra, S.; Yadav, D.; Sharma, R. K.; Dwivedi, D.; Vijayan, N.; Tawale, J. S.; Shanker, V.; and Haranath, D. "High yield synthesis and characterization of aqueous stable zinc oxide nanocrystals using various precursors." Journal of Alloys and Compounds 571 (Sep 2013): 1-5.
- Sydam, R.; Deepa, M.; and Joshi, A. G. "A novel 1,1 '-bis 4-(5,6-dimethyl-1H-benzimidazole-1-yl)butyl -4,4 '-bipyridinium dibromide (viologen) for a high contrast electrochromic device." Organic Electronics 14 (Apr 2013): 1027-1036.
- Tawale, J. S.; Kumar, A.; Mohan, A.; and Srivastava, A. K. "Influence of silver and graphite on zinc oxide nanostructures for optical application." Optical Materials 35 (May 2013): 1335-1341.
- Thukral, K.; Vijayan, N.; Rathi, B.; Bhagavannaryana, G.; Verma, S.; Philip, J.; Krishna, A.; Jeyalakshmy, M. S.; and Halder, S. K. "Synthesis and single crystal growth of L-proline cadmium chloride monohydrate and its characterization for higher order harmonic generation applications." Crystengcomm 16 (2014): 2802-2809.
- Tiwari, B.; Pal, A.; and Awana, V. P. S. "Anomalous magnetism of Pr in PrCoAsO." AIP Advances 4 (Jan 2014): 7.
- Tiwari, J. P.; Pillai, S.; Parakh, S.; Ali, F.; Sharma, A.; and Chand, S. "A futuristic approach towards interface layer modifications for improved efficiency in inverted organic solar cells." Applied Physics Letters 104 (Jan 2014): 5.
- Tiwari, R.; Chandra, S.; and Chakraborty, B. R. "Preparation, characterization and application of RF sputter deposited boron doped silicon dioxide thin films." Materials Science in Semiconductor Processing 16 (Dec 2013): 2013-2020.
- Tiwari, R.; Rana, S.; Singh, S.; Arora, A.; Kaushik, R.; Agrawal, V. V.; Saxena, A. K.; and Nain, L. "Biological delignification of paddy straw and Parthenium sp using a novel micromycete Myrothecium roridum LG7 for enhanced saccharification." Bioresource Technology 135 (May 2013): 7-11.
- Tripathi, S. N.; Saini, P.; Gupta, D.; and Choudhary, V. "Electrical and mechanical properties of PMMA/reduced graphene oxide nanocomposites prepared via in situ polymerization." Journal of Materials Science 48 (Sep 2013): 6223-6232.
- Tripathi, S.; Prakash, J.; Chandran, A.; Joshi, T.; Kumar, A.; Dhar, A.; and Biradar, A. M. "Enhanced dielectric and electro-optical properties of a newly synthesised ferroelectric liquid crystal material by doping gold nanoparticle-decorated multiwalled carbon

nanotubes." Liquid Crystals 40 (Sep 2013): 1255-1262.

- Tsai, C. J., and Aggarwal, S. G. "Overview of the Gas and Aerosol Metrology." Mapan-Journal of Metrology Society of India 28 (Sep 2013): 141-143.
- Tyagi, G.; Jangir, D. K.; Singh, P.; Mehrotra, R.; Ganesan, R.; and Gopal, E. S. R. "Rapid determination of main constituents of packed juices by reverse phase-high performance liquid chromatography: an insight in to commercial fruit drinks." Journal of Food Science and Technology-Mysore 51 (Mar 2014): 476-484.
- Tyagi, G.; Pradhan, S.; Srivastava, T.; and Mehrotra, R. "Nucleic acid binding properties of allicin: Spectroscopic analysis and estimation of anti-tumor potential." Biochimica Et Biophysica Acta-General Subjects 1840 (Jan 2014): 350-356.
- Tyagi, P.; Kumar, A.; Giri, L. I.; Dalai, M. K.; Tuli, S.; Kamalasanan, M. N.; and Srivastava, R. "Exciton quenching by diffusion of 2,3,5,6-tetrafluoro7,7 ',8,8 '-tetra cyano quino dimethane and its consequences on joule heating and lifetime of organic light-emitting diodes." Optics Letters 38 (Oct 2013): 3854-3857.
- Tyagi, P.; Srivastava, R.; Kumar, A.; Tuli, S.; and Kamalasanan, M. N. "Effect of doping of cesium carbonate on electron transport in Tris(8-hydroxyquinolinato) aluminum." Organic Electronics 14 (May 2013): 1391-1395.
- Upadhayaya, A. K., and Mahajan, K. K. "Ionospheric F-2 region: Variability and sudden stratospheric warmings." Journal of Geophysical Research-Space Physics 118 (Oct 2013): 6736-6750.
- Varshney, S.; Ohlan, A.; Jain, V. K.; Dutta, V. P.; and Dhawan, S. K. "Synthesis of ferrofluid based nanoarchitectured polypyrrole composites and its application for electromagnetic shielding." Materials Chemistry and Physics 143 (Jan 2014): 806-813.
- Varshney, S.; Ohlan, A.; Singh, K.; Jain, V. K.; Dutta, V. P.; and Dhawan, S. K. "Robust Multifunctional Free Standing Polypyrrole Sheet for Electromagnetic Shielding." Science of Advanced Materials 5 (Jul 2013): 881-890.
- Verma, A., and Singh, P. K. "Sol-gel derived nanostructured niobium pentoxide thin films for electrochromic applications." Indian Journal of Chemistry Section a-Inorganic Bio-Inorganic Physical Theoretical & Analytical Chemistry 52 (May 2013): 593-598.
- Verma, A., and Vijayan, N. "Sol-gel-derived nanocrystalline aluminum-doped zinc oxide thin films for use as antireflection coatings in silicon solar cells." Journal of Materials Research 28 (Nov 2013): 2990-2995.
- Verma, D.; Sharma, S. N.; Kharkwal, A.; Bhagavannarayana, G.; Kumar, M.; Singh, S. N.; Singh, P. K.; Mehdib, S. S.; and Husain, M. "Role of nanocrystalline ZnO coating on the stability of porous silicon formed on textured (1 0 0) Si." Applied Surface Science 285 (Nov 2013): 564-571.
- Verma, K. C.; Gupta, V.; Kaur, J.; and Kotnala, R. K. "Raman spectra, photoluminescence, magnetism and magnetoelectric coupling in pure and Fe doped $BaTiO_3$ nanostructures." Journal of Alloys and Compounds 578 (Nov 2013): 5-11.
- Verma, K. C.; Kaur, J.; Negi, N. S.; and Kotnala, R. K. "Multiferroic and magnetoelectric properties of nanostructured $BaFe_{0.01}Ti_{0.99}O_3$ thin films obtained under polyethylene glycol conditions." Solid State Communications 178 (Jan 2014): 11-15.
- Verma, K. C.; Kumar, M.; and Kotnala, R. K. "Magnetoelectric, Raman, and XPS Properties of $Pb_{0.7}Sr_{0.3}$ $(Fe_{2/3}Ce_{1/3})$(0.012)Ti-0.988 0-3 and Pb0.7Sr0.3 $(Fe_{2/3}La_{1/3})$(0.012)Ti-0.988 0-3 Nanoparticles." Metallurgical and Materials Transactions a-Physical Metallurgy and Materials Science 45A (Mar 2014): 1409-1414.
- Verma, M.; Senthilkumaran, P.; Joseph, J.; and Kandpal, H. C. "Experimental study on modulation of Stokes parameters on propagation of a Gaussian Schell model beam in free space." Optics Express 21 (Jul 2013): 15432-15437.
- Verma, R.; Sood, S.; Singh, R.; Sumana, G.; Bala, M.; Sharma, V. K.; Samantaray, J. C.; Pandey, R. M.; and Malhotra, B. D. "Coupling electrochemical response of a DNA biosensor with PCR for Neisseria gonorrhoeae detection."

Diagnostic Microbiology and Infectious Disease 78 (Jan 2014): 16-23.

- Vijayan, N.; Madhurambal, G.; Bhagavannarayana, G.; Maurya, K. K.; and Mojumdar, S. C. "Thermal, Structural and Optical Analyses of Benzimidazole Single Crystal Grown with Organic Dopants for Nonlinear Optical Applications." Research Journal of Chemistry and Environment 17 (Jul 2013): 2-9.
- Vijayan, N.; Philip, J.; Haranath, D.; Rathi, B.; Bhagavannarayana, G.; Halder, S. K.; Roy, N.; Jayalakshmy, M. S.; and Verma, S. "Bulk growth of ninhydrin single crystals by solvent evaporation method and its characterization for SHG and THG applications." Spectrochimica Acta Part A-Molecular and Biomolecular Spectroscopy 122 (Mar 2014): 309-314.
- Vijayan, N.; Rani, N.; Madhurambal, G.; Bhagavannarayana, G.; Rathi, B.; Philip, R.; Safakath, K.; and Mojumdar, S. C. "Synthesis, growth, and characterization of iminodiacetic acid monohydrochloride." Journal of Thermal Analysis and Calorimetry 112 (May 2013): 1113-1119.
- Wang, D. H.; Kyaw, A. K. K.; Gupta, V.; Bazan, G. C.; and Heeger, A. J. "Enhanced Efficiency Parameters of Solution-Processable Small-Molecule Solar Cells Depending on ITO Sheet Resistance." Advanced Energy Materials 3 (Sep 2013): 1161-1165.
- Xu, D. W.; Haranath, D.; He, H. Y.; Mishra, S.; Bharti, I.; Yadav, D.; Sivaiah, B.; Gahtori, B.; Vijayan, N.; Dhar, A.; Zhu, J. J.; Shanker, V.; and Pandey, R. "Studies on phase stability, mechanical, optical and electronic properties of a new Gd_2CaZnO_5 phosphor system for LEDs." Crystengcomm 16 (2014): 1652-1658.
- Yadav, D.; Dwivedi, D.; Mishra, S.; Sivaiah, B.; Dhar, A.; Shanker, V.; and Haranath, D. "Investigation of Local Field Enhancement and Hot Electron Injection in Carbon Nano-Tube Doped Phosphor Nano-Composite for Ultra-Bright Electroluminescence." Science of Advanced Materials 6 (Feb 2014): 413-418.
- Yadav, D.; Mishra, S.; Shanker, V.; and Haranath, D. "Design and development of low-power driven hybrid electroluminescent lamp from carbon nanotube embedded phosphor material." Journal of Alloys and Compounds 581 (Dec 2013): 632-635.
- Yadav, K.; Singh, M. P.; Singh, H. K.; Razavi, F. S.; and Varma, G. D. "Effect of Nd doping on the magnetic properties of charge-ordered $Bi_{0.6-x}Nd_xCa_{0.4}MnO_3$ perovskite manganites." Applied Physics A-Materials Science & Processing 111 (Jun 2013): 845-851.
- Yadav, S.; Dabas, R. S.; Das, R. M.; Upadhayaya, A. K.; and Gwal, A. K. "Temporal and spatial variation of equatorial ionization anomaly by using multistation ionosonde data for the 19th solar cycle over the Indian region." Advances in Space Research 51 (Apr 2013): 1253-1265.
- Yadav, S.; Das, R. M.; Dabas, R. S.; and Gwal, A. K. "The response of sporadic E-layer to the total solar eclipse of July 22, 2009 over the equatorial ionization anomaly region of the Indian zone." Advances in Space Research 51 (Jun 2013): 2043-2047.
- Yang, X. S., and Deb, S. "Multiobjective cuckoo search for design optimization." Computers & Operations Research 40 (Jun 2013): 1616-1624.
- Yerpude, A. N.; Dhoble, S. J.; and Haranath, D. "Synthesis and characterization of blue long-lasting $BaCa_2Al_8O_{15}:Eu^{2+}$, Dy^{3+} phosphor." Luminescence 28 (Jul 2013): 437-441.
- Zimik, K.; Bhagavannarayana, G.; Kumar, R.; Chauhan, R. R.; Murari, K.; Malhan, N.; and Thakur, H. V. "A novel comparative study of crystalline perfection and optical homogeneity in Nd:GGG crystals grown by the Czochralski technique with different crystal/melt interface shapes." Journal of Applied Crystallography 46 (Dec 2013): 1640-1644.

Appendix - 2

Patents Filed in India

S.No	Title	NF No	Application No	Compl. Filing Date	Inventors
1	Improvement in power conversion efficiency in conjugated polymer modified PTB7- PC60BM based bulk heterojunction solar cells	0137NF2012	2650DEL2012	27/8/2013	Gupta Vinay, Bharti Vishal, Chaudhary Neeraj, Chand Suresh
2	Light weight carbon foam as electromagnetic interference (EMI) shielding and thermal interface material	0168NF 2012	3615DEL2012	25/11/2013	Sanjay Rangnath Dhakate, Rajeev Kumar, Rakesh Behari Mathur, Parveen Saini
3	Resistive type porous magnesium ferrite humidity sensor	0138NF2012	2528DEL2013	27/08/2013	Ravinder Kumar Kotnala, Jyoti Shah, Hari Kishan, Bhikham Singh
4	A process for the removal of pesticides from contaminated water	0042NF2013	2184DEL2013	23/07/2013	Singh Nahar,Gupta Suman, Tripathy Sushree Swarupa, Rashmi, Singh Sukhvir, Gupta Prabhat Kumar
5	An improved process for the synthesis of nanostructured p-type copper-selenide (Cu_2Se) as a cheap and non-toxic thermoelectric material with a high thermoelectric figure-of-merit of 2 at 1000 K.	0143NF2013	2693DEL2013	12/09/2013	Bhasker Gahtori, Bathula Sivaiah, Avanish Kumar Srivastava, Kriti Tyagi, Ajay Dhar, Ramesh Chandra Budhani
6	Magnetic Nanoparticles Decorated Activated Carbon Nanocomposites for purification of Water	178NF2013	2891DEL2013	09/09/2013 Prov.	Saini Parveen, Arora Manju, Kotnala Ravinder Kumar, Barala Sunil Kumar, Pant Rajendra Prasad, Chandni Puri
7	Electromagnetic Interference (EMI) Shielding Nanocomposites with Enhanced Absorption Based on Superparamagnetic particles Decorated Porous Carbon	179NF 2013	2754DEL2013	9/09/2013 Prov.	Parveen Saini, R. K. Kotnala, Sunil Kumar Barala, Manju Arora, R. P. Pant
8	Boron doped manganese antimonide as a useful permanent magnet material	0177NF20133	3078DEL2013	17/10/2013 Prov.	Nidhi Singh, Kanika Anand, Jiji Thomas Joseph Pulikkotil, Ajay Dhar and Ramesh Chandra Budhani
9	PPY-AG nanocomposite impregnated activated carbon membrane useful for the removal of E.Coli from water	189NF2013	2955DEL2013	4.10.2013 Prov.	S K Dhawan, Hema Bhandari, Swati Varsheny, Brijesh Sharma, R K Kotnala
10	Conducting polymer composites for corrosion protection in marine environment	0170NF2013	3813DEL2013	30.12.2013 Prov.	S K Dhawan, Mukesh Kumar, Avanish Pratap Singh, Kuldeep Singh, Bipin Gupta, Vasudha Agarwal, G A Basheed, R K Kotnala

Patents Granted in India

S.No	Title	NF No	Application No	Grant Date	Patent No	Inventors
1	A process for joining oxide-superconducting tubes with a superconducting joint	0172NF2006/IN	0198DEL2007	30/10/2013	257738	Ekbote Shrikant Narayan, Padam Gursharan Kaur, Arora Narendra Kumar, Sharma Mukul, Sethi Ramesh
2	An improved sol-gel process for the preparation of nanocrystalline $CeTi_2O_6$ powder	0010NF2007/IN	0279DEL2007	26/03/2014	259736	Amita Verma, Suhasini Avinash Agnihotry

Patents Filed Abroad

S.No	Title	NF No	Application No	Compl. Filing Date	Inventors
1	Improvement in power conversion efficiency in conjugated polymer modified PTB7- PC60BM based bulk heterojunction solar cells	0137NF2012/WO	PCT/IN2013/000519	27/08/2013	Gupta Vinay, Bharti Vishal, Chaudhary Neeraj, Chand Suresh
2	A process for the removal of arsenic and chromium from water	0158NF2009/US	13/960311	08/06/2013	Singh Nahar, Rashmi, Singh Sukhvir, Soni Daya, Pashricha Renu, Gupta Prabhat Kumar
3	Light weight carbon foam as electromagnetic interference (EMI) shielding and thermal interface	0168NF2012/WO	PCT/IN2013/000714	26/11/2013	Sanjay Rangnath Dhakate, Rajeev Kumar, Rakesh Behari Mathur, Parveen Saini
4	Nanostructured copper-selenide (Cu_2Se) with high thermoelectric figure-of-merit and process for the preparation thereof	0143NF2013/WO	PCT/IN2014/000161	12/03/2014	Gahtori Bhasker, Bathula Sivaiah, Tyagi Kriti, Srivastava Avanish Kumar, Dhar Ajay, Budhani Ramesh Chandra

Patents Granted Abroad

S.No	Title	NF No	Application No	Grant Date	Patent No	Inventors
1	A process for preparing of nanowires of metal oxide —in lower valence state	0034NF2007_CN	200810098697.5	14/8/2013	ZL200810098697.5	Harish Chander, V Shanker, Divi Haranath, Pooja Sharma
2	An improved process to deposit diamond like carbon as protective coating on inner surface of bottles	0179NF2008/EP	10704976.9	7/8/2013	EP2398933	Kumar Sushil, Dixit Prakash Narain, Rauthan Chandra Mohan Singh
3	Process for growing an electron injection layer to improve the efficiency of organic light emitting diodes	0045NF2010/US	13/077029	23/07/2013	US8491820	Modeeparampil; Kamalasanan Narayanan, Srivastava; Ritu , Grover; Rakhi, Dhawan; Sundeep Kumar, Chand; Suresh, Bawa; S. S.

4	Process for the preparation of oxide superconducting rods	0179NF2007/US	12/290581	10/09/2013	US8530389	Arora Narinder Kumar, Padam Gursharan Kaur, Sethi Ramesh, Sharma Mukul, Ekbote Shrikant Narayan
5	A novel method for joining oxide-superconducting tubes with a superconducting joint	0172NF2006_KR	1020097018209	19/03/2014	10-1378171	Ekbote Shrikant Narayan, Padam Gursharan Kaur, Arora Narendra Kumar, Sharma Mukul, Sethi Ramesh
6	Process for the preparation of photoluminescent nanostructured silicon thin films using radio frequency plasma discharge	0097NF2007/US	12/810920	19/11/2013	US8586151	Sushil Kumar, P.N. Dixit, C.M.S. Rauthan
7	Process for preparing of nanowires of metal oxides with dopants in lower valence state	0034NF2007/US	12/134635	17/12/2013	US8609053	Chander; Harish, Shanker; Virendra, Haranath; Divi , Sharma; Pooja
8	An improved process to deposit diamond like carbon as protective coating on inner surface of bottles	0179NF2008/FR	10704976.9	7/8/2013	2398933	Kumar Sushil, Dixit Prakash Narain, Rauthan Chandra Mohan Singh
9	Process for preparing zinc peroxide nanoparticles	0158NF2009/US	13/960311	06/05/2014	8,715,612	Singh Nahar, Rashmi, Singh Sukhvir, Soni Daya, Pashricha Renu, Gupta Prabhat Kumar

Appendix-3

R & D Collaborations

COLLABORATING INSTITUTE	RESEARCH AREA
ISRO, Dept of Space	Development of Rubidium Atomic Clock
Department of Physics, ARSD College, University of Delhi (South Campus), New Delhi-110021, India	Degenerate gases: a new tool for frequency detection
LNE-SYRTE, Paris, France (LNE International Technical Collaboration Program)	Atomic fountains
NPL, UK	Atomic fountains
Bharti Automation Pvt. Ltd., New Delhi	Water flow measurement
LPEM, France	Two dimensional electron gas physics in oxide heterostructures
SINP, Kolkatta	Superconducting & Magnetic Materials
CNR/INFM-LAMIA, Genova, Italy	Superconducting Materials
JNU, New Delhi	Superconducting Materials
MAX Super Specialty Hospital, New Delhi	Tumor Diagnosis
Anna University, Chennai – CAP-14 (PI)	Crystal Growth and Characterization
Crystal Growth Centre, SSN College of Engg., Chennai, CAP-18 (PI)	Crystal Growth and Characterization
Jamia Millia Islamia, CAP-24. (PI)	Crystal Growth and Characterization

Appendix 4

Sponsored and supported R & D projects
New /Continuing /Completed Projects

COMPLETED PROJECTS

Sr. No	TITLE OF THE PROJECT	AGENCY	Receipts April 2013-March 2014 (₹ In Lakhs)
1	Development of Acoustic Equipment for object detection for divers	National Institute of Ocean Tech. (Min. of earth Science), (NIOT)	2.900
2	A novel way to reduce platinum metal loading in a carbon nano-composite electrode to produce low cost-high efficiency commercially viable Polymer Electroyte Membrane (PEM) fuel cells	DST (Indo-Australia)	0.000
3	Development of grain Ferroelectric Nanocomposites and Investigation of size effect on varous Ferroelectric Parameters	DST, New Delhi	9.500

Continuing PROJECTS

1	Operation of the South Asian Regional Research Centre (SAS-RRC) for Study of Global Change Under SASCOM	International START Secretariat, Washington, USA.	0.000
2	To Conduct Inter-Laboratory Proficiency Testing Amongst the NABL Accredited Calibration Laboratories in India	DST (NABL), New Delhi	0.000
3	Coherent Radio Beacon Experiment (CRABEX) for Tomographic Studies of the Ionosphere on Board GSAT-II Satellite	VSSC, Thiruvanthapuram Dept. of Space)	0.000
4	Investigation Study on Microwave Sintering of Beta Alumina Tubes	DST, New Delhi	0.000
5	Low cost technology for High efficiency Silicon Solar Cell	DST,Under Indo-Bulgarian Inter Govt.Prog	0.000
6	Generic Development of Nanometrology for Nanotechnology	Department of Information Technology, (DIT), New Delhi	0.000
7	Assessment of Effects of High Particulate on Pulmonary pollutants Health Status in Selected Megacities of South Asia	Asia-Pacific Network, (APN, Japan)	0.000
8	High rate deposition of the microcry-stalline silicon films using high density microwave plasma and its application to efficient to large area thin film solar cells	DST, New Delhi	0.000
9	Integrated campaign for aerosols, gases & radiation budget	VSSC, Thiruvanthapuram Dept. of Space)	0.000

10	Formation of Alkali Metal nanostructures on reconstructed low and high index Silicon Surfaces (under SERC FAST TRACK Proposals)	DST, New Delhi	0.000
11	Growth and structural characterization of nearly perfect single crystals of oxide materials for scintillation applications	DST (Under Indo-Russian Joint Project)	0.000
12	Development of Rubidium Atomic Clock by NPL & SAC	Department of Space, Space Application Centre, DSSAC, Ahmedabad	0.000
13	Centre on Bio-Molecular Electronics	DST, New Delhi	0.000
14	Nano-metrology: surface roughness (under USERS Scheme)	DST, New Delhi	0.000
15	Innovative Product Development Centre	DST, New Delhi	3.620
16	Multicentric collaborative study on the impact of global warming and ultra violet radiation (UVR) exposure on ocular health in India	Indian Council of Medical Research (Min. of Health & Family Welfare), (ICMR)	0.000
17	Morphological study of polar region ionosphere with special emphasis on space weather events	Department of Space Bangalore, (DOS)	0.000
18	J C Bose National Fellowship	DST, New Delhi	13.000
19	Ramanna Fellowship, A new High Resolution X-ray	DST, New Delhi	13.400
20	Preparation of energy sector GHG Emission Inventory and assessment of heat stress vulnerability under future climate change scenarios in India	Centre for Mathematical Modelling and Computer Simulation, NAL Belur Campus, Bangalore, (CSIR, CCMMCS)	12.236
21	Development of hybrid electroluminescent materials and low power driven lamps (Women Scientist Scheme)	DST, New Delhi	0.000
22	Preparation and characterization of silicon for solar energy applications	DST, New Delhi	0.000
23	Development of gold micro-electrode array with nanometer size opening for use in biosensor at physiological conditions	Department of Biotechnology	0.000
24	Advancing the Efficiency and Production Potential of Excitonic Solar Cells (APEX)	DST (Indo-UK)	1.827
25	Development of continuous nanofibers by electro-spinning	DST, New Delhi	9.500
26	Band gap engineering of nanophosphors for use in energy saving lighting applications	DST, New Delhi	8.000
27	Upper Tropospheric and Lower Stratospheric water vapour distribution	Department of Space Bangalore, (DOS)	5.768

	and variability over Tropical region : Implication on Stratosphere-Troposphere Exchange		
28	SAARC-PTB collaboration in the field of quality infrastructure to promote regional cooperation in metrology	PTB-Germany	0.000
29	Chemical characteristics and source apportionment of Atmospheric organic aerosols in Delhi region	DST (Fund received from Science & Engineering Research Board, New Delhi)	3.500
30	Seasonal variation of column aerosol properties, aerosol radiation forcing and the assessment of the impact of absorbing (BC)and desert dust aerosols in the mega-city of Delhi	Vikram Sarabhai Space Centre, Thiruvanan (ISRO)	5.000
31	R&D on Thin Film Solar Cells	Ministry of New and Renewable Energy (MNRE)	0.000
32	Standardization for Nanoscience and Technology	DST, New Delhi	0.000
33	Study of magnetic anisotopy in magnetic nanoparticles, thin film and heterostructures	DST New Delhi	0.000
34	Determination of the impact of oxidizing capacity of troposphere on the abundance of carbon monoxide and methane with special reference to India	Ministry of Earth Science (MoES)	0.000
35	Modification and designing of fly ash composites in building materials for energy conservation & sheilding application	Ministry of Environment & Forests, (ME&F)	0.000
36	Comparative study of space weather at terrestrial planets	Physical Research Laboratory, (PRL) Ahmedabad	3.888
37	Synthesis and development of graphene based polymer composite: Its application in polymer electroyte membrane fuel cell	DST (Under Women Scientists Scheme)	6.000
38	Development of high temperature silicon carbide material suitable for microwave susceptor applications	DST (Under Sci and Eng.Research Board)	0.000
39	Study of seasonal variation of ozone precursor in relation with surface ozone over Delhi, a mega city	Physical Research Laboratory, Navrangpura	0.000
40	Two dimensional electron gas physics in oxide heterostructures	Indo-French Centre Promotion of Advanced Research (IFCPAR)	21.098
41	Enhancement of solar cell effciencies using tapered ZnO nanorod-CdTe polycry stalline thin film structure	DST, New Delhi, (SERB)	0.000
42	DAE-SRC outstanding Investigaltor Award Fellowship	Department of Atomic Energy (DAE)	0.000

43	Fellowship for INSPIRE Faculty	DST New Delhi	0.000
44	Preparation and characterization of ferrofluids for energy conversion applications	DST, New Delhi	0.000
45	Development & characterization of bulk aluminium-alumina (Al-Al_2O_3) nano-composites-study of their nano-sintering with respect to densification & grain growth	DST, New Delhi (Indo-Hungary)	0.000
46	Studies of electron correlations at low temperatures and high magnetic fields in tailored interfaces and heterostructures	DST, New Delhi	0.00
47	Synthesis and characterisation of nanostructured electroluminescent materials for improved performance of optoelectronics devices and allied technologies	DST (Under Women Sci Scheme A WOS-A)	0.000

NEW PROJECTS

1	Infrared Spectroscopic study for Tumor Diagnosis-Phase II	DST, New Delhi	27.417
2	Implementation of Teleclock Service at Controller of Certifying Authority (CCA)	Controller of Certifying Authorities (CCA)(Ministry of Communication and Information technology)	8.820
3	Novel magnetic structures and excitations in multilayers, interface nanoparticles and bulk	Indo-US Science & Technology Forum	12.843
4	Implementation of Teleclock Service at Institute for Development & Research in Banking Technology (IDRBT)	Development & Research in Banking Technology,(IDRBT)	2.213
5	Nano-medicine for head and neck cancer	Indo-US Science & Technology Forum	17.938
6	Strengthening the quality infrastructure in Environmental analytics-Cooperation on Environmental Measurement in India (CEMI) (Phase -II)	Physikalish-Technische-Bundesanstalt Dept. of Tech Cooperation, Germany (PTB Germany)	8.735
7	Synthesis and characterization of Nanocrystalline Iridum Oxide Thin Films for pH Sensor Application	Science & Engineering Research Board, (DST)	6.000
8	Temperature and magnetic field dependent neutron studies on Cu_2OSCO_3	UGC-DAE Consortium for Scientific Research	0.350
9	Defect Engineered Flourescence from Nono-Diamond for Nano-photonics and Bio-Imaging	DST, New Delhi	19.0000

Appendix -5

CONSULTANCY PROJECTS 2013-14

₹ (In lakhs)

Project Code	Sr. No.	Client	Title	Contract Value	Amount Received 2013-14
NEW*					
CNP120132	1.	M/s Emerald Jewel Industry India, Coimbatore	Recovery of Gold and Silver from process waste	2.24	2.24
CNP 130132	2.	M/s. Mysore Paints & Varnish Limited, New Bannimantop Extension, Mysore-570015	Quantitative & Qualitative process improvement and demonstration for the recovery of silver from indelible ink process waste	6.74	6.74
CNP 130232	3.	M/s. Electronics Regional Test Laboratory (North), S – Block, Okhla, Industrial Area, Phase - II, New Delhi – 110 020	Metrological Characterization of a Dual Range Piston Gauge	3.70	3.70
CNP 130332	4.	M/s. InsPIRE Network for Environment, S-212, Second Floor, Panchsheel Park, New Delhi-110017	Preparation of Third National Communication (TNC) and other new information to the UNFCCC": Biennial update report	26.22	9.44
CNP 130432	5.	The Controller, Legal Metrology, Vikas Bhavan, Thiruvananthapuram – 695 033	Setting up of working standards laboratory for verification of sphygmomanometers in Kerala	15.17	15.17
CNP 130532	6.	M/s. InsPIRE Network for Environment, S-212, Second Floor, Panchsheel Park, New Delhi-110017 (for MoEF, GOI)	Preparation of Third National Communication (TNC) and other new information to the UNFCCC" Project : India's First Biennial Update Report – Mitigation Actions – Waste Sector	10.00	4.00
NEARING COMPLETION**					
CNP051032	1	M/s CPCB, Agra, Lucknow Zone	Inversion/mixing height studies at CPCB, Agra	9.99	0.00
CNP060632	2	M/s MN Dastur & Co. Ltd, Kolkatta	Mixing height determination at Paradeep, Orissa	2.76	0.00

CNP070432	3	M/s Regional Reference Standard Laboratory (RRSL), Guwahati	Setting up of torque standard machine at RRSL, Guwahati	14.29	0.00
CNP070932	4	Regional Reference Standard Laboratory (RRSL), Bangalore	Design, develop and fabricate torque primary standards from 2 Nm-200 Nm within uncertainty of 0.05 %	31.00	0.00
CNP071132	5	Regional Reference Standard Laboratory (RRSL), Ahmedabad	Design, primary and secondary torque measuring facility at RRSL, Ahmedabad	14.29	0.00
CNP071232	6	Regional Reference Standard Laboratory (RRSL), Bhubaneswar	Supply of one number of secondary torque measurement facility at RRSL, Bhubaneswar	14.29	0.00
CNP071332	7	M/s MN Dastur & Co. Kolkatta	Mixing height determination at Keonjhar, Orissa	5.25	0.00
CNP071732	8	M/s Tata Steel, Jamshedpur	Inversion study for Tata Steel Plant at Jamshedpur	4.10	0.00
CNP090332	9	M/s Raipur Tar Product, Raipur, Chhattisgarh, MP	General consultancy relating to reduction of QI from high QI coal tar pitch	0.98	0.00
CNP100132	10	M/s SIMCO Calibration Laboratory, Hyderabad	Guidance in Implementing of quality system dimensional parameters as per ISO 17025	1.37	0.00
CNP100532	11	M/s Rajesh & Rajesh Std. Lab, Konark Apartment, Tal Panvel, Dist. Raigad (Maharashtra)	Set-up of laboratory of mass measurement for NABL accreditation	2.49	0.00
CNP110132	12	M/s ABB Limited, 32, NIT, Faridabad	Weighing scale validation project	4.33	0.00
CNP110232	13	M/s Electronics Regional Test Laboratory (North), New Delhi	Metrological characterization of a dual range piston gauge	3.26	0.00
CNP110332	14	M/s Electronics Test and Development Centre, Guwahati	Determination of metrological parameters of hydraulic and pneumatic dead weight testers	5.40	0.00
ACCOMPLISHED***					
CNP050232	1	M/s Regional Reference Standard Laboratory (RRSL), Ahmedabad	Design, Fabrication and installation of load cell testing machine	16.44	0.00

CONTINUING *****

CNP070832	1.	M/s Aeronautical Development Agency (ADA), Bangalore	Certification of reference blocks of various materials as per 1,2mm FBH standards of ASTM E 127-PV3/PV5 (59/704)	9.36	0.00
			TOTAL	200.91	41.29

Pl. note: * New Projects during 2013-14;
** Nearing Completion (Intellectual fee yet to be distributed);
*** Accomplished (Intellectual fee distributed);
***** Continuing during the year 2013-14

Appendix -6

EARNING FROM CALIBRATION & TESTING
(Year 2013-14)

Material Physics & Engineering

Sub-Division No	Sub-Division	Charges or Actual Amount Received, inclusive of all Taxes (In lacs)	No. of Reports
D2.02	Physics & Engineering of Carbon	00.40	2
D2.04	Multiferroics & Magnetics	05.24	33
D2.07	Piezoelectric Sensors & Actuators	00.34	10
	TOTAL	5.98	45

Time & Frequency

Sub-Division No	Sub-Division	Charges or Actual Amount Received, inclusive of all Taxes (In lacs)	No. of Reports
D4.03	Precise Timing System	04.09	13
	TOTAL	04.09	13

Apex Level Standards, Metrology & Electrical Standards

Sub-Division No	Sub-Division	Charges or Actual Amount Received, inclusive of all Taxes (In lacs)	No. of Reports
D5.01	Mass Standards	90.83	343
D5.02	Standard of Dimension	64.17	290
D5.03	Temp & Humidity Standards	38.09	89
D5.04	Optical Radiation Standards	78.00	517
D5.05	Force & Hardness Standards	109.05	696
D5.06	Pressure & Vaccum Standards	48.69	118
D5.07	Acoustic, Ultrasonics, Shock and Vibration Standards	22.72	119
D5.09	LF & HF Impedance & DC Standards	27.35	123
D5.10	LF & HF Voltage, Current & Microwave Standards	32.36	79
D5.11	AC High Voltage & AC High Current Standards	54.72	78
D5.12	AC Power & Energy Standards	47.29	154
	TOTAL	613.27	2606

Quantum Phenomena and Applications

Sub-Division No	Sub-Division	Charges or Actual Amount Received, inclusive of all Taxes (In lacs)	No. of Reports
D6.03	Nanoscale Measurements	0.37	1
	TOTAL	0.37	1

Sophisticated and Analytical Instruments

Sub-Division No	Sub-Division	Charges or Actual Amount Received, inclusive of all Taxes (In lacs)	No. of Reports
SD7.01.02	Electron & Ion Microscopy	2.05	15
SD7.01.04	Analytical Chemistry	23.67	102
	Total	25.72	117

Appendix - 7

ANNUAL EXPENDITURE

Annual Expenditure 2013-14				
Sr. No.	Budget Heads	Grant	LRF	Total
1	Pay and Allowances	5231.94	102.842	5334.782
2	Contingencies	603.437	101.92	705.357
3	Human Resource Development			0
4	Maintenance	250.883	91.023	341.906
5	Chemicals	142.34	41.873	184.213
6	Works & Services	847	0.932	847.932
7	Apparatus & Equipment/Computers	9.545	85.311	94.856
8	Machine/Office Equipment/ Furnitures		4.886	4.886
9	Library Books	55	1.227	56.227
10	Staff Quarters	111.871	10.201	122.072
11	Network Projects	5143.87	0.94	5144.81
	Total	12395.886	441.155	12837.041

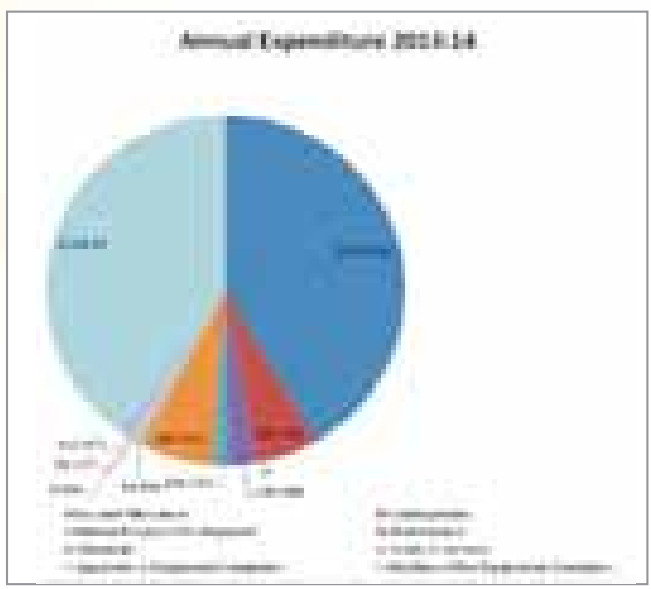

Appendix -8

Recognitions, Honours and Awards

Dr. Sanjay Kumar Srivastava and Dr. P. K. Saini received CSIR Young Scientist Award 2013 in Physical Sciences and Engineering Sciences respectively including instrumentation. The award consists of a citation, cash prize of Rs. 50,000 and a plaque.

Dr. O. S.Panwar - Member of Editorial Board of "Advanced Carbon" Journal, American Scientific Publisher, USA and his Biography included in "Marquis Who's Who in the World" Vol. 31(2014), New Jersey, U.S.A.

Dr. S.K. Dhawan received ASDF Global Award in December 2013 from Association of Scientists, Developers and Faculties

Dr Sonal received Dr G C Jain Memorial Prize for the Best PhD Thesis in Materials Science for the year 2014 by Materials Research Society of India (MRSI)

Dr D Haranath has been invited as a Jury Member for DST's INSPIRE scheme by Department of Science & Technology (DST) and also in National Level CBSE Science Exhibition conducted by Central Board of Secondary Education (CBSE)

Dr. R. K. Kotnala	-	Associate Editorship of Journal of Applied Physics, American Institute of Physics, Newark, USA
	-	Member of Editorial Board of Journal of Nanoparticle Research, Springer Publishers, Netherlands
	-	Fellow-APAM, Asia Pecific Academy of Materials

Mr. Vipin Jain has been invited to conduct "Metallica 2013" an Inter-School Quiz Competition, Indian Institute of Metals, Delhi Chapter

Dr. K. P. Chaudhary	-	Chairman, Engineering Metrology Sectional Committee, PG 25, Expert- PG 32 and PGDC in Bureau of Indian Standards (BIS).
	-	General Secretary, Metrology Society of India
	-	Governing Body, M.M. Engineering College, M, M, University, Mullana
	-	Chairman core Committee and supplementary Committee of NABL
Dr. V.N. Ojha	-	Member, MTD -33 and ET-01, Sectional Committee, BIS
	-	Alternate Chairman Core Committee and supplementary Committee of NABL

Dr. G. Bhagavannarayana spotted as 2nd top scientist in the area of crystal growth in terms of publications with 245 SCI publications in international journals, Indian Association for Crystal Growth

Dr Sukhvir Singh has been nominated as Chairman of Educational Instruments and Equipment Sectional Committee, PGD 22 of BIS

Dr R P Pant (ICMf13)	-	International Steering Committee member of magnetic fluid, ISCMF 2013
	-	Guest editor for the special issue of Magnetohydrodynamics journal
Dr. Shankar G. Aggarwal	-	Guest Editor for a special issue of MAPAN-Journal of Metrology Society of India

Appendix - 9

Distinguished Foreign Visitors at CSIR-NPL

(April 2013- March 2014)

S. N.	Name of the Scientists/Events	Period
1.	23 delegates from 17 countries under "Management Development Programme on Operation, Maintenance and Repair of Optical/Ophthalmic Equipment" sponsored by Ministry of External Affairs , Govt. of India under ITEC/ SCAAP Programme at CSIO, CSIR Complex , New Delhi	2/4/2013
2.	5 members delegation from Tanzania	8/4/2013
3.	Dr. Kamal Hossain of National Physical Laboratory, Teddington, UK	17/4/2013
4.	4 member Ukrainian delegation	23/4/2013
5.	34 participants from developing countries attending International Training Programme on "Standardization and Quality Assurance for Developing Countries" This training programme was organized by National Institute of Training for Standardization (NITS) of Bureau of Indian Standards.(BIS) under Min. of Consumer Affairs, Food & Public Distribution under Indian Technical & Economic cooperation(ITEC) & special Common Wealth Assistance for African Programme (SCAAP) of Ministry of External Affairs	7/5/2013
6.	17 delegates from 17 developing countries under "Management Development Programme on Operation, Maintenance and Repair of Optical/ Ophthalmic Equipment "sponsored by Ministry of External Affairs , Govt. of India under ITEC/ SCAAP Programme at CSIO, CSIR Complex , New Delhi	23/9/2013
7	Prof. Samuel D. Bader, COPI, Indo-US project, USA	8/12/2013 to 11/12/2013
8	A two member delegation from Ministry of Science & Technology, Govt. of Vietnam led by Ms. Pham Thi Mai Huong, General Editor of the Science & Development Newspaper – Leader & Dr. Tran Dong, Deputy Chief of the High Technology Department- Member	11/12/2013
9	20 delegates from 17 countries under "Management Development Programme on Operation, Maintenance and Repair of Optical/Ophthalmic Equipment" sponsored by Ministry of External Affairs , Govt. of India under ITEC/ SCAAP Programme at CSIO, CSIR Complex , New Delhi	2/1/2014
10	Dr. Ilya Budovsky, Section Manager of Electricity, National Measurement Institute of Australia	6/2/2014
11	10 members US delegation from various Universities of US	19/3/2014
12	Two members Myanmar delegation (Dr. Nyi Aung- Structure & Construction, MSTRD & Dr. Min Thu San – Head of Metrology Division , MSTRD)	31/3/2014

No. of CSIR-NPL Scientists visited abroad during 2013-14 : 43

No. of SRF & Project Assistant visited abroad during 2013-14: 05

Appendix 10

Ph.D awards based on the research work done at NPL

S.No.	Name of the Student	Supervisor	University
1.	Mr. Deepak Kr. Jangir	Dr. Ranjana Mehrotra	Delhi University
2.	Ms. Gunjan Tyagi	Dr. Ranjana Mehrotra	Delhi University
3.	Ms. Arti Singh	Dr. Y.P. Singh	CCS University
4.	Ms. Jhuma Gope	Dr. Sushil Kumar	BHU
5.	Mr. Neeraj Dwivedi	Dr. Sushil Kumar	IIT , Delhi
6.	Mr. Anuj Kumar	Dr. VPS Awana	Delhi University
7.	Mr. Shiv Kumar Singh	Dr. VPS Awana	Jamia Millia Islamia
8.	Mr. Anand Pal	Dr. VPS Awana	Jamia Millia Islamia
9.	Mr. Jagdish Kumar	Dr. VPS Awana	H.P. University
10.	Mr. Saurabh Srivastava	Dr. G. Sumana	BHU
11.	Mr. Nitu Kumar	Dr. R.K. Kotnala	IIT, Kurukshetra
12.	Mr. Amit Kumar	Dr. H.K. Singh	BHU
13.	Mr. Manoj Kumar Srivastava	Dr. H.K. Singh	Delhi University
14.	Mr. Pawan Kumar	Dr. H.K. Singh	Jaypee Inst. of Information Technology

Appendix 11

HUMAN RESOURCE DEVELOPMENT GROUP

The various activities of the Group are as follows:

1. Organization of Industrial Training Courses

Organisation of Training Courses on various physical parameters in the area of Metrology / Standards, as well as on other specialized topics is an important activity of the HRD Group. These courses are primarily meant for the personnel belonging to various industries, Testing & Calibration laboratories and other S&T organisations. However, the NPL staff members are also encouraged to attend these courses, where ever found fit.

The Training Courses consist of theory lectures on various scientific & technical aspects of the training course, followed by practical demonstration and hands-on training on the related instruments / apparatus / machines.

Six (06) Training Programmes on various physical parameters in the area of Metrology / Standards, as well as on other specialized topics were organised by NPL during the period from 1st April 2013 to 31st March, 2014, the details of which are as follows:

1. Training Programme on Calibration & Evaluation of uncertainty Measurement in Dimensional Parameter : *14-15 May 2013*
2. Training Programme on Mass Metrology, *20-22 August 2013*
3. Training Programme on Force, Torque & Hardness Metrology, *4-6 September 2013*
4. Residential Training Programme for Legal Metrology Officers on Mass, Volume, Density & Length, Blood Pressure Measurements & Clinical Thermometers, *18-22 November 2013*.
5. Workshop on Coordinate Metrology, *17-18 December 2013*
6. Residential Training Programme for Legal Metrology Officers on Laboratory Quality Management System, *28-31 January, 2014*.

This activity led to an ECF generation of ₹ 73,72,160

2. Placement, Ph.D. Registration and other Support to Research Fellows

One of the most prominent activities of the NPL is to provide help and support to Research Fellows (JRFs / SRFs), starting from the time they join NPL till the time they leave NPL. This includes their placement in a suitable Division / Group and helping them in getting Hostel accommodation, if required. This also includes their Ph.D. registration, assessment for continuance / upgradation, deputation to attend conferences, etc. Sometimes, the help to the Research Fellows starts even before they join NPL. This refers to the cases wherein they are invited and inspired to join NPL for their Ph.D. programme.

During the period from 1st April 2013 to 31st March, 2014, 41 research fellows (Project staff/JRFs/ SRFs) were inspired to join NPL, resulting in a total strength of Research Fellows in NPL to be 115, as on 31.03.2014. Most of these students are registered under AcSIR.

3. Organization of Institutional Visits to NPL

Organization of institutional visits involving students / teachers / faculty members / personnel belonging to schools / colleges / universities / technical institutes / S&T organisations is an important activity of the NPL. The basic objective is to provide the visitors a glimpse of the NPL activities and achievements, and thus enhance visibility of NPL in the society.

During the period from 1st April 2013 to 31st March 2014, Five (05) institutional visits were organized by NPL, which involved around 150 students from different schools/Colleges/Universities.

4. Organization of Students' Training at NPL

NPL provides Training (6 months & above) to students pursuing M.Sc./M.Tech./MCA, or their equivalent degree programmes, at different educational institutions spread all across the country, in the areas of research activities being carried out at NPL. The basic objective is to provide the students a feel and importance of the various activities, as well as to motivate them towards scientific research as the career.

During the period from 1st April 2013 to 31th March 2014, 151 students were provided training oriented towards the fulfillment of their academic degree requirements in different areas of research under the guidance of senior scientists.

This activity led to an ECF generation of ₹ 5,55,000/-.

5. Deputation of NPL Staff Members to Attend Conferences / Similar Events

NPL encourages and supports its staff members, including the students like JRFs, SRFs, PAs, RIs, RAs, SRAs, etc., to attend and present papers at national / international conferences / symposia / seminars / workshops, organised by different agencies in areas relevant to research activities being carried out at NPL. This is primarily meant to enable the staff members to put forward their views and research results before the leading national / international experts and interact with them on the latest developments in their research areas.

During the period from 1st April 2013 to 31th March 2014, 314 cases of NPL scientists and other staff members including research scholars, were nominated to participate in various conferences / similar events and different Training Courses held across the country.

6. AcSIR and M.Tech. Programme Related Activities

All activities related to M.Tech programme for Advanced Material Physics & Engineering and AcSIR Ph.D Students including Interviews , Admission Process, Classes (theory/tutorial/ practical), Examinations and Evaluation are handled by the HRD Group in consultation with the AcSIR-NPL Coordinator.
During the above mentioned duration, (07) M. Tech students joined CSIR-NPL for "Advanced Material Physics & Engineering" Course under the IMP Category and 41 Students were enrolled for Ph.D. in AcSIR in current financial year.

7. Organization of National Science Day Function

The 'National Science Day' was celebrated at National Physical Laboratory, New Delhi on February 28, 2014 in the form of **"Poster Presentation Symposium"** with great enthusiasm and commitment. Prof. R. C. Budhani Director, NPL addressed the scientists and students and introduced the chief guest for the

science day function, Dr. R. Muralidharan, Director, Solid State Physics Laboratory, New Delhi. The insightful and informative lecture by the chief guest on the topic 'Electronic Materials and Devices – Enablers for Defense Technology' was highly appreciated. Director, NPL honored the chief guest with a shawl and NPL memento. The lecture was followed by poster presentation by the research students to mark the quality research going on in NPL.

One hundred & fifteen (115) posters were displayed by students which were visited by the scientific fraternity, thus fostering scientific temperament among the students. The posters were also evaluated by the jury and four students were awarded "the best poster awards".

Appendix - 12

CSIR-NPL Colloquium Series

1. "Recent Trends in Ultra-flat Electronics" by Dr. Arindam Ghosh, Department of Physics, IISc, Bangalore

   Date: Friday, 21st June, 2013

2. "Crystalline Silicon Solar Cell Technology" by Dr. Kaustuv Chakrabarty, Jawaharlal Nehru Engineering College, Aurangabad

   Date: Friday, 11th Oct., 2013

3. "Spintronics: Implications for Energy, Information & Medical Technologies" by Prof. Samuel D. Bader, Argonne Distinguished Fellow and Associate Director,Argonne National Laboratory, USA

   Date: Tuesday, 10th December, 2013,

Appendix - 13

Invited talks and Lectures by CSIR-NPL Scientists

Sl. No.	Speaker's Name	Topic	Event and Venue
1	Dr. Suresh Chand	Alternate Acceptors and Transport Layers in Organic Solar Cells	Indo-US workshop on organic solar cells jointly sponsored by the Indo-US Science and Technology Forum (IUSSTF) in India and the US National Science Foundation (NSF) in the USA organized at Indian Institute of Technology (IIT) Kanpur on 20th and 21st March, 2014
2		Recent Advances in Organic Photovoltaics at CSIR-NPL and India Conext	Joint Indo-US Workshop on Organic Photovoltaics Materials and Devices Golden, Colorado, USA, June24-26, 2013
3		Advances in Efficiency at CSIR-NPL in Organic Solar Cells	Indo-UK Workshop and meet on Indo-UK joint Energy initiative at University of Cambridge, July 4-5, 2013.
4		Recent advances in Organic Solar cells – a bright future	RCET, Bhillai, Dec 28th, 2013.
5		Organic Solar Cells for a Bright Future	Rise -14 Silchar: 11.1.2014
6		Recent advances in Organic Solar cells	NCRTP, Raipur 11-14 March 2014.
7		New Development in Organic Solar cells – a bright future	Conference on Material Development Amity University 30.10.2013
8		Latest Developments in Organic Solar Cells for a Bright Future	IT Mandi, Kamand Campus, Major District Road 23, Suran, Himachal Pradesh 175005,Dec 3rd 2013.
9		High efficiency in small molecule based organic PV	IUMRS-ICA 2013, Indian Institute of Science, Bangalore, India, Dec 16-20,2013
10	Dr. O. S. Panwar	Synthesis of Multilayer Graphene by Filtered Cathodic Vacuum Arc Technique"	17th IWPSD on Physics of Semiconductor Devices held at Amity University, Noida, UP from December 10-13, 2013.
11	Dr.Ritu Srivastava	Organic Semiconductor and its applications	"Recent developments in Physics (NCRDP-2014)" on 29th and 30th March 2014 at Department of Physics SD (PG) College, Panipat
12		Application of new LED technologies leading to power	National seminar on"Applications of Engineering and Technology In Energy

		saving	Management", on 25th and 26th Feb 2014 at IIMT, Greater Noida
13	Dr. Sushil Kumar	Plasma Processing of Materials, Devices & Systems	Refresher Course on Physics, at GJ University of Science & Technology, Hisar (9 May 2013)
14		Thin Film Technology & Solar Cells	Refresher Course on Physics, at GJ University of Science & Technology, Hisar (9 May 2013)
15		Thin Film Silicon Solar Cell Technology	Continuing Education Programme (CEP), at SSPL, Delhi (18 Sept. 2013)
16	Dr. S. Sudhakar	Thin Film Solar Cells – Challenges and Opportunities	International conference on Recent advances in Physics, Sir Vidya Mandir Arts and Science College, Uthangarai (12-13 August 2013)
17		Thin Films: Technology and Applications	National Workshop on Recent trends in physics, Mother Teresa University, Kodaikanal (30 September 2013)
18		Plasma enhanced chemical vapor deposition of phosphorous doped micro/nanocrystalline Si thin films and their characterization	International workshop on Electronic Materials Technology, Anna University-Chennai (13-15 March 2014)
19	Dr. Vandana	Measurements in PV Devices and Materials	2nd National Conference on "Micro and Nano Electronic Systems and Devices-2013" (MINO-2013), Jaipur 8-9 August, 2013.
		Advancement in Silicon PV Technology and Solar Cell Measurements	"ESDM workshop, HMRITM, Hamidpur, Delhi, 9-10 October 2013"
20	Dr. P.K. Singh	Enabling Nanotechnology in Silicon Based Photovoltaic	Indo-Norwegian Workshop on Advanced Materials for Solar Cell Application, CIT, Coimbatore, 10 - 12 July 2013
21		Nanotechnology: A Platform for New Silicon Solar Cell Structures	2nd National Conference on "Micro and Nano Electronic Systems and Devices-2013"; VIT Campus, Jaipur, 8-9 Aug. 2013
22		Solar Energy: The Ultimate Source of Energy	Hansraj College, University of Delhi, Delhi, Sept 5, 2013
23		Solar PV Research: Current Status and Directions	PSGTech, Centre for Solar PV Research, Oct 08, 2013
24	Dr. S.K. Srivastava	Silicon nanowire arrays: A promising material for silicon solar cells	2nd TAPSUN Conference: ADVANCES IN FUTURISTIC SOLAR ENERGY MATERIALS & TECHNOLOGIES, held at CLRI Chennai during 13-14 Sept. 2013.

25		Silicon nanowire arrays: A promising approach for silicon solar cells	International conference on Nano materials with special reference to energy security (NMES-2014) (Under the auspices of Asia Pacific Academy of Materials (APAM) Department of Physics, Banaras Hindu University, Varanasi-221005, March 12-14, 2014
26	Dr . Govind	Growth of GaN and AlN/GaN by PAMBE & Their Characterization	National Workshop on Nitride Semiconductors (NWNS-2013), April 6, 2013, Indian Institute of Technology, Delhi
27		Nitrides: Material for Futuristic Optoelectronics & Photovoltaic Devices	QUARK-14, Hindu College, Delhi University, Delhi, January 3, 2014
28	Dr. S.K. Dhawan	Designing of nanoferromagnetic conducting composites for EMI Shielding Applications	International Conference on Recent Trends in Materials and Devices-ICRTMD 2013 (October 2013), Amity University, Noida
29	Dr. S.R. Dhakate	Development of carbon material in generation and storage of clean energy	IUMRS-ICA 2013, IISc, Bangalore, 16-20 December 2013.
30	Dr. Bhanu Pratap Singh	Carbon Nanotubes: Synthesis and Applications in Li-Ion Batteries	National Conference on Advances in material science for energy applications (AMSEA-14), University of Petroleum and Energy Studies, Dehradun, India from 9th to 10th Jan 2014
31	Dr.Virendra Shanker	Recent advances in Electro-Luminescent Materials for Display Applications	National Conference on Luminescence and its Applications (NCLA-2014) held at Department of Physics, Rani Durgavati University, Jabalpur during Feb 5-7, 2014
32	Dr. Santa Chawla	Light emitting nanoparticles and Plasmon enhanced fluorescence	International conference on Nanomaterials with special reference to Energy Security (NMES-2014)Under UGC Networking Programme. Department of Physics, B.H.U. Varanasi, March 11-17, 2014
33		Development of luminescent nanoparticles for lighting, display and energy harvesting applications	International Conference on Emerging trends in Science & Technology Impact on Environment & Society for inclusive growth (ICETST-14), AISECT University, Bhopal, 14,15 February 2014
34	Dr. D Haranath	Present and Future of Luminescent Quantum Dots	National Conference in Applied Physics and Materials Science (APMS-2013) held at Department of Physics, Vasavi College of Engineering, Hyderabad during July 19-20, 2013.

35		A New Rare-Earth Free Phosphor for Cost Effective LEDs	National Conference in Applied Physics and Materials Science (APMS-2013) held at Department of Physics, Vasavi College of Engineering, Hyderabad during July 19-20, 2013.
36		Semiconductor Quantum Dots: Current Status and Future Perspectives	National Conference on Luminescence and its Applications (NCLA-2014) held at Department of Physics, Rani Durgavati University, Jabalpur during Feb 5-7, 2014.
37	Dr. Bipin Kumar Gupta	Basics of X-ray diffraction: Structure determination of advanced nano and bulk materials	National Conference on Materials Science: Trends & Future-2014 (NCMS), held at Department of Physics, Bharatiya Mahavidyalaya, Amravati, Nagpur, January 10-11, 2014.
38		Broad Spectrum and Scope of Standardization in Luminescent Nanomaterials: Synthesis, Characterization and Nanoindustry	Workshop on " Nano Materials with particular reference to Energy Security" held at Department of Physics, Banaras Hindu University, Varanasi -221005, Under UGC Networking Programme during the period March 11-17, 2014.
39		Hydrogen as a Freedom Fuel: A New Era in India	National Workshop on Fuel Cell Technology (from Basic Science to applications) held at Energy Centre MANIT, Bhopal March 24-25, 2014
40	Dr. A. Sen Gupta	An Introduction to Atomic clocks	Public Lecture delivered at the Space Application Centre (ISRO), Ahmedabad on 9th July 2013
41		Atomic Clocks and their Application in Navigation Satellites	Invited lecture at the India Meteorological Society, Lodi Road, New Delhi on 25th July, 2013
42		Generation & Dissemination of Indian Standard Time at CSIR- NPL, India	Invited Lecture at the AdMet-2014 held at the Thapar Institute, Patiala on 19 Feb 2014
43		Atomic Clocks - How do they work and why do we need them?	Inaugural address at the National Workshop on Basic Optics, Fiber Optics and Optical Communication held at the Delhi University on 8th March, 2014
44	Dr Ashish Agarwal	The Atomic Clocks	DST-INSPIRE LECTURE, Raj Kumar Goel Institute of Technology, Ghaziabad, January 2014
45		The story of the most accurate clocks on earth - the Atomic Clocks	DST-INSPIRE LECTURE, Raj Kumar Goel Institute of Technology for Women, Ghaziabad, January 2014

46	Dr. P. Arora	Time-keeping and Atomic Clocks	Invited talk, CSIR-HRDC, Ghaziabad, 2013
47		Atomic Clocks at CSIR-NPL	Invited talk, RCI, DRDO, Hyderabad, India, Nov. 30 2013
48	Dr. S. De	Atomic Clocks from Indian Perspective	Cold atoms workshop at HRI Allahabad, India, Feb. 15, 2014
49		Atomic Clocks – Time and frequency standards in India	Colloquium, IISER Pune, India, Jan. 06, 2014
50		Atomic Clocks – Time and frequency standards in India	Colloquium, ISI Chennai, India, 17 Dec. 2013
51		Atomic clocks: R&D on frequency standards at CSIR-NPL, India.	Physics Dept. Colloquium, IIT Delhi, India, 12 Nov. 2013
52	Mr. Anil Kumar	Importance of mass standards	The ASEAN – INDIA Program on Quality System in manufacturing on April 09, 2013
53		Significance of measurement in life	National Seminar on Recent Trends in Mechanical Measurement on May 06, 2013 organized by H R Institute of Technology, Ghaziabad
54		Mass Measurements	National Conference on Advancements in Mechanical Engineering on Aug 22-23, 2013 organized by Al-Falah School of Engineering & Technology, Faridabad
55		Effect of Buoyancy in Mass Determination	3rd National Conference on Advancement in Metrology on Feb 18-21, 2014 organized by Thapar University, Patiala
56	Mr. Goutam Mandal	Weighing techniques and calibration of weights	CSIR - CSIO Complex on Dec 30, 2013
57		Calibration of balances	CSIR - CSIO Complex on Dec 30, 2013
58		Importance of mass metrology	National Seminar on Precision Engineering, Metrology, Quality Assurance, NABL Accreditation organized on Jan 31, 2014 by MSI-ER
59	Mr. Harish Kumar	Recent development of some precision force transducers	National Seminar on Recent Trends in Mechanical Measurement on May 06, 2013 in H R Institute of Technology, Ghaziabad
60	Dr. K.P. Choudhary	Dimensional Metrology in nano regime	Industry laboratory Summit on Testing and calibration at CMTI, Bangalore on December 06, 2013

61	Dr. K. P. Chaudhary	Application of LASER in Bio-Medical Instrumentation	Management Development Programme on operation, maintenance & repair of Bio-medical equipment sponsored by MEA at CSIO, New Delhi on September 09, 2013
62		LASER and its use in Opthalmology	Management Development Programme on operation, maintenance & repair of Analytical equipment sponsored by MEA at CSIO, New Delhi on December 17, 2013
63		Calibration Measurement: Criticality in R & D	Orientation Training Programme for Technical Group III personnel at HRDG, CSIR, Ghaziabad on April 10, 2013
64		Dimnesional Metrology, Principles of Metrology, Industrial Metrology	45th International Training Program on Standardization and Quality Assurance at Lemon Tree Hotel, Ghaziabad on April 30, 2013
65		Proficiency Testing, Root Cause Analysis and its Significance for Traceability and Quality Improvement	3rd National Conference on Advances in Metrology (AdMet - 2014) at Patiala on February 20, 2014
66		Dimensions and Length Metrology	PreAdMet tutorial on Basics in Metrology at Patiala on February 19, 2014
67	Dr. Y.P. Singh	Temperature standards and metrology at National Physical Laboratory	Training Programme on 'Calibration of Laboratory Equipment and Quality Assurance in Cement, Construction and Process Industries', NCCBM, Ballabhgarh (Haryana), (10-11 July 2013)
68		Temperature standards and metrology	Training Programme for Legal metrology officers At CSIR-NPL on Mass, Dimension, Pressure and Temperature", 18-22 Nov. 2013
69		Advanced temperature Measurement Techniques	National Symposin an Emergency plasma techniques for materials processing and Industrial Applications (N-SEPMI-2014), University of Pune, Feb. 13-15, 2014.
70		*1.* Temperature standards and metrology *as per ITS-90 at CSIR-NPL*	1st hands on training program on calibration and NABL assessor conclave held on Feb.12-14, at CMTI, Bangalore
		2. "Thermocouple thermometry for High Temperature metrology	
71		Recent trends in t*emperature* standards and precision metrology	AdMet-2014, Thapar University, Patiala, Feb. 19-21, 2014.

72	D.D. Shivagan	Realization of Zn freezing point using using SPRT	AdMet-2014, Thapar University, Patiala, Feb. 19-21, 201
73		Resistance thermometry: traceability and calibration of SPRT, RTD and and LIGT"	"Training Programme for Legal metrology Officers on Mass, Dimension, Pressure Temperature", 18-22 Nov. 2013.
74	Dr. A.K. Bandyopadhyay	New Raman spectrometer of CSIR-NPL for the advanced characterization of the novel materials	National conference on novel materials for advanced technology (NMAT-13), NRI Institute of Research and Technology, Bhopal
75	Dr. Sanjay Yadav	Fundamentals of Metrology and the Role of NMI in NMS: Calibrations of Pressure Measuring Instruments	Training Programme on Calibration of Laboratory Equipment and Quality Assurance, NCCBM, Ballabhgarh, Haryana on July 10, 2013
76		Indian National Pressure Standards, their Traceability and Global Metrological Equivalence	3rd National AdMet Conference (AdMet-2014), Thapar University, Patiala, Punjab, Feb. 19-21, 2014
77		Status of Existing NPL Pressure and Vacuum Standards, Their Traceability and Approved CMCs in KCDB of BIPM	1st Hand on Training Programme on Calibration of Mass, Volume, Density, Force, Torque and Pressure and NABL Assessors Conclave, CMTI, Bangalore, Feb. 12-14, 2014.
78		Standard Procedure for Calibration of Pressure Gauges	1st Hand on Training Programme on Calibration of Mass, Volume, Density, Force, Torque and Pressure and NABL Assessors Conclave, CMTI, Bangalore, Feb. 12-14, 2014.
79	Dr. Ranjana Mehrotra	Fundamentals of Infrared Spectroscopy	Biomedical Instrumentation Programme, CSIO, New Delhi, 4/4/2013
80		Fundamentals and applications of Infrared Spectroscopy	Management Development Programme on Operation Maintenance & Repair of Analytical Equipment, CSIO, New Delhi, 23/12/13
81		Design of experiment	Programme for Technical Group III personnel at HRDG, Ghaziabad, 11/12/13
82		Infrared spectroscopic study for tumor diagnosis	IRDE, DRDO, Dehradun, 1/2/2014
83		Near Infrared spectroscopy and its applications	Application of NIR technology for tea quality analysis, CDAC, Kolkata & Jadavpur University, 5/3/14
84	Dr. H.C. Kandpal	Quantum Standards and other Standards Activities in NPL 16, 2013	Refresher Course for University Teachers, ASC, JNU, New Delhi, Sept.

85		Evaluation and Estimation of Uncertainty in the Measurement of Photometric Parameters for Automotive Lighting	International Symposium on Automotive Lighting, ISoL 2013, International Centre on Advanced Technology, Maneshar, Harayana, Nov. 28-29, 2013
86		Standards and Measurement Traceability for LEDs and SSLs	AdMet 2014, Thapar University, Patiala Feb. 19- 21, 2014
87		Photon Correlation Spectroscopy of Single photon Sources using Superconducting Nanowire Single Photon Detectors	National Seminar on Nanophysics PNBGSC, Indore, Feb. 25-26, 2014
88		Evolution of radiometry and photometry from classical to quantum - NPLI's perspective	International Conference on Optics and Optoelectrnics, IRDE, Dehradun, March 5-8, 2014
89	Dr. Anurag Gupta	Critical current density and pinning properties of in-situ bulk MgB_2 with excess Mg and non-Carbon additives	IUMRS- ICA 2013, Indian Institute of Science, Bangalore, India, Dec. 16-19, 2013
90	Dr.V.N. Ojha	Advances in quantum metrology	3rd National Conference on Advances in Metrology (AdMet-2014) at Patiala on Feb 20, 2014.
91	Dr.G. Bhagavannarayana	Advanced X-ray characterization Techniques	Phys. Dept., Banaras Hindu University during June 21 & 22, 2013.
92		An introductory overview on Renewable energy Harvesting and Conservation	A special talk delivered to all the staff of NPL arranged by the Sophisticated Analytical Instruments Division, NPL on July 11, 2013.
93		An introductory overview on Renewable energy Harvesting and Conservation	Invited talk delivered in a special seminar held at Madurai Kamaraj University on July 26, 2013
94		Thin films and nano-scale device structures: characterization by high-resolution XRD, GITXRD and RSM	Invited talk delivered at 42nd National Seminar on Crystallography held at Jawaharlal Nehru University during Nov. 21-23, 2013.
95		In-house developed high-resolution multicrystal X-ray diffractometer and its role in crystal growth activity in India	Invited talk delivered at 42nd National Seminar on Crystallography held at Jawaharlal Nehru University during Nov. 21-23, 2013.
96		Synthesis, growth and structural analyses of iminodiacetic acid complexes for nonlinear optical applications.	Invited talk delivered in DST sponsored INSPIRES Programme held at Andhra University on Dec. 24, 2013
97		Building up of Developed India – Role of Young Students through Innovative Research	Invited talk delivered in DST sponsored SERC School held at SSN College of Engineering, Chennai on Feb. 21, 2014.

98		X-ray Crystallography and X-ray characterization Techniques for purity, composition, structure and perfection for advanced materials including single crystals and thin film devices	Chief Guest address delivered at XVIII National Seminar on Crystal Growth held at SSN College of Engineering, Chennai during Feb. 24-26, 2014 Chennai during Feb. 24-26, 2014
99		Crystal Growth-An overview in Indian Context	Invited talk delivered at XVIII National Seminar on Crystal Growth held at SSN College of Engineering, Chennai during Feb. 24-26, 2014.
100		Enhancement of crystalline perfection of CZ-grown single crystals by doping, necking, seeding, seed rotation, reduction, poling and annealing	Invited talk delivered at XVIII National Seminar on Crystal Growth held at SSN College of Engineering, Chennai during Feb. 24-26, 2014.
101		Growth of single crystals for second and third harmonic generation applications	Invited talk delivered at Phys. Dept., Loyola College, Chennai on Feb. 26, 2014.
102		X-ray Crystallography and X-ray characterization Techniques for purity, composition, structure and perfection for advanced materials including single crystals and thin film devices	Chief Guest address delivered in Workshop on Advanced Materials held at Phys. Dept., PSG College of Technology on Feb. 28, 2014 as a part of National Science Day.
103		Advanced Materials with a special emphasis on bulk and nano crystals	Invited talk delivered at Workshop on Advanced Materials held at Phys. Dept., PSG College of Technology on Feb. 28, 2014 as a part of National Science Day
104		An overview on crystal growth and X-ray characterization	Invited talk delivered at conference on "Nano Materials with Special Reference to Energy Security (NMES-2014)" held at Phys. Dept., Banaras Hind University during 12-14 March, 2014.
105	Dr. Rashmi	Hundred years of Moseley Law and X-ray Spectrometry	42nd National Seminar on Crystallography and Application of X-ray Diffraction for Drug Discovery, held at JNU, New Delhi during 21st-23rd November, 2013
106	Dr. N. Vijayan	Characterization of nonlinear optical Single crystals by X-ray Topography, photopyroelectric and other optical methods	International Conference on Perspectives in Vibrational Spectroscopy, held at Dept. of Physics, Bishop Moore College, Mavelikkara during Aug 7-9, 2013.

107		Experimental determination of induction period, metastable zone width and other characterization analyses of some nonlinear optical single crystals	National Conference on Advances in Materials Science held at Dept. of Physics, GAC, Pudukottai during 6-7, Aug. 2013
108		Recent Trends in Nonlinear Optical Materials	National Conference on Materials Science and its Applications held at Dept. of Physics, Kalasalingam University, Srivilliputhur, during 28th Feb. 2014-1st March 2014
109		Growth of high quality Single Crystals for Technological Applications	Special Lecture Organized by PSN College of Engineering, Tirunelveli during 27th Feb. 2014.
110		Growth of Single Crystals for Second and Third Harmonic Generation Applications	National Seminar on Crystal Growth held at SSN College of Engineering during 24-26th March 2014.
111		Growth of high quality single crystals by high temperature melt growth techniques	International Conference on Materials and Characterization techniques held at VIT University, Vellore, during 10-12th March 2014.
112	Dr. Vidyanand Singh	Growth and characterization of Cu_2ZnSnS_4 thin films by co-sputtering of metal targets and sulfurization in H_2S	International Conference on structural and physical properties of solid (SPPS 2013), organized by Indian School of Mines, Dhanbad on 18th to 20th November 2013
113	Dr. S. P. Singh	Nanomedicine: New Paradigms of Materials in Biomedical Science.	National conference NCSCAAN-2014, January 17-19, 2014 at Mathura
114		Safety assessment of metal and graphene oxide	Indo-UK Seminar on 6 Environmental Impact and Hazard Identification of Engineered Nanomaterials, 24-26th February, 2014, at Institute of Life Sciences, Ahmedabad University, Ahmedabad, India
115		Nanotechnology: Solution for Global Clean Water Challenge	International Workshop on Water Quality & Microbes: Detection to Remediation, 7th November, 2013 at CSIR-IITR, Lucknow.
116		Electrochemical Biosensors	Workshop on "Science and Technology of Sensors and E-nose"in Acharya Narendra Dev College (University of Delhi), 14 – 15 October 2013.
117		Nanomedicines: New Paradigms in Health Care	National conference on Recent Advances in Biotechnology & Nanobiotechnology, held on October 29 - 30, 2013 at Amity University Madhya Pradesh, Gwalior.

118		नैने औषधियाँ - कैंसर कलविक्षेत्र में नए याम, बायो-मेडिकल विज्ञान एवं प्रौदयोगिकी पर राष्ट्रीय सम्मेलन	21-22 नवंबर, 2013 स्थान, सीएसआईआर -राष्ट्रीय भैतिक प्रयोगशाला, नई दिल्ली.
119	Dr. Prabhat K. Gupta	Status of MiC in India	ASEAN-India Project for Quality Systems in Manufacturing: Standards at NPL India – An overview and understanding, NPL, April 9, 2013
120		Status of MiC in India	ASEAN-India Project for Quality Systems in Manufacturing: Certified Reference Materials (CRM) activities NPL, INSA, April 11, 2013
121		Metrology in Chemistry (MiC) for Life, Our Future	3rd National conference on Advances in Metrology' (AdMet-2014), Thapar Univ., Patiala, 19-21 Feb. 2014
122	Dr. Shankar G. Aggarwal	MiC at NPL India: Recent progress and action plan for 2013	BAM, Germany, April 11, 2013
123		Status of MiC activities at NPLI	APMP2013 TCQM meeting, Taipei, Taiwan, November 26, 2013
124		A brief review of metrology and current work at NPLI	NCTU, Hsinchu, Taiwan, November 28, 2013
125		Metrology in Chemistry: Issues in Air Quality Measurements	MSI-ERC National Seminar, NTH, Kolkata, January 31, 2014

Appendix -14

Human resources
(as on 31.03.2014)

GROUP IV	
Director	1
Outstanding Scientist	1
Chief Scientist	34
Sr. Principal Scientist	13
Principal Scientist	27
Sr. Scientist	36
Scientist	52
Jr. Scientist	7
Sub-Total :	171
GROUP III	
Principal Technical Officer	11
Supt. Engg. & Asst. Engg.	4
Sr. Technical Officer (3)	27
Sr. Technical Officer (2)	9
Sr. Technical Officer (1)	13
Technical Officer	14
Tech Asstt Gr III(2)	1
Tech Asstt Gr III(1)	57
Sub-Total :	136

GROUP II Sub-Total :	143
GROUP I Sub-Total :	52
ADMN-A	9
ADMN-B	57
ADMN-C	27
ADMN-C (Cafeteria Staff)	8
ADMN-D	91
ADMN-D (Cafeteria Staff)	7
Sub-Total :	200
GRAND TOTAL :	701

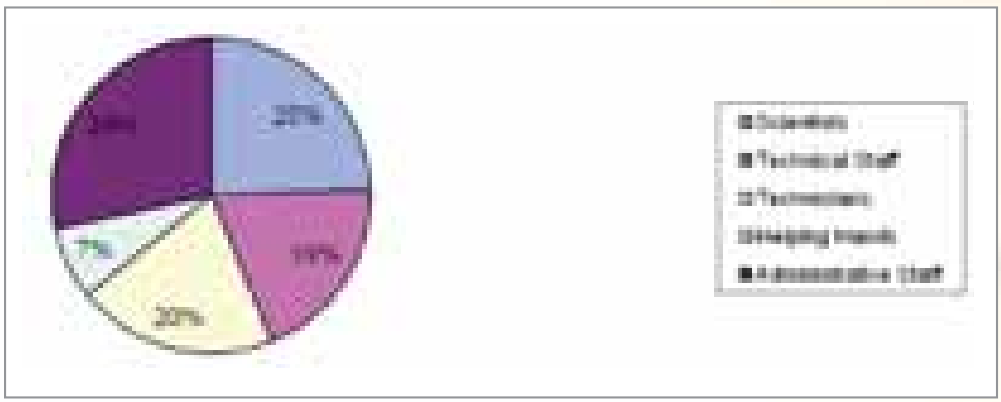

SCIENTISTS AND OFFICERS AS ON 31.03.2014

Director

Prof R C Budhani

Physics of Energy Harvesting

Head : Dr Suresh Chand

Name	Designation
Dr S T Lakshmikumar	Chief Scientist
Dr Suresh Chand	Chief Scientist
Dr Parakram Kumar Singh	Chief Scientist
Dr Omvir Singh Panwar	Chief Scientist
Dr Abdul Mobin	Chief Scientist
Dr S M Shivaprasad	Chief Scientist
Sh C MS Rauthan	Sr Principal Scientist
Dr KMK Srivatsa	Sr Principal Scientist
Dr Sushil Kumar	Principal Scientist
Dr Amish G Joshi	Principal Scientist
Dr Jeya Kumar Ramanujam	Principal Scientist
Dr Shailesh Narayan Sharma	Principal Scientist
Dr Suraj Prakash Khanna	Principal Scientist
Sh Chockalingam Sreekumar	Sr Scientist
Dr Govind	Sr Scientist
Dr (Ms) Ritu Srivastava	Sr Scientist
Dr Asit Patra	Sr Scientist
Sh Kamlesh Patel	Scientist
Dr Vinay Gupta	Scientist
Ms Vandana	Scientist
Dr Muthusamy Senthil Kumar	Scientist
Dr Mahesh Kumar	Scientist
Sh Sanjay Kumar Srivastava	Scientist
Dr Rajiv Kr. Singh	Scientist
Dr Praveen Kumar Siwach	Scientist
Dr Prabir Pal	Scientist
Dr Preetam Singh	Scientist
Dr Jai Prakash Tiwari	Scientist
Dr Ajay Kumar Shukla	Scientist
Dr Chandra Kant Suman	Scientist

Dr P Prathap	Scientist
Dr S Sudhakar	Scientist
Dr (Ms) Rachna Kumar	Scientist
Dr Mukesh Javeria	Scientist
Dr Srinivas Rao Ragam	Scientist
Sh Gauri Datt Sharma	Sr. Technical Officer (3)
Dr V K Hans	Sr. Technical Officer (3)
Sh Murari Lal Sharma	Sr. Technical Officer (3)
Sh Bhikham Singh	Sr. Technical Officer (3)
Sh Jagdish Chand	Sr. Technical Officer (2)

Materials Physics and Engineering
Head : Dr A M Biradar

Name	Designation
Dr Rakesh Behari Mathur	Chief Scientist
Dr Virendra Shanker	Chief Scientist
Dr Ashok Manikrao Biradar	Chief Scientist
Dr R K Kotnala	Chief Scientist
Dr S K Dhawan	Chief Scientist
Dr Ajay Dhar	Chief Scientist
Dr Sher Singh Rajput	Chief Scientist
Dr (Ms) Santa Chawla	Sr Principal Scientist
Sh Sanjay Rangnate Dhakate	Sr Principal Scientist
Dr Divi Haranath	Principal Scientist
Dr Rajesh	Sr Scientist
Sh Vipin Jain	Sr Scientist
Dr Aloysius R P	Sr Scientist
Dr (Ms) G Sumana Gajala	Sr Scientist
Dr Nirmalya Karar	Sr Scientist
Dr (Ms) Nidhi Singh	Sr Scientist
Sh Bhanu Pratap Singh	Sr Scientist
Sh Parveen Saini	Sr Scientist
Dr Dinesh Kumar Misra	Sr Scientist
Dr Ved Varun Agrawal	Scientist
Sh Pankaj Kumar	Scientist
Sh Bathula Sivaiah	Scientist
Sh M Saravanan	Scientist
Dr Bipin Kumar Gupta	Scientist
Dr (Ms) Priyanka Heda Maheshwari	Scientist

Dr Bhasker Gahtori	Scientist
Dr Kiran Mahadevgan	Scientist
Dr (Ms) Saroj Kumari	Jr Scientist
Sh Rajiv Sikand	Principal Technical Officer
Sh Pinaki Ranjan Sengupta	Principal Technical Officer
Sh Chander Kant	Sr. Technical Officer (3)
Sh Rajesh Kumar Seth	Sr. Technical Officer (2)
Sh Vinod Kumar Tanwar	Sr. Technical Officer (1)
Sh Manoj Kumar Pandey	Technical Officer

Radio and Atmospheric Sciences
Head : Dr M V S N Prasad

Name	Designation
Dr Bhuwan Chandra Arya	Chief Scientist
Dr M V S N Prasad	Chief Scientist
Dr(Ms) Meena Jain	Sr Principal Scientist
Dr Chhemendra Sharma	Principal Scientist
Dr Tuhin Mandal	Principal Scientist
Dr Sachidanand Singh	Principal Scientist
Dr (Ms) Monika J. Kulshrestha	Sr Scientist
Sh Ashish Ranjan	Sr Scientist
Dr Arun Kumar Upadhayaya	Sr Scientist
Sh Rupesh M Das	Scientist
Sh Sumit Kumar Mishra	Scientist
Dr Sudhir Kumar Sharma	Scientist
Dr Rajesh Agnihotri	Scientist
Dr Radhakrishnan Soman Radha	Scientist
Sh Arun Kumar Ghoghar	Sr. Technical Officer (3)
Sh Shambhu Nath	Sr. Technical Officer (3)
Mrs Shiv Kumari Bhatia	Sr. Technical Officer (3)
Mrs Beena Gupta	Sr. Technical Officer (3)
Sh Vinod Kumar Sharma	Sr. Technical Officer (3)
Sh Man Mohan Gupta	Sr. Technical Officer (3)
Sh Alok Mukherjee	Sr. Technical Officer (1)
Ms Smriti Tiwari	Technical Officer

Time and Frequency Standards
Head : Dr A Sengupta

Name	Designation
Dr Amitava Sengupta	Outstanding Scientist
Ms Arundhati Chatterjee	Sr Principal Scientist
Dr Ashish Agarwal	Sr Scientist
Dr Subhasis Panja	Sr Scientist
Dr (Ms) Poonam Arora	Scientist
Ms Pranalee Premdas Thorat	Scientist
Dr Subhadeep De	Scientist
Sh Anil Kumar Suri	Principal Technical Officer

Apex Level Standards & Industrial Metrology
Head : Dr A K Bandhyopadhyay

Name	Designation
Dr Ashis Kumar Bandyopadhyay	Chief Scientist
Sh Mukesh Kumar Mittal	Chief Scientist
Dr K P Chaudhary	Chief Scientist
Dr Yesh Pal Singh	Chief Scientist
Sh Anil Kishore Saxena	Chief Scientist
Sh Anil Kumar	Chief Scientist
Dr Tushya Kumar Saxena	Chief Scientist
Sh Thomas John	Chief Scientist
Sh Pramendra Singh Negi	Chief Scientist
Dr Mahavir Singh	Sr Principal Scientist
Sh Joges Chandra Biswas	Sr Principal Scientist
Sh D Arun Vijayakumar	Principal Scientist
Dr Sanjay Yadav	Principal Scientist
Dr (Ms) Nita Dilawar	Principal Scientist
Dr Seela Kumar Titus	Principal Scientist
Sh Rajesh Kumar	Principal Scientist
Sh M A Ansari	Principal Scientist
Sh Shiv Kumar Jaiswal	Sr Scientist
Sh Saood Ahmed	Sr Scientist
Sh Goutam Mandal	Sr Scientist

Sh Naveen Garg	Sr Scientist
Ms Priyanka Jain	Sr Scientist
Dr Ashok Kumar	Sr Scientist
Dr Premshankar Kedarnath Dubey	Sr Scientist
Sh Dilip Dhondiram Shivagan	Scientist
Sh Harish Kumar	Scientist
Dr (Ms) Kirti Soni	Scientist
Dr Satya Kesh Dubey	Scientist
Sh Satish	Jr Scientist
Sh K P S Yadav	Sr. Supt. Engnr.(Elect)
Sh Ravi Khanna	Principal Technical Officer
Sh Gurbir Singh	Principal Technical Officer
Ms Reeta Gupta	Principal Technical Officer
Dr Yudhisther Kumar Yadav	Principal Technical Officer
Sh Kul Bhushan Ravat	Principal Technical Officer
Sh Gurcharanjit Singh	Sr. Technical Officer (3)
Sh Mohammad Saleem	Sr. Technical Officer (3)
Sh Jagan Nath Prasad	Sr. Technical Officer (3)
Sh Ishwar Singh Taak	Sr. Technical Officer (3)
Sh Avdhesh Kumar Goel	Sr. Technical Officer (3)
Sh Rakesh Khanna	Sr. Technical Officer (3)
Sh Jokhan Ram	Sr. Technical Officer (3)
Sh Mukesh Kumar	Sr. Technical Officer (2)
Sh Om Prakash	Sr. Technical Officer (2)
Sh Jai Pal Singh	Sr. Technical Officer (2)
Sh Bijendra Pal	Sr. Technical Officer (2)
Sh Sudama	Sr. Technical Officer (2)
Sh Mahargha Baran Das	Sr. Technical Officer (2)
Ms Usha kiran	Sr. Technical Officer (1)
Dr Bharat Kumar Yadav	Sr. Technical Officer (1)
Sh Harish Kumar	Sr. Technical Officer (1)
Sh Sridhar Lingam	Sr. Technical Officer (1)
Ms Poonam Sethi Bist	Sr. Technical Officer (1)
Sh Manoj Kumar	Sr. Technical Officer (1)
Sh Rasik Behari Sibal	Technical Officer
Sh Anoop Singh Yadav	Technical Officer
Sh Mohammad Arif Sanjid	Technical Officer
Sh Vikram	Technical Officer
Ms Archna Sahu	Technical Officer
Sh Abhishek Singh	Technical Officer

Quantum Phenomena and Applications
Head : Dr H C Kandpal

Name	Designation
Dr Hem Chandra Kandpal	Chief Scientist
Dr Vijay Narain Ojha	Chief Scientist
Dr (Ms) Ranjana Mehrotra	Chief Scientist
Dr (Ms) P L Upadhyay	Sr Principal Scientist
Dr (Ms) Rina Sharma	Principal Scientist
Dr Veerpal Singh Awana	Principal Scientist
Dr Anurag Gupta	Principal Scientist
Dr Hari Krishna Singh	Principal Scientist
Ms Manju Singh	Principal Scientist
Dr Jiji Thomas Joseph Pulikkotil	Principal Scientist
Ms Deepti Chaddha	Sr Scientist
Sh Rajendra Singh Meena	Sr Scientist
Dr (Ms) Sangeeta Sahoo	Sr Scientist
Sh Virendra Kumar Jaiswal	Sr Scientist
Dr (Ms) Anjana Dogra	Scientist
Dr Parag Sharma	Scientist
Dr Sudhir Husale	Scientist
Dr Rajib Kr. Rakshit	Scientist
Dr Vijay Kr. Toutam	Scientist
Dr Ajeet Kumar	Scientist
Dr Ashok Kumar	Jr Scientist
Ms Girja Moona	Jr Scientist
Ms Santhya Malikar Patel	Jr Scientist
Dr (Ms) Manju Arora	Principal Technical Officer
Sh Manikandan R M	Technical Officer

Administration

Head : Sh Vijay Kumar Kaushika

Name	Designation
Sh Vijay Kumar Kaushika	COA
Sh M C Meena	AO

Ms Manju	Hindi Officer
Sh Jay Narayan Upadhyay	Hindi Officer
Ms Bhawna Guglani	S O(G)
Sh Anil Kumar	S O(G)
Sh Hari Narain Meena	SO(G)
Sh S K Yadav	S O(G)
Sh A K Handa	SO(G)
Sh Mange Ram	PS
Ms. Paramjit Kaur	PS
Sh Amar Singh	PS
Sh Ram Gopal Meena	PS
Ms Saroj Gandhi	PS
Sh R Subramanian	PS
Sh Ramesh Panjwani	PS

Finance & Accounts
Head : Sh M K Jain

Name	Designation
Sh M K Jain	COFA
Sh. S N Gulia	F&AO
Sh Upender kumar	F&AO
Sh Ajay Kumar	S O (F&A)
Sh S K Thakur	S O (F&A)
Sh R P Meena	S O (F&A)
Ms Sumit Kumari Panwar	S O (F&A)

Stores And Purchase
Head : Sh Tariq Badar

Name	Designation
Sh Tariq Badar	COSP
Sh Kuldeep Kaushik	SPO
Sh Jai Singh	S O (str & pur)
Sh Mahesh Kumar Bangar	S O (str & pur)

Works and Services
Head : Sh Rakesh Kumar Bindal

Name	Designation
Sh Rakesh Kumar Bindal	Sr. Supt. Engnr.
Dr Sanjeev Sinha	Principal Scientist
Sh Deepak Bansal	Sr. Technical Officer (3)
Sh Mohan Chandra Singh	Sr. Technical Officer (3)
Sh Gurdeep Singh Lamba	Sr. Technical Officer (3)
Sh Anand Kumar Mishra	Asstt. Exe.Engineer (Civil)
Sh Rambir Singh	Asstt.Exe. Engineer
Dr Harish Chandra	Sr. Technical Officer (1)
Sh Bendale Deepak Shaligram	Technical Officer

Workshop
Head : Dr T D Senguttuvan

Name	Designation
Sh Rajeev Sharma	Sr. Technical Officer (1)
Sh Virendra Kumar Gupta	Technical Officer

Computation and Network Facility
Head : Dr Ravi Mehrotra

Name	Designation
Dr Ravi Mehrotra	Chief Scientist
Sh Nitin Sharma	Sr Scientist
Ms Anjali Sharma	Scientist
Sh Trilok Bhardwaj	Scientist
Sh Vijay Sharma	Sr. Technical Officer (3)
Sh Kanwaljit Singh	Sr. Technical Officer (3)

Directorate
Head : Prof. R C Budhani

Name	Designation
Prof R C Budhani	Director
Dr Godavarthi Bhagavannarayana	Chief Scientist
Sh Prabhat Kumar Gupta	Chief Scientist
Dr (Ms) Rashmi	Chief Scientist
Dr Rajendra Prasad Pant	Sr Principal Scientist
Dr Sukhvir Singh	Sr Principal Scientist
Dr (Ms) Renu Pasricha	Principal Scientist
Dr Avanish K Srivastava	Principal Scientist
Dr T D Senguttuvan	Principal Scientist
Dr Kamlesh Kumar Maurya	Principal Scientist
Ms Santosh Singh Golia	Sr Scientist
Dr Nahar Singh	Sr Scientist
Dr (Ms) Prabha Johri	Sr Scientist
Dr Shankar Gopal Aggarwal	Sr Scientist
Dr Narayanaswamy Vijayan	Sr Scientist
Dr Surendra Pal Singh	Scientist
Dr (Ms) Sushree Swarupa Tripathy	Scientist
Dr (Ms) Daya Soni	Scientist
Dr Vidya Nand Singh	Scientist
Dr Gounda Abdul Basheed	Scientist
Dr Manas kumar Dalai	Jr Scientist
Sh Niranjan Singh	Principal Technical Officer
Sh V D Arora	Principal Technical Officer
Sh Kedar Nath Sood	Sr. Technical Officer (3)
Sh Rajiv Kumar Saxena	Sr. Technical Officer (3)
Sh Ashok Kumar	Sr. Technical Officer (3)
Sh Amar Singh	Sr. Technical Officer (1)
Sh Dinesh Singh	Sr. Technical Officer (1)
Ms Anita Sharma	Technical Officer
Dr Khem Singh	Technical Officer
Ms Jyoti Pokhariyal	Technical Officer

Intellectual Property and Human Resource
Head : Dr K P Chaudhary

Name	Designation
Dr Rajeev Chopra	Chief Scientist
Dr Krishan Kumar Saini	Chief Scientist
Dr (Ms) Jyoti Lata Pandey	Chief Scientist
Dr D P Bhatt	Sr Principal Scientist
Dr. Vijay Kumar (Gumber)	Sr Principal Scientist
Sh N K Wadhwa	Principal Scientist
Ms Anuradha Sengar	Principal Scientist
Dr R G Mathur	Scientist
Sh Abhishek Sharma	Jr Scientist
Sh Ashwani Kumar Suri	Sr. Technical Officer (3)
Sh Rajpal Zamaji Walke	Sr. Technical Officer (2)
Ms Neetu Chandra	Sr. Technical Officer (1)

Retired Persons	
Sh Rajbir Singh	Principal Scientist
Mrs Mohini Nebhnani	Asstt (G) Grade -1 (ACP3)
Sh Rupender Chakraborty	Sr. Technician (2)
Sh Jai Kumar Singh	Asst (Str & pur) Grade III
Sh H L Gera	Sr Stenographer (ACP3)
Sh Bhagwan Das	Sr. Technician (2)
Dr Ashok Kumar	Chief Scientist
Sh T Raghavendra	Chief Scientist
Sh Vinay Sharma	S O (str & pur)
Dr Sunil Kumar Singhal	Chief Scientist
Sh Ram Sharan	Sr. Technician (2)
Sh Jai Prakash Ram	Sr. Technician (2)
Sh Giriver Singh	Sr. Technician (2)
Sh Subhash Chander	Sr. Technician (2)
Sh Subodh Kumar Singhal	Chief Scientist
Sh Pattamatta Subrahmanyam	Chief Scientist
Sh Fahimuddin	Sr. Technician (2)
Sh Shyam Narain	Record Keeper (ACP3)
Sh Bhola Shankar	Asstt (G) Grade -1 (ACP3)
Sh Trilok Singh Negi	Sr. Technician (2)

Sh Jai Dav Chawla	Sr. Technician (2)
Sh B C Mallick	Sr. Technician (2)
Dr Jugdish Chandra Sharma	Chief Scientist
Ms Savtantr Rani	Asst.(str and Pur.) Grad 1
Sh Mukul Sharma	Principal Technical Officer
Sh Vijinder Singh	Karya Sahayak (ACP2)
Sh T V Joshua	COA
Sh Bhim Singh Rawat	Sr. Technician (2)
Sh Jagdish Prasad	Sr. Technical Officer (3)
Sh Prem Prakash	Asst. (Str & Pur) Grade I
Sh Ram Dev	Lab Assistant
Sh Surinder Pal Singh Bajaj	Sr. Technician (2)
Ms Naina Awatramani	PS
Sh Virendra Babu	Principal Technical Officer
Dr Sushil Kumar Jain	Chief Scientist
Sh Ram Kumar	Lab Assistant
Dr (Ms) Kiran Jain	Chief Scientist

Obituaries

Sh Anup Kumar Agnihotri	Sr. Technician (1)

Scientists Fellow & Emeritus Scientists

Dr S K Aggarwal	Emeritus Sci.
Dr S K Haldar	Emeritus Sci.
Dr B R Chakraborty	Emeritus Sci.
Dr S K Sarkar	Emeritus Sci.
Dr Hari Kishan	Emeritus Sci.
Dr S K Singhal	Emeritus Sci.
Dr K K Mahajan	INSA Honorary Sci
Dr Krishan Lal	INSA Sr. Sci.
Dr.Preeti Bijlani	Part time Medical Officer
Dr M L Moga	Part time Medical Officer
Dr Sudesh K Chug	Part time Medical Officer
Dr S K Joshi	Platinum Jub. Emr. Sci
Dr Anuj Kumar	Post Doctoral Fellow
Sh Brajesh Tiwari	Post Doctoral Fellow
Dr Vikram Soni	Research Sci C
Dr Gopal Bhatia	Project Adviser

Sh R C Anandani	Project Adviser
Sh Kavindra Pant	Project Adviser
Dr H R Singh	Project Adviser
Dr O P Bahl	Project Adviser / Co-ordinator
Dr. (Ms) Shubhra Kala	Scientist Fellow
Dr Koushik Samanta	Scientist Fellow
Dr Prasun Ganguly	Scientist Fellow - CSIR Nehru Science PDR Fellowship
Dr Deepak Garg	Ad-hoc Scientist

Research Fellows / Associates / Interns

Ms Mansi Sharma	JRF (NPL)
Ms Deepika Chaudhary	JRF (NPL)
Ms Jeevan Jyoti	JRF (NPL)
Sh Rahul Singh Bhauryal	JRF (NPL)
Ms Sonia	JRF (NPL)
Sh Komal Jain	JRF (NPL)
Ms Anupam Shakya	JRF (NPL)
Ms Srishti Chugh	JRF (NPL)
Ms Arti Rawat	JRF (NPL)
Ms Bhumika Ray	JRF (NPL)
Ms Neha Gupta	JRF (NPL)
Ms Pooja Singh	JRF (NPL)
Ms Renchu Scaria	JRF (UGC)
Sh Avirup Sen	JRF- SPMF (Shyama Prasad Mukherjee Fellowship)
Ms Pratibha Goel	JRF(CSIR)
Sh Shijin Babu P.	JRF(CSIR)
Sh Suraj Singh Saini	JRF(CSIR)
Sh Prakash Ranjan Singh	JRF(CSIR)
Ms Shweta Agarwal	JRF(CSIR)
Sh Shahjad	JRF(CSIR)
Sh Shashank Tripathi	JRF(CSIR)
Sh Raman M	JRF(CSIR)
Ms Swati	JRF(CSIR)
Ms Shobhita Singal	JRF(CSIR)
Ms Chanchal Gupta	JRF(CSIR)
Ms Kumari Vijeta	JRF(CSIR)

Sh Prashant Singh	JRF(CSIR)
Sh Anurag Reddy	JRF(CSIR)
Sh Shobhit Goel	JRF(CSIR)
Ms Amrita Soni	JRF(CSIR)
Ms Vijay Prajapati	JRF(CSIR)
Ms Neha Gupta	JRF(UGC)
Sh Akash Yadav	JRF(UGC)
Ms Kanika Thukral	JRF(UGC)
Sh Hitesh Gautam Borkar	JRF(UGC)
Sh Aniket Rana	JRF(UGC)
Ms Shipra Solanki	JRF(UGC)
Ms Sweeti	JRF(UGC)
Sh Abhiram Lochan	JRF(UGC)
Sh Pawan Kumar	JRF(UGC-RGNF)
Sh Chandra Shekhar Gohiya	JRF(UGC-RGNF)
Ms Nisha Prakash	JRF(UGC-RGNF)
Sh Ashutosh Sharan Sinha	JRF-GATE
Sh Afaqul Zafer	JRF-GATE
Ms Santawana Pati	JRF-GATE
Ms Akansha	JRF-GATE
Sh Lalit Mohan Kandpal	JRF-INSPIRE
Sh Ravi Kant Tripathi	JRF-MNRE
Ms Aarti Mehta	JRF-MNRE
Dr Farman Ali	P.I. (INSPIRE Faculty)
Dr Priti Singh	P.I. (INSPIRE Faculty)
Dr Dilip Kumar Singh	P.I. (INSPIRE Faculty)
Dr (Ms) Punita Singh	P.I.(WOS-A)
Ms Munu Borah	P.I.(WOS-A)
Ms Deepika Yadav	Quick Hire Scientist (Trainee)
Sh Dilip Kumar Kaushik	Quick Hire Scientist (Trainee)
Sh Aswin V.	Quick Hire Scientist (Trainee)
Sh Vattikonda Bharath	Quick Hire Scientist (Trainee)
Sh Anuj Krishna	Quick Hire Scientist (Trainee)
Sh Ratneshwar Thakur	Quick Hire Scientist (Trainee)
Sh Achu Chandran	Quick Hire Scientist (Trainee)
Sh Dibyajyoti Mohanty	Quick Hire Scientist (Trainee)
Ms Indu Elizabeth	Quick Hire Scientist (Trainee)
Ms Neha Kapoor Singhal	RA

Ms Naseema Begum	RA
Ms Indrani Coondoo	RA
Ms Kavita Sharma	RA
Ms. Taranuum Bano	RA
Dr (Ms) Jyoti Shah	RA
Ms Nirmal Prabhakar	RA
Dr Gajala Ruhi	RA
Dr Sandhya Dwevedi	RA
Dr (Mrs) Maumita Das	RA
Sh Ankur Anand	RA
Dr Divya Khetarpal	RA
Sh M Raju	RA
Sh Pradeep kumar Pandey	Res. Intern
Ms Kanika Anand	Res. Intern
Sh Virendra Singh Manral	Res. Intern
Ms Ankita Rajput	Res. Intern
Sh Venkata Swamy Gollapothu	Res. Intern
Sh Mohammad Israfil	Res. Intern
Ms Ambika Bawa	Res. Intern
Ms Poonam Gupta	Res. Intern
Sh Abhinav Agnihotri	Res. Intern
Ms Sathi Chakraborty	Res. Intern
Ms Tanika Agrawal	Res. Intern
Sh Abhishek Kumar	Res. Intern
Sh Sourav Das	Res. Intern
Ms Shiva Maheshwari	Res. Intern
Sh Vigil Varghese	Res. Intern
Ms Kritika Anand	Res. Intern
Ms Geetanjali Sharma	Res. Intern
Ms Poonam Rani	Res. Intern
Ms Naina Narang	Res. Intern
Ms Chandni Puri	Res. Intern
Ms Sheetal Rajput	Res. Intern
Sh Anshul Jain	Res. Intern
Ms Vasudha Agarwal	Res. Intern
Ms Rupali Das	Res. Intern
Sh Rajeev Kumar	Res. Intern
Sh Sanjeev Kumar	Research Assistant

Dr (Ms) Suman	Sr. Res. Assoc.
Dr Manoj Kumar Srivastava	Sr. Res. Assoc.
Dr (Ms) Amita Verma	Sr. Res. Assoc.
Ms Richa Singh	SRF (CSIR)
Sh Prabal Pratap Singh Bhadauria	SRF (CSIR)
Sh Ranjit Kumar	SRF (CSIR)
Mrs. K Jayanti	SRF (CSIR)
Sh Monojit Chakraborty	SRF (CSIR)
Sh Vinod Kumar Chahar	SRF (CSIR)
Sh Ashish Gupta	SRF (CSIR)
Ms Richa Baronia	SRF (CSIR)
Ms Stuti Joshi	SRF (CSIR)
Sh Pramod Kumar	SRF (CSIR)
Ms Harjeet Kaur	SRF (CSIR)
Sh Ajay Kumar Kesarwani	SRF (CSIR)
Sh Subhash Chandra	SRF (CSIR)
Sh Ajay Shankar	SRF (CSIR)
Sh Manish Verma	SRF (CSIR)
Sh Sandeep Kumar	SRF (CSIR)
Sh Saurabh Srivastava	SRF (CSIR)
Ms Nidhi Puri	SRF (CSIR)
Sh Amit Kumar Chauhan	SRF (CSIR)
Ms Aditya Sharma	SRF (CSIR)
Ms Aneeta Kharkwal	SRF (CSIR)
Sh Kajal Kumar Dey	SRF (CSIR)
Sh Sandeep Kumar Pundir	SRF (CSIR)
Sh Surjeet Kumar Mishra	SRF (CSIR)
Sh Amit Kumar	SRF (CSIR)
Dr Razi Ahmad	SRF (CSIR)
Md. Azahar Ali	SRF (CSIR)
Ms Omwati	SRF (CSIR)
Ms Rakhi Grover	SRF (CSIR)
Sh Amitava Bandhyopadhyay	SRF (CSIR)
Sh Atif Khan	SRF (CSIR)
Sh Neelesh kumar Lodhi	SRF (CSIR)
Sh Pawan Kumar	SRF (CSIR)
Sh Rajesh Kumar	SRF (CSIR)
Sh Tajendra Kumar Gupta	SRF (CSIR)

Sh Nitu Kumar	SRF (CSIR)
Ms Sugandha Dogra	SRF (CSIR)
Ms Deepa Joshi	SRF (CSIR)
Ms Rajni	SRF (CSIR)
Sh Chandra Mouli Pandey	SRF (CSIR)
Ms Poonam Yadav	SRF (CSIR)
Ms Noor Jahan	SRF (CSIR)
Ms Priyanka Tyagi	SRF (CSIR)
Ms Hema Bhandari	SRF (CSIR-UGC)
Sh Ravi Kant Prashad	SRF (CSIR-UGC)
Sh Umesh kumar	SRF (CSIR-UGC)
Sh Deepak Kumar Jangir	SRF (Extnd)-CSIR, NPL
Sh Purushottam Bhawre	SRF (NPL)
Ms Savvi Mishra	SRF (Project)
Mr Nadarajah Muhunthan	SRF (UGC)
Sh Veeresh Kumar	SRF (UGC)
Sh Anoop Kumar S	SRF (UGC)
Sh Vishal Bharti	SRF (UGC)
Aman Bhardwaj	SRF (UGC)
Sh Ompal Singh	SRF (UGC)
Sh Sudhanshu Kumar	SRF (UGC)
Ms Rekha Gupta	SRF (UGC)
Sh Atul Bist	SRF (UGC)
Ms Rachna Sharma	SRF (UGC)
Sh Jitendra Gangwar	SRF (UGC)
Sh Tilak Joshi	SRF (UGC-NPL)
Sh Ajay Kumar	SRF (UGC-NPL)
Sh Vikash Agarwal	SRF-CSIR, NPL
Sh B Riscob	SRF-CSIR, NPL
Sh Rajveer Jha	SRF-CSIR, NPL
Ms Vasundha Agarwal	SRF-CSIR, NPL
Ms Neha Batra	SRF-CSIR, NPL
Ms Daisy Verma	SRF-CSIR, NPL
Ms Geetanjali	SRF-CSIR, NPL
Sh Prasanna Kumar Rout	SRF-CSIR, NPL
Ms Ruchi Singh	SRF-CSIR, NPL(Project)
Ms Sonika	SRF-DBT
Ms Gunjan Tyagi	SRF-ICMR, NPL

Sh Bighnaraj Sarangi	SRF-INSPIRE
Sh Anil Kumar	SRF-MNRE
Ms Monika Mishra	SRF-MNRE
Ms Rajni Porwal	SRF-NPL (Project)
Sh Ramesh Chandra Bhatt	SRF-NPL (Project)
Sh Kunal	SRF-NPL (Project)
Sh Dharam Pal Singh	SRF-RGN
Ms Arti Rani	SRF-RGN

Appendix - 15

NPL Research Council Members

01.	**Prof Ajay Kumar Sood** Chairman, Division of Physical and Mathematical Sciences, Dept of Physics, Indian Institute of Science, BANGALORE - 560 012	Chairman
02.	**Dr C S Sundar** Director, Materials Science Group, Indira Gandhi Centre for Atomic Research (IGCAR), KALPAKKAM - 603 102	Ext. Member
03.	**Prof Indranil Manna** Director, Indian Institute of Technology Kanpur KANPUR - 208 016	Ext. Member
04.	**Prof R K Shevgaonkar** Director. Indian Institute of Technology Delhi, Hauz Khas NEW DELHI – 110 016	Ext. Member
05.	**Prof Arun Kumar Grover** Vice Chancellor, Panjab University, CHANDIGARH – 160 014	Ext. Member
06.	**Prof D Narayana Rao** Director (Research), SRM University, KATHANKULATHUR - 603 203	Ext. Member
07.	**Dr Praveer Asthana** Mission Director (Nano Mission), Department of Science and Technology (DST), Technology Bhawan, New Mehrauli Road, NEW DELHI - 110 016	Agency Represent Member
08.	**Prof Gautam Biswas** CSIR-Central Mechanical Engineering Research Institute, Mahatma Gandhi Avenue, DURGAPUR - 713 209	Member DG's Nominee Director,

09.	**Dr Vijayamohanan K Pillai** Director, CSIR-Central Electrochemical Research Institute, **KARAIKUDI - 630 006**	Sister Lab Member
10.	**Dr Chandra Shekhar** Director, CSIR-Central Electronics Engineering Research Institute (CEERI), **PILANI – 333 031**	Cluster Director Member
11.	**Dr Sudeep Kumar** **Head** Planning & Performance Division, Council of Scientific & Industrial Research, Anusandhan Bhawan, 2 Rafi Marg, **NEW DELHI - 110 001**	Permanent Invitee Member
12.	**Prof R C Budhani** Director, CSIR-National Physical Laboratory, Dr K S Krishnan Marg, **NEW DELHI - 110 012**	**Director** Member
13.	**Dr T D Senguttuven** Head, Planning Monitoring & Evaluation, CSIR-National Physical Laboratory, Dr K S Krishnan Marg, **NEW DELHI - 110 012**	**Non-Member Secy.**

NPL Management Council Members

1.	Prof R.C. Budhani, Director, NPL	Chairman
2.	Dr. S. Gangopadhyay, Director, CRRI	Member
3.	Dr. H.C. Kandpal, Chief Scientist	Member
4.	Dr. Rajesh, Pri. Scientist	Member
5.	Dr. Ritu Srivastava, Sr. Scientist	Member
6.	Dr. G.A. Basheed, Scientist	Member
7.	Sh. R.K. Bindal, Pri.T.O. Gr.III(7)	Member
8.	Dr. T.D. Senguttuvan, Pri. Scientist	Member
9.	Sh. Upender Kumar, F& A O	Member
10.	Sh. V.K. Kaushika, COA	Member-Convenor

राष्ट्रीय भौतिक प्रयोगशाला, नई दिल्ली
(वैज्ञानिक तथा औद्योगिक अनुसंधान परिषद्)

NATIONAL PHYSICAL LABORATORY
(Council of Scientific and Industrial Research)

Dr. K.S. Krishnan Marg, New Delhi-110012
www.nplindia.org

गुणवत्ता नीति • Quality Policy

अन्तर्राष्ट्रीय मानकों के अनुरूप बनाए गए राष्ट्रीय मापन मानकों को सतत् अनुसंधान और विकास द्वारा स्थापित करना, उनका रख रखाव करना और उनका उन्नयन करना।

आई एस/आई एस ओ/ आई ई सी 17025:2005 के अनुसार शीर्ष स्तर का अंशाकन प्रदान करना एवं मानकों के प्रसार का कार्य करना जिससे गुणवत्ता प्रणाली का सजगता और दक्षता से पालन करते हुए मापों की अनुमार्गणीयता को बनाए रखना।

To establish, maintain and upgrade the national standards of measurement compatible to international standards through continuous research and development.

To provide apex level calibration and dissemination of standards for maintaining the traceability of measurement following Quality System as per IS/ISO/IEC 17025:2005 consciously and effectively.

उद्देश्य • Objectives

पूर्व निर्धारित अवधि में अंशाकन और परीक्षण का कार्य पूरा करना जिससे ग्राहक भी पूर्णतया संतुष्ट हों।

सभी अंशाकन व परीक्षण से सम्बन्धित कार्मिकों को गुणवत्ता प्रणाली की नीतियों और कार्य विधियों के प्रलेखन और कार्यान्वयन से अवगत कराना।

To provide calibration and testing within the spe-cified time, and to the satisfaction of the customers.

To familiarize all personnel concerned in calibration and testing with quality system documentation and implementation of policies and procedures.

प्रो. रमेश चन्द्र बुधानी
निदेशक

Prof. Ramesh Chandra Budhani
Director

निकटवर्ती प्रमुख लैंडमार्क
IMPORTANT NEARBY LANDMARK

पूसा कैम्पस (आईएआरआई)
PUSA CAPMUS (IARI)

राजेन्द्र प्लेस मेट्रो स्टेशन
RAJENDRA PLACE METRO STN.

- राजेन्द्र प्लेस मेट्रो स्टेशन : 01 किमी.
  Rajendra Place Metro Station : 01 km
- कनॉट प्लेस (राजीव चौक) : 05 किमी.
  Connaught Place (Rajiv Chowk) : 05 km
- नई दिल्ली रेलवे स्टेशन : 06 किमी.
  New Delhi Railway Station : 06 km
- अंतरराष्ट्रीय बस-अड्डा : 08 किमी.
  I.S.B.T. : 08 km
- पुरानी दिल्ली रेलवे स्टेशन : 09 किमी.
  Old Delhi Railway Station : 09 km
- इन्दिरा गांधी अंतरराष्ट्रीय हवाई-अड्डा :
  Indira Gandhi International Airport :
  - घरेलू (टर्मिनल) : 11 किमी.
    Domestic (Terminal) : 11 km
  - अंतरराष्ट्रीय (टर्मिनल) : 19 किमी.
    International (Terminal) : 19 km

निदेशक
Director

प्रो. आर. सी. बुधानी
Prof R C Budhani
+91-11-4560 9201/301
dnpl@nplindia.org
फैक्स: **+91-11-4560 9310**
Fax: +91-11-4560 9310

कार्य दिवस
Working Days

सोमवार से शुक्रवार
Monday to Friday

कार्य समय
Working Hours

प्रातः 9:00 बजे से सांय 5:30 बजे तक
9:00 am to 5:30 pm

सीएसआईआर-राष्ट्रीय भौतिक प्रयोगशाला
डॉ. के. एस. कृष्णन मार्ग, नई दिल्ली 110012

CSIR-National Physical Laboratory
Dr K S Krishnan Marg, New Delhi 110 012

www.nplindia.org